Signal Analysis

Time, Frequency, Scale, and Structure

RONALD L. ALLEN
DUNCAN W. MILLS

SIGNAL ANALYSIS

TIME, FREQUENCY, SCALE, AND STRUCTURE

Ronald L. Allen
Duncan W. Mills

IEEE PRESS

A John Wiley & Sons, Inc., Publication

SIGNAL ANALYSIS

IEEE Press
445 Hoes Lane
Piscataway, NJ 08854

SIGNAL ANALYSIS

TIME, FREQUENCY, SCALE, AND STRUCTURE

Ronald L. Allen
Duncan W. Mills

IEEE PRESS

A John Wiley & Sons, Inc., Publication

Published simultaneously in Canada.

Library of Congress Cataloging-in-Publication Data is available.

ISBN: 0-471-23441-9

Printed in the United States of America

10 9 8 7 6 5 4 3 2 1

To Beverley and to the memory of my parents, Mary and R.L. (Kelley).

R.L.A.

To those yet born, who will in some manner—large or small—benefit from the technology and principles described here. To the reader, who will contribute to making this happen.

D.W.M.

CONTENT

PREFACE

This text provides a complete introduction to signal analysis. Inclusion of fundamental ideas—analog and discrete signals, linear systems, Fourier transforms, and sampling theory—makes it suitable for introductory courses, self-study, and refreshers in the discipline. But along with these basics, *Signal Analysis: Time, Frequency, Scale, and Structure* gives a running tutorial on functional analysis—the mathematical concepts that generalize linear algebra and underlie signal theory. While the advanced mathematics can be skimmed, readers who absorb the material will be prepared for latter chapters that explain modern mixed-domain signal analysis: Short-time Fourier (Gabor) and wavelet transforms.

Quite early in the presentation, *Signal Analysis* surveys methods for edge detection, segmentation, texture identification, template matching, and pattern recognition. Typically, these are only covered in image processing or computer vision books. Indeed, the fourth chapter might seem like a detour to some readers. But the techniques are essential to one-dimensional signal analysis as well. Soon after learning the rudiments of systems and convolutions, students are invited to apply the ideas to make a computer understand a signal. Does it contain anything significant, expected, or unanticipated? Where are the significant parts of the signal? What are its local features, where are their boundaries, and what is their structure? The difficulties inherent in understanding a signal become apparent, as does the need for a comprehensive approach to signal frequency. This leads to the chapters on the frequency domain. Various continous and discrete Fourier transforms make their appearance. Their application, in turn, proves to be problematic for signals with transients, localized frequency components, and features of varying scale. The text delves into the new analytical tools—some discovered only in the last 20 years—for such signals. Time-frequency and time-scale transforms, their underlying mathematical theory, their limitations, how they differently reveal signal structure, and their promising applications complete the book. So the highlights of this book are:

- The signal analysis perspective;
- The tutorial material on advanced mathematics—in particular function spaces, cast in signal processing terms;
- The coverage of the latest mixed domain analysis methods.

We thought that there is a clear need for a text that begins at a basic level while taking a *signal analysis* as opposed to *signal processing* perspective on applications.

The goal of signal analysis is to arrive at a structural description of a signal so that later high-level algorithms can interpret its content. This differs from signal processing *per se*, which only seeks to modify the input signal, without changing its fundamental nature as a one-dimensional sequence of numerical values. From this viewpoint, signal analysis stands within the scope of artificial intelligence. Many modern technologies demand its skills. Human–computer interaction, voice recognition, industrial process control, seismology, bioinformatics, and medicine are examples.

Signal Analysis provides the abstract mathematics and functional analysis which is missing from the backgrounds of many readers, especially undergraduate science and engineering students and professional engineers. The reader can begin comfortably with the basic ideas. The book gradually dispenses the mathematics of Hilbert spaces, complex analysis, disributions, modern integration theory, random signals, and analog Fourier transforms; the less mathematically adept reader is not overwhelmed with hard analysis. There has been no easy route from standard signal processing texts to the latest treatises on wavelets, Gabor transforms, and the like. The gap must be spanned with knowledge of advanced mathematics. And this has been a problem for too many engineering students, classically-educated applied researchers, and practising engineers. We hope that *Signal Analysis* removes the obstacles. It has the signal processing fundamentals, the signal analysis perspective, the mathematics, and the bridge from all of these to crucial developments that began in the mid-1980s.

The last three chapters of this book cover the latest mixed-domain transform methods: Gabor transforms, wavelets, multiresolution analysis, frames, and their applications. Researchers who need to keep abreast of the advances that are revolutionizing their discipline will find a complete introductory treatment of time-frequency and time-scale transforms in the book. We prove the Balian-Low theorem, which pinpoints a limitation on short-time Fourier representations. We had envisioned a much wider scope for mixed-domain applications. Ultimately, the publication schedule and the explosive growth of the field prevented us from achieving a thorough coverage of all principal algorithms and applications—what might have been a fourth highlight of the book. The last chapter explains briefly how to use the new methods in applications, contrasts them with time domain tactics, and contains further references to the research literature.

Enough material exists for a year-long university course in signal processing and analysis. Instructors who have students captive for two semesters may cover the chapters in order. When a single semester must suffice, Chapters 1–3, 5, 7, 8, and 9 comprise the core ideas. We recommend at least the sections on segmentation and thresholding in Chapter 4. After some programming experiments, the students will see how hard it is to make computers do what we humans take for granted. The instructor should adjust the pace according to the students' preparation. For instance, if a system theory course is prerequisite—as is typical in the undergraduate engineering curriculum—then the theoretical treatments of signal spaces, the Dirac delta, and the Fourier transforms are appropriate. An advanced course can pick up the mathematical theory, the pattern recognition material in

Chapter 4, the generalized Fourier transform in Chapter 6, and the analog filter designs in Chapter 9. But the second semester work should move quickly to and concentrate upon Chapters 10–12. This equips the students for reading the research literature.

RONALD L. ALLEN
San José, California

DUNCAN W. MILLS
Mountain View, California

ACKNOWLEDGMENTS

We would like to thank the editorial and production staffs on John Wiley and Sons and IEEE Press for their efficiency, courtesy, patience, and professionalism while we wrote this book. We are especially grateful to Marilyn G. Catis and Anthony VenGraitis of IEEE Press for handling incremental submissions, managing reviews, and providing general support over the years. We are grateful to Beverley Andalora for help with the figures, to William Parker of Philips Speech Recognition Systems for providing digital speech samples, and to KLA-Tencor Corporation for reflectometry and scanning electron microscopy data samples.

RONALD L. ALLEN

DUNCAN W. MILLS

CHAPTER 1

Signals: Analog, Discrete, and Digital

Analog, discrete, and digital signals are the raw material of signal processing and analysis. Natural processes, whether dependent upon or independent of human control, generate analog signals; they occur in a continuous fashion over an interval of time or space. The mathematical model of an analog signal is a function defined over a part of the real number line. Analog signal conditioning uses conventional electronic circuitry to acquire, amplify, filter, and transmit these signals. At some point, digital processing may take place; today, this is almost always necessary. Perhaps the application requires superior noise immunity. Intricate processing steps are also easier to implement on digital computers. Furthermore, it is easier to improve and correct computerized algorithms than systems comprised of hard-wired analog components. Whatever the rationale for digital processing, the analog signal is captured, stored momentarily, and then converted to digital form. In contrast to an analog signal, a discrete signal has values only at isolated points. Its mathematical representation is a function on the integers; this is a fundamental difference. When the signal values are of finite precision, so that they can be stored in the registers of a computer, then the discrete signal is more precisely known as a digital signal. Digital signals thus come from sampling an analog signal, and—although there is such a thing as an analog computer—nowadays digital machines perform almost all analytical computations on discrete signal data.

This has not, of course, always been the case; only recently have discrete techniques come to dominate signal processing. The reasons for this are both theoretical and practical.

On the practical side, nineteenth century inventions for transmitting words, the telegraph and the telephone—written and spoken language, respectively—mark the beginnings of engineered signal generation and interpretation technologies. Mathematics that supports signal processing began long ago, of course. But only in the nineteenth century did signal theory begin to distinguish itself as a technical, engineering, and scientific pursuit separate from pure mathematics. Until then, scientists did not see mathematical entities—polynomials, sinusoids, and exponential functions, for example—as sequences of symbols or carriers of information. They were envisioned instead as ideal shapes, motions, patterns, or models of natural processes.

Signal Analysis: Time, Frequency, Scale, and Structure, by Ronald L. Allen and Duncan W. Mills
ISBN: 0-471-23441-9

The development of electromagnetic theory and the growth of electrical and electronic communications technologies began to divide these sciences. The functions of mathematics came to be studied as bearing information, requiring modification to be useful, suitable for interpretation, and having a meaning. The life story of this new discipline—signal processing, communications, signal analysis, and information theory—would follow a curious and ironic path. Electromagnetic waves consist of coupled electric and magnetic fields that oscillate in a sinusoidal pattern and are perpendicular to one another and to their direction of propagation. Fourier discovered that very general classes of functions, even those containing discontinuities, could be represented by sums of sinusoidal functions, now called a Fourier series [1]. This surprising insight, together with the great advances in analog communication methods at the beginning of the twentieth century, captured the most attention from scientists and engineers.

Research efforts into discrete techniques were producing important results, even as the analog age of signal processing and communication technology charged ahead. Discrete Fourier series calculations were widely understood, but seldom carried out; they demanded quite a bit of labor with pencil and paper. The first theoretical links between analog and discrete signals were found in the 1920s by Nyquist,[1] in the course of research on optimal telegraphic transmission mechanisms [2]. Shannon[2] built upon Nyquist's discovery with his famous sampling theorem [3]. He also proved something to be feasible that no one else even thought possible: error-free digital communication over noisy channels. Soon thereafter, in the late 1940s, digital computers began to appear. These early monsters were capable of performing signal processing operations, but their speed remained too slow for some of the most important computations in signal processing—the discrete versions of the Fourier series. All this changed two decades later when Cooley and Tukey disclosed their fast Fourier transform (FFT) algorithm to an eager computing public [4–6]. Digital computations of Fourier's series were now practical on real-time signal data, and in the following years digital methods would proliferate. At the present time, digital systems have supplanted much analog circuitry, and they are the core of almost all signal processing and analysis systems. Analog techniques handle only the early signal input, output, and conditioning chores.

There are a variety of texts available covering signal processing. Modern introductory systems and signal processing texts cover both analog and discrete theory [7–11]. Many reflect the shift to discrete methods that began with the discovery of the FFT and was fueled by the ever-increasing power of computing machines. These often concentrate on discrete techniques and presuppose a background in analog

[1]As a teenager, Harry Nyquist (1887–1976) emigrated from Sweden to the United States. Among his many contributions to signal and communication theory, he studied the relationship between analog signals and discrete signals extracted from them. The term *Nyquist rate* refers to the sampling frequency necessary for reconstructing an analog signal from its discrete samples.

[2]Claude E. Shannon (1916–2001) founded the modern discipline of information theory. He detailed the affinity between Boolean logic and electrical circuits in his 1937 Masters thesis at the Massachusetts Institute of Technology. Later, at Bell Laboratories, he developed the theory of reliable communication, of which the sampling theorem remains a cornerstone.

signal processing [12–15]. Again, there is a distinction between discrete and digital signals. Discrete signals are theoretical entities, derived by taking instantaneous—and therefore exact—samples from analog signals. They might assume irrational values at some time instants, and the range of their values might be infinite. Hence, a digital computer, whose memory elements only hold limited precision values, can only process those discrete signals whose values are finite in number and finite in their precision—digital signals. Early texts on discrete signal processing sometimes blurred the distinction between the two types of signals, though some further editions have adopted the more precise terminology. Noteworthy, however, are the burgeoning applications of digital signal processing integrated circuits: digital telephony, modems, mobile radio, digital control systems, and digital video to name a few. The first high-definition television (HDTV) systems were analog; but later, superior HDTV technologies have relied upon digital techniques. This technology has created a true digital signal processing literature, comprised of the technical manuals for various DSP chips, their application notes, and general treatments on fast algorithms for real-time signal processing and analysis applications on digital signal processors [16–21]. Some of our later examples and applications offer some observations on architectures appropriate for signal processing, special instruction sets, and fast algorithms suitable for DSP implementation.

This chapter introduces signals and the mathematical tools needed to work with them. Everyone should review this chapter's first six sections. This first chapter combines discussions of analog signals, discrete signals, digital signals, and the methods to transition from one of these realms to another. All that it requires of the reader is a familiarity with calculus. There are a wide variety of examples. They illustrate basic signal concepts, filtering methods, and some easily understood, albeit limited, techniques for signal interpretation. The first section introduces the terminology of signal processing, the conventional architecture of signal processing systems, and the notions of analog, discrete, and digital signals. It describes signals in terms of mathematical models—functions of a single real or integral variable. A specification of a sequence of numerical values ordered by time or some other spatial dimension is a time domain description of a signal. There are other approaches to signal description: the frequency and scale domains, as well as some—relatively recent—methods for combining them with the time domain description. Sections 1.2 and 1.3 cover the two basic signal families: analog and discrete, respectively. Many of the signals used as examples come from conventional algebra and analysis.

The discussion gets progressively more formal. Section 1.4 covers sampling and interpolation. Sampling picks a discrete signal from an analog source, and interpolation works the other way, restoring the gaps between discrete samples to fashion an analog signal from a discrete signal. By way of these operations, signals pass from the analog world into the discrete world and vice versa. Section 1.5 covers periodicity, and foremost among these signals is the class of sinusoids. These signals are the fundamental tools for constructing a frequency domain description of a signal. There are many special classes of signals that we need to consider, and Section 1.6 quickly collects them and discusses their properties. We will of course expand upon and deepen our understanding of these special types of signals

throughout the book. Readers with signal processing backgrounds may quickly scan this material; however, those with little prior work in this area might well linger over these parts.

The last two sections cover some of the mathematics that arises in the detailed study of signals. The complex number system is essential for characterizing the timing relationships in signals and their frequency content. Section 1.7 explains why complex numbers are useful for signal processing and exposes some of their unique properties. Random signals are described in Section 1.8. Their application is to model the unpredictability in natural signals, both analog and discrete. Readers with a strong mathematics background may wish to skim the chapter for the special signal processing terminology and skip Sections 1.7 and 1.8. These sections can also be omitted from a first reading of the text.

A summary, a list of references, and a problem set complete the chapter. The summary provides supplemental historical notes. It also identifies some software resources and publicly available data sets. The references point out other introductory texts, reviews, and surveys from periodicals, as well as some of the recent research.

1.1 INTRODUCTION TO SIGNALS

There are several standpoints from which to study signal analysis problems: empirical, technical, and theoretical. This chapter uses all of them. We present lots of examples, and we will return to them often as we continue to develop methods for their processing and interpretation. After practical applications of signal processing and analysis, we introduce some basic terminology, goals, and strategies.

Our early methods will be largely experimental. It will be often be difficult to decide upon the best approach in an application; this is the limitation of an intuitive approach. But there will also be opportunities for making technical observations about the right mathematical tool or technique when engaged in a practical signal analysis problem. Mathematical tools for describing signals and their characteristics will continue to illuminate this technical side to our work. Finally, some abstract considerations will arise at the end of the chapter when we consider complex numbers and random signal theory. Right now, however, we seek only to spotlight some practical and technical issues related to signal processing and analysis applications. This will provide the motivation for building a significant theoretical apparatus in the sequel.

1.1.1 Basic Concepts

Signals are symbols or values that appear in some order, and they are familiar entities from science, technology, society, and life. Examples fit easily into these categories: radio-frequency emissions from a distant quasar; telegraph, telephone, and television transmissions; people speaking to one another, using hand gestures; raising a sequence of flags upon a ship's mast; the echolocation chirp of animals such as bats and dolphins; nerve impulses to muscles; and the sensation of light patterns

striking the eye. Some of these signal values are quantifiable; the phenomenon is a measurable quantity, and its evolution is ordered by time or distance. Thus, a residential telephone signal's value is known by measuring the voltage across the pair of wires that comprise the circuit. Sound waves are longitudinal and produce minute, but measurable, pressure variations on a listener's eardrum. On the other hand, some signals appear to have a representation that is at root not quantifiable, but rather symbolic. Thus, most people would grant that sign language gestures, maritime signal flags, and even ASCII text could be considered signals, albeit of a symbolic nature.

Let us for the moment concentrate on signals with quantifiable values. These are the traditional mathematical signal models, and a rich mathematical theory is available for studying them. We will consider signals that assume symbolic values, too, but, unlike signals with quantifiable values, these entities are better described by relational mathematical structures, such as graphs.

Now, if the signal is a continuously occurring phenomenon, then we can represent it as a function of a time variable t; thus, $x(t)$ is the value of signal x at time t. We understand the units of measurement of $x(t)$ implicitly. The signal might vary with some other spatial dimension other than time, but in any case, we can suppose that its domain is a subset of the real numbers. We then say that $x(t)$ is an *analog signal*. Analog signal values are read from conventional indicating devices or scientific instruments, such as oscilloscopes, dial gauges, strip charts, and so forth.

An example of an analog signal is the seismogram, which records the shaking motion of the ground during an earthquake. A precision instrument, called a *seismograph*, measures ground displacements on the order of a micron (10^{-6} m) and produces the seismogram on a paper strip chart attached to a rotating drum. Figure 1.1 shows the record of the Loma Prieta earthquake, centered in the Santa Cruz mountains of northern California, which struck the San Francisco Bay area on 18 October 1989.

Seismologists analyze such a signal in several ways. The total deflection of the pen across the chart is useful in determining the temblor's magnitude. Seismograms register three important types of waves: the *primary*, or *P waves*; the *secondary*, or *S waves*; and the *surface waves*. P waves arrive first, and they are compressive, so their direction of motion aligns with the wave front propagation [22]. The transverse S waves follow. They oscillate perpendicular to the direction of propagation. Finally, the large, sweeping surface waves appear on the trace.

This simple example illustrates processing and analysis concepts. Processing the seismogram signal is useful to remove noise. Noise can be minute ground motions from human activity (construction activity, heavy machinery, vehicles, and the like), or it may arise from natural processes, such as waves hitting the beach. Whatever the source, an important signal processing operation is to smooth out these minute ripples in the seismogram trace so as to better detect the occurrence of the initial indications of a seismic event, the P waves. They typically manifest themselves as seismometer needle motions above some threshold value. Then the analysis problem of finding when the S waves begin is posed. Figure 1.1 shows the result of a signal analysis; it slices the Loma Prieta seismogram into its three constituent wave

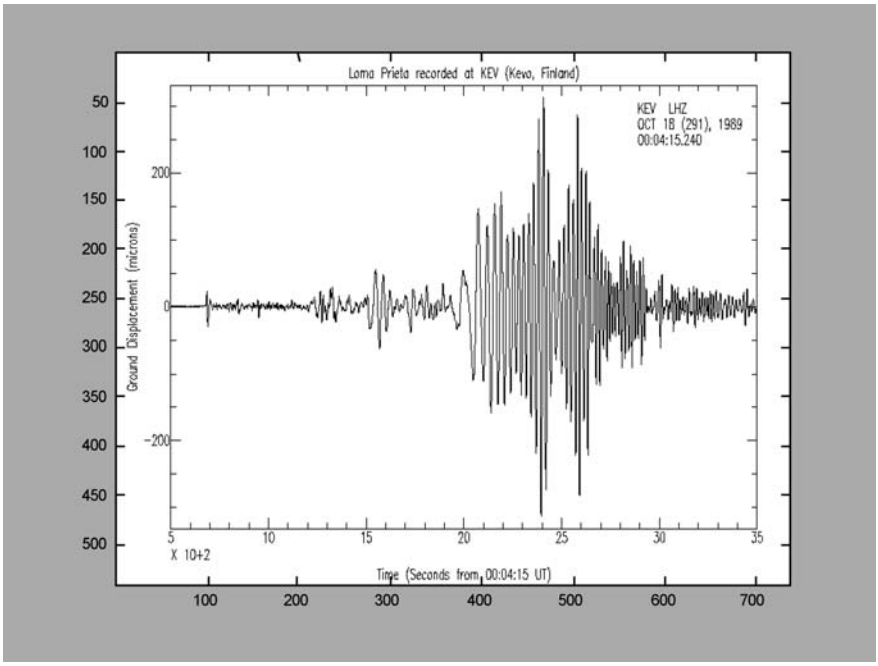

Fig. 1.1. Seismogram of the magnitude 7.1 Loma Prieta earthquake, recorded by a seismometer at Kevo, Finland. The first wiggle—some eight minutes after the actual event—marks the beginning of the low-magnitude P waves. The S waves arrive at approximately t = 1200 s, and the large sweeping surface waves begin near t = 2000 s.

trains. This type of signal analysis can be performed by inspection on analog seismograms.

Now, the time interval between the arrival of the P and S waves is critical. These undulations are simultaneously created at the earthquake's epicenter; however, they travel at different, but known, average speeds through the earth. Thus, if an analysis of the seismogram can reveal the time that these distinct wave trains arrive, then the time difference can be used to measure the distance from the instrument to the earthquake's epicenter. Reports from three separate seismological stations are sufficient to locate the epicenter. Analyzing smaller earthquakes is also important. Their location and the frequency of their occurrence may foretell a larger temblor [23]. Further, soundings in the earth are indicative of the underlying geological strata; seismologists use such methods to locate oil deposits, for example [24]. Other similar applications include the detection of nuclear arms detonations and avalanches. For all of these reasons—scientific, economic, and public safety—seismic signal intepretation is one of the most important areas in signal analysis and one of the areas in which new methods of signal analysis have been pioneered. These further signal interpretation tasks are more troublesome for human interpreters. The signal behavior that distinguishes a small earthquake from a distant nuclear detonation is not apparent. This demands thorough computerized analysis.

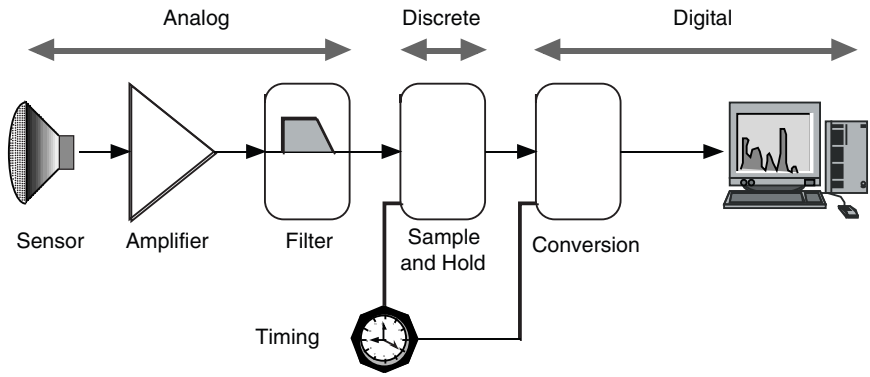

Fig. 1.2. Signal acquisition into a computer. Analog, discrete, and digital signals each occur—at least in principle—within such a system.

Suppose, therefore, that the signal is a discrete phenomenon, so that it occurs only at separate time instants or distance intervals and not continuously. Then we represent it as a function on a subset of the integers $x(n)$ and we identify $x(n)$ as a *discrete signal*. Furthermore, some discrete signals may have only a limited range of values. Their measurable values can be stored in the memory cells of a digital computer. The discrete signals that satisfy this further constraint are called *digital signals*.

Each of these three types of signals occurs at some stage in a conventional computerized signal acquisition system (Figure 1.2). Analog signals arise from some quantifiable, real-world process. The signal arrives at an interface card attached to the computer's input–output bus.

There are generally some signal amplification and conditioning components, all analog, at the system's front end. At the sample and hold circuit, a momentary storage component—a capacitor, for example—holds the signal value for a small time interval. The sampling occurs at regular intervals, which are set by a timer. Thus, the sequence of quantities appearing in the sample and hold device represents the discrete form of the signal. While the measurable quantity remains in the sample and hold unit, a digitization device composes its binary representation. The extracted value is moved into a digital acquisition register of finite length, thereby completing the analog-to-digital conversion process. The computer's signal processing software or its input–output driver reads the digital signal value out of the acquisition register, across the input–output bus, and into main memory. The computer itself may be a conventional general-purpose machine, such as a personal computer, an engineering workstation, or a mainframe computer. Or the processor may be one of the many special purpose *digital signal processors* (DSPs) now available. These are now a popular design choice in signal processing and analysis systems, especially those with strict execution time constraints.

Some natural processes generate more than one measurable quantity as a function of time. Each such quantity can be regarded as a separate signal, in which case

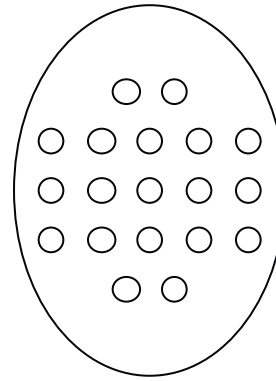

(a)

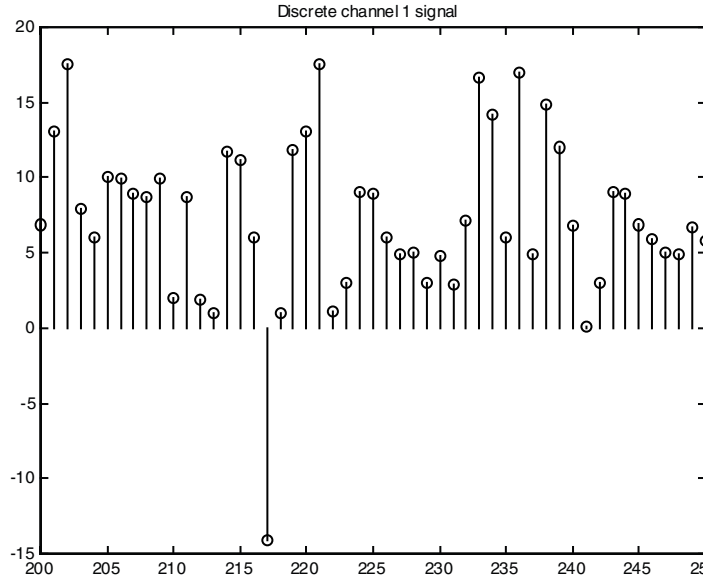

(b)

Fig. 1.3. A multichannel signal: The electroencephalogram (EEG) taken from a healthy young person, with eyes open. The standard EEG sensor arrangement consists of 19 electrodes (a). Discrete data points of channel one (b). Panels (c) and (d) show the complete traces for the first two channels, $x_1(n)$ and $x_2(n)$. These traces span an eight second time interval: 1024 samples. Note the jaggedness superimposed on gentler wavy patterns. The EEG varies according to whether the patient's eyes are open and according to the health of the individual; markedly different EEG traces typify, for example, Alzheimer's disease.

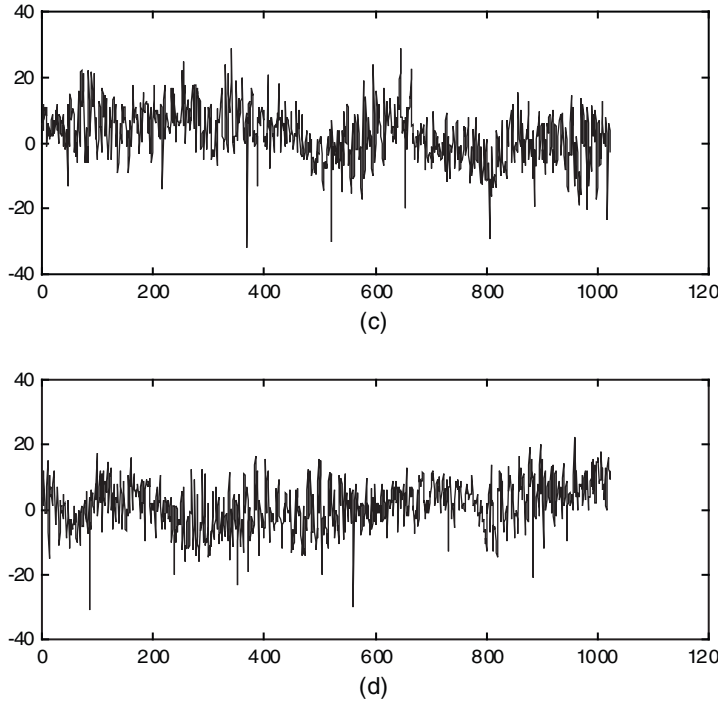

Fig. 1.3 (*Continued*)

they are all functions of the same independent variable with the same domain. Alternatively, it may be technically useful to maintain the multiple quantities together as a vector. This is called a *multichannel* signal. We use boldface letters to denote multichannel signals. Thus, if $\boldsymbol{x}$ is analog and has N channels, then $\boldsymbol{x}(t) = (x_1(t), x_2(t), \ldots, x_N(t))$, where the analog $x_i(t)$ are called the *component* or *channel* signals. Similarly, if $\boldsymbol{x}$ is discrete and has N channels, then $\boldsymbol{x}(n) = (x_1(n), x_2(n), \ldots, x_N(n))$.

One biomedical signal that is useful in diagnosing brain injuries, mental illness, and conditions such as Alzheimer's disease is the *electroencephalogram* (EEG) [25], a multichannel signal. It records electrical potential differences, or voltages, that arise from the interactions of massive numbers of neurons in different parts of the brain. For an EEG, 19 electrodes are attached from the front to the back of the scalp, in a two–five–five–five–two arrangement (Figure 1.3).

The EEG traces in Figure 1.3 are in fact digital signals, acquired one sample every 7.8 ms, or at a sampling frequency of 128 Hz. The signal appears to be continuous in nature, but this is due to the close spacing of the samples and linear interpolation by the plotting package.

Another variation on the nature of signals is that they may be functions of more than one independent variable. For example, we might measure air

temperature as a function of height: $T(h)$ is an analog signal. But if we consider that the variation may occur along a north-to-south line as well, then the temperature depends upon a distance measure x as well: $T(x, h)$. Finally, over an area with location coordinates (x, y), the air temperature is a continuous function of three variables $T(x, y, h)$. When a signal has more than one independent variable, then it is a *multidimensional* signal. We usually think of an "image" as recording light intesity measurements of a scene, but multidimensional signals—especially those with two or three independent variables—are usually called *images*. Images may be discrete too. Temperature readings taken at kilometer intervals on the ground and in the air produce a discrete signal $T(m, n, k)$. A discrete signal is a sequence of numerical values, whereas an image is an array of numerical values. Two-dimensional image elements, especially those that represent light intensity values, are called *pixels*, an acronym for *picture elements*. Occasionally, one encounters the term *voxel*, which is a three-dimensional signal value, or a *volume element*.

An area of multidimensional signal processing and analysis of considerable importance is the intepretation of images of landscapes acquired by satellites and high altitude aircraft. Figure 1.4. shows some examples. Typical tasks are to automatically distinguish land from sea; determine the amount and extent of sea ice; distinguish agricultural land, urban areas, and forests; and, within the agricultural regions, recognize various crop types. These are remote sensing applications.

Processing two-dimensional signals is more commonly called picture or image processing, and the task of interpreting an image is called image analysis or computer vision. Many researchers are involved in robotics, where their efforts couple computer vision ideas with manipulation of the environment by a vision-based machine. Consequently, there is a vast, overlapping literature on image processing [26–28], computer vision [29–31], and robotics [32].

Our subject, signal analysis, concentrates on the mathematical foundations, processing, and especially the intepretation of one-dimensional, single-valued signals. Generally, we may select a single channel of a multichannel signal for consideration; but we do not tackle problems specific to multichannel signal interpretation. Likewise, we do not delve deeply into image processing and analysis. Certain images do arise, so it turns out, in several important techniques for analyzing signals. Sometimes a daunting one-dimensional problem can be turned into a tractable two-dimensional task. Thus, we prefer to pursue the one-dimensional problem into the multidimensional realm only to the point of acknowledging that a straightforward image analysis will produce the intepretation we seek.

So far we have introduced the basic concepts of signal theory, and we have considered some examples: analog, discrete, multichannel, and multidimensional signals. In each case we describe the signals as sequences of numerical values, or as a function of an independent time or other spatial dimension variable. This constitutes a time-domain description of a signal. From this perspective, we can display a signal, process it to produce another signal, and describe its significant features.

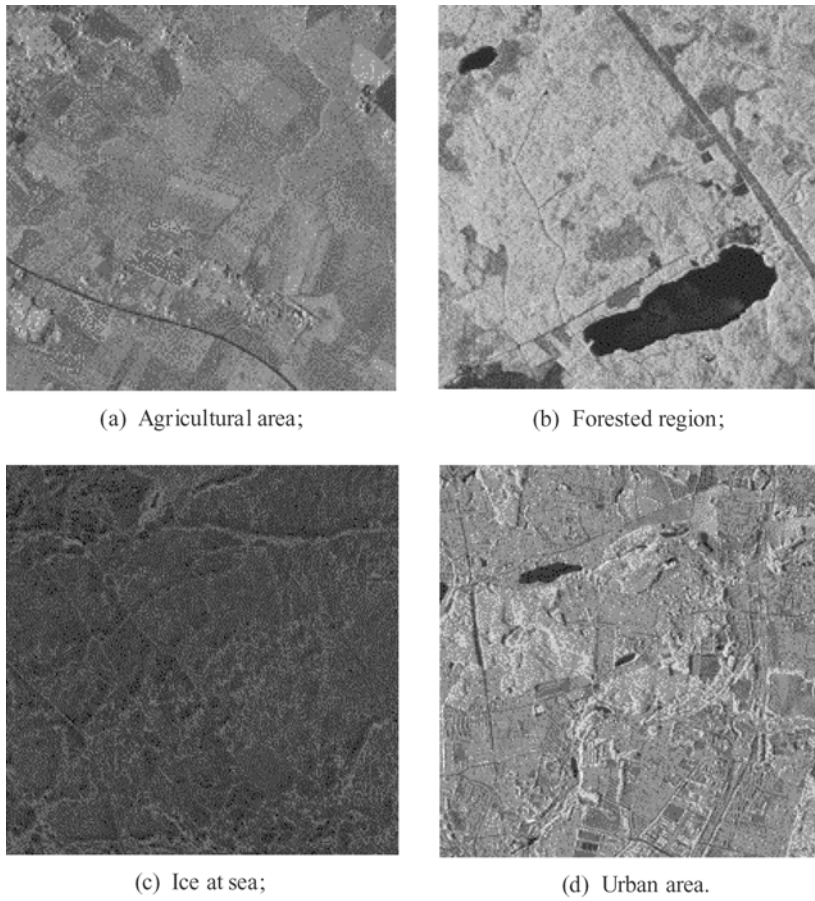

(a) Agricultural area; (b) Forested region; (c) Ice at sea; (d) Urban area.

Fig. 1.4. Aerial scenes. Distinguishing terrain types is a typical problem of image analysis, the interpretation of two-dimensional signals. Some problems, however, admit a one-dimensional solution. A sample line through an image is in fact a signal, and it is therefore suitable for one-dimensional techniques. (a) Agricultural area. (b) Forested region. (c) Ice at sea. (d) Urban area.

1.1.2 Time-Domain Description of Signals

Since time flows continuously and irreversibly, it is natural to describe sequential signal values as given by a time ordering. This is often, but not always, the case; many signals depend upon a distance measure. It is also possible, and sometimes a very important analytical step, to consider signals as given by order of a salient event. Conceiving the signal this way makes the dependent variable—the signal value—a function of time, distance, or some other quantity indicated between successive events. Whether the independent variable is time, some other spatial dimension, or a counting of events, when we represent and discuss a signal in terms of its ordered values, we call this the *time-domain* description of a signal.

Note that a precise time-domain description may elude us, and it may not even be possible to specify a signal's values. A fundamentally unknowable or random process is the source of such signals. It is important to develop methods for handling the randomness inherent in signals. Techniques that presuppose a theory of signal randomness are the topic of the final section of the chapter.

Next we look further into two application areas we have already touched upon: biophysical and geophysical signals. Signals from representative applications in these two areas readily illustrate the time-domain description of signals.

1.1.2.1 Electrocardiogram Interpretation. Electrocardiology is one of the earliest techniques in biomedicine. It also remains one of the most important. The excitation and recovery of the heart muscles cause small electrical potentials, or voltages, on the order of a millivolt, within the body and measurable on the skin. Cardiologists observe the regularity and shape of this voltage signal to diagnose heart conditions resulting from disease, abnormality, or injury. Examples include cardiac dysrhythmia and fibrillation, narrowing of the coronary arteries, and enlargement of the heart [33]. Automatic interpretation of ECGs is useful for many aspects of clinical and emergency medicine: remote monitoring, as a diagnostic aid when skilled cardiac care personnel are unavailable, and as a surgical decision support tool.

A modern electrocardiogram (ECG or EKG) contains traces of the voltages from 12 leads, which in biomedical parlance refers to a configuration of electrodes attached to the body [34]. Refer to Figure 1.5. The voltage between the arms is Lead I, Lead II is the potential between the right arm and left leg, and Lead III reads between the left arm and leg. The WCT is a common point that is formed by connecting the three limb electrodes through weighting resistors. Lead aVL measures potential difference between the left arm and the WCT. Similarly, lead aVR is the voltage between the right arm and the WCT. Lead aVF is between the left leg and the WCT. Finally, six more electrodes are fixed upon the chest, around the heart. Leads V1 through V6 measure the voltages between these sensors and the WCT. This circuit

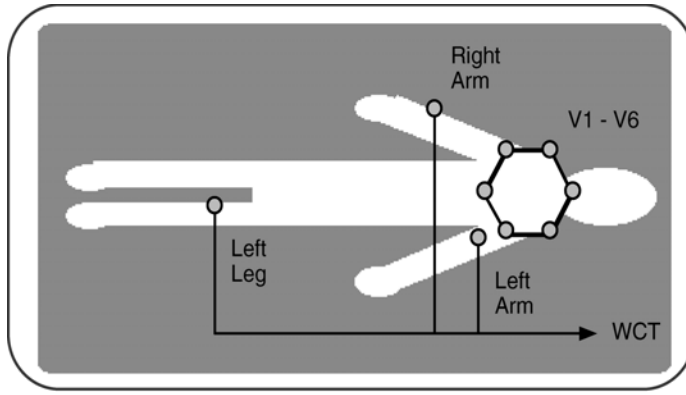

Fig. 1.5. The standard ECG configuration produces 12 signals from various electrodes attached to the subject's chest, arms, and leg.

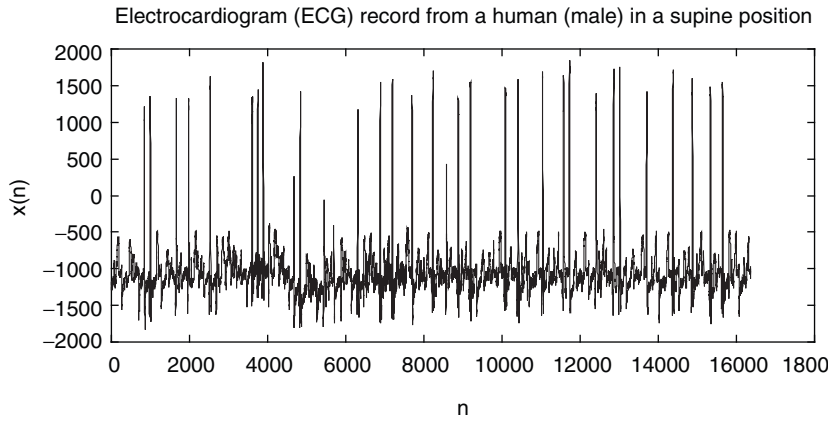

Fig. 1.6. One lead of an ECG: A human male in supine position. The sampling rate is 1 kHz, and the samples are digitized at 12 bits per sample. The irregularity of the heartbeat is evident.

arrangement is complicated; in fact, it is redundant. Redundancy provides for situations where a lead produces a poor signal and allows some cross-checking of the readings. Interpretation of 12-lead ECGs requires considerable training, experience, and expert judgment.

What does an ECG trace look like? Figure 1.6 shows an ECG trace from a single lead. Generally, an ECG has three discernible pulses: the P wave, the QRS complex, and the T wave. The P wave occurs upon excitation of the auricles of the heart, when they draw in blood from the body and lungs. The large-magnitude QRS complex occurs during the contraction of the vertricles as they contract to pump blood out of the heart. The Q and S waves are negative pulses, and the R wave is a positive pulse. The T wave arises during repolarization of the ventricles. The ECG signal is originally analog in nature; it is the continuous record of voltages produce across the various leads supported by the instrument. We could attach a millivoltmeter across an electrode pair and watch the needle jerk back and forth. Visualizing the signal's shape is easier with an oscilloscope, of course, because the instrument records the trace on its cathode ray tube. Both of these instruments display analog waveforms. If we could read the oscilloscope's output at regular time instants with perfect precision, then we would have—in principle, at least—a discrete representation of the ECG. But for computer display and automatic interpretation, the analog signal must be converted to digital form. In fact, Figure 1.6 is the result of such a digitization. The signal $v(n)$ appears continuous due to the large number of samples and the interpolating lines drawn by the graphics package that produced the illustration.

Interpreting ECGs is often difficult, especially in abnormal traces. A wide literature describing the 12-lead ECG exists. There are many guides to help technicians, nurses, and physicians use it to diagnose heart conditions. Signal processing and analysis of ECGs is a very active research area. Reports on new techniques, algorithms, and comparison studies continue to appear in the biomedical engineering and signal analysis literature [35].

One technical problem in ECG interpretation is to assess the regularity of the heart beat. As a time-domain signal description problem, this involves finding the separation between peaks of the QRS complex (Figure 1.6). Large time variations between peaks indicates dysrhythmia. If the time difference between two peaks, $v(n_1)$ and $v(n_0)$, is $\Delta_T = n_1 - n_0$, then the instantaneous heart rate becomes $60(\Delta_T)^{-1}$ beats/m. For the sample in Figure 1.6, this crude computation will, however, produce a wildly varying value of doubtful diagnostic use. The application calls for some kind of averaging and summary statistics, such as a report of the standard deviation of the running heart rate, to monitor the dysrhythmia.

There remains the technical problem of how to find the time location of QRS peaks. For an ideal QRS pulse, this is not too difficult, but the signal analysis algorithms must handle noise in the ECG trace. Now, because of the noise in the ECG signal, there are many local extrema. Evidently, the QRS complexes represent signal features that have inordinately high magnitudes; they are mountains above the forest of small-scale artifacts. So, to locate the peak of a QRS pulse, we might select a threshold M that is bigger than the small artifacts and smaller than the QRS peaks. We then deem any maximal, contiguous set of values $S = \{(n, v(n))\colon v(n) > M\}$ to be a QRS complex. Such regions will be disjoint. After finding the maximal value inside each such QRS complex, we can calculate Δ_T between each pair of maxima and give a running heart rate estimate. The task of dividing the signal up into disjoint regions, such as for the QRS pulses, is called signal *segmentation*. Chapter 4 explores this time domain procedure more thoroughly.

When there is poor heart rhythm, the QRS pulses may be jagged, misshapen, truncated, or irregulary spaced. A close inspection of the trace in Figure 1.7 seems to reveal this very phenomenon. In fact, one type of ventricular disorder that is

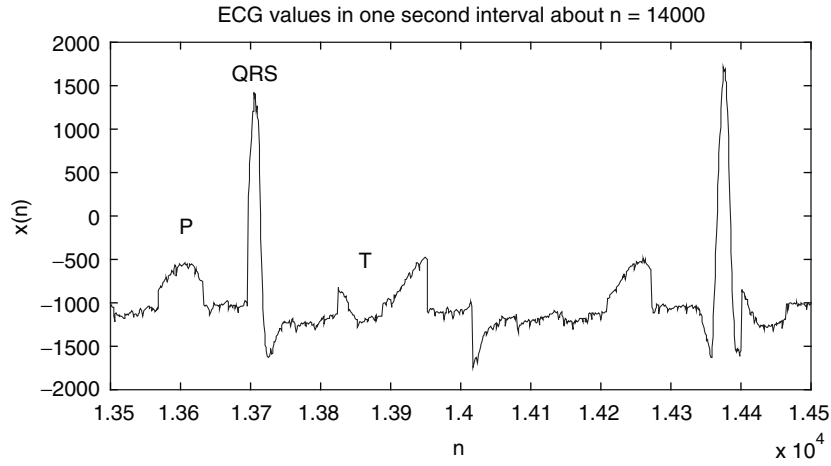

Fig. 1.7. Electrocardiogram of a human male, showing the fundametal waves. The 1-s time span around sample n = 14,000 is shown for the ECG of Figure 1.6. Note the locations of the P wave, the QRS complex, and—possibly—the T wave. Is there a broken P wave and a missing QRS pulse near the central time instant?

detectable in the ECG, provided that it employs a sufficiently high sampling rate, is *splintering* of the QRS complex. In this abnormal condition, the QRS consists of many closely spaced positive and negative transitions rather than a single, strong pulse. Note that in any ECG, there is a significant amount of signal noise. This too is clearly visible in the present example. Good peak detection and pulse location, especially for the smaller P and T waves, often require some data smoothing method. Averaging the signal values produces a smoother signal $w(n)$:

$$w(n) = \frac{1}{3}[v(n-1) + v(n) + v(n+1)]\,. \tag{1.1}$$

The particular formula (1.1) for processing the raw ECG signal to produce a less noisy $w(n)$ is called *moving average smoothing* or *moving average filtering*. This is a typical, almost ubiquitous signal processing operation. Equation (1.1) performs averaging within a symmetric window of width three about $v(n)$. Wider windows are possible and often useful. A window that is too wide can destroy signal features that bear on interpretation. Making a robust application requires judgment and experimentation.

Real-time smoothing operations require asymmetric windows. The underlying reason is that a symmetric smoothing window supposes knowledge of future signal values, such as $v(n + 1)$. To wit, as the computer monitoring system acquires each new ECG value $v(n)$, it can calculate the average of the last three values:

$$w(n) = \frac{1}{3}[v(n-2) + v(n-1) + v(n)]\,; \tag{1.2}$$

but at time instant n, it cannot possibly know the value of $v(n+1)$, which is necessary for calculating (1.1). If the smoothing operation occurs offline, after the entire set of signal values of interest has already been acquired and stored, then the whole range of signal values is accessible by the computer, and calculation (1.1) is, of course, feasible. When smoothing operations must procede in lockstep with acquisition operations, however, smoothing windows that look backward in time (1.2) must be applied.

Yet another method from removing noise from signals is to produce a signal whose values are the median of a window of raw input values. Thus, we might assign

$$w(n) = \text{Median}\{v(n-2), v(n-1), v(n), v(n+1), v(n+2)\} \tag{1.3}$$

so that $w(n)$ is the input value that lies closest to the middle of the range of five values around $v(n)$. A median filter tends to be superior to a moving average filter when the task is to remove isolated, large-magnitude spikes from a source signal. There are many variants. In general, smoothing is a common early processing step in signal analysis systems. In the present application, smoothing reduces the jagged noise in the ECG trace and improves the estimate of the QRS peak's location.

Contemplating the above algorithms for finding QRS peaks, smoothing the raw data, and estimating the instantaneous heart rate, we can note a variety of design choices. For example, how many values should we average to smooth the data? A span too small will fail to blur the jagged, noisy regions of the signal. A span too large may erode some of the QRS peaks. How should the threshold for segmenting QRS pulses be chosen? Again, an algorithm using values too small will falsely identify noisy bumps as QRS pulses. On the other hand, if the threshold values chosen are too large, then valid QRS complexes will be missed. Either circumstance will cause the application to fail. Can the thresholds be chosen automatically? The chemistry of the subject's skin could change while the leads are attached. This can cause the signal as a whole to trend up or down over time, with the result that the original threshold no longer works. Is there a way to adapt the threshold as the signal average changes so that QRS pulses remain detectable? These are but a few of the problems and tradeoffs involved in time domain signal processing and analysis.

Now we have illustrated some of the fundamental concepts of signal theory and, through the present example, have clarified the distinction between signal processing and analysis. Filtering for noise removal is a processing task. Signal averaging may serve our purposes, but it tends to smear isolated transients into what may be a quite different overall signal trend. Evidently, one aberrent upward spike can, after smoothing, assume the shape of a QRS pulse. An alternative that addresses this concern is median filtering. In either case—moving average or median filtering—the algorithm designer must still decide how wide to make the filters and discover the proper numerical values for thresholding the smoothed signal. Despite the analytical obstacles posed by signal noise and jagged shape, because of its prominence, the QRS complex is easier to characterize than the P and T waves.

There are alternative signal features that can serve as indicators of QRS complex location. We can locate the positive or negative transitions of QRS pulses, for example. Then the midpoint between the edges marks the center of each pulse, and the distance between these centers determines the instantaneous heart rate. This changes the technical problem from one of finding a local signal maximum to one of finding the positive- or negative-transition edges that bound the QRS complexes. Signal analysis, in fact, often revolves around edge detection. A useful indicator of edge presence is the discrete derivative, and a simple threshold operation identifies the significant changes.

1.1.2.2 Geothermal Measurements. Let us investigate an edge detection problem from geophysics. Ground temperature generally increases with depth. This variation is not as pronounced as the air temperature fluctuations or biophysical signals, to be sure, but local differences emerge due to the geological and volcanic history of the spot, thermal conductivity of the underlying rock strata, and even the amount of radioactivity. Mapping changes in ground termperature are important in the search for geothermal energy resources and are a supplementary indication of the underlying geological structures. If we plot temperature versus depth, we have a

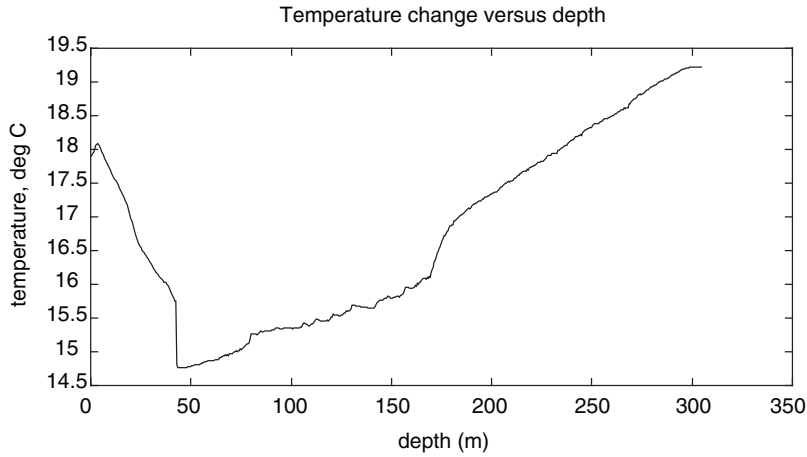

Fig. 1.8. A geothermal signal. The earth's temperature is sampled at various depths to produce a discrete signal with a spatially independent variable.

signal—the *geothermal gradient*—that is a function of distance, not time. It ramps up about 10°C per kilometer of depth and is a primary indicator for geothermal prospecting. In general, the geothermal gradient is higher for oceanic than for continental crust. Some 5% of the area of the United States has a gradient in the neighborhood of 40°C per kilometer of depth and has potential for use in geothermal power generation.

Mathematically, the geothermal gradient is the derivative of the signal with respect to its independent variable, which in this case measures depth into the earth. A very steep overall gradient may promise a geothermal energy source. A localized large magnitude gradient, or edge, in the temperature profile marks a geological artifact, such as a fracture zone. An example of the variation in ground temperature as one digs into the earth is shown in Figure 1.8.

The above data come from the second of four wells drilled on the Georgia–South Carolina border, in the eastern United States, in 1985 [36]. The temperature first declines with depth, which is typical, and then warmth from the earth's interior appears. Notice the large-magnitude positive gradients at approximately 80 and 175 m; these correspond to fracture zones. Large magnitude deviations often represent physically significant phenomena, and therein lies the importance of reliable methods for detecting, locating, and interpreting signal edges. Finding such large deviations in signal values is once again a time-domain signal analysis problem.

Suppose the analog ground temperature signal is $g(s)$, where s is depth into the earth. We seek large values of the derivative $g'(s) = dg/ds$. Approximating the derivative is possible once the data are digitized. We select a sampling interval $D > 0$ and set $x(n) = g(nD)$; then $x'(n) = x(n+1) - x(n-1)$ approximates the geothermal gradient at depth nD meters. It is further necessary to identify a threshold M for what constitutes a significant geothermal gradient. Threshold selection may rely upon expert scientific knowledge. A geophysicist might suggest significant gradients

for the region. If we collect some statistics on temperature gradients, then the outlying values may be candidates for threshold selection. Again, there are local variations in the temperature profile, and noise does intrude into the signal acquisition apparatus. Hence, preliminary signal smoothing may once again be useful. Toward this end, we may also employ discrete derivative formulas that use more signal values:

$$x'(n) = \frac{1}{12}[x(n-2) - 8x(n-1) + 8x(n+1) - x(n+2)]\,. \tag{1.4}$$

Standard numerical analysis texts provide many alternatives [37]. Among the problems at the chapter's end are several edge detection applications. They weigh some of the alternatives for filtering, threshold selection, and finding extrema.

For now, let us remark that the edges in the ECG signal (Figure 1.6) are far steeper than the edges in the geothermal trace (Figure 1.8). The upshot is that the signal analyst must tailor the discrete derivative methods to the data at hand. Developing methods for edge detection that are robust with respect to sharp local variation of the signal features proves to be a formidable task. Time-domain methods, such as we consider here, are usually appropriate for edge detection problems. There comes a point, nonetheless, when the variety of edge shapes, the background noise in the source signals, and the diverse gradients cause problems for simple time domain techniques. In recent years, researchers have turned to edge detection algorithms that incorporate a notion of the size or scale of the signal features. Chapter 4 has more to say about time domain signal analysis and edge detection, in particular. The later chapters round out the story.

1.1.3 Analysis in the Time-Frequency Plane

What about signals whose values are symbolic rather than numeric? In ordinary usage, we consider sequences of signs to be signals. Thus, we deem the display of flags on a ship's mast, a series of hand gestures between baseball players, DNA codes, and, in general, any sequence of codes to all be "signals." We have already taken note of such usages. And this is an important idea, but we shall not call such a symbolic sequence a signal, reserving for that term a narrow scientific definition as an ordered set of numbers. Instead, we shall define a sequence of abstract symbols to be a structural interpretation of a signal.

It is in fact the conversion of an ordered set of numerical values into a sequence of symbols that constitutes a signal interpretation or analysis. Thus, a microphone receives a logitudinal compressive sound wave and converts it into electrical impulses, thereby creating an analog signal. If the analog speech signal is digitized, processed, and analyzed by a speech recognition engine, then the output in the form of ASCII text characters is a symbolic sequence that interprets, analyzes, or assigns meaning to the signal. The final result may be just the words that were uttered. But, more likely, the speech interpretation algorithms will generate a variety of intermediate representations of the signal's structure. It is common to build a large hierarchy of interpretations: isolated utterances; candidate individual word sounds within the utterances; possible word recognition results; refinements from grammatical rules and application context; and, finally, a structural result.

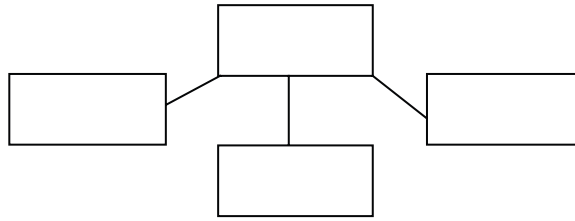

Fig. 1.9. Elementary graph structure for seismograms. One key analytical parameter is the time interval between the P waves and the S waves.

This framework applies to the applications covered in this section. A simple sequence of symbols representing the seismometer background, P waves, S waves, and surface waves may be the outcome of a structural analysis of a seismic signal (Figure 1.9).

The nodes of such a structure may have further information attached to them. For instance, the time-domain extent of the region, a confidence measure, or other analytical signal features can be inserted into the node data structure. Finding signal edges is often the prelude to a structural description of a signal. Figure 1.10

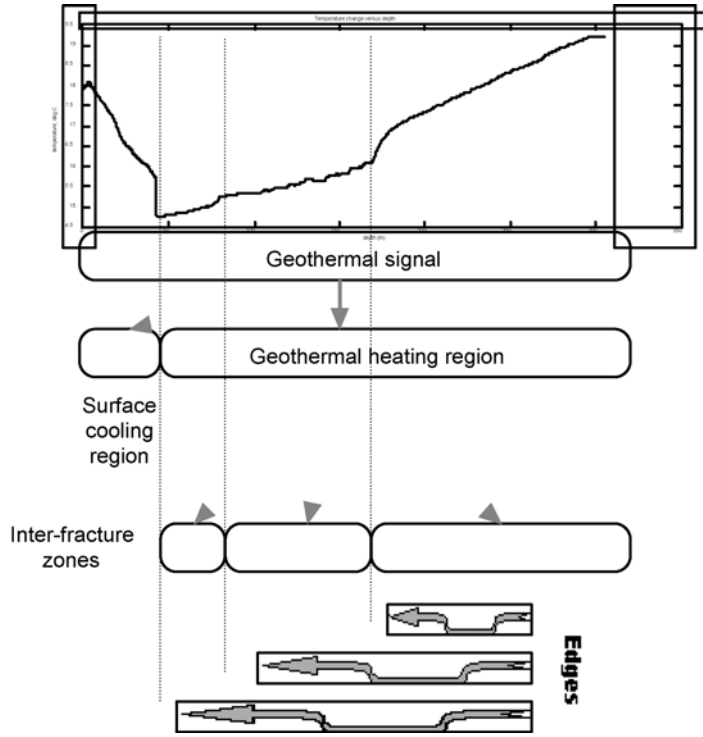

Fig. 1.10. Hypothetical geothermal signal structure. The root note of the interpretive structure represents the entire time-domain signal. Surface strata exhibit a cooling trend. Thereafter, geothermal heating effects are evident. Edges within the geothermal heating region indicate narrow fracture zones.

illustrates the decomposition of the geothermal profile from Figure 1.8 into a relational structure.

For many signal analysis problems, more or less flat relational structures that divide the signal domain into distinct regions are sufficient. Applications such as natural language understanding require more complicated, often hierarchical graph structures. Root nodes describe the coarse features and general subregions of the signal. Applying specialized algorithms to these distinct regions decomposes them further. Some regions may be deleted, further subdivided, or merged with their neighbors. Finally, the resulting graph structure can be compared with existing structural models or passed on to higher-level artificial intelligence applications.

1.1.4 Other Domains: Frequency and Scale

While we can achieve some success in processing and analyzing signals with elementary time-domain techniques, applied scientists regularly encounter applications demanding more sophisticated treatment. Thinking for a moment about the seismogram examples, we considered one aspect of their interpretation: finding the time difference between the arrival of the P and S waves. But how can one distinguish between the two wave sets? The distinction between them, which analysis algorithms must find, is in their oscillatory behavior and the magnitude of the oscillations. There is no monotone edge, such as characterized the geothermal signal. Rather, there is a change in the repetitiveness and the sweep of the seismograph needle's wiggling. When the oscillatory nature of a signal concerns us, then we are interested in its periodicity—or in other words, the reciprocal of period, the *frequency.*

Frequency-domain signal descriptions decompose the source signals into sinusoidal components. This strategy does improve upon pure time domain methods, given the appropriate application. A frequency-domain description uses some set of sinusoidal signals as a basis for describing a signal. The frequency of the sinusoid that most closely matches the signal is the principal frequency component of the signal. We can delete this principal frequency component from the source signal to get a difference signal. Then, we iterate. The first difference signal is further frequency analyzed to get a secondary periodic component and, of course, a second difference signal. The sinusoidal component identification and extraction continue until the difference signal consists of nothing but small magnitude, patternless, random perturbations—noise. This is a familiar procedure. It is just like the elementary linear algebra problem of finding the expansion coefficients of a given vector in terms of a basis set.

Thus, a frequency-domain approach is suitable for distinguishing the P waves from the S waves in seismogram interpretation. But, there is a caveat. We cannot apply the sinusoidal signal extraction to the whole signal, but rather only to small pieces of the signal. When the frequency components change radically on the separate, incoming small signal pieces, then the onset of the S waves must be at hand. The subtlety is to decide how to size the small signal pieces that will be subject to frequency analysis. If the seismographic station is far away, then the time interval

between the initial P waves and the later S waves is large, and fairly large subintervals should suffice. If the seismographic station is close to the earthquake epicenter, on the other hand, then the algorithm must use very small pieces, or it will miss the short P wave region of the motion entirely. But if the pieces are made too small, then they may contain too few discrete samples for us to perform a frequency analysis. There is no way to know whether a temblor that has not happened yet will be close or far away. And the dilemma is how to size the signal subintervals in order to analyze all earthquakes, near and far, and all possible frequency ranges for the S and P waves.

It turns out that although such a frequency-domain approach as we describe is adequate for seismic signals, the strategy has proven to be problematic for the interpretation of electrocardiograms. The waves in abnormal ECGs are sometimes too variable for successful frequency-domain description and analysis.

Enter the notion of a *scale-domain* signal description. A scale-domain description of a signal breaks it into similarly shaped signal fragments of varying sizes. Problems that involve the time-domain size of signal features tend to favor this type of representation. For example, a scale-based analysis can offer improvements in electrocardiogram analysis; in this field it is a popular redoubt for researchers that have experimented with time domain methods, then frequency-domain methods, and still find only partial success in interpreting ECGs.

We shall also illustrate the ideas of frequency- and scale-domain descriptions in this first chapter. A complete understanding of the methods of frequency- and scale-domain descriptions requires a considerable mathematical expertise. The next two sections provide some formal definitions and a variety of mathematical examples of signals. The kinds of functions that one normally studies in algebra, calculus, and mathematical analysis are quite different from the ones at the center of signal theory. Functions representing signals are often discontinuous; they tend to be irregularly shaped, blocky, spiky, and altogether more ragged than the smooth and elegant entities of pure mathematics.

1.2 ANALOG SIGNALS

At the scale of objects immediately present to human consciousness and at the macroscopic scale of conventional science and technology, measurable phenomena tend to be continuous in nature. Hence, the raw signals that issue from nature—temperatures, pressures, voltages, flows, velocities, and so on—are commonly measured through analog instruments. In order to study such real-world signals, engineers and scientists model them with mathematical functions of a real variable. This strategy brings the power and precision of mathematical analysis to bear on engineering questions and problems that concern the acquisition, transmission, interpretation, and utilization of natural streams of numbers (i.e., signals).

Now, at a very small scale, in contrast to our perceived macroscopic world, natural processes are more discrete and quantized. The energy of electromagnetic radiation exists in the form of individual quanta with energy $E = h/\lambda$, where h is

Planck's constant,[3] and λ is the wavelength of the radiation. Phenomena that we normally conceive of possessing wave properties exhibit certain particle-like behaviors. On the other hand, elementary bits of matter, electrons for instance, may also reveal certain wave-like aspects. The quantization of nature at the subatomic and atomic levels leads to discrete interactions at the molecular level. Lumping ever greater numbers of discretized interactions together, overall statistics take priority over particular interactions, and the continuous nature of the laws of nature at a large scale then become apparent.[4] Though nature is indeed discrete at the microlevel, the historical beginnings of common sense, engineering, and scientific endeavor involve reasoning with continuously measurable phenomena. Only recently, within the last century have the quantized nature of the interactions of matter and energy become known. And only quite recently, within our own lifetimes, have machines become available to us—digital computers—that require for their application the discretization of their continuous input data.

1.2.1 Definitions and Notation

Analog signal theory proceeds directly from the analysis of functions of a real variable. This material is familiar from introductory calculus courses. Historically, it also precedes the development of discrete signal theory. And this is a curious circumstance, because the formal development of analog signal theory is far more subtle—some would no doubt insist the right term is perilous—than discrete time signal processing and analysis.

Definition (Analog Signals). An *analog signal* is a function $x: \mathbb{R} \to \mathbb{R}$, where $\mathbb{R}$ is the set of real numbers, and $x(t)$ is the signal value at time t. A *complex-valued* analog signal is a function $x: \mathbb{R} \to \mathbb{C}$. Thus, $x(t) = x_r(t) + jx_i(t)$, where $x_r(t)$ is the real part of $x(t)$; $x_i(t)$ is the imaginary part of $x(t)$; both of these are real-valued signals; and $j^2 = -1$.

Thus, we simply identify analog signals with functions of a real variable. Ordinarily, analog signals, such the temperature of an oven varying over time, take on real values. In other cases, where signal timing relationships come into question, or the frequency content of signals is an issue, complex-valued signals are often used. We will work with both real- and complex-valued signals in this section. Section 1.7 considers the complex number system, complex-valued signals, and the mathematics of complex numbers in more detail. Complex-valued signals arise primarily in the study of signal frequency.

[3]To account for the observation that the maximum velocity of electrons dislodged from materials depended on the frequency of incident light, Max Planck (1858–1947) conjectured that radiant energy consists of discrete packets, called *photons* or *quanta*, thus discovering the quantum theory.

[4]This process draws the attention of philosophers (N. Hartmann, *New Ways of Ontology*, translator R. C. Kuhn, Chicago: Henry Regnery, 1953) and scientists alike (W. Zurek, "Decoherence and the transition from quantum to classical," *Physics Today*, vol. 44, no. 10, pp. 36–44, October 1991).

Of course, the independent variable of an analog signal does not have to be a time variable. The pneumatic valve of a bicycle tire follows a sinusoidal course in height above ground as the rider moves down the street. In this case the analog signal is a function of distance ridden rather than time passed. And the geothermal gradient noted in the previous section is an example of a signal that is a function of depth in the earth's crust.

It is possible to generalize the above definition to include multichannel signals that take values in $\mathbb{R}^n$, $n \geq 2$. This is a straightforward generalization for all of the theory that we develop. Another way to generalize to higher dimensionality is to consider signals with domains contained in $\mathbb{R}^n$, $n \geq 2$. This is the discipline of image processing, at least for $n = 2$, 3, and 4. As a generalization of signal processing, it is not so straightforward as multichannel theory; the extra dimension in the independent signal variable leads to complications in signal interpretation and imposes severe memory and execution time burdens for computer-based applications.

We should like to point out that modeling natural signals with mathematical functions is an inherently flawed step; many functions do not correspond to any real-world signal. Mathematical functions can have nonzero values for arbitrarily large values of their independent variable, whereas in reality, such signals are impossible; every signal must have a finite past and eventually decay to nothing. To suppose otherwise would imply that the natural phenomenon giving rise to the signal could supply energy indefinitely. We can further imagine that some natural signals containing random noise cannot be exactly characterized by a mathematical rule associating one independent variable with another dependent variable.

But, is it acceptable to model real-world signals with mathematical models that eventually diminish to zero? This seems unsatisfactory. A real-world signal may decay at such a slow rate that in choosing a function for its mathematical model we are not sure where to say the function's values are all zero. Thus, we should prefer a theory of signals that allows signals to continue forever, perhaps diminishing at an allowable rate. If our signal theory accomodates such models, then we have every assurance that it can account for the wildest natural signal that the real world can offer. We will indeed pursue this goal, beginning in this first chapter. With persistence, we shall see that natural signals do have mathematical models that reflect the essential nature of the real-world phenomenon and yet are not limited to be zero within finite intervals. We shall find as well that the notion of randomness within a real-world signal can be accommodated within a mathematical framework.

1.2.2 Examples

The basic functions of mathematical analysis, known from algebra and calculus, furnish many elementary signal models. Because of this, it is common to mix the terms "signal" and "function." We may specify an analog signal from a formula that relates independent variable values with dependent variable values. Sometimes the formula can be given in closed form as a single equation defining the signal values. We may also specify other signals by defining them piecewise on their domain. Some functions may best be described by a geometric definition. Still other

functions representing analog signals may be more convenient to sketch rather than specify mathematically.

1.2.2.1 Polynomial, Rational, and Algebraic Signals. Consider, for example, the *polynomial* signal,

$$x(t) = \sum_{k=0}^{N} a_k t^k. \tag{1.5}$$

$x(t)$ has derivatives of all orders and is continuous, along with all of its derivatives. It is quite unlike any of nature's signals, since its magnitude, $|x(t)|$, will approach infinity as $|t|$ becomes large. These signals are familiar from elementary algebra, where students find their roots and plot their graphs in the Cartesian plane. The domain of a polynomial $p(t)$ can be divided into disjoint regions of concavity: concave upward, where the second derivative is positive; concave downward, where the second derivative is negative; and regions of no concavity, where the second derivative is zero, and $p(t)$ is therefore a line. If the domain of a polynomial $p(t)$ contains an interval $a < t < b$ where $\frac{d^2}{dt^2}p(t) = 0$ for all $t \in (a, b)$, then $p(t)$ is a line. However familiar and natural the polynomials may be, they are not the signal family with which we are most intimately concerned in signal processing. Their behavior for large $|t|$ is the problem. We prefer mathematical functions that more closely resemble the kind of signals that occur in nature: Signals $x(t)$ which, as $|t|$ gets large, the signal either approaches a constant, oscillates, or decays to zero. Indeed, we expend quite an effort in Chapter 2 to discover signal families—called *function* or *signal spaces*—which are faithful models of natural signals.

The concavity of a signal is a very important concept in certain signal analysis applications. Years ago, the psychologist F. Attneave [38] noted that a scattering of simple curves suffices to convey the idea of a complex shape—for instance, a cat. Later, computer vision researchers developed the idea of assemblages of simple, oriented edges into complete theories of low-level image understanding [39–41]. Perhaps the most influential among them was David Marr, who conjectured that understanding a scene depends upon the extraction of edge information [39] over a range of visual resolutions from coarse to fine multiple scales. Marr challenged computer vision researchers to find processing and analysis paradigms within biological vision and apply them to machine vision. Researchers investigated the applications of concavity and convexity information at many different scales. Thus, an intricate shape might resolve into an intricate pattern at a fine scale, but at a coarser scale might appear to be just a tree. How this can be done, and how signals can be smoothed into larger regions of convexity and concavity without increasing the number of differently curved regions, is the topic of scale-space analysis [42,43]. We have already touched upon some of these ideas in our discussion of edges of the QRS complex of an electrocardiogram trace and in our discussion of the geothermal gradient. There the scale of an edge corresponded to the number of points incorporated in the discrete derivative computation. This is precisely the notion we are

trying to illustrate, since the scale of an edge is a measure of its time-domain extent. Describing signal features by their scale is most satisfactorily accomplished using special classes of signals (Section 1.6). At the root of all of this deep theory, however, are the basic calculus notion of the sign of the second derivative and the intuitive and simple polynomial examples.

Besides motivating the notions of convexity and concavity as component building blocks for more complicated shapes, polynomials are also useful in signal theory as interpolating functions. The theory of splines generalizes linear interpolation. It is one approach to the modern theory of wavelet transforms. Interpolating the values of a discrete signal with continuous polynomial sections—connecting the dots, so to speak—is the opposite process to sampling a continuous-domain signal.

If $p(t)$ and $q(t)$ are polynomials, then $x(t) = p(t)/q(t)$ is a *rational* function. Signals modeled by rational functions need to have provisions made in their definitions for the times t_0 when $q(t_0) = 0$. If, when this is the case, $p(t_0) = 0$ also, then it is possible that the limit,

$$\lim_{t \to t_0} \frac{p(t)}{q(t)} = r_0 = x(t_0), \tag{1.6}$$

exists and can be taken to be $x(t_0)$. This limit does exist when the order of the zero of $p(t)$ at $t = t_0$ is at least the order of the zero of $q(t)$ at $t = t_0$.

Signals that involve a rational exponent of the time variable, such as $x(t) = t^{1/2}$, are called *algebraic* signals. There are often problems with the domains of such signals; to the point, $t^{1/2}$ does not take values on the negative real numbers. Consequently, we must usually partition the domain of such signals and define the signal piecewise. One tool for this is the upcoming unit step signal $u(t)$.

1.2.2.2 Sinusoids. A more real-to-life example is a *sinusoidal* signal, such as $\sin(t)$ or $\cos(t)$. Of course, the mathematician's sinusoidal signals are synthetic, ideal creations. They undulate forever, whereas natural periodic motion eventually deteriorates. Both $\sin(t)$ and $\cos(t)$ are differentiable: $\frac{d}{dt}\sin(t) = \cos(t)$ and $\frac{d}{dt}\cos(t) = -\sin(t)$. From this it follows that both have derivatives of all orders and have Taylor[5] series expansions about the origin:

$$\sin(t) = t - \frac{t^3}{3!} + \frac{t^5}{5!} - \frac{t^7}{7!} + \cdots \tag{1.7a}$$

$$\cos(t) = 1 - \frac{t^2}{2!} + \frac{t^4}{4!} - \frac{t^6}{6!} + \cdots . \tag{1.7b}$$

[5]The idea is due to Brook Taylor (1685–1731), an English mathematician, who—together with many others of his day—sought to provide rigorous underpinnings for Newton's calculus.

So, while $\sin(t)$ and $\cos(t)$ are most intuitively described by the coordinates of a point on the unit circle, there are also formulas (1.7a)–(1.7b) that define them. In fact, the Taylor series, where it is valid for a function $x(t)$ on some interval $a < t < b$ of the real line, shows that a function is the limit of a sequence of polynomials: $x(a)$, $x(a) + x^{(1)}(a)(t-a)$, $x(a) + x^{(1)}(t-a) + x^{(2)}(t-a)^2/2!$, … , where we denote the nth-order derivative of $x(t)$ by $x^{(n)}(t)$.

The observation that $\sin(t)$ and $\cos(t)$ have a Taylor series representation (1.7a)–(1.7b) inspires what will become one of our driving principles. The polynomial signals may not be very lifelike, when we consider that naturally occurring signals will tend to wiggle and then diminish. But sequences of polynomials, taken to a limit, converge to the sinusoidal signals. The nature of the elements is completely changed by the limiting process. This underscores the importance of convergent sequences of signals, and throughout our exposition we will always be alert to examine the possibility of taking signal limits. Limit processes constitute a very powerful means for defininining fundamentally new types of signals.

From their geometric definition on the unit circle, the sine and cosine signals are periodic; $\sin(t + 2\pi) = \sin(t)$ and $\cos(t + 2\pi) = \cos(t)$ for all $t \in \mathbb{R}$. We can use the trigonometric formulas for $\sin(s + t)$ and $\cos(s + t)$, the limit $\frac{\sin(t)}{t} \to 1$ as $t \to 0$, and the limit $\frac{\cos(t)-1}{t} \to 0$ as $t \to 0$ to discover the derivatives and hence the Taylor series. Alternatively, we can define $\sin(t)$ and $\cos(t)$ by (1.7a)–(1.7b), whence we derive the addition formulas; define π as the unique point $1 < \pi/2 < 2$, where $\cos(t) = 0$; and, finally, show the periodicity of sine and cosine [44].

1.2.2.3 Exponentials.

Exponential signals are of the form

$$x(t) = Ce^{at}, \tag{1.8}$$

where C and a are constants, and e is the real number b for which the exponential $x(t) = b^t$ has derivative $\frac{d}{dt}x(t) = 1$ for $t = 0$. For $C = a = 1$, we often write $x(t) = \exp(t)$. The derivative of $\exp(t)$ is itself. This leads to the Taylor series expansion about $t = 0$:

$$e = \exp(t) = 1 + t + \frac{t^2}{2!} + \frac{t^3}{3!} + \cdots = \sum_{k=0}^{\infty} \frac{t^k}{k!}. \tag{1.9}$$

Notice once more that a polynomial limit process creates a signal of a completely different genus. Instead of a periodic signal, the limit in (1.9) grows rapidly as $t \to \infty$ and decays rapidly as $t \to -\infty$.

If $C > 0$ and $a > 0$ in (1.9), then the graph of the exponential signal is an ever-increasing curve for $t > 0$ and an ever-decaying curve for $t < 0$. Since it has non-zero derivatives of arbitrarily high orders, such an exponential grows faster than any polynomial for positive time values. For $a < 0$, the graph of the exponential reflects across the y-axis (Figure 1.11).

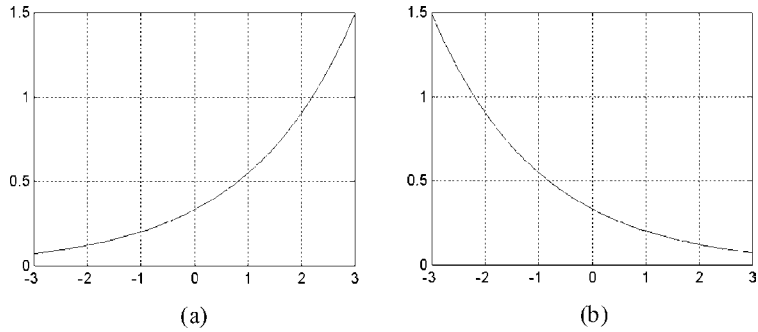

Fig. 1.11. Analog exponential signals. Panel (a) shows the exponential exp(*t*/2)/3, and (b) is its reflection across the *y*-axis, exp(−*t*/2)3.

A particularly valuable relation for signal theory is the *Laplace*[6] *identity*; we take the exponent in (1.9) to be purely imaginary:

$$e^{js} = \exp(js) = \cos(s) + j\sin(s), \tag{1.10}$$

where s is real. Why this is true can be seen from the unit circle in the complex plane (Figure 1.12) and by examining the expansion (1.10) of e^{js} in the series (1.9). First, substitute js for t in the expansion (1.9). Next, group the real and

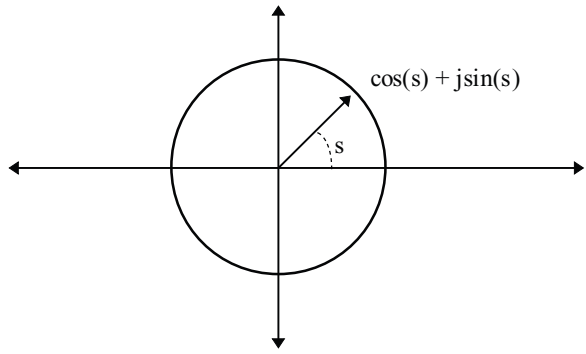

Fig. 1.12. Laplace's relation on the unit circle of the complex plane. By comparing Taylor series expansions, we find $e^{js} = \cos(s) + j\sin(s)$, and this corresponds to a point at arc distance s, counterclockwise on the unit circle from the positive x-axis.

[6]Pierre Simon Laplace (1749–1827), a French mathematician, physicist, and astronomer, theorized (along with German philosopher Immanuel Kant) that the solar system coalesced from a rotating gas cloud. The Laplace transform (Chapter 9) is named for him.

imaginary terms together. Observe that the sine and cosine Taylor series are in fact intermixed into the expansion of e^{js}, just as (1.10) expresses. The Laplace identity generalizes to any complex exponent $x + jy$: $e^{x+jy} = e^{x}[\cos(y) + j\sin(y)]$, where x and y are real. This is the most important formula in basic algebra.

The exponential signal is important in solving differential equations, such as arise from the study of heat transport and electromagnetism. For instance, the *heat diffusion equation* describes the propagation of heat $T(t, s)$ along a straight wire at time t and distance s from the end of the wire:

$$\frac{\partial T}{\partial t} = D\frac{\partial^2 T}{\partial s^2}, \tag{1.11}$$

where D is the *diffusion constant*. Solutions to (1.11) are $T(t, s) = e^{-\lambda t}e^{-jks}$, where λ and k are such that $D = \lambda/k^2$. The diffusion equation will make an unexpected appearance in Chapter 4 when we consider how to smooth a signal so that new regions of concavity do not appear as the smoothing progresses. Now, in electromagnetism, the electric and magnetic fields are vectors, $\boldsymbol{E}$ and $\boldsymbol{H}$, respectively, that depend upon one another. Maxwell's equations[7] for a vacuum describe this interaction in terms of space and time derivatives of the field vectors as follows:

$$\nabla \times \boldsymbol{E} = -\mu_0 \frac{\partial \boldsymbol{H}}{\partial t}, \tag{1.12a}$$

$$\nabla \times \boldsymbol{H} = \varepsilon_0 \frac{\partial \boldsymbol{E}}{\partial t}, \tag{1.12b}$$

$$\nabla \bullet \boldsymbol{E} = \nabla \bullet \boldsymbol{H} = 0. \tag{1.12c}$$

Equations (1.12a)–(1.12b) tell us that the curl of each field is proportional to the time derivative of the other field. The zero divergences in (1.12c) hold when there is no charge present. Constants μ_0 and ε_0 are the *magnetic permeability* and *electric permittivity* of space, respectively. By taking a second curl in (1.12a) and a second time derivative in (1.12b), separate equations in $\boldsymbol{E}$ and $\boldsymbol{H}$ result; for example, the electric field must satisfy

$$\nabla^2 \boldsymbol{E} = \mu_0 \varepsilon_0 \frac{\partial^2 \boldsymbol{E}}{\partial t^2}. \tag{1.13a}$$

For one spatial dimension, this becomes

$$\frac{\partial^2 \boldsymbol{E}}{\partial s^2} = \mu_0 \varepsilon_0 \frac{\partial^2 \boldsymbol{E}}{\partial t^2}. \tag{1.13b}$$

[7]Scottish physicist James Clerk Maxwell (1831–1879) is known best for the electromagnetic theory, but he also had a significant hand in the mechanical theory of heat.

Solutions to (1.13b) are sinusoids of the form $E(t, s) = A\cos(bs - \omega t)$, where $(b/\omega)^2 = \mu_0\varepsilon_0$, and b, ω, and A are constants.

Another signal of great importance in mathematics, statistics, engineering, and science is the *Gaussian.*[8]

Definition (Analog Gaussian). The *analog Gaussian* signal of mean μ and standard deviation σ is

$$g_{\mu,\sigma}(t) = \frac{1}{\sigma\sqrt{2\pi}} e^{-\frac{(t-\mu)^2}{2\sigma^2}}. \tag{1.14}$$

These terms are from statistics (Section 1.7). For now, however, let us note that the Gaussian $g_{\mu,\sigma}(t)$ can be integrated over the entire real line. Indeed, since (1.14) is always symmetric about the line $t = \mu$, we may take $\mu = 0$. The trick is to work out the square of the integral, relying on Fubini's theorem to turn the consequent iterated integral into a double integral:

$$\begin{aligned}\left(\int_{-\infty}^{\infty} g_{0,\sigma}(t)\,dt\right)^2 &= \left(\frac{1}{\sqrt{2\pi}\sigma}\int_{-\infty}^{\infty} e^{-\frac{t^2}{2\sigma^2}}dt\right)\left(\frac{1}{\sqrt{2\pi}\sigma}\int_{-\infty}^{\infty} e^{-\frac{s^2}{2\sigma^2}}ds\right)\\ &= \frac{1}{2\pi\sigma^2}\int_{-\infty}^{\infty}\int_{-\infty}^{\infty} e^{-\frac{s^2+t^2}{2\sigma^2}}dtds\end{aligned} \tag{1.15}$$

Changing to polar coordinates cracks the hard integral on the right-hand side of (1.15): $r^2 = t^2 + s^2$ and $dtds = rdrd\theta$. Hence,

$$\left(\int_{-\infty}^{\infty} g_{0,\sigma}(t)\,dt\right)^2 = \frac{1}{2\pi\sigma^2}\int_0^{2\pi}\int_0^{\infty} e^{-\frac{r^2}{2\sigma^2}} r\,drd\theta = \frac{1}{2\pi}\int_0^{2\pi}\left(-e^{-\frac{r^2}{2\sigma^2}}\Big|_0^{\infty}\right)d\theta \tag{1.16}$$

and we have

$$\left(\int_{-\infty}^{\infty} g_{0,\sigma}(t)\,dt\right)^2 = \frac{1}{2\pi}\int_0^{2\pi}(0-(-1))\,d\theta = \frac{1}{2\pi}(\theta)\Big|_0^{2\pi} = 1. \tag{1.17}$$

[8]Karl Friedrich Gauss (1777–1855) is a renowned German mathematician, physicist, and astronomer.

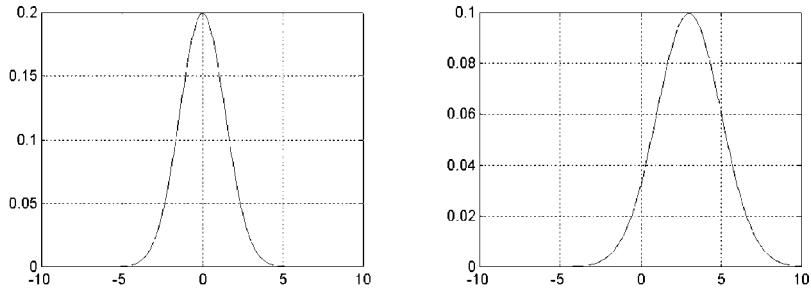

Fig. 1.13. Gaussian signals. The pulse on the left is $g_{0,2}(t)$, the Gaussian with mean μ equals 0, and the standard deviation σ equals 2. The pulse $g_{3,4}(t)$ is on the right. It has a wider spread than $g_{0,2}(t)$, and takes its smaller maximum value at $t = 3$.

Thus, there is unit area under the Gaussian curve. The Gaussian $g_{\mu,\sigma}(t)$ (1.14) is a bell-shaped curve (Figure 1.13), peaking at $t = \mu$, and symmetric about this line. The Gaussian decays forever as $|t| \to \infty$, but $g_{\mu,\sigma}(t) > 0$ for any $t \in \mathbb{R}$.

We define

$$g(t) = g_{0,1}(t) = \frac{1}{\sqrt{2\pi}} e^{-\frac{t^2}{2}}, \tag{1.18}$$

so that any Gaussian (1.14) is a scaled, shifted, and dilated version of $g(t)$:

$$g_{\mu,\sigma}(t) = \frac{1}{\sigma\sqrt{2\pi}} e^{-\frac{(t-\mu)^2}{2\sigma^2}} = \frac{1}{\sigma} g\left(\frac{t-\mu}{\sigma}\right). \tag{1.19}$$

The multiplying factor $(1/\sigma)$ governs the *scaling*, which may increase or decrease the height of the Gaussian. The same factor inside $g((t-\mu)/\sigma)$ *dilates* the Gaussian; it adjusts the spread of the bell curve according to the scale factor so as to preserve the unit area property. The peak of the bell shifts by the mean μ.

If we multiply a complex exponential $\exp(-j\omega t)$ by a Gaussian function, we get what is known as a *Gabor*[9] *elementary* function or signal [45].

[9]Dennis Gabor (1900–1979) analyzed these pulse-like signals in his 1946 study of optimal time and frequency signal representations. He is more famous outside the signal analysis discipline for having won the Nobel prize by inventing holography.

Definition (Gabor Elementary Functions). The *Gabor elementary function* $G_{\mu,\sigma,\omega}(t)$ is

$$G_{\mu,\,\sigma,\,\omega}(t) \;=\; g_{\mu,\,\sigma}(t)e^{j\omega t}. \tag{1.20}$$

Note that the real part of the Gabor elementary function $G_{\mu,\sigma,\omega}(t)$ in (1.20) is a cosine-like undulation in a Gaussian envelope. The imaginary part is a sine-like curve in a Gaussian envelope of the same shape (Figure 1.14). The time-frequency Gabor transform (Chapter 10) is based on Gabor elementary functions.

Interest in these signals surged in the mid-1980s when psychophysicists noticed that the modeled some aspects of the brain's visual processing. In particular, the receptive fields of adjacent neurons in the visual cortex seem to have profiles that resemble the real and imaginary parts of the Gabor elementary function. A controversy ensued, and researchers—electrical engineers, computer scientists, physiologists, and psychologists—armed with the techniques of mixed-domain signal decomposition continue to investigate and debate the mechanisms of animal visual perception [46, 47].

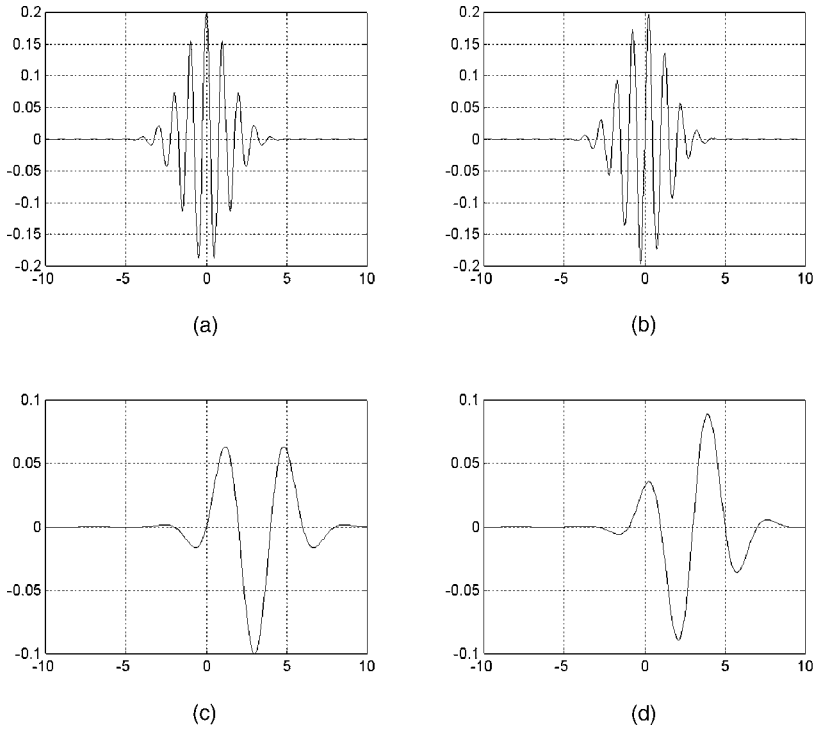

Fig. 1.14. Gabor elementary signals, real and imaginary parts. The pair on the top (a, b) are the real and imaginary parts of $g_{0,2}(t)\exp(j2\pi t)$. Below (c, d) is the Gabor pulse $G_{3,4,.5\pi}$. Note that if two Gabor elementary signals have the same sinusoidal frequency, but occupy Gaussian envelopes of different variances, then they have fundamentally different shapes.

1.2.3 Special Analog Signals

Several of the analog signal examples above are familiar from elementary algebra and calculus. Others, perhaps the Gabor elementary functions, are probably unfamiliar until one begins the formal study of signal processing and analysis. Some very simple analog signals play pivotal roles in the theoretical development.

1.2.3.1 Unit Step. We introduce the unit step and some closely related signals. The unit step signal (Figure 1.15) finds use in chopping up analog signals. It is also a building block for signals that consist of rectangular shapes and square pulses.

Definition (Unit Step). The *unit step* signal $u(t)$ is defined:

$$u(t) = \begin{cases} 1 & \text{if } t \geq 0, \\ 0 & \text{if } t < 0. \end{cases} \tag{1.21}$$

To chop up a signal using $u(t)$, we take the product $y(t) = x(t)u(t - c)$ for some $c \in \mathbb{R}$. The nonzero portion of $y(t)$ has some desired characteristic. Typically, this is how we zero-out the nonintegrable parts of signals such as $x(t) = t^{-2}$.

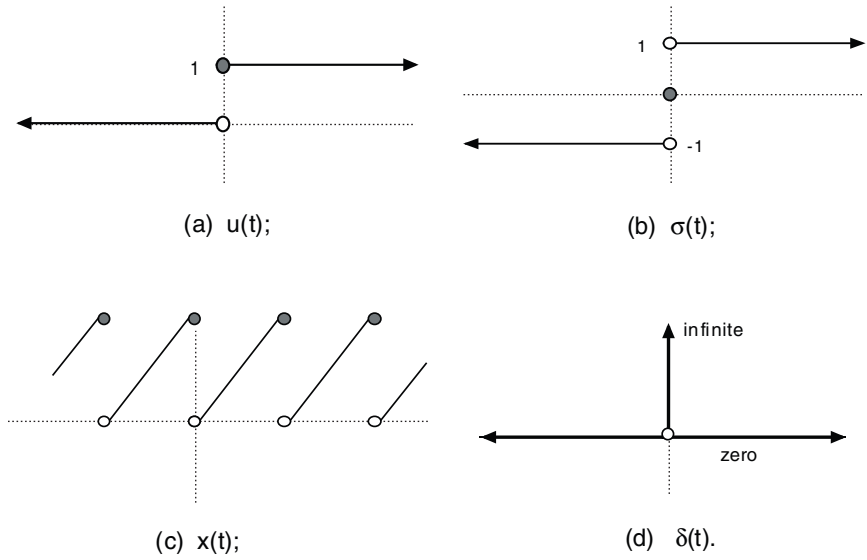

Fig. 1.15. Special Utility signals. (a) $u(t)$. (b) $\sigma(t)$. (c) $x(t)$. (d) $\delta(t)$. The unit step (a), signum (b), and sawtooth (c) are useful for constructing other signals and modeling their discontinuities. The Dirac delta (d) is "infinitely high" at $t = 0$ and zero otherwise; thus, it is not a bona fide analog signal. Chapters 3 and 5 provide the mathematical underpinnings of a valid, formal treatment of $\delta(t)$.

Definition (Signum). The *signum* signal $\sigma(t)$ is a cousin to the unit step:

$$\sigma(t) = \begin{cases} 1 & \text{if } t > 0, \\ 0 & \text{if } t = 0, \\ -1 & \text{if } t < 0. \end{cases} \tag{1.22}$$

Definition (Sawtooth). A sawtooth signal is a piecewise linear signal (Figure 1.15). For example, the infinite sawtooth $x(t)$ is

$$x(t) = \begin{cases} t & \text{if } t \geq 0, \\ 0 & \text{if } t < 0. \end{cases} \tag{1.23}$$

1.2.3.2 Dirac Delta. The *Dirac*[10] *delta* is really more of a fiction than a function. Nonetheless, it is a useful fiction. It can be made mathematically precise without losing its utility, and its informal development is familiar to many scientists and engineers.

For $n > 0$ let us define a sequence of analog signals $\delta_n(t)$:

$$\delta_n(t) = \begin{cases} \dfrac{n}{2} & \text{if } t \in \left[-\dfrac{1}{n}, \dfrac{1}{n}\right], \\ 0 & \text{if otherwise.} \end{cases} \tag{1.24}$$

The signals (1.24) are increasingly tall square spikes centered around the origin. Consider a general analog signal $x(t)$ and the integral over $\mathbb{R}$ of $x(t)\delta_n(t)$:

$$\int_{-\infty}^{\infty} x(t)\delta_n(t)\, dt = \int_{-1/n}^{1/n} x(t)\frac{n}{2}\, dt = \frac{1}{1/n - (-1/n)} \int_{-1/n}^{1/n} x(t)\, dt \tag{1.25}$$

The last term in (1.25) is the average value of $x(t)$ over $[-1/n, 1/n]$. As $n \to \infty$,

$$\lim_{n \to \infty} \int_{-\infty}^{\infty} x(t)\delta_n(t)\, dt = x(0). \tag{1.26}$$

The casual thought is to let $\delta(t)$ be the limit of the sequence $\{\delta_n(t): n > 0\}$ and conclude that the limit operation (1.26) can be moved inside the integral (Figure 1.16):

$$\lim_{n \to \infty} \int_{-\infty}^{\infty} x(t)\delta_n(t)\, dt = \int_{-\infty}^{\infty} x(t) \lim_{n \to \infty} \delta_n(t)\, dt = \int_{-\infty}^{\infty} x(t)\delta(t)\, dt = x(0). \tag{1.27}$$

[10]British physicist Paul Adrian Maurice Dirac (1902–1984) developed the theory of quantum electrodynamics. He received the Nobel prize in 1933.

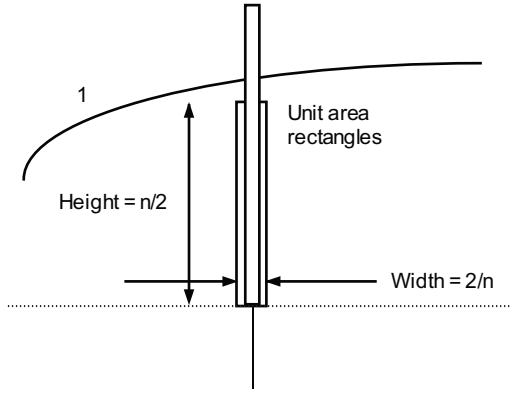

Fig. 1.16. Informal conception of the Dirac delta function. It is useful to think of $\delta(t)$ as the limit of a sequence of rectangles growing higher and narrower.

This idea is fundamentally mistaken, however. There is no pointwise limit of the sequence $\delta_n(t)$ at $t = 0$, and the limit of this signal sequence does not exist. The interchange of limit operations attempted in (1.27) is invalid. It is perhaps best to think of the final integral in (1.27) as an abbreviation for the valid limit operation in (1.26).

The Dirac delta can be shifted to any point t_0 in the domain of signal $x(t)$ and a similar argument applied. This gives the informal *sifting property* of the Dirac delta:

$$\int_{-\infty}^{\infty} x(t)\delta(t - t_0)\, dt \;=\; x(t_0)\,. \tag{1.28}$$

Again, mathematical prudence suggests that we think of the sifting property as special way of writing a limit of integrals. We can add another story to this mythology: The Dirac delta is the derivative of the unit step $u(t)$. Let $n > 0$ and consider the following sequence of continuous signals $u_n(t)$ approximating the unit step.

$$u_n(t) \;=\; \begin{cases} 1 & \text{if} \quad \dfrac{1}{n} < t, \\ \dfrac{(nt+1)}{2} & \text{if} \; -\dfrac{1}{n} \le t \le \dfrac{1}{n}, \\ 0 & \text{if} \quad t < -\dfrac{1}{n}. \end{cases} \tag{1.29}$$

Note that as $n \to \infty$, $u_n(t) \to u(t)$ for all $t \neq 0$. Also, for all $t \notin [-1/n, 1/n]$,

$$\frac{d}{dt}u_n(t) \;=\; \delta_n(t)\,. \tag{1.30}$$

We set aside our mathematical qualms and take limits as $n \to \infty$ of both sides of (1.30). The *derivative property* of the unit step results:

$$\lim_{n \to \infty} \frac{d}{dt} u_n(t) = \frac{d}{dt} \lim_{n \to \infty} u_n(t) = \frac{d}{dt} u(t) = \lim_{n \to \infty} \delta_n(t) = \delta(t). \tag{1.31}$$

The convergence of a sequence of functions must be *uniform* in order that interchange of limit operations, such as (1.27) and (1.30), be valid. Advanced calculus texts cover this theory [44]. The mathematical theory of *distributions* [48, 49] provides a rigorous foundation for the idea of a Dirac delta, as well as the sifting and derivative properties.

1.3 DISCRETE SIGNALS

Now that we have looked at some functions that serve as models for real-world analog signals, let us assume that we have a method for acquiring samples. Depending upon the nature of the analog signal, this may be easy or difficult. To get a discrete signal that represents the hourly air temperature, noting the reading on a thermometer is sufficient. Air temperature varies so slowly that hand recording of values works just fine. Rapidly changing analog signals, in contrast, require faster sampling methods. To acquire digital samples over one million times per second is not at all easy and demands sophisticated electronic design.

In signal processing, both analog and digital signals play critical roles. The signal acquisition process takes place at the system's front end. These are electronic components connected to some sort of transducer: a microphone, for instance. An analog value is stored momentarily while the digitization takes place. This sample-and-hold operation represents a discrete signal. An analog-to-digital converter turns the stored sample into a digital format for computer manipulation. We will, however, not ordinarily deal with digital signals, because the limitation on numerical precision that digital form implies makes the theoretical development too awkward. Thus, the discrete signal—actually an abstraction of the key properties of digital signals that are necessary for mathematical simplicity and flexibility—turns out to be the most convenient theoretical model for real-life digital signals.

1.3.1 Definitions and Notation

Unlike analog signals, which have a continuous domain, the set of real numbers $\mathbb{R}$, discrete signals take values on the set of integers $\mathbb{Z}$. Each integer n in the domain of x represents a time instant at which the signal has a value $x(n)$. Expressions such as $x(2/3)$ make no sense for discrete signals; the function is not even defined there.

Definition (Discrete and Digital Signals). A *discrete-time* (or simply *discrete*) signal is a real-valued function $x\colon \mathbb{Z} \to \mathbb{R}$. *x(n)* is the signal value at time instant n. A *digital* signal is an integer-valued function $x\colon \mathbb{Z} \to [-N, N]$, with domain $\mathbb{Z}$, $N \in \mathbb{Z}$, and $N > 0$. A complex-valued discrete-time signal is a function $x\colon \mathbb{Z} \to \mathbb{C}$, with domain $\mathbb{Z}$ and range included in the complex numbers $\mathbb{C}$.

Digital signals constitute a special class within the discrete signals. Because they can take on only a finite number of output values in the dependent variable, digital signals are rarely at the center of signal theory analyses. It is awkward to limit signal values to a finite set of integers, especially when arithmetic operations are performed on the signal values. Amplification is an example. What happens when the amplified value exceeds the maximum digital value? This is saturation, a very real problem for discrete signal processing systems. Some approach for avoiding saturation and some policy for handling it when it does occur must enter into the design considerations for engineered systems. To understand the theory of signals, however, it is far simpler to work with real-valued signals that may become arbitrarily small, arbitrarily large negative, and arbitrarily large positive. It is simply assumed that a real machine implementing signal operations would have a sufficiently high dynamic range within its arithmetic registers.

Notation. We use variable names such as "n", "m", and "k" for the independent variables of discrete signals. We prefer that analog signal independent variables have names such as "t" and "s". This is a tradition many readers will be comfortable with from Fortran computer programming. On those occasions when the discussion involves a sampling operation, and we want to use like names for the analog source and discrete result, we will subscript the continuous-domain signal: $x_a(t)$ is the analog source, and $x(n) = x_a(nT)$ is the discrete signal obtained from $x_a(t)$ by taking values every T time units.

With discrete-time signals we can tabulate or list signal values—for example, $x(n) = [3, 2, 1, \underline{5}, 1, 2, 3]$ (Figure 1.17). The square brackets signify that this is a discrete signal definition, rather than a set of integers. We must specify where the independent variable's zero time instant falls in the list. In this case, the value at $n = 0$ is

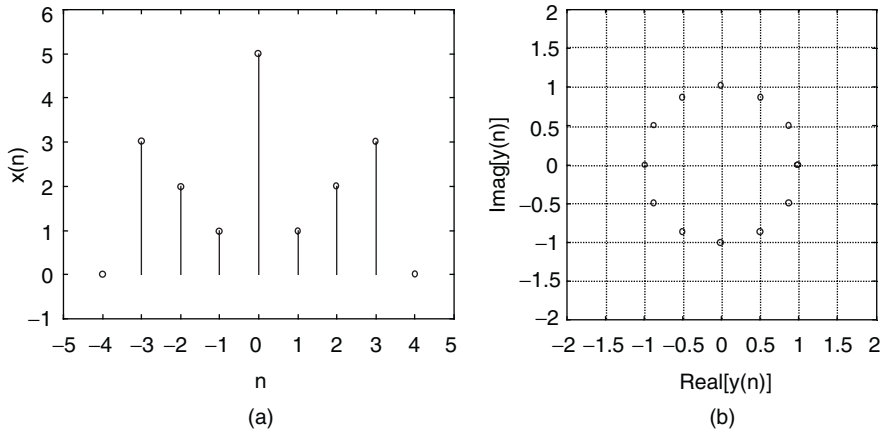

Fig. 1.17. Discrete signals. Panel (a) shows the signal $x(n) = [3, 2, 1, \underline{5}, 1, 2, 3]$. Signals may also be complex-valued, in which case their graphs are plotted in the complex plane. In (b), points of the signal $y(n) = \cos(n\pi/6) + j\sin(n\pi/6)$ are shown as pairs, (Real[$y(n)$], Imag[$y(n)$]).

underlined, and $x(0) = 5$, $x(-1) = 1$, $x(1) = 1$, and so on. For time instants not shown, signal values are zero. Thus, for discrete signals with an infinite number of nonzero values, we must provide a formula or rule that relates time instances to signal values, just as with analog signals.

1.3.2 Examples

We can derive straightforward discrete equivalents from the examples of analog signals above. A few curious properties relating to periodicity and derivatives arise.

1.3.2.1 Polynomials and Kindred Signals. There are discrete polynomial, rational, and algebraic signals. Discrete polynomials have the form

$$x(n) = \sum_{k=0}^{N} a_k n^k. \tag{1.32}$$

We cannot form the instantaneous derivative of $x(n)$ in (1.32) as with analog signals; instead discrete approximations must suffice. A variety of sometimes useful, but often problematic, notions of discrete derivatives do exist. For example, the left-hand discrete derivative of (1.32) is defined by $x_{\text{left}}(n) = x(n) - x(n-1)$. And a right-hand derivative exists too: $x_{\text{right}}(n) = x(n+1) - x(n)$. We can continue taking discrete derivatives of discrete derivatives. Note that there is no worry over the existence of a limit, since we are dividing the difference of successive signal values by the distance between them, and that can be no smaller than unity. Thus, discrete signals have (discrete) derivatives of all orders.

The domain of a polynomial $p(n)$ can be divided into disjoint regions of concavity: concave upward, where the second discrete derivative is positive; concave downward, where the second discrete derivative is negative; and regions of no concavity, where the second discrete derivative is zero, and $p(n)$ is therefore a set of dots on a line. Here is a first example, by the way, of how different analog signals can be from their discretely sampled versions. In the case of nonlinear analog polynomials, inflection points are always isolated. For discrete polynomials, though, there can be whole multiple point segments where the second derivative is zero.

If $p(n)$ and $q(n)$ are polynomials, then $x(n) = p(n)/q(n)$ is a *discrete rational* function. Signals modeled by discrete rational functions need to have provisions made in their definitions for the times n_0 when $q(n_0) = 0$. If, when this is the case, $p(n_0) = 0$ also, then it is necessary to separately specify the value of $x(n_0)$. There is no possibility of resorting to a limit procedure on $x(n)$ for a signal value, as with analog signals. Of course, if both $p(n)$ and $q(n)$ derive via sampling from analog ancestors, then such a limit, if it exists, could serve as the missing datum for $x(n_0)$.

Signals that involve a rational exponent of the time variable, such as $x(n) = n^{1/2}$, are called *discrete algebraic* signals. Again, there are problems with the domains of such signals; $n^{1/2}$ does not take values on the negative real numbers, for example. Consequently, we must usually partition the domain of such signals and define the signal piecewise.

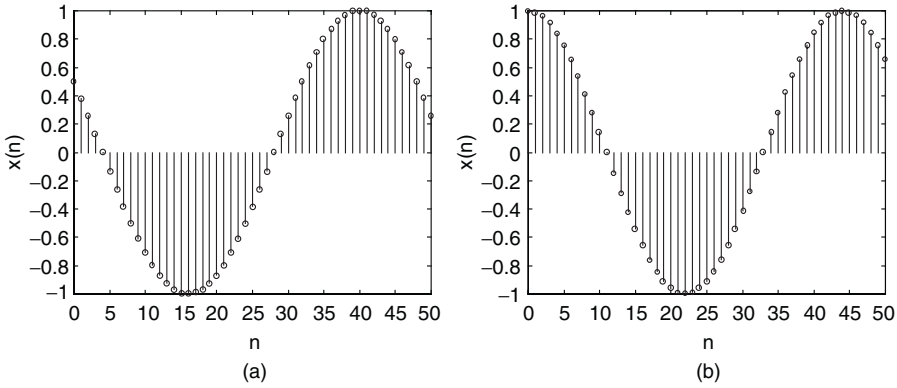

Fig. 1.18. Discrete sinusoids. Panel (a) shows the signal $x(n) = \cos(\omega n + \phi)$, with $\omega = \pi/24$ and $\phi = \pi/3$. Signal $x(n)$ has period $T = 48$. Panel (b,) on the other hand, shows the signal $y(n) = \cos(\omega n + \phi)$, with $\omega = 1/7$. It is not periodic.

1.3.2.2 Sinusoids. Discrete sinusoidal signals, such as $\sin(\omega n)$ or $\cos(\omega n)$, arise from sampling analog sinusoids (Figure 1.18). The function $\sin(\omega n + \phi)$ is the *discrete sine* function of *radial frequency* ω and phase ϕ. We will often work with $\cos(\omega n + \phi)$—and call it a sinusoid also—instead of the sine function. Note that—somewhat counter to intuition—discrete sinusoids may not be periodic! The periodicity depends upon the value of ω in $\cos(\omega n + \phi)$. We will study this nuance later, in Section 1.5.

1.3.2.3 Exponentials. Discrete exponential functions take the form

$$x(n) = Ce^{an} = C\exp(an), \tag{1.33}$$

where C and a are constants. Discrete exponentials (Figure 1.19) are used in frequency domain signal analysis (Chapters 7–9).

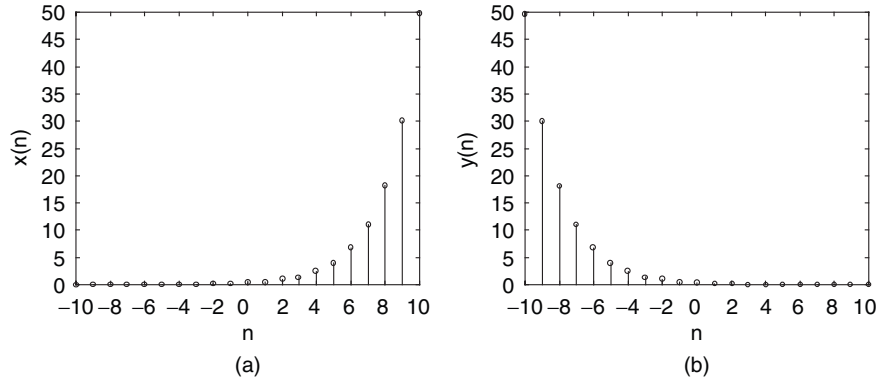

Fig. 1.19. Discrete exponential signals. Panel (a) shows the exponential $x(n) = \exp(n/2)/3$, and (b) is its reflection across the y-axis, $y(n) = \exp(-n/2)/3$.

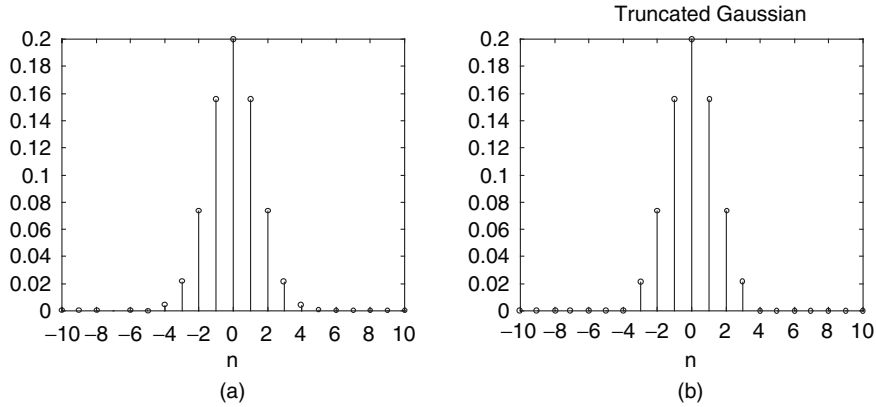

Fig. 1.20. Discrete Gaussian signals. The discrete pulse in (a) is $g_{0,2}(n)$, the Gaussian with mean μ equals 0 and standard deviation σ equals 2. Panel (b) illustrates a typical truncated Gaussian pulse.

The *discrete Gaussian* signal is

$$g_{\mu,\sigma}(n) = \frac{1}{\sigma\sqrt{2\pi}} e^{-\frac{(n-\mu)^2}{2\sigma^2}}. \tag{1.34}$$

Truncating the discrete Gaussian so that it is zero outside of some interval $[-N, N]$ is a discrete signal processing commonplace (Figure 1.20). This assumes that $g_{\mu,\sigma}(n)$ is small for $|n| > N$. As a signal with a finite number of nonzero values, the truncated discrete Gaussian serves as a noise removal filter. We can use it instead of the moving average filter (Section 1.1), giving preference to local signal values, for example. Also, for noise removal it makes sense to normalize the nonzero values so that their sum is unity. This preserves the average value of the raw signal.

There are also discrete versions of the Gabor elementary functions:

$$G_{\mu,\sigma,\omega}(n) = g_{\mu,\sigma}(n) e^{j\omega n}. \tag{1.35}$$

1.3.3 Special Discrete Signals

Discrete delta and unit step present no theoretical difficulties.

Definition (Discrete Delta). The *discrete delta* or *impulse* signal $\delta(n)$ is

$$\delta(n) = \begin{cases} 1 & \text{if } n = 0, \\ 0 & \text{if } n \neq 0. \end{cases} \tag{1.36}$$

There is a *sifting property* for the discrete impulse:

$$\sum_{n=-\infty}^{\infty} x(n)\delta(n-k) = x(k). \tag{1.37}$$

Discrete summation replaces the analog integral; this will become familiar.

Definition (Discrete Unit Step). The *unit step* signal $u(n)$ is

$$u(n) = \begin{cases} 1 & \text{if } n \geq 0, \\ 0 & \text{if } n < 0. \end{cases} \tag{1.38}$$

Note that if $m > k$, then $b(n) = u(n-k) - u(n-m)$ is a square pulse of unit height on $[k, m-1]$. Products $s(n)b(n)$ extract a chunk of the original discrete signal $s(n)$. And translated copies of $u(n)$ are handy for creating new signals on the positive or negative side of a signal: $y(n) = x(n)u(n-k)$.

1.4 SAMPLING AND INTERPOLATION

Sampling and interpolation take us back and forth between the analog and digital worlds. Sampling converts an analog signal into a digital signal. The procedure is straightforward: Take the values of the analog source at regular intervals. Interpolation converts a discrete signal into an analog signal. Its procedure is almost as easy: make some assumption about the signal between known values—linearity for instance—and fill them in accordingly. In the sampling process, much of the analog signal's information appears to be lost forever, because an infinite number of signal values are thrown away between successive sampling instants. On the other hand, interpolation appears to make some assumptions about what the discrete signal ought to look like between samples, when, in fact, the discrete signal says nothing about signal behavior between samples. Both operations would appear to be fundamentally flawed.

Nevertheless, we shall eventually find conditions upon analog signals that allow us to reconstruct them exactly from their samples. This was the discovery of Nyquist [2] and Shannon [3] (Chapter 7).

1.4.1 Introduction

This section explains the basic ideas of signal sampling: Sampling interval, sampling frequency, and quantization. The *sampling interval* is the time (or other spatial dimension measure) between samples. For a time signal, the *sampling frequency* is measured in hertz (Hz); it is the reciprocal of the sampling interval, measured in seconds (s). If the signal is a distance signal, on the other hand, with the sampling interval given in meters, then the sampling frequency is in units of (meters).$^{-1}$

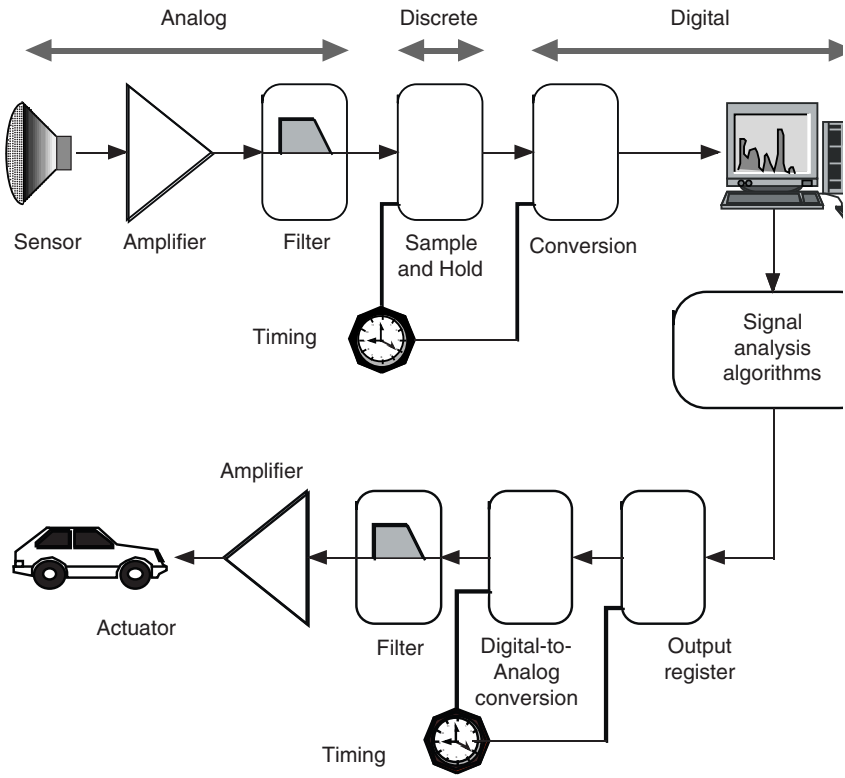

Fig. 1.21. Analog-to-digital conversion. Conversion of analog signals to digital signals requires several steps. Once digitized, algorithms running on the computer can analyze the signal. There may exist a closed loop with the analog world. For example, a digital output signal is converted back into analog form to control an actuator, such as anti-skid brakes on an automobile.

Discrete signals are more convenient for theoretical work, but for computer processing only a finite number of bits can represent the value in binary form. The signal must be digitized, or, in other words, the signal values must be *quantized*. By squeezing the signal value into an N-bit register, some fraction of the true signal value is lost, resulting in a *quantization error*. The number of possible digital signal values is called the *dynamic range* of the conversion.

If $x_a(t)$ is an analog signal, then $x(n) = x_a(n)$ defines a discrete signal. The time interval between $x(n)$ values is unity. We can also take more widely or narrowly spaced samples from $x_a(t)$: $x(n) = x_a(nT)$, where $T > 0$. In an actual system, electronic clock circuits set the sampling rate (Figure 1.21).

An N-bit register can hold non-negative digital values from 0 to $2^N - 1$. The smallest value is present when all bits are clear, and the largest value is when all bits are set. The two's complement representation of a digital value most common for storing signed digital signal values. Suppose there are N bits available in the input register, and the quantized signal's bit values are b_{N-1}, b_{N-2}, …, b_1, b_0. Then, the digital value is

$$D = -b_{N-1}2^{N-1} + b_{N-2}2^{N-2} + \cdots + b_2 2^2 + b_1 2^1 + b_0 2^0. \tag{1.39}$$

In this form, a register full of zeros represents a digital zero value; a single bit in the low-order position, $b_0 = 1$, represents unity; and a register having all bits set contains -1. The dynamic range of an N-bit register is 2^N.

There are several popular analog-to-digital converter (ADC) designs: Successive approximation, flash, dual-slope integration, and sigma–delta. The popular successive approximation converter operates like a balance beam scale. Starting at half of the digital maximum, it sets a bit, converts the tentative digital value to analog, and compares the analog equivalent to the analog input value. If the analog value is less than the converted digital guess, then the bit remains set; otherwise, the bit is cleared. The process continues with the next highest bit position in succession until all bits are tested against the input value. Thus, it adds and removes half-gram weights, quarter-gram weights, and so forth, until it balances the two pans on the beam. Successive approximation converters are accurate, slow, and common. A flash converter implements a whole bank of analog comparators. These devices are fast, nowadays operating at sampling rates of over 250 MHz. However, they have a restricted dynamic range. Dual-slope integration devices are slower, but offer better noise rejection. The sigma–delta converters represent a good design compromise. These units can digitize to over 20 bits and push sampling rates to almost 100 MHz.

1.4.2 Sampling Sinusoidal Signals

Let us consider sampling a sinusoid, $x_a(t) = \cos(\omega t)$, as in Figure 1.22. We sample it at a variety of rates T: $x(n) = x_a(nT)$. For high sampling rates, the discrete result resembles the analog original. But as the sampling interval widens, the resemblance fades. Eventually, we cannot know whether the original analog signal, or, possibly, one of much lower frequency was the analog source for $x(n)$.

To answer the simple question—what conditions can we impose on an analog signal $x_a(t)$ in order to recover it from discrete samples $x(n)$?—requires that we develop both the analog and discrete Fourier transform theory (Chapters 5–7).

1.4.3 Interpolation

Why reconstruct an analog signal from discrete samples? Perhaps the discrete signal is the original form in which a measurement comes to us. This is the case with the geothermal signals we considered in Section 1.1. There, we were given temperature values taken at regular intervals of depth into the earth. It may be of interest—especially when the intervals between samples are very wide or irregular—to provide estimates of the missing, intermediate values. Also, some engineered systems use digital-to-analog converters to take a discrete signal back out into the analog world again. Digital communication and entertainment devices come to mind. So, there is an impetus to better understand and improve upon the analog conversion process.

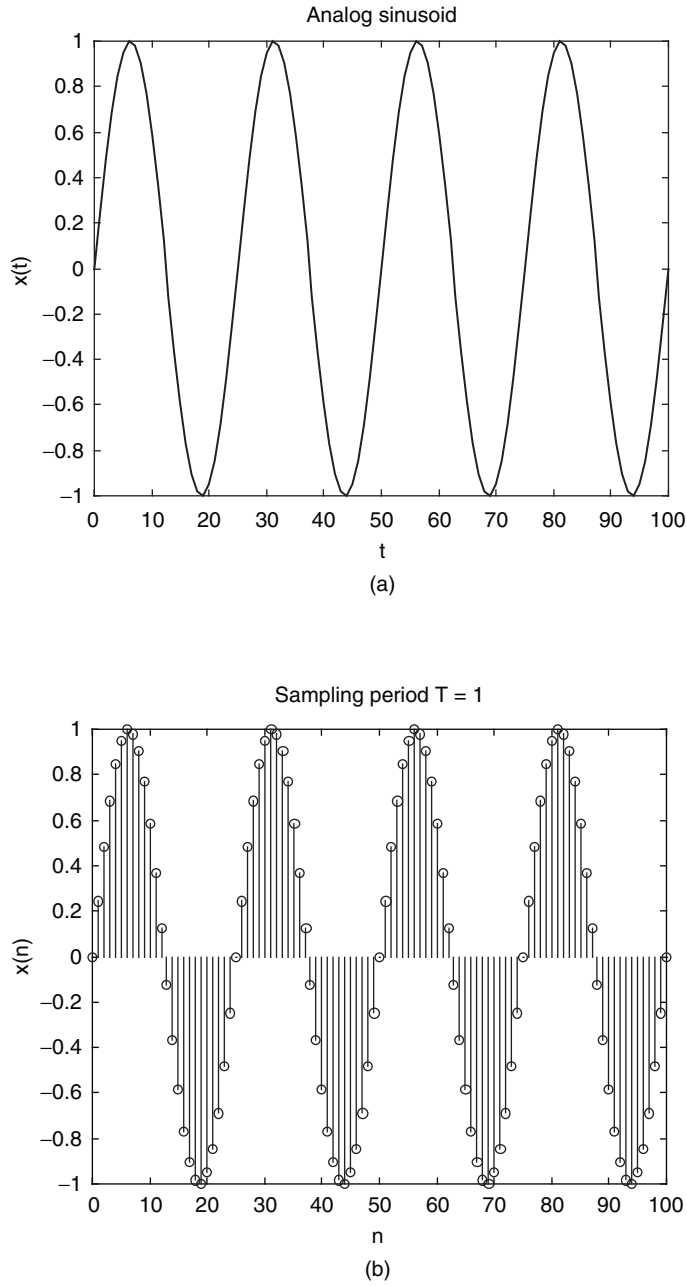

Fig. 1.22. Impossible to reconstruct. The original sinusoid (a) is first sampled at unit intervals (b). Sampling at a slower rate (c) suggests the same original $x(t)$ But when the rate falls, lower-frequency analog sinusoids could be the original signal (d).

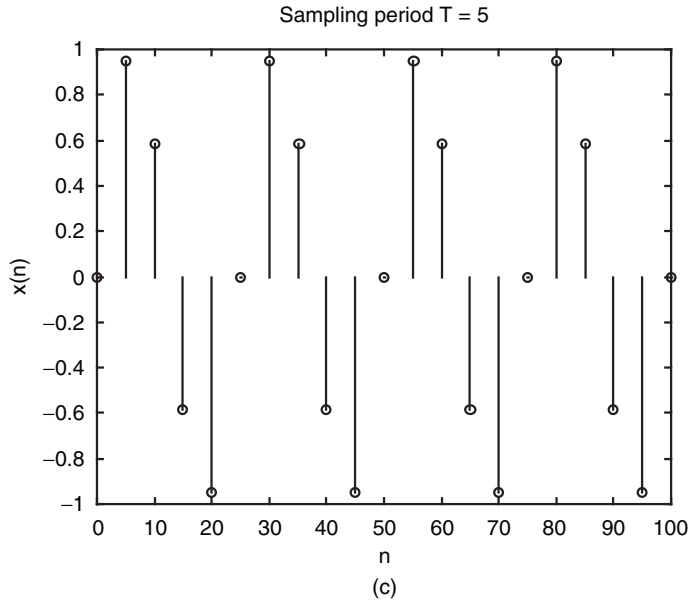

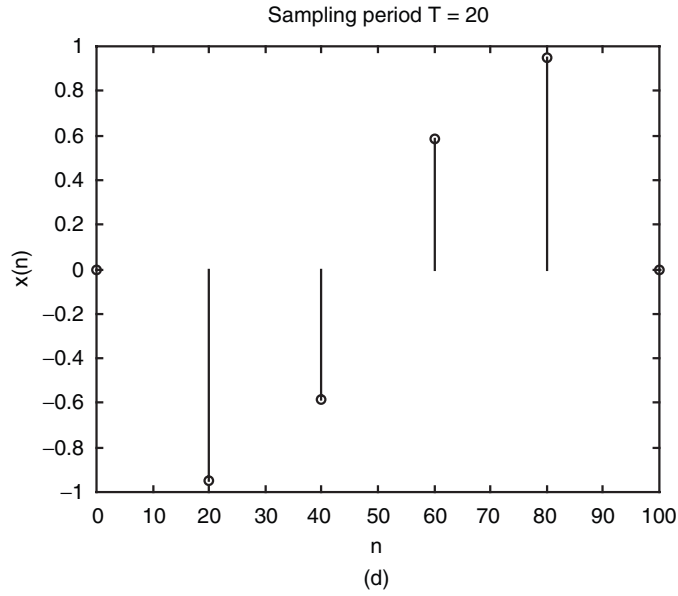

Fig. 1.22 (*Continued*)

1.4.3.1 Linear. Perhaps the simplest method of constructing an analog signal from discrete values is to use *linear interpolation* (Figure 1.23). Let $y_n = x(n)$, and define

$$x(t) = y_n + (y_{n+1} - y_n)(t - n) \tag{1.40}$$

for $t \in (n, n+1)$. The given samples are called *knots*, as if we were tying short sections of rope together. In this case, the analog signal passes through the knots. Observe that this scheme leaves corners—discontinuities in the first derivative—at the knots. The analog signal constructed from discrete samples via linear interpolation may therefore be unrealistic; nature's signals are usually smooth.

1.4.3.2 Polynomial. Smooth interpolations are possible with quadratic and higher-order polynomial interpolation.

Theorem (Lagrange[11] Interpolation). There is a unique polynomial $p(t)$ of degree $N > 0$ whose graph $(t, p(t))$ contains the distinct points $P_k = (n_k, x(n_k))$ for

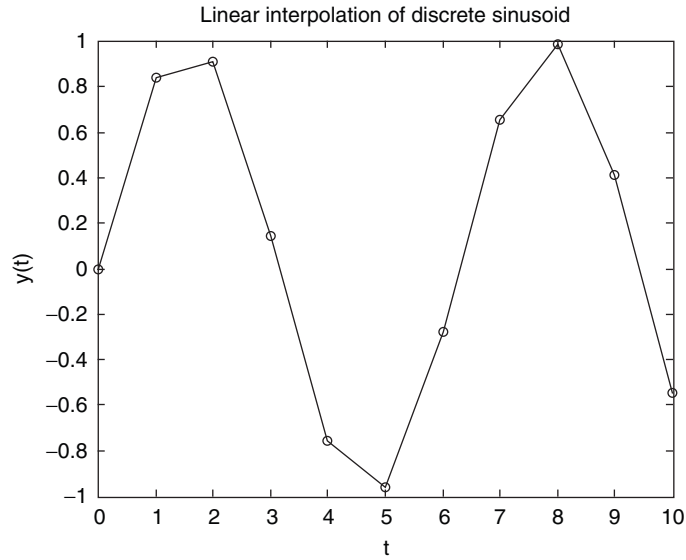

Fig. 1.23. Linear interpolation. Consider the signal $x(n) = \sin(n)$. Linear interpolation of this discrete sinusoid produces a jagged analog result.

[11]Joseph Louis Lagrange (1736–1813)—professor at Turin, Berlin, and Paris—was, with Euler, one of the great number theorists of the eighteenth century.

$0 \leq k \leq N$:

$$p(t) = \sum_{k=0}^{N} x(n_k) \prod_{\substack{m=0, \\ m \neq k}}^{N} \frac{(t - n_m)}{(n_k - n_m)} \tag{1.41}$$

Proof: Clearly $p(t)$ is of degree N and its graph passes through the points P_k. If $q(t)$ is another polynomial like this, then $d(t) = p(t) - q(t)$ is of degree N and has zeros at the $N + 1$ places: n_k, $0 \leq k \leq N$. Since a nonzero polynomial of degree N has at most N roots, the difference $d(t)$ must be identically zero. ■

Lagrange interpolation is not completely satisfactory. If N is large, then the method depends on a quotient of products of many terms; it is thereby subject to numerical round-off errors in digital computation. Furthermore, it is only valid for a restricted interval of points in a discrete signal. We may delete some points, since the interval between successive knots does not need to be unity in (1.41). However, we are still left with a polynomial approximation to a small part of the signal. If the signal is zero outside an interval, then however well the interpolant matches the nonzero signal region, $p(t)$ still grows large in magnitude with $|t|$.

An alternative is to compute quadratic polynomials on sequential triples of points. This provides some smoothness, but at every other knot, there is the possibility of a discontinuity in the derivative of the interpolants. Another problem is that the interpolation results vary depending on the point at which one starts choosing triples. To the point, how should we smooth the unit step signal $u(n)$ with interpolating quadratics? The interpolants are lines, except near the origin. If we begin with the triple (−2, −1, 0) and fit it with a quadratic polynomial, then our first interpolant will be concave up. If, on the other hand, we begin interpolating with the triad (−1, 0, 1), then our first quadratic approximation will be concave down. The exercises explore this and other questions entailed by quadratic interpolation. There is, however, a better way.

1.4.4 Cubic Splines

Perhaps the best method to make an analog signal out of discrete samples is to interpolate with spline[12] functions. The idea is to use a cubic polynomial between each successive pair of knots, $(n_k, x(n_k))$ and $(n_{k+1}, x(n_{k+1}))$ and yet match the first derivatives of cubics on either side of a knot.

To understand how this might work, let us first allow that the distance between known points need not be unity. Perhaps the system that collects the discrete samples cannot guarantee a regular sampling interval. The irregular sampling

[12]Architects and engineers once used a jointed, flexible ruler—known as a *spline*—to draw curves. These tools were made from sections of wood or plastic, attached together by brass rivets; modern splines, however, are almost always made of software.

notwithstanding, it is desirable to compose an analog signal that models the discrete data as a continuous, naturally occurring phenomenon. Later, it may even be useful to sample the analog model at regular intervals. So we assume that there are $N+1$ data points $(n_k, x(n_k))$, $0 \le k \le N$. Next, we set $\Delta_k = n_{k+1} - n_k$, $y_k = x(n_k)$, and we consider a polynomial $p_k(t)$ between the knots (n_k, y_k) and (n_{k+1}, y_{k+1}), for $0 \le k < N$. If the polynomial is quadratic or of higher degree and it contains the knots, then we need additional conditions to specify it. We prefer no sharp corners at the knots; thus, let us also stipulate that the derivatives of successive polyomials, $p_k'(t)$ and $p_{k+1}'(t)$, agree on their common knots: $p_k'(n_{k+1}) = p_{k+1}'(n_{k+1})$. Now there are four conditions on any interpolant: It must pass through two given knots and agree with its neighbors on endpoint derivatives. This suggests a cubic, since there are four unknowns. Readers might suspect that something more is necessary, because a condition on a polynomial's derivative is much less restrictive than requiring it to contain a given point.

Indeed, we need two further conditions on the second derivative in order to uniquely determine the interpolating polynomial. This reduces the search for a set of interpolating cubics to a set of linear equations. The two supplementary conditions are that we must have continuity of the second derivatives at knots, and we must specify second derivative values at the endpoints, (n_0, y_0) and (n_N, y_N). Then the equations are solvable [37, 50].

We write the interpolant on the interval $[n_k, n_{k+1}]$ in the form

$$p_k(t) = a_k(t-n_k)^3 + b_k(t-n_k)^2 + c_k(t-n_k) + y_k. \tag{1.42}$$

Then the derivative is

$$p_k'(t) = 3a_k(t-n_k)^2 + 2b_k(t-n_k) + c_k, \tag{1.43}$$

and the second derivative is

$$p_k''(t) = 6a_k(t-n_k) + 2b_k. \tag{1.44}$$

We define $D_k = p_k''(n_k)$ and $E_k = p_k''(n_{k+1})$. From (1.44),

$$D_k = 2b_k \tag{1.45}$$

and

$$E_k = 6a_k(n_{k+1} - n_k) + 2b_k = 6a_k\Delta_k + 2b_k, \tag{1.46}$$

with $\Delta_k = n_{k+1} - n_k$. Thus, we can express b_k and a_k in terms of Δ_k, which is known, and D_k and E_k, which are as yet unknown. Using (1.42), we can write c_k as follows:

$$c_k = \frac{y_{k+1} - y_k}{\Delta_k} - a_k\Delta_k^2 - b_k\Delta_k. \tag{1.47}$$

For $0 \le k < N$, (1.45)–(1.47) imply

$$c_k = \frac{y_{k+1} - y_k}{\Delta_k} - \frac{E_k - D_k}{6}\Delta_k - \frac{D_k}{2}\Delta_k = \frac{y_{k+1} - y_k}{\Delta_k} - \frac{\Delta_k}{6}(E_k + 2D_k). \quad (1.48)$$

To make a system of linear equations, we need to express this in terms of the second derivatives, D_k and E_k. The derivatives, $p_k'(t)$ and $p_{k+1}'(t)$, are equal for $t = n_{k+1}$; this is a required property of the interpolating cubics. Hence,

$$p_k'(n_{k+1}) = 3a_k(\Delta_k)^2 + 2b_k(\Delta_k) + c_k = p_{k+1}'(n_{k+1}) = c_{k+1}. \quad (1.49)$$

Inserting the expressions for c_{k+1}, c_k, b_k, and a_k in terms of second derivatives gives

$$6\frac{y_{k+2} - y_{k+1}}{\Delta_{k+1}} - 6\frac{y_{k+1} - y_k}{\Delta_k} = \Delta_k(2E_k + D_k) + \Delta_{k+1}(2D_{k+1} + E_{k+1}). \quad (1.50)$$

Now, $E_k = p_k''(n_{k+1}) = D_{k+1} = p_{k+1}''(n_{k+1})$, by invoking the continuity assumption on second derivatives. We also set $E_{N-1} = D_N$, producing a linear equation in D_k, D_{k+1}, and D_{k+2}:

$$6\frac{y_{k+2} - y_{k+1}}{\Delta_{k+1}} - 6\frac{y_{k+1} - y_k}{\Delta_k} = \Delta_k(2D_{k+1} + D_k) + \Delta_{k+1}(2D_{k+1} + D_{k+2}). \quad (1.51)$$

This system of equations has $N + 1$ variables, $D_0, D_1, \ldots, D_N$. Unfortunately, (1.51) has only $N - 1$ equations, for $k = 0, 1, \ldots, N - 2$. Let us lay them out as follows:

$$\begin{bmatrix} \Delta_0 & 2(\Delta_0 + \Delta_1) & \Delta_1 & 0 & 0 & \cdots & 0 \\ 0 & \Delta_1 & 2(\Delta_1 + \Delta_2) & \Delta_2 & 0 & \cdots & 0 \\ 0 & 0 & \Delta_2 & \cdots & \cdots & \cdots & 0 \\ 0 & 0 & 0 & \cdots & \cdots & \cdots & \cdots \\ \cdots & \cdots & \cdots & \cdots & \cdots & \Delta_{N-2} & 0 \\ 0 & 0 & 0 & 0 & \Delta_{N-2} & 2(\Delta_{N-2} + \Delta_{N-1}) & \Delta_{N-1} \end{bmatrix} \begin{bmatrix} D_0 \\ D_1 \\ D_2 \\ D_4 \\ \cdots \\ D_N \end{bmatrix}$$

$$= 6\begin{bmatrix} \frac{y_2 - y_1}{\Delta_1} - \frac{y_1 - y_0}{\Delta_0} \\ \frac{y_3 - y_2}{\Delta_2} - \frac{y_2 - y_1}{\Delta_1} \\ \cdots \\ \cdots \\ \cdots \\ \frac{y_N - y_{N-1}}{\Delta_{N-1}} - \frac{y_{N-1} - y_{N-2}}{\Delta_{N-2}} \end{bmatrix}. \quad (1.52)$$

From linear algebra, the system (1.52) may have no solution or multiple solutions [51, 52]. It has a unique solution only if the number of variables equals the number of equations. Then there is a solution if and only if the rows of the coefficient matrix—and consequently its columns—are linearly independent. Thus, we must reduce the number of variables by a pair, and this is where the final condition on second derivatives applies.

We specify values for D_0 and D_N. The most common choice is to set $D_0 = D_N = 0$; this gives the so-called *natural spline* along the knots (n_0, y_0), (n_1, y_1), …, (n_N, y_N). The coefficient matrix of the linear system (1.52) loses its first and last columns, simplifying to the symmetric system (1.53). Other choices for D_0 and D_N exist and are often recommended [37, 50]. It remains to show that (1.53) always has a solution.

$$\begin{bmatrix} 2(\Delta_0+\Delta_1) & \Delta_1 & 0 & 0 & 0 & \dots & 0 \\ \Delta_1 & 2(\Delta_1+\Delta_2) & \Delta_2 & 0 & 0 & \dots & 0 \\ 0 & \Delta_2 & 2(\Delta_2+\Delta_3) & \Delta_3 & \dots & \dots & 0 \\ 0 & 0 & \Delta_3 & \dots & \dots & \dots & \dots \\ \dots & \dots & \dots & \dots & \dots & \dots & \Delta_{N-2} \\ 0 & 0 & \dots & \dots & 0 & \Delta_{N-2} & 2(\Delta_{N-2}+\Delta_{N-1}) \end{bmatrix} \begin{bmatrix} D_1 \\ D_2 \\ D_3 \\ D_4 \\ \dots \\ D_{N-1} \end{bmatrix}$$

$$= 6 \begin{bmatrix} \dfrac{y_2 - y_1}{\Delta_1} - \dfrac{y_1 - y_0}{\Delta_0} \\ \dfrac{y_3 - y_2}{\Delta_2} - \dfrac{y_2 - y_1}{\Delta_1} \\ \dots \\ \dots \\ \dots \\ \dfrac{y_N - y_{N-1}}{\Delta_{N-1}} - \dfrac{y_{N-1} - y_{N-2}}{\Delta_{N-2}} \end{bmatrix}. \tag{1.53}$$

Theorem (Existence of Natural Splines). Suppose the points (n_0, y_0), (n_1, y_1), …, (n_N, y_N) are given and $n_0 < n_1 < \dots < n_N$. Let $\Delta_k = n_{k+1} - n_k$. Then the system $A\boldsymbol{v} = \boldsymbol{y}$ in (1.53) has a solution $\boldsymbol{v} = [D_1, D_2, \dots, D_{N-1}]^T$.

Proof: Gaussian elimination solves the system, using row operations to convert $\boldsymbol{A} = [A_{r,c}]$ into an upper-triangular matrix. The elements on the diagonal of the coefficient matrix are called the *pivots*. The first pivot is $P_1 = 2\Delta_0 + 2\Delta_1$, which is *positive*. We multiply the first row of $\boldsymbol{A}$ by the factor $f_1 = \frac{-\Delta_1}{2\Delta_0 + 2\Delta_1}$ and add it to

the second row, thereby annihilating $A_{2,1}$. A second pivot P_2 appears in place of $A_{2,2}$:

$$P_2 = 2\Delta_1 + 2\Delta_2 + \Delta_1 f_1 = \Delta_1 \frac{-\Delta_1}{(2\Delta_0 + 2\Delta_1)} + 2\Delta_1 + 2\Delta_2$$
$$= \frac{3\Delta_1^2 + 4\Delta_0\Delta_1}{(2\Delta_0 + 2\Delta_1)} + 2\Delta_2. \tag{1.54}$$

We update the vector $\boldsymbol{y}$ according to the row operation as well. Notice that $P_2 > 2\Delta_2 > 0$. The process produces another positive pivot. Indeed, the algorithm continues to produce positive pivots P_r. These are more than double the coefficient $A_{r+1,r}$, which the next row operation will annihilate. Thus, this process will eventually produce an upper-triangular matrix. We can find the solution to (1.53) by back substitution, beginning with D_{N-1} on the upper-triangular result. ■

Figure 1.24 shows how nicely cubic spline interpolation works on a discrete sinusoid. Besides their value for reconstructing analog signals from discrete samples, splines are important for building multiresolution signal decompositions that support modern wavelet theory [53] (Chapters 11 and 12).

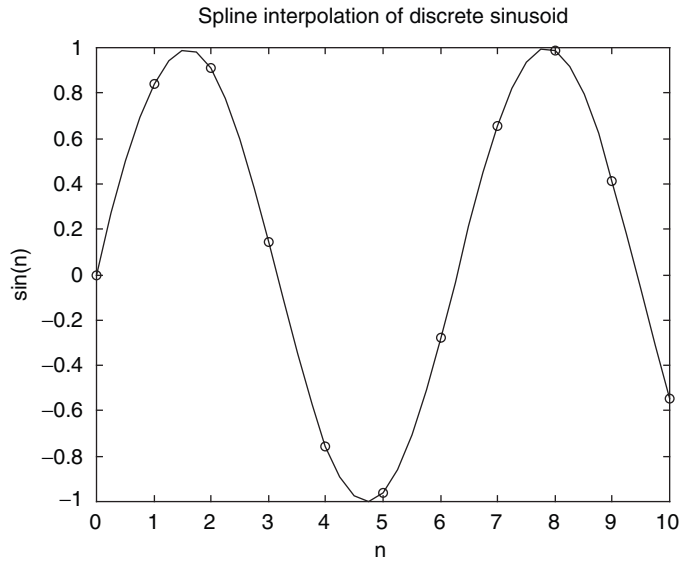

Fig. 1.24. Cubic spline interpolation. Again, discrete samples of the signal $x(n) = \sin(n)$ are used for the knots. Cubic spline interpolation offers a smooth model of the undulations and clearly captures the sinusoidal behavior of the original analog signal.

1.5 PERIODIC SIGNALS

Periodic signals, whether analog or discrete, repeat their values over intervals. The most familar ones are sinusoids. These signals arise from the mechanics of circular motion, in electric and magnetic interactions, and they are found in many natural phenomena. For instance, we considered the solution of Maxwell's equations, which describe the relation between the electric and magnetic fields. There we showed how to derive from the field equations a set of differential equations whose solution involves sinsusoidal functions. Radio waves propagate through empty space as electric and magnetic sinusoids at right angles to one another.

1.5.1 Fundamental Period and Frequency

The interval over which a signal repeats itself is its period, and the reciprocal of its period is its frequency. Of course, if a signal repeats itself over an interval, then it also repeats itself over any positive integral multiple of that interval; we must characterize a periodic signal by the smallest such interval of repetition.

Definition (Periodicity). An analog signal $x(t)$ is *periodic* if there is a $T > 0$ with $x(t + T) = x(t)$ for all t. A discrete signal $x(n)$ is periodic if there is an integer $N > 0$ with $x(n) = x(n + N)$ for all n. The smallest value for which a signal is periodic is called the *fundamental period.*

Definition (Analog Sinusoid). The signal

$$x(t) = A\cos(\Omega t + \phi) \tag{1.55}$$

is an *analog sinusoid*. A is the *amplitude* of $x(t)$, which gives its maximum value; Ω is its *frequency* in radians per second; and ϕ is its *phase* in radians. $\Omega = 2\pi F$, where F is the frequency in hertz.

Example. If $x(t) = A\cos(\Omega t + \phi)$, then $x(t) = x(t + \frac{2\pi}{\Omega})$, from the 2π-periodicity of the cosine function. So $T = \frac{2\pi}{\Omega} = \frac{1}{F}$ is the fundamental period of $x(t)$.

The sinusodal signals in nature are, to be sure, never the perfect sinusoid that our mathematical models suggest. Electromagnetic propagation through space comes close to the ideal, but always present are traces of matter, interference from other radiation sources, and the minute effects of gravity. Noise corrupts many of the phenomena that fall under our analytical eye, and often the phenomena are only vaguely sinusoidal. An example is the periodic trends of solar activity—in particular, the 11-year sunspot cycle, which we consider in more detail in the next section. But signal noise is only one aspect of nature's refusal to strictly obey our mathematical forumulas.

Natural sinusoidal signals decay. Thus, for it to be a faithful mathematical model of a naturally occurring signal, the amplitude of the sinusoid (1.55) should decrease. Its fidelity to nature's processes improves with a time-varying amplitude:

$$x(t) = A(t)\cos(\Omega t + \phi)\,. \tag{1.56}$$

The earliest radio telephony technique, *amplitude modulation* (AM), makes use of this idea. The AM radio wave has a constant *carrier frequency*, $F = \frac{\Omega}{2\pi}$ Hz, but its amplitude $A(t)$ is made to vary with the transmitted signal. Electronic circuits on the receiving end tune to the carrier frequency. The amplitude cannot jump up and down so quickly that it alters the carrier frequency, so AM is feasible only if F greatly exceeds the frequency of the superimposed amplitude modulation. This works for common AM content—voice and music—since their highest useful frequencies are about 8 and 25 kHz, respectively. In fact, limiting voice frequencies to only 4 kHz produces a very lifelike voice audio, suitable for telephony. Accordingly, the AM radio band, 550 kHz to 1600 kHz, is set well above these values. The signal looks like a sine wave whose envelope (the curve that follows local signal maxima) matches the transmitted speech or music.

Natural and engineered systems also vary the frequency value in (1.55). The basic *frequency-modulated* (FM) signal is the chirp, wherein the frequency increases linearly. Animals—birds, dolphins, and whales, for example—use frequency varying signals for communication. Other animals, such as bats, use chirps for echolocation. Some natural languages, such as Chinese, use changing tones as a critical indication of word meaning. In other languages, such as English and Russian, it plays only an ancillary role, helping to indicate whether a sentence is a question or a statement. Thus, we consider signals of the form

$$x(t) = A\cos(2\pi F(t) + \phi)\,, \tag{1.57}$$

where $F(t)$ need not be linear. An FM signal (1.57) is not a true sinusoid, but it provides the analyst with a different kind of signal model, suitable for situations where the frequency is not constant over the time region of interest. Applications that rely on FM signals include such systems as radars, sonars, seismic prospecting systems, and, of course, communication systems.

A *phase-modulated* signal is of the form

$$x(t) = A\cos(2\pi F + \phi(t))\,. \tag{1.58}$$

There is a close relation between phase and frequency modulation, namely, that the derivative of the phase function $\phi(t)$ in (1.58) is the *instantaneous frequency* of the signal $x(t)$ [54, 55]. The idea of instantaeous frequency is that there is a sinusoid that best resembles $x(t)$ at time t. It arose as recently as the late 1930s in the context of FM communication systems design, and its physical meaning has been the subject of some controversy [56]. If we fix F in (1.58) and allow $\phi(t)$ to vary, then the

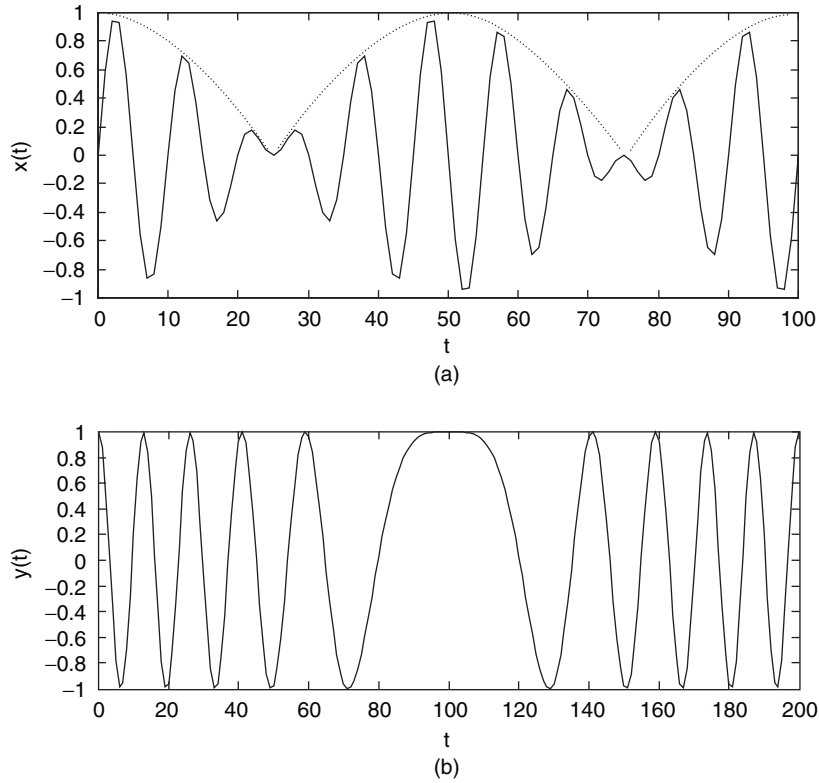

Fig. 1.25. AM and FM signals. Panel (a) shows a sinusoidal carrier modulated by a sinusoidal signal. The information-bearing part of the signal is given by the envelope of the signal, shown by dotted lines. In (b), a simple FM signal with the frequency varying sinusoidally is shown. Note that the oscillations bunch up and spread out as time passes, indicating rising and falling signal frequency, respectively.

frequency of the cosine wave changes. Over Δt seconds, the radial frequency of $x(t)$ changes by amount $[\Omega + \phi(t + \Delta t)] - [\Omega + \phi(t)] = \phi(t + \Delta t) - \phi(t)$, where $\Omega = 2\pi f$. The average change in Hertz frequency over this time interval is $\frac{\phi(t+\Delta t)-\phi(t)}{2\pi\Delta t}$. As $\Delta t \to 0$, this value becomes the derivative $\frac{d}{dt}\phi(t)$, the instantaneous frequency of the phase modulated signal $x(t)$.

If it seems odd that the derivative of phase is the signal frequency, then perhaps thinking about the familiar Doppler[13] effect can help reveal the connection. Suppose a train whistle makes a pure sinusoidal tone. If the train is standing still, then someone within earshot hears a sound of pure tone that varies neither in amplitude nor pitch. If the train moves while the whistle continues to blow, however, then the

[13]Austrian physicist Christian Doppler (1803–1853) discovered and described this phenomenon, first experimenting with trumpeters on a freight train.

tone changes. Coming toward us, the train whistle mechanically reproduces the same blast of air through an orifice, but the signal that we hear is different. The pitch increases as the train comes toward us. That means the signal frequency is increasing, but all that it takes to accomplish that is to move the train. In other words, a change in the phase of the whistle signal results in a different frequency in sound produced. A similar effect occurs in astronomical signals with the red shift of optical spectral lines from distant galaxies. In fact, the further they are away from us, the more their frequency is shifted. This means that the further they are from earth, the more rapidly is the phase changing. Objects further away move away faster. This led Hubble[14] to conclude that the universe is expanding, and the galaxies are spreading apart as do inked dots on an inflating balloon.

Some signals, natural and synthetic, are superpositions of sinusoids. In speech analysis, for example, it is often possible to model vowels as the sum of two sinusoidal components, called *formants*:

$$x(t) = x_1(t) + x_2(t) = A_1 \cos(\Omega_1 t + \phi_1) + A_2 \cos(\Omega_2 t + \phi_2) . \tag{1.59}$$

Generally, $x(t)$ in (1.59) is not sinusoidal, unless $\Omega_1 = \Omega_2 = \Omega$. A geometric argument demonstrates this. If the radial frequencies of the sinusoidal components are equal, then the vectors $\boldsymbol{v}_1 = (A_1 \cos(\Omega t + \phi_1), A_1 \sin(\Omega t + \phi_1))$ and $\boldsymbol{v}_2 = (A_2 \cos(\Omega t + \phi_2), A_2 \sin(\Omega t + \phi_2))$ rotate around the origin at equal speeds. This forms a parallelogram structure, rotating about the origin at the same speed as $\boldsymbol{v}_1$ and $\boldsymbol{v}_2$ (Figure 1.26), namely Ω radians per unit time. The x-coordinates of $\boldsymbol{v}_1$ and

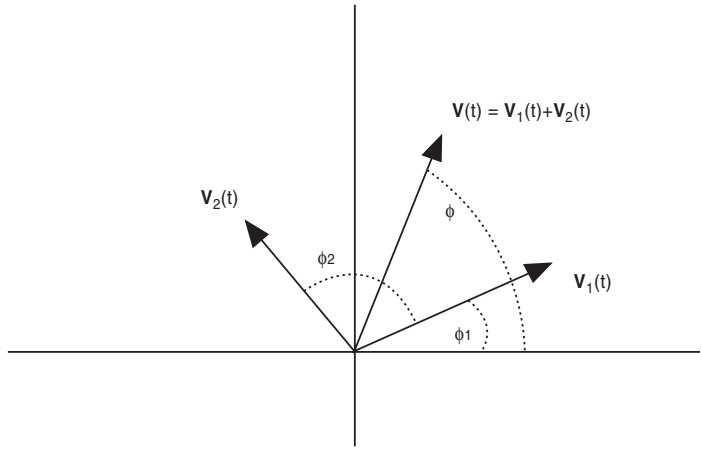

Fig. 1.26. Sinusoidal summation. Vector $\boldsymbol{v} = \boldsymbol{v}_1 + \boldsymbol{v}_2$ has length $\|\boldsymbol{v}\| = A$. Its x-coordinate, as a function of t, is a sinusoid of radial frequency Ω and phase $\phi = (\phi_2 - \phi_1)/2$.

[14]Working at the Mount Wilson Observatory near Los Angeles, Edwin Powell Hubble (1889–1953) discovered that galaxies are islands of stars in the vast sea of space, the red shift relates velocity to distance, and the universe itself expands in all directions.

$\boldsymbol{v}_2$ are the values of $x_1(t)$ and $x_2(t)$, respectively. The sum $x(t)$ is the x-coordinate of $\boldsymbol{v}_1 + \boldsymbol{v}_2$. Now, $\|\boldsymbol{v}_1 + \boldsymbol{v}_2\| = \|\boldsymbol{v}\| = A$, where

$$\begin{aligned} A^2 &= A_1^2 + A_2^2 + 2A_1A_2\cos(\Omega t + \phi_1)\cos(\Omega t + \phi_2) \\ &\quad + 2A_1A_2\sin(\Omega t + \phi_1)\cos(\Omega t + \phi_2) \\ &= A_1^2 + A_2^2 + 2A_1A_2\cos(\phi_1 - \phi_2). \end{aligned} \tag{1.60}$$

We also see from Figure 1.26 that the sum lies half way between $\boldsymbol{v}_1$ and $\boldsymbol{v}_2$. Thus, the phase of $\mathbf{v}$ is $\phi = \frac{\phi_2 - \phi_1}{2}$, and we have $x(t) = A\cos(\Omega t + \phi)$.

1.5.2 Discrete Signal Frequency

Due to the gap between successive signal values, discrete periodic signals have several properties that distinguish them from analog periodic waveforms:

(i) Discrete periodic signals have lower limits on their period; it makes no sense to have a discrete signal with period less than unity, because the discrete world does not even define signals at intervals smaller than unity.

(ii) A discrete signal with unit period is constant.

(iii) For sinusoids, the restriction to unit periods or more means that they have a maximum frequency: $|\Omega| = \pi$.

(iv) Not all sinusoids are periodic; periodicity only obtains when the frequency of the sampled signal is matched to the sampling interval.

This section covers these idiosyncrasies.

Proposition (Discrete Period). The smallest period for a discrete signal is $T = 1$. The largest frequency for a discrete sinusoid is $|\Omega| = \pi$, or equivalently, $|F| = 1$, where $\Omega = 2\pi F$ is the frequency in radians per sample.

Proof: Exercise. ■

Proposition (Periodicity of Discrete Sinusoids). Discrete sinusoid $x(n) = A\cos(\Omega n + \phi)$, $A \neq 0$, is periodic if and only if $\Omega = 2\pi p$, where $p \in \mathbb{Q}$, the rational numbers.

Proof: First, suppose that $\Omega = 2\pi p$, where $p \in \mathbb{Q}$. Let $p = m/k$ where $m, k \in \mathbb{N}$. If $m = 0$, then $x(n)$ is periodic; in fact, it is constant. Therefore, suppose $m \neq 0$ and choose $N = |k/m|$. Then,

$$\begin{aligned} x(n+N) &= A\cos\left(\Omega n + \Omega\left|\frac{k}{m}\right| + \phi\right) = A\cos\left(\Omega n + 2\pi\frac{m}{k}\left|\frac{k}{m}\right| + \phi\right) \\ &= A\cos(\Omega n + 2\pi(\pm 1) + \phi) = A\cos(\Omega n + \phi) = x(n) \end{aligned}$$

by the 2π-periodicity of the cosine function. Thus, $x(n)$ is periodic with period N. Conversely, suppose that for some $N > 0$, $x(n + N) = x(n)$ for all n. Then, $A\cos(\Omega n + \phi) = A\cos(\Omega n + \Omega N + \phi)$. Since $A \neq 0$, we must have

$\cos(\Omega n + \phi) = \cos((\Omega n + \phi) + \Omega N)$. And, since cosine can only assume the same values on intervals that are integral multiples of π, we must have $\Omega N = m\pi$ for some $m \in \mathbb{N}$. Then, $\Omega = m\pi/N$, so that Ω is a rational multiple of π. ■

Let us reinforce this idea. Suppose that $x(n) = x_a(Tn)$, where $x_a(t) = A\cos(\Omega t + \phi)$, with $A \neq 0$. Then $x_a(t)$ is an analog periodic signal. But $x(n)$ is not necessarily periodic. Indeed, $x(n) = A\cos(\Omega nT + \phi)$, so by the proposition, $x(n)$ is periodic only if ΩT is a rational multiple of π. Also, the discrete sinusoid $x(n) = \cos(2\pi fn)$ is periodic if and only if the frequency $f \in \mathbb{Q}$. The analog signal $s(t) = \cos(2\pi ft)$, $f > 0$, is always periodic with period $1/f$. But if $f = m/k$, with $m, k \in \mathbb{N}$, and m and k are relatively prime, then $x(n)$ has period k, not $1/f$. It takes time to get used to the odd habits of discrete sinusoids.

1.5.3 Frequency Domain

Having introduced analog and discrete sinusoids, fundamental period, and sinusoidal frequency, let us explain what it means to give a frequency-domain description of a signal. We already know that signals from nature and technology are not always pure sinusoids. Sometimes a process involves superpositions of sinusoids. The signal amplitude may vary too, and this behavior may be critical to system understanding. A variant of the pure sinusoid, the amplitude-modulated sine wave, models this situation. Another possibility is a variable frequency characteristic in the signal, and the frequency-modulated sine wave model accounts for it. There is also phase modulation, such as produced by a moving signal source. Finally, we must always be cognizant of, prepare for, and accommodate noise within the signal. How can we apply ordinary sinusoids to the study of these diverse signal processing and analysis applications?

1.5.3.1 Signal Decomposition. Many natural and synthetic signals contain regular oscillatory components. The purpose of a frequency-domain description of a signal is to identify these components. The most familar tool for aiding in identifying periodicities in signals are the sinusoidal signals, $\sin(t)$ and $\cos(t)$. Thus, a frequency-domain description presupposes that the signal to be analyzed consists of a sum of a few sinusoidal components. Perhaps the sum of sinusoids does not exactly capture the signal values, but what is left over may be deemed noise or background. We consider two examples: sunspot counts and speech. If we can identify some simple sinusoidal components, then a frequency-domain description offers a much simpler signal description. For instead of needing a great number of time domain values to define the signal, we need only a few triplets of real numbers—the amplitude, frequency, and phase of each substantive component—in order to capture the essence of the signal.

Consider the signal $x(n)$ of Figure 1.27, which consists of a series of irregular pulses. There appears to be no rule or regularity of the values that would allow us to describe it by more that a listing of its time-domain values. We note that certain regions of the signal appear to be purely sinusoidal, but the juxtaposition of unfamiliar, oddly shaped pulses upsets this local pattern.

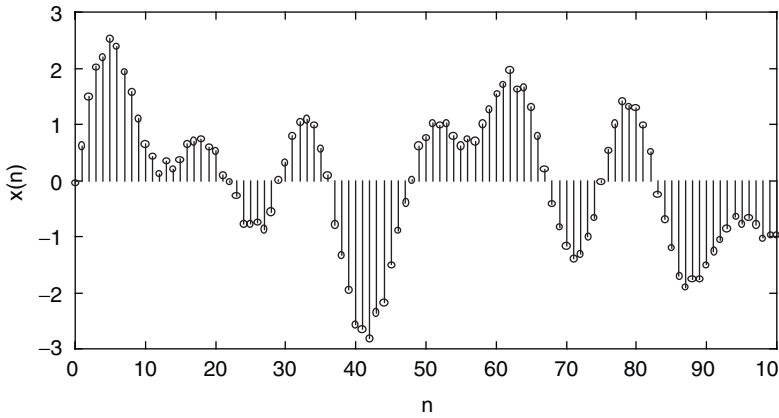

Fig. 1.27. Efficiency of freqency-domain signal description. An irregular signal, appearing to lack any regular description beyond a listing of its time-domain values, turns out to be the sum of three sinusoids and a small background noise signal.

The signal does, however, have a concise description as a sum of three sinusoids and a small noise component:

$$x(n) = \sin\left(\frac{2\pi n}{15}\right) + \sin\left(\frac{2\pi n}{25}\right) + \sin\left(\frac{2\pi n}{50}\right) + N(n)\,. \tag{1.61}$$

Thus, signal description, and hence the further analysis of signals, is often made more powerful by representing signals in terms of an established set of prototype signals. For a frequency domain signal description, sinusoidal models are appropriate. Some background noise may elude an immediate description in terms of sinusoidal components. Depending on the application, of course, this residual signal may be negligible because it has a much lower magnitude than the source signal of interest. If the sinusoidal trends are localized within a signal, the arithmetic of superposition may allow us to describe them even with sinusoids of longer duration, as Figure 1.27 illustrates.

1.5.3.2 Sunspots. One periodic phenomenon with which we are familiar is the sunspot cycle, an example of a natural periodic trend. Sunspots appear regularly on the sun's surface as clusters of dark spots and, at their highest intensities, disrupt high-frequency radio communication. Scientists have scrutinized sunspot activity, because, at its height during the 11-year cycle, it occasionally hampers very high frequency radio communication. Until recently, the mechanism responsible for this phenomenon was not known. With temperature of 3800 °K, they are considerably cooler than the rest of the sun's surface, which has an average temperature of some 5400 °K.

Ancient people sometimes observed dark spots on the solar disk when it was obscured by fog, mist, or smoke. Now we check for them with a simple telescope

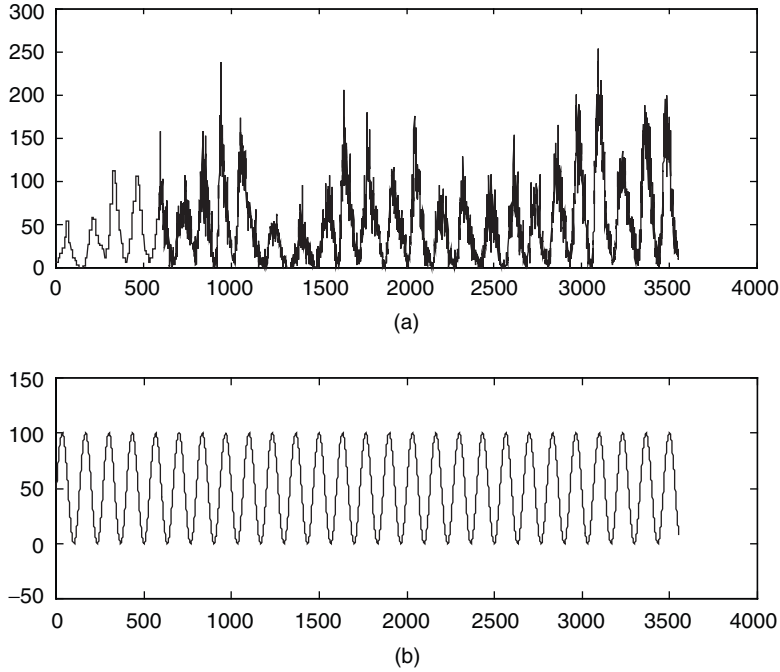

Fig. 1.28. Wolf sunspot numbers. Panel (a) plots the time-domain values of $w(n) = 10G(n) + S(n)$ for each month from 1700 through 1995. We compare the oscillation with sinusoids, for example, when period $T = 11.1$ years as in (b).

that projects the sun's image onto a white plate. Galileo[15] was the first to do so. His observations upset the prevailing dogma of seventeenth century Europe insisting that the sun was a perfect disk. Standardized sunspot reports began in the mid-1700s, and the earlier values given in our data plots (Figure 1.28) are assumptions based on informal observations.

Sunspot activity can be formulated as a discrete signal by counting the number of groups of sunspots. In 1848, the Swiss astronomer, Johann Rudolph Wolf, introduced a daily measurement of sunspot number. His method, which is still used today, counts the total number of spots visible on the face of the sun and the number of groups into which they cluster, because neither quantity alone satisfactorily measures sunspot activity. The *Wolf*[16] *sunspot number* is $w(n) = 10G(n) + S(n)$, where $G(n)$ is the average number of sunspot groups and $S(n)$ is the average number of spots. Individual observational results do vary greatly, however, since the measurement strongly depends on interpretation, experience, and the stability of the earth's atmosphere

[15]In addition to finding solar blemishes in 1610, Galileo Galilei (1564–1642) used his telescope to resolve the Milky Way into faint stars and, with his discovery of the phases of Venus, confirmed Copernicus's heliocentric theory.

[16]After Swiss astronomer Johann Rudolph Wolf (1816–1893).

above the observing site. The use of the earth as a platform from which to record these numbers contributes to their variability, too, because the sun rotates and the evolving spot groups are distributed unevenly across solar longitudes. To compensate for these limitations, each daily international number is computed as a weighted average of measurements made from a network of cooperating observatories.

One way to elucidate a frequency-domain description of the sunspot signal $w(n)$ is to compare it with a sinusoidal signal. For example, we can align sinusoids of varying frequency with $w(n)$, as shown in Figure 1.28b. Thus, the sinusoids are models of an ideal sunspot cycle. This ideal does not match reality perfectly, of course, but by pursuing the mathematical comparison between the trignonometric model and the raw data, we can get a primitive frequency-domain description of the sunspot cycle. What we want to derive in a frequency-domain description of a signal is some kind of quantification of how much a signal resembles model sinusoids of various frequencies. In other words, we seek the relative weighting of supposed frequency components within the signal. Thinking of the signal values as a very long vector, we can compute the inner product of $w(n)$ with the unit vectors whose values are given by sinusoids

$$s(n) = 50 + 50\sin\left(\frac{2\pi n}{12T}\right), \tag{1.62}$$

where T varies from 0.1 year to 16 years. Then we compute the difference $e_T(n) = w(n) - s(n)$, an error term which varies with periodicity of the sinusoid (1.62) determined by T. Now, we take evalutate the norm of the vector $e_T(n)$, which has length $12 \times 296 = 3552 : \|e_T\|$. If we plot the norm of the error vectors with respect to the supposed period T of the sinusoidal model, we see that there is a pronounced minimum near $T = 11$ (Figure 1.29).

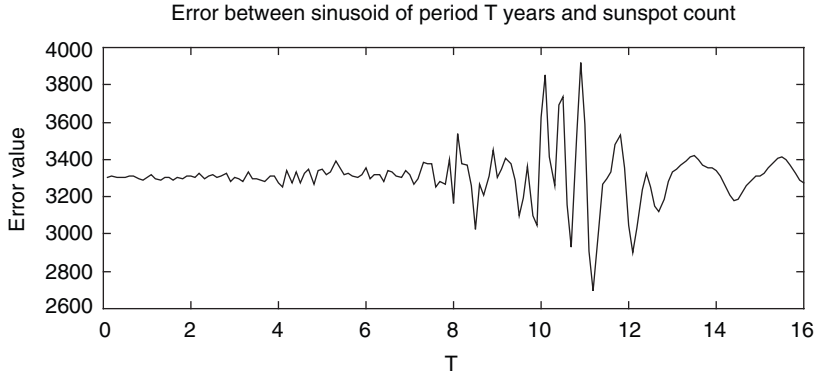

Fig. 1.29. Comparing sinusoids with sunspot numbers. The minimal error between such sinusoids and the sunspot oscillations occurs just above $T = 11$. Note that there are other local minima both below and above $T = 11$. In point of fact, sometimes the sunspot cycle peaks a few months early and sometimes a few months later.

Note that we have exploited a few specific facts about the sunspot numbers in this analysis. In particular, we have not worried about the relative position of the sinusoidal model. That is, we have not taken the relative phases of the sinusoid $s(n)$ and the discrete sunspot signal $w(n)$ into account. Could a slightly shifted sinusoid result in a smaller error term? This is indeed quite a likely possibility, and we avoid it for two reasons. First, it turns the minimization of the error term into a two-dimensional problem. This is a practical, application-oriented discussion. Although we want to explain the technical issues that arise in signal analysis problems, we do not want to stray into two-dimensional problems. Our focus is one-dimensional—signal analysis, not image analysis—problems. In fact, with more powerful tools, such as the discrete Fourier transform (Chapter 7), we we can achieve a frequency domain analysis in one dimension that handles the relative phase problem.

1.5.3.3 Speech. Scientists and engineers have long attempted to build commercial speech recognition products. Such products now exist, but their applicability remains limited. Computers are so fast, mathematics so rich, and the investigations so deep: How can there be a failure to achieve? The answers seem to lie in the fundamental differences between how signal analyzing computers and human minds—or animal minds in general, for that matter—process the acoustical signals they acquire. The biological systems process data in larger chunks with a greater application of top-down, goal-directed information than is presently possible with present signal analysis and artificial intelligence techniques.

An interesting contrast to speech recognition is speech generation. Speech synthesis is in some sense the opposite of recognition, since it begins with a structural description of a signal—an ASCII text string, for instance—and generates speech sounds therefrom. Speech synthesis technology has come very far, and now at the turn of the century it is found in all kinds of commercial systems: telephones, home appliances, toys, personal computer interfaces, and automobiles. This illustrates the fundamental asymmetry between signal synthesis and analysis. Speech recognition systems have become increasingly sophisticated, some capable of handling large vocabularies [57–59]. In recent years, some of the recognition systems have begun to rely on artificial neural networks, which mimic the processing capabilities of biological signal and image understanding systems [60].

To begin to understand this fundamental difference and some of the daunting problems faced by speech recognition researchers, let us consider an example of digitized voice (Figure 1.30). Linguists typically classify speech events according to whether the vocal cords vibrate during the pronunciation of a speech sound, called a *phone* [61]. Phones are speech fragments. They are realizations of the basic, abstract components of a natural language, called *phonemes*. Not all natural languages have the same phonemes. Speakers of one language sometimes have extreme difficulties hearing and saying phonemes of a foreign tongue. And within a given language, some phonemes are more prevalent than others. The most common strategy for speech recognition technology is to break apart a digital speech sample into separate phones and then identify phonemes among

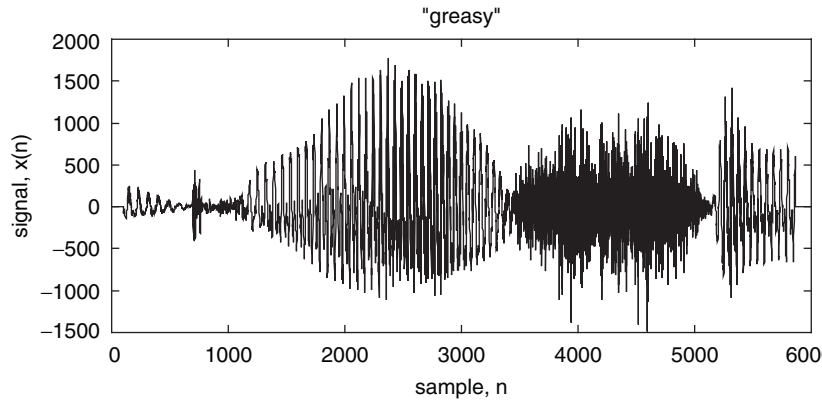

Fig. 1.30. A digitized voice signal, the word "greasy". The sampling rate is 16 kHz. It is difficult, even to the trained eye, to recognize the spoken content of a signal from its time-domain signal values.

them [59, 62]. The speech fragment of Figure 1.30 contains five phonemes. Sometimes the preliminary sequence of phonemes makes no sense; a sophisticated algorithm may merge or further segment some of the phones for a better result. A higher-level process uses the phoneme stream to extract whole words. Perhaps some posited word does not fit the application's context. Still higher-level algorithms—and at this point the application has removed itself from signal processing and analysis proper to the realm of artificial intelligence—may substitute one phoneme for another to improve the interpretation. This is called *contextual analysis*. Although we will consider speech analysis in more detail in later chapters, topics such as contextual analysis blend into artificial intelligence, and are outside the scope of our presentation. It is nevertheless interesting to note that computers are generally better than humans at recognizing individual phonemes, while humans are far superior when recognizing complete words [63], a hint of the power of contextual methods.

Linguists separate phonemes into two categories: *voiced* and *unvoiced*, according to whether the vocal cords vibrate or not, respectively. Vowels are voiced, and it turns out that a frequency-domain description helps to detect the presence of a vowel sound. Vowel sounds typically contain two sinusoidal components, and one important early step in speech processing is to determine the frequency components of the signal. We can see this in a digital speech sample of a vowel (Figure 1.31). There are clearly two trends of oscillatory behavior in the signal.

Thus, depending upon the relative strength of the two components and upon their actual frequency, a frequency domain description can identify this phone as the /u/ phoneme. There are complicating factors of course. The frequency components change with the gender of the speaker. And noise may corrupt the analysis. Nevertheless, a frequency-domain description is an important beginning point in phoneme recognition.

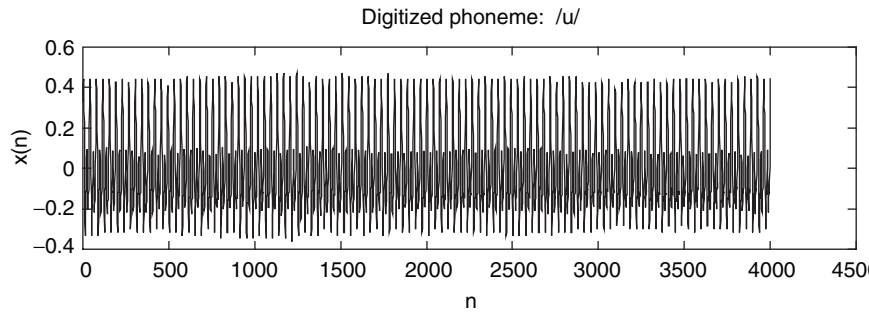

Fig. 1.31. A vowel phoneme, the sound "*u*", sampled at 8 kHz. Note the two sinusoids in the time-domain trace. The lower frequency component has a higher amplitude. Principal frequency components are at approximately 424 Hz and at 212 Hz.

1.5.4 Time and Frequency Combined

Until we develop the formal theory for the frequency analysis of signals—the Fourier transform, in particular—we continue to illustrate signals in terms of their time-domain values. We can nonetheless identify the oscillatory components by inspection. Parts of a given signal resemble a sinusoid of a given frequency. Sometimes the oscillations continue throughout the time span of the signal. For such signals, the Fourier transform (Chapters 5 and 6, and introduced from a practical standpoint in Chapter 4) is the appropriate tool.

Sometimes, however, the oscillatory components die out. This makes the game interesting, because our ordinary sinusoidal models continue oscillating forever. We can arbitrarily limit the time domain extent for our sinusoidal models, and this happens to be effective for applications such as speech analysis. Special mathematical tools exist that can decompose a signal into a form that exposes its frequency components within distinct time intervals. Among these tools is the Gabor transform, one of several time-frequency transforms that we explore in Chapter 10. Until the theoretical groundwork is laid for understanding these transforms, however, we must content ourselves with intuitive methods for describing the frequency content of signals.

Let us also remark that frequency-domain methods have been extensively explored in electrocardiography and electroencephalography—applications we considered at the beginning of the chapter. This seems a natural approach for the ECG, since the heartbeat is a regular pulse. Perhaps surprisingly, for heartbeat irregularities, frequency-domain techniques have been found to be problematic. In EEG work, the detection of certain transients and their development into regular waves is important for diagnosing epilepsy. And here again frequency-domain tools—even those that employ an explicit mixed time-frequency analysis strategy—do not address all of the difficulties [35, 64–66]. Like problems arise in seismic signal interpretation [67, 68]. In fact, problems in working with time-frequency analysis

methods for seismic soundings analysis in petroleum prospecting led to the discovery of the scale-based wavelet transform in the mid-1980s [69].

Researchers have thus begun to investigate methods that employ signal shape and scale as a tool, rather than frequency. Unlike the sinusoidal components that are the basis for a frequency-domain signal description, the components for a scale-based description are limited in their time-domain extent. The next section considers several special signal classes, among them several types which are time-limited. Of these, the finite-energy signals are particularly attractive, as later chapters demonstrate, for signal descriptions based on scale.

1.6 SPECIAL SIGNAL CLASSES

This section covers some special signal classes: finitely supported signals, even and odd signals, absolutely summable signals, finite energy signals, and finite average power signals. The finite-energy signals are by far the most important. This signal class has a particularly elegant structure. The finite energy signals are usually at the center of theoretical signal processing and analysis discussions.

It is from such signal families that the notion of a scale-domain description of a signal arises. A scale-domain description decomposes a signal into parts based on shape over a given length of time. All of the parts contain the same shape, even though the time-domain extent of the shape element varies. In order for a shape element to be so localized, the component signal must eventually die out; it becomes zero, or at least effectively zero. Thus, signals that oscillate forever, as do the sinusoids, do not directly serve a scale-domain analysis. Signals that diminish near infinity, such as Gaussians, Gabor elementary functions, and the like, are used for scale-domain description.

1.6.1 Basic Classes

Useful distinguishing properties of signals are their symmetry and their behavior near infinity.

1.6.1.1 Even and Odd Signals. One of the important characteristics of a signal is its symmetry. Symmetries allow us to simplify the description of a signal; we only need to know about the shape of the signal over some restricted domain. Uncovering symmetries can also be a first step to decomposing a signal into constituent parts. For brevity, this section primarily discusses discrete signals, but for analog signals, similar definitions and properties follow easily.

Definition (Symmetry, Even and Odd Signals). A discrete signal $x(n)$ is *symmetric* about the time instant $n = p$ if $x(p + n) = x(p - n)$ for all $n \in \mathbb{Z}$. And $x(n)$ is *antisymmetric* about the time instant p if $x(p + n) = -x(p - n)$ for all nonzero $n \in \mathbb{Z}$. A discrete signal $x(n)$ is *even* if it is symmetric about $n = 0$. Similarly, if $x(n)$ is antisymmetric about $n = 0$, then x is *odd*.

Corresponding definitions exist for symmetries of analog signals $x(t)$.

Definition (Even and Odd Part of Signals). Let $x(n)$ be a discrete signal. Then the *even part* of $x(n)$ is

$$x_e(n) = \frac{x(n) + x(-n)}{2}. \tag{1.63a}$$

The *odd part* of $x(n)$ is

$$x_o(n) = \frac{x(n) - x(-n)}{2}. \tag{1.63b}$$

There are corresponding definitions for the even and odd parts of analog signals as well.

Proposition (Even/Odd Decomposition). If $x(n)$ is a discrete signal, then

(i) $x_e(n)$ is even;
(ii) $x_o(n)$ is odd;
(iii) $x(n) = x_e(n) + x_o(n)$.

Proof: Exercise. ■

Examples. $\sin(t)$ is odd; $\cos(t)$ is even; and the Gaussian, $g_{\mu,\sigma}(t)$ of mean μ and standard deviation σ (1.14), is symmetric about μ.

Of course, some signals are neither even nor odd. For complex-valued signals, we often look at the real and imaginary components for even and odd symmetries.

1.6.1.2 *Finitely Supported Signals.*

The set of time values over which a signal x is nonzero is called the *support* of x. *Finitely supported* signals are zero outside some finite interval. For analog signals, a related concept is also useful—compact support.

Definition (Finite Support). A discrete signal $x(n)$ is *finitely supported* if there are integers $M < N$ such that $x(n) = 0$ for $n < M$ and $n > N$.

If $x(n)$ is finitely supported, then it can be specified via square brackets notation: $x = [k_M, \ldots, \underline{kd_0}, \ldots, k_N]$, where $x(n) = k_n$ and $M \leq 0 \leq N$.

For analog signals, we define the concept of finite support as we do with discrete signals; that is, $x(t)$ is of *finite support* if it is zero outside some interval $[a, b]$ on the real line. It turns out that our analog theory will need more specialized concepts from the topology of the real number line [44, 70].

Definition (Open and Closed Sets, Open Covering, Compactness). A set $S \subseteq \mathbb{R}$ is *open* if for every $s \in S$, there is an open interval *(a, b)* such that $s \in (a, b) \subseteq S$. A set is *closed* if its complement is open. An *open covering* of a $S \subseteq \mathbb{R}$ is a family of open sets $\{O_n \mid n \in \mathbb{N}\}$ such that $\bigcup_{n=0}^{\infty} O_n \supseteq S$. Finally, a set $S \subseteq \mathbb{R}$ is *compact* if for every open covering of S, $\{O_n \mid n \in \mathbb{N}\}$, there is a finite subset that also contains S:

$$\bigcup_{n=0}^{N} O_n \supseteq S, \tag{1.64}$$

for some $\{n \in \mathbb{N}\}$.

Definition (Compact Support). An analog signal $x(t)$ has *compact support* if $\{t \in \mathbb{R} \mid x(t) \neq 0\}$ is compact.

It is easy to show that a (finite) sum of finitely supported discrete signals is still of finite support; that is, the class of finitely supported signals is closed under addition. We will explore this and other operations on signals, as well as the associated closure properties in Chapters 2 and 3. The following theorem connects the idea of compact support for analog signals to the analogous concept of finite support for discrete signals [44, 70].

Theorem (Heine–Borel). $S \subseteq \mathbb{R}$ is compact if and only if it is closed and contained within some finite interval $[a, b]$ (that is, it is *bounded*).

Proof: The exercises outline the proof. ■

1.6.2 Summable and Integrable Signals

Compact support is a very strong constraint on a signal. This section introduces the classes of absolutely summable (discrete) and absolutely integrable (analog) signals. Their decay is sufficiently fast so that they are often neglible for large time values. Their interesting values are concentrated near the origin, and we can consider them as having localized shape.

Definition (Absolutely Summable Signals). A discrete signal $x(n)$ is *absolutely summable* (or simply *summable*) if the sum of its absolute values is finite:

$$\sum_{n=-\infty}^{\infty} |x(n)| < \infty. \tag{1.65}$$

Another notation for this family of discrete signals is l^1. Finite support implies absolutely summability.

Definition (Absolutely Integrable Signals). A signal $x(t)$ is *absolutely integrable* (or simply *integrable*) if the integral of its absolute value over $\mathbb{R}$ is finite:

$$\int_{-\infty}^{\infty} |x(t)|\ dt < \infty\,. \tag{1.66}$$

Other notations for this analog signal family are L^1 or $L^1[\mathbb{R}]$. Signals that are integrable of an interval $[a, b]$ are in $L^1[a, b]$. They satisfy

$$\int_{a}^{b} |x(t)|\ dt < \infty\,. \tag{1.67}$$

1.6.3 Finite-Energy Signals

The most important signal classes are the discrete and analog finite energy signals.

Definition (Finite–Energy Discrete Signals). A discrete signal $x(n)$ has *finite energy* or is *square-summable* if

$$\sum_{n=-\infty}^{\infty} |x(n)|^2 < \infty\,. \tag{1.68}$$

Another notation for this family of discrete signals is l^2. Note that a discrete signal that is absolutely summable must also be finite energy. We require the square of the absolute value $|x(n)|^2$ in (1.68) to accomodate complex-valued signals.

Definition (Finite-Energy Analog Signals). An analog signal $x(t)$ is *finite-energy* (or *square-integrable*) if

$$\int_{-\infty}^{\infty} |x(t)|^2\ dt < \infty. \tag{1.69}$$

Alternative names for this family are L^2 or $L^2[\mathbb{R}]$. $L^1[a, b]$ signals satisfy

$$\int_{a}^{b} |x(t)|^2\ dt < \infty. \tag{1.70}$$

The term "finite-energy" has a physical meaning. The amount of energy required to generate a real-world signal is proportional to the total squares of its values. In classical electromagnetic theory, for example, a radio wave carries energy that is

proportional to the sum of the squares of its electric and magnetic fields integrated over the empty space through which the fields propagate.

Discrete and analog finite-energy signals are central to the later theoretical development. The next two chapters generalize the concept of a vector space to infinite dimensions. A discrete signal is like a vector that is infinitely long in both positive and negative directions. We need to justify mathematical operations on signals so that we can study the processes that operate upon them in either nature or in engineered systems. The goal is to find classes of signals that allow infinite support, yet possess all of the handy operations that vector space theory gives us: signal sums, scalar multiplication, inner (dot) product, norms, and so forth.

1.6.4 Scale Description

Only recently have we come to understand the advantages of analyzing signals by the size of their time-domain features. Before the mid-1980s, signal descriptions using frequency content predominated. Sometimes the frequency description was localized, but sometimes these methods break down. Other applications naturally invite an analysis in terms of the feature scales. At a coarse scale, only large features of the signal are evident. In a speech recognition application, for example, one does not perform a frequency decomposition or further try to identify phonemes if a coarse-scale inspection of the signal reveals only the presence of low-level background noise. At a finer scale, algorithms separate words. And at even higher resolution, the words may be segmented into phonemes that are finally subjected to recognition efforts. Although a frequency-domain analysis is necessary to identify phonemes, therefore, some kind of scale-domain analysis may be appropriate for the initial decomposition of signal.

Figure 1.32 shows an example from image analysis. One-dimensional analysis is possible by extracting lines from the image. In fact, many image analysis applications approach the early segmentation steps by using one-dimensional methods at a series of coarse scales. The time-consuming, two-dimensional analysis is thus postponed as long as possible.

1.6.5 Scale and Structure

Signal description at many scales is one of the most powerful methods for exposing a signal's structure. Of course, a simple parsing of a signal into time-domain subsets that do and do not contain useful signal represents a structural decomposition. However, when this type of signal breakdown is presented a different scales, then an artificial intelligence algorithm can home in on areas of interest, perform some goal-directed interpretation, and proceed—based upon the coarse scale results—to focus on minute details that were ignored previously. Thus, the structural description of a signal resembles a tree, and this tree, properly constructed, becomes a guide for the interpretation of the signal by high-level algorithms.

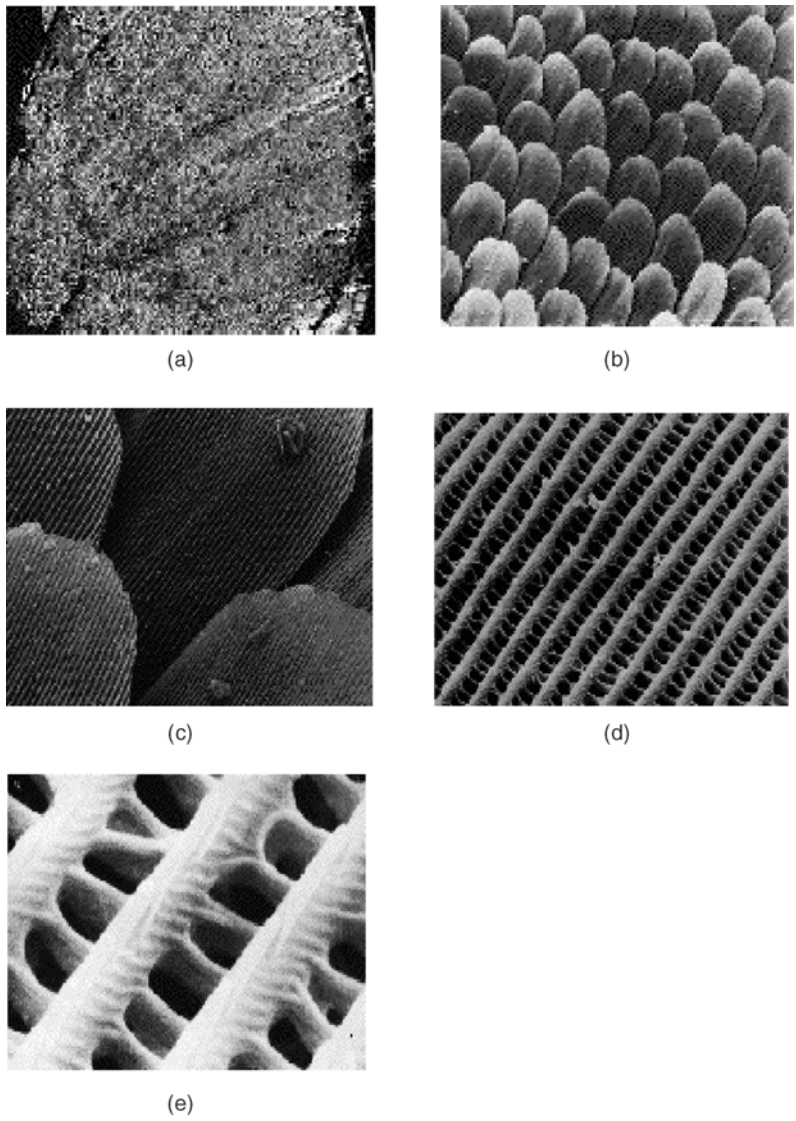

Fig. 1.32. A butterfly and a scanning electron microscope (SEM) teach us the concept of scale. The first image (a), which looks like a butterfly wing is taken at a magnification of 9×. (b) The SEM, at a power of 330×, reveals a scaly pattern. (c) At 1700× the scales appear to possess striations. (d) This confirms the existence of striations at 8500× and hints of small-scale integuments between the principal linear structures. (e) This exposes both the coarse-scale striations and the fine-scale integuments between them at 40,000× magnification.

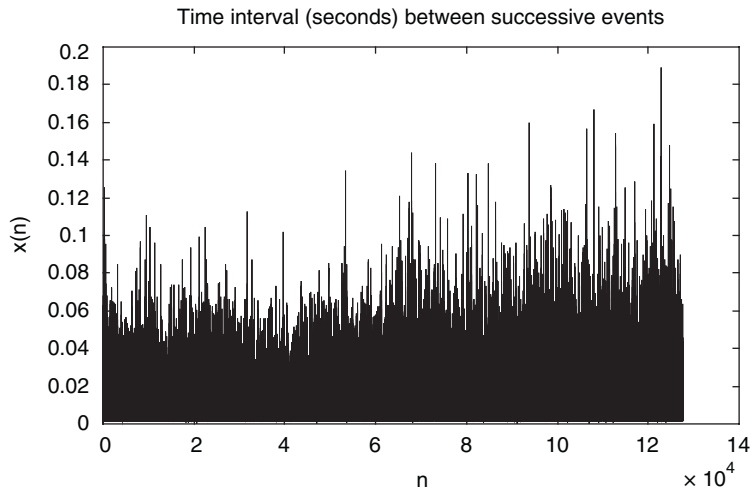

Fig. 1.33. Fractal behavior of an auditory neuron. From a single neuron in the hearing pathways of an anesthesized cat, researchers recorded the time intervals between successive neural discharge events in the presence of a tone stimulus. Note in particular that the independent variable represents not the flow of time or an ordering by distance but rather an enumeration of successive neural discharge events.

Two methods of structural description rely on signal shape models:

(i) Using self-similar shape models over a range of scales
(ii) Using a library of special shapes

Applications using self-similar shape models have begun to draw the attention of researchers in recent years. This approach makes possible a fractal analysis of a signal pattern. A fractal application attempts to understand to what degree the same shape occurs within a signal at different scales.

Sometimes, naturally occurring signals unexpectedly reveal fractal properties (Figure 1.33). This signal monitors neurons in the auditory pathway of an anesthetized cat. The signal's independent variable is not temporally dimensioned. Rather, each signal instant represents the next neural event, and the value of the signal is the time interval between such events. This twist in the conventional way of sketching a signal is key to arriving at the fractal behavior of the neuron.

Representing the signal in this special way provides insight into the nature of the neural process [71]. The discharge pattern reveals fractal properties; its behavior at large scales (in this case, over a span of many discharge events) resembles its behavior over small scales. Recently, signal analysts have brought their latest tools—among them the wavelet transform (Chapter 11), which breaks down a signal according to its frequency content within a telescoping family of scales—to bear on fractal analysis problems [53, 69].

1.7 SIGNALS AND COMPLEX NUMBERS

Complex numbers are useful for two important areas of signal theory:

(i) Computation of timing relationships (phase) between signals;
(ii) Studying the frequency content of signals.

1.7.1 Introduction

To understand why complex numbers are computationally useful, let us consider the superposition of two sinusoidal waves. Earlier, we considered this important case. It occurs in electrical circuits, where two voltages are summed together; in speech recognition, where vowel phonemes, for example, are represented by a sinusoidal sum; and in optics, where two optical wavefronts combine and interfere with one another to produce an interference pattern. Introducing complex numbers into the mathematical description of signal phenomena makes the analysis much more tractable [72].

Let $x(t) = x_1(t) + x_2(t) = A_1\cos(\Omega_1 t + \phi_1) + A_2\cos(\Omega_2 t + \phi_2)$. An awkward geometric argument showed earlier that if $\Omega_1 = \Omega_2 = \Omega$, then $x(t)$ remains sinusoidal. Why should a purely algebraic result demand a proof idea based on rotating parallelograms? Complex numbers make it easier. We let $x_1(t)$ and $x_2(t)$ be the real parts of the complex exponentials: $x_1(t) = \mathrm{Real}[z_1(t)]$ and $x_2(t) = \mathrm{Real}[z_2(t)]$, where

$$z_1(t) = A_1\exp(j[\Omega t + \phi_1]), \tag{1.71a}$$

$$z_2(t) = A_2\exp(j[\Omega t + \phi_2]). \tag{1.71b}$$

Then $x(t) = \mathrm{Real}[z_1(t) + z_2(t)] = \mathrm{Real}[z(t)]$. We calculate

$$\begin{aligned} z(t) &= A_1\exp(j[\Omega t + \phi_1]) + A_2\exp(j[\Omega t + \phi_2]) \\ &= \exp(j\Omega t)[A_1\exp(j\phi_1) + A_2\exp(j\phi_2)] \end{aligned} \tag{1.72}$$

Notice that the sum (1.72) has radial frequency Ω radians per second; the $\exp(j\Omega t)$ term is the only one with a time dependence. To calculate $\|z(t)\|$, note that $\left\|e^{j\Omega t}\right\| = 1$, and so $z(t) = \left\|A_1\exp(j\phi_1) + A_2\exp(j\phi_2)\right\|$. As before, we find

$$\|z(t)\|^2 = A_1^2 + A_2^2 + 2A_1A_2\cos(\phi_2 - \phi_1). \tag{1.73}$$

Thus, complex arithmetic takes care of the phase term for us, and this is one reason why complex arithmetic figures in signal theory. Of course, we understand that only the real part of the complex-valued signal model corresponds to any physical reality.

Now let us consider complex-valued functions, $f: \mathbb{C} \to \mathbb{C}$, and develop the ideas of calculus for them. Such functions may at first glance appear to bear a strong resemblance to signals defined on pairs of real numbers: $f: \mathbb{R} \times \mathbb{R} \to \mathbb{C}$, for example. To pursue the idea for a moment, we can let $z = x + jy$, where $j^2 = -1$. Then, $f(z) = f(x + jy)$, and f is a function of the real pair (x, y). The function f is complex-valued, of course, but we can take its real and imaginary parts: $f(z) = \text{Real}[f(x + jy)] + j\text{Imag}[f(x + jy)]$. Now $f(z)$ looks suspiciously like a sum of two multidimensional signals—a sum of two images—one of which is scaled by the imaginary square root of -1. If we were to define differentiation of $f(z)$ with respect to x and y, where $z = x + jy$, then this would indeed be the case; our theory of complex analysis would look a lot like ordinary real analysis. But when we define differentiation with respect to the complex variable z, what a huge difference it makes! A seemingly innocuous distinction about how to define differentiation makes the calculus of complex variables rich, novel, and powerful.

1.7.2 Analytic Functions

The existence of a derivative is a very special and far-reaching property for a complex function $f(z)$.

Definition (Differentiation, Derivative). Let $S \subseteq \mathbb{C}$ and $f: S \to \mathbb{C}$. Then f is *differentiable* at a point $z \in S$ if the limit,

$$f'(z) = \lim_{w \to z} \frac{f(w) - f(z)}{w - z} \tag{1.74}$$

exists. As in calculus, the limit $f'(z) = \frac{d}{dz} f(z)$ is called the *derivative* of f at z.

Definition (Analyticity). Let $w \in \mathbb{C}$. If there is an $R > 0$ such that $f(z)$ is differentiable for all at all z such that $|w - z| < R$, then f is *analytic* at w. If $f(z)$ is analytic at every $w \in S$, then $f(z)$ is analytic in S.

Proposition (Differentiation). Let f and g be differentiable at $z \in \mathbb{C}$. Then

(i) f is continuous at z.
(ii) If $c \in \mathbb{C}$, then cf is differentiable at z, and $(cf)'(z) = cf'(z)$.
(iii) $f+g$ is differentiable at z, and $(f + g)'(z) = f'(z) + g'(z)$.
(iv) fg is differentiable at z, and $(fg)'(z) = fg'(z) + f'g(z)$.
(v) If $g(z) \neq 0$, then f/g is differentiable at z, and

$$(f/g)'(z) = \frac{g(z)f'(z) - f(z)g'(z)}{g^2(z)}. \tag{1.75}$$

Proof: As in calculus of a real variable [44]; also see complex analysis texts [73– 75]. ■

Proposition (Chain Rule). Let f be differentiable at $z \in \mathbb{C}$ and let g be differentiable at $f(z)$. Then the composition of the two functions, $(g \circ f)(z) = g(f(z))$, is also differentiable, and $(g \circ f)'(z) = g'(f(z))f'(z)$.

Proof: Refer to Refs. [44] and [73–75]. ■

Power series of a complex variable are useful for the study of discrete *systems*, signal processing entities that modify discrete signals. A system takes a signal as an input and produces another signal as an output. A special complex power series, called the *z-transform* of a signal, is studied in Chapters 8 and 9.

Definition (Power and Laurent Series). A *complex power series* is a sum of scaled powers of the complex variable z:

$$\sum_{n=0}^{\infty} a_n z^n, \tag{1.76a}$$

where the a_n are (possibly complex) coefficients. Sometimes we expand a complex power series about a point $w \in \mathbb{C}$:

$$\sum_{n=0}^{\infty} a_n (z-w)^n. \tag{1.76b}$$

A *Laurent series* is two-sided:

$$\sum_{n=-\infty}^{\infty} a_n z^n \tag{1.77a}$$

and can be expanded about $w \in \mathbb{C}$:

$$\sum_{n=-\infty}^{\infty} a_n (z-w)^n. \tag{1.77b}$$

[The z-transform of $x(n)$ is in fact a Laurent expansion on the values of the discrete signal: $x(n) = a_n$ in (1.77a).]

We define special complex functions in terms of power series:

$$\sin(z) = z - \frac{z^3}{3!} + \frac{z^5}{5!} - \frac{z^7}{7!} + \cdots; \tag{1.78a}$$

$$\cos(z) = 1 - \frac{z^2}{2!} + \frac{z^4}{4!} - \frac{z^6}{6!} + \cdots; \tag{1.78b}$$

and the most important function in mathematics,

$$\exp(z) = 1 + z + \frac{z^2}{2!} + \frac{z^3}{3!} + \frac{z^4}{4!} + \cdots = e^z. \tag{1.79}$$

Their convergence criteria are similar to those of real power series. The following theorem says that a convergent power series is differentiable and its derivative may be computed by termwise differentiation.

Proposition (Power Series Differentiation). Suppose that

$$p(z) = \sum_{n=0}^{\infty} a_n (z-w)^n \tag{1.80}$$

converges in $S = \{z : |z-w| < R\}$. Then $p(z)$ is analytic (differentiable at every point) inside S, and

$$p'(z) = \sum_{n=1}^{\infty} n a_n (z-w)^{n-1}. \tag{1.81}$$

Proof: References [44] and [73–75]. ■

The next theorem suggests that complex function calculus is very different from conventional real variable theory [73–75].

Theorem (Cauchy–Riemann Equations). Suppose that $f(z) = u(x, y) + jv(x, y)$, where u and v are the real and imaginary parts, respectively, of $f(z)$. If f is differentiable at $z = w$, then the partial derivative $\partial u/\partial x, \partial u/\partial y, \partial v/\partial x$, and $\partial v/\partial y$ all exist; furthermore,

$$\frac{\partial u}{\partial x}(w) = \frac{\partial v}{\partial y}(w), \tag{1.82a}$$

$$\frac{\partial u}{\partial y}(w) = \frac{\partial v}{\partial x}(w). \tag{1.82b}$$

Proof: We can compute the derivative $f'(w)$ in two different ways. We can approach w along the real axis or along the imaginary axis. Thus, we see that the following limit gives $f'(w)$ when we approach w from values $w + h$, where h is real:

$$\lim_{h \to 0} \frac{f(w+h) - f(w)}{h} = \lim_{h \to 0} \frac{u(x+h, y) - u(x, y)}{h} + j \lim_{h \to 0} \frac{v(x+h, y) - v(x, y)}{h}. \tag{1.83a}$$

But $f'(w)$ can also be computed by taking the limit along the imaginary axis; we now approach w from values $w+jk$, where k is real. Consequently,

$$\lim_{k \to 0} \frac{f(w + jk) - f(w)}{jk} = \lim_{k \to 0} \frac{u(x, y + k) - u(x, y)}{jk} + j \lim_{k \to 0} \frac{v(x, y + k) - v(x, y)}{jk}. \tag{1.83b}$$

The limit (1.83a) is

$$f'(w) = \frac{\partial u}{\partial x}(x, y) + j\left[\frac{\partial v}{\partial x}(x, y)\right], \tag{1.84a}$$

whereas (1.83b) is

$$f'(w) = -j\left[\frac{\partial u}{\partial y}(x, y)\right] + \frac{\partial v}{\partial y}(x, y). \tag{1.84b}$$

Since $f'(w)$ has to be equal to both limits, the only way to reconcile (1.84a) and (1.84b) is to equate their real and imaginary parts, which gives (1.82a)–(1.82b). ■

Remark. The Cauchy–Riemann equations imply that some surprisingly simple complex functions, $f(z) = f(x + jy) = x - jy$, for example, are not differentiable.

The converse to the theorem requires an additional criterion on the partial derivatives, namely that they be continuous.

Theorem (Cauchy–Riemann Converse). Let $f(z) = u(x, y) + jv(x, y)$, where u and v are the real and imaginary parts, respectively, of $f(z)$. Furthermore, let the partial derivatives $\partial u/\partial x$, $\partial u/\partial y$, $\partial v/\partial x$, and $\partial v/\partial y$ all exist and be continuous and satisfy the Cauchy–Riemann equations (1.82a)–(1.82b) at $z = w$. Then $f'(w)$ exists.

Proof: Not too difficult [73–75]. ■

Corollary. Let $f(z) = u(x, y) + jv(x, y)$, where u and v are the real and imaginary parts, respectively, of $f(z)$. If $f'(w)$ and $f''(w)$ exist, then the partial derivatives of u and v obey the Laplace equation:

$$\frac{\partial^2 \phi}{\partial x^2} + \frac{\partial^2 \phi}{\partial y^2} = 0. \tag{1.85}$$

Proof: By the Cauchy–Riemann theorem, u and v satisfy (1.82a)–(1.82b). Applying the theorem again to the deriviatives, and using the fact from calculus that

mixed partial derivatives are equal where they are continuous, we find

$$\frac{\partial}{\partial x}\frac{\partial u}{\partial x}(w) = \frac{\partial}{\partial x}\frac{\partial v}{\partial y}(w) = \frac{\partial}{\partial y}\frac{\partial v}{\partial x}(w) = -\frac{\partial}{\partial y}\frac{\partial u}{\partial y}(w) \tag{1.86a}$$

Similarly,

$$\frac{\partial}{\partial y}\frac{\partial v}{\partial y}(w) = -\frac{\partial}{\partial x}\frac{\partial v}{\partial x}(w). \tag{1.86b}$$

The Laplace equations for both u and v follow. ■

This is an intriguing result. Complex differentiability leads to a second-order partial differential equation. That is, if a function *f(z)* is twice differentiable, then it is harmonic in a set $S \subseteq \mathbb{C}$. Thus, complex differentiation is already seen to be a much more restricted condition on a function than real differentiation. Laplace's equation appears in many applications of physics and mechanics: heat conduction, gravitation, current flow, and fluid flow, to name a few. The import of the corollary is that complex functions are a key tool for understanding such physical systems. For applications to the theory of fluid flow, for example, see Ref. 75.

Even stronger results are provable. The next section outlines the development of complex integration theory. It seems quite backwards to prove theorems about differentiation by means of integration theory; but in the exotic realm of complex analysis, that is exactly the course we follow. Using contour integration in the complex plane, it is possible to prove that an analytic function (differentiable in a region) has continuous derivatives of all orders. That is, every analytic function expands in a Taylor series.

1.7.3 Complex Integration

This section continues our sweep through complex analysis, turning now to integration in the complex plane. Given the results of the previous section, one might imagine that complex integration should also have special properties unlike anything in real analysis. Such readers will not be disappointed; the theory of complex integration is even more amazing than differentiation.

Definition (Contour). A *curve* in the complex plane is a function $s : [a, b] \to \mathbb{C}$, where $[a, b] \subset \mathbb{R}$. We say that *s parameterizes* its range. If the real and imaginary parts of $s(t)$ are continuously differentiable, then s is called an *arc*. If $s(a) = s(b)$, then the curve s is *closed*. And if $s(t_1) = s(t_2)$ on (a, b) implies $t_1 = t_2$, then the curve s is *simple*. A sequence of arcs $\{s_n(t) : [a_n, b_n] \to C : 1 \le n \le N\}$ is a *contour* if $s_n(b_n) = s_{n+1}(a_{n+1})$, for $n = 1, 2, \ldots, N-1$.

Remarks. A curve is a complex-valued analog signal, defined on a closed interval of the real line. An arc is a continuously differentiable, complex-valued analog signal. A simple curve does not intersect itself, save at its endpoints. We often denote

an arc in the complex plane by its range, $C = \{z : z = s(t), \text{ for some } a \le t \le b\}$, and the defining curve function is implicit. Our purpose is to define integration along a contour [76].

Definition (Contour Integral). If the complex function $f(z)$ is continuous in a region containing an arc C, then the contour integral of f over C is defined by

$$\oint_C f(z)\, dz = \int_a^b f[s(t)]s'(t)\, dt\,, \tag{1.87}$$

where $s(t)$ is the function that parameterizes C.

Since $f(z)$, $s(t)$, and $s'(t)$ are all continuous, the integrand in (1.87) is Riemann integrable. The function $f[s(t)]s'(t)$ is complex-valued; we therefore perform the real integration (that is, with respect to t) twice, once for the real part and once for the imaginary part of the integrand. Observe that the change of integration variable, $z = s(t)$ and $dz = s'(t)\, dt$, converts the integral's definition with respect to z in (1.87) to one with respect to t.

The main result of this section is Cauchy's integral theorem. There is an interpretation of contour integration that provides an intuitive link to the familiar theory of integration from calculus and an informal argument for the theorem [77]. Readers seeking rigor and details will find them in the standard texts [73–76]. We first consider the case where C is a circle around the origin, which is a simple, closed arc. Then we shall argue the extension to general arcs, by supposing the arcs to be the limit of a local tiling of the region by adjacent triangles. From this, the extension to contours, which are a sequence of arcs, follows directly.

Theorem (Cauchy Integral for a Circle). Suppose $f(z)$ is analytic in a region containing the closed circle C, with radius R and center $z = (0, 0)$. Then,

$$\frac{1}{2\pi j}\oint_C z^m dz = \begin{cases} 0 & \text{if } m \neq 1, \\ 1 & \text{if } m = -1. \end{cases} \tag{1.88}$$

Proof: In calculus courses [44], Riemann integrals are the limits of Riemann sums. For the case of a contour integral, such a sum is a limit:

$$\oint_C f(z)dz = \lim_{N\to\infty} \sum_{n=1}^{N} f(w_n)[z_{n+1} - z_n]\,. \tag{1.89}$$

where $s : [a, b] \to \mathbb{C}$ parameterizes the arc C; $a = t_1 < t_2 < \cdots < t_N < t_{N+1} = b$ partitions $[a, b]$; $z_n = s(t_n)$; and $w_n = s(t)$ for some $t \in [t_n, t_{n+1}]$. Suppose further that we select the t_n so that $|z_{n+1} - z_n| = \varepsilon_N = \text{Length}(C)/N = L_C/N$. Then we have

$$\oint_C f(z)dz = \lim_{N\to\infty} \sum_{n=1}^{N} f(w_n)\frac{[z_{n+1}-z_n]}{|z_{n+1}-z_n|}|z_{n+1}-z_n|$$
$$= \lim_{N\to\infty} \varepsilon_N \sum_{n=1}^{N} f(w_n)\frac{[z_{n+1}-z_n]}{|z_{n+1}-z_n|} = L_C \lim_{N\to\infty} \frac{1}{N} \sum_{n=1}^{N} f(w_n)\frac{[z_{n+1}-z_n]}{|z_{n+1}-z_n|}. \tag{1.90}$$

Note that as $N \to \infty$, we have $w_n \to z_n$, and $(z_{n+1}-z_n)/|z_{n+1}-z_n|$ approaches a complex value whose real and imaginary parts are the components of the unit tangent vector to C at z_n, $\boldsymbol{T}(z_n)$. Since C has radius R, $\boldsymbol{T}(z_n) = jz/R$ and $L_C = 2\pi R$. Therefore, the final sum in (1.90) approaches $L_C \times \{\text{average over } C \text{ of } f(z)\boldsymbol{T}(z)\}$. We conclude

$$\frac{1}{L_C}\oint_C f(z)\, dz = \text{Avg}_{z\in C}[f(z)\boldsymbol{T}(z)]. \tag{1.91}$$

Now suppose $m = -1$, so that $f(z) = z^{-1}$. Then

$$\frac{1}{2\pi R}\oint_C f(z)\, dz = \text{Avg}_{z\in C}\left[\frac{\boldsymbol{T}(z)}{z}\right] = \text{Avg}_{z\in C}\left[\frac{jz}{Rz}\right] = \text{Avg}_{z\in C}\left[\frac{j}{R}\right] = \frac{j}{R}. \tag{1.92}$$

To show the other possibility in (1.88), we let $m \neq -1$ and find

$$\frac{1}{2\pi R}\oint_C f(z)\, dz = \text{Avg}_{z\in C}\left[\frac{jz^{m+1}}{R}\right] = \frac{j}{R}\text{Avg}_{z\in C}[z^{m+1}]. \tag{1.93}$$

But, the average of all values z^{m+1} over the circle $|z| = R$ is zero, which demonstrates the second possibility of (1.88) and concludes the proof. ■

Note that the informal limit (1.89) is very like the standard calculus formulation of the Riemann integral. The definition of the contour integral is thus a plausible generalization to complex-valued functions.

We will apply this result in Chapter 8 to derive one form of the inverse z-transform. This produces discrete signal values $x(n)$ from the complex function $X(z)$ according to the rule:

$$x(n) = \frac{1}{2\pi j}\oint_C X(z)z^{n-1}dz. \tag{1.94}$$

The Cauchy residue theorem leads to the following concepts.

Definition (Poles and Zeros). A complex function $f(z)$ has a *pole* of order k at $z = p$ if there is a $g(z)$ such that $f(z) = g(z)/(z-p)^k$, $g(z)$ is analytic in an open set containing $z = p$, and $g(p) \neq 0$. We say that $f(z)$ has a *zero* of order k at $z = p$ if there is a $g(z)$ such that $f(z) = g(z)(z-p)^k$, $g(z)$ is analytic in a region about $z = p$, and $g(p) \neq 0$.

Definition (Residue). The *residue* of $f(z)$ at the pole $z = p$ is given by

$$\text{Res}(f(z), p) = \begin{cases} \left[\dfrac{1}{(k-1)!} f^{(k-1)}(p)\right] & \text{if } p \in \text{Interior}(C), \\ 0 & \text{if otherwise,} \end{cases} \tag{1.95}$$

where k is the order of the pole.

Theorem (Cauchy Residue). Assume that $f(z)$ is a complex function, which is analytic on and within a curve C; $a \notin C$; and $f(z)$ is finite (has no pole) at $z = a$. Then

$$\frac{1}{2\pi j}\oint_C \frac{f(z)}{(z-a)^{m-1}}\, dz = \begin{cases} \left[\dfrac{1}{(m-1)!} f^{(m-1)}(a)\right] & \text{if } a \in \text{Interior}(C), \\ 0 & \text{if otherwise.} \end{cases} \tag{1.96}$$

More generally, we state the following theorem.

Theorem (Cauchy Residue, General Case). Assume that C is a simple, closed curve; $a_m \notin C$ for $1 \le m \le M$; and $f(z)$ is analytic on and within C, except for poles at each of the a_m. Then

$$\frac{1}{2\pi j}\oint_C f(z)\, dz = \sum_{m=1}^{M} \text{Res}(f(z), a_m), \tag{1.97}$$

Proof: References 73–76. ■

1.8 RANDOM SIGNALS AND NOISE

Up until now, we have assumed a close link between mathematical formulas or explicit rules and our signal values. Naturally occurring signals are inevitably corrupted by some random noise, and we have yet to capture this aspect of signal processing in our mathematical models. To incorporate randomness and make the models more realistic, we need more theory.

We therefore distinguish between *random* signals and *deterministic* signals. Deterministic signals are those whose values are completely specified in terms of their independent variable; their exact time domain description is possible. The signal may be discrete or continuous in nature, but as long as there is a rule or formula that relates an independent variable value to a corresponding signal value, then the signal is deterministic. In contrast, a random signal is one whose values are not known in terms of the value of its independent variable. It is best to think of time-dependent signals to understand this. For a random signal, we cannot know the value of the signal in advance; however, once we measure the signal at a particular

time instant, only then do we know its value. Deterministic signals are good for carrying information, because we can reliably insert and extract the information we need to move in a reliable fashion. Nature is not kind, however, to our designs. A random component—for example, a measurement error, digitization error, or thermal noise—corrupts the deterministic signal and makes recovery of the signal information more difficult.

This situation often confronts electrical communication engineers. There are many sources of noise on telephone circuits, for example. If the circuits are physically close, electromagnetic coupling between them occurs. Faint, but altogether annoying, voices will interfere with a conversation. One might argue that this is really a deterministic interference: someone else is deliberately talking, and indeed, if the coupling is strong enough, the other coversation can be understood. However, it is in general impossible to predict when this will occur, if at all, and telephony engineers allow for its possibility by considering models of random signal interference within their designs. Thermal noise from the random motion of electrons in conductors is truly random. It is generally negligible. But it becomes significant when the information-bearing signals are quite weak, such as at the receiving end of a long line or wireless link.

An important signal analysis problem arises in communication system design. In a conversation, a person speaks about 35% of the time. Even allowing that there are two persons talking and that both may speak at once, there is still time available on their communication channel when nobody speaks. If circuitry or algorithms can detect such episodes, the channel can be reused by quickly switching in another conversation. The key idea is to distinguish voice signals from the channel's background noise. There is one quirk: When the conversation is broken, the telephone line sounds dead; one listener or the other invariably asks, "Are you still there?" In order to not distress subscribers when the equipment seizes their channel in this manner, telephone companies actually synthesize noise for both ends of the conversation; it sounds like the connection still exists when, in fact, it has been momentarily broken for reuse by a third party. This is called *comfort noise* generation. A further problem in digital telephony is to estimate the background noise level on a voice circuit so that the equipment can synthesize equivalent noise at just the right time.

Now let us provide some foundation for using random signals in our development. Our treatment is quite compact; we assume the reader is at least partly familiar with the material. Readers can gain a deeper appreciation for discrete and continuous probability space theory from standard introductory texts [78–81]. Random signal theory is covered by general signal processing texts [13, 14] and by books that specialize in the treatment of random signals [82, 83].

1.8.1 Probability Theory

This section introduces the basic principles and underlying definitions of probability theory, material that should already be familiar to most readers.

Consider the noise in the 12-lead electrocardiogram signal. Close inspection of its trace shows small magnitude jaggedness, roughness of texture, and spiky artifacts. Variations in the patient's physical condition and skin chemistry, imperfections in the sensors, and flaws in the electronic signal conditioning equipment impose an element of randomness and unknowability on the ECG's value at any time. We cannot know the exact voltage across one of the ECG leads in advance of the measurement. Hence, at any time t, the voltage across a chosen ECG lead $v(t)$ is a *random variable*. All of the possible activities of ECG signal acquisition constitute the *sample space*. An *event* is a subset of the the sample space. For instance, recording the ECG signal at a moment in time is an event. We assign numerical likelihoods or probabilities to the ECG signal acquisition events.

1.8.1.1 Basic Concepts and Definitions. In order that probability and random signal theory work correctly, the events must obey certain rules for separating and combining them.

Definition (Algebra and σ-Algebra). An *algebra* over a set Ω is a collection of subsets of Ω, $\Sigma \subseteq \wp(\Sigma) = \{A : A \subseteq \Omega\}$, with the following properties:

(i) The empty set is in Σ: $\varnothing \in \Sigma$.
(ii) If $A \in \Sigma$, then the complement of A is in Σ: $A' \in \Sigma$.
(iii) If $A, B \in \Sigma$, then $A \cup B \in \Sigma$.

A σ-*algebra* over a set Ω is an algebra Σ with a further property:

(iv) If $A_n \in \Sigma$ for all $n \in \mathbb{N}$, then their union is in Σ:

$$\bigcup_{n=0}^{\infty} A_n \in \Sigma. \tag{1.98}$$

It is easy to verify that in an algebra Σ, $\Omega \in \Sigma$, the union of any finite set of its elements is still in Σ, and Σ is closed under finite intersections. A σ-algebra is also closed under the intersection of infinite families of elements as in (1.98).

The probability measure must have certain mathematical properties.

Definition (Probability Measure). A *probability measure* on a σ-algebra Σ over Ω is a function $P: \Sigma \to [0, 1]$ such that

(i) $P(\Omega) = 1$;
(ii) P sums on disjoints unions; that is, if $\{A_n : n \in I\} \subseteq \Sigma$, where $I \subseteq \mathbb{N}$, and $A_n \cap A_m = \varnothing$, when $n \neq m$, then

$$P(\bigcup_{n \in I} A_n) = \sum_{n \in I} P(A_n). \tag{1.99}$$

Definition (Probability Space). A *probability space* is an ordered triple (Ω, Σ, P), where Ω is a set of experimental outcomes, called the *sample space*; Σ is a σ-algebra over Ω, the elements of which are called *events*; and P is a probability measure on Σ. The event $\varnothing$ is called the *impossible* event, and the event Ω is called the *certain* event.

Alternative approaches to probability exist. The earliest theories are drawn from the experiments of early gambler-mathematicians, such as Cardano and Pascal.[17] Their dice and card games, run through many cycles—sometimes to the point of financial ruin of the investigator—inspired an alternative definition of probability. It is the value given by the limiting ratio of the number of times the event occurs divided by the number of times the experiment has been tried:

$$P(X) = \lim_{n \to \infty} \frac{O_{X,n}}{n}, \tag{1.100}$$

where $O_{X,n}$ is the number of observations through n trials where X occurred. This intuition serves as a foundation for probability. The exercises supply some flavor of the theoretical development. More widely accepted, however, is the axiomatic approach we follow here. Soviet mathematicians—notably Kolmogorov[18]—pioneered this approach in the 1930s. Through William Feller's classic treatise [79] the axiomatic development became popular outside the Soviet Union. Most readers are probably familiar with this material; those who require a complete treatment will find [78–81] helpful.

1.8.1.2 Conditional Probability.

Conditional probability describes experiments where the probability of one event is linked to the occurrence of another.

Definition (Conditional Probability, Independence). Suppose A and B are two events. The probability that A will occur, given that B has occurred, is defined as

$$P(A \mid B) = P\frac{(A \cap B)}{P(B)}. \tag{1.101}$$

The quotient $P(A|B)$ is called the *conditional probability* of event A given B.

[17]Girolamo Cardano (1501–1576) led a scandalous life as a gambler, but learned enough to found the theory of probability decades before Fermat and Pascal. Blaise Pascal (1623–1662) was a French mathematician and philosopher. See O. Ore, *Cardano, The Gambling Scholar*, New York: Dover, 1953; also, O. Ore, Pascal and the invention of probability theory, *American Mathematical Monthly*, vol. 67, pp. 409–419, 1960.

[18]Andrei Nikolaevich Kolmogorov (1903–1987) became professor of mathematics at Moscow University in 1931. His foundational treatise on probability theory appeared in 1933.

B must occur with nonzero probability for the conditional probability $P(A|B)$ to be defined.

Definition (Independent Events). Suppose A and B are two events. If $P(A|B) = P(A)P(B)$, then A and B are said to be *independent* events.

Proposition. If A and B are independent, then

(i) A and $\sim B$ are independent;
(ii) $\sim A$ and $\sim B$ are independent.

Proof: Exercise. ■

Proposition (Total Probability). Suppose $\{B_n: 1 \le n \le N\}$ is a partition of Ω and $P(B_n) > 0$ for all n. Then for any A,

$$P(A) = \sum_{n=1}^{N} P(B_n)P(A \mid B_n). \tag{1.102}$$

Proof: $A = (A \cap B_1) \cup (A \cap B_2) \cup \ldots \cup (A \cap B_N)$, which is a disjoint union. The definition of conditional probability entails

$$P(A) = \sum_{n=1}^{N} P(A \cap B_n) = \sum_{n=1}^{N} P(B_n)P(A \mid B_n). \tag{1.103}$$

■

1.8.1.3 Bayes's Theorem. An important consequence of the total probability property, known as Bayes's[19] theorem, is central to a popular pattern classification scheme (Chapter 4).

Theorem (Bayes's). Suppose $\{C_n: 1 \le n \le N\}$ is a partition of Ω and $P(C_n) > 0$ for all n. If $P(A) > 0$ and $1 \le k \le N$

$$P(C_k \mid \mathrm{A}) = \frac{P(C_k)P(A \mid C_k)}{\sum_{n=1}^{N} P(C_n)P(A \mid C_n)}. \tag{1.104}$$

[19]A friend of Thomas Bayes (1703–1761) published the Nonconformist minister's theorem in a 1764 paper before the Royal Society of London.

Proof: The definition of conditional probability implies

$$P(C_k \mid \mathrm{A}) = \frac{P(A \cap C_k)}{P(A)} = \frac{P(C_k)P(A \mid C_k)}{P(A)} = \frac{P(C_k)P(A \mid C_k)}{\sum_{n=1}^{N} P(C_n)P(A \mid C_n)}. \quad (1.105)$$

■

Example (Phoneme Classification). Consider the application of Bayes's theorem to a phoneme classification system. Phonemes fall into a fixed number of classes, C_1, C_2, …, C_N, given by the application domain. There are also a set of signal features that the application computes for each candidate phoneme. Let us suppose that there are M features, A_1, A_2, …, A_M, and the application design is so well done that, for any phoneme-bearing signal, it is possible to both reliably distinguish the phonemes from one another and to assign one of the classes A_m as the principal feature of the signal. A typical feature might be a set of sinusoidal frequencies (formants) that dominate the energy contained in the signal. In any case, we are interested in the phoneme class C_n to which a given input signal belongs. Suppose that the dominant feature is $A = A_m$. We calculate each of the probabilities: $P(C_1|A)$, $P(C_2|A)$, …, $P(C_N|A)$. The highest of these probabilities is the answer—the *Bayes classification*.

How can we calculate these N probabilities? Evidently, we must know $P(C_n)$ for each n. But any of the features might be the dominant one within a signal. Therefore, we must know $P(A_m|C_n)$ for each m and n. And, finally, we must know $P(A_m)$ for each m. A working Bayes classifier requires many probabilities to be known in advance. It is possible to develop these statistics, however, a step called the classifier *training phase*. We gather a large, representative body of speech for the application. If we classify the phonemes manually, in an offline effort, then the relative frequencies of each phoneme can be used in the real-time application. This gives us $P(C_n)$, $1 \le n \le N$. Once we identify a phoneme's class, then we find its predominant feature. For each phoneme C_n, we calculate the number of times that feature A_m turns out to be its predominant feature, which approximates $P(A_m|C_n)$. Lastly, we compute the number of times that each feature is dominant and thus estimate $P(A_m)$. Now all of the numbers are available from the training phase to support the execution of the phoneme classifier on actual data. The more sample phonemes we process and the more genuinely the training data reflects the actual application sources, the better should be our probability estimates.

It is unfortunately often the case that one cannot discover any predominant feature from a set of signal data. What we usually encounter is a feature vector $\boldsymbol{a} = (a_1, a_2, ..., a_M)$, where the a_m represent numerical values or scores indicating the presence of each feature A_m. We can compute the probability of a vector of features, but that can only be done after a little more development.

1.8.2 Random Variables

A *random variable* is a function that maps events to numerical values.

Definition (Random Variable). Suppose that (Ω, Σ, P) is a probability space. A *random variable* x on Ω is a function $\boldsymbol{x} : \Omega \to \mathbb{R}$, such that for all $r \in \mathbb{R}$, $\{\omega \in \mathbb{R}: \boldsymbol{x}(\omega) \le r\} \in \Sigma$.

Notation. $\boldsymbol{x} \le r$ or $\{\boldsymbol{x} \le r\}$ is standard for the event $\{\omega \in \mathbb{R}: \boldsymbol{x}(\omega) \le r\} \in \Sigma$. Similarly, we write $\boldsymbol{x} > r$, $\boldsymbol{x} = r$, $r < \boldsymbol{x} \le s$, and so on. Using the properties of a σ-algebra, we can show these too are events in S. It is also possible to consider complex-valued random variables, $\boldsymbol{z} : \Omega \to \mathbb{C}$.

Definition (Distribution Function). Suppose that (Ω, Σ, P) is a probability space and $\boldsymbol{x}$ is a random variable $\boldsymbol{x} : \Omega \to \mathbb{R}$. Then the *probability distribution function*, or simply the *distribution function*, for $\mathbf{x}$ is defined by $F_{\boldsymbol{x}}(r) = P(\boldsymbol{x} \le r)$.

Since there is no ordering relation on the complex numbers, there is no distribution function for a complex-valued random variable. However, we can consider distribution functions of the real and imaginary part combined; this topic is explored later via the concept of multivariate distributions.

Proposition (Distribution Function Properties). Let $\boldsymbol{x} : \Omega \to \mathbb{R}$ be a random variable in the probability space (Ω, Σ, P), and let $F_{\boldsymbol{x}}(r)$ be its distribution function. Then the following properties hold:

(i) If $r < s$, then $F_{\boldsymbol{x}}(r) \le F_{\boldsymbol{x}}(s)$.
(ii) $\lim_{r \to \infty} F_{\boldsymbol{x}}(r) = 1$ and $\lim_{x \to \infty} F_{\boldsymbol{x}}(r) = 0$.
(iii) $P(\boldsymbol{x} > r) = 1 - F_x(r)$.
(iv) $P(r < \boldsymbol{x} \le s) = F_x(s) - F_x(r)$.
(v) $P(\boldsymbol{x} = r) = F_x(r) - \lim_{s > 0,\, s \to 0} F_x(r - s)$.
(vi) $P(r \le \boldsymbol{x} \le s) = F_x(s) - \lim_{t > 0,\, t \to 0} F_x(r - t)$.
(vii) If $F_x(r)$ is a continuous function of r, then $P(\boldsymbol{x} = r) = 0$ for all r.

Proof: Exercise [81]. ■

The proposition's first statement (i) is a *monotonicity* property.

The distribution function of a random variable may be computed by experiment or may be assumed to obey a given mathematical rule. Special mathematical properties are often assumed for the distribution function; this facilitates mathematical investigations into the behavior of the random variable. One common assumption is that the distribution function is differentiable. This motivates the next definition.

Definition (Density Function). Suppose that (Ω, Σ, P) is a probability space and $\boldsymbol{x}$ is a random variable on Ω. If $F_x(r)$ is differentiable, then the derivative with respect to r of $F_x(r)$, denoted with a lowercase letter f,

$$f_{\boldsymbol{x}}(r) = \frac{d}{dr} F_{\boldsymbol{x}}(r), \tag{1.106}$$

is called the *probability density* function or simply the *density* function of x.

Only functions with specific properties can be density functions. The exercises explore some specific cases.

Proposition (Density Function Properties). Let $\boldsymbol{x} : \Omega \to \mathbb{R}$ be a random variable in the probability space (Ω, Σ, P) with distribution function $F_{\boldsymbol{x}}(r)$. Then

(i) $0 \leq f_{\boldsymbol{x}}(r)$ for all $r \in \mathbb{R}$.

(ii)

$$\int_{-\infty}^{\infty} f_x(t)\, dt = 1. \tag{1.107}$$

(iii)

$$F_{\boldsymbol{x}}(r) = \int_{-\infty}^{r} f_x(t)\, dt. \tag{1.108}$$

(iv)

$$P(r < x \leq s) = F_x(s) - F_x(r) = \int_{s}^{r} f_x(t)\, dt. \tag{1.109}$$

Proof: Property (i) follows from the monotonicity property of the distribution function. Property (iv) follows from the fundamental theorem of calculus [44], where we let the lower limit of the integral pass to infinity in the limit. Properties (ii) and (ii) derive from (iv) via the distribution function limit properties. ■

In the proposition, (i) and (ii) are the conditions that a general function $f : \mathbb{R} \to \mathbb{R}$ must satisfy in order to be a density function. One may also prove an existence theorem that constructs a random variable from such a density function [81]. Random variables divide into two classes: discrete and continuous, based on the continuity of the distribution function. (There is also a *mixed distribution* that has aspects of both, but it is outside our scope.)

1.8.2.1 Discrete Random Variables. Discrete random variables prevail within discrete signal theory.

Definition (Discrete Random Variable). The random variable $\boldsymbol{x}$ is *discrete* if its distribution function is a step function.

In this case, there is a set $M = \{r_n : n \in \mathbb{Z}\}$, such that $m < n$ implies $r_m < r_n$, the set of half-open intervals $[r_m, r_n)$ partition $\mathbb{R}$, and $F_{\boldsymbol{x}}(r)$ is constant on each $[r_m, r_n)$.

Proposition (Discrete Random Variable Characterization). Let $\boldsymbol{x}$ be a random variable in the probability space (Ω, Σ, P) with distribution function $F_{\boldsymbol{x}}(r)$. Set $M = \{r \in \mathbb{R} : \mathrm{P}(\mathrm{x} = \mathrm{r}) > 0\}$. Then, $\boldsymbol{x}$ is discrete if and only if

$$\sum_{r \in M} P_x(\mathrm{x} = \mathrm{r}) = 1 . \tag{1.110}$$

Proof: By the definition, we see that $P(\boldsymbol{x} \le r_n) = P(\boldsymbol{x} < r_{n+1})$. This occurs if and only if $P(r_n \le \boldsymbol{x} \le r_{n+1}) = P(\boldsymbol{x} = r_n)$. Therefore the sum (1.110) is

$$\sum_{r \in M} P_x(\mathrm{x} = \mathrm{r}) = \lim_{r \to \infty} F_{\boldsymbol{x}}(r) + \lim_{r \to -\infty} F_{\boldsymbol{x}}(r) = 1 \tag{1.111}$$

by the distribution function properties. ■

If the random variable $\boldsymbol{x}$ is discrete, then the $F_{\boldsymbol{x}}(r)$ step heights approach zero as $r \to -\infty$ and approach unity as $r \to \infty$. Because a step function is not differentiable, we cannot define a density function for a discrete random variable as in the previous section. However, we can separately define the density function for a discrete random variable as discrete impulses corresponding to the transition points between steps.

Definition (Discrete Density Function). Suppose the random variable $\boldsymbol{x}$ is discrete, and its distribution function $F_x(r)$ is constant on half-open intervals $[r_n, r_m)$ that partition R. Its density function $f_x(r)$ is defined:

$$f_x(r) = \begin{cases} F_x(r_{n+1}) - F_x(r_n) & \text{if } r = r_n, \\ 0 & \text{if otherwise.} \end{cases} \tag{1.112}$$

Example (Dice). Consider an experiment where two fair dice are thrown, such as at a Las Vegas craps table. Each die shows one to six dots. The probability of any roll on one die is, given honest dice, 1/6. The throw's total is the sum, a random variable $\boldsymbol{x}$. The values of $\boldsymbol{x}$ can be 2, 12, or any natural number in between. There are 36 possible rolls, and the probability of the event that either 2 or 12 is rolled is 1/36. Lucky seven is the most common event—with probability 6/36—as it occurs through the following tosses: (1, 6), (2, 5), (3, 4), (4, 3), (5, 2), or (6, 1). Figure 1.34 shows the distribution function and the density functions for the dice toss.

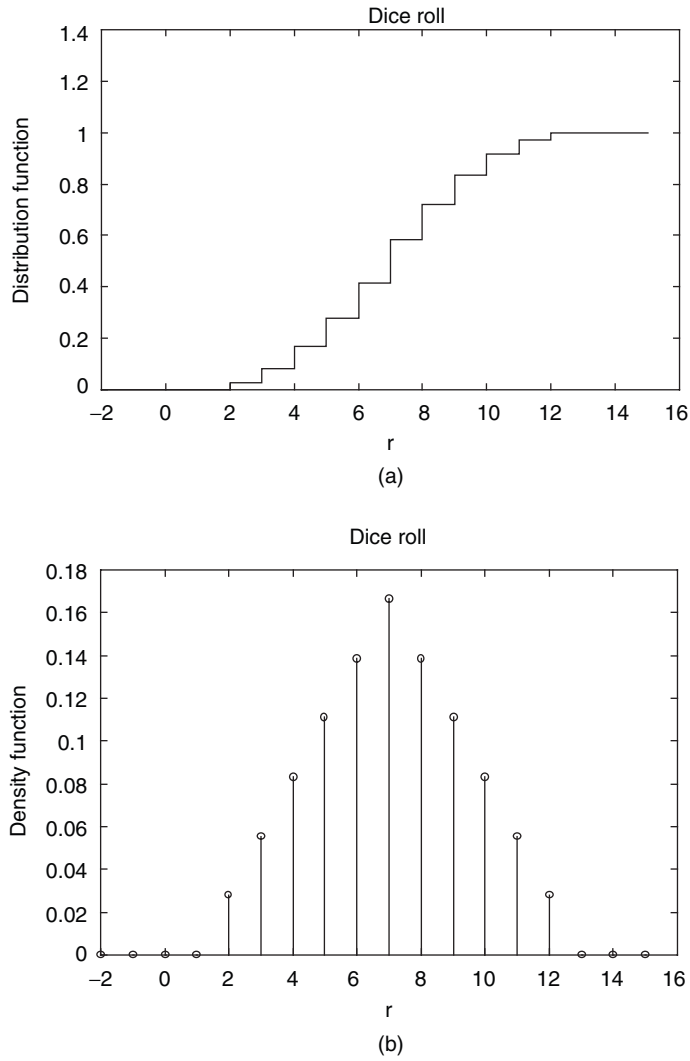

Fig. 1.34. Distribution (a) and density functions (b) for tossing a pair of dice.

Discrete signal theory commonly assumes a density or distribution function for a random variable. If the density or distribution is unknown, it can be measured, of course, but that is sometimes impractical. Instead, one typically approximates it by a distribution that has tractable mathematical properties.

Definition (Binomial Distribution). Suppose that the discrete random variable x has $\text{Range}(\boldsymbol{x}) \subseteq \{0, 1, 2, \ldots, n\}$. Then $\boldsymbol{x}$ has a *binomial distribution* of order n if

there are non-negative values p and q, such that $p + q = 1$, and

$$P(\boldsymbol{x} = k) = \binom{n}{k} p^k q^{n-k}. \tag{1.113}$$

Definition (Poisson[20] Distribution). Suppose the discrete random variable $\boldsymbol{x}$ has $\text{Range}(\boldsymbol{x}) \subseteq \{0, 1, 2, \ldots, n\}$ and $a > 0$. Then $\boldsymbol{x}$ has a *Poisson distribution* with parameter a if

$$P(\boldsymbol{x} = k) = \frac{a^k}{k!} e^{-a}. \tag{1.114}$$

We cannot know the value that a random variable will assume on an event before the event occurs. However, we may know enough about the trend of the random variable to be able to specify its average value over time and how well grouped about its average the random values tend to be. There are a variety of parameters associated with a random variable; these we calculate from its distribution or density functions. The most important of these are the mean and standard deviation.

Definition (Discrete Mean). If the random variable $\boldsymbol{x}$ is discrete and $M = \{r \in \mathbb{R}: P(\boldsymbol{x} = r) > 0\}$, then the *mean* or *expectation* of $\boldsymbol{x}$, written $E[x]$, is

$$E(x) = \sum_{r \in M} rP(\boldsymbol{x} = r). \tag{1.115}$$

Definition (Discrete Variance, Standard Deviation). Let the random variable $\boldsymbol{x}$ be discrete, $M = \{r \in \mathbb{R}: P(\boldsymbol{x} = r) > 0\}$, and $\mu = E[\boldsymbol{x}]$. Then the *variance* of $\boldsymbol{x}$, σ_x^2, is

$$\sigma_x^2 = \sum_{r \in M} (r - \mu)^2 P(\boldsymbol{x} = r). \tag{1.116}$$

The *standard deviation* of $\boldsymbol{x}$ is the square root of the variance: σ_x.

1.8.2.2 Continuous Random Variables. The distribution function may have no steps.

Definition (Continuous Random Variable). The random variable $\boldsymbol{x}$ is *continuous* if its distribution function $F_{\boldsymbol{x}}(r)$ is continuous.

Proposition (Continuous Random Variable Characterization). Let x be a continuous random variable in the probability space (Ω, Σ, P) with distribution function $F_{\boldsymbol{x}}(r)$. Then, $P(\boldsymbol{x} = r) = 0$ for all $r \in \mathbb{R}$.

[20]This distribution was first described in 1837 by French mathematician Siméon-Denis Poisson (1781–1840).

Proof: By continuity $F_x(r) = \lim_{s>0,\, s\to 0} F_x(r-s)$. But the distribution function properties entail that $P(\boldsymbol{x} = r) = F_x(r) - \lim_{s>0,\, s\to 0} F_x(r-s)$. So, $P(\boldsymbol{x} = r) = 0$.

■

Assuming a particular form of the density function and then integrating it to get a distribution is common in analytical work. The only restrictions are that the density function must be non-negative and that its integral over the entire real line be unity. This implies that density functions for continuous random variables are in fact absolutely integrable. There are many distribution functions useful for analog signal theory, but the normal or Gaussian distribution is of paramount importance.

Definition (Normal Distribution). The random variable x is *normally* or *Gaussian* distributed if its probability density function is of the form

$$f_x(r) = \frac{1}{\sigma\sqrt{2\pi}} \exp\left(-\frac{(r-\mu)^2}{2\sigma^2}\right). \tag{1.117}$$

where μ and σ are the mean and standard deviation of the Gaussian (1.117), respectively.

Definition (Exponential Distribution). The random variable $\boldsymbol{x}$ has an *exponential distribution* with parameter $a > 0$ if its density function is of the form

$$f_x(r) = \begin{cases} a\exp(-ar) & \text{if } r > 0, \\ 0 & \text{if } r \le 0. \end{cases} \tag{1.118}$$

Definition (Gamma Distribution). The random variable x has a *gamma distribution* with *scale* parameter $a > 0$ and *shape* parameter $b > 0$ if its density function is of the form

$$f_x(r) = \begin{cases} \dfrac{a^b r^{b-1}\exp(-ar)}{\Gamma(b)} & \text{if } r > 0, \\ 0 & \text{if } r \le 0, \end{cases} \tag{1.119}$$

where $\Gamma(t)$ is the gamma function [80]:

$$\Gamma(t) = \int_0^\infty s^{t-1}\exp(-s)\, ds, \tag{1.120}$$

defined for $t > 0$.

Definition (Continuous Mean). If the random variable $\boldsymbol{x}$ is continuous and has density function $f_x(r)$ and if $xf_x(r)$ is in $L^1(\mathbb{R})$, then the *mean* or *expectation* of $\boldsymbol{x}$,

written $E[\boldsymbol{x}]$, is

$$E(x) = \int_{-\infty}^{\infty} r f_x(r)\, dr. \tag{1.121}$$

Definition (Continuous Variance, Standard Deviation). Suppose that the random variable $\boldsymbol{x}$ is continuous, $xf_x(r)$ is in $L^1(\mathbb{R})$, $\mu = E[\boldsymbol{x}]$, and $x^2 f_x(r)$ is in $L^1(\mathbb{R})$. Then the *variance* of $\boldsymbol{x}$, σ_x^2, is

$$\sigma_x^2 = \int_{-\infty}^{\infty} (r-\mu)^2 f_x(r)\, dr. \tag{1.122}$$

1.8.2.3 Multivariate Distributions. This section considers the description of random vectors, entities that consist of two or more random components. Much of the development follows from a direct, albeit somewhat messy, extension of the ideas from the single random variables.

Definition (Multivariate Distributions). Let $\boldsymbol{x}$ and $\boldsymbol{y}$ be random variables in the probability space (Ω, Σ, P). Their joint distribution function is defined by $F_{\boldsymbol{x},\boldsymbol{y}}(r, s) = P[(\boldsymbol{x} \le r) \cap (\boldsymbol{y} \le s)]$. This generalizes to an arbitrary finite number of random variables, $\boldsymbol{r} = (\boldsymbol{r}_1, \boldsymbol{r}_2, \ldots, \boldsymbol{r}_M)$. For continuous random variables, the *joint density* of $\boldsymbol{x}$ and $\boldsymbol{y}$ is

$$f_{x,y}(r, s) = \frac{\partial^2}{\partial x \partial y} F_{x,y}(r, s). \tag{1.123}$$

We can define joint probability density functions for families of random variables too. This requires vector and matrix formulations in order to preserve the properties of density and distribution functions. For example, for the multivariate normal density, we have the following definition.

Definition (Joint Normal Density). Suppose that $\boldsymbol{X} = (\boldsymbol{x}_1, \boldsymbol{x}_2, \ldots, \boldsymbol{x}_M)$ is a vector of M random variables on the probability space (Ω, Θ, P). We define the *joint normal density* function $f_{\boldsymbol{X}}(r)$ by

$$f(r) = \frac{\exp\left[-\frac{1}{2}(\boldsymbol{r}-\mu)^T \Sigma^{-1} (\boldsymbol{r}-\mu)\right]}{\sqrt{\det(\Sigma)(2\pi)^M}}, \tag{1.124}$$

where $\boldsymbol{r} = (\boldsymbol{r}_1, \boldsymbol{r}_2, \ldots, \boldsymbol{r}_M)$ is a vector of length M; $\mu = (E[\boldsymbol{x}_1], E[\boldsymbol{x}_2], \ldots, E[\boldsymbol{x}_M])$ is the vector of means; $(\boldsymbol{r}-\mu)^T$ is the transpose of $\boldsymbol{r}-\mu$; Σ is the $M \times M$ covariance matrix for $\boldsymbol{X}$, $\Sigma = [\sigma_{m,n}] = E[(x_m - \mu_m)(x_n - \mu_n)]$; $\det(\Sigma)$ is its determinant; and its inverse is Σ^{-1}.

Earlier we considered how to apply Bayes's theorem to the problem of signal classification. However, we noted that it is not easy to distinguish signals by one feature alone, and our one-dimensional statistical classification breaks down. Now let's consider how to use statistical information about feature vectors and classes of signals to develop statistical discriminant functions. Suppose that we know the *a priori* probability of occurrence of each of the classes C_k, $P(C_k)$. Suppose further that for each class C_k we know the probability density function for the feature vector $\boldsymbol{v}$, $p(\boldsymbol{v}|C_k)$. The conditional probability $P(\boldsymbol{v}|C_k)$ provides the likelihood that class k is present, given that the input signal has feature vector $\boldsymbol{v}$. If we could compute $P(C_k|\boldsymbol{v})$ for each C_k and $\boldsymbol{v}$, then this would constitute a statistical basis for selecting one class over another for categorizing the input signal f.

We can restate Bayes's theorem for the multivariate case as follows.

Theorem (Multivariate Bayes). Suppose that for K signal classes C_k we know the *a priori* probability of occurrence of each of the classes $P(C_k)$ and the probability density function for the feature vector $\boldsymbol{v}$, $P(\boldsymbol{v}|C_k)$. Then

$$P(C_k \mid \boldsymbol{v}) = \frac{p(\boldsymbol{v} \mid C_k)P(C_k)}{p(\boldsymbol{v})} = \frac{p(\boldsymbol{v} \mid C_k)P(C_k)}{\sum_{i=1}^{K} p(\boldsymbol{v} \mid C_i)P(C_i)}, \tag{1.125}$$

where $p(\boldsymbol{v})$ is the probability density function for feature vector $\boldsymbol{v}$.

1.8.3 Random Signals

The ideas of random variables, their distribution and density functions, and the principal parameters that describe them are the basis for a definition of a random signal.

When we say that a signal is random, that is not to say that we know nothing of its values; in fact, we might know that the value of the signal at a time instant is almost certain to be in a given range. We might know that the signal remains, at other times, in some other range. It should be possible to provide a table that specifies the possible ranges of the signal and furnishes rough measures for how likely the signal value is to fall within that range. Every time the signal is measured or evaluated at a time, the signal is different, but we have an approximate idea of how these values behave. We can find one set of signal values, one instance of the random signal, but the next instance will differ. Thus, our concept of a random signal is embodied by a family of signals, and each member of the family represents a possible measurement of the signal over its domain. In probabilty theory, this is known as a *random* or *stochastic process*.

Definition (Random Signal). Suppose that (Ω, Σ, P) is a probability space. Let $\boldsymbol{X} = \{x(r): t \in T\}$ be a family of random variables on (Ω, Σ, P) indexed by the set T. Then $\boldsymbol{X}$ is a *stochastic process* or *random signa*l. If the index set T is the integers, then we say that $\boldsymbol{X}$ is a *discrete* random signal. If T is the real numbers, then we call $\boldsymbol{X}$ an *analog* random signal.

1.9 SUMMARY

There are two distinct signal categories: those with a continuous independent variable and those with a discrete independent variable. Natural signals are generally analog, and they become discrete—or more precisely, digital—by means of a conversion apparatus or by the way in which they are collected. The electrocardiogram source is analog, and it could be displayed in such a mode on an oscilloscope, for example. But nowadays it is often digitized for computer analysis. Such digital signals have a finite range. They are the true objects of digital signal processing on computers, but they are awkward for theoretical development. The temperature of the earth is a continuous function of depth, and it could be continuously recorded on a strip chart. But since the changes in the geothermal signal are so slow, it is more practical to collect isolated measurements. It is therefore discrete from the beginning. We rely on mathematical model for signal theory: continuous time functions, defined on the real numbers, for analog signals, and discrete time functions, defined on the integers, for discrete signals.

There is also a notion of the units of the interval between numerical signal values; This is called the independent variable. It is often a time variable, measured in seconds, minutes, hours, and so on, and this is natural, because time of occurrence provides a strict, irreversible ordering of events. So often are signals based on time that we get imprecise and routinely speak in temporal terms of the independent variable. On occasion, the independent variable that defines earlier and later signal values is a distance measure. The geothermal signal has an independent variable typically measured in meters, or even kilometers, of depth into the earth. Despite the fact that the independent variable is a distance measure, we often casually refer to the list of the signal's values as its "time-domain" specification.

The dependent variable of the signal is generally a real value for analog and discrete signals, and it is an integral value for digital signals. These are the signal values, and we stipulate that they assume numerical values, so that we can apply mathematical methods to study them. So the terminology here follows that from the mathematical notions of the independent and dependent variable for a mathematical function. We reserve the idea of a sequence of symbols, which is sometimes called a signal in ordinary language, for our concept of a signal interpretation.

We are concerned mainly with signals that have a one-dimensional independent and dependent variables. It is possible for a signal's dependent measurement to depend on multiple independent measurements. Image processing performs conditioning operations on two-dimensional signals. Computer vision analyzes multidimensional signals and produces a structural description or interpretation of them. We distinguish between single channel and multiple channel signals. If a signal produces a one-dimensional value, then it is single channel. An example is the temperature versus depth measurement. Signals that generate multidimensional values are called multichannel signals. An example is the 12-lead ECG. Multichannel signals have multidimensional range values. They arise in many applications, but we confine our discussions primarily to single-channel signals and refer interested readers to the more specialized literature on sensor fusion.

1.9.1 Historical Notes

A popular introduction to signal theory with historical background is Ref. 84. One of the latest discoveries in signal analysis is wavelet theory—a relatively recent and exciting approach for time-scale analysis [85]. An overview of wavelets and related time-frequency transforms is Ref. 69.

Several practical inventions spurred the early development of signal processing and analysis. The telegraph, invented by the American portrait painter Samuel F. B. Morse (1791–1872) in 1835, transmitted messages comprised of a sequence of isolated pulse patterns, or symbols, standing for letters of the English alphabet. The symbols themselves were (and still are, for the Morse code has been amended slightly and standardized internationally) a finite sequence of short and long electrical pulses, called dots and dashes, respectively. Shorter symbols represent the more prevalent English letters. For example, single dot and single dash represent the most common English letters, E and T, respectively. Morse's signaling scheme is an essentially discrete coding, since there is no continuous transition between either the full symbols or the component dots and dashes. Moreover, as a means of communication it could be considered to be digital, since the code elements are finite in number. But it would eventually be supplanted by analog communication technologies—the telephone and voice radio—which relied on a continuously varying representation of natural language.

Alexander Graham Bell (1847–1922), the famed U.S. inventor and educator of the deaf, discovered the telephone in the course of his experiments, undertaken in the mid-1870s, to improve the telegraph. The telegraph carried a single signal on a single pair of conductors. Bell sought to multiplex several noninterfering telegraphic messages onto a single circuit. The economic advantages of Bell's Harmonic Telegraph would have been tremendous, but the results were modest. Instead, Bell happened upon a technique for continuously converting human voices into electrical current variations and accurately reproducing the voice sounds at a remote location. Bell patented the telephone less than a year later, in March 1876; verified the concept six months later in sustained conversations between Boston and Cambridgeport, Massachusetts; and built the first commerical telephone exhange, at New Haven, Connecticut in January 1878. Bell's patent application points to the analog nature of telephony as clearly distinguishing it from discrete telegraphy.

Wireless telegraphy—and eventually wireless telephony—were the fruit of persistent efforts by yet another scientific layperson, Guglielmo Marconi (1874–1937). The young Italian inventor was aware of both J. C. Maxwell's theory of electromagnetic waves[21]and H. R. Hertz's demonstration[22] of precisely this radiation with a spark coil transmitter and wire loop receiver. But Hertz's apparatus was too weak for practical use. Marconi's improvements—a telegraph key to control the firing of the spark gap, a long wire antenna and earth ground for greater signal strength, and

[21]Scottish physicist James Clerk Maxwell (1831–1879) announced his electromagnetic field theory to a skeptical scientific community in 1864.

[22]With a small spark coil, German physicist Heinrich Rudolf Hertz (1857–1894) generated the first electromagnetic waves at the University of Karlsruhe and verified Maxwell's theory.

the crystal detector for improved reception—enabled him to demonstrate radio telegraphy in 1895. Unheralded in his native Italy, Marconi took his technology to England, received a patent in 1896, formed his own company a year later, and received the Nobel prize in 1909. These techniques could only serve discrete modes of telecommunication, however. Analog communication awaited further improvements in radio communication, in particular the radio-frequency alternator.

These practical advances in analog technologies were complemented by the discovery of the richness within Jean-Baptiste Fourier's discovery, long past, that even signals containing discontinuities could be represented by sums of smoothly undulating sinusoids. Fourier developed his theory for the purpose of studying heat propagation. In particular, it remains a principal tool for solving the differential equations governing such phenomena as heat conduction, Fourier's original problem [1]. Thus, at the turn of the last century, the most important signal technologies and the most important signal theories revolved around analog methods.

Theory would not link the analog and discrete realms of signal processing until the early twentieth century, when Nyquist [2], Shannon [3], and Vladimir Kotelnikov[23] developed the sampling theory. Nyquist's original research article focused on telegraphy, and it established a first theoretical link between discrete and analog communication methods. In particular, he showed that a continuous domain signal containing but a limited variety of frequencies could be captured and regenerated with a discrete signal. But analog practice and analog theory ruled supreme, and Nyquist's contribution was largely overlooked. Only when Shannon proved that error-free digital communication—even in the presence of noise—was possible did the attention of scientists and engineers turn once more to discrete modes of communication. The contributions of Nyquist and Shannon did firmly establish signal theory as a distinct scientific and engineering discipline. Both analog and discrete signal theory were soundly fixed upon mathematical foundations and shared a link through the Shannon–Nyquist results.

One seemingly insurmountable problem remained. The frequency analysis of analog signals was possible using conventional analog instruments such as a frequency analyzer. But discrete signal frequencies could not be calculated fast enough to keep pace with the arrival of discrete values to a processing apparatus. Therefore, although mathematicians developed a considerable complement of tools for understanding discrete signals, engineers remained preoccupied with analog tools which could handle their signals in real time.

The discovery of the fast Fourier transform (FFT) by J. W. Cooley and J. W. Tukey in 1965 shattered the analog tradition in signal processing. By eliminating duplicate computations in the DFT, it became possible to produce the frequency spectrum of a signal with N data points in $N\log_2 N$ operations; real-time digital signal spectrum analysis became feasible [4–6].

[23]Vladimir A. Kotelnikov (1908–), a Russian communications engineer, independently discovered the sampling theorem in 1933. His work was largely unknown outside the Soviet Union.

1.9.2 Resources

A vast array of resources—commercial products, inexpensive shareware applications, and public-domain software—are available nowadays for studying signal theory. Researchers, university laboratories, private firms, and interested individuals have also made available signal and image processing data sets. Some of these have become standards for experimentation, algorithm development, and performance comparisons.

1.9.2.1 Signal Processing Tools. Commercial packages used for this chapter's examples include:

- *Matlab*, available from The MathWorks, Inc., 24 Prime Park Way, Natick, MA, 01760, USA [86].
- *Mathematica*, available from Wolfram Research, Inc., 100 Trade Center Drive, Champaign, IL, 61820, USA [87].

Public-domain packages include the following:

- *Wavelab*, which uses Matlab and includes several popular research data sets, available free of charge from Stanford University: `http://playfair.stanford.edu/~wavelab`.
- *Khoros*, available free of charge via anonymous ftp from the University of New Mexico: `ftp.eece.unm.edu` [88].

1.9.2.2 Data. There are many data sets available over the internet, including several smaller data archives, maintained by individual researchers, tapped for examples in this chapter.

Among the larger repositories are the following:

- Rice University, Houston, TX, in conjunction with the Institute of Electrical and Electronic Engineers (IEEE), supports the Signal Processing Information Base (SPIB): `http://spib.rice.edu/spib.html`. SPIB contains a variety of signal and image data sets, several of which found their way into the examples of this text.
- The University of California at Irvine, Irvine, CA supports a machine intelligence database.

Every effort has been made to use example data sets that are available to the reader. Readers should be able to find this chapter's signal data examples within the public domain. Figure 1.1 is on the web site of the Princeton Earth Physics Project (`http://www.gns.cri.nz/quaketrackers/curr/seismic_waves.htm`). The EEG signals of Figure 1.3 are from Krishna Nayak's Florida State University web

site, `http://www.scri.fsu.edu`. The aerial scenes of Figure 1.4 are from the Danish Center for Remote Sensing, `http://www.dcrs.dk`. The ECG signal of Figure 1.6 is from SPIB. The geothermal data of Figure 1.8 comes from the Appalachian Deep Core Hole project and is available at the ADCOH web site [36]. The auditory neuron pulse train data are from SPIB.

1.9.3 Looking Forward

Now that we have introduced the basic raw material, signals, we proceed in Chapters 2 and 3 to introduce the machinery, systems. The term "system" is a very broad term, but in signal theory it is used in a quite specific sense. A *system* is the mathematical entity that accomplishes signal processing; it takes a signal as input and produces a signal as output. A system is a function that operates on signals.

An understanding of signals requires ideas from basic mathematics, algebra, calculus, a dose of complex analysis, and some random variable theory. In contrast, a firm understanding of the ideas of systems—the mechanisms that convert one signal into another, signal processing in other words—depends upon ideas from advanced mathematical analysis. In particular, we must draw upon the concepts of functional analysis—especially Hilbert space theory—topics normally taught at the university graduate mathematics level. For practical-minded scientists and engineers, this seems ominous. But the good news is that this development is straightforward for discrete signals. Thus, in Chapter 2 we concentrate exclusively on discrete signal spaces, of which discrete Hilbert spaces are a special case.

To most of us, the mastery of analog signal processing theory comes less readily than a thorough understanding of discrete theory. Readers need to understand both developments, even though the analog theory is more mathematically involved. However, scientists, applied mathematicians, and engineers who are looking further toward modern mixed-domain signal processing methods need a good foundation in signal spaces and an advanced presentation of analog signal analysis. Chapter 3 presents the prerequisite background in continuous-domain signal spaces.

1.9.4 Guide to Problems

All of the chapters provide problems. They range in difficulty from simple exercises that recall basic ideas from the text to more complicated problems that extend and develop the chapter's material. Some of them are outlines of research projects that may involve several weeks of work. The student may need to make simplifying assumptions, discover constraints, and—quite likely—will not arrive at a once-and-for-all answer to the problems posed.

REFERENCES

1. J.-B. J. Fourier, *The Analytical Theory of Heat*, translated by A. Freeman, New York: Dover, 1955.
2. H. Nyquist, Certain topics in telegraph transmission theory, *Transactions of the AIEE*, vol. 47, pp. 617–644, 1928.
3. C. E. Shannon, A mathematical theory of communication, *Bell Systems Technical Journal*, vol. 27, pp. 379–423 and pp. 623–656, 1948.
4. J. W. Cooley and J. W. Tukey, An algorithm for the machine calculation of complex Fourier series," *Mathematics of Computation*, vol. 19, pp. 297–301, April 1965.
5. J. W. Cooley, P. A. Lewis, and P. D. Welch, Historical notes on the fast Fourier transform, *IEEE Transactions on Audio and Electroacoustics*, vol AU-15, pp. 76–79, June 1967.
6. J. W. Cooley, How the FFT gained acceptance, *IEEE SP Magazine*, pp. 10–13, January 1992.
7. H. Baher, *Analog and Digital Signal Processing*, New York: Wiley, 1990.
8. J. A. Cadzow and H. F. van Landingham, *Signals, Systems, and Transforms*, Englewood Cliffs, N J: Prentice-Hall, 1989.
9. L. B. Jackson, *Signals, Systems, and Transforms*, Reading, MA: Addison-Wesley, 1991.
10. A. V. Oppenheim, A. S. Willsky, and S. H. Nawab, *Signals and Systems*, 2nd ed., Englewood Cliffs, NJ: Prentice-Hall, 1989.
11. R. E. Ziemer, W. H. Tranter, and D. R. Fannin, *Signals and Systems*: *Continuous and Discrete*, New York: Macmillan, 1989.
12. L. B. Jackson, *Digital Filters and Signal Processing*, Boston: Kluwer Academic Publishers, 1989.
13. A. V. Oppenheim and R. W. Shafer, *Discrete-Time Signal Processing*, Englewood Cliffs, NJ: Prentice-Hall, 1989.
14. J. G. Proakis and D. G. Manolakis, *Digital Signal Processing: Principles, Algorithms, and Applications*, 2nd ed., New York: Macmillan, 1992.
15. L. R. Rabiner and B. Gold, *Theory and Application of Digital Signal Processing*, Englewood Cliffs, NJ: Prentice-Hall, 1975.
16. K.-S. Lin, ed., *Digital Signal Processing Applications with the TMS320 Family*, vol. 1, Dallas, TX: Texas Instruments, 1989.
17. R. J. Simpson, *Digital Signal Processing Using the Motorola DSP Family*, Englewood Cliffs, NJ: Prentice-Hall, 1994.
18. Motorola, Inc., *DSP56000/DSP56001 Digital Signal Processor User's Manual*, Phoenix, AZ: Motorola Literature Distribution, 1990.
19. R. J. Higgins, *Digital Signal Processing in VLSI*, Englewood Cliffs, NJ: Prentice-Hall, 1990.
20. A. Mar, ed., *Digital Signal Processing Applications Using the ADSP-2100 Family*, Englewood Cliffs, NJ: Prentice-Hall, 1990.
21. V. K. Madisetti, *VLSI Digital Signal Processors: An Introduction to Rapid Prototyping and Design Synthesis*, Piscataway, NJ: IEEE Press, 1995.
22. B. A. Bolt, *Earthquakes and Geologic Discovery*, New York: Scientific American Library, 1990.

23. O. Kulhanek, *Anatomy of Seismograms*, Amsterdam: Elsevier, 1990.
24. J. F. Claerbout, *Fundamentals of Geophysical Data Processing: With Applications to Petroleum Prospecting*, Boston: Blackwell Scientific, 1985.
25. M. Akay, *Biomedical Signal Processing*, San Diego, CA: Academic Press, 1994.
26. J. C. Russ, *The Image Processing Handbook*, Boca Raton, FL: CRC Press, 1995.
27. A. Rosenfeld and A. C. Kak, *Digital Picture Processing*, vols. 1 and 2, Orlando, FL: Academic Press, 1982.
28. A. K. Jain, *Fundamentals of Digital Image Processing*, Englewood Cliffs, NJ: Prentice-Hall, 1989.
29. R. J. Schalkoff, *Digital Image Processing and Computer Vision*, New York: Wiley, 1989.
30. D. H. Ballard and C. M. Brown, *Computer Vision*, Englewood Cliffs, NJ: Prentice-Hall, 1982.
31. R. M. Haralick and L. G. Shapiro, *Computer and Robot Vision*, vols. 1 and 2, New York: Addison-Wesley, 1992.
32. B. K. P. Horn, *Robot Vision*, Cambridge, MA: MIT Press, 1986.
33. M. J. Goldman, *Principles of Clinical Electrocardiography*, Los Altos, CA: Lange Medical Publications, 1986.
34. D. B. Geselowitz, On the theory of the electrocardiogram, *Proceedings of the IEEE*, vol. 77, no. 6, pp. 857–872, June 1989.
35. M. Unser and A. Aldroubi, A review of wavelets in biomedical applications, *Proceedings of the IEEE*, vol. 84, no. 4, pp. 626–638, April 1996.
36. J. K. Costain and E. R. Decker, Heat flow at the proposed Appalachian Ultradeep Core Hole (ADCOH) site: Tectonic implications, *Geophysical Research Letters*, vol. 14, no. 3, pp. 252–255, 1987.
37. C .F. Gerald and P. O. Wheatley, *Applied Numerical Analysis*, Reading, MA: Addison-Wesley, 1990.
38. F. Attneave, Some informational aspects of visual perception, *Psychological Review*, vol. 61, pp. 183–193, 1954.
39. D. Marr, *Vision*, New York: W. H. Freeman and Company, 1982.
40. H. Asada and M. Brady, The curvature primal sketch, *IEEE Transactions on Pattern Analysis and Machine Intelligence*, vol. PAMI-8, no. 1, pp. 2–14, January 1986.
41. I. Biedermann, Human image understanding: Recent research and a theory," *Computer Vision, Graphics, and Image Processing*, vol. 32, pp. 29–73, 1985.
42. A. P. Witkin, Scale-space filtering, *Proceedings of the 8th International Joint Conference on Artificial Intelligence*, Karlsruhe, W. Germany, 1983. See also A. P. Witkin, Scale-space filtering, in *From Pixels to Predicates*, A. P. Pentland, ed., Norwood, NJ: Ablex, 1986.
43. T. Lindeberg, Scale space for discrete signals, *IEEE Transactions on Pattern Analysis and Machine Intelligence*, vol. 12, no. 3, pp. 234–254, March 1990.
44. M. Rosenlicht, *Introduction to Analysis*, New York: Dover, 1978.
45. D. Gabor, Theory of communication, *Journal of the Institute of Electrical Engineers*, vol. 93, pp. 429–457, 1946.
46. D. A. Pollen and S. F. Ronner, Visual cortical neurons as localized spatial frequency filters, *IEEE Transactions on Systems, Man, and Cybernetics*, vol. SMC-13, no. 5, pp. 907–916, September–October 1983.

47. J. J. Kulikowski, S. Marcelja, and P. O. Bishop, Theory of spatial position and spatial frequency relations in the receptive fields of simple cells in the visual cortex, *Biological Cybernetics*, vol. 43, pp. 187–198, 1982.
48. A. H. Zemanian, *Distribution Theory and Transform Analysis*, New York: Dover, 1965.
49. M. J. Lighthill, *Introduction to Fourier Analysis and Generalized Functions*, New York: Cambridge University Press, 1958.
50. J. Stoer and R. Bulirsch, *Introduction to Numerical Analysis*, 2nd ed., New York: Springer-Verlag, 1993.
51. S. Lang, *Linear Algebra*, Reading, MA: Addison-Wesley, 1968.
52. G. Strang, *Linear Algebra and Its Applications*, 2nd ed., New York: Academic Press, 1980.
53. S. G. Mallat, A theory for multiresolution signal decomposition: The wavelet representation, *IEEE Transactions on Pattern Analysis and Machine Intelligence*, vol. 11, no. 7, pp. 674–693, July 1989.
54. J. Carson and T. Fry, Variable frequency electric circuit theory with applications to the theory of frequency modulation, *Bell Systems Technical Journal*, vol. 16, pp. 513–540, 1937.
55. B. Van der Pol, The fundamental principles of frequency modulation, *Proceedings of the IEE*, vol. 93, pp. 153–158, 1946.
56. J. Shekel, Instantaneous frequency, *Proceedings of the IRE*, vol. 41, p. 548, 1953.
57. F. Jelinek, Continuous speech recognition by statistical methods, *Proceedings of the IEEE*, vol. 64, no. 4, pp. 532–556, April 1976.
58. S. Young, A review of large-vocabulary continuous-speech recognition, *IEEE Signal Processing Magazine*, vol. 13, no. 5, pp. 45–57, September 1996.
59. L. Rabiner and B.-H. Juang, *Fundamentals of Speech Recognition*, Englewood Cliffs, NJ: Prentice-Hall, 1993.
60. N. Morgan and H. Bourlard, Continuous speech recognition, *IEEE Signal Processing Magazine*, vol. 12, no. 3, pp. 25–42, May 1995.
61. B. Malmberg, *Phonetics*, New York: Dover, 1963.
62. J. L. Flanagan, *Speech Analysis, Synthesis, and Perception*, 2nd ed., New York: Springer-Verlag, 1972.
63. N. Deshmukh, R. J. Duncan, A. Ganapathiraju, and J. Picone, Benchmarking human performance for continuous speech recognition, *Proceedings of the Fourth International Conference on Spoken Language Processing*, Philadelphia, pp. SUP1-SUP10, October 1996.
64. J. R. Cox, Jr., F. M. Nolle, and R. M. Arthur, Digital analysis of electroencephalogram, the blood pressure wave, and the electrocardiogram, *Proceedings of the IEEE*, vol. 60, pp. 1137–1164, 1972.
65. L. Khadra, M. Matalgah, B. El-Asir, and S. Mawagdeh, Representation of ECG-late potentials in the time frequency plane, *Journal of Medical Engineering and Technology*, vol. 17, no. 6, pp. 228–231, 1993.
66. F. B. Tuteur, Wavelet transformations in signal detection, in *Wavelets: Time-Frequency Methods and Phase Space*, J. M. Combes, A. Grossmann, and P. Tchamitchian, eds., 2nd ed., Berlin: Springer-Verlag, pp. 132–138, 1990.

67. G. Olmo and L. Lo Presti, Applications of the wavelet transform for seismic activity monitoring, in *Wavelets: Theory, Applications, and Applications*, C. K. Chui, L. Montefusco, and L. Puccio, eds., San Diego, CA: Academic Press, pp. 561–572, 1994.
68. J. L. Larsonneur and J. Morlet, Wavelets and seismic interpretation, in *Wavelets*: *Time-Frequency Methods and Phase Space*, J. M. Combes, A. Grossmann, and P. Tchamitchian, eds., 2nd ed., Berlin: Springer-Verlag, pp. 126–131, 1990.
69. Y. Meyer, *Wavelets: Algorithms and Applications*, Philadelphia: SIAM, 1993.
70. A. N. Kolmogorov and S. V. Fomin, *Introductory Real Analysis*, New York: Dover, 1975.
71. M. C. Teich, D. H. Johnson, A. R. Kumar, and R. Turcott, Fractional power law behavior of single units in the lower auditory system, *Hearing Research*, vol. 46, pp. 41–52, May 1990.
72. R. P. Feynman, R. B. Leighton, and M. Sands, *The Feynman Lectures on Physics*, vol. 1, Reading, MA: Addison-Wesley, 1977.
73. L. V. Ahlfors, *Complex Analysis*, 2nd ed., New York: McGraw-Hill, 1966.
74. E. Hille, *Analytic Function Theory*, vol. 1, Waltam, MA: Blaisdell, 1959.
75. N. Levinson and R. M. Redheffer, *Complex Variables*, San Francisco: Holden-Day, 1970.
76. R. Beals, *Advanced Mathematical Analysis*, New York: Springer-Verlag, 1987.
77. A. Gluchoff, A simple interpretation of the complex contour integral, *Teaching of Mathematic*s, pp. 641–644, August–September 1991.
78. A. O. Allen, *Probability, Statistics, and Queueing Theory with Computer Scinece Applications*, Boston: Academic, 1990.
79. W. Feller, *An Introduction to Probability Theory and Its Applications*, New York: Wiley, 1968.
80. E. Parzen, *Modern Probability Theory and Its Applications*, New York: Wiley, 1960.
81. A. Papoulis, *Probability, Random Variables, and Stochastic Processes*, New York: McGraw-Hill, 1984.
82. R. E. Mortensen, *Random Signals and Systems*, New York: Wiley, 1984.
83. W. B. Davenport and W. L. Root, *An Introduction to the Theory of Random Signals and Noise*, New York: McGraw-Hill, 1958.
84. J. R. Pierce and A. M. Noll, *Signals: The Science of Telecommunications*, New York: Scientific American Library, 1990.
85. B. B. Hubbard, *The World According to Wavelets*, Wellesley, MA: A. K. Peters, 1996.
86. A. Biran and M. Breiner, *Matlab for Engineers*, Harlow, England: Addison-Wesley, 1995.
87. S. Wolfram, *The Mathematica Book*, 3rd ed., Cambridge, UK: Cambridge University Press, 1996.
88. K. Konstantinides and J. R. Rasure, The Khoros software development environment for image and signal processing, *IEEE Transactions on Image Processing*, vol. 3, no. 3, pp. 243–252, May 1994.

PROBLEMS

1. Which of the following signals are analog, discrete, or digital? Explain.

(a) The temperature reading on a mercury thermometer, as a function of height, attached to a rising weather balloon.

(b) The time interval, given by a mechanical clock, between arriving customers at a bank teller's window.

(c) The number of customers that have been serviced at a bank teller's window, as recorded at fifteen minutes intervals throughout the workday.

2. Which of the following constitute time domain, frequency domain, or scale domain descriptions of a signal? Explain.

(a) A listing of the percentages of 2-kHz, 4-kHz, 8-kHz, and 16-kHz tones in a ten second long tape recording of music.

(b) The atmospheric pressure readings reported from a weather balloon, as it rises above the earth.

(c) From a digital electrocardiogram, the number of QRS pulses that extend for 5, 10, 15, 20, 25, and 30 ms.

3. Sketch the following signals derived from the unit step $u(t)$:

(a) $u(t-1)$

(b) $u(t+2)$

(c) $u(-t)$

(d) $u(-t-1)$

(e) $u(-t+2)$

(f) $u(t-2)-u(t-8)$

4. Sketch the following signals derived from the discrete unit step $u(n)$:

(a) $u(n-4)$

(b) $u(n+3)$

(c) $u(-n)$

(d) $u(-n-3)$

(e) $u(-n+3)$

(f) $u(n-2)-u(n-8)$

(g) $u(n+6)-u(n-3)$

5. Describe the difference between the graphs of a signal $x(t)$; the shifted version of $x(t)$, $y(t) = x(t-c)$; and the reflected and shifted version, $z(t) = x(-t-c)$. Consider all cases for $c > 0$, $c < 0$, and $c = 0$.

6. Suppose that an N-bit register stores non-negative digital values ranging from 0 (all bits clear) to all bits set. The value of bit b_n is 2^n, $n = 0, 1, ..., N-1$. Show that the largest possible value is $2^N - 1$.

7. Consider the two's complement representation of a digital value in an N-bit register. If the bits are $b_{N-1}, b_{N-2}, ..., b_1, b_0$, then the digital value is $-b_{N-1}2^{N-1} + b_{N-2}2^{N-2} + \cdots + b_2 2^2 + b_1 2^1 + b_0 2^0$.

(a) Find the largest positive value and give its bit values.

(b) Find the most negative value and give its bit values.

(c) Show that the dynamic range is 2^N.

8. Suppose that an N-bit register uses the most significant bit b_{N-1} as a sign bit: If $b_{N-1} = 1$, then the value is -1 times the value in first $N-1$ bits; otherwise the value is positive, 1 times the value in first $N-1$ bits. The remaining $N-1$ bits store a value as in Problem 6.

(a) Again, find the largest possible positive value and the most negative value.

(b) What is the dynamic range for this type of digital storage register? Explain the result.

9. Suppose discrete signal $x(n)$ is known at distinct points $(n_k, x(n_k)) = (n_k, y_k)$, where $0 \le k \le N$. Suppose too that there are interpolating cubic polynomials over the $[n_k, n_{k+1}]$:

$$p(t) = a_k(t-n_k)^3 + b_k(t-n_k)^2 + c_k(t-n_k) + d_k. \tag{1.126}$$

(a) If the interpolants passes through the knots (n_k, y_k), then show $y_k = d_k$.

(b) Compute the derivatives, $p_k'(t)$ and $p_k''(t)$ for each k, and show that if $D_k = p_k''(n_k)$ and $E_k = p_k''(n_{k+1})$, then a_k and b_k can be written in terms of D_k and E_k.

(c) Suppose that for some k, we know both D_k and E_k. Show that we can then give the coefficients of the interpolating cubic, $p_k(t)$ on $[n_k, n_{k+1}]$.

10. Let $x(t) = 5\sin(2400t + 400)$, where t is a (real) time value in seconds. Give:

(a) The amplitude of x

(b) The phase of x

(c) The frequency of x in Hz (cycles/second)

(d) The frequency of x in radians/second

(e) The period of x

11. Consider a discrete signal $x(n) = A\cos(\Omega n + \phi)$ for which there is an $N>0$ with $x(n)=x(n+N)$ for all n.

(a) Explain why the smallest period for all discrete signals is $N=1$, but there is no such lowest possible period for the class of analog signals.

(b) Show that if $x(n)$ is a sinusoid, then the largest frequency it can have is $|\Omega| = \pi$ or, equivalently, $|F| = 1$, where $\Omega = 2\pi F$.

12. Let $s(n) = -8\cos\left(\frac{21}{2}n + 3\right)$ be a discrete signal. Find the following:

(a) The amplitude of s

(b) The phase of s

(c) The frequency of s in radians/sample

(d) The frequency of s in Hz (cycles/sample)

(e) Does s have a period? Why?

13. Find the frequency of the following discrete signals. Which ones are even, odd, finitely supported? Which ones are equal?

(a) $a(n) = 5\cos\left(n\frac{\pi}{4}\right)$.

(b) $b(n) = 5\cos\left(-n\frac{\pi}{4}\right)$.

(c) $c(n) = 5\sin\left(n\frac{\pi}{4}\right)$.

(d) $d(n) = 5\sin\left(-n\frac{\pi}{4}\right)$.

14. Prove that a signal decomposes into its even and odd parts. If $x(n)$ is a discrete signal, then show that:

(a) $x_e(n)$ is even.

(b) $x_o(n)$ is odd.

(c) $x(n) = x_e(n) + x_o(n)$.

15. Consider the signal $x(n) = [3, 2, 1, -1, -1, \underline{-1}, 0, 1, 2]$. Write $x(n)$ as a sum of even and odd discrete functions.

16. Show the following:

(a) $\sin(t)$ is odd.

(b) $\cos(t)$ is even.

(c) $g_{\mu,\sigma}(t)$ of mean μ and standard deviation σ (1.14) is symmetric about μ.

(d) Suppose a polynomial $x(t)$ is even; what can you say about $x(t)$? Explain.

(e) Suppose a polynomial $x(t)$ is odd; what can you say about $x(t)$? Explain.

(f) Show that the norm of the Gabor elementary function $\left\|G_{\mu,\sigma,\omega}(t)\right\|$ (1.20) is even.

(g) Characterize the real and imaginary parts of $G_{\mu,\sigma,\omega}(t)$ as even or odd.

17. Show that rational signal $x(t) = 1/t$ is neither integrable nor square-integrable in the positive real half-line $\{t : t > 0\}$. Show that $s(t) = t^{-2}$, however, is integrable for $\{t : t > 1\}$.

18. Show that $f(z) = f(x + jy) = x - jy$, the complex conjugate function, is not differentiable at a general point $z \in \mathbb{C}$.

19. Suppose that $f(z) = z$ and C is the straight line arc from a point u to point v in the complex plane.

(a) Find the contour integral

$$\oint_C f(z)\,dz. \tag{1.127}$$

(b) Suppose that $f(z) = z^{-1}$; again evaluate the contour integral in part (a); what assumptions must be made? Explain.

20. Suppose Σ is an algebra over a set Ω.

(a) Show that $\Omega \in \Sigma$.

(b) Show that Σ is closed under finite unions; that is, show that a finite union of elements of Σ is still in Σ.

(c) Show that Σ is closed under finite intersections.

(d) Supposing that Σ is a σ-algebra as well and that $S_n \in \Sigma$ for all natural numbers $n \in \mathbb{N}$, show that

$$\bigcap_{n \in \mathbb{N}} S_n \in \Sigma. \tag{1.128}$$

21. Suppose that (Ω, Σ, P) is a probability space. Let S and T be events in Σ. Show the following:

(a) $P(\varnothing) = 0$.

(b) $P(S) = 1 - P(S')$, where S' is the complement of S inside Ω.

(c) If $S \subseteq T$, then $P(S) \leq P(T)$.

(d) $P(S \cup T) = P(S) + P(T) - P(S \cap T)$.

22. Suppose that Ω is a set.

(a) What is the smallest algebra over Ω?

(b) What is the largest algebra over Ω?

(c) Find an example set Ω and an algebra Σ over Ω that is not a σ-algebra;

(d) Suppose that every algebra over Ω is also a σ-algebra. What can you say about Ω? Explain.

23. If A and B are independent, show that

(a) A and $\sim B$ are independent.

(b) $\sim A$ and $\sim B$ are independent.

24. Let $\boldsymbol{x}$ be a random variable and let r and s be real numbers. Then, by the definition of a random variable, the set $\{\omega \in \Omega : \boldsymbol{x}(\omega) \leq r\}$ is an event. Provide definitions for the following and show that they must be events:

(a) $\boldsymbol{x} > r$.

(b) $r < \boldsymbol{x} \leq s$.

(c) $\boldsymbol{x} = r$.

25. Find constants A, B, C, and D so that the following are probability density functions:

(a) $x(n) = A \times [\underline{4}, 3, 2, 1]$.

(b) $f(r) = B[u(r) - u(r-2)]$, where $u(t)$ is the analog unit step signal.

(c) The Rayleigh density function is

$$f(r) = \begin{cases} Cr\exp\left(-\dfrac{r^2}{2}\right) & \text{if } r \geq 0, \\ 0 & \text{if } r < 0. \end{cases} \tag{1.129}$$

(d) $f(r)$ is defined as follows:

$$f(r) = \begin{cases} \dfrac{D}{\sqrt{1-r^2}} & \text{if } |r| < 1, \\ 0 & \text{if } r \geq 1. \end{cases} \tag{1.130}$$

The following problems are more involved and, in some cases, expand upon ideas in the text.

26. Let $x(t) = A\cos(\Omega t)$ and $y(t) = A\cos(\Phi t)$ be continuous-domain (analog) signals. Find conditions for A, B, Ω, and Φ so that the following statement is true, and then prove it: If $x(t) = y(t)$ for all t, then $A = B$ and $\Omega = \Phi$.

27. Explain the following statement: There is a unique discrete sinusoid $x(n)$ with radial frequency $|\omega| \leq \pi$.

28. The following steps show that the support of a signal $x(t)$ is compact if and only if its support is both closed and bounded [44, 70].

(a) Show that a convergent set of points in a closed set S converges to a point in S.

(b) Prove that a compact $S \subset \mathbb{R}$ is bounded.

(c) Show that a compact $S \subset \mathbb{R}$ has at least one cluster point; that is, there is a t in S such that any open interval (a, b) containing t contains infinitely many points of S.

(d) Using (a) and (b), show that a compact set is closed.

(e) If $r > 0$ and $S \subset \mathbb{R}$ is bounded, show S is contained in the union of a finite number of closed intervals of length r.

(f) Show that if $S \subset \mathbb{R}$ is closed and bounded, then S is compact.

29. The *average power* of the discrete signal $x(n)$ is defined by

$$P_x = \lim_{N \to \infty} \left[\frac{1}{2N+1} \sum_{n=-n}^{n} |x(n)|^2 \right]. \tag{1.131}$$

If the limit defining P_x exists, then we say that $x(n)$ has *finite average power.* Show the following.

(a) An exponential signal $x(n) = Ae^{j\omega n}$, where A is real and nonzero, has finite average power, but not finite energy.

(b) If $x(n)$ is periodic and $x(n)$ is non-zero, then $x(n)$ is neither absolutely summable nor square summable.

(c) If $x(n)$ is periodic, then $x(n)$ has finite average power.

30. Show that under any of the following conditions, the differentiable function $f(z)$ must be constant on $\mathbb{C}$.

(a) Real$[f(z)]$ is constant.

(b) Imag$[f(z)]$ is constant.

(c) $|f(z)|$ is constant.

31. Show that a discrete polynomial $p(k)$ may have consecutive points, k_0, k_1, ..., and so on, where the discrete second derivative is zero.

(a) For a given degree n, what is the limit, if any, on the number of consecutive points where the discrete second derivative is zero? Explain.

(b) For a discrete polynomial $p(k)$ of degree n, find formulas for the first, second, and third derivatives of $p(k)$.

(c) Show that a polynomial $p(t)$ of degree $n > 1$ has only isolated points, t_0, t_1, ..., t_N, where the second derivative is zero. What is N?

32. Prove the proposition on distribution function properties of Section 1.8.2 [81].

33. Suppose the discrete random variable $\boldsymbol{x}$ has a binomial distribution (1.113).

(a) Find the density function $f_{\boldsymbol{x}}(r)$.

(b) Find the distribution function $F_{\boldsymbol{x}}(r)$.

(c) Find the mean $E[\boldsymbol{x}]$.

(d) Find the variance $(\sigma_{\boldsymbol{x}})^2$.

(e) Discuss the case where p or q is zero in (1.113).

34. Suppose the discrete random variable **x** has a Poisson distribution with parameter $a > 0$ (1.114).

(a) Find the density function $f_{\boldsymbol{x}}(r)$.

(b) Find the distribution function $F_{\boldsymbol{x}}(r)$.

(c) Find the mean $E[\boldsymbol{x}]$.

(d) Find the variance $(\sigma_{\boldsymbol{x}})^2$.

The next several problems consider electrocardiogram processing and analysis.

35. Develop algorithms for calculating the running heart rate from a single ECG lead.

(a) Obtain the ECG trace of Figure 1.6 from the Signal Processing Information Base (see Section 1.9.2.2). Plot the data set using a standard graphing package or spreadsheet application. For example, in Matlab, execute the command lines: `load ecg.txt; plot (ecg)`. As an alternative, develop C or C++ code to load the file, plot the signal, and print out the time-domain values. Identify the QRS complexes and give a threshold value M which allows you to separate QRS pulses from noise and other cardiac events.

(b) Give an algorithm that reads the data sequentially; identifies the beginning of a QRS complex using the threshold M from (a); identifies the end of the QRS pulse; and finds the maximum value over the QRS event just determined.

(c) Suppose two successive QRS pulse maxima are located at n_0 and n_1, where $n_1 > n_0$. Let the sampling interval be T seconds. Find the elapsed time (seconds) between the two maxima, $v(n_1)$ and $v(n_0)$. Give a formula for the heart rate from this single interval; let us call this value $H(n_1)$.

(d) Critique the algorithm for instantaneous heart rate above. Explain any assumptions you have made in the algorithm. Calculate the instantaneous heart rate $H(n_i)$, for all successive pairs of QRS pulses beginning at n_{i-1}. Plot this $H(n_i)$ value over the entire span of the signal. What do you observe? What if the threshold you choose in (a) is different? How does this affect your running heart rate value?

(e) Suppose that the running heart rate is computed as the average of the last several $H(n_i)$ values—for example, $H_3(n_i) = [H(n_i) + H(n_{i-1}) + H(n_{i-2})]/3$. Is the instantaneous heart rate readout better? Is there a practical limit to how many past values you should average?

36. Explore the usefulness of signal averaging when computing the instantaneous heart rate.

(a) Use a symmetric moving average filter on the raw ECG trace:

$$w(n) = \frac{1}{3}[v(n-1) + v(n) + v(n+1)]\,. \tag{1.132}$$

Calculate the running heart rates as in the previous problem using $w(n)$ instead of $v(n)$.

(b) How does an asymmetric smoothing filter,

$$w(n) = \frac{1}{3}[v(n) + v(n-1) + v(n-2)]\,, \tag{1.133}$$

affect the results? Explain.

(c) Sketch an application scenario which might require an asymmetric filter.

(d) Try symmetric moving average filters of widths five and seven for the task of part (a). Graph the resulting ECG traces. Are the results improved? Is the appearance of the signal markedly different?

(e) Why do signal analysts use symmetric filters with an odd number of terms?

(f) When smoothing a signal, such as the ECG trace $v(n)$, would it be useful to weight the signal values according to how close they are to the most recently acquired datum? Contemplate filters of the form

$$w(n) = \frac{1}{4}v(n-1) + \frac{1}{2}v(n) + \frac{1}{4}v(n+1)\,, \tag{1.134}$$

and discuss their practicality.

(g) Why do we choose the weighting coefficients in the equation of part (f) to have unit sum? Explain.

(h) Finally, consider weighted filter coefficients for asymmetric filters. How might these be chosen, and what is the motivation for so doing? Provide examples and explain them.

37. Develop algorithms for alerting medical personnel to the presence of cardiac dysrhythmia. A statistical measure of the variability of numerical data is the standard deviation,

(a) What is the average heart rate over the entire span of the ECG trace, once again using the distance between QRS pulse peaks as the basis for computing the instantaneous heart rate.

(b) Calculate the standard deviation of time intervals between QRS pulses. How many pulses are necessary for meaningful dysrhythmia computations?

38. Find algorithms for detecting the presence of the P wave and T wave in an ECG. One approach is to again identify QRS pulses and then locate the P wave pulse prior to the detected QRS complex and the T wave pulse subsequent to the detected QRS complex.

(a) Find the presence of a QRS pulse using a threshold method as before. That is, a QRS pulse is indicated by signal values above a threshold T_q.

(b) However, to locate P and T waves adjacent to the QRS complex, we must develop an algorithm for finding the time domain extent, that is the *scale*, of QRS pulses in the ECG trace. Develop an algorithm that segments the signal into the QRS pulse regions and non-QRS pulse regions. How do you handle the problem of noise that might split a QRS region? Is the method robust to extremely jagged QRS pulses—that is, *splintering* of the QRS complex?

(c) Show how a second, smaller threshold T_p can be used to find the P wave prior to the QRS complex. Similarly, a third threshold T_t can be used to find the T wave after the falling edge of the QRS complex.

(d) Should the thresholds T_p and T_t be global constants, or should they be chosen according to the signal levels of the analog and discrete signal acquisition procedures? Explain.

CHAPTER 2

Discrete Systems and Signal Spaces

The first chapter introduced many different sorts of signals—simple, complicated, interesting, boring, synthetic, natural, clean, noisy, analog, discrete—the initial mixed stock of fuel for the signal analysis machinery that we are going to build. But few signals are ends in themselves. In an audio system, for example, the end result is music to our ears. But that longitudinal, compressive signal is only the last product of many transformations of many representations of the sound on its path from compact disc to cochlea. It begins as a stretch of some six billion tiny pits on a compact disc. A laser light strobes the disc, with its reflection forming a pair of 16-bit sound magnitude values 44,000 times each second. This digital technique, known as *Pulse Code Modulation* (PCM), provides an extremely accurate musical tone rendition. Filtering circuits remove undesirable artifacts from the digital signal. The digital signal is converted into analog form, filtered again, amplified, bandpass filtered through the graphic equalizer, amplified again, and finally delivered strong and clean to the speakers. The superior sound quality of digital technology has the drawback of introducing some distortion at higher frequencies. Filtering circuits get rid of some distortion. Since we are human, though, we cannot hear the false notes; such interference occurs at frequencies above 22 kHz, essentially outside our audio range. Of the many forms the music signal takes through the stereo equipment, all but the last are transitional, intended for further conversion, correction, and enhancement. Indeed, the final output is pleasant only because the design of the system incorporates many special intermediate processing steps. The abstract notion of taking an input signal, performing an operation on it, and obtaining an output is called a *system*. Chapter 2 covers systems for discrete signals.

As a mathematical entity, a system is analogous to a vector-valued function on vectors, except that, of course, the "vectors" have an infinite extent. Signal processing systems may require a single signal, a pair of signals, or more for their inputs. We shall develop theory primarily for systems that input and output a single signal. Later (Chapter 4) we consider operations that accept a signal as an input but fundamentally change it or break it down somehow to produce an output that is not a signal. For example, the output could be a structural description, an interpretation, or

Signal Analysis: Time, Frequency, Scale, and Structure, by Ronald L. Allen and Duncan W. Mills
ISBN: 0-471-23441-9

just a number that indicates the type of the signal. We will call this a *signal analysis system* in order to distinguish it from the present case of *signal processing systems*.

Examples of systems abound in electronic communication technology: amplifiers, attenuators, modulators, demodulators, coders, decoders, and so on. A radio receiver is a system. It consists of a sequence of systems, each accepting an input from an earlier system, performing a particular operation on the signal, and passing its output on to a subsequent system. The entire cascade of processing steps converts the minute voltage induced at the antenna into sound waves at the loudspeaker. In modern audio technology, more and more of the processing stages operate on digital signal information. The compact disc player is a wonderful example, embodying many of the systems that we cover in this chapter. Its processed signals take many forms: discrete engravings on the disc, light pulses, digital encodings, analog voltages, vibration of the loudspeaker membrane, and finally sound waves.

Although systems that process on digital signals may not be the first to come to mind—and they are certainly not the first to have been developed in electronic signal conditioning applications—it turns out that their mathematical description is much simpler. We shall cover the two subjects separately, beginning here with the realm that is easier realm to conquer: discrete signal spaces and systems. Many signal processing treatments combine the introduction of discrete and continuous time systems [1–4]. Chapter 3 covers the subtler theory of analog systems.

2.1 OPERATIONS ON SIGNALS

This section explores the idea of a discrete system, which performs an operation on signals. To help classify systems, we define special properties of systems, provide examples, and prove some basic theorems about them. The proofs at this level are straightforward.

A discrete system is a function that maps discrete signals to discrete signals. Systems may be defined by rules relating input signals to output signals. For example, the rule $y(n) = 2x(n)$ governs an *amplifier* system. This system multiplies each input value $x(n)$ by a constant $A \geq 1$. If H is a system and $x(n)$ is a signal, then $y = H(x)$ is the output of the system H, given the input signal x. More compact and common, when clarity permits, is $y = Hx$. To highlight the independent variable of the signals we can also say $y(n) = H(x(n))$. But there should be no misunderstanding: The system H operates on the whole signal x not its individual values $x(n)$, found at time instants n. Signal flow diagrams, with arrows and boxes, are good for visualizing signal processing operations (Figure 2.1).

Not every input signal to a given system produces a valid output signal. Recall that a function on the real numbers might not have all real numbers in its domain. An example is $f(t) = \sqrt{t}$ with $\text{Domain}(f) = \{t \in \mathbb{R}\colon t \geq 0\}$. Consider now the *accumulator* system $y = Hx$ defined by the rule

$$y(n) = \sum_{k=-\infty}^{n} x(k)\,. \tag{2.1}$$

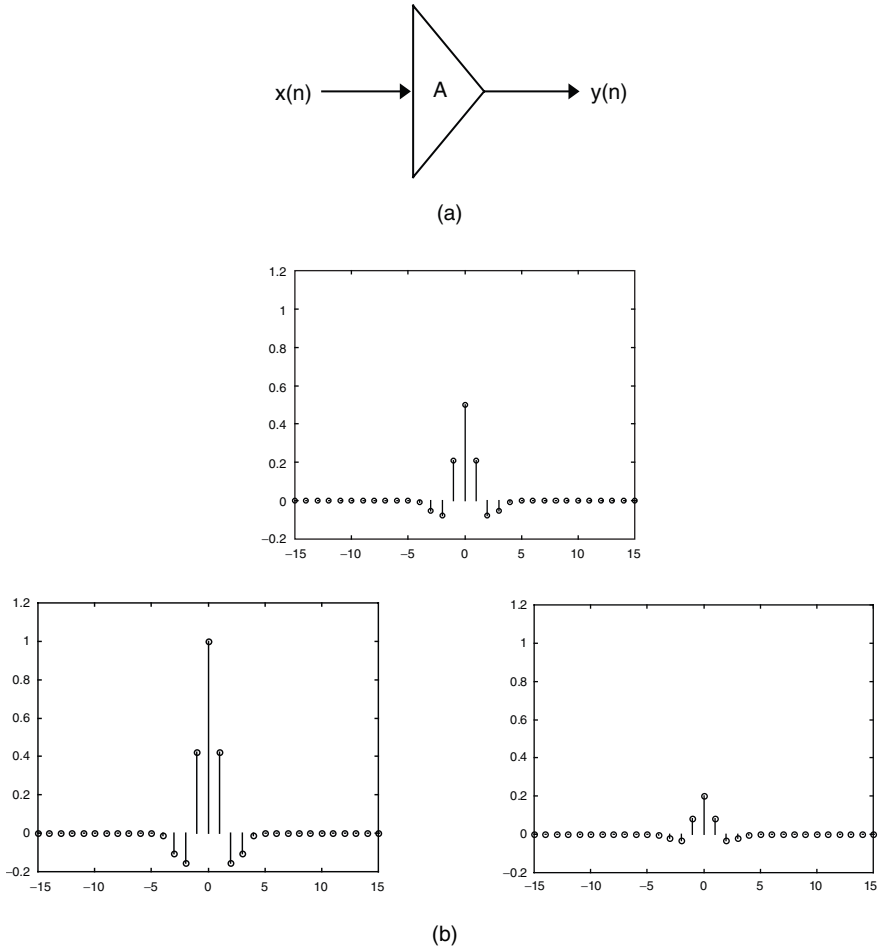

Fig. 2.1. (a) Amplifier system symbol. (b) A sinusoidal pulse, amplification by factor $A = 2$, and attenuation by factor $A = 0.4$.

With $x(n) = 1$ for all n, H has no output. So, as with functions on the real numbers, it is best to think of a system as a partial function on discrete signals.

2.1.1 Operations on Signals and Discrete Systems

There are many types of operations on signals and the particular cases that happen to be discrete systems. We list a variety of cases, some quite simple. But it will turn out that many types of discrete systems decompose into such simple system components, just as individual signals break down into sums of shifted impulses.

Definition (Discrete System). A *discrete system* H is a partial function from the set of all discrete signals to itself. If $y(n)$ is the signal output by H from the input $x(n)$, then $y = Hx$ or $y = H(x)$. It is common to call y the *response* of the system H to input

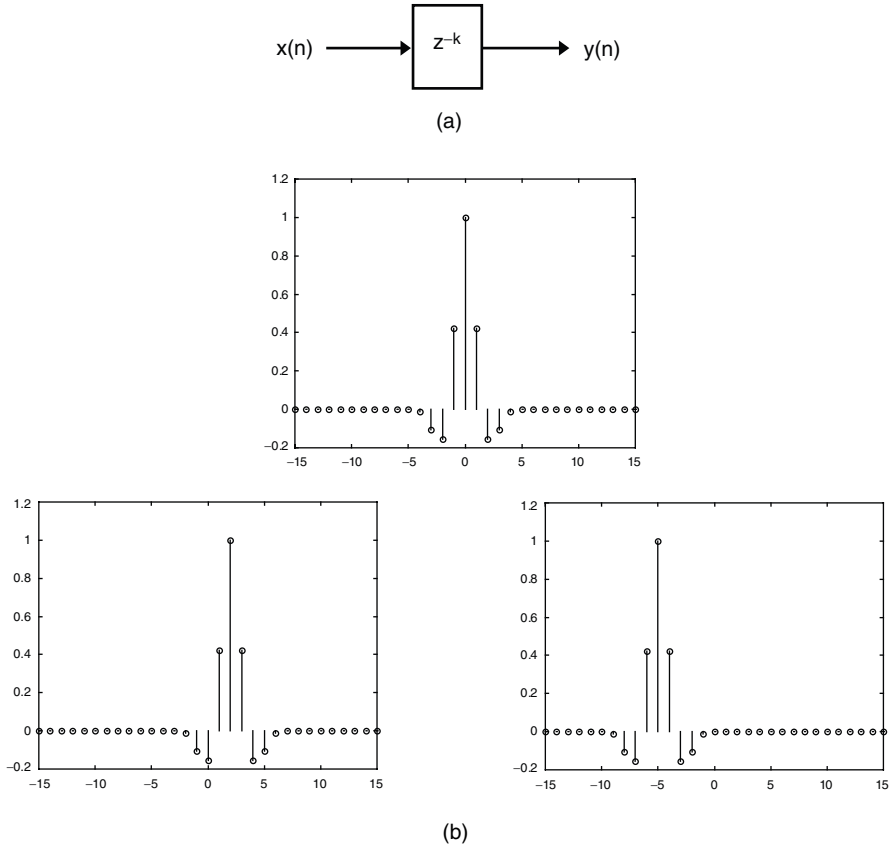

Fig. 2.2. Translation systems. (a) Diagram for a translation system, $y(n) = x(n-k)$. (b) discrete sinusoidal pulse within a Gaussian envelope, $x(n)$; $x(n-k)$, with $k = 2$; and $x(n-k)$ with $k = -5$.

x. The set of signals x for which some $y = Hx$ is the *domain* of the system H. The set of signals y for which $y = Hx$ for some signal x is the *range* of H.

One simple signal operation is to multiply each signal value by a constant (Figure 2.1). If H is the system and $y = Hx$, then the output values $y(n)$ are related to input values by $y(n) = Ax(n)$. This operation *inverts* the input signal when $A < 0$. When $|A| > 1$, the system *amplifies* the input. When $|A| < 1$, the system *attenuates* the input signal. This system is also referred to as a *scaling* system. (Unfortunately, another type of system, one that dilates a signal by distorting its independent variable, is also called a scaling system. Both appellations are widespread, but the two notions are so different that the context is usually enough to avoid confusion.)

The domain of an amplification system is all discrete signals. Except for the case $A = 0$, the range of all amplification systems is all discrete signals.

Another basic signal operation is to delay or advance its values (Figure 2.2). Thus, if $x(n)$ is an input signal, this system produces an output signal $y(n) = x(n-k)$

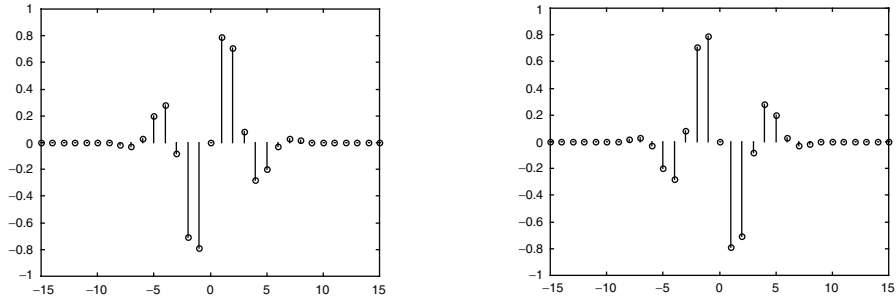

Fig. 2.3. Time reversal $y(n) = x(-n)$. There does not seem to be a conventional block diagram symbol for time reversal, perhaps owing to its physical impossibility for time-based signals.

for some integer k. This is called a *time shift* when the signal's independent variable indicates a time instant or a translation when the independent variable stands for a non-time quantity, such as distance. If $k > 0$, then the shift operation is a *delay.* If $k < 0$, then this system *advances* the signal. The diagram notation z^{-k} is inspired by the notions of the impulse response of the translation system, which we shall discover later in this chapter, and the z-transform (Chapter 8).

The set of all translates of a signal is closed under the translation operation. This system is also commutative; the order of two successive translations of a signal does not matter. Translations cause no domain and range problems. If T is a translation system, then $Domain(T) = \text{Range}(T) = \{s(n)$: *s is a discrete signal*$\}$.

Signal *reflection* reverses the order of signal values: $y(n) = x(-n)$. For time signals, we will call this a *time reversal* system (Figure 2.3). It flips the signal values $x(n)$ around the instant $n = 0$. Note that the reflection and translation operations do not commute with one another. If H is a reflection system and G is a translation $y(n) = x(n - k)$, then $H(Gx) \neq G(Hx)$ for all x unless $k = 0$. Notice also that we are careful to say "for all x" in this property. In order for two systems to be identical, it is necessary that their outputs are identical when their inputs are identical. It is not enough that the system outputs coincide for a particular input signal.

Signal *addition* or *summation* adds a given signal to the input, $y(n) = x(n) + x_0(n)$, where $x_0(n)$ is a fixed signal associated with the system H (Figure 2.4). If we allow systems with two inputs, then we can define $y = H(v,w) = v + w$.

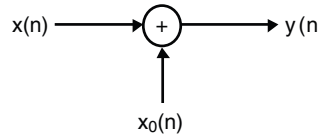

Fig. 2.4. System $y = Hx$ adds another (fixed) signal to the input.

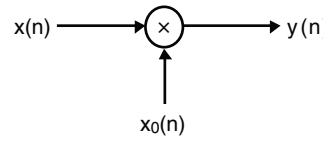

Fig. 2.5. System $y = Hx$ multiplies the input term-by-term with another (fixed) signal. This also called *modulation*, especially in communication theory.

Another type of system, called a *multiplier* or *modulator*, forms the termwise product of the input, $y(n) = x(n)x_0(n)$, where $x_0(n)$ is a fixed signal associated with the system H (Figure 2.5). Note carefully that the product system is *not* written with an asterisk operator $y = x*h$. This is the notation for convolution, a more important signal operation, which we will cover below.

The *correlation* of two signals is the sum of their termwise products:

$$C = \sum_{n=-\infty}^{\infty} x(n)\overline{y(n)}\,. \tag{2.2}$$

Signals $x(n)$ and $y(n)$ may be complex-valued; in this case, we take the complex conjugate of the second operand. The correlation of a signal with itself, the *autocorrelation*, will then always be a non-negative real number. In (2.2) the sum is infinite, so the limit may not exist. Also note that (2.2) does not define a system, because the output is a number, not a signal. When we study abstract signal spaces later, we will call correlation the *inner product* of the two signals. It is a challenge to find classes of signals, not necessarily having finite support, for which the inner product always exists.

The *cross-correlation system* is defined by the input–output relation

$$y(n) = (x \circ h)(n) = \sum_{k=-\infty}^{\infty} x(k)h(n+k)\,. \tag{2.3}$$

In (2.3) the signal $h(n)$ is translated before the sum of products correlation is computed for each $y(n)$. If the signals are complex-valued, then we use the complex conjugate of $h(n)$:

$$y(n) = (x \circ h)(n) = \sum_{k=-\infty}^{\infty} x(k)\overline{h(n+k)}\,. \tag{2.4}$$

This makes the autocorrelation have a non-negative real value for $n = 0$; if $x = h$,

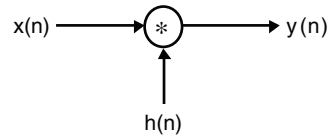

(a)

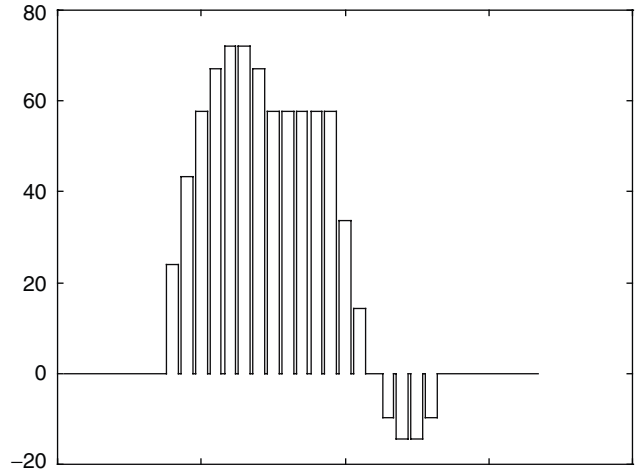

(b)

Fig. 2.6. Convolution. (a) The system $y = Hx = (h*x)(n)$. (b) An example convolving two finitely supported signals a square pulse $h(n) = 4.8[u(n-8) - u(n-20)]$ and a triangular pulse $x(n) = (6-n)[u(n-1) - u(n-9)]$.

$$y(0) = (x \circ h)(0) = \sum_{k=-\infty}^{\infty} x(k)\overline{x(nk)} = \|x\|_2^2, \tag{2.5}$$

the square of the l^2 norm of x, which will become quite important later.

Convolution seems strange at first glance—a combination of reflection, translation, and correlation:

$$y(n) = (x * h)(n) = \sum_{k=-\infty}^{\infty} x(k)h(n-k). \tag{2.6}$$

But this operation lies at the heart of linear translation invariant system theory, transforms, and filtering. As Figure 2.6 shows, in convolution one signal is flipped and then shifted relative to the other. At each shift position, a new $y(n)$ is calculated as the sum of products.

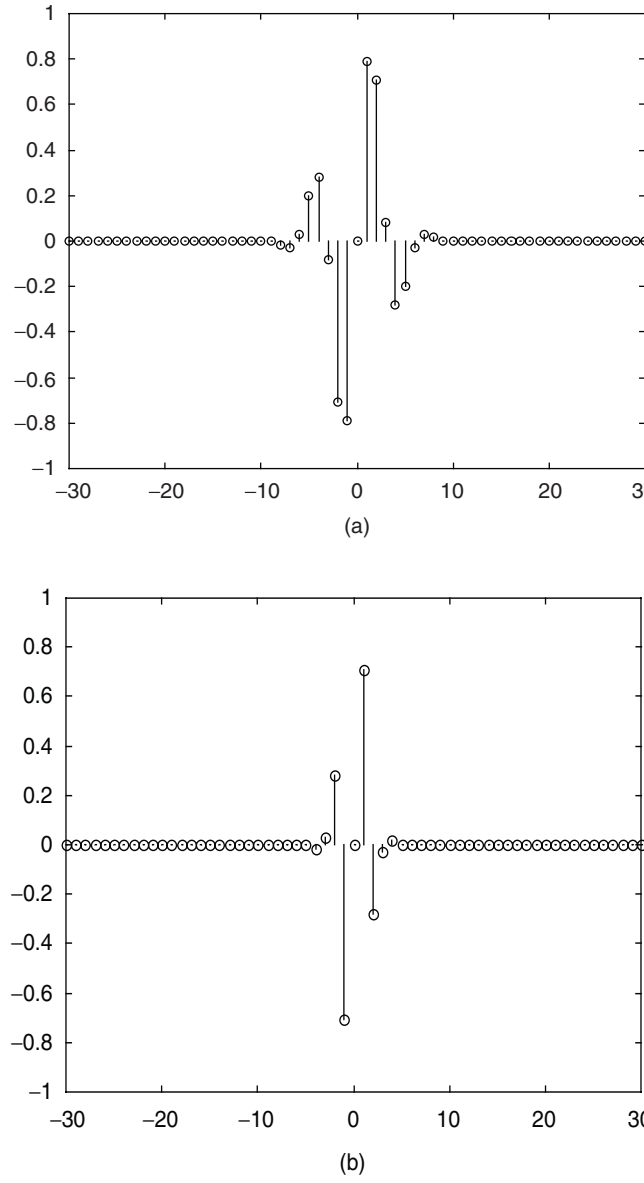

Fig. 2.7. Uniform sampling.

A *subsampling* or *downsampling* system skips over samples of the input signal: $y(n) = x(kn)$, where $k > 0$ is the *sampling interval*. This is *uniform* sampling (Figure 2.7). In nonuniform sampling, the intervals between samples vary. Both forms of signal sampling have proven handy in applications.

Sampling is useful when the content of a signal contains less information than the density of the samples warrants. In uniform sampling, the relevant signal information is adequately conveyed by every kth sample of the input. Thus, subsampling is a preliminary signal compression step. Scientists and engineers, attempting to squeeze every bit of digital information through narrow bandwidth communication channels, have been seeking better ways to compress signals and images in recent years [5]. Technologies such as network video and cellular radio communications hinge on the efficiency and integrity of the compression operations. Also, in signal and image analysis applications, we can filter signals and subsample them at multiple rates for coarse-to-fine recognition. One outcome of all the research is that if the filtering and subsampling operations are judiciously chosen, then the sampled signals are adequate for exact reconstruction of the original signal. Progressive transmission is therefore feasible. Moreover, there is an unexpected, intimate connection between multirate signal sampling and the modern theory of time-scale transforms, or wavelet analysis [6]. Later chapters detail these aspects of signal subsampling operations. Nonuniform sampling is useful when some local regions of a signal must be more carefully preserved in the sampled output. Such systems have also become the focus of modern research efforts [7].

An *upsampling* operation (Figure 2.8) inserts extra values between input samples to produce an output signal. Let $k > 0$ be an integer. Then we form the upsampled output signal $y(n)$ from input signal $x(n)$ by

$$y(n) = \begin{cases} x\left(\frac{n}{k}\right) & \text{if } \frac{n}{k} \in \mathbb{Z}, \\ 0 & \text{if otherwise.} \end{cases} \tag{2.7}$$

A *multiplexer* merges two signals together:

$$y(n) = \begin{cases} x_0(n) & \text{if } n \text{ is even,} \\ x_1(n) & \text{if } n \text{ is odd.} \end{cases} \tag{2.8}$$

A related system, the *demultiplexer*, accepts a single signal $x(n)$ as an input and produces two signals on output, $y_0(n)$ and $y_1(n)$. It also is possible to multiplex and demultiplex more than two signals at a time. These are important systems for communications engineering.

Thresholding is an utterly simple operation, ubiquitous as well as notorious in the signal analysis literature. Given a threshold value T, this system segments a signal:

$$y(n) = \begin{cases} 1 & \text{if } x(n) \geq T, \\ 0 & \text{if } x(n) < T. \end{cases} \tag{2.9}$$

The threshold value T can be any real number; however, it is usually positive and a thresholding system usually takes non-negative real-valued signals as inputs. If the input signal takes on negative or complex values, then it may make sense to first produce its magnitude $y(n) = |x(n)|$ before thresholding.

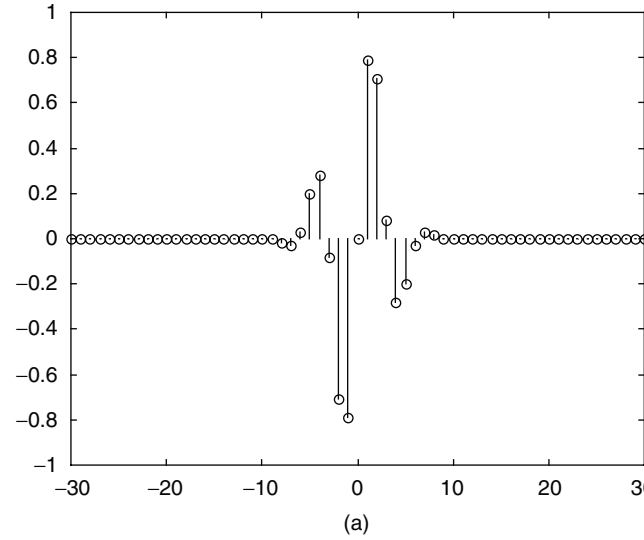

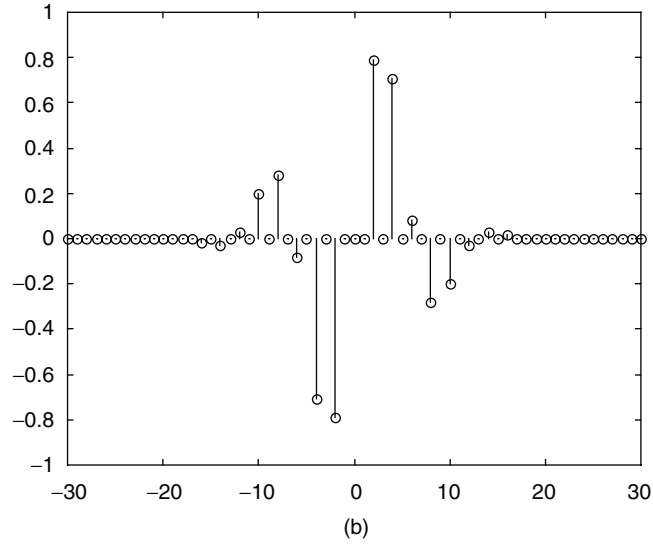

Fig. 2.8. Upsampling operation.

The thresholding operation of (2.9) is an elementary signal analysis system. Input signals $x(n)$ are labeled by the output signal $y(n)$ which takes on two values, 0 or 1. Thus, 1 indicates the presence of meaningful information, and 0 indicates the presence of nonmeaningful information in $x(n)$. When we say that the thresholding operation *segments* the signal into useful and nonuseful portions, we mean that the system partitions the input signal's domain. Typically, we use thresholding as a crude method for removing background noise from signals. A problem with brute-force thresholding is that signals may contain noise impulses that are as large in magnitude as some meaningful signal values. Furthermore, the noise magnitude may be as large as the interesting signal values and thresholding therefore fails completely. Chapter 4 elaborates on thresholding subtleties.

Threshold selection dramatically affects the segmentation. Thresholding usually follows the filtering or transforming of an input signal. The trick is choosing the proper threshold so that the output binary image correctly marks signal regions. To gain some appreciation of this, let's consider a thresholding problem on a two-dimensional discrete signal—that is an 8-bit, 256 gray scales image. Figure 2.9 shows the original image, a parcel delivery service's shipping label. A very thoroughly studied image analysis problem is to interpret the text on the label so that automated systems can handle and route the parcel to its destination. Optical character recognition (OCR) systems read the individual characters. Since almost all current OCR engines accept only binary image data, an essential first step is to convert this gray scale image to binary form [8, 9]. Although the image itself is fairly legible, only the most careful selection of a single threshold for the picture suffices to correctly binarize it.

The *accumulator* system, $y = Hx$, is given by

$$y(n) = \sum_{k=-\infty}^{n} x(k). \tag{2.10}$$

The accumulator outputs a value that is the sum of all input values to the present signal instant. Any signal with finite support is in the domain of the accumulator system. But, as already noted, not all signals are in the accumulator's domain. If a signal is absolutely summable (Section 1.6.2), then it is in the domain of the accumulator. Some finite-energy signals are not in the domain of the accumulator. An example that cannot be fed into an accumulator is the finite-energy signal

$$x(n) = \begin{cases} 0 & \text{if } n \geq 0, \\ -\dfrac{1}{n} & \text{if } n < 0. \end{cases} \tag{2.11}$$

A system may extract the nearest integer to a signal value. This called a *digitizer* because in principle a finite-length storage register can hold the integral values produced from a bounded input signal. There are two variants. One kind of digitizer produces a signal that contains the integral *ceiling* of the input,

$$y(n) = \lceil x(n) \rceil = \text{least integer} \geq x(n). \tag{2.12}$$

The other variant produces the integral *floor* of the input,

$$y(n) = \lfloor x(n) \rfloor = \text{greatest integer} \leq x(n)\,. \tag{2.13}$$

The moving average system, $y = Hx$, is given by

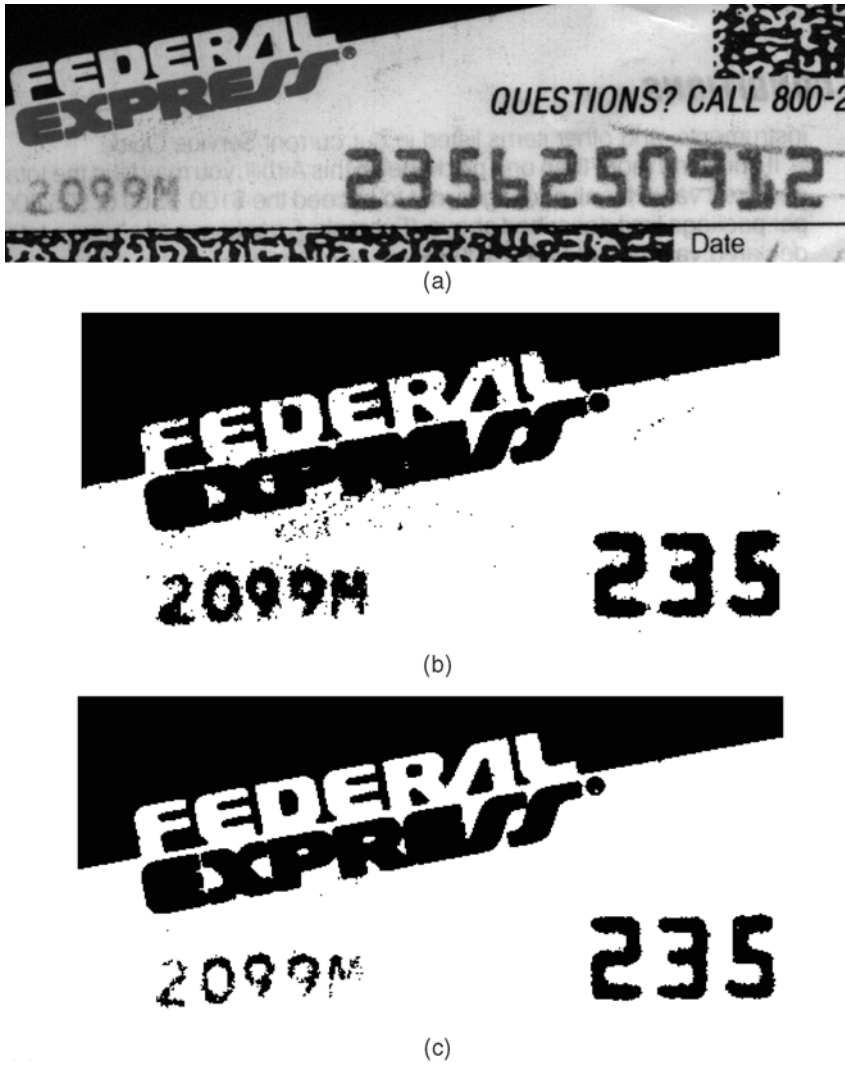

Fig. 2.9. Thresholding. An 8-bit, 256 gray scales image of a shipping label (a). First threshold applied (b). Here the threshold results in an image that is too dark. The company logo is only marginally readable. With a different threshold (c), the logo improves, but the shipping code beneath begins to erode. It is difficult to pick an appropriate global threshold for the image.

$$y(n) = \frac{1}{2N+1} \sum_{k=-N}^{N} x(k). \tag{2.14}$$

This system outputs a signal that averages the $2N + 1$ values around each $x(n)$. This smoothes the input signal, and it is commonly used to improve the signal-to-noise ratio of raw signals in data acquisition systems.

2.1.2 Operations on Systems

We can build more complicated systems by combining the systems, taking the output of one system and using it as an input to another.

Definition (System Composition). Let H and G be systems. Then the *composite system GH* is the system defined by $y(n) = G(H(x(n))$. GH is called the *composition* or the *cascade* of G with H.

Remark. In general, the order of system composition is important. Many signal operations—however intuitive and simple they may seem—may not commute with one another. In particular, note again that the shift operation does not commute with reflection. If G is a shift operation, $G(x(n)) = x(n - k)$, k is nonzero, and H is a reflection, then $GH \neq HG$.

2.1.3 Types of Systems

Now let us categorize the various systems we have considered. These characterizations will prove useful for understanding the behavior of a system in an application. Some systems, because of the form of their definition, may seem impossible to implement on a computer. For example, the accumulator (2.9) is defined with an infinite sum that uses every earlier input signal value. We have observed already that it is an example of a system in which not every input produces a meaningful output. Do we need an infinite set of memory locations to store input signal values? No, we can still implement an accumulator on a computer by exploiting the recurrence relation $y(n) = y(n - 1) + x(n)$. It is only necessary to know an initial value of $y(n)$ at some past time instant $n = n_0$. The accumulator belongs to a class of systems—called *recursive* systems—that can be implemented by reusing output values from previous time instants.

Now we develop some basic categories for systems: static and dynamic systems, recursive systems, and causal systems.

We can start by distinguishing systems according to whether they require computer memory for signal values at other than the current instant for their implementation. Let H be a system $y = Hx$. H is *static* if $y(n)$ can always be found from the current value of input signal $x(n)$ and n itself. That is, H is *static* when $y(n) = F(x(n))$ for some defining function or rule F for H. H is *dynamic* when it must use values $x(m)$ or $y(m)$ for $m \neq n$ in order to specify $y(n)$.

A system that depends on future values of the input signal $x(n)$ is dynamic too. This seems impossible, if one thinks only of signals that have a time-related independent variable. But signals can independent variables of distance, for example. So the values of $x(n + k)$, $k > 0$, that need to be known to compute $y(n)$ are just values of the input signal in a different direction. Systems for two-dimensional signals (i.e., images) are in fact a very widely studied case of signals whose values may depend on "future" values of the input.

Example. The accumulator is a dynamic system because, for a general input $x(n)$, it cannot be implemented without knowing either

(i) $x(n)$ and all previous values of the input signal; or
(ii) for some $k > 1$, $y(n - k)$ and all $x(n - k + p)$ for $p = 0, ..., k$.

Dynamic systems require memory units to store previous values of the input signal. So static systems are also commonly called *memoryless* systems.

A concept related to the static versus dynamic distinction is that of a *recursive* system. Pondering the accumulator system once more, we note that this dynamic system cannot be implemented with a finite set of memory elements that only contain previous values of $x(n)$. Let H be a system, $y = Hx$. H is *nonrecursive* if there is an $M > 0$, such that $y(n)$ can always be found as a function of $x(n)$, $x(n - 1)$, ..., $x(n - M)$. If $y(n)$ depends on $y(n - 1)$, $y(n - 2)$, ..., $y(n - N)$, for some $N > 0$, and perhaps upon $x(n - 1)$, ..., $x(n - M)$, for some M, then H is *recursive*.

A system $y = Hx$ is *causal* if $y(n)$ can always be computed from present and past inputs $x(n)$, $x(n - 1)$, $x(n - 2)$, ... Real, engineered systems for time-based signals must always be causal, and, if for no other reason, causality is important. Nevertheless, where the signals are not functions of discrete time variables, noncausal signals are acceptable. A nonrecursive system is causal, but the converse is not true.

Examples (System Causality)

(i) $y(n) = x(n) + x(n - 1) + x(n - 2)$ is causal and nonrecursive.
(ii) $y(n) = x(n) + x(n + 1)$ is not causal.
(iii) $y(n) = x(2 - n)$ is noncausal.
(iv) $y(n) = x(|n|)$ is noncausal.
(v) The accumulator (2.10) is causal.
(vi) The moving average system (2.14) is not causal.

2.2 LINEAR SYSTEMS

Linearity prevails in many signal processing systems. It is desirable in entertainment audio systems, for example. Underlying the concept of linearity are two ideas, and they are both straightforward:

(i) When the input signal to the system is larger (or smaller) in amplitude, then the output signal from the system produces is proportionally larger (or smaller). This is the *scaling* property of linearity. In other words, if a signal is amplified or attenuated and then input to a linear system, then the output is a signal that is amplified or attenuated by the same amount.

(ii) Furthermore, if two signals are added together before input, then the result is just the sum of the outputs that would occur if each input component were passed through the system independently. This is the *superposition* property.

Obviously, technology cannot produce a truly linear system; there is a range within which the linearity of a system can be assumed. Real systems add noise to any signal. When the input signal becomes too small, the output may disappear into the noise. The input could become so large intensity that the output is distorted. Worse, the system may fail if subjected to huge input signals. Practical, nearly linear systems are possible, however, and engineers have discovered some clever techniques to make signal amplification as linear as possible.

When amplification factors must be large, the nonlinearity of the circuit components—vacuum tubes, transistors, resistors, capacitors, inductors, and so on—becomes more and more of a factor affecting the output signal. The discrete components lose their linearity at higher power levels. A change in the output proportional to the change in the input becomes very difficult to maintain for large amplification ratios. Strong amplification is essential, however, if signals must travel long distances from transmitter to repeater to receiver. One way to lessen the distortion by amplification components is to feed back a tiny fraction of the output signal, invert it, and add it to the input signal. Subject to a sharp attenuation, the feedback signal remains much closer to true linearity. When the output varies from the amplification setting, the input biases in the opposite direction. This restores the amplified signal to the required magnitude. An illustration helps to clarify the concept (Figure 2.10).

From Figure 2.10 we can see that the output signal is $y(n) = A(x(n) - By(n-1))$. Assuming that the output is relatively stable, so that $y(n) \approx y(n-1)$, we can express

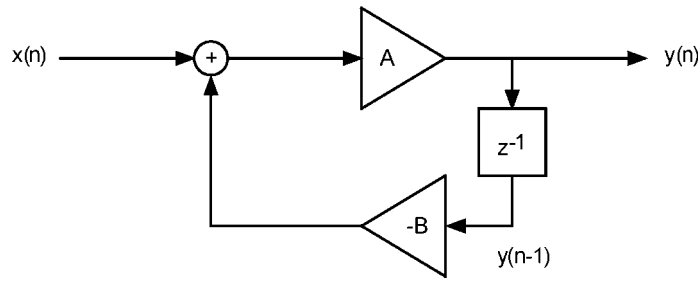

Fig. 2.10. Feedback amplifier.

the system gain as follows:

$$y(n) = \frac{A}{AB+1}x(n) = \frac{1}{B+A^{-1}}x(n). \tag{2.15}$$

Evidently, if the amplification factor A is large, then A^{-1} is small, and the system gain depends mostly on the inverse of the attenuation factor in the feedback. It is approximately B^{-1}. Due to its low power levels, the feedback circuit is inherently more linear, and it improves the overall linearity of the system immensely. Achieving good linearity was an early stumbling block in the development of the telephone system.[1]

Since many important results and characterizations about systems follow from the assumption of linearity, it is a central object of our study in signal processing and analysis.

2.2.1 Properties

Let us formalize these ideas and explore the properties of linear systems.

Definition (Linear System). Let $y = Hx$, and let A be a scalar (real or complex number). The system H is *linear* if it obeys the scaling and superposition properties:

(i) *Scaling*:

$$H(Ax) = AH(x). \tag{2.16}$$

(ii) *Superposition*:

$$H(x+y) = Hx + Hy. \tag{2.17}$$

There is a useful criterion for system linearity.

Proposition (Linearity Criterion). If system H is linear, $x(n) = 0$ for all n, and $y = Hx$, then $y(n) = 0$ for all n also.

Proof: Although it seems tricky to many who are not familiar with this type of argument, the proof is quite simple. If $x(n) = 0$ for all n, then $x(n) = x(n) + x(n)$. Hence, $y(n) = H(x(n) + x(n)) = H(x(n))$. But $H(x + x) = Hx + Hx$ by superposition. So $Hx + Hx = Hx$; the consequence, subtracting Hx from both sides of this equation, is that $0 = Hx = y$. That is, $y(n)$ is the zero signal, and the criterion is proven. Note,

[1]The big technical breakthrough came when a Bell Laboratories engineer, Harold Black, had a flash of insight on the ferry from Hoboken, New Jersey, to work in New York City on a summer morning in 1927 [J. R. Pierce and A. M. Noll, *Signals: The Science of Telecommunications*, New York: Scientific American Library, 1990].

by the way, that this last equality is an equality of signals and that the "0" in the equation is really the signal $y(n)$ that is zero for all time instants n. ■

Examples. To show a system is linear, we must check that it satisfies both the scaling and superposition properties. The linearity criterion is helpful for exposing nonlinear systems.

(i) The system $y(n) = 5 + x(n)$ is nonlinear, an easy application of the criterion.
(ii) The system $y(n) = x(n)x(n)$ is nonlinear. The criterion does not help with this example. However, the system violates both the scaling and superposition properties.
(iii) The reflection system $y(n) = x(-n)$ is linear.
(iv) The system $y(n) = \cos(n)x(n)$ is linear. Note this example. The idea of linearity is that systems are linear in their input signals. There may be nonlinear functions, such as $\cos(t)$, involved in the definition of the system relation. Nevertheless, as long as the overall relation between input and output signals obeys both scaling and superposition (and this one does indeed), then the system is linear.

2.2.2 Decomposition

A very useful mathematical technique is to resolve complicated entities into simpler components. For example, the Taylor series from calculus resolves differentiable functions into sums of polynomials. Linear systems can defy initial analysis because of their apparent complexity, and our goal is to break them down into elementary systems more amenable to study. There are two steps:

(i) We first break down signals into sums of scaled, shifted unit impulse signals.
(ii) This decomposition can it turn be used to resolve the outputs of linear systems into sums of simple component outputs.

Proposition (Decomposition). Let $x(n)$ be a discrete signal and define the constants $c_k = x(k)$. Then $x(n)$ can be decomposed into a sum of scaled, shifted impulse signals as follows:

$$x(n) = \sum_{k=-\infty}^{\infty} c_k \delta(n-k)\,. \tag{2.18}$$

Proof: Let $w(n)$ be the right-hand side of (2.18). Then $w(k) = c_k$, since all of the terms $\delta(n-k)$ are zero, unless $n = k$. But this is just $x(k)$ by the definition of the constants c_k. So $w(k) = x(k)$ for all k, completing the proof. ■

The next definition prepares us for a theorem that characterizes discrete linear systems. From the examples above, linear systems can come in quite a few varieties. Sometimes the system's linear nature is nonintuitive. However, any general linear system is completely known by its behavior on one type of input signal: a shifted impulse. (Our proof is informal, in that we assume that scaling and superposition apply to infinite sums and that a convergent series can be rearranged without affecting its limit.)

Definition (Output of Shifted Input). Let H be a linear system and $y = Hx$. Define $y(n, k) = H(x(n-k))$ and $h(n, k) = H(\delta(n-k))$, where δ is the discrete unit impulse signal.

Theorem (Linearity Characterization). Let H be a linear system, $x(n)$ a signal, $c_k = x(k)$, and $y = Hx$. Then

$$y(n) = \sum_{k=-\infty}^{\infty} c_k h(n, k). \tag{2.19}$$

Proof: By the decomposition of discrete signals into impulses, we know that $x(n) = \sum_{k=-\infty}^{\infty} c_k \delta(n-k)$. So with $y(n) = H(x(n))$, it follows from superposition that

$$\begin{aligned} y(n) &= H\left(\sum_{k=-\infty}^{\infty} c_k \delta(n-k)\right) \\ &= H\left(\sum_{k=1}^{\infty} c_k \delta(n-k)\right) + H(c_0 \delta(n)) + H\left(\sum_{k=-\infty}^{-1} c_k \delta(n-k)\right). \end{aligned} \tag{2.20}$$

And then by the scaling property applied to the middle term of (2.20),

$$\begin{aligned} y(n) &= H\left(\sum_{k=-\infty}^{\infty} c_k \delta(n-k)\right) \\ &= H\left(\sum_{k=1}^{\infty} c_k \delta(n-k)\right) + c_0 h(n, 0) + H\left(\sum_{k=-\infty}^{-1} c_k \delta(n-k)\right). \end{aligned} \tag{2.21}$$

Repeatedly using the linearity properties to break out middle terms in (2.21) gives the desired result. ■

2.3 TRANSLATION INVARIANT SYSTEMS

In many real-life systems, the outputs do not depend on the absolute time at which the inputs were done. For example, a compact disc player is a reasonably good time-invariant system. The music played from a compact disc on Monday will not differ substantially when the same disc played on Tuesday. Loosely put, time-invariant systems produce identically shifted outputs from shifted inputs. Since not all systems, of course, are time-based, we prefer to call such systems *translation-invariant*.

To formalize this idea, we need to carefully distinguish between the following:

- The signal $y(n, k)$ is the output of a system, given a delay (or advance, depending on the sign of k) of the input signal $x(n)$ by k time units.
- On the other hand, $y(n - k)$ is the signal obtained by finding $y = Hx$ and then shifting the resulting output signal, $y(n)$, by k.

These two results may not be the same. An example is the system $y(n) = x(n) + n$. It is easy to find input signals $x(n)$ which for this system give $y(n-k) \neq y(n, k)$. Hence, the important definition:

Definition (Translation-Invariant Systems). Let H be the system $y = Hx$. Then, if for all signals $x(n)$ in $Domain(H)$, if $y(n, k) = H(x(n - k)) = y(n - k)$, then H is *translation-invariant*. Another term is *shift-invariant*. For time-based signals, it is common to say *time-invariant*.

To show a system is translation-invariant, we must compare the shifted output, $y(n - k)$, with the output from the shifted input, $H(x(n - k))$. If these are equal for all signals in the system's domain, then H is indeed translation-invariant. It is very easy to confuse these two situations, especially for readers new to signal processing. But there is a simple, effective technique for showing translation-invariance: we rename the input signal after it is shifted, hiding the shift amount.

Examples (Translation-Invariance). Let us try this technique on the systems we checked for linearity earlier.

(i) The system $y(n) = 5 + x(n)$ is translation-invariant. If $y = Hx$, then the output shifted by k is $y(n - k) = 5 + x(n - k)$. We just substitute "$n - k$" for "n" at each instance in the defining rule for the system's input–output relation. What if we translate the input by k units also? This produces $x(n - k)$. We rename it $w(n) = x(n - k)$. This hides the shift amount within the new name for the input signal. It is easy to see what H does to any signal, be it named x, w, u, v, or whatever. H adds the constant 5 to each signal value. Hence we see $y(n, k) = H(w(n)) = 5 + w(n)$. Now we put the expression for x in terms

of w back into the expression: $y(n, k) = 5 + x(n - k)$. So $y(n - k) = y(n, k)$, and the system is translation-invariant.

(ii) The system $y(n) = x(n)x(n)$ is translation-invariant. The output shifted by k is $y(n - k) = x(n - k)x(n - k)$. We rename once more the shifted input $w(n) = x(n - k)$. Then $y(n, k) = H(w(n)) = w(n)w(n) = x(n - k)x(n - k)$. Again, the system is translation-invariant.

(iii) The reflection system $y(n) = x(-n)$ is not translation-invariant. The shifted output in this case is $y(n - k) = x(-(n - k)) = x(k - n)$. We make a new name for the shifted input, $w(n) = x(n - k)$. Then $y(n, k) = H(w(n)) = w(-n)$. But $w(-n) = x(-n - k)$. Thus, $y(n - k) \neq y(n, k)$ in general. In particular, we can take $x(n) = \delta(n)$, the unit impulse signal, and $k = 1$. Then $y(n - k) = \delta(1 - n)$, although $y(n, k) = \delta(-1 - n)$.

(iv) The system $y(n) = \cos(n)x(n)$ is not translation-invariant. The shifted output in this case is $y(n - k) = \cos(n - k)x(n - k)$. Once more, we rename the shifted input $w(n) = x(n - k)$. Then $y(n, k) = H(w(n)) = \cos(n)w(n) = \cos(n)x(n - k)$. Again, $y(n - k) \neq y(n, k)$ in general.

2.4 CONVOLUTIONAL SYSTEMS

The most important systems obey both the linearity and translation-invariance properties. Many physical systems are practically linear and practically translation-invariant. If these special properties can be assumed for a physical system, then the analysis of that system simplifies tremendously. The key relationship, it turns out, is that linear translation-invariant systems are fully characterized by one signal associated with the system, the impulse response. By way of contrast, think again of the characterization of linear systems that was given in Section 2.2. For a linear system, there is a characterization of the system's outputs as sums of scaled signals $h(n, k)$. However, there are in general an infinite number of $h(n, k)$ components. This infinite set reduces to just one signal if the system is translation-invariant too.

2.4.1 Linear, Translation-Invariant Systems

This is the most important type of system in basic signal processing theory.

Definition (LTI System). A system H that is both linear and translation-invariant is called an *LTI system*. When signals are functions of an independent time variable, we may say *linear, time-invariant*, but the abbreviation is the same. Some authors use the term *shift-invariant* and refer to *LSI* systems.

Definition (Impulse Response). Let H be an LTI system and $y = Hx$. Then we define the impulse response of the system as $h(n) = H(\delta(n))$, where δ is the discrete unit impulse signal.

Theorem (Convolution). Let H be an LTI system, $y = Hx$, and $h = H\delta$. Then

$$y(n) = \sum_{k=-\infty}^{\infty} x(k)h(n-k)\,. \tag{2.22}$$

Proof: With H linear, there follows the decomposition

$$y(n) = \sum_{k=-\infty}^{\infty} x(k)h(n,k) = \sum_{k=-\infty}^{\infty} x(k)H(\delta(n-k))\,. \tag{2.23}$$

But since H is translation-invariant, $h(n-k) = H(\delta(n-k))$. Inserting this into (2.23) proves the theorem. ■

Remarks. Note that (2.22) is the convolution of the input signal $x(n)$ and the impulse response $\delta(n)$ of the LTI system H: $y(n) = (x*h)(n)$. For this reason, we call LTI systems *convolutional*. Although it is a simple result, the importance of the theorem cannot be overemphasized. In order to understand a system, we must know how it operates on its input signals. This could be extremely complicated. But for LTI systems, all we need to do is find one signal—the system's impulse response. Then, for any input, the output can be computed by convolving the input signal and the impulse response. There is some more theory to cover, but let us wait and give an application of the theorem.

Example (System Determination). Consider the LTI system $y = Hx$ for which only two test cases of input–output signal pairs are known: $y_1 = Hx_1$ and $y_2 = Hx_2$, where $y_1 = [-2, 2, \underline{0}, 2, -2]$, $x_1 = [2, \underline{2}, 2]$, $y_2 = [1, -2, \underline{2}, -2, 1]$, $x_2 = [-1, \underline{0}, -1]$. (Recall from Chapter 1 the square brackets notation: $x = [n_{-M}, ..., n_{-1}, \underline{n_0}, n_1, ..., n_N]$ is the finitely supported signal on the interval $[M, N]$ with $x(0) = n_0$, $x(-1) = n_{-1}$, $x(1) = n_1$, and so on. The underscored value indicates the zero time instant value.) The problem is to find the output $y = Hx$ when x is the ramp signal $x = [1, \underline{2}, 3]$. An inspection of the signal pairs reveals that $2\delta(n) = x_1 + 2x_2$. Thus, $2h = Hx_1 + 2Hx_2 = y_1 + 2y_2$ by the linearity of H. The impulse response of H must be the signal $(y_1 + 2y_2)/2 = h = [-1, \underline{2}, -1]$. Finding the impulse response is the key. Now the convolution theorem implies that the response of the system to $x(n)$ is the convolution $x*h$. So $y = [-1, 0, \underline{0}, 4, -3]$.

Incidentally, this example previews some of the methods we develop extensively in Chapter 4. Note that the output of the system takes zero values in the middle of the ramp input and large values at or near the edges of the ramp. In fact, the impulse response is known as a *discrete Laplacian operator*. It is an elementary example of a signal *edge detector*, a type of signal analysis system. They produce low magnitude outputs where the input signal is constant or uniformly changing, and they produce large magnitude outputs where the signal changes abruptly. We could proceed further to find a threshold value T for a signal analysis system that would mark the signal edges with nonzero values. In fact, even this easy example gives us a taste of

the problems with picking threshold values. If we make T large, we will only detect the large step edge of the ramp input signal above. If we make T small enough to detect the beginning edge of the ramp, then there are two instants at which the final edge is detected.

2.4.2 Systems Defined by Difference Equations

A discrete difference equation can specify a system. Difference equations are the discrete equivalent of differential equations in continuous-time mathematical analysis, science, and engineering. Consider the LTI system $y = Hx$ where the input and output signals always satisfy a linear, constant-coefficient difference equation:

$$y(n) = \sum_{k=1}^{K} a_k y(n-k) + \sum_{m=0}^{M} b_m x(n-m). \tag{2.24}$$

The output $y(n)$ can be determined from the current input value, recent input values, and recent output values.

Example. Suppose the inputs and outputs of the LTI system H are related by

$$y(n) = ay(n-1) + x(n), \tag{2.25}$$

where $a \neq 0$. In order to characterize inputs and outputs of this system, it suffices to find the impulse response. There are, however, many signals that may be the impulse response of a system satisfying (2.25). If $h = H\delta$, is an input–output pair that satisfies (2.25), with $x = \delta$ and $y = h$, then a single known value of $h(n_0)$ determines all of $h(n)$. Let us say that $h(0) = c$. Then repeatedly applying (2.25) we can find $h(1) = ac + \delta(1) = ac$; $h(2) = a^2c$; and, for non-negative k, $h(k) = a^k c$. Furthermore, by writing the equation for $y(n-1)$ in terms of $y(n)$ and $x(n)$, we have

$$y(n-1) = \frac{y(n) - x(n)}{a}. \tag{2.26}$$

Working with (2.26) from the initial known value $h(0) = c$ gives $h(k) = a^k(c-1)$, for $k < 0$. So

$$h(n) = \begin{cases} a^n c & \text{if } n \geq 0, \\ a^n (c-1) & \text{if } n < 0. \end{cases} \tag{2.27}$$

From the convolution relation, we now know exactly what LTI systems satisfy the difference equation (2.25). It can be shown that if the signal pair (δ, h) satisfies the difference equation (2.24), then the pair (x, $h*x$) also satisfies (2.24).

Example. Not all solutions (x, y) of (2.24) are an input–output pair for an LTI system. To see this, let $a \neq 0$ and consider the *homogeneous* linear difference equation

$$y(n) - ay(n-1) = 0. \tag{2.28}$$

Clearly, any signal of the form $y(n) = da^n$, where d is a constant, satisfies the homogeneous equation. If (x, y) is a solution pair for (2.25), and y_h is a solution of the homogeneous equation, then $(x, y + y_h)$ is yet another solution of (2.25). We know by the linearity criterion (Section 2.2) that for an LTI system, the only possible input–output pair (x, y) when $x(n) = 0$ for all n is $y(n) = 0$ for all n. In particular, $(0, da^n)$ is a solution of (2.25), but not an input–output pair on any LTI system.

2.4.3 Convolution Properties

Although it seems at first glance to be a very odd operation on signals, convolution is closely related to two quite natural conditions on systems: linearity and translation-invariance. Convolution in fact enjoys a number of algebraic properties: associativity, commutativity, and distributivity.

Proposition (Convolution Properties). Let x, y, and z be discrete signals. Then

(i) (*Associativity*) $x*(y*z) = x*(y*z)$.
(ii) (*Commutativity*) $x*y = y*x$.
(iii) (*Distributivity*) $x*(y+z) = x*y + x*z$.

Proof: We begin with associativity. Let $w = y*z$. Then, by the definition of convolution, we have $[x*(y*z)](n) = (x*w)(n)$. But, x convolved with w is

$$\begin{aligned}\sum_{k=-\infty}^{\infty} x(k)w(n-k) &= \sum_{k=-\infty}^{\infty} x(k) \sum_{l=-\infty}^{\infty} y(l)z((n-k)-l) \\ &= \sum_{l=-\infty}^{\infty}\sum_{k=-\infty}^{\infty} x(k)y(l)z((n-k)-l). \end{aligned} \tag{2.29}$$

Let $p = k + l$ so that $l = p - k$, and note that $p \to \pm\infty$ as $l \to \pm\infty$. Then make the change of summation in (2.29):

$$\begin{aligned}(x * w)(n) = (x * (y * z))(n) &= \sum_{p=-\infty}^{\infty}\sum_{k=-\infty}^{\infty} x(k)y(p-k)z(n-p) \\ &= \sum_{p=-\infty}^{\infty}\left(\sum_{k=-\infty}^{\infty} x(k)y(p-k)\right)z(n-p) \\ &= \sum_{p=-\infty}^{\infty}(x * y)(p)z(n-p) = ((x * y) * z)(n). \end{aligned} \tag{2.30}$$

Commutativity is likewise a matter of juggling summations:

$$\begin{aligned}(x * y)(n) &= \sum_{k=-\infty}^{\infty} x(k)y(n-k) = \sum_{k=-\infty}^{\infty} y(n-k)x(k) \\ &= \sum_{k=\infty}^{-\infty} y(n-k)x(k) = \sum_{p=-\infty}^{\infty} y(p)x(n-p) = (y*x)(n). \end{aligned} \tag{2.31}$$

Finally, distributivity is the easiest property, since

$$\begin{aligned}(x * (y+z))(n) &= \sum_{k=-\infty}^{\infty} x(k)(y+z)(n-k) = \sum_{k=-\infty}^{\infty} [x(k)y(n-k) + x(k)z(n-k)] \\ &= \sum_{k=-\infty}^{\infty} x(k)y(n-k) + \sum_{k=-\infty}^{\infty} x(k)z(n-k) \\ &= (x * y)(n) + (x * z)(n). \end{aligned} \tag{2.32}$$

This completes the theorem. ■

The convolution theorem has a converse, which means that convolution with the impulse response characterizes LTI systems.

Theorem (Convolution Converse). Let $h(n)$ be a discrete signal and H be the system defined by $y = Hx = x*h$. Then H is LTI and $h = H\delta$.

Proof: Superposition follows from the distributive property. The scaling property of linearity is straightforward (exercise). To see that H is translation-invariant, note that the shifted output $y(n-l)$ is given by

$$y(n-l) = \sum_{k=-\infty}^{\infty} x(k)h((n-l)-k). \tag{2.33}$$

We compare this to the response of the system to the shifted input, $w(n) = x(n-l)$:

$$\begin{aligned}H(x(n-l)) &= (Hw)(n) = \sum_{k=-\infty}^{\infty} w(k)h(n-k) = \sum_{k=-\infty}^{\infty} x(k-l)h(n-k) \\ &= \sum_{p=-\infty}^{\infty} x(p)h(n-(p+l)) = \sum_{p=-\infty}^{\infty} x(p)h((n-l)-p) = y(n-l). \end{aligned} \tag{2.34}$$

So H is indeed translation-invariant. It is left to the reader to verify that $h = H\delta$. ■

Definition (FIR and IIR Systems). An LTI system H having an impulse response $h = H\delta$ with finite support is called a *finite impulse response* (*FIR*) system. If the LTI system H is not FIR, then it is called *infinite impulse response* (*IIR*).

Remarks. FIR systems are defined by a convolution sum that may be computed for any input signal. IIR systems will have some signals that are not in their domain. IIR systems may nevertheless have particularly simple implementations. This is the case when the system can be implemented via a difference equation, where previous known output values are stored in memory for the computation of current response values. Indeed, an entire theory of signal processing with IIR systems and their compact implementation on digital computers has been developed and is covered in signal processing texts [10].

2.4.4 Application: Echo Cancellation in Digital Telephony

In telephone systems, especially those that include digital links (almost all intermediate- and long-distance circuits in a modern system), *echo* is a persistent problem. Without some special equipment—either echo suppressors or echo cancellers—a speaker can hear a replica of his or her own voice. This section looks at an important application of the theory of convolution and LTI systems for constructing effective echo cancellers on digital telephone circuits.

Echo arises at the connection between two-wire telephone circuits, such as found in a typical residential system, and four-wire circuits, that are used in long-haul circuits. The telephone circuits at the subscriber's site rely on two wires to carry the near-end and far-end speakers' voices and an earth ground as the common conductor between the two circuit paths. The earth ground is noisy, however, and for long-distance circuits, quite unacceptable. Good noise immunity requires a four-wire circuit. It contains separate two-wire paths for the far-end and near-end voices. A device called a *hybrid transformer*, or simply a *hybrid*, effects the transition between the two systems [11]. Were it an ideal device, the hybrid would convert all of the energy in a signal from the far-end speaker into energy on the near-end two-wire circuit. Instead, some of the energy leaks through the hybrid (Figure 2.11) into the circuit that carries the near-end voice outbound to the far-end speaker. The result

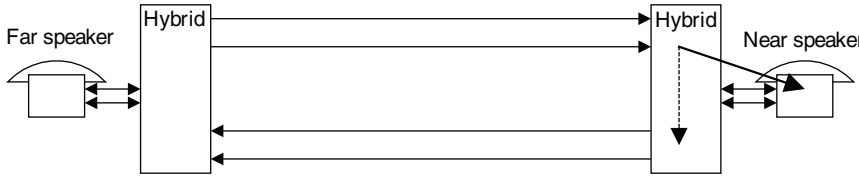

Fig. 2.11. Impedance mismatches in the four-wire to two-wire hybrid transformer allow an echo signal to pass into the speech signal from the near-end speaker. The result is that the far-end speaker hears an echo.

is that far-end speakers hear echoes of their own voices. Since the system design is often symmetrical, the echo problem is symmetrical too, and near-end speakers also suffer annoying echoes. The solution is to employ an *echo suppression* or *echo cancellation* device.

Echo suppression is the older of the two approaches. Long-haul telephone circuits are typically digital and, in the case of the common North American T1 standard, multiplex upwards of 24 digital signals on a single circuit. Since the echo removal is most economically viable at telephone service provider central offices, the echo removal equipment must also be digital in nature. A digital echo suppressor extracts samples from the far-end and near-end digital voice circuits. It compares the magnitudes of the two signals, generally using a threshold on the difference in signal amplitudes. It opens the near-end to far-end voice path when there is sufficient far-end speech detected to cause an echo through the hybrid, but insufficient near-end speech to warrant maintaining the circuit so that the two speakers talk at once. (This situation, called *double-talk* in telephone engineering parlance, occurs some 30% of the time during a typical conversation.) Thus, let $T > 0$ be a threshold parameter, and suppose that M far-end samples and N near-end samples are compared to decide a suppression action. Let $x(n)$ and $s(n)$ be the far- and near-end digital signals, respectively. If $|x(n)| + |x(n-1)| + \cdots + |x(n-M+1)| > T(|s(n)| + |s(n-1)| + \cdots + |s(n-N+1)|)$ at time instant n, then the suppressor mutes the near-end speaker's voice. Now, this may seem crude.

And echo suppression truly is crude. When both people speak, there is echo, but it is less noticeable. The suppressor activates only when the near-end speaker stops talking. Hence, unless the threshold T, the far-end window size M, and the near-end window size N are carefully chosen, the suppressor haphazardly interrupts the near-end signal and makes the resultant voice at the far-end sound choppy. Even granting that these parameters are correct for given circuit conditions, there is no guarantee that system component performances will not drift, or that one speaker will be unusually loud, or that the other will be unusually soft-voiced. Moreover, the suppressor design ought to provide a noise matching capability, whereby it substitutes *comfort noise* during periods of voice interruption; otherwise, from the utter silence, the far-end listener also gets the disturbing impression that the circuit is being repeatedly broken and reestablished. Chapter 4 will study some methods for updating such parameters to maintain good echo suppressor performance. For now, however, we wish to turn to the echo canceller, a more reliable and also more modern alternative.

An echo canceller builds a signal model of the echo which slips through the hybrid. It then subtracts the model signal from the near-end speaker's outbound voice signal (Figure 2.12). How can this work? Note that the hybrid is an approximately linear device. If the far-end speaker's signal $x(n)$ is louder, then the echo gets proportionally louder. Also, since telephone circuit transmission characteristics do not change much over the time of a telephone call, the echo that the far-end signal produces at one moment is approximately the same as it produces at another moment. That is, the hybrid is very nearly translation-invariant. This provides an opportunity to invoke the convolution theorem for LTI systems.

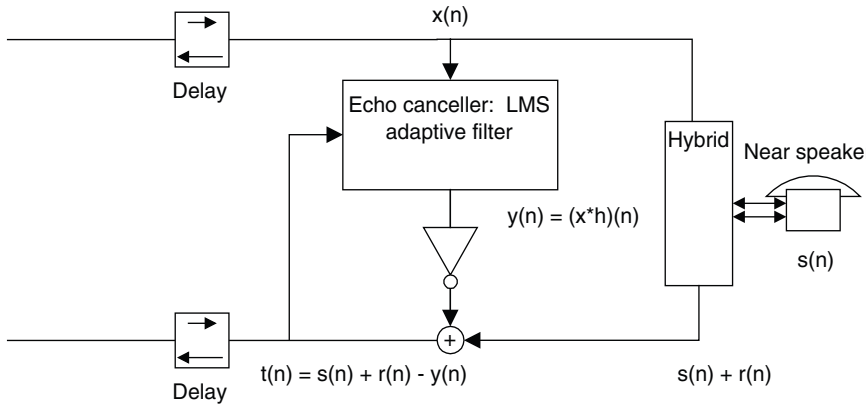

Fig. 2.12. An echo canceller holds a set of coefficients from which it can approximately model the echo signal $r(n)$. Assuming that the hybrid leakage is both linear and translation-invariant, we can apply the convolution theorem for LTI systems. The canceller stores the impulse response of the inbound far-end voice signal $h(n)$ and computes the echo as $y(n) = (x*h)(n)$. Subtracting $y(n)$ from the near-end speech and echo signal, $s(n) + r(n)$, gives the transmitted digital voice signal $t(n) = s(n) + r(n) - y(n)$.

Let H be the hybrid system, so that $r = Hx$ is LTI, where $x(n)$ is the inbound signal from the far-end speaker, and $r(n)$ is the echo through the hybrid. Suppose that the canceller stores the impulse response of the inbound far-end voice signal $h(n)$. Then it can approximate the echo as $y(n) = (x*h)(n)$, and this is the crux of the design. Subtracting $y(n)$ from the near-end speech and echo signal, $s(n) + r(n)$, gives the transmitted digital voice signal $t(n) = s(n) + r(n) - y(n)$ with echo largely removed. Digital signal processors can perform these convolution and subtraction steps in real time on digital telephony circuits [12]. Alternatively, echo cancellation can be implemented in application-specific integrated circuits [13].

An intriguing problem is how to establish the echo impulse response coefficients $h(k)$. The echo may change based on the connection and disconnection of equipment on the near-end circuit, including the two-wire drop to the subscriber. Thus, it is useful to allow $h(k)$ to change slowly over time. We can allow $h(k)$ to adapt so as to minimize the residual error signal, $e(n) = r(n) - y(n)$, that occurs when the near-end speaker is silent, $s(n) = 0$. Suppose that discrete values up to time instant n have been received and the coefficients must be adjusted so that the energy of the error $e(n)$ is a minimum. The energy of the error signal's last sample is $e^2(n)$. Viewing $e^2(n)$ as a function of the coefficients $h(k)$, the maximum decrease in the error is in the direction of the negative gradient, given by the vector with components

$$-\nabla e^2(n)_k = -\frac{\partial}{\partial h(k)}(e^2(n)) = 2r(n)x(n-k). \tag{2.35}$$

To smoothly converge on a good set of $h(k)$ values, it is best to use some proportion parameter η; thus, we adjust $h(k)$ by adding $2\eta r(n)x(n-k)$. This is an adaptive

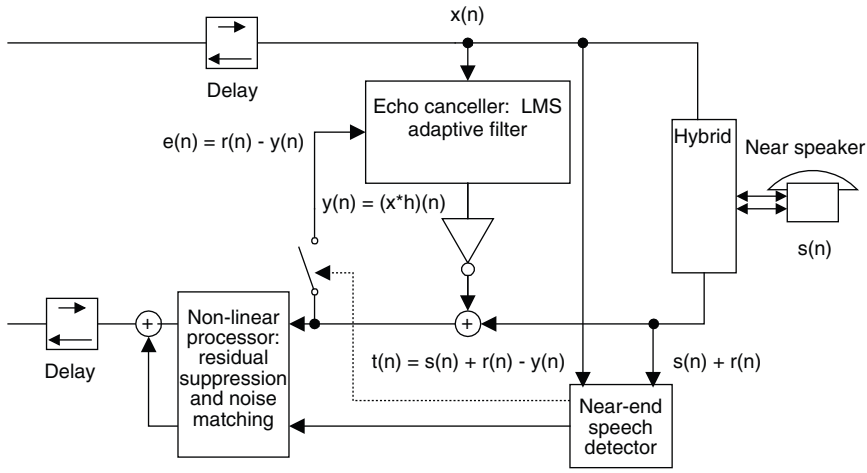

Fig. 2.13. An advanced echo canceller implements some of the design ideas from echo suppressors. The nonlinear processor mutes residual echo (the signal $t(n)$ after cancellation) when it exceeds a threshold. Noise matching supplies comfort noise to the outbound circuit so that the far-end listener does not suspect a dead line.

filtering algorithm known in the research literature as the *least mean squares* (*LMS*) *algorithm* [14].

An improvement in echo cancellation results from implementing some of the ideas from echo suppressor designs. A component commonly called the nonlinear processor (NLP) performs muting and noise insertion in the advanced canceller. Referring to Figure 2.13, note that the NLP mutes residual echo $t(n)$ when it falls below a small threshold and there is no near-end speech. NLP noise matching supplies comfort noise to the outbound circuit so the far-end listener does not suspect a dead line. Finally, the adaptation of the coefficients $h(n)$ should cease during periods of double-talk; otherwise, just as does genuine echo, the large magnitude near-end speech will be seen as echo by the canceller. The upshot is that the $h(n)$ coefficients will diverge from their proper settings, and a burst of echo will occur when the near speaker stops talking.

2.5 THE l^p SIGNAL SPACES

The remainder of the chapter develops the mathematical foundation for discrete signal processing theory. Vector calculus relies on such a foundation. But it is so intuitive, however, that many students do not even realize that the finite-dimensional vector spaces, $\mathbb{R}^n$ and $\mathbb{C}^n$, underlie multivariable calculus. The theories of differentiation, integration, limits, and series easily generalize to work with vectors instead of just scalars. Our problems are much more complicated now, since the objects of our theory—signals—are like vectors that are infinitely long and extend in two

directions. We cannot, for example, carelessly generalize the dot product from finite dimensional vector spaces to signals; the resulting sum may not converge.

2.5.1 l^p Signals

What signal operations must our formal framework support? We have discovered that convolution operations play a pivotal role in the study of LTI systems. Since the summation in this important operation is infinite, we may ask under what circumstances one can compute the limit which it represents. It is clear that if the system is FIR, then the convolution sum is computable for any input signal. From a practical perspective, every signal encountered in engineering is finitely supported and cannot continue with nonzero values forever. However, it is reassuring to know that this is not a fundamental limitation of the theory we develop for signals. By looking a little deeper into the mathematics of signals and operations on them, we can in fact find classes of signals, not finitely supported, that allow us to compute convolutions for IIR systems.

Definition (l^p Signal Spaces). Let $p \geq 1$ be a real number. Then l^p is the set of all real-valued (or complex-valued) signals $x(n)$ such that

$$\sum_{n=-\infty}^{\infty} |x(n)|^p < \infty . \tag{2.36}$$

We sometimes call the l^p signals *p-summable*. If $x(n)$ is in l^p, then its l^p*-norm* is

$$\|x(n)\|_p = \left(\sum_{n=-\infty}^{\infty} |x(n)|^p \right)^{\frac{1}{p}} . \tag{2.37}$$

There is an l^p *distance measure* as well: $d_p(x, y) = \|x - y\|_p$. There is a special case of l^p signals, the bounded signals. A discrete signal $x(n)$ is *bounded* if there is a positive real number M_x such that for all n,

$$|x(n)| \leq M_x . \tag{2.38}$$

It is customary to denote the class of bounded signals as l^∞. (This notation allows an elegant formulation of an upcoming theorem.) Finally, we define the l^∞ *norm* of a signal to be its least upper bound:

$$\|x(n)\|_\infty = \min \{M: x(n) \leq M \text{ for all } n\}. \tag{2.39}$$

The l^p signal classes share a number of important properties that we need in order to do signal processing within them. This and the next section comprise a tutorial on the mathematical discipline known as *functional analysis* [15], which studies the properties of mathematical functions from a geometric standpoint. It is a

generalization of finite-dimensional real and complex vector space theory. In fact, we already know some examples of l^p spaces.

Example (Finite-Energy Signals). The l^2 signals are precisely the finite energy, or square-summable discrete signals. The l^2 norm is also the square root of the energy of the signal. We will find that l^2 is a standout l^p space, since it supports an inner product relation that generalizes the dot product on signals. There are signal spaces for finite energy analog signals too (Chapter 3). Furthermore, we will find in Chapter 7 that it is possible to build a complete theory for the frequency analysis of l^2 signals [16]. Chapter 11 explains the recent theory of multiresolution analysis for finite energy signals—a recent advance in signal analysis and one kind of signal decomposition based on wavelets [17].

Example (Absolutely Summable Signals). The l^1 signal space is the set of absolutely summable signals. It too enjoys a complete signal frequency theory. Interestingly, for any p, $1 \le p \le 2$, there is an associated frequency analysis theory for the space of l^p signals [16]. Since signal processing and analysis uses mainly l^1 and l^2, however, we will not elaborate the Fourier transform theory for l^p, $1 < p < 2$.

2.5.2 Stable Systems

The notion of the l^p signal spaces applies readily to study of stable systems.

Definition (Stability). The system H is *stable* if $y = Hx$ is bounded whenever x is bounded. Another term for stable is *bounded input–bounded output* (*BIBO*).

Thus, the response of a stable system to an l^∞ input signal is still an l^∞ signal. The next theorem is useful for discovering whether or not an LTI system is stable. This result depends on an important property of the real number system: Every sequence that has a upper bound has a least upper bound [18].

Theorem (Stability Characterization). An LTI system H is stable if and only if its impulse response, $h = H\delta$, is in l^1 (absolutely summable).

Proof: First, suppose $h = H\delta$ is in l^1, and $x(n)$ is an l^∞ input signal with $|x(n)| \le M$. Let $y = Hx$. Then,

$$|y(n)| = \left| \sum_{k=-\infty}^{\infty} h(k)x(n-k) \right| \le \sum_{k=-\infty}^{\infty} |h(k)||x(n-k)| \le \sum_{k=-\infty}^{\infty} |h(k)|M$$
$$= M \sum_{k=-\infty}^{\infty} |h(k)| = M\|h\|_1 < \infty. \tag{2.40}$$

So $y(n)$ is bounded, proving that H is stable. Conversely, suppose the system H is stable, but the impulse response $h(n)$ is not in l^1. Now, the expression (2.37) for

the l^1-norm of h is in fact a limit operation on a monotonically increasing sequence of sums. This sequence is either bounded or it is not. If it is bounded, then it would have a least upper bound, which must be the limit of the infinite sum (2.37). But we are assuming this limit does not exist. Thus, the sum must in fact be unbounded. And the only way that the limit cannot exist is if it diverges to infinity. That is,

$$\|h\|_1 = \sum_{k=-\infty}^{\infty} |h(k)| = \infty. \tag{2.41}$$

Let us consider the bounded input signal $x(n)$ defined

$$x(n) = \begin{cases} \dfrac{h(-n)}{|h(-n)|} & \text{if } h(-n) \neq 0, \\ 0 & \text{if } h(-n) = 0. \end{cases} \tag{2.42}$$

What is the response of our supposedly stable system to the signal $x(n)$? The convolution theorem for LTI systems tells us that we can find, for example, $y(0)$ to be

$$y(0) = \sum_{k=-\infty}^{\infty} h(k)x(0-k) = \sum_{k=-\infty}^{\infty} h(k)\frac{h(k)}{|h(k)|} = \sum_{k=-\infty}^{\infty} |h(k)| = \|h\|_1 = \infty. \tag{2.43}$$

This shows that y is unbounded, so that H is not stable, contradicting the assumption. Consequently, it must be the case that h is in l^1. ■

2.5.3 Toward Abstract Signal Spaces

One of the first things to verify is the closure of the l^p spaces under certain arithmetic or algebraic signal operations. This involves two steps:

(i) Verifying that the result of the operation is still a signal; that is, we can compute the value of the result at any time instant (if one of the signal values becomes infinite, then it is not a signal).
(ii) Verifying that the resulting signal is in the signal space of the operands.

2.5.3.1 Closure Properties. The closure property for a signal operation shows that we can process l^p space signals through systems that are defined by the given operation. For example, the proof of the following closure proposition is easy and left as an exercise. What it shows is that an l^p signal can be fed into an amplifier system and yet it remains an l^p signal. Similarly, a delay or advance system preserves the l^p nature of its input signals.

Proposition (Closure of l^p Spaces). Let $x(n)$ be a signal in l^p, $1 \le p \le \infty$, let c be a real (or complex) number, and let k be an integer. Then:

(i) $cx(n)$ is in l^p and $\|cx\|_p = |c|\ \|x\|_p$.
(ii) $x(k-n)$ is in l^p and $\|x(k-n)\|_p = \|x(n)\|_p$.

Proof: Exercise. ■

Proposition (Closure of l^1 Spaces). Let $x(n)$ and $y(n)$ be l^1 signals. Then $w(n) = x(n) + y(n)$ is in l^1 also.

Proof: To show that $\|w(n)\|_1$ is finite, we only need to generalize the *triangle inequality* from arithmetic, $|x + y| \le |x| + |y|$, to infinite sums, and this is straightforward. ■

Proposition (Closure of l^∞ Spaces). Let $x(n)$ and $y(n)$ be l^∞ signals. Then $w(n) = x(n) + y(n)$ is in l^∞ also.

Proof: $\|w(n)\|_\infty$ is the least upper bound of $\{|w(n)|: n \text{ an integer}\}$. The arithmetic triangle inequality extends to infinite sets for upper bounds as well. ■

2.5.3.2 Vector Spaces. Before getting into the thick of abstract signal spaces, let us review the properties of a vector V space over the real numbers $\mathbb{R}$. There is a zero vector. Vectors may be added, and this addition is commutative. Vectors have additive inverses. Vectors can be multiplied by scalars, that is, elements of $\mathbb{R}$. Also, there are distributive and associative rules for scalar multiplication of vectors. One vector space is the real numbers over the real numbers: not very provocative. More interesting is the space with vectors taken from $\mathbb{R} \times \mathbb{R} = \{(a, b): a, b \in \mathbb{R}\}$. This set of real ordered pairs is called the *Cartesian product*, after Descartes,[2] but the concept was also pioneered by Fermat.[3] In general, we can take the Cartesian

[2]Forming a set of ordered pairs into a structure that combines algebraic and geometric concepts originates with Rene Descartes (1596–1650) and Pierre Fermat (1601–1665) [D. Struik, ed., *A Source Book in Mathematics,* 1200–1800, Princeton, NJ: Princeton University Press, 1986]. Descartes, among other things, invented the current notation for algebraic equations; developed coordinate geometry; inaugurated, in his *Meditations*, the epoch of modern philosophy; and was subject to a pointed critique by his pupil, Queen Christina of Sweden.

[3]Fermat is famous for notes he jotted down while perusing Diophantus's *Arithmetic*. One was a claim to the discovery of a proof for his Last Theorem: There are no nonzero whole number solutions of $x^n + y^n = z^n$ for $n > 1$. Historians of science, mathematicians, and the lay public for that matter have come to doubt that the Toulouse lawyer had a "marvelous demonstration," easily inserted but for the tight margins left by the printer. Three centuries after Fermat's teasing marginalia, A. Wiles of Princeton University followed an unexpected series of deep results from mathematicians around the world with his own six-year assault and produced a convincing proof of Fermat's Last Theorem [K. Devlin, *Mathematics: The Science of Patterns*, New York: Scientific American Library, 1994.]

product any positive number of times. The vector space exemplar is in fact the set of ordered n-tuples of real numbers $(a_1, a_2, \ldots, a_n) \in \mathbb{R}^n$. This space is called *Euclidean n-space*.[4]

Ideas of linear combination, span, linear independence, basis, and dimension are important; we will generalize these notions as we continue to lay our foundation for signal analysis. When a set of vectors $S = \{\boldsymbol{u}_i : i \in I\}$ *spans V*, then each vector $\boldsymbol{v} \in V$ is a *linear combination* of some of the $\boldsymbol{u}_i$: there are real numbers a_i such that $\boldsymbol{v} = a_1\boldsymbol{u}_1 + \cdots + a_N\boldsymbol{u}_N$. If S is finite and spans V, then there is a *linearly independent* subset of S that spans V. In other words, there is some $B \subseteq S$, $B = \{\boldsymbol{b}_i : 1 \le i \le N\}$, B spans V, and no nontrivial linear combination of the $\mathbf{b_i}$ is the zero vector: $\mathbf{0} = a_1\mathbf{u}_1 + \cdots + a_N\mathbf{u}_N$ implies $a_i = 0$. A spanning, linearly independent set is called a *basis* for V. If V has a finite basis, then every basis for V contains the same number of vectors—the *dimension* of V. A vector in Euclidean n-space has a *norm*, or *length*, which is the square root of the sum of the squares of its elements.

There is also an *inner product*, or *dot product*, for $\mathbb{R}^n$: $\langle \boldsymbol{a}, \boldsymbol{b} \rangle = \sum_{i=1}^{n} a_i b_i = \boldsymbol{a} \cdot \boldsymbol{b}$.

The dot product is a means of comparing two vectors via the relation $\langle \boldsymbol{a}, \boldsymbol{b} \rangle = \|\boldsymbol{a}\| \|\boldsymbol{b}\| \cos\theta$, where θ is the angle between the two vectors.

The vector space may also be defined over the complex numbers $\mathbb{C}$ in which casewe call it a *complex vector space*. The set of n-tuples of complex numbers $\mathbb{C}^n$ is called *unitary n-space*, an n-dimensional complex vector space. All of the vector space definitions and properties carry directly over from real to complex vector spaces, except for those associated with the inner product. We have to define $\langle \boldsymbol{a}, \boldsymbol{b} \rangle = \sum_{i=1}^{n} a_i \overline{b}_i = \boldsymbol{a} \cdot \boldsymbol{b}$, where $\overline{c}$ is the complex conjugate. A classic reference on vector spaces (and modern algebra all the way up to the unsolvability of quintic polynomials by radicals $\sqrt[n]{r}$, roots of order n) is Ref. 19.

2.5.3.3 Metric Spaces.

A *metric space* is an abstract space that incorporates into its definition only the notion of a distance measure between elements.

Definition (Metric Space). Suppose that M is a set and d maps pairs of elements of M into the real numbers, $d: M \times M \to \mathbb{R}$. Then M is a *metric space* with *metric*, or *distance measure d,* if:

(i) $d(u, v) \ge 0$ for all u, v in M.
(ii) $d(u, v) = 0$ if and only if $u = v$.
(iii) $d(u, v) = d(v, u)$ for all u, v in M.
(iv) For any u, v, and w in M, $d(u, v) \le d(u, w) + d(w, v)$.

[4]The ancient Greek mathematician Euclid (ca. 300 B.C.) was (probably) educated at Plato's Academy in Athens, compiled the *Elements*, and founded a school at Alexandria, Egypt.

Items (i) and (ii) are known as the *positive-definiteness* conditions; (iii) is a *symmetry* condition; and (iv) is the *triangle inequality*, analogous to the distances along sides of a triangle.

Example (Euclidean, Unitary Metric Spaces). Clearly the Euclidean and unitary spaces are metric spaces. We can simply take the metric to be the Euclidean norm: $d(\mathbf{u}, \mathbf{v}) = \|\mathbf{u} - \mathbf{v}\|$.

Example (City Block Metric). But other distance measures are possible, too. For example, if we set $d((u_1, v_1), (u_2, v_2)) = |u_1 - u_2| + |v_1 - v_2|$, then this is a metric on $\mathbb{R}^2$, called the *city block distance*. This is easy to check and left as an exercise. Note that the same set of elements can underlie a different metric space, depending upon the particular distance measure chosen, as the city block distance shows. Thus, it is common to write a metric space as an ordered pair (M, d), where M is the set of elements of the space, and d is the distance measure.

The triangle inequality is a crucial property. It allows us to form groups of metric space elements, all centered around a single element. Thus, it is the mathematical foundation for the notion of the proximity of one element to another. It makes the notion of distance make sense: You can jump from u to v directly, or you can jump twice, once to w and thence to v. But since you end up in the same place, namely at element v, a double jump should not be a shorter overall trip.

We would like to compare two signals for similarity—for instance, to match one signal against another (Chapter 4). One way to do this is to subtract the signal values from each other and calculate the size or magnitude of their difference. We can't easily adapt our inner product and norm definitions from Euclidean and unitary spaces to signals because signals contain an infinite number of components. Intuitively, a finitely supported signal could have some norm like a finite-dimensional vector. But what about other signals? The inner product sum we are tempted to write for a discrete signal becomes an infinite sum if the signal is not finitely supported. When does this sum converge? What about bases and dimension? Can the span, basis, and dimension notions extend to encompass discrete signals too?

2.5.4 Normed Spaces

This section introduces the *normed space*, which combines the ideas of vector spaces and metric spaces.

Definition (Normed Space). A *normed space*, or *normed linear space*, is a vector space V with a norm $\|v\|$ such that for any u and v in V,

(i) $\|v\|$ is real and $\|v\| \geq 0$.
(ii) $\|v\| = 0$ if and only if $v = \mathbf{0}$, the zero vector in V.

(iii) $\|av\| = |a|\,\|v\|$, for all real numbers a.
(iv) $\|u + v\| \leq \|u\| + \|v\|$.

If $S \subseteq V$ is a vector subspace of V, then we may define a norm on S by just taking the norm of V restricted to S. Then S becomes a normed space too. S is called a *normed subspace* of V.

We adopt Euclidean and unitary vector spaces as our inspiration. The goal is to take the abstract properties we need for signals from them and define a special type of vector space that has at least a norm. Now, we may not be able to make the class of all signals into a normed space; there does not appear to be any sensible way to define a norm for a general signal with infinite support. One might try to define a norm on a restricted set of signals in the same way as we define the norm of a vector in $\mathbb{R}^3$. The l^2 signals have such a norm defined for them. The problem is that we do not yet know whether the l^2 signals form a vector space. In particular, we must show that a sum of l^2 signals is still an l^2 signal (additive closure). Now, we have already shown that the l^1 signals with the norm $\|x\|_1$ do form a normed space. Thus, our strategy is to work out the specific properties we need for signal theory, specify an abstract space with these traits, and then discover those concrete classes of signals that fulfill our axiom system's requirements. This strategy has proven quite successful in applied mathematics.[5] The discipline of *functional analysis* provides the tools we need [15, 20–23]. There is a complete history as well [24]. We start with a lemma about conjugate exponents [15].

Definition (Conjugate Exponents). Let $p > 1$. If $p^{-1} + q^{-1} = 1$, then q is a *conjugate exponent* of p. For $p = 1$, the conjugate exponent of p is $q = \infty$.

Let us collect a few simple facts about conjugate exponents.

Proposition (Conjugate Exponent Properties). Let p and q be conjugate exponents. Then

(i) $(p + q)/pq = 1$.
(ii) $pq = p + q$.
(iii) $(p - 1)(q - 1) = 1$.
(iv) $(p - 1)^{-1} = q - 1$.
(v) If $u = tp^{-1}$, then $t = uq^{-1}$.

[5]Several mathematicians—among them Wiener, Hahn, and Banach—simultaneously and independently worked out the concept and properties for a normed space in the 1920s. The discipline of functional analysis grew quickly. It incorporated the previous results of Hölder and Minkowski, found applications in quantum mechanics, helped unify the study of differential equations, and, within a decade, was the subject of general treatises and reviews.

Lemma (Conjugate Exponents). Let $a > 0$ and $b > 0$ be real numbers. Let p and q be conjugate exponents. Then $ab \leq p^{-1}a^p + q^{-1}b^q$.

Proof: The trick is to see that the inequality statement of the lemma reduces to a geometric argument about the areas of regions bounded by the curve $u = tp^{-1}$. Note that

$$\frac{a^p}{p} = \int_0^a t^{p-1}dt, \tag{2.44}$$

$$\frac{b^q}{q} = \int_0^b u^{q-1}du. \tag{2.45}$$

Definite integrals (2.44) and (2.45) are areas bounded by the curve and the t- and u-axis, respectively (Figure 2.14). The sum of these areas is not smaller than the area of the rectangle defined by (0,0) and (a,b) in any case. ■

Our first nontrivial closure result on l^p spaces, Hölder's[6] inequality [15], shows that it is possible to form the product of signals from conjugate l^p spaces.

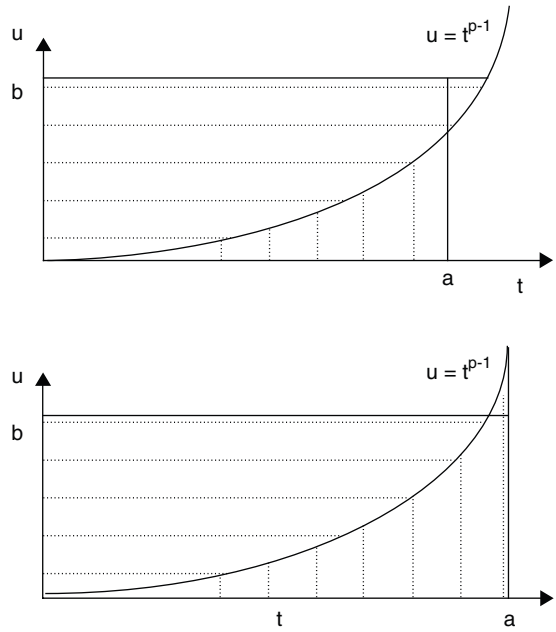

Fig. 2.14. There are two cases: Either point (a, b) is below the curve (bottom) or above the curve (top). In either case the area of the rectangle determined by the origin and (a, b) has a smaller area than the total area of regions bounded by the curve and the t- and u-axes.

[6]German mathematician Otto Ludwig Hölder (1859–1937) discovered the relation in 1884.

Theorem (Hölder's Inequality). Let $x(n)$ be in l^p and let $h(n)$ in l^q, where p and q are conjugate exponents. Then $y(n) = x(n)h(n)$ is in l^1 and $\|y\|_1 \le \|x\|_p \|h\|_q$.

Proof: Since the inequality clearly holds if $\|x\|_p = 0$ or $\|h\|_q = 0$, we assume that these signals are not identically 0. Next, let $x'(n) = \frac{x(n)}{\|x\|_p}$ and $h'(n) = \frac{h(n)}{\|h\|_q}$, and set $y'(n) = x'(n)h'(n)$. By the lemma,

$$|x'(n)||h'(n)| \le \frac{|x'(n)|^p}{p} + \frac{|h(n)|^q}{q}. \tag{2.46}$$

Putting (2.46) into the expression for $\|y'\|_1$, we find that

$$\begin{aligned} \|y'\|_1 &= \sum_{n=-\infty}^{\infty} |x'(n)||h'(n)| \le \sum_{n=-\infty}^{\infty} \frac{|x'(n)|^p}{p} + \sum_{n=-\infty}^{\infty} \frac{|h'(n)|^q}{q} \\ &= \frac{1}{p} \sum_{n=-\infty}^{\infty} \frac{|x(n)|^p}{\|x\|_p} + \frac{1}{q} \sum_{n=-\infty}^{\infty} \frac{|h(n)|^q}{\|h\|_q} = \frac{1}{p} + \frac{1}{q} = 1. \end{aligned} \tag{2.47}$$

Hence,

$$\|y'\|_1 = \frac{\|xh\|_1}{\|x\|_p \|h\|_q} = \frac{\|y\|_1}{\|x\|_p \|h\|_q} \le 1 \tag{2.48}$$

and the Hölder inequality follows. ■

Remarks. From the Hölder inequality, it is easy to show that there are IIR systems that have large classes of infinitely supported signals in their domains. This shows that our theory of signals can cope with more than FIR systems. In particular, the space of finite-energy signals is contained within the domain of any LTI system with a finite-energy impulse response.

Theorem (Domain of l^q Impulse Response Systems). Suppose H is an LTI system and $h = H\delta$ is in l^q. Then any $x(n)$ in l^p, where p and q are conjugate exponents, is in *Domain*(H).

Proof: By the convolution theorem for LTI systems, the response of H to input x is $y = x * h$. Thus,

$$|y(n)| = \left| \sum_{k=-\infty}^{\infty} x(k)h(n-k) \right| \le \sum_{k=-\infty}^{\infty} |x(k)||h(n-k)|. \tag{2.49}$$

Since the q-summable spaces are closed under translation and reflection, $h(n-k)$ is in l^q for all n. So the Hölder inequality implies that the product signal $w_n(k) = x(k)h(n-k)$ is in l^1. Computing $\|w_n\|_1$, we see that it is just the right-hand side of (2.49). Therefore, $|y(n)| \le \|w_n\|_1$ for all n. The convolution sum (2.49) converges. ■

Corollary (Cauchy–Schwarz[7] Inequality). Suppose $x(n)$ and $h(n)$ are in l^2. Then the product $y(n) = x(n)h(n)$ is in l^1 and

$$\|y\|_1 = \sum_{n=-\infty}^{\infty} |x(n)||h(n)| \le \sqrt{\sum_{n=-\infty}^{\infty} |x(n)|^2}\sqrt{\sum_{n=-\infty}^{\infty} |h(n)|^2} = \|x\|_2\|h\|_2 . \quad (2.50)$$

Proof: Take $p = q = 2$ in the Hölder inequality. ■

Theorem (Minkowski[8] Inequality). If x and y are in l^p, then $w = x + y$ is in l^p, and $\|w\|_p \le \|x\|_p + \|y\|_p$.

Proof: Assume $p > 1$. Then,

$$|w(n)|^p = |w(n)|^{p-1}|x(n) + y(n)| \le |w(n)|^{p-1}(|x(n)| + |y(n)|) . \quad (2.51)$$

Summing over all n gives

$$\sum_{n=-\infty}^{\infty} |w(n)|^p \le \sum_{n=-\infty}^{\infty} |x(n)||w(n)|^{p-1} + \sum_{n=-\infty}^{\infty} |y(n)||w(n)|^{p-1} . \quad (2.52)$$

The Hölder inequality applies to the first sum on the right-hand side of (2.52) with $q = p/(p-1)$ as follows:

$$\sum_{n=-\infty}^{\infty} |x(n)||w(n)|^{p-1} \le \left(\sum_{n=-\infty}^{\infty} |x(n)|^p\right)^{\frac{1}{p}}\left(\sum_{n=-\infty}^{\infty} [|w(n)|^{p-1}]^q\right)^{\frac{1}{q}}$$
$$= \left(\sum_{n=-\infty}^{\infty} |x(n)|^p\right)^{\frac{1}{p}}\left(\sum_{n=-\infty}^{\infty} |w(n)|^p\right)^{\frac{1}{q}} . \quad (2.53)$$

Similarly, for the second sum of the right-hand side of (2.52), we have

$$\sum_{n=-\infty}^{\infty} |y(n)||w(n)|^{p-1} \le \left(\sum_{n=-\infty}^{\infty} |y(n)|^p\right)^{\frac{1}{p}}\left(\sum_{n=-\infty}^{\infty} |w(n)|^p\right)^{\frac{1}{q}} . \quad (2.54)$$

Putting (2.52)–(2.54) together gives

$$\sum_{n=-\infty}^{\infty} |w(n)|^p \le \left[\left(\sum_{n=-\infty}^{\infty} |x(n)|^p\right)^{\frac{1}{p}} + \left(\sum_{n=-\infty}^{\infty} |y(n)|^p\right)^{\frac{1}{p}}\right]\left(\sum_{n=-\infty}^{\infty} |w(n)|^p\right)^{\frac{1}{q}} . \quad (2.55)$$

[7]After French mathematician Augustin-Louis Cauchy (1789–1857) and German mathematician Hermann Amandus Schwarz (1843–1921).

[8]Although he was born in what is now Lithuania, Hermann Minkowski (1864–1909) spent his academic career at German universities. He studied physics as well as pure mathematics. He was one of the first to propose a space-time continuum for relativity theory.

Finally, (2.55) entails

$$\frac{\sum_{n=-\infty}^{\infty} |w(n)|^p}{\left(\sum_{n=-\infty}^{\infty} |w(n)|^p\right)^{\frac{1}{q}}} = \left(\sum_{n=-\infty}^{\infty} |w(n)|^p\right)^{1-\frac{1}{q}} = \left(\sum_{n=-\infty}^{\infty} |w(n)|^p\right)^{\frac{1}{p}}$$

$$= \|w\|_p \leq \left(\sum_{n=-\infty}^{\infty} |x(n)|^p\right)^{\frac{1}{p}} + \left(\sum_{n=-\infty}^{\infty} |y(n)|^p\right)^{\frac{1}{p}} = \|x\|_p + \|y\|_p, \tag{2.56}$$

completing the proof. ■

Now, it's easy to check that the norms associated with the l^p signal spaces, $\|x\|_p$, are in fact norms under the above abstract definition of a normed linear space:

Theorem (l^p Spaces Characterization). The l^p spaces are normed spaces for $1 \leq p \leq \infty$. ■

So far we find that the l^p spaces support several needed signal operations: addition, scalar multiplication, and convolution. Sometimes the result is not in the same class as the operands, but it is still in another related class; this is not ideal, but at least we can work with the result. Now let us try to incorporate the idea of signal convergence—limits of sequences of signals—into our formal signal theory.

2.5.5 Banach Spaces

In signal processing and analysis, we often consider sequences of signals $\{x_k(n)\}$. For example, the sequence could be a series of transformations of a source signal. It is of interest to know whether the sequence of signals converges to another limiting signal. In particular, we are concerned with the convergence of sequences of signals in l^p spaces, since we have already shown them to obey special closure properties, and they have a close connection with such signal processing ideas as stability. We have also shown that the l^p signal spaces are normed spaces. We cannot expect every sequence of signals to converge; after all, not every sequence of real numbers converges. However, we recall from calculus the Cauchy condition for convergence: A sequence of real (or complex) numbers $\{a_k\}$ is a *Cauchy sequence* if for every $\varepsilon > 0$, there is an $N > 0$ such that for $k, l > N$, $|a_k - a_l| < \varepsilon$. Informally, this means that if we wait long enough, the numbers in the sequence will remain arbitrarily close together. An essential property of the real line is that every Cauchy sequence of converges to a limit [18]. If we have an analogous

property for signals in a normed space, then we call the signal space a Banach[9] space [15].

Definition (Banach Space). A Banach space B is a normed space that is *complete*. That is, any sequence $\{x_k(n)\}$ of signals in B that is a Cauchy sequence converges in B to a signal $x(n)$ also in B. Note that $\{x_k(n)\}$ is a *Cauchy sequence* if for every $\varepsilon > 0$, there is an $N > 0$ so that whenever $k, l > N$, we have $\|x_k - x_l\| < \varepsilon$. If $S \subseteq B$ is a complete normed subspace of B, then we call S a *Banach subspace* of B.

Theorem (Completeness of l^p Spaces). The l^p spaces are complete, $1 \le p \le \infty$.

Proof: The exercises sketch the proofs. ■

Banach spaces have historically proven difficult to analyze, evidently due to the lack of an inner product relation. Breakthrough research has of late cleared up some of the mysteries of these abstract spaces and revealed surprising structure. The area remains one of intense mathematical research activity. For signal theory, we need more analytical power than what Banach spaces furnish. In particular, we need some theoretical framework for establishing the similarity or dissimilarity of two signals—we need to augment our abstract signal theory space with an inner product relation.

Examples

(i) An example of a Banach subspace is l^1, which is a subspace of all l^p $1 \le p \le \infty$.

(ii) The set of signals in l^p that are zero on a nonempty subset $Y \subseteq \mathbb{Z}$ is easily shown to be a Banach space. This is a proper subspace of l^p for all p.

(iii) The normed subspace of l^p that consists of all finitely supported p-summable signals is not a Banach subspace. There is a sequence of finitely supported signals that is a Cauchy sequence (and therefore converges inside l^p) but does not converge to a finitely supported signal.

Recall from calculus the ideas of open and closed subsets of the real line. A set $S \subseteq \mathbb{R}$ is *open* if for every point p in S, there is $\varepsilon > 0$ such that $Ball(p, \varepsilon) = \{x \in \mathbb{R}: |x - p| < \varepsilon\} \subseteq S$. That is, every point p of S is contained in an open ball that is contained in S. A set $S \subseteq \mathbb{R}$ is *closed* if its complement is open. Let V be a normed space. Then a set $S \subseteq V$ is *open* if for every point p in S, there is $\varepsilon > 0$ such that $Ball(p, \varepsilon) = \{x \in V: \|x - p\| < \varepsilon\} \subseteq S$. That is, every point p of S is contained in an open ball that is contained in S.

Theorem (Banach Subspace Characterization). Let B be a Banach space and S a normed subspace of B. Then S is a Banach subspace if and only if S is closed in B.

[9]The Polish mathematician S. Banach (1892–1945) developed so much of the initial theory of complete normed spaces that the structure is named after him. Banach published one of the first texts on functional analysis in the early 1930s.

Proof: First suppose that S is a Banach subspace. We need to show that S is closed in B. Let $p \in B$, and $p \notin S$. We claim that there is an $\varepsilon > 0$ such that the open ball $Ball(p, \varepsilon) \cap S = \varnothing$. If not, then for any integer $n > 0$, there is a point $s_n \in S$ that is within the ball $Ball(p, 1/n)$. The sequence $\{s_n: n > 0\}$ is a Cauchy sequence in S. Since S is Banach, this sequence converges to $s \in S$. However, this means we must have $s = p$, showing that $p \in S$, a contradiction.

Conversely, suppose that S is closed and $\{s_n: n > 0\}$ is a Cauchy sequence in S. We need to show that $\{s_n\}$ converges to an element in S. The sequence is still a Cauchy sequence in all of B; the sequence converges to $p \in B$. We claim $p \in S$. If not, then since p is in the complement of S and S is closed, there must be an $\varepsilon > 0$ and an open ball $Ball(p, \varepsilon) \subseteq S'$. This contradicts the fact that $d(s_n, s) \to 0$, proving the claim and the theorem. ■

2.6 INNER PRODUCT SPACES

Inner product spaces have a binary operator for measuring the similarity of two elements. Remember that in linear algebra and vector calculus over the normed spaces $\mathbb{R}^n$, the inner (or dot) product operation has a distinct geometric interpretation. We use it to find the angle between two vectors in $\mathbb{R}^n$: $\langle u, v\rangle = \|u\|\|v\|\cos(\theta)$, where θ is the angle between the vectors. From the inner product, we define the notion of orthogonality and of an orthogonal set of basis elements. Orthogonal bases are important because they furnish a very easy set of computations for decomposing general elements of the space.

2.6.1 Definitions and Examples

Once again, we abstract the desired properties from the Euclidean and unitary spaces.

Definition (Inner Product Space). An *inner product space* I is a vector space with an inner product defined on it. The inner product, written with brackets notation $\langle x, y\rangle$, can be real- or complex-valued, according to whether I is a real or complex vector space, respectively. The inner product satisfies these five rules:

(i) $0 \le \langle x, x\rangle$ for all $x \in I$.
(ii) For all $x \in I$, $0 = \langle x, x\rangle$ if and only if $x = 0$ (that is, x is the zero vector).
(iii) For all $x, y \in I$, $\langle x, y\rangle = \overline{\langle y, x\rangle}$, where $\overline{c}$ is the complex conjugate of c.
(iv) For all $c \in \mathbb{C}$ (or just $\mathbb{R}$, if I is a real inner product space) and all $x, y \in I$, $\langle cx, y\rangle = c\langle x, y\rangle$.
(v) For all $w, x, y \in I$, $\langle w + x, y\rangle = \langle w, y\rangle + \langle x, y\rangle$.

If $S \subseteq I$, then S becomes an inner product space by taking its inner product to be the inner product of I restricted to S. We call S an *inner product subspace* of I.

Remarks. Note that the inner product is linear in the first component, but, when the inner product spaces are complex, it is *conjugate linear* in the second component. When the definition speaks of "vectors," these are understood to be abstract elements; they could, for example, be infinitely long or functions from the integers to the real numbers (discrete signals).

Examples (Inner Product Spaces)

(i) The normed space R^n, Euclidean n-space, with inner product defined $\langle x, y\rangle = \sum_{k=1}^{n} x_k y_k$ is a real inner product space. This space is familiar from linear algebra and vector calculus.

(ii) The normed space $\mathbb{C}^n$ with inner product defined $\langle x, y\rangle = \sum_{k=1}^{n} x_k \overline{y_k}$ is a complex inner product space. (We take complex conjugates in the definition so that we can define $\|x\|$ on $\mathbb{C}^n$ from the inner product.)

(iii) The signal space l^2 is an inner product space when we define its inner product

$$\langle x, y\rangle = \sum_{n=-\infty}^{\infty} x(n)\overline{y(n)}\,. \tag{2.57}$$

Remarks. Notice that the Cauchy–Schwarz result (2.50) implies convergence of (2.57). Furthermore, since we know that the l^p spaces are Banach spaces and therefore complete, l^2 is our first example of a *Hilbert space*[10] (Figure 2.15).

The ideas underlying Banach and Hilbert spaces are central to understanding the latest developments in signal analysis: time-frequency transforms, time-scale transforms, and frames (Chapters 10–12).

[10]D. Hilbert studied the special case of l^2 around 1900. Later, in a landmark 1910 paper, F. Riesz generalized the concept and defined the l^p spaces we know today. The Cauchy–Schwarz inequality was known for discrete finite sums (i.e., discrete signals with finite support) by A. Cauchy in the early nineteenth century. H. Schwarz proved the analagous result for continuous signals (we see this in the next chapter, when the summations become integrals) and used it well in a prominent 1885 paper on minimal surfaces. V. Buniakowski had in fact already discovered Schwarz's integral form of the inequality in 1859, but his result drew little attention. O. Hölder published a paper containing his inequality in 1889. H. Minkowski disclosed the inequality that now bears his name as late as 1896; it was, however, restricted to finite sums. Riesz's 1910 paper would extend both the Hölder and Minkowski results to analog signals, for which integrals replace the discrete sums.

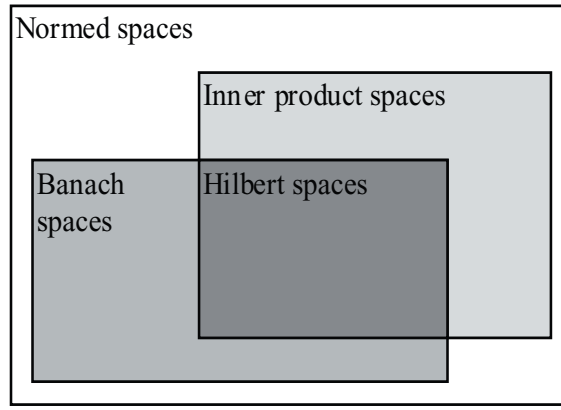

Fig. 2.15. Relationships between signal spaces. Hilbert spaces are precisely the inner prodct spaces that are also Banach spaces.

2.6.2 Norm and Metric

An inner product space I has a natural *norm* associated with its inner product: $\|x\| = \sqrt{\langle x, x\rangle}$. With this definition, the triangle inequality follows from the Cauchy–Schwarz relation, and the other normed space properties follow easily. There is also a natural distance measure: $d(x,y) = \|x - y\|$.

Theorem (Cauchy–Schwarz Inequality for Inner Product Spaces). Let I be an inner product space and $u,v \in I$. Then

$$|\langle u, v\rangle| \le \|u\|\|v\| \tag{2.58}$$

Furthermore, $|\langle u, v\rangle| = \|u\|\|v\|$ if and only if u and v are linearly dependent.

Proof: First, suppose that u and v are linearly dependent. If, say, $v = 0$, then both sides of (2.58) are zero. Also, if $u = cv$ for some scalar (real or complex number) c, then $|\langle u, v\rangle| = c\|v\|^2 = \|u\|\|v\|$, proving (2.58) with equality. Next, let us show that there is strict inequality in (2.58) if u and v are linearly independent. We resort to a standard trick. By linear independence, $u + cv \neq 0$ for any scalar c. Hence,

$$0 < \|u - cv\|^2 = \langle u, u\rangle - \bar{c}\langle u, v\rangle - c\langle v, u\rangle - |c|^2\langle v, v\rangle \tag{2.59}$$

for any c. In particular, by taking $c = \frac{\overline{\langle v, u\rangle}}{\langle v, v\rangle}$ in (2.59),

$$0 < \|u\|^2 - \frac{|\langle u, v\rangle|^2}{\|v\|^2}. \tag{2.60}$$

The Cauchy–Schwarz inequality follows. ■

We can now show that with $\|x\| = \sqrt{\langle x, x\rangle}$, I is a normed space. All of the properties of a normed space are simple, except for the triangle inequality. By expanding the inner products in $\|u + v\|^2$, it turns out that

$$\|u + v\|^2 = \|u\|^2 + \|v\|^2 + 2Real(\langle u, v\rangle) \le \|u\|^2 + \|v\|^2 + 2|\langle u, v\rangle|, \qquad (2.61)$$

where $Real(c)$ is the real part of $c \in \mathbb{C}$. Applying Cauchy–Schwarz to (2.61),

$$\|u + v\|^2 \le \|u\|^2 + \|v\|^2 + 2\|u\|\|v\| = (\|u\| + \|v\|)^2, \qquad (2.62)$$

and we have shown the triangle inequality for the norm.

The natural distance measure $d(x,y) = \|x - y\|$ is indeed a metric. That is, for all $x, y \in I$ we have $d(x, y) \ge 0$. Also, $d(x, y) = 0$ if and only if $x = y$. Symmetry exists: $d(x, y) = d(y, x)$. And the triangle inequality holds: Given $z \in I$, $d(x, y) \le d(x, z) + d(z, y)$. We use the distance metric to define convergent sequences in I: If $\{x_n\}$ is a sequence in I, and $d(x_n, x) \to 0$ as $n \to \infty$, then we say $x_n \to x$. The inner product in I is continuous (exercise), another corollary of the Cauchy–Schwarz inequality.

Proposition (Parallelogram Rule). Let I be an inner product space, let x and y be elements of I, and let $\|x\| = \sqrt{\langle x, x\rangle}$ be the the inner product space norm. Then $\|x + y\|^2 + \|x - y\|^2 = 2\|x\|^2 + 2\|y\|^2$.

Proof: Expanding the norms in terms of their definition by the inner product gives

$$\|x + y\|^2 = \|x\|^2 + \langle x, y\rangle + \langle y, x\rangle + \|y\|^2, \qquad (2.63)$$

$$\|x - y\|^2 = \|x\|^2 - \langle x, y\rangle - \langle y, x\rangle + \|y\|^2. \qquad (2.64)$$

Adding (2.63) and (2.64) together gives the rule. ■

The reason for the rule's name lies in a nice geometric interpretation (Figure 2.16). The parallelogram rule is an abstract signal space equivalent of an elementary

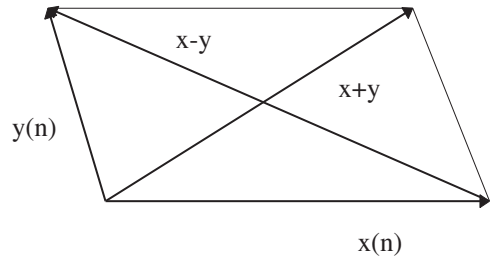

Fig. 2.16. Parallelogram rule. This simple geometric relationship between signals in an inner product space imposes a severe constraint on the l^p spaces. Only subspaces of l^2 support an inner product relation for our signal theory.

property from plane geometry. This shows the formal and conceptual power of the function space approach to signal theory. We can derive the algebraic rule from blind manipulations, and we can also resort to geometric constructs for insights into the relationships between the abstractions.

There is a negative consequence of the parallelogram rule: Except for l^2, none of the l^p spaces support an inner product definition that is related to the norm, $\| \ \|_p$. To verify this, consider the signals $x = [\underline{0}, 1]$, $y = [\underline{1}, 0]$, and compute $\|x\|_p^2 = \|y\|_p^2 = 1$ and $\|x + y\|_p^2 = \|x - y\|_p^2 = 2^{2/p}$. By the rule, we must have $2 = 2^{2/p}$, so that $p = 2$. The consequence is that although we have developed a certain body of theory for p-summable signals, found closure rules for basic operations like signal summation, amplification, and convolution, and shown that Cauchy sequences of p-summable signals converge, we cannot have an inner product relation for comparing signals unless $p = 2$. One might worry that l^2 is a signal analysis monoculture—it lacks the diversity of examples, counterexamples, classes, and conditions that we need to run and maintain the signal analysis economy. The good news is that the square-summable signal space is quite rich and that we can find in its recesses the exceptional signals we happen to need.

2.6.3 Orthogonality

The inner product relation is the key to decomposing a signal into a set of simpler components and for characterizing subspaces of signals. The pivotal concept for inner product signal spaces, as with simple Euclidean and unitary vector spaces, is orthogonality.

2.6.3.1 Definition and Examples. If we consider inner product spaces of discrete signals, then the inner product is a measure of the similarity of two signals. Signals are similar to themselves, and so nonzero signals have a positive inner product with themselves: $\langle u, u \rangle > 0$. Two signals that are not at all alike, following this intuition, have zero inner product with each other: $\langle u, u \rangle = 0$.

Definition (Orthogonality). In an inner product space *I,* two elements—*u* and *v*— are *orthogonal* if $\langle u, v \rangle = 0$; in this case, we write $u \perp v$. If u is orthogonal to every element of a set S, we write $u \perp S$. The set of all u in I such that for all s in S, we have $u \perp s$ is called the *orthogonal complement* of S; it is written $S^{\perp}$. A set S of nonzero elements of I is an *orthogonal* set if $u \perp v$ for *u, v* in S, $u \neq v$. If S is an orthogonal set such that $\|u\| = 1$ for all u in S, then S is an *orthonormal* set.

Example (Unit Impulses). The shifted unit impulse signals $S = \{\delta(n - k)\}$ form an orthonormal set in the inner product space l^2.

Notice that we do not say that the unit impulse signals are a *basis* for the square-summable signals. In finite-dimensional vector spaces, bases span the entire space; thus, every vector is a linear combination of a finite number of elements from the basis set. This is not true for general l^2 signals and the shifted unit impulses. No finite set of shifted unit impulses can span the whole Hilbert space. Moreover, some signals—those without finite support—cannot be a linear combination of a finite number of shifted unit impulses. While we were able to smoothly migrate most of the ideas from finite-dimensional vector spaces to inner product spaces, we now find that the concept of a basis did not fare so well. The problem is that general inner product spaces (among them our remaining l^p space, l^2) may have an "infinite" dimension.

We must loosen up the old idea of basis considerably. Let us reflect for a moment on the shifted unit impulses and a signal $x \in l^2$. Since $\|x\|_2 < \infty$, given $\varepsilon > 0$, we can find $N > 0$, so that the energy of the outer fringes of the signal—$x(n)$ values for $n > N$—have energy less than ε. This means that some linear combination of shifted impulses comes arbitrarily close to x in l^2 norm. Here then is where we loosen the basis concept so that it works for inner product spaces. We allow that a linear combination come arbitrarily close to signal x. This is the key idea of *completeness*: A set of elements S is *complete* or *total* if every element of the space I is the limit of a sequence of elements from the linear span of S. We also say that S is *dense* in I. The term "complete" for this idea is terrible, but standard. In a space with a distance measure, "complete" means that every Cauchy sequence converges to an element in the space. For example, the real number line is complete this sense. Now we use the same term for something different, namely the existence of a Cauchy sequence of linear combinations. The better term is "total" [15]. The only good advice is to pay close attention to the context; if the discussion is about bases, then "complete" probably signifies this new sense. So we could stipulate that a *basis* for I is a linearly independent set of signals whose linear span is dense in I.

Should we also assert that the shifted unit samples are a basis for the square-integrable signals? Notice that we are talking here about convergence in a general inner product space. Some inner product spaces are not complete. So, we will postpone the proper definition of completeness and the generalization of the basis concept that we need until we develop more inner product space theory.

Example (Rademacher[11] Signals). Consider the signals $e_0 = [\underline{1}, -1]$, $e_1 = [\underline{1}, 1, -1, -1]$, $e_2 = [\underline{1}, 1, 1, 1, -1, -1\ -1, -1]$, and so on. These signals are orthogonal. Notice that we can shift e_0 by multiples of 2, and the result is still orthogonal to all of the e_i. And we can delay e_1 by $4k$ for some integer k, and it is still orthogonal to all of the e_i and all of the shifted versions of e_0. Let us continue to use $e_{i,k}$ to denote the signal e_i delayed by amount k. Then the set $\{e_{i,k}$*: i is a natural number and* $k = m^{2i+1}$*, for some* $m\}$ is orthogonal. Notice that the sum of signal values of a linear combination

[11]Although not Jewish, but rather a pacifist, German number theorist and analyst Hans Rademacher (1892–1969) was forced from his professorship at Breslau in 1934 by the Nazi regime and took refuge in the United States.

of Rademacher signals is always zero. Hence, the Rademacher signals are not complete. The signal $\delta(n)$, for instance, is not in the closure of the linear span of the Rademacher signals. Note too that the Rademacher signals are not an orthonormal set. But we can orthonormalize them by dividing each $e_{i,k}$ by its norm, 2^{i+1}.

We will use the notion of orthogonality extensively. Note first of all that this formal definition of orthogonality conforms to our geometric intuition. The Pythagoras[12] relation for a right triangle states that the square of the length of the hypoteneuse is equal to the sum of the squares of the other two sides. It is easy to show that $u \perp v$ in an inner product space entails $\|u\|^2 + \|v\|^2 = \|u+v\|^2$. This also generalizes to an arbitrary finite orthogonal set. Other familiar inner product properties from the realm of vector spaces reappear as well:

(i) If $x \perp u_i$ for $i = 1, ..., n$, then x is orthogonal to any linear combination of the u_i.
(ii) If $x \perp u_i$ for i in the natural numbers, and $u_i \to u$, then $x \perp u$.
(iii) If $x \perp S$ (where S is an orthogonal set), u_i is in S, and $u_i \to u$, then $x \perp u$.

Orthonormal sets can be found that span the inner product signal spaces I that we commonly use to model our discrete (and later, analog) signals. The idea of spanning an inner product space generalizes the same notion for finite-dimensional vector spaces. We are often interested in decomposing a signal $x(n)$ into linear combination of simpler signals $\{u_0, u_1, ...\}$. That is, we seek scalars c_k such that $x(n) = \sum c_k u_k(n)$. If the family $\{c_k\}$ is finite, we say that $x(n)$ is in the *linear span* of $\{u_0, u_1, ...\}$. Orthonormal sets are handy for the decomposition because the scalars c_k are particularly easy to find. If $x(n) = \sum c_k u_k(n)$ and the u_k are orthonormal, then $c_k = \langle x, u_k \rangle$. For example, the shifted unit impulse signals $S = \{\delta(n - k)\}$ form an orthonormal set in the inner product space l^2. Decomposing $x(n)$ on the orthonormal shifted unit impulses is trivial: $c_k = x(k)$. The unit impulses are not a very informative decomposition of a discrete signal, however, because they do not provide any more information about the signal than its values contain at time instants. The problem of signal decomposition becomes much more interesting and useful when the composition elements become complicated. Each u_k then encapsulates more elaborate information about $x(n)$ within the decomposition. We may also interpret $|c_k|$ as a measure of how much alike are $x(n)$ and $u_k(n)$.

Example (Discrete Fourier Transform). To illustrate a nontrivial orthonormal decomposition, let $N > 0$ and consider the windowed exponential signals

$$u(n) = \frac{\exp\left(2\pi jk\frac{n}{N}\right)}{\sqrt{N}}[u(n) - u(n-N)], \tag{2.65}$$

[12]This property of right triangles was known to the Babylonians long before the mystic Greek number theorist Pythagoras (fl. ca. 510 B.C.) [B. L. van der Waerden, *Science Awakening*, translator. A. Dresden, Groningen, Holland: Nordhoff, 1954].

where $u(n)$ is the unit step signal. They form an orthonormal set on $[0, N-1]$. Suppose $x(n)$ also has support in $[0, N-1]$. We will show later that $x(n)$ is in the linear span of $\{u_k(n): 0 \le k \le N-1\}$ (Chapter 7). Since x, u_1, ..., u_{N-1} are in l^2, we have

$$x(n) = \sum_{k=0}^{N-1} c_k u_k = \sum_{k=0}^{N-1} \langle x, u_k \rangle u_k . \tag{2.66}$$

This decomposes $x(n)$ into a sum of scaled frequency components; we have, in fact, quite easily discovered the *discrete Fourier transform* (DFT) using a bit of inner product space theory. Fourier transforms in signal processing are a class of signal operations that resolve an analog or discrete signal into its frequency components—sinusoids or exponentials. The components may be called "Fourier components" when the underlying orthonormal set is not made up of sinusoidal or exponential components. Thus we have the definition: If $\{u_k(n): 0 \le k \le N-1\}$ is an orthonormal set and x is a signal in an inner product space, then $c_k = \langle x, u_k \rangle$ is the kth Fourier coefficient of $x(n)$ with respect to the $\{u_k\}$. If $x(n) = \sum c_k u_k$, then we say that x is represented by a *Fourier series* in the $\{u_k\}$.

Note that the DFT system is linear, but, owing to the fixed decomposition window, not translation-invariant. There are a great many other properties and applications of the DFT (Chapter 7).

2.6.3.2 Bessel's Inequality. Geometric intuition about inner product spaces can tell us how we might use Fourier coefficients to characterize a signal. From (2.66) we can see that each Fourier coefficient indicates how much of each $u_k(n)$ there is in the signal $x(n)$. If $0 = \langle x, u_k \rangle$, then there is nothing like $u_k(n)$ in $x(n)$; if $|\langle x, u_k \rangle|$ is large, it means that there is an important u_k-like element in $x(n)$; and when $|\langle x, u_k \rangle|$ is large and the rest of the Fourier coefficients are small, it means that as a signal $x(n)$ has a significant similarity to $u_k(n)$. Given an orthonormal set $S = \{u_k\}$ and a signal $x(n)$, what do the Fourier coefficients of $x(n)$ with respect to S look like? It is clear from (2.66) that when $\|x(n)\|$ is large, then the norms of the Fourier coefficients also become large. How large can the Fourier coefficients be with respect to $\|x(n)\|$? If the set S is infinite, are most of the Fourier coefficients zero? Is it possible for the Fourier coefficients of $x(n)$ to be arbitrarily large? Perhaps the $\langle x, u_k \rangle \to 0$ as $k \to \infty$? If not, then there is an $\varepsilon > 0$, such that for any $N > 0$, there is a $k > N$ with $|\langle x, u_k \rangle| > \varepsilon$. In other words, can the significant Fourier components in $x(n)$ with respect to S go on forever? The next set of results, leading to Bessel's theorem for inner product spaces, helps to answer these questions.

Consider a signal $x(n)$ and an orthonormal set $S = \{u_k(n): 0 \le k < N\}$ in an inner product space I. $x(n)$ may be in the linear span of S, in which case the Fourier coefficients tell us the degree of similarity of $x(n)$ to each of the elements u_k. But if $x(n)$ is not in the linear span of S, then we might try to find the $y(n)$ in the linear span of S that is the closest signal to $x(n)$. In other words, if S cannot give us an exact breakdown of $x(n)$, what is the best model of $x(n)$ that S can provide? Let c_k be complex numbers,

and let $y = \sum c_k u_k$. $y(n)$ is a linear combination of elements of S which we want to be close to $x(n)$. Then, after some inner product algebra and help from Pythagoras,

$$\|x - y\|^2 = \left\langle x - \sum c_k u_k, x - \sum c_k u_k \right\rangle = \|x\|^2 - \sum \left| c_k - \langle u_k, x \rangle \right|^2 - \sum \left| \langle u_k, x \rangle \right|^2. \tag{2.67}$$

By varying the c_k, $y(n)$ becomes any general signal in the linear span of S. The minimum distance between $x(n)$ and $y(n)$ occurs when the middle term of (2.67) is zero: $c_k = \langle u_k, x \rangle$. With this choice of $\{c_k\}$, $y(n)$ is the best model S can provide for $x(n)$.

We can apply this last result to answer the question about the magnitude of Fourier coefficients for a signal $x(n)$ in an inner product space. We would like to find an orthogonal set S so that its linear span contains every element of the inner product space. Then, we might characterize a signal $x(n)$ by its Fourier coefficients with respect to S. Unfortunately, as with the Rademacher signals, the linear span of an orthonormal set may not include the entire inner product space. Nevertheless, it is still possible to derive Bessel's inequality for inner product spaces.

Theorem (Inner Product Space Bessel[13] Inequality). Let I be an inner product space, let $S = \{u_k\}$ an orthonormal family of signals in I, and let $x \in I$. Then

$$\|x\|^2 \geq \sum \left| \langle u_k, x \rangle \right|^2. \tag{2.68}$$

Proof: Proceeding from (2.67), we set $c_k = \langle u_k, x \rangle$. Then, $\sum \left| c_k - \langle u_k, x \rangle \right|^2 = 0$, and $\|x - y\|^2 = \|x\|^2 - \sum \left| \langle u_k, x \rangle \right|^2$. But $\|x - y\|^2 \geq 0$. Thus, $\|x\|^2 - \sum \left| \langle u_k, x \rangle \right|^2 \geq 0$ and (2.68) follows. ■

2.6.3.3 Summary. We use the inner product relation as a measure of the similarity of signals, just as we do with finite-dimensional vectors. Orthonormal families of signals $S = \{u^k\}$ are especially convenient for decomposing signals $x(n)$, since the coefficients of the decomposition sum are readily computed as the inner product $c_k = \langle u_k, x \rangle$. It may well be that $x(n)$ cannot be expressed as a sum (possibly infinite) of elements of S; nevertheless, we can find the coefficients c_k that give us the closest signal to $x(n)$. From Bessel's relation, we see that the Fourier coefficients for a general signal $x(n)$ with respect to an orthonormal family S are bounded by $\|x\|$. One does not find a monstrous Fourier coefficient unless the original signal itself is monstrous. Moreover, the sum in (2.68) could involve an infinite number of nonzero terms. Then the fact that the sum converges indicates that the Fourier coefficients must eventually become arbitrarily small. No signal has Fourier coefficients with respect to S that get arbitrarily large. When S is infinite, every signal has Fourier coefficients $c_k = \langle u_k, x \rangle$ such that $c_k \to 0$ as $k \to \infty$. Bessel's inequality guarantees that the Fourier coefficients for $x(n)$ are well-behaved.

[13]After German mathematician and astronomer Friedrich Wilhelm Bessel (1794–1846).

Under what conditions does $x = \sum c_k u_k$, with $c_k = \langle u_k, x \rangle$? That is, we are interested in whether $x(n)$ has a Fourier series representation with respect to the $\{u_k\}$. If the orthonormal set S is finite and x is in the linear span of S, then this is true. If, on the other hand, S is infinite, then the sum becomes (possibly) infinite and the problem becomes whether the limit that formally defines this summation exists. Recall that calculus explains convergence of infinite sums in terms of Cauchy sequences of partial series sums. Thus, $\sum a_k = a$, if $\lim A_n = a$, where $A_n = \sum_{k=1}^{n} a_k$. If every Cauchy sequence has a limit, then the abstract space is called *complete*. Banach spaces are normed spaces that are complete. If we add completeness to the required properties of an inner product space, then what we get is the abstract structure known as a *Hilbert space*—one of the most important tools in applied mathematics, signal analysis, and physics.

2.7 HILBERT SPACES

In addition to the many excellent treatments of inner product and Hilbert spaces in functional analysis treatises, Hilbert space theory is found in specialized, introductory texts [25, 26].

2.7.1 Definitions and Examples

Definition (Hilbert Space). A *Hilbert space* is a complete inner product space. If $S \subseteq H$ is an inner product subspace of H and every Cauchy sequence of elements of S converges to an element of S, then S is a *Hilbert subspace* of H.

Recall that $\{x_k(n)\}$ is a Cauchy sequence if for every $\varepsilon > 0$, there is an $N > 0$ so that whenever $k, l > N$, we have $d(x_k, x_l) = \|x_k - x_l\| < \varepsilon$. Completeness means that every Cauchy sequence of signals in the space converges to a signal also in that space. Since we are working with inner product spaces, this norm must be interpreted as the inner product space norm. The least special of all the spaces is the normed space. Within its class, and distinct from one another, are the inner product and Banach spaces. The Banach spaces that are blessed with an inner product are the Hilbert spaces (Figure 2.15).

Examples (Hilbert Spaces). The following are Hilbert spaces:

(i) l^2 with the inner product defined

$$\langle x, y \rangle = \sum_{n=-\infty}^{\infty} x(n)\overline{y(n)}. \tag{2.69}$$

(ii) The set of signals in l^2 that are zero on a nonempty subset $Y \subseteq \mathbb{Z}$.

(iii) The inner product space $\mathbb{R}^n$, Euclidean n-space, with the standard dot product.

(iv) Similarly, the unitary space $\mathbb{R}^n$ with the standard inner product is a complex Hilbert space.

(v) Consider some subset of the shifted unit impulse signals $S = \{\delta(n-k)\}$. The linear span of S is an inner product subspace of l^2. If we take the set of limit points of Cauchy sequences of the linear span of S, then we get a Hilbert subspace of l^2. These subspaces are identical to those of (ii).

2.7.2 Decomposition and Direct Sums

The notions of orthogonality, basis, and subspace are interlinked within Hilbert space theory. The results in this section will show that l^2 Hilbert space looks very much like an "infinite-dimensional" extension of our finite-dimensional Euclidean and unitary n-spaces.

2.7.2.1 Subspace Decomposition.

The following theorem is basic.

Theorem (Hilbert Space Decomposition). Let H be a Hilbert space, let X be a Hilbert subspace of H, and let $Y = X^{\perp}$ be the orthogonal complement of X in H. Then for any h in H, $h = x + y$, where $x \in X$ and $y \in Y$.

Proof: Let $h \in H$ and consider the distance from the subspace X to h. This number, call it $\delta = d(h, X)$, is the greatest lower bound of $\{\|x - h\|: x \text{ in } X\}$. Since we can find elements $x \in X$ whose distance to h differs by an arbitrarily small value from δ, there must be a sequence $\{x_n: x_n \text{ in } X, n > 0\}$ with $\|x_n - h\| < 1/n + \delta$.

We claim that $\{x_n\}$ is a Cauchy sequence in X. By applying the parallelogram rule to $x_n - h$ and $x_m - h$, we have

$$\|(x_n - h) + (x_m - h)\|^2 + \|x_n - x_m\|^2 = 2\|(x_n - h)\|^2 + 2\|(x_m - h)\|^2. \tag{2.70}$$

Since X is closed under addition and scalar multiplication, we have $\frac{x_n + x_m}{2} \in X$, and therefore

$$\|(x_n - h) + (x_m - h)\| = \|x_n + x_m - 2h\| = 2\left\|\frac{x_n + x_m}{2} - 2\right\| \geq 2\delta. \tag{2.71}$$

Putting the inequality (2.71) into (2.70) and rearranging gives

$$\|x_n - x_m\|^2 \leq 2\left(\delta + \frac{1}{n}\right) + 2\left(\delta + \frac{1}{m}\right) - \|x_n - h + x_m - h\|^2. \tag{2.72}$$

Consequently,

$$\|x_n - x_m\|^2 \le 4\left(\frac{\delta}{n}\right) + \frac{2}{n^2} + 4\left(\frac{\delta}{m}\right) + \frac{2}{m^2}, \tag{2.73}$$

which shows $\{x_n\}$ is Cauchy, as claimed. Since X is complete and contains this sequence, there must be a limit point: $x_n \to x \in X$. Let $y = h - x$. We claim that $y \in X^{\perp} = Y$. To prove this claim, let $0 \neq w \in X$. We must show that $\langle y, w\rangle = 0$. First note that since $\delta = d(h, X)$ and $x \in X$, we have

$$\delta \le \|y\| = \|h - x\| = \left\|h - \lim_{k\to\infty} x_k\right\| \le \frac{1}{n} + \delta \tag{2.74}$$

for all n. Thus, $\delta = \|y\| = \langle y, y\rangle^{1/2}$. Next, let a be a scalar. Closure properties of X imply that $x + aw \in X$ so that $\|y - aw\| = \|h - (x + aw)\| \ge \delta$. Expanding this last inequality in terms of the inner product on H gives

$$\langle y, y\rangle - \bar{a}\langle y, w\rangle - a\langle w, y\rangle + |a|^2\langle w, w\rangle \ge \delta^2. \tag{2.75}$$

Because $\langle y, y\rangle = \delta^2$, we can simplify (2.75) and then take $a = \frac{\langle y, w\rangle}{\langle w, w\rangle}$, which greatly simplifies to produce $|\langle y, w\rangle|^2 \le 0$. This must mean that $0 = \langle y, w\rangle$, $y \perp w$, and $y \in X^{\perp}$. This proves the last claim and completes the proof. ■

Let us list a few facts that follow from the theorem:

(i) The norm of element y is precisely the distance from h to the subspace X, $\|y\| = \delta = d(h, X)$. This was shown in the course of the proof.
(ii) Also, the decomposition of $h = x + y$ is unique (exercise).
(iii) One last corollary is that a set S of elements in H is complete (that is, the closure of its linear span is all of H) if and only if the only element that is orthogonal to all elements of S is the zero element.

Definition (Direct Sum, Projection). Suppose that H is a Hilbert space with $X, Y \subseteq H$. Then H is the *direct sum* of X and Y if every $h \in H$ is a unique sum of a signal in X and a signal in Y: $h = x + y$. We write $H = X \oplus Y$ and, in this case, if $h = x + y$ with $x \in X$ and $y \in Y$, we say that x is the *projection* of h onto X and y is the projection of h onto Y.

The decomposition theorem tells us that a Hilbert space is the direct sum of any Hilbert subspace and its orthogonal complement. The direct sum decomposition of a Hilbert space leads naturally to a linear system.

Definition (Projection System). Let H be a Hilbert space and X a Hilbert subspace of H. The *projection from H to X* is the mapping $T: H \to X$ defined by $T(h) = x$, where $h = x + y$, with $y \in X^{\perp}$.

Remark. This definition makes sense (in other words, the mapping is *well-defined*) because there is a unique $x \in X$ that can be associated with any $h \in H$.

2.7.2.2 Convergence Criterion. Combining the decomposition system with orthogonality gives Hilbert space theory much of the power it has for application in signal analysis. Consider an orthonormal set of signals $\{u_k(n)\}$ in a Hilbert space H, a set of scalars $\{a_k\}$, and the sum

$$x(n) = \sum_{k=-\infty}^{\infty} a_k u_k(n). \tag{2.76}$$

This sum may or may not converge in H. If the sequence of partial sums $\{s_N(n)\}$

$$s_N(n) = \sum_{k=-N}^{N} a_k u_k(n). \tag{2.77}$$

is a Cauchy sequence, then (2.76) has a limit.

Theorem (Series Convergence Criterion). The sum (2.76) converges in Hilbert space H if and only if the signal $a(n) = a_n$ is in l^2.

Proof: Let $N > M$ and take the difference $s_N - s_M$ in (2.77). Then,

$$\|s_N - s_M\|^2 = |a_{-N}|^2 + |a_{-N+1}|^2 + \cdots + |a_{-M-1}|^2 + |a_{M+1}|^2 + \cdots + |a_N|^2, \tag{2.78}$$

because of the orthonormality of the $\{u_k(n)\}$ signal family. Thus, $d(s_N, s_M)$ tends to zero if and only if the sums of squares of the $|a_n|$ tend to zero. ■

Note too that if (2.76) converges, then the a_n are the Fourier coefficients of x with respect to the orthonormal family $\{u_k(n)\}$. This follows from taking the inner product of x with a typical u_k:

$$\langle x, u_k \rangle = \left\langle \sum_{i=-\infty}^{\infty} a_i u_i(n), u_k \right\rangle = \left\langle \lim_{N\to\infty} \sum_{i=-N}^{N} a_i u_i(n), u_k \right\rangle = a_k \langle u_k, u_k \rangle = a_k. \tag{2.79}$$

Therefore,

$$x(n) = \sum_{k=-\infty}^{\infty} \langle x, u_k \rangle u_k(n). \tag{2.80}$$

Thus, if the orthonormal family $\{u_k(n)\}$ is complete, then any $x(n)$ in H can be written as a limit of partial sums, and the representation (2.80) holds.

The theorem shows that there is a surprisingly close relationship between a general Hilbert space and the square-summable sequences l^2.

Orthonormal families and inner products are powerful tools for finding the significant components within signals. When does a Hilbert space have a complete orthonormal family? It turns out that every Hilbert space has a complete orthonormal family, a result that we will explain in a moment. There is also a method whereby any linearly independent set of signals in an inner product space can be converted into an orthonormal family.

2.7.2.3 Orthogonalization. Let us begin by showing that there is an algorithm, called *Gram–Schmidt*[14] *orthogonalization*, for converting a linearly independent set of signals into an orthormal family. Many readers will recognize the procedure from linear algebra.

Theorem (Gram–Schmidt Orthogonalization). Let H be a Hilbert space containing a linearly independent family $\{u_n\}$. Then there is an orthonormal family $\{v_n\}$ with each v_n in the linear span of $\{u_k: 0 \le k \le n\}$.

Proof: The proof is by induction on n. For $n = 0$, we can take $v_0 = \dfrac{u_0}{\|u_0\|}$. Now suppose that the algorithm works for $n = 0, 1, ..., k$. We want to show that the orthonormal elements can be expanded one more time, for $n = k + 1$. Let U be the subspace of H that consists of the linear span of $\{u_0, u_1, ..., u_k\}$. This is a Hilbert subspace; for instance, it is closed and therefore complete. Let $V = U^{\perp}$. By linear independence, u_{k+1} is not in U. This means that in the unique decomposition $u_{k+1} = u + v$, with u in U and v in V, we must have $v \neq 0$, the zero signal. If we set $v_{k+1} = \dfrac{v}{\|v\|}$, then $\|v_{k+1}\| = 1$; $v_{k+1} \in U^{\perp}$; and, because $v = u_{k+1} - u$, v_{k+1} is in the linear span of $\{u_i: 0 \le i \le k + 1\}$. ■

It is easier to find linearly independent than fully orthogonal signal families. So the Gram–Schmidt method is useful. The Gram–Schmidt procedure shows that if the linearly independent family is complete, then the algorithm converts it into a complete, orthonomal family.

[14]Erhard Schmidt (1876–1959), to whom the algorithm had been attributed, was Hilbert's student. Schmidt specified the algorithm in 1907. But it was discovered later that Jorgen Pedersen Gram (1850–1916) of Denmark had resorted to the same technique during his groundbreaking 1883 study on least squares approximation problems.

2.7.3 Orthonormal Bases

We now show how to build complete orthonormal families of signals in Hilbert space. That is, we want every element in the space to be approximated arbitrarily well by some linear combination of signals from the orthonormal family. Euclidean and unitary n-dimensional vector spaces all have orthonormal bases. This is a central idea in linear algebra. We are close to having shown the existence of orthonormal bases for general Hilbert spaces, too. But to get there with the Gram–Schmidt algorithm, we need to start with a complete (total) linearly independent family of signals. At this point, it is not clear that a general Hilbert space should even have a total linearly independent set.

Definition (Orthonormal Basis). In a Hilbert space, a complete orthonormal set is called an *orthonormal basis*.

We have already observed that the shifted unit sample signals are an orthonormal basis for the Hilbert space l^2. Remember the important distinction between this looser concept of basis and that for the finite-dimensional Euclidean and unitary spaces. In the cases of $\mathbb{R}^n$ and $\mathbb{C}^n$, the bases span the entire space. For some Hilbert spaces, however—and l^2 is a fine example—the linear combinations of the orthonormal basis signals only come arbitrarily close in norm to some signals.

2.7.3.1 Set Theoretic Preliminaries. There are some mathematical subtleties involved in showing that every Hilbert space has an orthonormal basis. The notions we need hinge on some fundamental results from mathematical set theory. A very readable introduction to these ideas is [27]. Most readers are probably aware that there are different orders of infinity in mathematics. (Those that are not may be in for a shock.) The number of points on a line (i.e., the set of real numbers) is a larger infinity than the natural numbers, because $\mathbb{R}$ cannot be placed in a one-to-one correspondence with $\mathbb{N}$. We say that two sets between which a one-to-one map exists have the same *cardinality*. The notation for the cardinality of a set X is $|X|$. In fact, the natural numbers, the integers, the rational numbers, and even all the real numbers which are roots of rational polynomials have the same cardinality, $|\mathbb{N}|$. They are called *countable* sets, because there is a one-to-one and onto map from $\mathbb{N}$, the counting set, to each of them. The real numbers are an *uncountable* set. Also uncountable is the set of subsets of the natural numbers, called the *power set* of $\mathbb{N}$, written $\mathcal{P}(\mathbb{N})$. It turns out that $|\mathcal{P}(\mathbb{N})| = |\mathbb{R}|$. The discovery of different orders of infinity—different cardinalities—is due to Cantor.[15]

[15]Georg Cantor (1845–1918) worked himself to the point of physical, emotional, and mental exhaustion trying to demonstrate the *continuum hypothesis*: there is no cardinality of sets in between $|\mathcal{N}|$ and $|\mathcal{R}|$. He retreated from set theory to an asylum, but never proved or disproved the continuum hypothesis. It is a good thing, too. In 1963, Paul Cohen proved that the continuum hypothesis is independent of the usual axioms of set theory; it can be neither proved nor disproved! [K. Devlin, *Mathematics: The Science of Patterns*, New York: Scientific American Library, 1994.]

Some basic facts about countable sets are as follows (exercises):

(i) The Cartesian product $X \times Y$ of two countable sets is countable.
(ii) The Cartesian product $X_1 \times X_2 \times \cdots \times X_n$ of a finite number of countable sets is countable.
(iii) A countable union of countable sets is countable.
(iv) The set that consists of all finite subsets of a countable set is countable.
(v) The set of all subsets of a set X always has a larger cardinality than X; in other words, $|X| < |\mathcal{P}(X)|$.

Observe carefully that indexing notation presupposes a one-to-one, onto map from the indexing set to the indexed set. Suppose X is a countable set—for example, the set of shifted impulses, $X = \{\delta(n-k)\colon k \text{ an integer}\}$. We can index X by $\mathbb{N}$ with the map $f(k) = \delta(n-k)$. Trivially, f is a one-to-one and onto map of $\mathbb{N}$ to X. Now let $Y = \{a\delta(n)\colon a \text{ is a real number}\}$ be the set of amplified unit impulse signals. It is impossible to index Y with the natural numbers, because Y has the same cardinality as the real line. Instead, if it is necessary to index such a collection, we must pick an indexing set that has the same cardinality as Y.

2.7.3.2 Separability. We draw upon these set theoretic ideas in order to show that every Hilbert space has an orthonormal basis. In particular, we need to bring the notion of cardinality into the discussion of Hilbert space and to invoke another concept from set theory—the Axiom of Choice.

Definition (Separable Hilbert Space). A Hilbert space is *separable* if it contains a countable dense set.

Notice that l^2 is a separable Hilbert space. The set of shifted impulse signals is an orthonormal basis for l^2. Now the set of all scalar multiples of linear combinations of the shifted impulses is not countable, because there are an uncountable number of magnitude values possible. However, we can get arbitrarily close to a linear combination of shifted impulses with a linear combination that has rational coefficients. There are a countable number of rationals. The set of finite sequences of rationals is therefore countable. Thus, the set of linear combinations of shifted impulses with rational coefficients is a countable dense subset of l^2.

Let's continue this line of reasoning and assume that we have a countable dense subset S of a Hilbert space H. We wish to fashion S into an orthonormal basis. We may write the dense family using the natural numbers as an indexing set: $S = \{s_n\colon n \text{ is in } \mathbb{N}\}$. If S is a linearly independent family, then the Gram–Schmidt procedure applies, and we can construct from S an orthonormal family that is still dense in H. Thus, in this case, H has a countable basis. If S is has some linear dependency, we can pick the first element of S, call it d_0, that is a linear combination of the previous ones. We delete d_0 from S to form S_0, which still has the same linear span, and hence is just as dense as S in H. Continue this process for all natural numbers,

finding d_{n+1} and cutting it from S_n to produce S_{n+1}. The result is a linearly independent set, S_ω. If S_ω is not linearly independent, then there is an element that is a linear combination of the others; call it t. We see immediately a contradiction, because t had to be chosen from the orthogonal complement of the elements that we chose before it and because the elements that were chosen later had to be orthogonal—and therefore linearly independent—to t. We note as well that S_ω has a linear span which is dense in H; and, using the Gram–Schmidt algorithm, it can be sculpted into an orthonormal basis for H.

Without separability of the Hilbert space H, the above argument breaks down. We could begin an attack on the problem by assuming a dense subset $S \subseteq H$. But what subsets, other than H itself, can we assume for a general, abstract Hilbert space? Examining the separable case's argument more closely, we see that we really built up a linearly independent basis incrementally, beginning from the bottom $s_0 \in S$. Here we can begin with some nonzero element of H, call it s_a, where we index by some other set A that has sufficient cardinality to completely index the orthonormal set we construct. If the linear span of $\{s_a\}$ includes all of H, then we are done; otherwise, there is an element in the orthogonal complement of the Hilbert subspace spanned by $\{s_a\}$. Call this element s_b. Then $\{s_a, s_b\}$ is a linearly independent set in H. Continue the process: Check whether the current set of linearly independent elements has a dense linear span; if not, select a vector from the orthogonal complement, and add this vector to the linearly independent family. In the induction procedure for the case of a separable H, the ultimate completion of the construction was evident. Without completion a contradiction arises. For if our "continuation" on the natural numbers does not work, can we find a least element that is a linear combination of the others, leading to a contradiction. But how can we find a "least" element of the index set A in the nonseparable case? We do not even know of an ordering for A. Thus there is a stumbling block in showing the existence of an orthonormal basis for a nonseparable Hilbert space.

2.7.3.3 Existence. The key is an axiom from set theory, called the *Axiom of Choice*, and one of its related formulations, called *Zorn's lemma.*[16] The Axiom of Choice states that the Cartesian product of a family of sets $\{S_a : a \in A\}$ is not empty. That is, $P = \{(s_a, s_b, s_c, \ldots) : s_a \in S_a, s_b \in S_b, \ldots\}$ has at least one element. The existence of an element in P means that there is a way to simultaneously choose one element from each of the sets S_a of the collection S. Zorn's lemma seems to say nothing like this. The lemma states that if a family of sets $S = \{S_a : a \in A\}$ has the property that for every chain $S_a \subseteq S_b \subseteq \ldots$ of sets in S, there is a T in S that is a superset of each of the chain elements, then S itself has an element that is contained properly in no other element of S; that is, S has a *maximal* set. Most people are inclined to think that the Axiom of Choice is obviously true and that Zorn's lemma is very suspicious, if not an outright fiction. On the contrary: Zorn's lemma is true if and only if the Axiom of Choice is true [27].

[16]Algebraist Max Zorn (1906–1993) used his *maximal set principle* in a 1935 paper.

Let us return now to our problem of constructing a dense linearly independent set in a Hilbert space H and apply the Zorn's lemma formulation of the Axiom of Choice. In a Hilbert space, the union of any chain of linearly independent subsets is also linearly independent. Thus, H must have, by Zorn, a maximal linearly independent set S. We claim that K, the linear span of S, is dense. Suppose not. Now K is a Hilbert subspace. So there is a vector v in the orthogonal complement to K. Contradiction is imminent. The set $S \cup \{v\}$ is linearly independent and properly includes S; this is impossible since S was selected to be maximal. So S must be complete (total). Its linear span is dense in H. Now we apply the Gram–Schmidt procedure to S. One final obstacle remains. We showed the Gram–Schmidt algorithm while using the natural numbers as an index set, and thus implicitly assumed a countable collection! We must not assume this now. Instead we apply Zorn's lemma to the Gram–Schmidt procedure, finding a maximal orthonormal set with same span as S. We have, with the aid of some set theory, finally shown the following.

Theorem (Existence of Orthonormal Bases). Every Hilbert space contains an orthonormal basis. ■

If the Hilbert space is spanned by a finite set of signals, then the orthonormal basis has a finite number of elements. Examples of finite-dimensional Hilbert spaces are the familiar Euclidean and unitary spaces. If the Hilbert space is separable, but is not spanned by a finite set, then it has a countably infinite orthonormal basis. Lastly, there are cases of Hilbert spaces which are not separable.

2.7.3.4 Fourier Series. Let us complete this chapter with a theorem that wraps up many of the ideas of discrete signal spaces: orthonormal bases, Fourier coefficients, and completeness.

Theorem (Fourier Series Representation). Let H be a Hilbert space and let $S = \{u_a : a \in A\}$ be an orthonormal family in H. Then,

(i) Any $x \in H$ has at most countably many nonzero Fourier coefficients with respect to the u_a.

(ii) S is complete (its linear span is dense in H) if and only if for all signals $x \in H$ we have

$$\|x\|^2 = \sum_{a \in A} \left|\langle x, u_a \rangle\right|^2, \tag{2.81}$$

where the sum is taken over all a, such that the Fourier coefficient of x with respect to u_a is not zero.

(iii) (Riesz–Fischer Theorem[17]) If $\{c_a : a \in A\}$ is a set of scalars such that

[17]Hungarian Frigyes Riesz (1880–1956) and Austrian Ernst Sigismund Fischer (1875–1954) arrived at this result independently in 1907 [22].

$$\sum_{a \in A} |c_a|^2 < \infty, \tag{2.82}$$

then there is a unique x in H such that $\langle x, u_a \rangle = c_a$, and

$$x = \sum_{a \in A} c_a u_a. \tag{2.83}$$

Proof: We have already used most of the proof ideas in previous results.

(i) The set of nonzero Fourier coefficients of x with respect to the u_a is the same as the set of Fourier coefficients that are greater than $1/n$ for some integer n. Since there can only be finitely many Fourier coefficients that are greater than $1/n$, we must have a countable union of finite sets, which is still countable. Therefore, there may only be a countable number of $\langle x, u_a \rangle \neq 0$.

(ii) Suppose first that S is complete and $x \in H$. Since there can be at most a countably infinite number of nonzero Fourier coefficients, it is possible to form the series sum,

$$s = \sum_{a \in A} \langle x, u_a \rangle u_a. \tag{2.84}$$

This sum converges by the Bessel inequality for inner product spaces. Consider $t = s - x$. It is easy to see that $t \in S^{\perp}$ by taking the inner product of t with each $u_a \in S$. But since S is complete, this means that there can be no nonzero element in its orthogonal complement; in other words, $t = 0$ and $s = x$. Now, since $\langle u_a, u_b \rangle \neq 0$ when $a \neq b$, we see that

$$\|x\|^2 = \langle x, x \rangle = \left\langle \sum_{a \in A} \langle x, u_a \rangle u_a, \sum_{a \in A} \langle x, u_a \rangle u_a \right\rangle = \sum_{a \in A} \langle x, u_a \rangle \overline{\langle x, u_a \rangle}. \tag{2.85}$$

Next, suppose that the relation (2.81) holds for all x. Assume for the sake of contradiction that S is not complete. Then by the Hilbert space decomposition theorem, we know that there is some nonzero $x \in S^{\perp}$. This means that $\langle x, u_a \rangle = 0$ for all u_a and that the sum (2.81) is zero. The contradiction is that now we must have $x = 0$, the zero signal.

(iii) If $\{c_a : a \in A\}$ is a set of scalars such that (2.82) holds, then at most a countable number of them can be nonzero. This follows from an argument similar to the proof of (i). Since we have a countable collection in (2.82), we may use the Hilbert space series convergence criterion, which was stated (implicitly at that point in the text) for a countable collection. ■

An extremely powerful technique for specifying discrete systems follows from these results. Given a Hilbert space, we can find an orthonormal basis for it. In the case of a separable Hilbert space, there is an iterative procedure to find a linearly independent family and orthogonalize it using the Gram–Schmidt algorithm. If the

Hilbert space is not separable, then we do not have such a construction. But the existence of the orthonormal basis $U = \{u_a : a \in A\}$ is still guaranteed by Zorn's lemma. Now suppose we use the orthonormal basis to analyze a signal. Certain of the basis elements, $V = \{v_b : b \in B \subseteq A\}$, have features we seek in general signals, x. We form the linear system $T(x) = y$, defined by

$$Tx = y = \sum_{b \in B} \langle x, v_b \rangle v_b . \tag{2.86}$$

Now the signal y is that part of x that resembles the critical basis elements. Since the theorem guarantees that we can expand any general element in terms of the orthonormal basis U, we know that the sum (2.86) converges. We can tune our linear system to provide precisely the characteristics we wish to preserve in or remove from signal x by selecting the appropriate orthonormal basis elements. Once the output $y = Tx$ is found, we can find the features we desire in x more easily in y. Also, y may prove that x is desirable in some way because it has a large norm; that is $\|x\| \approx \|y\|$. And, continuing this reasoning, y may prove that x is quite undesirable because $\|y\|$ is small.

In its many guises, we will be pursuing this idea for the remainder of the book.

2.8 SUMMARY

This chapter began with a practical—perhaps even naïve—exploration of the types of operations that one can perform on signals. Many of these simple systems will arise again and again as we develop methods for processing and interpreting discrete and continuous signals. The later chapters will demonstrate that the most important type of system we have identified so far is the linear, time-invariant system. In fact, the importance of the characterization result, the convolution theorem for LTI systems, cannot be overemphasized. This simple result underlies almost all of our subsequent work. Some of the most important concepts in signal filtering and frequency analysis depend directly on this result.

Our explorations acquire quite a bit of mathematical sophistication, however, when we investigate the closure properties of our naively formulated signal processing systems. We needed some good answers for what types of signals can be used with certain operations. It seems obvious enough that we would like to be able to sum any two signals that we consider, and this is clearly feasible for finitely supported signals. For other signals, however, this simple summing problem is not so swiftly answered. We need a formal mathematical framework for signal processing and analysis. Inspired by basic vector space properties, we began a search for the mathematical underpinnings of signal theory with the idea of a normed space. The l^p Banach spaces conveniently generalize some natural signal families that we first encountered in Chapter 1. Moreover, these spaces are an adequate realm for developing the theory of signals, stable systems, closure, convolution, and convergence of signals.

Unfortunately, except for l^2, none of the l^p spaces support an inner product definition that is related to the norm, $\| \|_p$. This is a profoundly negative result. But it once again shows the unique nature of the l^2 space. Of the l^p Banach spaces, only l^2 can be equipped with an inner product that makes it into a Hilbert space. This explains why finite-energy signals are so often the focus of signal theory. Only the l^2 Hilbert space, or one of its closed subspaces, has all of the features from Euclidean vector spaces that we find so essential for studying signals and systems.

We see that all Hilbert spaces have orthonormal bases, whether they are finite, countable, or uncountable. Furthermore, a close link exists between orthonormal bases for Hilbert spaces and linear systems that map one signal to another yet retain only desirable properties of the input. We will see in the sequel that it is possible to find special orthonormal bases that provide for the efficient extraction of special characteristics of signals, help us to find certain frequency and scale components of a signal, and, finally, allow us to discover the structure and analyze a signal.

REFERENCES

1. A. V. Oppenheim, A. S. Willsky, and S. H. Nawab, *Signals and Systems*, 2nd ed., Upper Saddle River, NJ: Prentice-Hall, 1997.
2. J. A. Cadzow and H. F. Van Landingham, *Signals, Systems, and Transforms*, Englewood Cliffs, NJ: Prentice-Hall, 1983.
3. H. Baher, *Analog and Dignal Signal Processing*, New York: Wiley, 1990.
4. R. E. Ziemer, W. H. Tranter, and D. R. Fannin, *Signals and Systems*: *Continouous and Discrete*, 3rd ed., New York: Macmillan, 1993.
5. P. P. Vaidyanathan, Multirate digital filters, filter banks, polyphase networks, and applications: A tutorial, *Proceedings of the IEEE*, vol. 78, pp. 56–93, January 1990.
6. O. Rioul and M. Vetterli, Wavelets and signal processing, *IEEE SP Magazine*, pp. 14–38, October 1991.
7. M. R. K. Khansari and A. Leon-Garcia, Subband decomposition of signals with generalized sampling, *IEEE Transactions on Signal Processing*, vol. 41, pp. 3365–3376, December 1993.
8. M. Kamel and A. Zhao, Extraction of binary character/graphics images from grayscale document images, *CVGIP: Graphical Models and Image Processing*, vol. 55, no. 3, pp. 203–217, 1993.
9. P. K. Sahoo, S. Soltani, and A. K. C. Wong, A survey of thresholding techniques, *Computer Vision, Graphics, and Image Processing*, vol. 41, pp. 233–260, 1988.
10. J. G. Proakis and D. G. Manolakis, *Digital Signal Processing*, 2nd ed., New York: Macmillan, 1992.
11. L. W. Couch, *Digital and Analog Communication Systems*, 4th ed., Upper Saddle River, NJ: Prentice-Hall, 1993.
12. D. Messerschmitt, D. Hedberg, C. Cole, A. Haoui, and P. Winsip, Digital voice echo canceller with a TMS32020, *Digital Signal Processing Applications with the TMS320 Family*: *Theory, Applications, and Implementations*, Dallas: Texas Instruments, Inc., pp. 415–454, 1989.

13. D. L. Duttweiler and Y. S. Chen, A single-chip VLSI echo canceller, *Bell System Technical Journal*, vol. 59, no. 2, pp. 149–160, February 1980.
14. B. Widrow, J. Kaunitz, J. Glover, and C. Williams, Adaptive noise cancelling: Principles and applications, *Proceedings of the IEEE*, vol. 63, pp. 1692–1716, December 1975.
15. E. Kreysig, *Introductory Functional Analysis with Applications*, New York: Wiley, 1989.
16. D. C. Champeney, *A Handbook of Fourier Theorems*, Cambridge: Cambridge University Press, 1987.
17. S. Mallat, A theory for multiresolution signal decomposition: The wavelet decomposition, *IEEE Transactions on Pattern Analysis and Machine Intelligence*, vol. 11, pp. 674–693, July 1989.
18. M. Rosenlicht, *An Introduction to Analysis*, New York: Dover, 1978.
19. G. Birkhoff and S. MacLane, *A Survey of Modern Algebra*, New York: Macmillan, 1965.
20. K. Yosida, *Functional Analysis*, 6th ed., Berlin: Springer-Verlag, 1980.
21. W. F. Rudin, *Functional Analysis*, 2nd ed., New York: McGraw-Hill, 1991.
22. F. Riesz and B. Sz.-Nagy, *Functional Analysis*, New York: Dover, 1990.
23. L. Kantorovich and G. Akilov, *Functional Analysis*, Oxford: Pergamon, 1982.
24. J. Dieudonne, *History of Functional Analysis*, Amsterdam: North-Holland, 1981.
25. N. Young, *An Introduction to Hilbert Space*, Cambridge: Cambridge University Press, 1968.
26. L. Debnath and P. Mikusinski, *Introduction to Hilbert Spaces with Applications*, 2nd ed., San Diego, CA: Academic Press, 1999.
27. P. Halmos, *Naive Set Theory*, New York: Van Nostrand, 1960.

PROBLEMS

1. Find the domain and range of the following systems:

(a) The amplifier system: $y(n) = Ax(n)$.

(b) A translation system: $y(n) = x(n - k)$.

(c) The discrete system on real-valued signals, $y(n) = x(n)^{1/2}$.

(d) The discrete system on complex-valued signals, $y(n) = x(n)^{1/2}$.

(e) An adder: $y(n) = x(n) + x_0(n)$.

(f) Termwise multiplication (modulation): $y(n) = x(n)x_0(n)$.

(g) Convolution: $y(n) = x(n)*h(n)$.

(h) Accumulator: $y(n) = x(n) + y(n - 1)$.

2. Consider the LTI system $y = Hx$ that satisfies a linear, constant-coefficient difference equation

$$y(n) = \sum_{k=1}^{K} a_k y(n-k) + \sum_{m=0}^{M} b_m x(n-m)\,. \tag{2.87}$$

Show that any K successive values of the output $h = H\delta$ are sufficient to characterize the system.

3. Consider an LTI system $y = Hx$ that satisfies the difference equation (2.87).

(a) Give the homogeneous equation corresponding to (2.87).

(b) Show that if (x, y) is a solution pair for (2.87) and y_h is a solution of its homogeneous equation, then $(x, y+ y_h)$ is a solution of the difference equation.

(c) Show that if (x, y_1) and (x, y_2) are solution pairs for (2.87), then $y_1 - y_2$ is a solution to the homogeneous equation in (a).

4. Consider the LTI system $y = Hx$ that satisfies a linear, constant-coefficient difference equation (2.87). Prove that if the signal pair (δ, h) satisfies the difference equation and $y = x*h$, then the pair (x, y) also satisfies the difference equation.

5. Prove the converse of the convolution theorem for LTI Systems: Let $h(n)$ be a discrete signal and H be the system defined by $y = Hx = x*h$. Then H is LTI and $h = H\delta$.

6. Suppose $x(n)$ is in l^p, $1 \le p \le \infty$. Let c be a scalar (real or complex number) and let k be an integer. Show the following closure rules:

(a) $cx(n)$ is in l^p and $\|cx\|_p = |c|\ \|x\|_p$.

(b) $x(k-n)$ is in l^p and $\|x(k-n)\|_p = \|x(n)\|_p$.

7. Show that the signal space l^p is a normed space. The triangle inequality of the norm is proven by Minkowski's inequality. It remains to show the following:

(a) $\|x\|_p \ge 0$ for all x.

(b) $\|x\|p = 0$ if and only if $x(n) = 0$ for all n.

(c) $\|ax\|_p = |a|\ \|x\|_p$ for all scalars a and all signals $x(n)$.

8. Let p and q be conjugate exponents. Show the following:

(a) $(p + q)/pq = 1$.

(b) $pq = p + q$.

(c) $(p-1)(q-1) = 1$.

(d) $(p-1)^{-1} = q - 1$.

(e) If $u = t^{p-1}$, then $t = uq^{-1}$.

9. Show that the l^p spaces are complete, $1 \le p < \infty$. Let $\{x_k(n)\}$ be a Cauchy sequence of signals in l^p.

(a) Show that for any integer n, the values of the signals in the sequence at time instant n are a Cauchy sequence. That is, with n fixed, the sequence of scalars $\{x_k(n)$: k an integer$\}$ is a Cauchy sequence.

(b) Since the real (complex) numbers are complete, we can fix n, and take the limit

$$c_n = \lim_{k \to \infty} x_k(n)\,. \tag{2.88}$$

Show that the signal defined by $x(n) = c_n$ is in l^p.

(c) Show that

$$\lim_{k \to \infty} \|x_k - x\|_p = 0, \tag{2.89}$$

so that the signals x_k converge to x in the l^p distance measure d_p.

10. Show that the l^∞ signal space is complete.

11. Let I be an inner product space. Show that the inner product is continuous in I; that is if $x_n \to x$ and $y_n \to y$, then $\langle x_n, y_n \rangle \to \langle x, y \rangle$.

12. Show that orthogonal signals in an inner product space are linearly independent.

13. Let I be an inner product space and $d(u, v) = \|u - v\|$ be its distance measure. Show that with the distance measure $d(u, v)$, I is a metric space:

(a) $d(u, v) \geq 0$ for all u, v.

(b) $d(u, v) = 0$ if and only if $u = v$.

(c) $d(u, v) = d(v, u)$ for all u, v.

(d) For any w, $d(u, v) \leq d(u, w) + d(w, v)$.

14. Show that the *discrete Euclidean* space $\mathbb{Z}^n = \{(k_1, k_2, \cdots, k_n) \mid k_i \text{ is in } \mathbb{Z}\}$ is a metric space. Is it a normed linear space? Explain.

15. Show that if for the Euclidean space $\mathbb{R}^n$, we define the metric $d((u_1, u_2, ..., u_n), (v_1, v_2, \cdots, v_n)) = |u_1 - v_1| + |u_2 - v_2| + \cdots + |u_n - v_n|$, then $(\mathbb{R}^n, d)$ is a metric space.

16. Show that the following sets are countable.

(a) The integers $\mathbb{Z}$ by arranging them in two rows:

0, 2, 4, 6, ...

1, 3, 5, 7, ...

and enumerating them with a zigzag traversal.

(b) All ordered pairs in the Cartesian product $\mathbb{N} \times \mathbb{N}$.

(c) The rational numbers $\mathbb{Q}$.

(d) All ordered k-tuples of a countable set X.

(e) Any countable union of countable sets.

CHAPTER 3

Analog Systems and Signal Spaces

This chapter extends linear systems and Hilbert space ideas to continuous domain signals, filling the gap Chapter 2 left conspicuous. Indeed, noting that an integral over the real line displaces an integral summation, the definitions, theorems, and examples are quite similar in form to their discrete-world cousins. We mainly verify that after replacing summations with integrations we can still construct analog signal spaces that support signal theory.

The initial presentation is informal, not rigorous, and takes a quicker pace. We require normed vector space operations for analog signals: the capability to add, scalar multiply, and measure the size of a signal. The signal spaces should also support limit operations, which imply that arbitrarily precise signal approximations are possible; we find that we can construct analog Banach spaces, too. More important is the measure of similarity between two analog signals—the inner product relation—and we take some care in showing that our abstract structures survive the transition to the analog world. There is an analog Hilbert space theory, for which many of the purely algebraic results of Chapter 2 remain valid. This is convenient, because we can simply quote the same results for analog signals. Hilbert spaces, principally represented by the discrete and analog finite energy signals, will prove to be the most important abstract structure in the sequel. Introductory texts that cover analog signal theory include Refs. 1–5.

The last two sections are optional reading; they supply rigor to the analog theory. One might hope that it is only necessary to replace the infinite summations with infinite integrations, but subtle problems thwart this optimistic scheme. The Riemann integral, familiar from college calculus, cannot handle signals with an infinite number of discontinuities, for example. Its behavior under limit operations is also problematic. Mathematicians faced this same problem at the end of the nineteenth century when they originally developed function space theories. The solution they found—the Lebesgue integral—works on exotic signals, has good limit operation properties, and is identical to the Riemann integral on piecewise continuous functions. Lebesgue measure and integration theory is covered in Section 3.4. In another area, the discrete-world results do not straightforwardly generalize to the analog world: There is no bona fide continuous-time delta function. The intuitive

Signal Analysis: Time, Frequency, Scale, and Structure, by Ronald L. Allen and Duncan W. Mills
ISBN: 0-471-23441-9

treatment, which we offer to begin with, does leave the theory of linear, translation-invariant systems with a glaring hole. It took mathematicians some time to put forward a theoretically sound alternative to the informal delta function concept as well. The concept of a distribution was worked out in the 1930s, and we introduce the theory in Section 3.5.

The chapter contains two important applications. The first, called the matched filter, uses the ideas of inner product and orthogonalization to construct an optimal detector for an analog waveform. The second application introduces the idea of a frame. Frames generalize the concept of a basis, and we show that they are the basic tool for numerically stable pattern detection using a family of signal models. The next chapter applies matched filters to the problem of recognizing signal shapes. Chapter 10 develops frame theory further in the context of time-frequency signal transforms.

3.1 ANALOG SYSTEMS

This section introduces operations on analog signals. Analog signals have a continuous rather than discrete independent time-domain variable. Analog systems operate on analog systems, and among them we find the familiar amplifiers, attenuators, summers, and so on. This section is a quick read for readers who are already familiar with analog systems.

3.1.1 Operations on Analog Signals

For almost every discrete system there corresponds an analog system. We can skim quickly over these ideas, so similar they are to the discrete-world development in the previous chapter.

Definition (Analog System). An analog system H is a partial function from the set of all analog signals to itself. If $x(t)$ is a signal and $y(t)$ is the signal output by H from the input $x(t)$, then $y = Hx$, $y(t) = (Hx)(t)$, or $y(t) = H(x(t))$. As with discrete signals, we call $y(t)$ the response of the system H to input $x(t)$. The set of signals $x(t)$ for which some $y = Hx$ is determined is the domain of the system H. The set of signals y for which $y = Hx$ for some signal x is the range of H.

3.1.2 Extensions to the Analog World

Let us begin by enumerating some common, but not unimportant, analog operations that pose no theoretical problems. As with discrete signals, the operations of scaling (in the sense of amplification and attenuation) and translation (or shifting) an analog signal are central.

We may amplify or attenuate an analog signal by multiplying its values by a constant:

$$y = Ax(t). \tag{3.1}$$

This is sometimes called a scaling operation, which introduces a possible confusion with the notion of dilation $y(t) = x(At)$, which is also called "scaling." The scaling operation inverts the input signal when $A < 0$, amplifies the signal when $|A| > 1$, and attenuates the signal when $|A| < 1$. The domain of a scaling system is all analog signals, as is the range, as long as $A = 0$.

An analog signal may be translated or shifted by any real time value:

$$y = x(t - t_0). \tag{3.2}$$

When $t_0 > 0$ the translation is a delay, and when $t_0 < 0$ the system can more precisely be called an advance. As in the discrete world, translations cause no domain and range problems. If T is an analog time shift, then $\mathrm{Dom}(T) = \mathrm{Ran}(T) = \{s(t)\colon s \text{ is an analog signal}\}$.

Analog signal reflection reverses the order of signal values: $y(t) = x(-\mathrm{t})$. For analog time signals, this time reversal system reflects the signal values $x(t)$ around the time $t = 0$. As with discrete signals, the reflection and translation operations do not commute.

The basic arithmetic operations on signals exist for the analog world as well. Signal addition or summation adds a given signal to the input, $y(t) = x(t) + x_0(t)$, where $x_0(t)$ is a fixed signal associated with the system H. We can also consider the system that takes the termwise product of a given signal with the input, $y(t) = x(t)x_0(t)$.

One benefit of a continuous-domain variable is that analog signals allow some operations that were impossible or at least problematic in the discrete world.

Dilation always works in the analog world. We can form $y(t) = x(at)$ whatever the value of $a \in \mathbb{R}$. The corresponding discrete operation, $y(n) = x(bn)$, works nicely only if $b \in \mathbb{Z}$ and $|b| \geq 1$; when $0 < |b| < 1$ and $b \in \mathbb{Q}$ we have to create special values (typically zero) for those $y(n)$ for which $b \in \mathbb{Z}$. As noted earlier, dilation is often called scaling, because it changes the scale of a signal. Dilation enlarges or shrinks signal features according to whether $|a| < 1$ or $|a| > 1$, respectively.

Another analog operation is differentiation. If it is smooth enough, we can take the derivative of an analog signal:

$$y(t) = \frac{dx}{dt} = x'(t). \tag{3.3}$$

If the signal $x(t)$ is only piecewise differentiable in (3.3), then we can assign some other value to $y(t)$ at the points of nondifferentiability.

3.1.3 Cross-Correlation, Autocorrelation, and Convolution

The correlation and convolution operations depend on signal integrals. In the discrete world, systems that implement these operations have input–output relations that involve infinite summations over the integers. In continuous-domain signal processing, the corresponding operations rely on integrations over the entire real line.

These do pose some theoretical problems—just as did the infinite summations reminiscent of Chapter 2; we shall address them later when we consider signal spaces of analog signals.

The analog *convolution* operation is once again denoted by the * operator: $y = x*h$. We define:

$$y(t) = (x*h)(t) = \int_{-\infty}^{\infty} x(s)h(t-s)\,ds. \tag{3.4}$$

The *cross-correlation* system is defined by the rule $y = x\circ h$, where

$$y(t) = (x\circ h)(t) = \int_{-\infty}^{\infty} x(s)h(t+s)\,ds. \tag{3.5}$$

The analog *autocorrelation* operation on a signal is $y = x\circ x$, and when the signals are complex-valued, we use the complex conjugate of the kernel function $h(t)$:

$$y(t) = (x\circ h)(t) = \int_{-\infty}^{\infty} x(s)\overline{h(t+s)}\,ds. \tag{3.6}$$

The autocorrelation is defined by $y(t) = (x\circ x)(t)$. One of the applications of functional analysis ideas to signal processing, which we shall provide below, is to show the existence of the correlation and autocorrelation functions for square-integrable signals $x(t)$ and $h(t)$.

We can show that linear translation invariant analog systems are again characterized by the convolution operation. This is not as easy as it was back in the discrete realm. We have no analog signal that corresponds to the discrete impulse, and discovering the right generalization demands that we invent an entirely new theory: distributions.

3.1.4 Miscellaneous Operations

Let us briefly survey other useful analog operations.

A subsampling or downsampling system continuously expands or contracts an analog signal: $y(t) = x(at)$, where $a > 0$ is the scale or dilation factor. Tedious as it is to say, we once more have a terminology conflict; the term "scale" also commonly refers in the signal theory literature to the operation of amplifying or attenuating a signal: $y(t) = ax(t)$.

Analog thresholding is a just as simple as in the discrete world:

$$y(t) = \begin{cases} 1 & \text{if } x(t) \geq T, \\ 0 & \text{if } x(t) < T. \end{cases} \tag{3.7}$$

The accumulator system, $y = Hx$, is given by

$$y(t) = \int_{-\infty}^{t} x(s)\, ds. \tag{3.8}$$

The accumulator outputs a value that is the sum of all input values to the present signal instant. As already noted, not all signals are in the domain of an accumulator system. The exercises explore some of these ideas further.

The moving average system is given by

$$y(t) = \frac{1}{2a} \int_{t-a}^{t+a} x(s)\, ds, \tag{3.9}$$

where $a > 0$. This system averages $x(s)$ around in an inteval of width $2a$ to output $y(t)$.

3.2 CONVOLUTION AND ANALOG LTI SYSTEMS

The characterization of a linear, translation-invariant analog system as one given by the convolution operation holds for the case of continuous domain signals too. We take aim at this idea right away. But, the notion of an impulse response—so elementary it is an embarassment within discrete system theory—does not come to us so readily in the analog world. It is not an understatement to say that the proper explication of the analog delta requires supplementary theory; what it demands is a complete alternative conceptualization of the mathematical representation of analog signals. We will offer an informal definition for the moment, and this might be the prudent stopping point for first-time readers. We shall postpone the more abstruse development, known as distribution theory, until Section 3.5.

3.2.1 Linearity and Translation-Invariance

Analog systems can be classified much like discrete systems. The important discrete signal definitions of linearity and translation- (or shift- or time-) invariance extend readily to the analog world.

Definition (Linear System). An analog system H is linear if $H(ax) = aH(x)$ and $H(x + y) = H(x) + H(y)$. Often the system function notation drops the parentheses; thus, we write Hx instead of $H(x)$. $H(x)$ is a signal, a function of a time variable, and so we use the notation $y(t) = (Hx)(t)$ to include the independent variable of the output signal.

Definition (Translation-Invariant). An analog system H is translation-invariant if whenever $y = Hx$ and $s(t) = x(t - a)$, then $H(s) = y(t - a)$.

A linear system obeys the principles of scaling and superposition. When a system is translation-invariant, then the output of the shifted input is precisely the shifted output.

Definition (LTI System). An LTI system is both linear and translation-invariant.

Let us consider some examples.

Example. Let the system $y = Hx$ be given by $y(t) = x(t)\cos(t)$. The cosine term is a nonlinear distraction, but this system is linear. Indeed, $H(x_1 + x_2)(t) = [x_1(t) + x_2(t)]\cos(t) = x_1(t)\cos(t) + x_2(t)\cos(t) = H(x_1)(t) + H(x_2)(t)$. Also, $H(ax)(t) = [ax(t)]\cos(t) = a[x(t)\cos(t)] = a(Hx)(t)$.

Example. Let $y = Hx$ by given by $y(t) = tx(t)$. Then H is not translation-invariant. The decision about whether a system is or is not translation-invariant can sometimes bedevil signal processing students. The key idea is to hide the shift amount inside a new signal's definition: Let $w(t) = x(t - a)$. Then $w(t)$ is the shifted input signal. $(Hw)(t) = tw(t)$ by definition of the system H. But $tw(t) = tx(t - a)$. Is this the shifted output? Well, the shifted output is $y(t - a) = (t - a)x(t - a)$. In general, this will not equal $tx(t - a)$, so the system H is not shift-invariant.

Example. Let $y = Hx$, where $y(t) = x^2(t) + 8$. This system is translation-invariant. Again, let $w(t) = x(t - a)$, so that $(Hw)(t) = w^2(t) + 8 = x(t - a)x(t - a) + 8$ is the output of the translated input signal. Is this the translated output signal? Yes, because $y(t - a) = x^2(t - a) + 8 = (Hw)(t)$.

Example (Moving Average). Let $T > 0$ and consider the system $y = Hx$:

$$y(t) = \int_{t-T}^{t+T} x(s)\, ds. \tag{3.10}$$

Then H is LTI. The integration is a linear operation, which is easy to show. So let us consider a translated input signal $w(t) = x(t - a)$. Then $(Hw)(t)$ is

$$\int_{t-T}^{t+T} w(s)\, ds = \int_{t-T}^{t+T} x(s-a)\, ds = \int_{t-T-a}^{t+T-a} x(u)\, du, \tag{3.11}$$

where we have changed the integration variable with $u = s - a$. But note that the shifted output is

$$y(t-a) = \int_{t-a-T}^{t-a+T} x(s)\, ds, \tag{3.12}$$

and (3.12) is identical to (3.11).

3.2.2 LTI Systems, Impulse Response, and Convolution

Putting aside mathematical formalities, it is possible to characterize analog linear, translation-invariant systems by convolution of the input signal with the system impulse response.

3.2.2.1 Analog Delta and Impulse Response. Let us begin by developing the idea of the analog delta function, or Dirac[1] delta, $\delta(t)$. This signal should—like the discrete delta, $\delta(n)$—be zero everywhere except at time $t = 0$. Discrete convolution is a discrete sum, so $\delta(0) = 1$ suffices for sifting out values of discrete siganls $x(n)$. Analog convolution is an integral, and if $\delta(t)$ is a signal which is nonzero only at $t = 0$, then the integral of any integrand $x(s)\delta(t - s)$ in the convolution integral (3.4) is zero. Consequently, it is conventional to imagine the analog impulse signal as being infinite at $t = 0$ and zero otherwise; informally, then,

$$\delta(t) = \begin{cases} \infty & \text{if } t \neq 0, \\ 0 & \text{if otherwise.} \end{cases} \tag{3.13}$$

Another way to define the analog delta function is through the following convolutional identity:

Sifting Property. The analog impulse is the signal for which, given analog signal $x(t)$,

$$x(t) = (x^*\delta)(t) = \int_{-\infty}^{\infty} x(s)\delta(t-s)\, ds. \tag{3.14}$$

No signal satisfying (3.13) or having the property (3.14) exists, however. The choice seems to be between the Scylla of an impossible function or the Charybdis of an incorrect integration.

To escape this quandary, let us try to approximate the ideal, unattainable analog sifting property by a local average. Let $\delta_n(t)$ be defined for $n > 0$ by

$$\delta_n(t) = \begin{cases} n & \text{if } t \in \left[-\frac{1}{2n}, \frac{1}{2n}\right], \\ 0 & \text{if otherwise.} \end{cases} \tag{3.15}$$

[1]P. A. M. Dirac (1902–1984) applied the delta function to the discontinuous energy states found in quantum mechanics (*The Principles of Quantum Mechanics*, Oxford: Clarendon, 1930). Born in England, Dirac studied electrical engineering and mathematics at Bristol and then Cambridge, respectively. He developed the relativistic theory of the electron and predicted the existence of the positron.

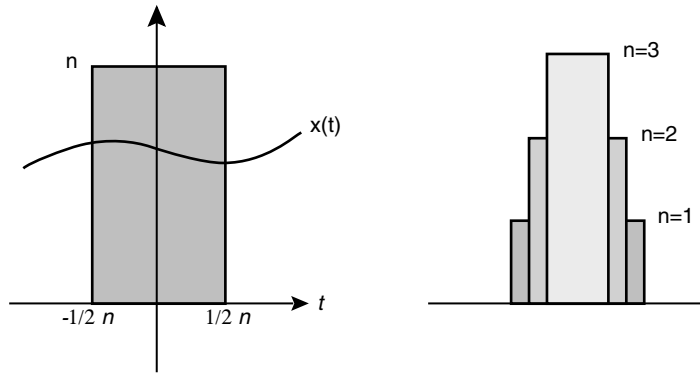

Fig. 3.1. Approximating the analog impulse, $\delta_n(t) = n$ on the interval of width $1/n$ around the origin.

Then, referring to Figure 3.1, $\delta_n(t)$ integrates to unity on the real line,

$$\int_{-\infty}^{\infty} \delta_n(t)\, dt = 1. \tag{3.16}$$

Furthermore, $\delta_n(t)$ provides a rudimentary sifting relationship,

$$\int_{-\infty}^{\infty} x(t)\delta_n(t)\, dt = \text{Average value of } x(t) \text{ on} \left[-\frac{1}{2n}, \frac{1}{2n}\right]. \tag{3.17}$$

To verify this, note that

$$\int_{-\infty}^{\infty} x(t)\delta_n(t)\, dt = n \int_{-1/2n}^{1/2n} x(t)\, dt, \tag{3.18}$$

while

$$\int_{a}^{b} x(t)\, dt = (b-a) \times \text{Average value of } x(t) \text{ on } \left[-\frac{1}{2n}, \frac{1}{2n}\right]. \tag{3.19}$$

Combining (3.18) and (3.19) proves that $\delta_n(t)$ has a sifting-like property. Note that as $n \to \infty$ the square impluse in Figure 3.1 grows higher and narrower, approximating an infinitely high spike. Under this limit the integral (3.17) is the average of $x(t)$ within an increasingly minute window around $t = 0$:

$$\lim_{n \to \infty} \int_{-\infty}^{\infty} x(t)\delta_n(t)\, dt = x(0). \tag{3.20}$$

This argument works whatever the location of the tall averaging rectangles defined by $\delta_n(t)$. We can conclude that

$$\lim_{n \to \infty} \int_{-\infty}^{\infty} x(s)\delta_n(t-s)\, ds = x(t). \tag{3.21}$$

An interchange of limit and integration in (3.21) gives

$$\lim_{n \to \infty} \int_{-\infty}^{\infty} x(s)\delta_n(t-s)\, ds = \int_{-\infty}^{\infty} x(s) \lim_{n \to \infty} \delta_n(t-s)\, ds. \tag{3.22}$$

Finally, and if we assume $\delta_n(t) \to \delta(t)$, that the square spikes converge to the Dirac delta, then the sifting property follows from (3.22).

Rigorously speaking, of course, there is no signal $\delta(t)$ to which the $\delta_n(t)$ converge, no such limit exists, and our interchange of limits is quite invalid [6]. It is possible to formally substantiate delta function theory with the theory of generalized functions and distributions [7–10]. Some applied mathematics texts take time to validate their use of Diracs [11–13]. In fact, the amendments follow fairly closely the informal motivation that we have provided above. Despite our momentary neglect of mathematical justification, at this point these ideas turn out to be very useful in analog signal theory; we shamelessly proceed to feed delta "functions" into linear, translation-invariant systems.

Definition (Impulse Response). Let H be an analog LTI system and $\delta(t)$ be the Dirac delta function. Then the impulse response of H is $h(t) = (H\delta)(t)$. Standard notation uses a lowercase "h" for the impulse response of the LTI system "H."

The next section applies these ideas toward a characterization of analog LTI systems.

3.2.2.2 LTI System Characterization. The most important idea in analog system theory is that a convolution operation—the input signal with the system's impulse response—characterizes LTI systems. We first rewrite an analog signal $x(t)$ as a scaled sum of shifted impulses. Why take a perfectly good—perhaps infinitely differentiable—signal and write it as a linear combination of these spikey, problematic components? This is how, in Chapter 2, we saw that convolution governs the input–output relation of an LTI discrete system.

To decompose $x(t)$ into Diracs, note that any integral is a limit of Riemann sums of decreasing width:

$$\int_{-\infty}^{\infty} f(s)ds = \lim_{Len(I) \to 0} \sum_{n=-\infty}^{\infty} f(a_n)Len(I_n), \tag{3.23}$$

where $I = \{I_n : n \in \mathbb{Z}\}$ is a partition of the real line, $I_n = [a_n, b_n]$, the length of interval I_n is $\text{Len}(I_n) = b_n - a_n$, and $\text{Len}(I) = \max\{\text{Len}(I_n) : n \in \mathbb{Z}\}$. If $f(s) = x(s)\delta(t-s)$, then

$$x(t) = \int_{-\infty}^{\infty} f(s)\, ds = \lim_{Len(I)\to 0} \sum_{n=-\infty}^{\infty} x(a_n)\delta(t-a_n)\, Len(I_n), \tag{3.24}$$

so that

$$\begin{aligned} y(t) = H(x)(t) &= H\left[\lim_{Len(I)\to 0} \sum_{n=-\infty}^{\infty} x(a_n)\delta(t-a_n) Len(I_n)\right] \\ &= \lim_{Len(I)\to 0} \sum_{n=-\infty}^{\infty} x(a_n) H[\delta(t-a_n)] Len(I_n) \end{aligned} \tag{3.25}$$

Besides blithely swapping the limit and system operators, (3.25) applies linearity twice: scaling with the factor $x(a_n)$ and superposition with the summation. By translation-invariance, $H[\delta(t-a_n)] = (H\delta)(t-a_n)$. The final summation above is an integral itself, precisely the LTI system characterization we have sought:

Theorem (Convolution for LTI Systems). Let H be an LTI system, $y = Hx$, and $h = Hd$. Then

$$y(t) = (x^* h)(t) = \int_{-\infty}^{\infty} x(s)h(t-s)\, ds. \tag{3.26}$$

Now let us consider a basic application of the theorem to the study of stable and causal systems.

3.2.2.3 Stable and Causal Systems.

The same ideas of stability and causality, known from discrete system theory, apply to analog systems.

Definition (Bounded). A signal $x(t)$ is *bounded* if there is a constant M such that $|x(t)| < M$ for all $t \in \mathbb{R}$.

Definition (Absolutely Integrable). A signal $x(t)$ is *absolutely integrable* if

$$\int_{-\infty}^{\infty} |x(t)|\, dt < \infty. \tag{3.27}$$

The equivalent concept in Chapter 2 is *absolutely summable*.

Definition (Stable System). If $y = Hx$ is a bounded output signal whenever $x(t)$ is a bounded input signal, then the system H is *stable*.

Proposition (Stability Characterization). The LTI system $y = Hx$ is stable if and only if its impulse response $h = H\delta$ is absolutely integrable.

Proof: Suppose h is absolutely integrable and $|x(t)| < M$ for all $t \in \mathbb{R}$. Then

$$|y(t)| = \left| \int_{-\infty}^{\infty} x(s)h(t-s)\, ds \right| \leq \int_{-\infty}^{\infty} |x(s)h(t-s)|\, ds \leq M \int_{-\infty}^{\infty} |h(t-s)|\, ds. \tag{3.28}$$

Since the final integral in (3.28) is finite, $y(t)$ is bounded and H must be stable. Conversely, suppose that H is stable but $h = H\delta$ is not absolutely integrable:

$$\int_{-\infty}^{\infty} |h(t)|\, dt = \infty; \tag{3.29}$$

we seek a contradiction. If

$$x(t) = \begin{cases} \dfrac{\overline{h(-t)}}{|h(-t)|} & \text{if } h(-t) \neq 0, \\ 0 & \text{if otherwise,} \end{cases} \tag{3.30}$$

where we are allowing for the situation that $h(t)$ is complex-valued, then $x(t)$ is clearly bounded. But convolution with $h(t)$ governs the input-output relation of H, and that is the key. We can write $y = Hx$ as

$$y(t) = \int_{-\infty}^{\infty} x(s)h(t-s)\, ds = \int_{-\infty}^{\infty} \frac{\overline{h(-s)}}{|h(-s)|} h(t-s)\, ds. \tag{3.31}$$

So $y(t)$ is the output of stable system H given bounded input $x(t)$. $y(t)$ should be bounded. What is $y(0)$? Well,

$$\begin{aligned} y(0) &= \int_{-\infty}^{\infty} x(s)h(0-s)\, ds = \int_{-\infty}^{\infty} \frac{\overline{h(-s)}}{|h(-s)|} h(0-s)\, ds = \int_{-\infty}^{\infty} \frac{|h(-s)|^2}{|h(-s)|}\, ds \\ &= \int_{-\infty}^{\infty} \frac{|h(-s)|^2}{|h(-s)|}\, ds = \int_{-\infty}^{\infty} |h(-s)| ds. \end{aligned} \tag{3.32}$$

However, the final integral in (3.32) is infinite by (3.29). So $y(t)$ cannot be bounded, and this contradicts the converse's assumption. ■

To the discrete theory, there also corresponds an analog notion of causality. A system is causal if the future of the input signals have no bearing on their response.

Definition (Causal System). The system H is *causal* if $y = Hx$ can be found using only present and past values of $x(t)$.

Proposition (Causality Criterion). The LTI system $y = Hx$ is causal if its impulse response $h = H\delta$ satisfies $h(r) = 0$ for $r < 0$.

Proof: If $h(t - s) = 0$ for $s > t$, then jotting down the convolution integral shows

$$y(t) = \int_{-\infty}^{\infty} x(s)h(t-s)\, ds = \int_{-\infty}^{t} x(s)h(t-s)\, ds. \tag{3.33}$$

We have written $y(t)$ knowing only earlier $x(s)$ values, and so H must be causal. ■

Remark. For analog signals, the converse of the causality criterion is not true. The impulse response $h(t)$ could be nonzero at an isolated point, say $t = -2$, and so the convolution integral (3.33) does not depend on negative times.

Example. Let H be the system with impulse response

$$h(t) = \begin{cases} e^{-t} & \text{if } t \geq 0, \\ 1 & \text{if } t = -1, \\ 0 & \text{if otherwise.} \end{cases} \tag{3.34}$$

The system $y(t) = (x^*h)(t)$ is LTI, and H is causal, but it does not obey the converse of the causality criterion.

The causality criterion's lack of a converse distinguishes analog from discrete theory. In discrete system theory, an LTI system H is causal if and only if its impulse response $h(n)$ is zero for $n < 0$. We can improve on the proposition, by developing a stronger integral. Indeed, the fact that we might allow signals that have isolated finite impulses, or even a countably infinite number of finite impulse discontinuities points to the Riemann integral's inadequacy. This same defect troubled mathematicians in the early 1900s, when they first drew set theoretic concepts into analysis and began to demand limit operations from the integral. Modern measure and integration theory was the outcome, and we cover it in Section 3.4.

3.2.3 Convolution Properties

Convolution is the most important signal operation, since $y = h^*x$ gives the input–output relation for the LTI system H, where $h = H\delta$. This section develops basic theorems, these coming straight from the properties of the convolution integral.

Proposition (Linearity). The convolution operation is linear: $h^*(ax) = ah^*x$, and $h^*(x + y) = h^*x + h^*y$.

Proof: Easy by the linearity of integration (exercise). ■

Proposition (Translation-Invariance). The convolution operation is translation invariant: $h^*[x(t-a)] = (h^*x)(t-a)$.

Proof: It is helpful to hide the time shift in a signal with a new name. Let $w(t) = x(t-a)$, so that the translated input is $w(t)$. We are asking, what is the convolution of the shifted input? It is $(h^*w)(t)$. Well,

$$(h^*w)(t) = \int_{-\infty}^{\infty} h(s)w(t-s)\,ds = \int_{-\infty}^{\infty} h(s)x((t-a)-s)\,ds = (h^*x)(t-a), \quad (3.35)$$

which is the translation of the output by the same amount. ■

These last two propositions comprise a converse to the convolution theorem (3.26) for LTI systems: a system $y = h^*x$ is an LTI system. The next property shows that the order of LTI processing steps does not matter.

Proposition (Commutativity). The convolution operation is commutative: $x^*y = y^*x$.

Proof: Let $u = t - s$ for a change of integration variable. Then $du = -ds$, and

$$(x^*y)(t) = \int_{-\infty}^{\infty} x(s)y(t-s)\,ds = -\int_{\infty}^{-\infty} x(t-u)y(u)\,du = \int_{-\infty}^{\infty} x(t-u)y(u)\,du. \quad (3.36)$$

The last integral in (3.36) we recognize to be the convolution y^*x. ■

Proposition (Associativity). The convolution operation is associative: $h^*(x^*y) = h^*(x^*y)$.

Proof: Exercise. ■

Table 3.1 summarizes the above results.

TABLE 3.1. Convolution Properties

Signal Expression	Property Name
$(x^*y)(t) = \int_{-\infty}^{\infty} x(s)y(t-s)\,ds$	Definition
$h^*[ax+y] = ah^*x + h^*y$	Linearity
$h^*[x(t-a)] = (h^*x)(t-a)$	Translation- or shift-invariance
$x^*y = y^*x$	Commutativity
$h^*(x^*y) = (h^*x)^*y$	Associativity
$h^*(\delta(t-a)) = h(a)$	Sifting

3.2.4 Dirac Delta Properties

The Dirac delta function has some unusual properties. Although they can be rigorously formulated, they also follow from its informal description as a limit of ever higher and narrower rectangles. We maintain a heuristic approach.

Proposition. Let $u(t)$ be the unit step signal. Then $\delta(t) = \frac{d}{dt}[u(t)]$.

Proof: Consider the functions $u_n(t)$:

$$u_n(t) = \begin{cases} 1 & \text{if } t \geq \frac{1}{2n}, \\ 0 & \text{if } t \leq -\frac{1}{2n}, \\ nt + \frac{1}{2} & \text{if otherwise.} \end{cases} \tag{3.37}$$

Notice that the derivatives of $u_n(t)$ are precisely the $\delta_n(t)$ of (3.15) and that as $n \to \infty$ we have $u_n(t) \to u(t)$. Taking the liberty of assuming that in this case differentiation and the limit operations are interchangeable, we have

$$\delta(t) = \lim_{n \to \infty} \delta_n(t) = \lim_{n \to \infty} \frac{d}{dt} u_n(t) = \frac{d}{dt} \lim_{n \to \infty} u_n(t) = \frac{d}{dt} u(t). \tag{3.38}$$

■

Remarks. The above argument does stand mathematical rigor on its head. In differential calculus [6] we need to verify several conditions on a sequence of signals and their derivatives in order to conclude that the limit of the derivatives is the derivative of their limit. In particular, one must verify the following in some interval I around the origin:

(i) Each function in $\{x_n(t) \mid n \in \mathbb{N}\}$ is continuously differentiable on I.
(ii) There is an $a \in I$ such that $\{x_n(a)\}$ converges.
(iii) The sequence $\{x_n'(t)\}$ converges uniformly on I.

Uniform convergence of $\{y_n(t) \mid n \in \mathbb{N}\}$ means that for every $\varepsilon > 0$ there is an $N_\varepsilon > 0$ such that $m, n > N_\varepsilon$ implies $|y_n(t) - y_m(t)| < \varepsilon$ for all $t \in I$. The key distinction between uniform convergence and ordinary, or *pointwise*, convergence is that uniform convergence requires that an N_ε be found that pinches $y_n(t)$ and $y_m(t)$ together throughout the interval. If the N_ε has to depend on $t \in I$ (such as could happen if the derivatives of the $y_n(t)$ are not bounded on I), then we might find pointwise convergence exists, but that uniform convergence is lost. The exercises delve further into these ideas. Note also that a very important instance of this distinction occurs in Fourier series convergence, which we detail in Chapters 5 and 7. There we show that around a discontinuity in a signal $x(t)$ the Fourier series is pointwise but not uniformly convergent. Connected with this idea is the famous ringing artifact of Fourier series approximations, known as the *Gibbs phenomenon*.

The next property describes the scaling or time dilation behavior of $\delta(t)$. Needless to say, it looks quite weird at first glance.

Proposition (Scaling Property). Let $u(t)$ be the unit step signal and $a \in \mathbb{R}$, $a \neq 0$. Then

$$\delta(at) = \frac{1}{|a|}\delta(t)\,. \tag{3.39}$$

Proof: Consider the rectangles approaching $\delta(t)$ as in Figure 3.1. If the $\delta_n(t)$ are dilated to form $\delta_n(at)$, then in order to maintain unit area, we must alter their height; this makes the integrals an average of $x(t)$. This intuition explains away the property's initial oddness. However, we can also argue for the proposition by changing integration variables: $s = at$. Assume first that $a > 0$; thus,

$$\int_{-\infty}^{\infty} x(t)\delta(at)\,dt = \int_{-\infty}^{\infty} x\left(\frac{s}{a}\right)\delta(s)\frac{1}{a}\,ds = \frac{1}{a}\int_{-\infty}^{\infty} x\left(\frac{s}{a}\right)\delta(s)\,ds = \frac{1}{a}x(0), \tag{3.40}$$

and $\delta(at)$ behaves just like $\frac{1}{|a|}\delta(t)$. If $a < 0$, then $s = at = -|a|t$, and

$$\int_{-\infty}^{\infty} x(t)\delta(at)\,dt = \int_{\infty}^{-\infty} x\left(\frac{s}{a}\right)\delta(s)\frac{-1}{|a|}\,ds = \frac{1}{|a|}\int_{-\infty}^{\infty} x\left(\frac{s}{a}\right)\delta(s)\,ds = \frac{1}{|a|}x(0). \tag{3.41}$$

Whatever the sign of the scaling parameter, (3.39) follows. ■

The Dirac is even: $\delta(-t) = \delta(t)$, as follows from the Dirac scaling proposition. The next property uses this corollary to show how to sift out the signal derivative (Table 3.2).

TABLE 3.2. Dirac Delta Properties

Signal Expression	Property Name
$x(t) = \int_{-\infty}^{\infty} x(s)\delta(t-s)\,ds$	Sifting
$\delta(t) = \frac{d}{dt}[u(t)]$	Derivative of unit step
$\delta(at) = \frac{1}{\|a\|}\delta(t)$	Scaling
$\delta(t) = \delta(-t)$	Even
$\int_{-\infty}^{\infty} x(t)\frac{d}{dt}\delta(t)\,dt = -\frac{d}{dt}x(t)\Big\|_{t=0}$	Derivative of Dirac

Proposition. Let $\delta(t)$ be the Dirac delta and $x(t)$ a signal. Then,

$$\int_{-\infty}^{\infty} x(t)\frac{d}{dt}\delta(t)\ dt = -\frac{d}{dt}(x(t))\bigg|_{t=0}. \tag{3.42}$$

Proof: We differentiate both sides of the sifting property equality to obtain

$$\frac{d}{dt}x(t) = \frac{d}{dt}\int_{-\infty}^{\infty} x(s)\delta(t-s)\ ds = \int_{-\infty}^{\infty} x(s)\frac{d}{dt}\delta(t-s)\ ds = \int_{-\infty}^{\infty} x(s)\frac{d}{dt}\delta(s-t)\ ds, \tag{3.43}$$

and the proposition follows by taking $t = 0$ in (3.43). ■

3.2.5 Splines

Splines are signals formed by interpolating discrete points with polynomials, and they are particularly useful for signal modeling and analysis. Sampling converts an analog signal into a discrete signal, and we can effect the reverse by stretching polynomials between isolated time instants. The term "spline" comes from a jointed wood or plastic tool of the same name used by architects to hand draw elongated, smooth curves for the design of a ship or building. Here we provide a brief overview of the basic splines, or *B-splines*. There are many other types of splines, but what now interests us in B-splines is their definition by repetitive convolution.

Definition (Spline). The analog signal $s(t)$ is a *spline* if there is a set of points $K = \{k_m : m \in \mathbb{Z}\}$ such that $s(t)$ is continuous and equal to a polynomial on each interval $[k_m, k_{m+1}]$. Elements of K are called *knots*. If $s(t)$ is a polynomial of degree n on each $[k_m, k_{m+1}]$, then $s(t)$ has degree n. A spline $s(t)$ of degree n is called *smooth* if it is $n-1$ times continuously differentiable.

Splines are interesting examples of analog signals, because they are based on discrete samples—their set of knots—and yet they are very well-behaved between the knots. Linear interpolation is probably everyone's first thought to get from a discrete to an analog signal representation. But the sharp corners are problematic. Splines of small order, say $n = 2$ or $n = 3$, are a useful alternative; their smoothness is often precisely what we want to model a natural, continuously occurring process.

Splines accomplish function approximation in applied mathematics [14, 15] and shape generation in computer graphics [16, 17]. They have become very popular signal modeling tools in signal processing and analysis [18, 19] especially in connection with recent developments in wavelet theory [20]. A recent tutorial is Ref. 21.

For signal processing, splines with uniformly spaced knots $K = \{k_m : m \in \mathbb{Z}\}$ are most useful. The knots then represent samples of the spline $s(t)$ on intervals of length $T = k_1 - k_0$. We confine the discussion to smooth splines.

Definition (B-Spline). The zero-order B-spline $\beta_0(t)$ is given by

$$\beta_0(t) = \begin{cases} 1 & \text{if } -\frac{1}{2} < t < \frac{1}{2}, \\ \frac{1}{2} & \text{if } |t| = \frac{1}{2}, \\ 0 & \text{if otherwise.} \end{cases} \tag{3.44}$$

The *B-spline of order n*, $\beta_n(t)$, is

$$\beta_n(t) = \underbrace{\beta_0(t) * \beta_0(t) * \ldots \beta_0(t)}_{n+1 \text{ times}}. \tag{3.45}$$

The B-splines are isolated pulses. The zeroth-order B-spline is a square, $\beta_1(t)$ is a triangle, and higher-order functions are Gaussian-like creatures (Figure 3.2).

Before proving some theorems about splines, let us recall a few ideas from the topology of the real number system $\mathbb{R}$ [6]. Open sets on the real line have soft edges; $S \subset \mathbb{R}$ is *open* if every $s \in S$ is contained in an open interval $I = (a, b)$ that is completely within S: $s \in I \subset S$. Closed sets have hard edges: S is *closed* if its complement is open. Unions of open sets are open, and intersections of closed sets are closed. S is *bounded* if it is contained in some finite interval (a, b). A set of open sets $O = \{O_n\}$ is an *open covering* of S if $\bigcup_n O_n \supset S$. Set S is *compact* if for every open

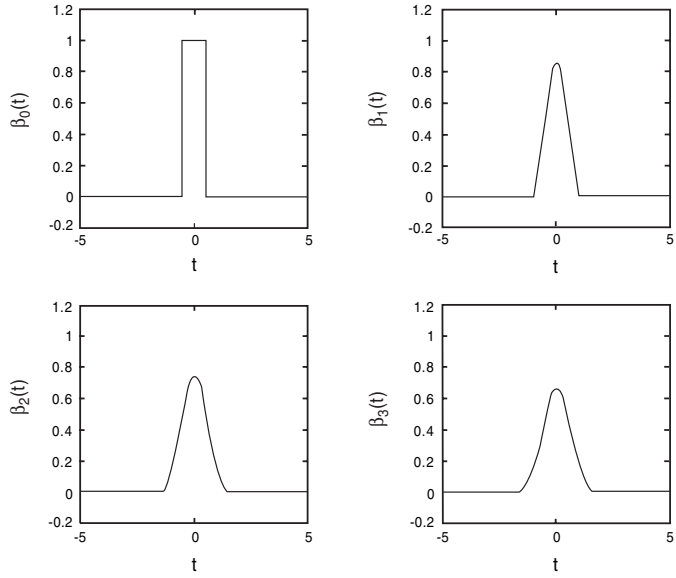

Fig. 3.2. The first four B-splines.

covering O of S there is a subset $P \subset O$ such that P is finite and P covers S. The famous Heine–Borel theorem[2] states that a set is compact if and only if it is closed and bounded [22, 23].

Definition (Support). Let $x(t)$ be an analog signal. Then $x(t)$ is *compactly supported* if $x(t) = 0$ outside some interval $[a, b]$. The *support* of $x(t)$, written Support(x), is the smallest closed set S such that $x(t) = 0$ if $t \notin S$.

Proposition. The n th-order B-spline $\beta_n(t)$ has compact support; that is, the smallest closed set which contains the domain over which set $\beta_n(t)$ is nonzero is closed and bounded.

Proof: By induction on the order (exercise). ■

The next result shows that general splines are linear combinations of shifted B-splines [14].

Theorem (Schoenberg). Let $x(t)$ be a spline having degree n and integral knots $K = \{m = k_m : m \in \mathbb{Z}\}$. Then there are constants c_m such that

$$s(t) = \sum_{m=-\infty}^{\infty} c_m \beta_n(t - m). \tag{3.46}$$

Proof: The proof is outside our present scope; we need Fourier transform tools (Chapters 5 and 6) for the arguments; interested readers will find some of the steps sketched in the latter chapter's problems. ■

The Schoenberg theorem shows that sums of simple shifts and scalings (amplification or attentuation) of the B-spline $\beta_n(t)$ will generate any spline of order n. Thus, the B-splines constitute a kind of signal atom. If signal $x(t)$ admits a spline model, then we can decompose the model into a sum of atoms. The relative abundance of each atom in the original signal at a time value $t = m$ is given by a simple coefficient c_m. This data reduction can be a great help to signal processing and analysis applications, such as filtering and pattern recognition. Notice too that as models of naturally occurring signals, B-splines have the realistic property that they decay to zero as time increases toward $\pm\infty$.

Once we develop more signal theory we shall explore B-spline ideas further. We require a more powerful tool: the full theory of signal frequency, which the Fourier transform provides. Looking forward, we will apply B-splines to construct windowed Fourier transforms (Chapter 10) and scaling functions for wavelet multiresolution analysis structures (Chapter 11).

[2]German analyst Heinrich Eduard Heine (1821–1881) first defined uniform continuity. Emile Borel (1871–1956) is mostly known for his contributions to topology and modern analysis. But he was also Minister of the French Navy (1925–1940) and received the Resistance Medal in 1945 for his efforts opposing the Vichy government during the war.

3.3 ANALOG SIGNAL SPACES

We must once again find sufficiently powerful mathematical structures to support the analog signal processing operations that we have been working with. For instance, convolution characterizes linear, translation-invariant analog systems. But how does one know that the convolution of two signals produces a genuine signal? Since convolution involves integration between infinite limits, there is ample room for doubt about the validity of the result. Are there classes of signals that are broad enough to capture the behavior of all the real-world signals we encounter and yet are closed under the convolution operation? We are thus once again confronted with the task of finding formal mathematical structures that support the operations we need to study systems that process analog signals.

3.3.1 L^p Spaces

Let us begin by defining the p-integrable signal spaces, the analog equivalents of the p-summable spaces studied in the previous chapter. Again, some aforementioned signal classes—such as the absolutely integrable, bounded, and finite-energy signals—fall into one of these families. The theory of signal frequency (Fourier analysis) in Chapters 5 and 7 uses these concepts extensively. These ideas also lie at the heart of recent developments in mixed-domain signal analysis: Gabor transforms, wavelets, and their applications, which comprise the final three chapters of the book.

3.3.1.1 Definition and Basic Properties. We begin with the definition of the p norm for analog signals. The norm is a measure of analog signal size. It looks a lot like the definition of the l^p norm for discrete signals, with an infinite integral replacing the infinite sum. Again, our signals may be real- or complex-valued.

Definition (L^p Norm or p Norm). If $x(t)$ is an analog signal and $p \geq 1$ is finite, then its L^p *norm* is

$$\|x\|_p = \left[\int_{-\infty}^{\infty} |x(t)|^p dt \right]^{\frac{1}{p}}, \tag{3.47}$$

if the Riemann integral exists. If $p = \infty$, then $\|x\|_\infty$ is the least upper bound of $\{|x(t)| \mid x \in \mathbb{R}\}$, if it exists. The L^p norm of $x(t)$ restricted to the interval $[a, b]$ is

$$\|x\|_{L^p[a,\,b]} = \left[\int_a^b |x(t)|^p dt \right]^{\frac{1}{p}}. \tag{3.48}$$

Other notations are $\|x\|_{p,\mathbb{R}}$ and $\|x\|_{p,[a,\,b]}$. The basic properties of the p-norm are the Hölder, Schwarz, and Minkowski inequalities; let us extend them to integrals.

Theorem (Hölder Inequality). Suppose $1 \leq p \leq \infty$ and p and q are conjugate exponents: $p^{-1} + q^{-1} = 1$. If $\|x\|_p < \infty$ and $\|y\|_q < \infty$, then $\|xy\|_1 \leq \|x\|_p \|y\|_q$.

Proof: Recall the technical lemma from Section 2.5.4: $ab \le p^{-1}a^p + q^{-1}b^q$, where p and q are conjugate exponents and $a, b > 0$. So by the same lemma,

$$\frac{|x(t)|}{\|x\|_p}\frac{|y(t)|}{\|y\|_q} \le \frac{|x(t)|^p}{p\|x\|_p^p} + \frac{|y(t)|^q}{q\|y\|_q^q}. \tag{3.49}$$

Integrating (3.49) on both sides of the inequality gives

$$\frac{1}{\|x\|_p\|y\|_q}\int_{-\infty}^{\infty}|x(t)||y(t)|\,dt \le \frac{1}{p\|x\|_p^p}\int_{-\infty}^{\infty}|x(t)|^p dt + \frac{1}{q\|y\|_q^q}\int_{-\infty}^{\infty}|y(t)|^q\,dt = \frac{1}{p}+\frac{1}{q} = 1. \tag{3.50}$$

The case $p = 1$ and $q = \infty$ is straightforward and left as an exercise. ■

Corollary (Schwarz Inequality). If $\|x\|_2 < \infty$ and $\|y\|_2 < \infty$, then $\|xy\|_1 \le \|x\|_2\|y\|_2$.

Proof: Because $p = q = 2$ are conjugate exponents. ■

Theorem (Minkowski Inequality). Let $1 \le p \le \infty$, $\|x\|_p < \infty$, and $\|y\|_p < \infty$. Then $\|x + y\|_p \le \|x\|_p + \|y\|_p$.

Proof: We prove the theorem for $1 < p < \infty$ and leave the remaining cases as exercises. Because $|x(t) + y(t)| \le |x(t)| + |y(t)|$ and $1 \le p$, we have $|x(t) + y(t)|^p \le (|x(t)| + |y(t)|)^p = (|x| + |y|)^{p-1}|x| + (|x| + |y|)^{p-1}|y|$. Integration gives

$$\begin{aligned}\int_{-\infty}^{\infty}|x(t)+y(t)|^p dt \le \int_{-\infty}^{\infty}(|x|+|y|)^p dt &= \int_{-\infty}^{\infty}(|x|+|y|)^{p-1}|x|\,dt \\ &\quad + \int_{-\infty}^{\infty}(|x|+|y|)^{p-1}|y|\,dt.\end{aligned} \tag{3.51}$$

Let $q = \dfrac{p}{p-1}$ so that p and q are conjugate exponents. Hölder's inequality then applies to both integrals on the right-hand side of (3.51):

$$\int_{-\infty}^{\infty}|x|(|x|+|y|)^{p-1}dt = \int_{-\infty}^{\infty}|x|(|x|+|y|)^{\frac{p}{q}}dt \le \|x\|_p\left[\int_{-\infty}^{\infty}(|x|+|y|)^p dt\right]^{\frac{1}{q}} \tag{3.52a}$$

and

$$\int_{-\infty}^{\infty}|y|(|x|+|y|)^{p-1}dt = \int_{-\infty}^{\infty}|y|(|x|+|y|)^{\frac{p}{q}}dt \le \|y\|_p\left[\int_{-\infty}^{\infty}(|x|+|y|)^p dt\right]^{\frac{1}{q}}. \tag{3.52b}$$

If the term in square brackets is zero, the theorem is trivially true; we assme otherwise. Putting (3.52a) and (3.52b) together into (3.51) and dividing through by the square-bracketed term gives

$$\frac{\int_{-\infty}^{\infty} (|x| + |y|)^p \, dt}{\left[\int_{-\infty}^{\infty} (|x| + |y|)^p \, dt\right]^{\frac{1}{q}}} = \left[\int_{-\infty}^{\infty} (|x| + |y|)^p \, dt\right]^{p - \frac{1}{q}} \leq \|x\|_p + \|y\|_p . \tag{3.53}$$

Since $p - \frac{1}{q} = \frac{1}{p}$, the middle term in (3.53) is $\| \, |x| + |y| \, \|_p$. But $\|x + y\|_p \leq \| \, |x| + |y| \, \|_p$ and we are done. ■

Now we can define the principal abstract spaces for signal theory. The definition is provisional only, since it relies upon the Riemann integral for the idea that $\|x\|_p < \infty$. We offer two refinements in what follows.

Definition ($L^p(\mathbb{R})$, $L^p[a, b]$). Let $1 \leq p \leq \infty$. For $p < \infty$, the p-integrable space of analog signals or functions defined on the real numbers is $L^p(\mathbb{R}) = \{x(t) \mid x\colon \mathbb{R} \to \mathbb{K}$ and $\|x\|_p < \infty\}$, where $\| \cdot \|$ is the L^p norm and $\mathbb{K}$ is either the real numbers $\mathbb{R}$ or the complex numbers $\mathbb{C}$. Also if $a < b$, then $L^p[a, b] = \{x(t) \mid x\colon [a, b] \to \mathbb{K}$ and $\|x\|_{p,[a,b]} < \infty\}$. If $p = \infty$, then $L^\infty(\mathbb{R})$ and $L^\infty[a, b]$ are the bounded signals on $\mathbb{R}$ and $[a, b]$, respectively.

It is conventional to use uppercase letters for the analog p-integrable spaces and lowercase letters for the discrete p-summable signal spaces. It is also possible to consider half-infinite L^p spaces: $L^p(-\infty, a]$ and $L^p[a, +\infty)$.

These ideas have signal processing significance. The absolutely integrable signals can be used with other L^p signals under the convolution operation [12]. The following proposition tells us that as long as its impulse response $h = H\delta$ is absolutely integrable, an LTI system will produce an L^1 output from an L^1 input.

Proposition. If $x, h \in L^1(\mathbb{R})$, then $y = x * h \in L^1(\mathbb{R})$, and $\|y\|_1 \leq \|x\|_1 \|h\|_1$.

Proof

$$\int_{-\infty}^{\infty} |y(t)| \, dt = \int_{-\infty}^{\infty} \left| \int_{-\infty}^{\infty} x(s) h(t - s) \, ds \right| dt \leq \int_{-\infty}^{\infty} \int_{-\infty}^{\infty} |x(s) h(t - s)| \, ds dt. \tag{3.54}$$

From the Fubini–Tonelli theorem [24], if the two-dimensional integrand is either absolutely integrable or non-negative, then the double integral equals either iterated integral. Thus,

$$\|y\|_1 \leq \int_{-\infty}^{\infty} |x(s)| \left[\int_{-\infty}^{\infty} |h(t-s)| \, dt \right] ds = \|x\|_1 \|h\|_1 . \tag{3.55}$$

■

The next proposition concerns the concept of uniform continuity, which readers may recall from calculus [6]. A function $y(t)$ is *uniformly continuous* means that for any $e > 0$ there is a $\delta > 0$ such that $|t - s| < \delta$ implies $|y(t) - y(s)| < \varepsilon$. The key idea is that for any $\varepsilon > 0$, it is possible to find a $\delta > 0$ that works for all time values. When the interval width δ must depend on $t \in \mathbb{R}$, then we may have ordinary continuity, but not necessarily uniform continuity. An example of a signal that is uniformly continuous on $\mathbb{R}$ is $\sin(t)$. A signal that is continuous, but not uniformly so, is t^2.

Proposition. If $x \in L^2(\mathbb{R})$ and $y = x \circ x$, then $|y(t)| \leq \|x\|_2^2$. Furthermore, $y(t)$ is uniformly continuous.

Proof: We apply the Schwarz inequality, $\|fg\|_1 \leq \|f\|_2 \|g\|_2$:

$$|y(t)| \leq \int_{-\infty}^{\infty} |x(s)| \left| \overline{x(t+s)} \right| \, ds \leq \|x(s)\|_2 \|x(t+s)\|_2 = \|x\|_2^2 . \tag{3.56}$$

To show uniform continuity, let us consider the magnitude $|y(t + \Delta t) - y(t)|$:

$$|y(t+\Delta t) - y(t)| \leq \int_{-\infty}^{\infty} |x(s)| \overline{|x(t+\Delta t+s) - x(t+s)|} \, ds. \tag{3.57}$$

Invoking the Schwarz inequality on the right-hand side of (3.57) and changing the integration variable with $\tau = t + s$, we obtain

$$|y(t+\Delta t) - y(t)| \leq \|x\|_2 \left[\int_{-\infty}^{\infty} |x(\tau + \Delta t) - x(\tau)|^2 d\tau \right]^{\frac{1}{2}} . \tag{3.58}$$

The limit, $\lim_{\Delta t \to 0} y(t + \Delta t) - y(t)$, concerns us. From integration theory—for instance, Ref. 24, p. 91—we know that

$$\lim_{\tau \to 0} \int_{-\infty}^{\infty} |x(\tau + \Delta t) - x(\tau)| \, d\tau = 0, \tag{3.59}$$

and since this limit does not depend upon t, $y(t)$ is uniform continuous. ■

Proposition. Let $1 \leq p \leq \infty$, $x \in L^p(\mathbb{R})$, and $h \in L^1(\mathbb{R})$. Then $y = x * h \in L^p(\mathbb{R})$, and $\|y\|_p \leq \|x\|_p \|h\|_1$.

Proof: Exercise. ■

The criterion upon which the definition rides depends completely on whether $|x(t)|^p$ is integrable or not; that is, it depends how powerful an integral we can roust up. The Riemann integral, of college calculus renown, is good for functions that are piecewise continuous. Basic texts usually assume continuity of the integrand, but their theory generalizes easily to those functions having a finite number of discontinuities; it is only necessary to count the pieces and perform separate Riemann integrals on each segment. A refinement of the definition is possible, still based on Riemann integration. We make this refinement after we discover how to construct Banach spaces out of the L^p-normed linear spaces given by the first defintion of $\|x\|_p$. We issue the following warning: The Riemann integral will fail to serve our signal theoretic needs. We will see this as soon as we delve into the basic abstract signal structures: normed linear, Banach, inner product, and Hilbert spaces. The modern Lebesgue integral replaces it. Our final definition, which accords with modern practice, will provide the same finite integral criterion, but make use of the modern Lebesgue integral instead. This means that although the above definition will not change in form, when we interpret it in the light of Lebesgue's rather than Riemann's integral, the L^p spaces will admit a far wider class of signals.

3.3.1.2 Normed Linear Spaces. A normed linear space allows basic signal operations such as summation and scalar multiplication (amplification or attenuation) and in addition provides a measure of signal size, the norm operator, written $\|\cdot\|$. Normed spaces can be made up of abstract elements, but generally we consider those that are sets of analog signals.

Definition (Norm, Normed Linear Space). Let X be a vector space of analog signals over $\mathbb{K}$ ($\mathbb{R}$ or $\mathbb{C}$). Then a *norm*, written $\|\cdot\|$, is a map $\|\cdot\|: X \to \mathbb{R}$ such that

(i) (Non-negative) $0 \leq \|x\|$ for all $x \in X$.
(ii) (Zero) $\|x\| = 0$ if and only if $x(t) = 0$ for all t.
(iii) (Scalar multiplication) $\|ax\| = |c|\,\|x\|$ for every scalar $c \in \mathbb{K}$.
(iv) (Triangle inequality) $\|x + y\| \leq \|x\| + \|y\|$.

If X is a vector space of analog signals and $\|\cdot\|$ is a norm on X, then $(X, \|\cdot\|)$ is a *normed linear space*. Other common terms are normed vector space or simply normed space.

One can show that the norm is a continuous map. That is, for any $x \in X$ and $\varepsilon > 0$ there is a $\delta > 0$ such that for all $y \in X$, $\|y - x\| < \delta$ implies $|\,\|y\| - \|x\|\,| < \varepsilon$. The algebraic operations, addition and scalar multiplication, are also continuous.

Example. Let $a < b$ and consider the set of continuous functions $x(t)$ on $[a, b]$. This space, denoted $C^0[a, b]$ is a normed linear space with the following norm: $\|x(t)\| = \sup\{|x(t)|: t \in [a, b]\}$. Since the closed interval $[a, b]$ is compact, it is closed and bounded (by the Heine–Borel theorem), and a continuous function therefore achieves a maximum [6]. Thus, the norm is well-defined.

Example. Let $C^0(\mathbb{R})$ the set of bounded continuous analog signals. This too is a normed linear space, given the supremum norm: $\|x(t)\| = \sup\{|x(t)|: t \in \mathbb{R}\}$.

Example. Different norms can be given for the same underlying set of signals, and this results in different normed vector spaces. For example, we can choose the energy of a continuous signal $x(t) \in C^0[a, b]$ as a norm:

$$\|x\| = E_x = \left[\int_a^b |x(t)|^2 dt\right]^{\frac{1}{2}}. \tag{3.60}$$

The next proposition ensures that the L^p-norm is indeed a norm for continuous signals.

Proposition. Let X be the set of continuous, p-integrable signals $x : \mathbb{R} \to \mathbb{K}$, where $\mathbb{K}$ is either $\mathbb{R}$ or $\mathbb{C}$. Then $\|x\|_p$ is a norm, and $(X, \|x\|_p)$ is a normed linear space.

Proof: The continuous signals are clearly an Abelian (commutative) group under addition, and obey the scalar multiplication rules for a vector space. Norm properties (i) and (iii) follow from basic integration theory. For (ii), note that if $x(t)$ is not identically zero, then there must be some t_0 such that $x(t_0) = \varepsilon \neq 0$. By continuity, in an interval $I = (a, b)$ about t_0, we must have $|x(t)| > \varepsilon/2$. But then the norm integral is at least $[\varepsilon(b - a)/2]^p > 0$. The last property follows from Minkowski's inequality for analog signals. ■

Proposition. Let X be the set of continuous, p-integrable signals x: $[a, b] \to \mathbb{K}$, where $a < b$. Then $(X, \|x\|_{p,[a,b]})$ is a normed linear space.

Proof: Exercise. ■

Must analog signal theory confine itself to continuous signals? Some important analog signals contain discontinuities, such as the unit step and square pulse signals, and we should have enough confidence in our theory to apply it to signals with an infinite number of discontinuities. Describing signal noise, for example, might demand just as much. The continuity assumption enforces the zero property of the norm, (ii) above; without presupposing continuity, signals that are zero except on a finite number of points, for example, violate (ii). The full spaces, $L^p(\mathbb{R})$ and $L^p[a,b]$, are not—from discussion so far—normed spaces.

A *metric space* derives naturally from a normed linear space. Recall from the Chapter 2 exercises that a *metric* $d(x, y)$ is a map from pairs of signals to real numbers. Its four properties are:

(i) $d(x, y) \geq 0$ for all x, y.
(ii) $d(x, y) = 0$ if and only if $x = y$.

(iii) $d(u, v) = d(v, u)$ for all u, v.

(iv) For any s, $d(x, y) \leq d(x, s) + d(s, y)$.

Thus, the L^p-norm generates a metric. In signal analysis matching applications, a common application requirement is to develop a measure of match between candidate signals and prototype signals. The candidate signals are fed into the analysis system, and the prototypes are models or library elements which are expected among the inputs. The goal is to match candidates against prototypes, and it is typical to require that the match measure be a metric.

Mappings between normed spaces are also important in signal theory. Such maps abstractly model the idea of filtering a signal: signal-in and signal-out. When the normed spaces contain analog signals, or rather functions on the real number line, then such maps are precisely the analog systems covered earlier in the chapter. For applications we are often interested in linear maps.

Definition (Linear Operator). Let X and W be normed spaces over $\mathbb{K}$ ($\mathbb{R}$ or $\mathbb{C}$) and $T\colon X \to W$ such that for all $x, y \in X$ and any $a \in \mathbb{K}$ we have

(i) $T(x + y) = T(x) + T(y)$.

(ii) $T(ax) = aT(x)$.

Then T is called a *linear operator* or *linear map*. Dropping parentheses is widespread: $Tx \equiv T(x)$. If the operator's range is included in $\mathbb{R}$ or $\mathbb{C}$, then we more specifically call T a *linear functional*.

Proposition (Properties). Let X and W be normed spaces over $\mathbb{K}$ and let $T\colon X \to W$ be a linear operator. Then

(i) Range(T) is a normed linear subspace of W.

(ii) The null space of T, $\{x \in X \mid Tx = 0\}$ is a normed linear subspace of X.

(iii) The inverse map $T^{-1}\colon \text{Range}(T) \to X$ exists if and only if the null space of T is precisely $\{0\}$ in X.

Proof: Exercise. ■

Definition (Continuous Operator). Let X and W be normed spaces over $\mathbb{K}$ and $T\colon X \to W$. Then T is *continuous at* x if for any $\varepsilon > 0$ there is a $\delta > 0$ such that if $\|y - x\| < \delta$, then $\|Ty - Tx\| < \varepsilon$. T is *continuous* if it is continuous at every $x \in X$.

Definition (Norm, Bounded Linear Operator). Let X and W be normed spaces over $\mathbb{K}$ and $T\colon X \to W$ be a linear operator. Then we define the *norm* of T, written $\|T\|$, by $\|T\| = \sup\{\|Tx\|/\|x\| \colon x \in X, x \neq 0\}$. If $\|T\| < \infty$, then T is a *bounded linear operator.*

Theorem (Boundedness). Let X and W be normed spaces over $\mathbb{K}$ and T: $X \to W$ be a linear operator. Then the following are equivalent:

(i) T is bounded.
(ii) T is continuous.
(iii) T is continuous at $0 \in X$.

Proof: The easy part of this proof is not hard to spot: (ii) obviously implies (iii). Let us therefore assume continuity at zero (iii) and show that T is bounded. Let $\delta > 0$ such that $\|Tx - 0\| = \|Tx\| < 1$ when $\|x - 0\| = \|x\| < \delta$. Let $y \in X$ be nonzero. Then $\left\| \frac{\delta y}{2\|y\|} \right\| = \frac{\delta}{2} < \delta$, so that $\left\| \frac{T(\delta y)}{2\|y\|} \right\| < 1$ and $\|Ty\| < \frac{2\|y\|}{\delta}$; T is bounded. Now we assume T is bounded (i) and show continuity. Note that $\|Tx - Ty\| = \|T(x - y)\| \leq \|T\| \, \|x - y\|$, from which continuity follows. ■

The boundedness theorem seems strange at first glance. But what $\|T\| < \infty$ really says is that T amplifies signals by a limited amount. So there cannot be any sudden jumps in the range when there are only slight changes in the domain. Still, it might seem that a system could be continuous without being bounded, since it could allow no jumps but still amplify signals by arbitrarily large factors. The linearity assumption on T prevents this, however.

3.3.1.3 Banach Spaces. Analog Banach spaces are normed linear spaces for which every Cauchy sequence of signals converges to a limit signal also in the space. Again, after formal developments in the previous chapter, the main task here is to investigate how analog spaces using the L^p norm can be complete. Using familiar Riemann integration, we can solve this problem with an abstract mathematical technique: forming the completion of a given normed linear space. But this solution is unsatisfactory because it leaves us with an abstract Banach space whose elements are quite different in nature from the simple analog signals with which we began. Interested readers will find that the ultimate solution is to replace the Riemann with the modern Lebesgue integral.

Recall that a sequence of signals $\{x_n(t)\colon n \in \mathbb{Z}\}$ is Cauchy when for all $\varepsilon > 0$ there is an N such that if $m, n > N$, then $\|x_m - x_n\| < \varepsilon$. Note that the definition depends on the choice of norm on the space X. That is, the signals get arbitrarily close to one another; as the sequence continues, signal perturbations become less and less significant—at least as far as the norm can measure. A signal $x(t)$ is the limit of a sequence $\{x_n(t)\}$ means that for any $\varepsilon > 0$ there is an $N > 0$ such that $n > N$ implies $\|x_n - x\| < \varepsilon$. A normed space X is complete if for any Cauchy sequence $\{x_n(t) : n \in \mathbb{N}\}$ there is an $x(t) \in X$ such that $x(t)$ is the limit of $\{x_n(t)\}$. A complete normed space is also called a Banach space.

In the previous section, we considered the continuous analog signals on the real line, or on an interval, and showed that with the L^p norm, they constituted normed linear spaces. Are they also Banach spaces? The answer is no, unfortunately;

Cauchy sequences of continuous signals may converge to signals that are not continuous, as the counterexample below illustrates.

Example. If $p < \infty$, then the signal space $(C^0[-1, 1], \|\cdot\|_{p,[-1,1]})$, consisting of all continuous signals on $[-1, 1]$ with the L^p norm, is not complete. The claim is secure if we can exhibit a Cauchy sequence of continuous functions that converges to a discontinuous function. A sequence that approximates the unit step on $[-1, 1]$ is

$$x_n(t) = \begin{cases} 0 & \text{if } t < -\dfrac{1}{n}, \\ \dfrac{tn}{2} + \dfrac{1}{2} & \text{if } -\dfrac{1}{n} \le t \le \dfrac{1}{n}, \\ 1 & \text{if } t > \dfrac{1}{n}. \end{cases} \tag{3.61}$$

The $\{x_n(t)\}$, shown in Figure 3.3, clearly converge pointwise. Indeed, for any $t_0 < 0$, $x_n(t_0) \to 0$; for any $t_0 > 0$, $x_n(t_0) \to 1$; and for $t_0 = 0$, $x_n(t_0) = 1/2$ for all n. Now, if we assume that $n < m$, then

$$\int_{-1}^{1} \left|x_m(t) - x_n(t)\right|^p dt = \int_{-1/n}^{1/n} \left|x_m(t) - x_n(t)\right|^p dt \le \frac{2}{n}\left(\frac{1}{2^p}\right). \tag{3.62}$$

The sequence is Cauchy, but converges to a discontinuous signal. The same reasoning applies to $L^p[a, b]$, where $a < b$, and to $L^p(\mathbb{R})$.

Example. Now consider $C^0[a, b]$ the set of bounded continuous analog signals on $[a, b]$ with the supremum or L^∞ norm: $\|x(t)\|_\infty = \sup\{|x(t)| : t \in [a, b]\}$. This space's norm avoids integration, so $(C^0[a, b], \|\cdot\|_\infty)$ earns Banach space status. To see this, note that if $\{x_n(t)\}$ is Cauchy and $\varepsilon > 0$, then there is an $N > 0$ such that for all $m, n > N$ we have $\|x_n - x_m\|_\infty < \varepsilon$. Fixing $t_0 \in [a, b]$, the sequence of real numbers $\{x_n(t_0)\}$ is Cauchy in $\mathbb{R}$. Calculus teaches that Cauchy sequences of real numbers converge to a limit in $\mathbb{R}$; for each $t \in [a, b]$, we may therefore set $x(t) = \lim_{n \to \infty} x_n(t)$. We claim $x(t)$ is continuous. Indeed, since the sequence $\{x_n(t)\}$ is Cauchy in the L^∞ norm, the sequence must converge not just pointwise, but uniformly to $x(t)$. That is, for any $\varepsilon > 0$, there is an $N > 0$ such that $m, n > N$ implies $|x_m(t) - x_n(t)| < \varepsilon$ for all $t \in [a, b]$. Uniformly convergent sequences of continuous functions converge to a continuous limit [6] $x(t)$ must therefore be continuous, and $C^0[a, b]$ is a Banach space.

Analog signal spaces seem to leave us in a quandary. We need continuity in order to achieve the basic properties of normed linear spaces, which provide a basic signal size function, namely the norm. Prodded by our intuition that worldly processes—at least at our own perceptual level of objects, forces between them, and their motions—are continuously defined, we might proceed to develop analog signal theory from

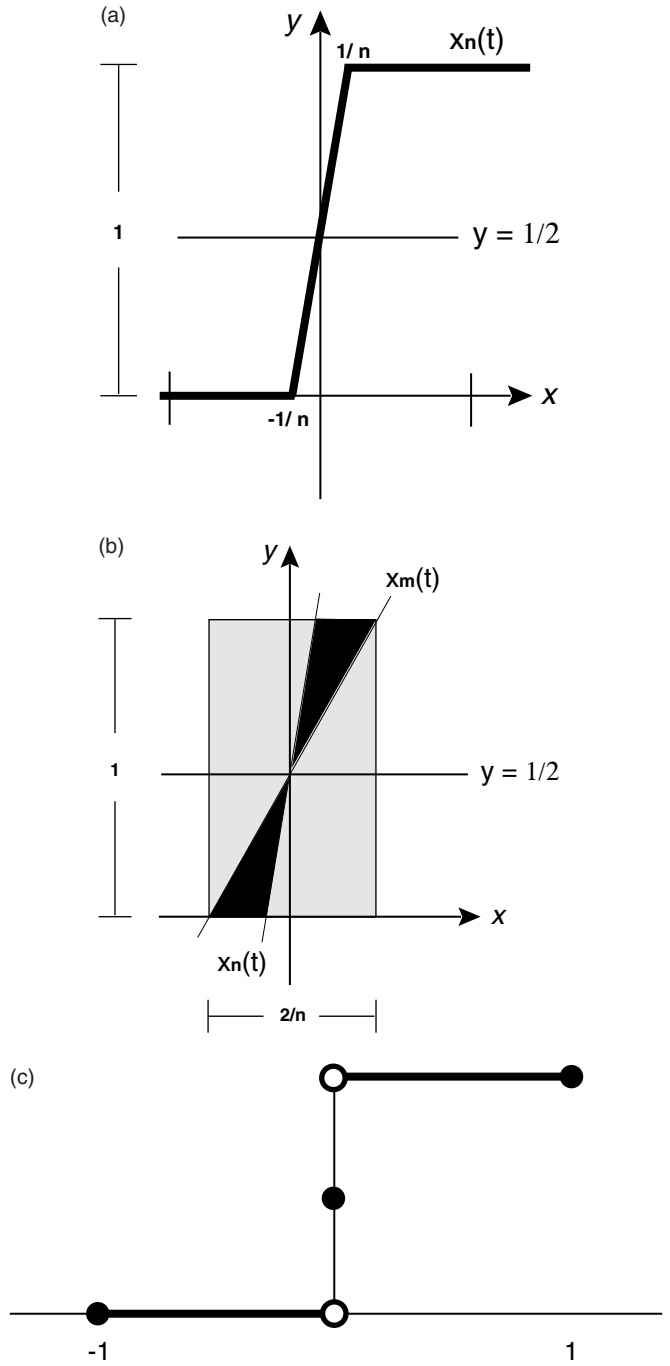

Fig. 3.3. (a) A Cauchy sequence of continuous signals in $L^p[-1, 1]$. (b) Detail of the difference between x_m and x_n. Assuming $n < m$, the signals differ by at most 1/2 within the rectangular region, which has width $2/n$. (c) Diagram showing discontinuous limit.

continuous signals alone. However, arbitrarily precise signal approximations depend on the mathematical theory of limits, which in turn begs the question of the completeness for our designated theoretical base, $(C^0[-1, 1], \|\cdot\|_p)$ for example. But the first above example shows that we cannot get completeness from families of continuous signals with the L^p-norm, where $p < \infty$.

What about working with the supremum norm, $\|\cdot\|_\infty$? This is a perfectly good norm for certain signal analysis applications. Some matching applications rely on it, for example. Nonetheless, the next section shows that L^∞ does not support an inner product. Inner products are crucial for much of our later development: Fourier analysis, windowed Fourier (Gabor) transforms, and wavelet transforms. Also many applications presuppose square-integrable physical quantities. It would appear that the supremum norm would confine signal theory to a narrow range of processing and analysis problems.

Let us persist: Can we only allow sequences that do converge? As the exercises explain, uniformly convergent sequences of continuous signals converge to a continuous limit. The problem is when the signal values, say $x_n(t_0)$, converges for every $t_0 \in [-1, 1]$, then we should expect that x_n itself converges to an allowable member of our signal space. Alternatively, since Cauchy sequences of continuous signals lead us to discontinuous entities, can we just incorporate into our foundational signal space the piecewise continuous signals that are p-integrable? We would allow signals with a finite number of discontinuities. The Riemann integral extends to them, and it serves the L^p-norm definition (3.47). We would have to give up one of the criteria for a normed linear space; signals would differ, but the norm of their difference would be zero. Frustratingly, this scheme fails, too, as the next example shows [25].

Example. Consider the signals $\{x_n(t)\}$ defined on $[-1, 1]$ defined by

$$x_n(t) = \lim_{m \to \infty} [\cos(n!\pi t)]^{2m} = \begin{cases} 1 & \text{if } n!t \in \mathbb{Z}, \\ 0 & \text{if otherwise.} \end{cases} \tag{3.63}$$

Note that $x_n(t)$ is zero at all but a finite number of points in $[-1, 1]$; $x_n(t)$ is Riemann-integrable, and its Riemann integral is zero on $[-1, 1]$. Also $\|x_n(t) - x_m(t)\|_{p,[-1,1]} = 0$, which means that the sequence $\{x_n(t)\}$ is Cauchy. It converges, however, to

$$x(t) = \begin{cases} 1 & \text{if } t \in \mathbb{Q}, \\ 0 & \text{if otherwise .} \end{cases} \tag{3.64}$$

which is not Riemann-integrable.

3.3.1.4 Constructing Banach Spaces. An abstract mathematical technique, called completing the normed space, eliminates most of the above aggravations. The completion of a normed linear space X, is a Banach space B having a subspace C isometric to X. Two normed spaces, M and N, are isometric means there is a one-to-one,

onto map f: $M \to N$ such that f is a vector space isomorphism and for all $x \in M$, $\|x\|_M = \|f(x)\|_N$. Isometries preserve norms. The next theorem shows how to construct the completion of a general normed linear space.

Let us cover an algebraic idea which features in the completion result: equivalence relations [26].

Definition (Equivalence Relation). We say $a \sim b$ is an equivalence relation on a set S if it satisfies the following three properties:

(i) (Reflexive) For all $a \in S$, $a \sim a$.
(ii) (Symmetric) For all $a, b \in S$, if $a \sim b$, then $b \sim a$.
(iii) (Transitive) For all $a, b, c \in S$, if $a \sim b$ and $b \sim c$, then $a \sim c$.

Equivalence relations associate things in a collection that are similar in form.

Example. For example, we might consider ordered pairs of integers (m, n) with $n \neq 0$. If $p = (m, n)$ and $q = (i, k)$, then it is easy to check that the relation, $p \sim q$ if and only if $m{\cdot}k = n{\cdot}i$, is an equivalence relation. In fact, this is the equivalence relation for different forms of the same rational number: $\frac{7}{8} = \frac{42}{48}$, for instance. Rational numbers themselves are not pairs of integers, but are represented by an infinite collection of such pairs. This is an important idea.

Definition (Equivalence Class). Let $a \sim b$ be an equivalence relation on a set S. The equivalence class of $a \in S$ is $[a] = \{b \in S \mid a \sim b\}$.

If $a \sim b$ is an equivalence relation on a set S, then the equivalence classes form a partition of S. Every $a \in S$ belongs to one and only one equivalence class.

Example (Rational Numbers). From the previous example we can let $S = \{(m, n) \mid m, n \in \mathbb{Z} \text{ and } n \neq 0\}$. Let $\mathbb{Q} = \{[q] \mid q \in S\}$. We can define addition and multiplication on elements of $\mathbb{Q}$. This is easy. If $p = (m, n)$ and $q = (i, k)$, then we define $[p] + [q] = [(M, N)]$, where $\frac{M}{N} = \frac{m}{n} + \frac{i}{k}$. Constructing a rational multiplication operator is simple, too. These steps construct the rational numbers from the integers [26].

But for signal theory, so what? Well, equivalence relations are precisely what we need to deal with the problem that arises when making a normed linear space based on the L^p norm. Just a moment ago, we noted that the zero property of the norm—namely, that $\|x\|_p = 0$ if and only if $x(t) = 0$ identically—compelled us to use continuous signals for normed linear spaces. But we use and need piecewise continuous entities, such as the unit step, in signal processing. Also, signals with point discontinuities are also useful for modeling noise spikes and the like. The strategy is to begin with piecewise discontinuous signals, but to assemble them into equivalence classes for making the normed linear space.

Example (Signal Equivalence Classes). Let $1 \le p < \infty$, and suppose that we have extended the Riemann integral to piecewise continuous analog signals (that is, having at most a finite number of discontinuities) on the interval $[a, b]$. Strictly speaking, this class of signals is not a normed linear space using $\|\cdot\|_p$; the zero property of the norm fails. However, we let $[x] = \{y(t)\colon \|y\|_p = \|x\|_p\}$ and define $\underline{L}^p[a, b] = \{[x] \mid x \in L^p[a, b]\}$. Evidently, we have identified all signals that differ from one another by a finite number of discontinuities as being essentially the same. That is what lumping them into equivalence classes accomplishes. Now we can define signal addition, scalar multiplication, and the norm on equivalence classes. This reinterpretation of $L^p[a, b]$ in terms of equivalence classes is often implicit in many signal processing treatments. The same idea applies to $L^p(\mathbb{R})$. The exercises explore these ideas in greater depth.

Now let us turn to the problem of constructing a Banach space from a given normed linear space [22, 27]. This leads to a refined definition for the L^p spaces.

Theorem (Completion of Normed Linear Space). Let X be a normed linear space. Then there is a Banach space B and an isometry $f\colon X \to B$ such that $C = \text{Range}(f)$ is dense in B.

Proof: Let $S = \{x_n\}$ and $T = \{y_n\}$ be Cauchy sequences in X. We define the relation $S \sim T$ if and only if $\lim_{n\to\infty}\|x_n - y_n\| = 0$. It is not hard to show this is an equivalence relation (exercise). Let $[S] = \{T\colon T \sim S\}$ and set $B = \{[S]\colon\ S = \{x_n\}$ is Cauchy in $X\}$. Let $x \in X$ and define $f(x) = [\{x_n\}]$, where $x_n = x$ for all n; the image $f(x)$ is a constant sequence. There are several things we must show.

With appropriate definitions of addition, scalar multiplication, and norm, we can make B into a normed linear space. If $S = \{x_n\}$, $T = \{y_n\} \in B$, then we define an additon operation on B by $[S] + [T] = [\{x_n + y_n\}]$. This works, but there is a slight technical problem. Many different Cauchy sequences $\{a_n\}$ can be the source for a single equivalence class, say $[S]$. We must show that the definition of additon does not depend on which sequences in the respective equivalence classes, S and T, are taken for defining the sums in $\{x_n + y_n\}$. So suppose $S = [\{a_n\}]$ and $T = [\{b_n\}]$ so that $\{a_n\} \sim \{x_n\}$ and $\{b_n\} \sim \{y_n\}$. We claim that $[\{x_n + y_n\}] = [\{a_n + b_n\}]$; that is, our addition operation is well-defined. Because $\|(x_n + y_n) - (a_n + b_n)\| = \|(x_n - a_n) + (y_n - b_n)\| \le \|x_n - a_n\| + \|y_n - b_n\|$, and both of these last terms approach zero, we must have $\{x_n + y_n\} \sim \{a_n + b_n\}$, proving the claim. We define scalar multiplication by $c[S] = [\{cx_n\}]$. It is straightforward to show that these definitions make B into a vector space. For the norm, we define $\|[S]\| = \lim_{n\to\infty}\|x_n\|$. Justifying the definition requires that the limit exists and that the definition is independent of the sequence chosen from the equivalence class $[S]$. We have

$$\big|\|x_n\| - \|x_m\|\big| \le \|x_n - x_m\| \tag{3.65}$$

by the triangle inequality. Since $\{x_n\}$ is Cauchy in X, so must $\{\|x_n\|\}$ be in $\mathbb{R}$. Next, suppose that some other sequence $\{a_n\}$ generates the same equivalence class: $[\{a_n\}] = [S]$. We need to show that $\lim_{n\to\infty}\|x_n\| = \lim_{n\to\infty}\|a_n\|$. In fact, we know that $[\{a_n\}] \sim [\{x_n\}]$, since they are in the same equivalence class. Thus, $\lim_{n\to\infty}\|x_n - a_n\| = 0$. Since $\|x_n - a_n\| \geq \|\|x_n\| - \|a_a\|\|$, $\lim_{n\to\infty}[\|x_n\| - \|a_n\|] = 0$, and we have shown our second point necessary for a well-defined norm. Verifying the normed space properties remains, but it is straightforward and perhaps tedious.

Notice that the map f is a normed space isomorphism that preserves norms—an *isometry.* An *isomorphism* is one-to-one and onto, $f(x + y) = f(x) + f(y)$, and $f(cx) = cf(x)$ for scalars $c \in \mathbb{R}$ (or $\mathbb{C}$). In an isometry we also have $\|x\| = \|f(x)\|$.

Our major claim is that B is complete, but a convenient shortcut is to first show that Range(f) is dense in B. Given $[T] = [\{y_n\}] \in B$, we seek an $x \in X$ such that $f(x)$ is arbitrarily close to $[T]$. Since $\{y_n\}$ is Cauchy, for any $\varepsilon > 0$, there is an N_ε such that if $m, n > N_\varepsilon$, then $\|y_m - y_n\| < \varepsilon$. Let $k > N_\varepsilon$, and set $x = x_n = y_k$ for all $n \in \mathbb{N}$. Then $f(x) = [\{x_n\}]$, and $\|[\{y_n\}] - [\{x_n\}]\| = \lim_{n\to\infty}\|y_n - x_n\| = \lim_{n\to\infty}\|y_n - y_k\| \leq \varepsilon$. Since ε is arbitrary, $f(X)$ must be dense in B.

Finally, to show that B is complete, let $\{S_n\}$ be a Cauchy sequence in B; we have to find an $S \in B$ such that $\lim_{n\to\infty}S_n = S$. Since Range(f) is dense in B, there must exist $x_n \in X$ such that $\|f(x_n) - S_n\| < 1/(n + 1)$ for all $n \in \mathbb{N}$. We claim that $\{x_n\}$ is Cauchy in X, and if we set $S = [\{x_n\}]$, then $S = \lim_{n\to\infty}S_n$. Since f is an isometry,

$$\begin{aligned}\|x_n - x_m\| &= \|f(x_n) - f(x_m)\| = \|(f(x_n) - S_n) + (S_m - f(x_m)) + (S_n - S_m)\| \\ &\leq \|f(x_n) - S_n\| + \|S_m - f(x_m)\| + \|S_n - S_m\|. \end{aligned} \tag{3.66}$$

By the choice of $\{x_n\}$, the first two terms on the bottom of (3.66) are small for sufficiently large m, n. The final term in (3.66) is small too, since $\{S_n\}$ is Cauchy. Consequently, $\{x_n\}$ is Cauchy, and $S = [\{x_n\}]$ must be a bona fide element of B. Furthermore, note that $\|S_k - S\| \leq \|f(x_k) - S_k\| + \|f(x_k) - S\|$. Again, $\|f(x_k) - S_k\| < 1/(k + 1)$; we must attend to the second term. Let $y_n = x_k$ for all $n \in N$, so that $f(x_k) = [\{y_n\}]$. Then $\|f(x_k) - S\| = \|[\{y_n\}] - [\{x_n\}]\| = \lim_{n\to\infty}\|y_n - x_n\| = \lim_{n\to\infty}\|x_k - x_n\|$. But $\{x_n\}$ is Cauchy, so this last expression is also small for large n. ■

Corollary (Uniqueness). Let X be a normed linear space and suppose B is a Banach space with a dense subset C isometric to X. Then B is isometric to the completion of X.

Proof: Let f: $X \to C$ be the isometry and suppose $\overline{X}$ is the completion of X. Any element of B is a limit of a Cauchy sequence of elements in C: $b = \lim_{n\to\infty}c_n$. We can extend f to a map from $\overline{X}$ to B by $f(x) = b$, where $x = \lim_{n\to\infty} f^{-1}(c_n)$. We trust the further demonstration that this is an isometry to the reader (exercise). ■

The corollary justifies our referring to *the* completion of a normed linear space. Now we can refine the definition of the p-integrable signal spaces.

Definition ($L^p(\mathbb{R})$, $L^p[a, b]$). For $1 \leq p < \infty$, $L^p(\mathbb{R})$ and $L^p[a, b]$ are the completions of the normed linear spaces consisting of the continuous, Riemann p-integrable analog signals on $\mathbb{R}$ and $[a, b]$, respectively.

So the completion theorem builds up Banach spaces from normed linear spaces having only a limited complement of signals—consisting, for instance, of just continuous signals. The problem with completion is that it provides no clear picture of what the elements in completed normed space look like. We do need to expand our realm of allowable signals because limit operations lead us beyond functions that are piecewise continuous. We also seek constructive and elemental descriptions of such functions and hope to avoid invoking abstract, indirect operations such as with the completion theorem. Can we accomplish so much and still preserve closure under limit operations?

The Lebesgue integral is the key concept. Modern integration theory removes almost every burden the Riemann integral imposes, but some readers may prefer to skip the purely mathematical development; the rest of the text is quite accessible without Lebesgue integration. So we postpone the formalities and turn instead to inner products, Hilbert spaces, and ideas on orthonormality and basis expansions that we need for our later analysis of signal frequency.

3.3.2 Inner Product and Hilbert Spaces

Inner product and Hilbert spaces provide many of the theoretical underpinnings for time domain signal pattern recognition applicatins and for the whole theory of signal frequency, or Fourier analysis.

3.3.2.1 Inner Product Spaces.

An inner product space X is a vector space equipped with an inner product relation $\langle x, y \rangle$. The operation $\langle \cdot, \cdot \rangle$ takes pairs of elements in X and maps them to the real numbers or, more generally, the complex numbers. The algebraic content of Chapter 2's development is still valid; again, all we need to do is define the inner product for analog signals and verify that the properties of an abstract inner product space remain true.

Definition (Inner Product). Let $x(t)$ and $y(t)$ be real- or complex-valued analog signals. Then their inner product is $\langle x, y \rangle$:

$$\langle x, y \rangle = \int_{-\infty}^{\infty} x(t)\overline{y(t)}\, dt\,. \tag{3.67}$$

The inner product induces a norm, $\|x\| = (\langle x, x \rangle)^{1/2}$. So any inner product space thereby becomes a normed linear space. Readers mindful of Chapter 2's theorems will rightly suspect that the converse does not hold for analog signals. Recall that the inner product norm obeys the *parallelogram law*,

$$\|x + y\|^2 + \|x - y\|^2 = 2(\|x\|^2 + \|y\|^2)\,, \tag{3.68}$$

and the *polarization identity*,

$$4\langle x, y\rangle = \|x+y\|^2 - \|x-y\|^2 + j\|x+jy\|^2 - j\|x-jy\|^2. \tag{3.69}$$

It is not hard to show that the definition (3.67) satisfies the properties of an inner product. The main difficulty—as in the discrete world—is to find out for which abstract signal spaces the integral (3.67) actually exists. As with our earlier discrete results, we find that the space L^2 is special.

Example (Square-Integrable Signals). The spaces $L^2[a, b]$ and $L^2(\mathbb{R})$ are inner product spaces. Let $x(t)$ and $y(t)$ be real- or complex-valued analog signals. By the Schwarz inequality we know that if signals x and y are square-integrable, that is $\|x\|_2 < \infty$ and $\|y\|_2 < \infty$, then $\|xy\|_1 \le \|x\|_2\|y\|_2$. We must show that their inner product integral (3.67) exists. But,

$$|\langle x, y\rangle| = \left|\int_{-\infty}^{\infty} x(t)\overline{y(t)}\,dt\right| \le \int_{-\infty}^{\infty} \left|x(t)\overline{y(t)}\right| dt = \int_{-\infty}^{\infty} |x(t)||y(t)|\,dt = \|xy\|_1. \tag{3.70}$$

Schwarz's inequality shows the integration works. It states that if $\|x\|_2 < \infty$ and $\|y\|_2 < \infty$, then $\|xy\|_1 \le \|x\|_2\|y\|_2$. But (3.70) shows that $|\langle x, y\rangle| \le \|xy\|_1$. Requisite properties of an inner product are:

(i) $0 \le \langle x, x\rangle$ and $\langle x, x\rangle = 0$ if and only if $x(t) = 0$ for all t.
(ii) $\langle x + y, z\rangle = \langle x, z\rangle + \langle y, z\rangle$.
(iii) $\langle cx, y\rangle = c\langle x, y\rangle$, for any scalar c.
(iv) $\langle x, y\rangle = \overline{\langle y, x\rangle}$.

Their verification from (3.67) follows from the basic properties of Riemann integration (exercise).

Example (L^p spaces, $p \neq 2$). The spaces $L^p[a, b]$ and $L^p(\mathbb{R})$ are *not* inner product spaces with $\langle\cdot,\cdot\rangle$ defined in (3.67). Let $x(t)$ and $y(t)$ be the signals shown in Figure 3.4. Observe that $\|x\|_p = \|y\|_p = 2^{1/p}$, but $\|x + y\|_p = \|x - y\|_p = 2$. The parallelogram law holds in an inner product space, which for these signals implies $2 = 2^{2/p}$. This is only possible if $p = 2$.

3.3.2.2 Hilbert Spaces. An inner product space that is complete with respect to its induced norm is called a *Hilbert space*. All of the L^p signal spaces are Banach spaces, but only L^2 is an inner product space. So our generalization of linear algebra to encompass vectors that are infinitely long in both directions—that is, *signals*—succeeds but at the cost of eliminating all but an apparently narrow class of signals.

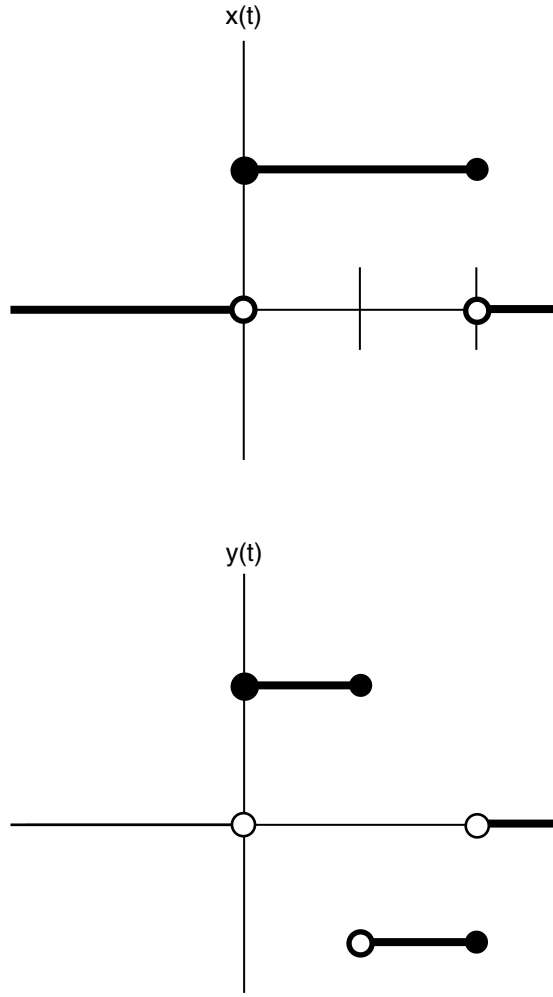

Fig. 3.4. Signals in the L^p Banach spaces: a square pulse $x(t)$ and a step signal $y(t)$.

Though it is true that square-integrable signals shall be our principal realm for signal theory, other classes do feature significantly in the sequel:

- Absolutely integrable signals, L^1;
- Bounded signals, L^∞;
- Certain subclasses of L^2, such as $L^1 \cap L^2$;
- Infinitely differentiable, rapidly decreasing signals.

It turns out that the L^1 signals constitute the best stepping-off point for constructing the Fourier transform (Chapter 5). This theory is the foundation of signal frequency analysis. With some extra effort, we can also handle L^2 signals, but we have

to resort to limit operations to so extend the Fourier transform. Boundedness connects with absolute integrability in the theory of stable linear, translation-invariant systems: $y = Hx$ is stable when its impulse response $h = H\delta \in L^1(\mathbb{R})$. L^∞ is a basic, but useful, signal class. For example, if $f \in L^\infty$ and $g \in L^p$, then $fg \in L^p$.

Example (Square-Integrable Signals). The spaces $L^2[a, b]$ and $L^2(\mathbb{R})$ are Hilbert spaces. All of the L^p spaces are complete, and L^2 has an inner product that corresponds to its standard p-norm. These and their discrete cousin, $l^2(\mathbb{Z})$, the square-summable discrete signals, are the most important Hilbert spaces for signal theory.

Example (Absolutely and Square-Integrable Signals). The inner product on $L^2(\mathbb{R})$, restricted to those signals that are also absolutely integrable, furnishes a $\langle \cdot, \cdot \rangle$ operation for $L^1 \cap L^2$. We have to define $\|x\| = \langle x, x \rangle^{1/2}$ on this space. Note too that any Cauchy sequence of signals in $L^1 \cap L^2$ is still Cauchy in L^1. Thus, the sequence converges to an absolutely integrable limit. This sequence and its limit is also square-integrable, and so the limit is also in L^2. Thus, $L^1 \cap L^2$ is complete. It is easy to show that the restrictions of the signal addition and scalar multiplication operations to $L^1 \cap L^2$ are closed on that space. So $L^1 \cap L^2$ is a Hilbert space. We can say more: $L^1 \cap L^2$ is a *dense* subspace of L^2; for every square integrable signal $x(t)$ and any $\varepsilon > 0$, there is $y(t) \in L^1 \cap L^2$ such that $\|y - x\| < \varepsilon$. In fact, if $x(t) \in L^2$, then we may take

$$x_n(t) = \begin{cases} x(t) & \text{if } -n \le t \le n, \\ 0 & \text{if otherwise.} \end{cases} \tag{3.71}$$

Then $\lim_{n\to\infty} x_n = x$, and $x_n \in L^1(\mathbb{R})$ are absolutely integrable because they are compactly supported.

Example (Schwarz Space). The Schwarz space S is the class of infinitely differentiable, rapidly decreasing functions of a real variable [28]. *Infinitely differentiable* means that each $x(t) \in S$ has derivatives of all orders. Thus, $x(t)$ and its derivatives are all continuous. *Rapidly decreasing* means that $\lim_{t\to\infty} t^m x^{(n)}(t) = 0$ for all $m, n \in \mathbb{N}$, where $x^{(n)}(t) = d^n x/dt^n$. Examples of signals in S are the Gaussians of mean μ and standard deviation $\sigma > 0$:

$$g_{\mu,\sigma}(t) = \frac{1}{\sigma\sqrt{2\pi}} e^{-\frac{(t-\mu)^2}{2\sigma^2}}. \tag{3.72}$$

Examples of signals not in S include rational signals such as $(\sigma^2 + t^2)^{-1}$; these are not rapidly decreasing. The even decaying exponentials $\exp(-\sigma|t|)$ rapidly decrease, but fail differentiability, so they are not in the Schwarz class. The Schwarz space is a plausible candidate for the mathematical models of continuously defined naturally occurring signals: temperatures, voltages, pressures, elevations, and like quantitative

phenomena. The Schwarz class strikes us as incredibly special and probably populated by very few signals. In fact, S is dense in both $L^1(\mathbb{R})$ and $L^2(\mathbb{R})$. To see this, it suffices to show that elements of S are arbitrarily close to square pulse functions. Since linear combinations of square pulses are precisely the step functions, and since step functions are dense in $L^1(\mathbb{R})$ and $L^2(\mathbb{R})$, this implies that S is dense as well. The trick is to blend the upper and lower ledge of a step together in an infinitely differentiable way [28]. The following function interpolates a unit step edge:

$$s(t) = \begin{cases} 0 & \text{if } t \le 0, \\ e^{-\frac{1}{t \exp\left[\frac{1}{t-1}\right]}} & \text{if } 0 < t < 1. \\ 1 & \text{if } 1 \le t. \end{cases} \tag{3.73}$$

Scalings and dilations of $s(t)$ interpolate a general step edge, and it is evident that arbitrary step functions are approximated to any precision by linear combinations of functions of the form (3.73).

There is a rich theory of linear operators and especially linear functionals on Hilbert spaces. Detailed explication of the ideas would take this presentation too far astray into abstract functional analysis; we refer the reader to the broad, excellent literature [13, 25, 26, 29] We shall be obliged to quote some of these results here, as elaborating some of our later signal analysis tools depends upon them.

Example (Inner Product). If we fix $h \in L^2(\mathbb{R})$, then the inner product $Tx = \langle x, h \rangle$ is a bounded linear functional with $\|T\| = \|h\|_2$. Indeed by Schwarz's inequality (3.70), $\|Tx\| = |\langle x, h \rangle| = \|xh\|_1 \le \|x\|_2 \|h\|_2$.

We have held up the inner product operation as the standard by which two signals may be compared. Is this right? It is conjugate linear and defined for square-integrable analog signals, which are desirable properties. We might well wonder whether any functional other than the inner product could better serve us as a tool for signal comparisons. The following theorem provides the answer.

Theorem (Riesz Representation). Let T be a bounded linear function on a Hilbert Space H. Then there is a unique $h \in H$ such that $Tx = \langle x, h \rangle$ for all $x \in H$. Futhermore, $\|T\| = \|h\|$.

Proof: See Ref. 29. ■

Inner products and bounded linear operators are very closely related. Using a generalization of the Riesz representation theorem, it is possible to show that every bounded linear Hilbert space operator $T : H \to K$ has a related map $S : K \to H$ which cross-couples the inner product.

Theorem. Let T: $H \to K$ be a bounded linear function on Hilbert space H and K. Then there is a bounded linear operator $S : K \to H$ such that:

(i) $\|T\| = \|S\|$.
(ii) For all $h \in H$ and $k \in K$, $\langle Th, k\rangle = \langle h, Sk\rangle$.

Proof: The idea is as follows. Let $k \in K$ and define the linear functional $L : H \to \mathbb{K}$ ($\mathbb{R}$ or $\mathbb{C}$) by $L(h) = \langle Th, k\rangle$. L is linear by the properties of the inner product. L is also bounded. The Riesz representation theorem applies, guaranteeing that there is a unique $g \in H$ such that $L(h) = \langle h, g\rangle$. Thus, we set $S(k) = g$. After verifying that S is linear and bounded, we see that it satisfies the two required properties [26]. ■

Definition (Adjoint). Let T: $H \to K$ be a bounded linear operator on Hilbert spaces H and K and S be the map identified by the previous theorem. Then S is called the *Hilbert adjoint operator* of T and is usually written $S = T^*$. If $H = K$ and $T^* = T$, then T is called *self-adjoint*.

Note that if T is self-adjoint, then $\langle Th, h\rangle = \langle h, Th\rangle$. So $\langle Th, h\rangle \in \mathbb{R}$ for all $h \in H$. This observation enables us to order self-adjoint operators.

Definition (Positive Operator, Ordering). A self-adjoint linear operator is *positive*, written $T \geq 0$, if for all h $\in H$, $0 \leq \langle Th, h\rangle$. If S and T are self-adjoint operators on a Hilbert space H with $T - S \geq 0$, then we say $S \leq$ T.

We shall use ordered self-adjoint linear operators when we study frame theory in Section 3.3.4.

Finally, important special cases of Hilbert operators are those that are isometries.

Definition (Isometry). If T: $H \to K$ is linear operator on Hilbert spaces H and K and for all $g, h \in H$ we have $\langle Tg, Th\rangle = \langle g, h\rangle$, then T is an *isometry.*

3.3.2.3 Application: Constructing Optimal Detectors. As an application of functional analysis ideas to signal analysis, consider the problem of finding a known or prototype signal $p(t)$ within a given, candidate signal $x(t)$. The idea is to convolve a kernel $k(t)$ with the input: $y(t) = (x * k)(t)$. Where the response $y(t)$ has a maximum, then hopefully $x(t)$ closely resembles the model signal $p(t)$. How should we choose $k(t)$ to make this work?

A commonly used approach is to let $k(t) = p(-t)$, the prototype pattern's reflection [30, 31]. Then $y(t) = (x * k)(t) = (x \circ p)(t)$, the correlation of $x(t)$ and $p(t)$. Since

$$\int_{-\infty}^{\infty}\int_{-\infty}^{\infty} (x(t) - p(t))^2\, dt = \int_{-\infty}^{\infty}\int_{-\infty}^{\infty} x^2(t)dt + \int_{-\infty}^{\infty}\int_{-\infty}^{\infty} p^2(t)dt - 2\int_{-\infty}^{\infty}\int_{-\infty}^{\infty} x(t)p(t)\, dt, \quad (3.74)$$

we see that minimizing the energy of the difference of $x(t)$ and $p(t)$ is equivalent to maximizing their inner product as long as the two signals have constant 2-norms. It is easy to do this for the prototype; we use the normalized signal $\tilde{p}(t) = p(t)/\|p\|_2$ as the model signal, for example. This step is called normalization, and so the method is often called *normalized cross-correlation*. If the entire candidate $x(t)$ is available at the moment of comparison, such as for signals acquired offline or as functions of a nontemporal independent variable, then we can similarly normalize $x(t)$ and compare it to $\tilde{p}(t)$. If, on the other hand, $x(t)$ is acquired in real time, then the feasible analysis works on past fragments of $x(t)$.

The Schwarz inequality tells us that equality exists if and only if the candidate and prototype are constant multiples of one another. If we subtract the mean of each signal before computing the normalized cross-correlation, then the normalized cross-correlation has unit magnitude if and only if the signals are related by $x(t) = Ap(t) + B$, for some constants A, B. Since $y(t) = (x * k)(t) = (x \circ p)(t)$ attains a maximum response when the prototype $p(t)$ matches the candidate $x(t)$, this technique is also known as matched filtering. It can be shown that in the presence of a random additive white noise signal, the optimal detector for a known pattern is still given by the matched filter [32].

Many signal and image processing applications depend upon matched filtering. In speech processing, one problem is to minimize the effect of reverberation from the walls and furnishings within a room on the recorded sound. This is an echo cancellation problem where there may be multiple microphones. The idea is to filter each microphone's input by the reflected impulse response of the room system [33].

Normalized cross correlation can be computationally demanding. When it is applied to images, this is especially the case. Consequently, many applications in image-based pattern matching use coarse resolution matched filtering to develop a set of likely match locations of the template against the input image. Then, finer resolution versions of the template and original image are compared [34]. Correlation techniques are also one of the cornerstones of image motion analysis [35].

3.3.3 Orthonormal Bases

In Chapter 2 a close relationship was established between general Hilbert spaces and the space of square-summable discrete signals. Here we list discuss four different orthogonal basis sets:

- Exponential signals of the form $\exp(jnt)$, where $n \in \mathbb{N}$
- Closely related sinusoids, which are the real and imaginary parts of the exponentials
- Haar basis, which consists of translations and dilations of a single, simple step function
- Sinc functions of the form $s_n(t) = \frac{1}{\sqrt{\pi}} \frac{\sin(At - n\pi)}{At - n\pi}$, where $A > 0$ and $n \in \mathbb{N}$

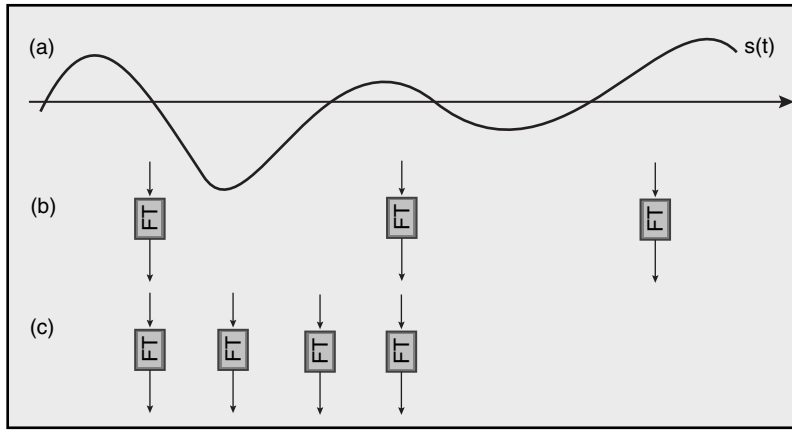

Fig. 3.5. Signal decomposition on an orthonormal basis (a). Sparse representations are better (b) than decompositions that spread signal energy across many different basis elements (c).

Orthonormal bases are fundamental signal identification tools. Given a signal $x(t)$, we project it onto the orthonormal basis set $\{e_n \mid n \in \mathbb{N}\}$ by taking the inner products $c_n = \langle x(t), e_n(t) \rangle$. Each c_n indicates the relative presence of the basis element e_n inside $x(t)$. The strategy is that—hopefully, at least—the set of coefficients $\{c_n \mid n \in \mathbb{N}\}$ is a simpler description of the original signal. If they are not, then we attempt to find an alternative basis set that better captures the character of anticipated input signals. We can say more, though. It works best for the signal recognition application if decomposition produces only a few significant c_n values for every typical $x(t)$ that we try to analyze. In other words, for the original signals $x(t)$ that we expect to feed into our analysis application, the energy of the decomposition coefficients is sparse and concentrated in a relative few values. On the other hand, dense decomposition coefficient sets make signal classification harder, because we cannot clearly distinguish which $e_n(t)$ factor most critically within $x(t)$. Figure 3.5 illustrates the idea. For signal identification, therefore, the upshot is that the statistics of the decomposition coefficients for typical system input signals are our guide for selecting an orthonormal basis set.

3.3.3.1 Exponentials. The most important basis for the L^2 Hilbert spaces is the exponential signals. We begin by considering the space $L^2[-\pi, \pi]$.

Let $\{e_n(t) \mid n \in \mathbb{N}\}$ be defined by $e_n(t) = (2\pi)^{-1/2}\exp(jnt)$. It can be easily shown that the $e_n(t)$ are indeed orthonormal (exercise). Similarly, if we set

$$e_n(t) = \frac{1}{\sqrt{b-a}} e^{2\pi jn\frac{t-a}{b-a}}, \tag{3.75}$$

then $B = \{e_n(t) \mid n \in \mathbb{N}\}$ is orthonormal in $L^2[a, b]$. We shall show in Chapter 5 that B is complete so that it is, in fact, a basis. Thus, for any square-integrable signal $x(t)$ on $[a, b]$ a linear combination of $\{e_n\}$ is arbitrarily close to $x(t)$; in other words,

$$x(t) = \sum_{n=-\infty}^{\infty} c_n e^{jnt} \tag{3.76}$$

for some constants $\{c_n \mid n \in \mathbb{N}\}$, called the Fourier series coefficients for $x(t)$. Note that c_n measures the similarity of $x(t)$ to the basis element $\exp(jnt)$: $\langle x(t), \exp(jnt)\rangle = c_n$ by orthonormality.

Now consider the case of $L^2(\mathbb{R})$. We can break up the real line into 2π-wide intervals $I_m = [(2m-1)\pi, (2m+1)\pi]$. Let X_m be the characteristic function on I_m, and set $e_{m,n}(t) = X_m(2\pi)^{-1/2}\exp(jnt)$. Then clearly $\{e_{m,n}(t) \mid m, n \in \mathbb{N}\}$ is an orthonormal basis for $L^2(\mathbb{R})$.

3.3.3.2 Sinusoids. There is an orthonormal basis for $L^2[-\pi, \pi]$ consisting entirely of sinusoids. Let us break up $e_n(t) = (2\pi)^{-1/2}\exp(jnt)$ into its real and imaginary parts using $\exp(jt) = \cos(t) = j\sin(t)$. We set $a_n = c_n + c_{-n}$ and $jb_n = c_{-n} - c_n$. Thus, (3.36) becomes

$$x(t) = \frac{a_0}{2} + \sum_{n=1}^{\infty} a_n \cos(nt) + \sum_{n=1} b_n \sin(nt), \tag{3.77}$$

and any $x(t) \in L^2[-\pi, \pi]$ can be expressed as a sum of sinusoids. Equation (3.77) shows that in addition to bona fide sinusoids on $[-\pi, \pi]$, we need one constant function to comprise a spanning set. That the sinusoids are also orthogonal follows from writing them in terms of exponentials:

$$\cos(t) = \frac{e^{jt} + e^{-jt}}{2} \tag{3.78a}$$

$$\sin(t) = \frac{e^{jt} - e^{-jt}}{2j} \tag{3.78b}$$

and using the orthonormality of the exponentials once more. As with exponentials, the sinusoids can be assembled interval-by-interval into an orthonormal basis for $L^2(\mathbb{R})$. The exercises further explore exponential and sinusoidal basis decomposition.

3.3.3.3 Haar Basis. The Haar[3] basis uses differences of shifted square pulses to form an orthonormal basis for square-integrable signals. It is a classic construction

[3]Hungarian mathematician Alfréd Haar (1885–1933) was Hilbert's graduate student at Göttingen. The results of his 1909 dissertation on orthogonal systems, including his famous basis set, were published a year later.

[36], dating from the early 1900s. It is also quite different in nature from the exponential and sinusoidal bases discussed above.

The sinusoidal basis elements consist of sinusoids whose frequencies are all integral multiples of one another—*harmonics*. As such, they all have different shapes. Thus, cos(t) follows one undulation on $[-\pi, \pi]$, and it looks like a shifted version of sin(t). Futhermore, $\cos(2t)$ and $\sin(2t)$ resemble one another as shapes, but they are certainly different from $\cos(t)$, $\sin(t)$, and any other basis elements of the form $\cos(nt)$ or $\sin(nt)$ where $n \neq 2$.

Haar's orthonormal family begins with a single step function, defined as follows:

$$h(t) = \begin{cases} 1 & \text{if } 0 \leq t < \frac{1}{2}, \\ -1 & \text{if } \frac{1}{2} \leq t \leq 1, \\ 0 & \text{if otherwise.} \end{cases} \tag{3.79}$$

Nowadays $h(t)$ is called a *Haar wavelet*. Haar's basis contains dilations and translations of this single atomic step function (Figure 3.6). Indeed, if we set $H = \{h_{m,n}(t) = 2^{n/2}h(2^n t - m) \mid m, n \in \mathbb{N}\}$, then we claim that H is an orthonormal basis for $L^2(\mathbb{R})$.

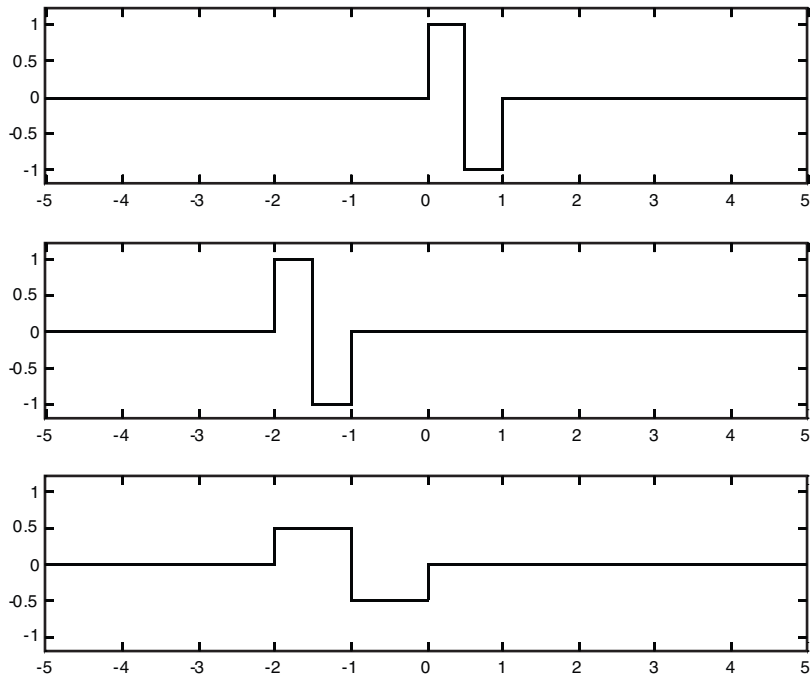

Fig. 3.6. Some examples of Haar basis elements.

Orthonormality is easy. If the supports of two unequal basis elements, $h_{m,n}(t)$ and $h_{p,q}(t)$, overlap, then we must have $n \neq q$; let us suppose $n > q$. Then the support of $h_{m,n}(t)$ will lie completely within one of the dyadic subintervals of Support $(h_{p,q}(t))$. The inner product must be zero: $\langle h_{m,n}(t), h_{p,q}(t) \rangle = 0$.

Completeness—that the closure of the span of $H = \{h_{m,n}(t) \mid m, n \in \mathbb{N}\}$ happens to be all of $L^2(\mathbb{R})$—is somewhat harder to show. Informally, any square-integrable signal can be approximated to arbitrary precision with a step function. Likewise, if we can approximate step functions with linear combinations of $\{h_{m,n}(t)\}$, then completeness follows. We first show that the unit square pulse, $s(t) = u(t-1) - u(t)$, is in Span(H). Indeed, one can check that for any $N \in \mathbb{N}$,

$$\sum_{n=-\infty}^{-1} 2^{\frac{n}{2}} h_{0,n}(t) = \begin{cases} 0 & \text{if } t \leq 0, \\ 1 & \text{if } 0 < t < 1, \\ 0 & \text{if } 2^N < t < 2^{N+1}. \end{cases} \tag{3.80}$$

So on all but a countably infinite set of points, the sum on the left-hand side of (3.80) is $s(t)$. When we study the Lebesgue integral, we shall see that these discontinuities do not affect the integral. Similarly, we can show that dyadic dilations and translations of $s(t)$ are in Span(H). Linear combinations of these dilations and translations can be arbitrarily close to a general step function, which justifies our completeness claim.

Practically, the importance of this is that it is good for finding one particular shape, which might manifest itself in different sizes or scales inside a signal. By contrast, the sinusoidal basis elements find various harmonics—distinct shapes—on the subintervals by which they divide the time domain. Of course, the elemental shape of the Haar basis is quite simple, but the basis elements are tuned to this shape at an infinite range of scales and an infinite set of positions. The two different types of basis in fact represent two different ways of analyzing signals. The sinusoidal and exponential bases find frequencies inside signals; they are *frequency-domain* tools for signal interpretation. The Haar basis finds a single atomic shape at different scales inside a signal, so it exemplifies *scale-domain* methods.

Recent books on wavelets [37, 38] cover Haar's basis. Until the mid-1980s, mathematicians believed that the only possible orthonormal bases for $L^2(\mathbb{R})$ which used dilations and translations of a single signal atom were those like Haar's construction where the atom has step discontinuities. The new wavelet theories, however, have completely toppled this long-standing conviction (Chapter 11).

3.3.3.4 Sinc Functions. Another important basis set consists of $\text{sinc}(t) = \sin(t)/t$ functions. In later chapters we shall have the tools in hand to show that the following family of functions is orthonormal: $\{s_n(t) \mid n \in \mathbb{N}\}$, where

$$s_n(t) = \frac{1}{\sqrt{\pi}} \frac{\sin(At - n\pi)}{At - n\pi} \tag{3.81}$$

and $A > 0$. We shall find that $\{s_n(t)\}$ defined in (3.81) spans an important Hilbert subspace of $L^2(\mathbb{R})$: a band-limited subspace that consists of signals whose spectral content lies entirely within a finite frequency range.

3.3.4 Frames

The concept of a frame generalizes the idea of an orthonormal basis in Hilbert space. Frame representations may be *overcomplete*. This means they may represent a signal in more than one way, and therefore they are not orthogonal. To understand why this might be useful and, indeed, why a signal analysis application based on frames can still be made workable, we have to reflect for a moment on the use of orthonormal bases for signal representation.

Many signal and image analysis applications need to recognize an unknown, candidate profile as an instance or combination of certain known prototypes. Probably the first approach that comes to mind is to decompose the candidate signal as a linear combination of the prototypical building blocks: $x(t) = \Sigma c_n e_n(t)$. The c_n represent the relative weight of each $e_n(t)$ in this linear signal combination. The application's desirable features are as follows:

(i) Incoming signals are uniquely represented by the coefficients $\langle x,\ e_n \rangle$; $x(t)$ does not have multiple identifying strings of weighting coefficients.
(ii) Two representations in terms of decomposition coefficients should permit a straightforward comparison of source signals for the differences between them.
(iii) Any original signal should be reconstructible from the stored coefficients; this is a completeness criterion.
(iv) Finally, the reconstruction of $x(t)$ from $\{c_n\}$ should be numerically stable; a small change in the coefficients results in a small change on the rebuilt signal.

These criteria suggest orthonormal bases. If we use an orthogonal set, such as the exponential functions $e_n(t) = e^{-jnt}$, then the four conditions hold in theory. The orthogonal character of the underlying special functions eases the computation of coefficients. However, a local change in the incoming signal leads to changes in the whole range of decomposition coefficients. Noise in signals, however sparse, drastically perturbs the stored digital form of the signal. This leads to practical difficulties in comparing two outwardly similar signals.

Sometimes, in an attempt to localize changes in signals to appropriate portions of the coefficient set, the decomposition functions are chosen to be windowed or "short-time" exponentials. These may take the form $e_{n,m}(t) = C_m e^{-jnt}$, where C_m is the characteristic function of the integral interval $[m,\ m + 1]$. The downfall of this tactic is that it adds high-frequency components to the decomposition. Relatively smooth signals decompose into sequences with unusually large coefficients for

large values of n. This problem can be ameliorated by choosing a smoother window function—a Gaussian instead of a square window, for example. This becomes a representation in terms of the Gabor elementary functions, which first chapter introduced. But a deeper problem with windowed exponentials arises. It turns out that one cannot construct an orthonormal basis out of Gaussian-windowed exponentials. Chapter 10 will cover this famous result, known as the Balian–Low theorem. Nonetheless, it is possible to make *frames* out Gabor elementary functions, and this is a prime reason for the technique's recent popularity.

Earlier, however, we noted that the statistics of the decomposition coefficients are an important consideration. Sparse sets are better than dense sets. We form vectors out of the decomposition coefficient sets of system input signals. The vectors comprise a library of signal models. Sparse decomposition coefficients imply short vectors, and short vectors mean that the library more succinctly represents the essential aspects of our signal models.

Unfortunately, it quite often happens that orthonormal bases produce nonsparse coefficient sets on fairly simple signals. For example, a decaying pulse signal, $x(t) = \exp(-At^2)\cos(Bt)$, contains a local frequency component set by the width of the Gaussian envelope. Now, $x(t)$ can be represented by the exponential or sinusoidal basis sets, but far from the origin there will always be large weighting coefficients. These distant, high-frequency sinusoidal wiggles have to cancel one another in order to correctly represent the negligible amplitude of $x(t)$ in their neighborhood. Libraries based on such orthonormal bases can also be problematic; when the signal changes a little bit, many decomposition coefficients must change globally to effect just the right weighting to cancel and reinforce the right signal components.

One surprising result from contemporary signal analysis research is that overcomplete representations—in particular, the frame decomposition that we cover here—can help in constructing sparse signal representations. Special techniques, such as the matching pursuit algorithm have been devised to cope with the overcompleteness [39, 40]. Originating in the 1950s [41, 42], frames are now widely used in connection with the recent development of the theory of time-frequency and time-scale transforms [38, 43].

First-time readers may skip this section. Visitors to the latest research literature on time-frequency and time-scale transform methods will, however, commonly encounter frame theoretic discussions. We shall cover frames more thoroughly in Chapters 10–12.

3.3.4.1 Definition and Basic Properties. This section defines the notion of a Hilbert space frame and provides some simple connections to the more specific and familiar concept of orthonormal basis. In what follows, we shall allow Hilbert spaces defined over the complex numbers.

Definition (Frame). Let $\{f_n: n \in \mathbb{Z}\}$ be signals in a Hilbert space H. If there are positive $A, B \in \mathbb{R}$ such that for all $x \in H$ we have

$$A\|x\|^2 \le \sum_{n=-\infty}^{\infty} \left|\langle x, f_n\rangle\right|^2 \le B\|x\|^2, \tag{3.82}$$

then the $\{f_n\}$ constitute a *frame* in H. The constants A and B are the *frame bounds*, *lower* and *upper*, respectively. The frame is *tight* if $A = B$. A frame is *exact* if it is no longer a frame following the deletion of a single element.

It is immediately clear that the frame condition (3.82) generalizes the idea of an orthonormal basis, makes the convergence unconditional, and ensures that a frame is a complete set (the closure of its linear span is all of H).

Proposition. Let $\{e_n: n \in \mathbb{Z}\}$ be an orthonormal basis for a Hilbert space H. Then $\{e_n\}$ is a tight exact frame having bounds $A = B = 1$.

Proof: Let $x \in H$. Parseval's relation for Hilbert spaces implies

$$\sum_{n=-\infty}^{\infty} \left|\langle x, e_n\rangle\right|^2 = \|x\|^2. \tag{3.83}$$

Therefore,

$$1 \cdot \|x\|^2 = \sum_{n=-\infty}^{\infty} \left|\langle x, e_n\rangle\right|^2 = 1 \cdot \|x\|^2, \tag{3.84}$$

which is precisely the frame condition (3.82), with $A = B = 1$. ■

Proposition (Unconditionality). Let $\{f_n : n \in \mathbb{Z}\}$ be a frame in a Hilbert space H. Then any rearrangement of the sequence $\{f_n\}$ is also a frame.

Proof: If $x \in H$, then $\{|\langle x, f_n\rangle|^2\}$ is a sequence of positive real numbers, and the convergence of the series

$$\sum_{n=-\infty}^{\infty} \left|\langle x, f_n\rangle\right|^2 \tag{3.85}$$

is absolute [6]. This means that the above sum converges to the same value under any rearrangement of the $\{f_n\}$. ■

Remark. Thus, we are free to renumber a frame with the natural numbers. Later, in Chapter 10, we shall find it convenient to use pairs of integers to index frame elements. This same idea is at work, as long as the index set has the same cardinality as the natural numbers.

Proposition (Completeness). Let $F = \{f_n : n \in \mathbb{Z}\}$ be a frame in a Hilbert space H. Then $\{f_n\}$ is a total set: $\overline{\text{Span}}\ \{f_n\} = H$.

Proof: Let $x \in H$, $\langle x, f_n \rangle = 0$ for all n, and $A > 0$ be the lower frame bound for F. By the definition of a frame,

$$0 \le A\|x\|^2 \le \sum_{n=-\infty}^{\infty} \left|\langle x, f_n \rangle\right|^2 = 0. \tag{3.86}$$

Equation (3.86) shows that $x = 0$. Since a subset X of H is complete if and only if no nonzero element is orthogonal to all elements of X, it must be the case that F is total in H. ■

3.3.4.2 Examples. In the following examples, H is a Hilbert space, and $\{e_n: n \in \mathbb{N}\}$ is an orthonormal basis in H.

Example (Overcompleteness). Let $F = \{f_n\} = \{e_0, e_0, e_1, e_1, e_2, e_2, ...\}$. Then F is a tight frame with bounds $A = B = 2$. Of course, it is not an orthonormal basis, although the subsequence $\{f_{2n}: n \in \mathbb{N}\}$ is orthonormal. It is also not exact. Elements of H have multiple decompositions over the frame elements.

Example (Orthogonal, Yet Not a Frame). $F = \{f_n\} = \{e_0, e_1/2, e_2/3, ...\}$ is complete and orthogonal. However, it is not a frame, because it can have no positive lower frame bound. To see this, assume instead that F is a frame and let $A > 0$ be its lower bound. Let N be large enough that $N^{-2} < A$ and set $x = e_N$. Then, (3.82) gives

$$A = A\|x\|^2 \le \sum_n \left|\langle x, f_n \rangle\right|^2 = \left|\langle e_N, f_N \rangle\right|^2 = \frac{1}{N^2} < A, \tag{3.87}$$

a contradiction.

Example (Tight Frame). $F = \{f_n\} = \{e_0, 2^{-1/2}e_1, 2^{-1/2}e_1, 3^{-1/2}e_2, 3^{-1/2}e_2, 3^{-1/2}e_2, ...\}$ is a tight frame with bounds $A = B = 1$. F is not exact.

Example (Exact But Not Tight). $F = \{f_n\} = \{2e_0, e_1, e_2, ...\}$ is a frame, with lower bound $A = 1$ and upper bound $B = 2$. F is exact but not tight.

3.3.4.3 Frame Operator. There is a natural bounded linear operator associated with a frame. In fact, if the decomposition set is a frame, then the basic signal analysis system that associates signals in a Hilbert space with their decomposition coefficients is just such an operator. This section gives their definition and properties. While they are mathematically elegant and abstract, frame operators also factor critically in using overcomplete frames in signal representation.

Definition (Frame Operator). If $F = \{f_n(t): m, n \in \mathbb{Z}\}$ is a frame in a Hilbert space H, then the associated frame operator $T_F: H \to l^2(\mathbb{Z})$ is defined by

$$T_F(x)(n) = \langle x, f_n \rangle. \tag{3.88}$$

In other words, $y = T_F(x) = T_F x$ is the complex-valued function defined on the integers such that $y(n) = \langle x, f_n \rangle$. When the frame is clear by the context we may drop the subscript on the frame operator: $y = Tx$.

Proposition. If $F = \{f_n(t): n \in \mathbb{Z}\}$ is a frame in a Hilbert space H, then the associated frame operator T given by (3.88) is linear and bounded. Furthermore, if B is the upper frame bound, then $\|T\| \leq B^{1/2}$.

Proof: Linearity is clear from inner product properties. If $x \in H$, then

$$\|Tx\| = \left(\sum_n \langle x, x_n \rangle \overline{\langle x, x_n \rangle} \right)^{\frac{1}{2}} = \left(\sum_n \left| \langle x, x_n \rangle \right|^2 \right)^{\frac{1}{2}} \leq \left(B \|x\|^2 \right)^{\frac{1}{2}} = B^{\frac{1}{2}} \|x\| . \tag{3.89}$$

■

Definition (Adjoint Frame Operator). Let $F = \{f_n(t) : n \in \mathbb{Z}\}$ be a frame in a Hilbert space H and let T be its associated frame operator T (3.88). The *adjoint frame operator* $S : l^2(\mathbb{Z}) \to H$ is defined for $y(n) \in l^2(\mathbb{Z})$ by

$$S(y) = \sum_{n=-\infty}^{\infty} y(n) f_n. \tag{3.90}$$

Proposition. Let S be given by (3.90). Then S is the Hilbert adjoint operator with respect to frame operator T of F: $S = T^*$.

Proof: That S is linear is left as an exercise. Let $x \in H$, T the frame operator for $F = \{f_n(t) : n \in \mathbb{Z}\}$, and let $y = \{y_n : n \in \mathbb{Z}\}$ be some sequence in l^2. Then

$$\langle x, Sy \rangle = \left\langle x, \sum_n y_n x_n \right\rangle = \sum_n \overline{y_n} \langle x, x_n \rangle, \tag{3.91}$$

and also

$$\langle Tx, y \rangle = \sum_n \langle x, x_n \rangle \overline{y_n} = \sum_n \overline{y_n} \langle x, x_n \rangle . \tag{3.92}$$

Together, (3.91) and (3.92) show that T and S cross-couple the inner products of the two Hilbert spaces. Therefore, $S = T^*$. ■

The next theorem, one of the classic results on frames and frame operators, offers a characterization of frames [41]. It uses the idea of a positive operator. Recall that an operator T on a Hilbert space H is *positive*, written $T \geq 0$, when $\langle Tx, x \rangle \geq 0$ for all $x \in H$. Also, if S and T are operators on H, then $T \geq S$ means that $T - S \geq 0$. Positive operators are self-adjoint [26, 29].

Theorem (Frame Characterization). Let $F = \{f_n : n \in \mathbb{Z}\}$ be a sequence in a Hilbert space H; $A, B > 0$; and let I be the identity operator on H. Then F is a frame with lower and upper bounds A and B, respectively, if and only if the operator S defined by

$$Sx = \sum_n \langle x, f_n \rangle f_n \tag{3.93}$$

is a bounded linear operator with

$$AI \le S \le BI\,. \tag{3.94}$$

Proof: Assume that (3.93) defines S and (3.94) holds. By the definition of $\le$ for operators, for all $x \in H$ (3.94) implies

$$\langle AIx, x\rangle \le \langle Sx, x\rangle \le \langle BIx, x\rangle\,. \tag{3.95}$$

However,

$$\langle AIx, x\rangle \;=\; A\|x\|^2 \tag{3.96a}$$

and

$$\langle BIx, x\rangle \;=\; B\|x\|^2\,. \tag{3.96b}$$

The middle term of (3.95) is

$$\langle Sx, x\rangle \;=\; \left\langle \sum_n \langle x, f_n\rangle f_n, x\right\rangle \;=\; \sum_n \langle x, f_n\rangle\,\overline{\langle f_n, x\rangle} \;=\; \sum_n \left|\langle x, f_n\rangle\right|^2. \tag{3.97}$$

Together (3.96a), (3.96b), and (3.97) can be inserted into (3.95) to show that the frame condition is satisfied for F.

Conversely, suppose that F is a frame. We must first show that S is well-defined—that is, the series (3.93) converges. Now, the Schwarz inequality implies that the norm of any $z \in H$ is $\sup\{|\langle z, y\rangle| : y \in H \text{ and } \|y\| = 1\}$. Let s_N represent partial sums of the series (3.93):

$$s_N(x) \;=\; \sum_{n\,=\,-N}^{N} \langle x, f_n\rangle f_n\,. \tag{3.98}$$

When $M \le N$ the Schwarz inequality applies again:

$$\|s_N - s_M\|^2 \;=\; \sup_{\|y\|\,=\,1}\left\{\left|\langle s_N - s_M, y\rangle\right|^2\right\} \;=\; \sup_{\|y\|\,=\,1}\left\{\left|\sum_{n\,=\,M+1}^{N} \langle x, f_n\rangle\,\langle f_n, y\rangle\right|^2\right\}. \tag{3.99}$$

Algebra on the last term above gives

$$\|s_N - s_M\|^2 \le \sup_{\|y\|\,=\,1}\left\{\sum_{n\,=\,M+1}^{N} \left|\langle x, f_n\rangle\right|^2 \sum_{n\,=\,M+1}^{N} \left|\langle f_n, y\rangle\right|^2\right\}. \tag{3.100}$$

By the frame condition,

$$\|s_N - s_M\|^2 \le \sup_{\|y\|\,=\,1} \sum_{n\,=\,M+1}^{N} \left|\langle x, f_n\rangle\right|^2 B\|y\|^2 = B \sum_{n\,=\,M+1}^{N} \left|\langle x, f_n\rangle\right|^2, \tag{3.101}$$

and the final term in (3.101) must approach zero as $M, N \to \infty$. This shows that the sequence $\{s_N \mid N \in \mathbb{N}\}$ is Cauchy in the Hilbert space H. H is complete, so the $\{s_N\}$ converge, the series must converge, and the operator S is well-defined.

Similarly,

$$\|Sx\|^2 \leq \sup_{\|y\| = 1} |\langle Sx, y\rangle|^2, \tag{3.102}$$

which entails $\|S\| \leq B$. From the frame condition and (3.93) the operator ordering, $AI \leq S \leq BI$ follows immediately. ■

Remark. Notice that for a frame $F = \{f_n : n \in \mathbb{Z}\}$ the theorem's operator S is the composite T^*T, where T is the frame operator and T^* is its adjoint. The following corollaries provides further properties of T^*T.

Corollary. Let $F = \{f_n : n \in \mathbb{Z}\}$ be a frame in a Hilbert space H and let T be the frame operator. Then the map $S = T^*T : L^2(\mathbb{R}) \to L^2(\mathbb{R})$ given by

$$(T^*T)(x) = \sum_{n=-\infty}^{\infty} \langle x, f_n\rangle f_n. \tag{3.103}$$

is positive and invertible.

Proof: Let A be the lower frame bound for F. Since $AI \leq S$, $S - AI \geq 0$, by the definition of the operator ordering relation. Also, since $A > 0$, $S/A - I \geq 0$. A property of positive operators is that if an operator, say U, is positive, $U \geq 0$, then $U + I$ is invertible [27]. Therefore, $S/A - I + I = S/A$ is invertible. Clearly then, S is invertible. Moreover, adding a positive operator I to $S/A - I$ still gives a positive operator. This shows that S is indeed positive. ■

Corollary. Let $F = \{f_n : n \in \mathbb{Z}\}$ be a frame in a Hilbert space H; let A and B be the lower and upper frame bounds, respectively, for F; let T be the frame operator; and let $S = T^*T$ be given by the previous corollary. Then $I/B \leq S^{-1} \leq I/A$.

Proof: The previous corollary shows that S^{-1} exists. Since S^{-1} commutes with I and with S, and since $AI \leq S \leq BI$, it follows that $S^{-1}AI \leq S^{-1}S \leq S^{-1}BI$. Upon rearrangment, this yields $B^{-1}I \leq S^{-1} \leq A^{-1}I$. ■

These results allow us to define the concept of the dual frame. The dual frame is the key concept for applying frames in signal analysis applications.

Definition (Dual Frame). Let $F = \{f_n : n \in \mathbb{Z}\}$ be a frame in a Hilbert space H and T be the frame operator. We define the *dual frame* to F by applying the inverse of T^*T to frame elements:

$$\tilde{F} = \left\{ (T^*T)^{-1}(f_n) \right\}_{n \in Z}. \tag{3.104}$$

Corollary. Let $F = \{f_n: n \in \mathrm{Z}\}$ be a frame in a Hilbert space H; let A and B the lower and upper frame bounds, respectively, for F; let T be the frame operator; and let $S = T^*T$. Then the sequence $\{S^{-1}f_n \mid n \in \mathbb{Z}\}$ in H is a frame with lower bound B^{-1} and upper bound A^{-1}.

Proof: S^{-1} exists and is positive. Let $x \in H$ and note that

$$S^{-1}x = S^{-1}(SS^{-1}x) = S^{-1}\left(\sum_n \langle S^{-1}x, f_n\rangle f_n\right) = \sum_n \langle S^{-1}x, f_n\rangle S^{-1}f_n \tag{3.105}$$

by the linearity and continuity of S^{-1}. Since every positive operator is self-adjoint (Hermitian) [29], S^{-1} is self-adjoint. Hence,

$$S^{-1}x = \sum_n \langle S^{-1}x, f_n\rangle S^{-1}f_n = \sum_n \langle x, S^{-1}f_n\rangle S^{-1}f_n\,. \tag{3.106}$$

Notice that (3.106) is precisely the form that the operator S^{-1} takes in (3.93) of the frame characterization theorem. That $B^{-1}I \le S^{-1} \le A^{-1}I$ follows from an earlier corollary. Thus, the theorem's condition applies, and $\{S^{-1}f_n\}$ is a frame in H. ■

Corollary. Under the assumptions of the previous corollary, any $x \in H$ can be written

$$x = \sum_n \langle x, S^{-1}f_n\rangle f_n = \sum_n \langle x, f_n\rangle S^{-1}f_n. \tag{3.107}$$

Proof: Using (3.105), (3.106), and $x = SS^{-1}x = S^{-1}Sx$, the result follows easily. ■

Corollary. Further assuming that the frame T is tight, we have $S = AI$, $S^{-1} = A^{-1}I$, and, if $x \in H$, then

$$x = A^{-1}\sum_n \langle x, f_n\rangle f_n. \tag{3.108}$$

Proof: Clear from the definition of tightness and the preceding corollaries. ■

3.3.4.4 Application: Stable Modeling and Characterization. These results shed light on our proposed requirements for a typical signal analysis system. Let us list what we know so far:

- The first requirement—that the representation be unique—was demonstrated not to hold for general frames by an easy counterexample.
- The second specification—that signal representations should permit a straightforward comparison of two incoming signals—is satisfied by the frame operator that maps signals to sequences of complex numbers allowing us to use the l^2 norm for comparing signals.

- The corollary (3.107) fulfills the requirement that the original signal should be reconstructible from the decomposition coefficients.
- The fourth requirement has been left rather vague: What does numerical instability mean?

We can understand numerical instability in terms of bounded operators. Let $F = \{f_n\}$ be a frame and $T = T_F$ its frame operator. If the inverse mapping T^{-1} is unbounded, then elements of l^2 of unit norm will be mapped back to elements of H having arbitrarily large norms. This is not at all desirable; signals of enormous power as well as signals of miniscule power will map to decomposition coefficients of small l^2-norm. *This is numerical instability.* The next result shows that frame-based signal decomposition realizes the fourth requirement of a signal analysis system.

Corollary. Let $F = \{f_n : n \in \mathbb{Z}\}$ be a frame in a Hilbert space H and let $T = T_F$ be the associated frame operator. Then the inverse T^{-1} exists and is bounded.

Proof: Let $S = T^*T$, as in the previous section. Then S^{-1} exists and $S^{-1}T^* = T^{-1}$ is the bounded inverse of T. Alternatively, (3.107) explicitly maps a square-summable sequence in $\mathbb{C}$ to H, and it inverts T. A straightforward calculation shows that the map is bounded with $\|T^{-1}\| \leq A^{-1/2}$. ■

Remarks. So the use of a frame decomposition for the signal analysis system allows a *stable reconstruction* of incoming signals from the coefficients obtained previously. In the case that the frame used in the signal processing system is tight, then the reconstruction is much simpler (3.108). We can reconstruct a signal from its decomposition coefficients using (3.108) alone; there is no need to invert $S = T^*T$ to get $S^{-1}f_n$ values.

We have substantiated all of the basic requirements of a signal analysis system, except for the first stipulation—that the coefficients of the decomposition be unique. The exercises elaborate some properties of exact frames that allow us to recover this uniqueness property. Briefly, if $F = \{f_n(t) : n \in \mathbb{Z}\}$ is a frame in a Hilbert space H, $T = T_F$ is its associated frame operator (3.88), and $S = T^*T$, then we know from the corollaries to the frame representation theorem that for any $x \in H$, if $a_n = \langle x, S^{-1}f_n \rangle$, then $x = \Sigma a_n f_n$. We can also show (exercises) that if there is some other representation of x, then it is no better than the the one we give in terms of the dual frame. That is, if there are $c_n \in C$ such that $x = \Sigma c_n f_n$, then

$$\sum_n |c_n|^2 = \sum_n |a_n|^2 + \sum_n |a_n - c_n|^2 ; \tag{3.109}$$

the representation by dual frame elements is the best in a least-squares sense. Later chapters (10–12) further cover frame representations and elaborate upon this idea.

To sum up. We began by listing the desired features of a signal analysis system. The notion of a frame can serve as a mathematical foundation for the decomposition, analysis, and reconstruction of signals. Orthonormal bases have very nice computational properties, but their application is often confounded by an undesirable

practicality: The representations may well not be sparse. Frame theoretic approaches are a noteworthy alternative trend in recent signal analysis research, offering improved representation density over orthonormal bases [39, 40, 43].

3.4 MODERN INTEGRATION THEORY

The Lebesgue integral offers several theoretical advantages over the Riemann integral. The modern integral allows us to define Banach spaces directly, rather than in terms of the completion of a simpler space based on continuous analog signals. Also, the Lebesgue integral widens considerably the class of functions for which we can develop signal theory. It supports a powerful set of limit operations. Practically speaking, this means that we can develop powerful signal approximation techniques where signal and error magnitudes are based upon Lebesgue integrals (here we have in mind, of course, the L^p-norm).

This material has not been traditionally included in the university engineering and science curricula. Until recently, these disciplines could get along quite well without the mathematician's full toolkit. Mixed domain transform methods, Gabor and wavelet transforms in particular, have entered into widespread use in signal processing and analysis in the last several years. And carried with them has been an increased need for ideas from abstract functional analysis, Hilbert space techniques, and their mathematical underpinnings, among them the Lebesgue integral.

First-time readers and those who are content to build Banach spaces indirectly, by completing a given normed linear space, may elect to skip the material on the modern integral. Frankly, much of the sequel will still be quite understandable. Occasionally, we may worry that a signal is nonzero, but has Lebesgue integral zero; the mathematical term is that the signal is zero *almost everywhere* on an interval $[a, b]$. This is the standard, albeit homely, term for a function with so many zero points that its L^1-norm with respect to the Lebesgue integral is zero. We also say two signals are *equal almost everywhere* when their difference is zero almost everywhere.

Standard mathematical analysis texts cover measure and integration theory in far more detail and generality than we need here [24, 44, 45]. A tutorial is contained in Ref. 25. We cover the basic theoretical development only in these settings: measures on subsets of the real line and complex plane, real- and complex-valued functions, and their integrals. So restricted, this treatment follows the classic approach of Ref. 44.

Calculus defines the Riemann[4] integral as a limit of sums of areas of rectangles [6, 25]. Another approach uses trapezoids instead of rectangles; it offers somewhat

[4]Georg Friedrich Bernhard Riemann (1826–1866) studied under a number of great German mathematicians of the nineteenth century, including Gauss and Dirichlet. In 1857 he assumed a professorship at Göttingen. He contributed important results to complex variable theory, within which the Cauchy–Riemann equations are fundamental, and to non-Euclidean geometries, whose Riemannian manifolds Einstein much later appropriated for modern cosmology. Riemann is most widely known, ironically perhaps, for a relatively minor accomplishment—formalizing the definition of the conventional integral from calculus [R. Dedekind, Biography of Riemann, in H. Weber, ed., *Collected Works of Bernhard Riemann*, New York: Dover, 1953].

better numerical convergence. Either approach produces the same result. For rectangular sums, let us recall the definition.

Definition (Riemann Integral). Let $x(t)$ be continuous on the interval $I = [a, b]$; $a = t_0 < t_1 < \cdots < t_N = b$ partition I; and, for each subinterval, $I_k = [t_k, t_{k+1}]$, let r_k and s_k be the minimum and maximum values, respectively, of $x(t)$ on I_k. Then the lower and upper Riemann sums for $x(t)$ and I are

$$R_{x,I} = \sum_{k=1}^{N} r_k(t_k - t_{k-1}). \tag{3.110a}$$

$$S_{x,I} = \sum_{k=1}^{N} s_k(t_k - t_{k-1}). \tag{3.110b}$$

The Riemann integral is defined by

$$\int_a^b x(t)\, dt = \lim_{\Delta_I \to 0} R_{x,I}, \tag{3.110c}$$

where $\Delta_I = \max\{t_k - t_{k-1} \mid k = 1, 2, \cdots, N\}$.

Calculus proves that limit (3.110c) remains the same whether we use upper or lower Riemann sums. The height of the rectangle may indeed be the function value at any point within the domain interval. We have chosen to define the Riemann integral using the extreme cases, because, in fact, the modern Lebesgue integral uses sums from below similar to (3.110c).

The base of the rectangle or trapezoid is, of course, an interval. So the Riemann integral partitions the function *domain* and lets that partition determine the range values used for computing little areas. The insight of modern integration is this: Partition the *range*, not the domain, and then look at the sets in the function's domain that it maps to the range regions. There is a way to measure the area of these domain sets (next section), and then their area is weighted by the range values in much the same way as the Riemann integral. The difference seems simple. The difference seems inconsequential. But the implications are enormous.

3.4.1 Measure Theory

The standard approach to the Lebesgue integral is to develop a preliminary theory of the *measure* of a set. This generalizes the notion of simple interval length to a much wider class of sets. Although the Lebesgue integral can be defined without first building a foundation in measure theory (cf. Refs. 13 and 25), the idea of a measure is not difficult. Just as the Riemann integral is a limit of sums of areas,

which are interval widths wide and function values high, the Lebesgue integral is a limit of sums of weighted measures—set measures scaled by function values.

Measurable sets, however, can be much more intricate than simple intervals. For example, the rational numbers $\mathbb{Q}$ is a measurable set, and its measure, or its *area* if you will, is zero. Furthermore, any countable set (i.e., a set that can be put into a one–one correspondence with the natural numbers $\mathbb{N}$) is measurable and has zero measure. The interval [0, 1] has unit measure, which is no doubt reassuring, and if we remove all the rational points from it, obtaining $[0, 1] \setminus \mathbb{Q}$, then the result is still measurable and still has unit measure. The rest of this section sketches the developments upon which these appealing ideas can be justified.

3.4.1.1 Rudiments of the Theory. Measure theory axiomatics are closely related to the ideas of a probability measure, which we covered in Chapter 1. We recall therefrom the concept of a σ-algebra Σ. These can be defined for abstract spaces, but we shall stick to sets of real or complex numbers, since these are the spaces for which we define analog signals. Let $\mathbb{K}$ be either $\mathbb{R}$ or $\mathbb{C}$. The four properties of Σ are:

(i) Elements of Σ are subsets of $\mathbb{R}$ (or $\mathbb{C}$): $\wp(\mathbb{K}) \supset \Sigma$.
(ii) The entire space is in Σ: $\mathbb{K} \in \Sigma$.
(iii) Closure under complement: If $A \in \Sigma$, then $\overline{A} = \{t \in \mathbb{K} \mid t \notin A\} \in \Sigma$.
(iv) Closure under countable union: If $\Sigma \supset \{A_n \mid n \in \mathbb{N}\}$, then $\bigcup_{n \in \mathrm{N}} A_n \in \Sigma$.

Examples. A couple of extreme examples of σ-algebras are as follows:

- $\Sigma_1 = \wp(\mathbb{R})$, the set of all subsets of $\mathbb{R}$.
- $\Sigma_0 = \{\varnothing, \mathbb{R}\}$.

There are equivalent examples for $\mathbb{C}$. We have a more interesting σ-algebra in mind, the Borel sets, and we will cover this class momentarily. Combining the closure under countable unions and complement rules, we can show (exercise) that σ-algebras are closed under countable intersections. Two basic concepts are that of a *measurable function*, which we interpret as a measurable signal, and of a *measure* itself, which is a map from a σ-algebra to the non-negative reals.

Definition (Measurable Function). A real- or complex-valued function $x(t)$ is measurable with respect to a σ-algebra Σ if $x^{-1}(A) = \{t \in \mathrm{R} \mid x(t) \in A\} \in \Sigma$ for all open sets A in $\mathbb{K}$.

Proposition. Let Σ be a σ-algebra and let $x : \mathbb{R} \to \mathbb{K}$ be a real- or complex-valued function. Let $\Theta = \{T \in \wp(\mathbb{K}) \mid x^{-1}(T) \in \Sigma\}$. Then Θ is a σ-algebra in $\mathbb{K}$.

Proof: Clearly, $\emptyset$ and $\mathbb{K} \in \Theta$. If $T \in \Theta$, then $S = x^{-1}(T) \in \Sigma$ and $\mathbb{R} \setminus S \in \Sigma$. But $\overline{T} = x(\mathbb{R} \setminus S)$, so $\mathbb{T} \in \Theta$. Finally, $x^{-1}(\cup_{n \in \mathbb{N}} T_n) = \cup_{n \in N} x^{-1}(T_n)$, so closure under countable unions holds as well. ■

The properties of a measure and limit theorems for the modern integral depend on an extension of the real numbers to include two infinite values: ∞ and $-\infty$. Formally, these are just symbols. Intuitively, however, ∞ is an abstract positive value that is larger than any than any real number and $-\infty$ is an abstract negative value that has larger magnitude than any real number. Let us first consider ∞. This value's arithmetic operations are limited. For example, $r + \infty = \infty$ for any $r \in$ R; $r \times \infty = \infty$ for any $r > 0$; if $r = 0$, then $r \times \infty = 0$; and addition and multiplication with ∞ are commutative. There is also a negative infinity element, $-\infty$, so that $r + (-\infty) = -\infty$ for any $r \in \mathbb{R}$. Furthermore, $r \times (-\infty) = -\infty$ for any $r > 0$; if $r = 0$, then $r \times (-\infty) = 0$; if $r < 0$, then $r \times \infty = -\infty$; and so on.

Note that subtraction, division, and cancellation operations only work with finite values. That is, $r - s$ is not defined if both r and s are infinite, and a similar restriction applies to r/s. If $rs = rt$, then we can conclude $s = t$ only if r is finite. A similar restriction applies to $r + s = r + t$.

We can also consider the extended real line, $\mathbb{R}^+ = \mathbb{R} \cup \{\infty\} \cup \{-\infty\}$. We consider $\mathbb{R}^+$ as having the additional open sets $(r, \infty]$ and $[-\infty, r)$ for any finite $r \in \mathbb{R}$. Of course, countable unions of open sets are open in the extended reals. Analog signals can be extended so that they take on infinite values at their singularities. Thus, a signal like $x(t) = t^{-2}$ is undefined at $t = 0$. In the extended reals, however, we may set $x(0) = \infty$. This makes the later limit theorems on modern integration (Section 3.4.3) into equalities. Note that we do not use the extended reals as the domain for analog signals. We only use the extension $\mathbb{R} \cup \{\infty\} \cup \{-\infty\}$ for defining the idea of a measure on σ-algebras and for extending the range of analog signals.

Definition (Measure). A *measure* on a σ-algebra Σ is a function $\mu : \Sigma \to [0, \infty]$ such that

$$\mu\left(\bigcup_{n=-\infty}^{\infty} A_n\right) = \sum_{n=-\infty}^{\infty} \mu(A_n) \tag{3.111}$$

whenever $\{A_n\}$ are pairwise disjoint.

Thus a measure is just like a probability measure, except that its values range in $[0, \infty]$ rather than in $[0, 1]$. A measure function gives a size value for a set. Thus, the measure might indicate the relative size of part of a signal's domain. We are also limiting the discussion to the real line, even though the ideas generalize to measures on σ-algebras in abstract metric spaces. Real analysis texts formalize these notions [24, 44, 45], but we prefer to limit the scope to just what we need for analog signal theory. Here are some easy examples.

Example (All or Nothing Measure). Let $\Sigma = \wp(\mathbb{R})$, and for $A \in \Sigma$ define $\mu(\varnothing) = 0$ and $\mu(A) = \infty$ if $A \neq \varnothing$. Then μ is a measure on Σ.

Example (Counting Measure). Again let $\Sigma = \wp(\mathbb{R})$, and for $A \in \Sigma$ define $\mu(A) = N$ if A contains exactly N elements and $\mu(A) = \infty$ otherwise. Then μ is a measure on Σ.

Proposition. Let μ be a measure on the σ-algebra Σ. Then

(i) (*Null set*) $\mu(\varnothing) = 0$.
(ii) (*Additivity*) If $A_p \cap A_q = \varnothing$ when $p \neq q$, then $\mu(A_1 \cup A_2 \cup \cdots \cup A_n) = \mu(A_1) + \mu(A_2) + \cdots + \mu(A_n)$.
(iii) (*Monotonicity*) If $B \supset A$, then $\mu(B) \geq \mu(A)$.

Proof: Similar to probability measure arguments. ■

3.4.1.2 Lebesgue Measurable Sets. There are lots of σ-algebras on the real line. Analog signal theory needs only the smallest σ-algebra that contains all the open sets in $\mathbb{R}$. We must show that such a smallest σ-algebra exists.

Theorem. There is a σ-algebra $\mathcal{B}$ on $\mathbb{R}$ such that:

(i) $\mathcal{B}$ contains all open subsets of $\mathbb{R}$.
(ii) If Σ is a σ-algebra containing all the open sets, then $\Sigma \supset \mathcal{B}$.

Proof: To begin with, the power set on the real line, $\wp(\mathbb{R})$, is itself is a σ-algebra and contains all open sets. Nonconstructively, we set $\mathcal{B}$ to be the intersection of all such σ-algebras. It is straightforward to show that this intersection is still a σ-algera. It is still a subset of $\wp(\mathbb{R})$. Since $\mathbb{R}$ must be in every σ-algebra, it is must be in the intersection of those containing the open sets. Closure under complement is also easy: if $A \in \Sigma$, where Σ is a any σ-algebra containing the open sets, then $\overline{A} \in \Sigma$; thus, $\overline{A}$ is in the intersection of all such σ-algebras. Finally, let $\mathcal{B} \supset \{A_n \mid n \in \mathbb{N}\}$. Then for all $n \in \mathbb{N}$, A_n is in every σ-algebra Σ that contains all the open sets in $\mathbb{R}$. Thus the countable family $\{A_n\}$ is a subset of every such σ-algebra. Hence $\bigcup_{n \in \mathrm{N}} A_n$ is in each of these σ-algebras; and, consequently, $\bigcup_{n \in \mathrm{N}} A_n$ is in the intersection $\mathcal{B}$. ■

Definition (Borel sets). The class of *Borel* or *Lebesgue measurable* sets is the smallest σ-algebra that contains every open set.

All the sets we normally use in signal theory are Borel sets. In fact, it takes a certain amount of craftiness to exhibit a set that is not Lebesgue measurable.

Example (Intervals). All of the open and closed sets, and the intervals (a, b) and $[a, b]$ in particular, are Lebesgue measurable. That closed sets are measurable follows from the σ-algebra's complement property. Also, since we take the half-infinite intervals $(a, \infty]$ and $[-\infty, a)$ to be open, these too are measurable. Finally, we can form countable unions involving these basic measurable sets. In the complex plane, open disks $\{z: |z| < r\}$, and closed disks $\{z: |z| \leq r\}$ are measurable as are half-infinite sets $\{z: |z| > r\}$, and so on.

Example (Countable Sets). Any countable set is measurable. For example, real singletons $\{a\}$ are measurable because they are closed. So any countable union of singletons is measurable.

Proposition. If $x(t)$ is measurable and T is a Lebesgue measurable set in $\mathbb{K}$ ($\mathbb{R}$ or $\mathbb{C}$), then $x^{-1}(T) \in \mathcal{B}$; in other words, $x^{-1}(T)$ is Lebesgue measurable in $\mathbb{R}$.

Proof: Let $\Theta = \{T \in \wp(\mathbb{K}) \mid x^{-1}(T) \in \mathcal{B}\}$. Since $x(t)$ is measurable, Θ contains all the open sets in $\mathbb{K}$. In the previous section, we showed that Θ is a σ-algebra, so it must contain all the Lebesgue measurable sets. ■

3.4.1.3 Lebesgue Measure.

There are lots of possible measures on σ-algebras in $\mathbb{R}$ (or $\mathbb{C}$). Again, we need only one of them: the *Lebesgue measure*. It applies to the Lebesgue measurable, or Borel sets.

Definition (Open Covering). Let S be a set and $O = \{A_n \mid n \in \mathbb{N}\}$ be a family of open sets. If $S \subset \bigcup_{n \in \mathrm{N}} A_n$, then O is an *open covering* for S.

Definition (Real Lebesgue Measure). Let $\mathcal{B}$ be the Lebesgue measurable sets on $\mathbb{R}$ and let the measure function μ be defined as follows:

(i) $\mu(a, b) = b - a$.

(ii) If S is an open set in R, then

$$\mu(S) = \inf_{S \subset \bigcup A_n} \left[\sum_{n=0}^{\infty} \mu(A_n) \right], \tag{3.112}$$

where the greatest lower bound is taken over all open coverings of S by intervals. The function μ is called the (real) *Lebesgue measure*.

Definition (Complex Lebesgue Measure). Let $\mathcal{B}$ be the Lebesgue measurable sets on $\mathbb{C}$. Let the measure function μ be defined as follows:

(i) If $B = \{z \in \mathbb{C} \mid |z - c| < r\}$, then $\mu(B) = \pi r^2$.

(ii) If S is an open set in $\mathbb{C}$, then

$$\mu(S) = \inf_{S \subset \bigcup B_n} \left[\sum_{n=0}^{\infty} \mu(B_n) \right], \tag{3.113}$$

where the greatest lower bound is taken over all open coverings of S by open balls. The function μ is called the (complex) *Lebesgue measure*.

Accepting that these definitions do produce functions that are indeed measures on the Borel sets, let us provide some examples of the measures of sets.

Example (Singletons). The measure of a singleton $\{a\}$ is zero. Let $\varepsilon > 0$. Then the single interval $I_\varepsilon = (a - \varepsilon, a + \varepsilon)$ covers $\{a\}$. The Lebesgue measure of I_ε is 2ε. Since ε was arbitrary and positive, the greatest lower bound of the lengths of all such intervals cannot be positive, so $\mu\{a\} = 0$.

Example (Intervals). The measure of a half-open interval $[a, b)$ is $b - a$. The measure of (a, b) is $b - a$, and the singleton $\{a\}$ has measure zero. Because (a, b) and $\{a\}$ are disjoint, $\mu(a, b) + \mu\{a\} = \mu[a, b) = b - a$. We also have $\mu(a, \infty] = \infty$; this is a consequence of the monotonicity property of a measure, since there are infinitely many disjoint intervals of unit length that are contained in a half-infinite interval.

Example (Countable Sets). Suppose A is a countable set $A = \{a_n \mid n \in \mathbb{N}\}$. Then for each $\varepsilon > 0$ we can find a set of intervals that covers A such that the sum of the lengths of the intervals is ε. For example, let $I_{n,\varepsilon} = (a_n - \varepsilon 2^{-n-2}, a_n + \varepsilon 2^{-n-2})$. Since ε is arbitrary, $\mu A = 0$.

Definition (Almost Everywhere). A property is said to hold *almost everywhere* on a measurable set A if the set of elements of A upon which is does not hold has Lebesgue measure zero.

Example (Nonmeasurable Set). To show that there are non-Lebesgue measurable sets, we recapitulate the example from Ref. 24. Consider the half-open unit interval $I = [0, 1)$, for which $\mu I = 1$. For $a, b \in I$, define $a \oplus b$ by

$$a \oplus b = \begin{cases} a + b & \text{if } a + b < 1, \\ a + b - 1 & \text{if } a + b \geq 1. \end{cases} \tag{3.114}$$

We can easily see that Lebesgue measure is translation invariant: If $\mu S = r$, then $\mu(S + a) = \mu\{s + a \mid s \in S\} = r$ for any $a \in \mathbb{R}$. Similarly, if we define $S \oplus a = \{s \oplus a \mid s \in S\}$, then $\mu(S \oplus a) = \mu(S)$. Now define an equivalence relation $a \sim b$ on I to mean $a - b \in \mathbb{Q}$, the rational numbers. Let $[a] = \{b \in I \mid a \sim b\}$ be the equivalence class of any $a \in I$ and $K = \{[a] \mid a \in I\}$. Define the set C to contain exactly one element from each equivalence class in K. Set theory's Axiom of Choice [46] ensures

that set C exists. Since $\mathbb{Q}$ is countable, we can index $\mathbb{Q} \cap I$ by $\{q_n \mid n \in \mathbb{N}\}$, with $q_0 = 0$. We set $C_n = C \oplus q_n$. The properties of the C_n are as follows:

(i) $C_0 = C$.

(ii) The C_n are disjoint; for if $r \in C_m \cap C_n$, then $r = c + q_m = d + q_n$ for some c, $d \in C$; so $c \sim d$, and since C was a choice set containing exactly one element from disjoint equivalence classes in K, we must have $m = n$.

(iii) $I = \bigcup_{n \in \mathbb{N}} C_n$; if $r \in I$, then there is an $[a] \in K$ with $r \in [a]$ and $a \in C$; this implies $r \sim a$ or $r - a \in \mathbb{Q} \cap I$; but $\{q_n\}$ indexes such rational numbers, so $r - a = q_n$ for some $n \in \mathbb{N}$; thus, $r = a + q_n \in C_n$.

If C is Lebesgue measurable, then by the properties of the Lebesgue measure under translations, for all $n \in \mathbb{N}$, C_n is measurable and $\mu C = \mu C_n$.

Thus,

$$\mu(I) = \mu\left(\bigcup_{n \in \mathbb{N}} C_n\right) = \sum_{n=0}^{\infty} \mu(C_n) = \sum_{n=0}^{\infty} \mu C = \begin{cases} \infty & \text{if } \mu C > 0 \\ 0 & \text{if } \mu C = 0 \end{cases} \tag{3.115}$$

However, we know $\mu I = 1$, so that (3.115) is a contradiction; it must be the case that the choice set C is not Lebesgue measurable.

Our intuition might well suggest an easy generalization of the idea of an interval's length to a length measure for any subset of the real line. This last example has shown that the task demands some care. We cannot have the proposed properties of a measure and still be able to measure the size (length or area) of all sets. Some functions must be outside our theory of analog signals. The characteristic function for the choice set C in the above example is a case in point. Nevertheless, the class of measurable sets is quite large, and so too is the class of measurable functions. Let us turn to integration of measurable functions and apply the modern integral to signal theory. Here we shall see how these mathematical tools sharpen the definitions of the basic analog signal spaces. Moreover, these concepts will support our later development of signal approximation and transform techniques.

3.4.2 Lebesgue Integration

The key distinction between the Lebesgue and Riemann integrals is that the modern integral partitions the range of function values, whereas the classic integral partitions the domain of the function. A seemingly inconsequential difference at first glance, this insight is critical.

To illustrate the idea, consider the task of counting the supply of canned goods on a cabinet shelf. (Perhaps the reader lives in a seismically active region, such as this book's Californian authors, and is assessing household earthquake preparedness.) One way to do this is to iterate over the shelf, left to right, front to back,

adding up the volume of each canned food item. No doubt, most people would count cans like this. And it is just how we Riemann integrate $x(t)$ by adding areas: for each interval $I = [a, b)$ in the domain partition, accumulate the area, say $x(a) \times (b - a)$; refine the partition; find a better Riemann sum; and continue to the limit. The other way to guage the stock of canned food is to first count all the cans of one size, say the small tins of tuna. Then proceed to the medium size soup cans. Next the large canned vegetables. Finally—and perhaps exhausting the reader's patience—we count the giant fruit juices. It might seem silly, but it works.

And this is also Lebesgue's insight for defining the integral. We slice up the range of $x(t)$, forming sums with the weighted measures $x(a) \times \mu[x^{-1}\{a\}]$, where $x^{-1}\{a\} = \{t \in \mathbb{R} \mid x(t) = a\}$ and μ is some measure of the size of $x^{-1}\{a\}$. Our remaining exposition omits many abstractions and details; mathematical treatises that excel in this area are readily available. Instead we seek a clear and simple statement of how the ideas on measure and measurable functions fit together to support the modern integral.

3.4.2.1 Simple Functions. Like the Riemann integral, the Lebesgue integral is also a limit. It is the limit of integrals of so-called simple functions.

Definition (Simple Function). If $x : \mathbb{R} \to \mathbb{R}$ is Lebesgue measurable and Range(x) is finite, then $x(t)$ is called a simple function.

Every Lebesgue measurable function can be approximated from below by such simple functions [44]. This theorem's proof uses the stereotypical Lebesgue integration technique of partitioning the range of a measurable function.

Theorem (Approximation by Simple Functions). If $x(t)$ is measurable, then there is a sequence of simple functions $s_n(t)$ such that:

(i) If $n \le m$, then $|s_n(t)| \le |s_m(t)|$.
(ii) $|s_n(t)| \le |x(t)|$.
(iii) $\lim_{n\to\infty} s_n(t) = x(t)$.

Proof: Since we can split $x(t)$ into its negative and non-negative parts, and these are still measurable, we may assume that $x(t) \in [0, \infty]$ for all $t \in \mathbb{R}$. The idea is to break Range(x) into two parts: $S_n = [0, n)$ and $T_n = [n, \infty]$ for each $n > 0$. We further subdivide S_n into $n2^n$ subintervals of length 2^{-n}: $S_{m,n} = [m2^{-n}, (m + 1)2^{-n})$, for $0 \le m < n2^n$. Set $A_n = x^{-1}(S_n)$ and $B_n = x^{-1}(T_n)$. Define

$$s_n(t) = n\chi_{B_n}(t) + \sum_{m=0}^{n2^n - 1} \frac{m}{2^n}\chi_{B_n}(t), \tag{3.116}$$

where χ_S is the characteristic function on the set S. The simple functions (3.116) satisfy the conditions (i)–(iii). ■

3.4.2.2 Definition and Basic Properties. We define the modern integral in increments: first for non-negative functions, then for functions that go negative, and finally for complex-valued functions.

Definition (Lebesgue Integral, Non-negative Functions). Let μ the Lebesgue measure, let A be a Lebesgue measurable set in $\mathbb{R}$, and let $x : \mathbb{R} \to [0, \infty]$ be a measurable function. Then the Lebesgue integral with respect to μ of $x(t)$ over A is

$$\int_A x(t)\, d\mu = \sup_{0 \le s(t) \le x(t)} \left\{ \int_A s(t)\, d\mu \right\}, \tag{3.117}$$

where the functions $s(t)$ used to take the least upper bound in (3.117) are all simple.

Definition (Lebesgue Integral, Real-Valued Functions). Let μ the Lebesgue measure, let A be a Lebesgue measurable set in $\mathbb{R}$, and let $x : \mathbb{R} \to \mathbb{R}$ be a measurable function. Furthermore, let $x(t) = p(t) - n(t)$, where $p(t) > 0$ and $n(t) > 0$ for all $t \in \mathbb{R}$. Then the Lebesgue integral with respect to μ of $x(t)$ over A is

$$\int_A x(t)\, d\mu = \int_A p(t)\, d\mu - \int_A n(t)\, d\mu \tag{3.118}$$

as long as one of the integrals on the right-hand side of (3.118) is finite.

Remarks. By the elementary properties of Lebesgue measurable functions, the positive, negative, and zero parts of $x(t)$ are measurable functions. Note that the zero part of $x(t)$ does not contribute to the integral. In general, definitions and properties of the Lebesgue integral must assume that the subtractions of extended reals make sense, such as in (3.118). This assumption is implicit in what follows.

Definition (Lebesgue Integral, Complex-Valued Functions). Let μ the Lebesgue measure; let A be a Lebesgue measurable set in $\mathbb{R}$, let x: $\mathbb{R} \to \mathbb{C}$ be a measurable function, and let $x(t) = x_r(t) + jx_i(t)$, where $x_r(t)$ and $x_i(t)$ are real-valued for all $t \in \mathbb{R}$. Then the Lebesgue integral with respect to μ of $x(t)$ over A is

$$\int_A x(t)\, d\mu = \int_A x_r(t)\, d\mu + j \int_A x_i(t)\, d\mu\,. \tag{3.119}$$

The modern Lebesgue integral obeys all the rules one expects of an integral. It also agrees with the classic Riemann integral on piecewise continuous functions. Finally, it has superior limit operation properties.

Proposition (Linearity). Let μ the Lebesgue measure, let A be a Lebesgue measurable set in $\mathbb{R}$, and let $x, y : \mathbb{R} \to \mathbb{C}$ be measurable functions. Then,

(i) (Scaling) For any $c \in \mathbb{C}$, $\int_A cx(t)\, d\mu = c \int_A x(t)\, d\mu$.

(ii) (Superposition) $\int_A [x(t) + y(t)]\ d\mu = \int_A x(t)\ d\mu + \int_A y(t)\ d\mu$.

Proof: The integral of simple functions and the supremum are linear. ■

Remark. If $x(t) = 0$ for all $t \in \mathbb{R}$, then (even if $\mu A = \infty$) $\int_A x(t)\ d\mu = 0$ by (i).

Proposition. Let μ be the Lebesgue measure, let $[a, b]$ be an interval on $\mathbb{R}$, and let x: $\mathbb{R} \to \mathbb{C}$ be a piecewise continuous function. Then the Lebesgue and Riemann integrals of $x(t)$ are identical:

$$\int_{[a,\,b]} x(t)\ d\mu = \int_a^b x(t)\ dt\,. \tag{3.120}$$

Proof: $x(t)$ is both Riemann integrable and Lebesgue integrable. The Riemann integral, computed as a limit of lower rectangular Riemann sums (3.110a), is precisely a limit of simple function integrals. ■

Proposition (Domain Properties). Let μ be the Lebesgue measure; let A, B be Lebesgue measurable sets in $\mathbb{R}$; and let x: $\mathbb{R} \to \mathbb{C}$ be a measurable function. Then,

(i) (Subset) If $B \supset A$ and $x(t)$ is non-negative, then $\int_B x(t)\ d\mu \geq \int_A x(t)\ d\mu$.

(ii) (Union) $\int_{A \cup B} x(t)\ d\mu = \int_A x(t)\ d\mu + \int_B x(t)\ d\mu - \int_{A \cap B} x(t)\ d\mu$.

(iii) (Measure Zero Set) If $\mu(A) = 0$, then $\int_A x(t)\ d\mu = 0$.

Remark. Note that $\int_A x(t)\ d\mu = 0$ in (iii) even if $x(t) = \infty$ for all $t \in \mathbb{R}$.

Proposition (Integrand Properties). Let μ the Lebesgue measure; let A be Lebesgue measurable in $\mathbb{R}$; let $\chi_A(t)$ be the characteristic function on A; and let x, y: $\mathbb{R} \to \mathbb{C}$ be measurable functions. Then,

(i) (Monotonicity) If $y(t) \geq x(t) \geq 0$ for all $t \in \mathbb{R}$, then $\int_A y(t)\ d\mu \geq \int_A x(t)\ d\mu$.

(ii) (Characteristic Function) $\int_A x(t)\ d\mu = \int_{\mathbb{R}} x(t)\chi_A(t)\ d\mu$.

Proof: The proofs of these propositions follows from the definition of simple functions and integrals as limits thereof. ■

3.4.2.3 Limit Operations with Lebesgue's Integral. The modern integral supports much more powerful limit operations than does the Riemann integral. We recall that sequence of functions can converge to a limit that is not Riemann

integrable. In order to simplify the discussion, we offer the following theorems without detailed proofs; the interested reader can find them in treatises on modern analysis, [13, 24, 25, 44, 45].

Theorem (Monotone Convergence). Let μ be the Lebesgue measure, let A be a measurable set in $\mathbb{R}$, and x_n: $\mathbb{R} \to \mathbb{R}$ be Lebesgue measurable for $n \in \mathbb{N}$. If $0 \leq x_n(t) \leq x_m(t)$ for $n < m$ and $\lim_{n\to\infty} x_n(t) = x(t)$ for all $t \in A$, then $x(t)$ is measurable and

$$\lim_{n \to \infty} \int_A x_n(t)\, d\mu = \int_A x(t)\, d\mu . \tag{3.121}$$

Proof: $x(t)$ is measurable, because for any $r \in \mathbb{R}$,

$$x^{-1}(r, \infty] = \bigcup_{n=0}^{\infty} x_n^{-1}(r, \infty] . \tag{3.122}$$

Hence, $\lim_{n \to \infty} \int_A x_n(t)\, d\mu \leq \int_A x(t)\, d\mu$. Arguing the inequality the other way [44] requires that we consider simple functions $s(t)$ such that $0 \leq s(t) \leq x(t)$ for all $t \in \mathbb{R}$. Let $0 < c < 1$ be constant and set $A_n = \{t \in \mathbb{R} \mid cs(t) \leq x_n(t)\}$. Then, $A_{n+1} \supset A_n$ for all $n \in \mathbb{N}$, and $A = \bigcup_{n=0}^{\infty} A_N$. Thus,

$$c \int_{A_n} s(t)\, d\mu \leq \int_A x_n(t)\, d\mu . \tag{3.123}$$

As $n \to \infty$ on the right-hand side of (3.123), we see

$$c \int_A s(t)\, d\mu \leq \lim_{n \to \infty} \int_A x_n(t)\, d\mu , \tag{3.124a}$$

which is true for every $0 < c < 1$. Let $c \to 1$, so that

$$\int_A s(t)\, d\mu \leq \lim_{n \to \infty} \int_A x_n(t)\, d\mu . \tag{3.124b}$$

But $s(t)$ can be any simple function bounding $x(t)$ below, so by the definition of Lebesgue integration we know $\lim_{n \to \infty} \int_A x_n(t)\, d\mu \geq \int_A x(t)\, d\mu$. ■

Corollary. Let μ the Lebesgue measure; let A be a measurable set in $\mathbb{R}$; let x_n: $\mathbb{R} \to \mathbb{R}$ be Lebesgue measurable for $n \in \mathbb{N}$; and, for all $t \in A$, suppose $\lim_{n\to\infty} x_n(t) = x(t)$. Then, $x(t)$ is measurable and

$$\lim_{n \to \infty} \int_A x_n(t)\, d\mu = \int_A x(t)\, d\mu . \tag{3.125}$$

Proof: Split $x(t)$ into negative and positive parts. ■

A similar result holds for complex-valued functions. The next corollary shows that we may interchange Lebesgue integration and series summation.

Corollary (Integral of Series). Let μ the Lebesgue measure; let A be a measurable set in $\mathbb{R}$; let x_n: $\mathbb{R} \to \mathbb{C}$ be Lebesgue measurable for $n \in \mathbb{N}$; and, for all $t \in A$, suppose $\Sigma_{n\to\infty} x_n(t) = x(t)$. Then,

$$\sum_{n=0}^{\infty} \int_A x_n(t)\, d\mu = \int_A x(t)\, d\mu\,. \tag{3.126}$$

Proof: Beginning with non-negative functions, apply the theorem to the partial sums in (3.126). Then extend the result to general real- and complex-valued functions. ■

The next theorem, Fatou's lemma,[5] relies on the idea of the lower limit of a sequence [23].

Definition (lim inf, lim sup). Let $A = \{a_n \mid n \in \mathbb{N}\}$ be a set of real numbers and let $A_N = \{a_n \mid n \geq \mathrm{N}\}$. Let $r_N = \inf A_N$ be the greatest lower bound of A_N in the extended real numbers $\mathbb{R} \cup \{\infty\} \cup \{-\infty\}$. Let $s_N = \sup A_N$ be the least upper bound of A_N in the extended real numbers. We define lim inf A and lim sup A by

$$\liminf \{a_n\} = \lim_{N\to\infty} r_N \tag{3.127a}$$

and

$$\limsup \{a_n\} = \lim_{N\to\infty} s_N\,. \tag{3.127b}$$

The main things anyone has to know are:

- $\liminf\{a_n\}$ is the smallest limit point in the sequence $\{a_n\}$;
- $\limsup\{a_n\}$ is the largest limit point in the sequence $\{a_n\}$;
- $\liminf\{a_n\} = \limsup\{a_n\}$ if and only if the sequence $\{a_n\}$ converges to some limit value $a = \lim_{n\to\infty}\{a_n\}$, in which case $a = \liminf\{a_n\} = \limsup\{a_n\}$;
- the upper and lower limits could be infinite, but they always exist;
- if $a_n \leq b_n$ then $\liminf\{a_n\} \leq \liminf\{b_n\}$;
- $\limsup\{-a_n\} = -\liminf\{a_n\}$.

Example. Consider the sequence $\{a_n\} = \{1^{-1}, 1, -1, 2^{-1}, 2, -2, 3^{-1}, 3, -3, \ldots\}$. This sequence has three limit points: $-\infty$, ∞, and 0. We have $\liminf\{a_n\} = -\infty$, $\limsup\{a_n\} = +\infty$, and $\lim_{n\to\infty}\{a_{3n}\} = 0$. Only this last sequence is a genuine Cauchy sequence, however.

Theorem (Fatou's Lemma). Let μ the Lebesgue measure; let A be a measurable set in $\mathbb{R}$; let x_n: $\mathbb{R} \to \mathbb{R}$ be Lebesgue measurable for $n \in \mathbb{N}$; and, for all $n \in \mathbb{N}$ and $t \in A$, $0 \leq x_n(t) \leq \infty$. Then,

$$\int_A \liminf[x_n(t)]\, d\mu \leq \liminf \int_A x_n(t)\, d\mu\,. \tag{3.128}$$

[5]Pierre Fatou (1878–1929), mathematician and astronomer at the Paris Observatory.

Proof: Define

$$y_n(t) = \inf_{k \geq n} \{x_k(t)\}, \tag{3.129}$$

so that the $y_n(t)$ approach $\liminf x_n(t)$ as $n \to \infty$ and $y_n(t) \leq y_m(t)$ when $n < m$. Note that for all $n \in \mathbb{N}$, $y_n(t) \leq x_n(t)$. Consequently,

$$\int_A y_n(t)\, d\mu \leq \int_A x_n(t)\, d\mu, \tag{3.130}$$

and thus,

$$\liminf \int_A y_n(t)\, d\mu \leq \liminf \int_A x_n(t)\, d\mu. \tag{3.131}$$

The left-hand side of (3.131) draws our attention. Since $\lim\{y_n(t)\} = \liminf\{x_n(t)\}$ and $\{y_n(t)\}$ are monotone increasing, Lebesgue's monotone convergence theorem implies

$$\liminf \int_A y_n(t)\, d\mu = \lim \int_A y_n(t)\, d\mu = \int_A \lim[y_n(t)]\, d\mu = \int_A \liminf[x_n(t)]\, d\mu. \tag{3.132}$$

Combining (3.131) and (3.132) completes the proof. ■

Theorem (Lebesgue's Dominated Convergence). Let μ be the Lebesgue measure, let A be a measurable set in $\mathbb{R}$, and let $x_n\colon \mathbb{R} \to \mathbb{C}$ be Lebesgue measurable for $n \in \mathbb{N}$, $\lim_{n\to\infty} x_n(t) = x(t)$ for all $t \in A$, and $|x_n(t)| \leq g(t) \in L^1(\mathbb{R})$. Then $x(t) \in L^1(\mathbb{R})$ and

$$\lim_{n\to\infty} \int_A x_n(t)\, d\mu = \int_A x(t)\, d\mu. \tag{3.133}$$

Proof: We borrow the proof from Ref. 44. Note first that limit $x(t)$ is a measurable function and it is dominated by $g(t)$, so $x(t) \in L^1(\mathbb{R})$. Next, we have $|x(t) - x_n(t)| \leq 2g(t)$ and we apply Fatou's lemma to the difference $2g(t) - |x_n(t) - x(t)|$:

$$2\int_A g(t)d\mu \leq \liminf_{n\to\infty} \int_A \{2g(t) - |x(t) - x_n(t)|\}d\mu. \tag{3.134a}$$

Manipulating the lower limit on the right-hand integral in (3.134a) gives

$$2\int_A g(t)\, d\mu \leq 2\int_A g(t)\, d\mu - \limsup_{n\to\infty} \int_A |x(t) - x_n(t)|\, d\mu. \tag{3.134b}$$

Subtracting $2\int_A g\, d\mu$ out of (3.134b), we have $\lim_{n\to\infty} \sup \int_A |x(t) - x_n(t)|\, d\mu \leq 0$ from which $\lim_{n\to\infty} \int_A |x(t) - x_n(t)|\, d\mu = 0$ and (3.133) follows. ■

Corollary (Interchange of Limits). Let μ the Lebesgue measure, let A be a measurable set in $\mathbb{R}$, and let x_n: $\mathbb{R} \to \mathbb{C}$ be Lebesgue measurable for $n \in \mathbb{N}$. Suppose that

$$\sum_{n=-\infty}^{\infty} \int_A |x_n(t)| \, d\mu < \infty . \tag{3.135}$$

Then the series $\Sigma_n x_n(t) = x(t)$ for almost all $t \in A$, $x(t) \in L^1(\mathbb{R})$, and

$$\sum_{n=-\infty}^{\infty} \int_A x_n(t) \, d\mu = \int_A x(t) \, d\mu . \tag{3.136}$$

Proof: Apply the dominated convergence theorem to partial series sums. ■

3.4.2.4 Lebesgue Integrals in Signal Theory. To this point, our definitions of L^p signal spaces were defined abstractly as completions of more rudimentary spaces. The new integral helps avoid such stilted formulations. We define both the L^p norm and L^p signals spaces using the Lebesgue integral.

Definition (L^p, L^p norm). Let μ the Lebesgue measure and let A be a measurable set in $\mathbb{R}$. Then $L^p(A)$ is the set of all Lebesgue measurable signals $x(t)$ such that

$$\int_A |x(t)|^p d\mu < \infty . \tag{3.137}$$

We define $\|x\|_{p,A}$ to be

$$\|x\|_{p,A} = \left(\int_A |x(t)|^p d\mu \right)^{\frac{1}{p}} \tag{3.138}$$

when the integral (3.137) exists. In the case of $p = \infty$, we take $L^\infty(A)$ to be the set of all $x(t)$ for which there exists M_x with $|x(t)| < M_x$ almost everywhere on A.

Now we can recast the entire theory of L^p spaces using the modern integral. We must still identify L^p space elements with the equivalence class of all functions that differ only by a set of measure zero. The basic inequalities of Holder, Minkowski, and Schwarz still hold. For instance, Minkowski's inequality states that $\|x + y\|_p \leq \|x\|_p + \|y\|_p$, where the p-norm is defined by Lebesgue integral. The more powerful limit theorems of the modern integral, however, allow us to prove the following completeness result [25, 44, 45].

Theorem. For Lebesgue measurable A, the $L^p(A)$ spaces are complete, $1 \leq p \leq \infty$.

Proof: We leave the case $p = \infty$ as an exercise. Let $\{x_n(t)\}$ be Cauchy in $L^p(A)$ We can extract a subsequence $\{y_n(t)\}$ of $\{x_n(t)\}$ with $\|y_{n+1} - y_n\|_p < 2^{-n}$ for all n. We then define $f_n(t) = |y_1(t) - y_0(t)| + |y_2(t) - y_1(t)| + \cdots + |y_{n+1}(t) - y_n(t)|$ and $f(t) = \lim_{n\to\infty} f_n(t)$.

The choice of the subsequence and Minkowski's inequality together imply $\|f_n(t)\|_p < 1$. Invoking Fatou's lemma (3.128) on $\{[f_n(t)]^p\}$, we obtain

$$\int_A [f(t)]^p d\mu = \int_A \liminf [f_n(t)]^p d\mu \le \liminf \int_A [f_n(t)]^p d\mu \le \liminf \{1^p\} = 1. \tag{3.139}$$

This also shows $f(t) < \infty$ almost everywhere on A. If $x(t)$ is given by

$$x(t) = y_0(t) + \sum_{n=0}^{\infty} (y_{n+1}(t) - y_n(t)), \tag{3.140}$$

then the convergence of $f(t)$ guarantees that $x(t)$ converges absolutely almost everywhere on A. Thus, $x(t) = \lim_{n\to\infty} y_n(t)$, the Cauchy sequence $\{x_n(t)\}$ has a convergent subsequence, and so $\{x_n(t)\}$ must have the same limit. ■

The next result concerns two-dimensional integrals. These occur often, even in one-dimensional signal theory. The Fubini theorem[6] provides conditions under which iterated one-dimensional integrals—which arise when we apply successive integral operators—are equal to the associated two-dimensional integral [24]. Functions defined on $\mathbb{R} \times \mathbb{R}$ are really two-dimensional signals—*analog images*—and generally outside the scope of this book. However, in later chapters our signal transform operations will mutate a one-dimensional signal into a two-dimensional transform representation. Opportunties to apply the following result will abound.

Theorem (Fubini). Let $x(s, t)$ be a measurable function on a measurable subset $A \times B$ of the plane $\mathbb{R}^2$. If either of these conditions obtains,

(i) $x(s, t) \in L^1(A \times B)$,
(ii) $0 \le x(s, t)$ on $A \times B$,

then the order of integration may be interchanged:

$$\int_A \left[\int_B x(s, t)\, dt\right] ds = \int_B \left[\int_A x(s, t)\, ds\right] dt. \tag{3.141}$$

Proof: Refer to Ref. 24.

3.4.2.5 Differentiation. It remains to explain the concept of a derivative in the context of Lebesgue integration. Modern integration seems to do everything backwards. First, it defines the sums for integration in terms of range values rather than domain intervals. Then, unlike conventional calculus courses, it leaves out the intuitively easier differentiation theory until the end. Lastly, as we shall see below, it defines the derivative in terms of an integral.

[6]Guido Fubini (1879–1943) was a mathematics professor at Genoa and Turin until anti-Semitic decrees issued by Mussolini's fascist regime compelled him to retire. Fubini moved to the United States from Italy, taking a position at the Institute for Advanced Study in Princeton, New Jersey in 1939.

Definition (Derivative). Let $y(t)$ be a Lebesgue measurable function. Suppose $x(t)$ is a Lebesgue measurable function such that

$$y(t) = \int_a^t x \, d\mu \,, \tag{3.142}$$

almost everywhere on any interval $[a, b]$ that contains t. Then we say $x(t)$ is the *derivative* of $y(t)$. With the usual notations, we write $\frac{dy}{dt} = y'(t) = y^{(1)}(t) = x(t)$. Second and higher derivatives may be further defined, and the notations carry through as well.

All of the differentiation properties of conventional calculus check out under this definition.

3.5 DISTRIBUTIONS

Distributions extend the utility of Hilbert space to embrace certain useful quantities which are not classically defined in Riemannian calculus. The most celebrated example of a distribution is the *Dirac delta*, which played a seminal role in the development of quantum mechanics and has been extended to other areas of quantitative science [7–11, 47–49]. The Dirac delta is easy to apply but its development within the context of distributions is often obscured, particularly at the introductory level. This section develops the foundations of distribution theory with emphasis on the Dirac delta. The theory and definitions developed here are also the basis for the generalized Fourier transform of Chapter 6.

3.5.1 From Function to Functional

Quantitative science is concerned with generating numbers and the notion of a function as a mapping from the one set of complex numbers to another is well-established. The inner product in Hilbert space is another tool for generating physically relevant data, and this Hilbert space mapping is conveniently generalized by the concept of a *functional*.

Definition (Functional). Let $\phi(t)$ be a function belonging to the class of so-called *test functions* (to be defined shortly). If the inner product

$$\langle f(t), \phi(t) \rangle \equiv \int_{-\infty}^{\infty} f(t)\phi^*(t) \, dy \tag{3.143}$$

converges, the quantity $f(t)$ is a *functional* on the space of test functions.

The test functions are defined as follows.

Definition (Rapid Descent). A function is said to be *rapidly descending* if for each positive integer N, the product

$$t^N \cdot f(t) \tag{3.144}$$

remains bounded as $|t| \to \infty$. A test function $\phi(t)$ will be classified as *rapidly decreasing* if $\phi(t)$ and all its derivatives are rapidly decreasing.

The derivatives are included in this definition to ensure that the concept of rapid descent is closed under this operation. Exponentials such as e^{-t}, and Gaussians e^{-t^2} are rapidly decreasing. On the other hand, polynomials, the exponential e^{t}, and $\sin t$, $\cos t$ are not rapidly decreasing. (These will be categorized shortly.) Furthermore, rapidly decreasing functions are integrable.

The condition of rapid descent can be guaranteed for a large class of functions by forcing them vanish identically for all t outside some interval $[t_1, t_2]$, that is,

$$f(t) \to f(t) \cdot [u(t - t_1) - u(t - t_2)]\,. \tag{3.145}$$

These *test functions of compact support* are a subset of all test functions of rapid descent.

Remark. The test functions are our slaves; by stipulating that they decay sufficiently rapidly, we can ensure that (3.143) converges for a sufficiently broad class of functionals $f(t)$. In many discussions, particularly general theoretical treatment of functionals, the exact form of the test function is immaterial; it is merely a vehicle for ensuring that the inner products on the space of $\phi(t)$ converge. Often, all that is required is the knowledge that a test function behaves in a certain way under selected operations, such as differentiation, translation, scaling, and more advanced operations such as the Fourier transform (Chapters 5 and 6). Whenever possible, it is advantageous to work in the space of compact support test functions since that eliminates any questions as to whether its descent is sufficiently rapid; if $\phi(t)$ has compact support, the product $\phi(t)f(t)$ follows suit, admitting a large set of $f(t)$ for which (3.143) generates good data. However, in some advanced applications, such as the generalized Fourier transform (Chapter 6), we do not have the luxury of assuming that all test functions are compactly supported.

3.5.2 From Functional to Distribution

A distribution is a subset of the class of functionals with some additional (and physically reasonable) properties imposed.

3.5.2.1 Defintion and Classification

Definition (Distribution). Let $\phi(t)$ be a test function of rapid descent. A functional $f(t)$ is a distribution if it satisfies conditions of continuity and linearity:

(i) *Continuity.* Functional $f(t)$ is continuous if when the sequence $\phi_k(t)$ converges to zero in the space of test functions, then $\lim_{k\to\infty} \langle f(t),\phi_k(t)\rangle \to 0$.

(ii) *Linearity.* Functional $f(t)$ is linear if for all complex constants c_1 and c_2 and for $\psi(t)$ of rapid descent,

$$\langle f(t),c_1\phi(t) + c_2\psi(t)\rangle = c_1\langle f(t),\phi(t)\rangle + c_2\langle f(t),\psi(t)\rangle. \tag{3.146}$$

Linearity plays such a central role to signal analysis that any functional that does not belong to the class of distributions is not useful for our applications. Distributions of all types are sometimes referred to as *generalized functions.*

Definition (Equivalent Distributions). Two functionals $f(t)$ and $g(t)$ are equivalent if

$$\langle f(t),\phi(t)\rangle = \langle g(t),\phi(t)\rangle \tag{3.147}$$

for all test functions.

A distribution $f(t)$ that is equivalent to a classically defined function $f_0(t)$ so that

$$\langle f(t),\phi(t)\rangle = \langle f_0(t),\phi(t)\rangle \tag{3.148}$$

is termed a *regular distribution*. Distributions that have no direct expression as a standard function belong to the class of *singular distributions*. The most celebrated example of a singular distribution is the Dirac delta, which we will study in detail.

Distributions $f(t)$ defined on the space of the rapidly descending test functions are *tempered distributions* or *distributions of slow growth.* The concept of slow growth applies equally well to regular and singular distributions. For the former, it can be illustrated with familiar concepts:

Definition (Slow Increase). A function is said to be *slowly increasing*, *tempered*, or of *slow growth* if for some positive integer M, the product

$$t^{-M}\cdot f(t) \tag{3.149}$$

remains bounded as $|t| \to \infty$.

In essence, a slowly increasing function is one that can be tamed (tempered) by a sufficiently high power of t in (3.149). Examples include the polynomials, the sine and cosine, as well as $\sin t/t$. The exponential e^t grows too rapidly to be tempered.

Remarks. Functions of slow growth are not generally integrable, a fact that later hinders the description of their spectral content via the integral Fourier transform.

We will demonstrate this difficulty in Chapter 5 and remedy the situation by defining a generalized Fourier transform in Chapter 6; of utility will be many of the concepts developed here.

Note that the product of a function of slow growth $g(t)$ and a function of rapid descent $f(t)$ is a function of rapid descent. This is easily demonstrated. According to (3.144) and (3.149), there is some M for which

$$\upsilon \cdot g(t)f(t) \tag{3.150}$$

remains bounded as $t \to \infty$ for any positive integer $\upsilon \equiv N - M$. Therefore $h(t) \equiv f(t)g(t)$ decreases rapidly. Such products are therefore integrable. For signal analysis applications, distributions of slow growth and test functions of rapid descent are the most useful set of *dual spaces* in the distribution literature. For alternative spaces, see Ref. 10.

3.5.2.2 Properties of Distributions. Many standard operations such as scaling, addition, and multiplication by constants have predictable effects on the inner product defining distributions. In selected cases these operations map distributions to distributions, giving us flexibility to add them, scale the independent variable, multiply by classically defined functions or constants, and take derivatives.

Proposition. Let $f(t)$ be a distribution. Then $\dfrac{df}{dt}$ is a functional which is continuous and linear.

Proof: By definition, a distribution $\dfrac{df}{dt}$ is a functional satisfying

$$\left\langle \frac{df}{dt},\phi(t) \right\rangle = f(t)\phi(t)\Big|_{-\infty}^{\infty} - \left\langle f(t),\frac{d\phi}{dt} \right\rangle = -\left\langle f(t),\frac{d\phi}{dt} \right\rangle \tag{3.151}$$

Continuity is assured by noting

$$\lim_{k \to \infty} \left\langle \frac{df}{dt},\phi_k(t) \right\rangle = -\lim_{k \to \infty} \left\langle f(t),\frac{d\phi_k}{dt} \right\rangle = 0\,, \tag{3.152}$$

which follows directly from the stipulations placed on the test function $\phi(t)$. Linearity is easy to establish and is left to the reader. ■

Derivatives of higher order follow in a similar manner. Consider the second derivative $\dfrac{d^2f}{dt^2}$. Let $g(t) = f'(t)$, where the prime denotes differentiation. Then for $g'(t) \equiv f''(t)$ the derivative rule leads to

$$\int_{-\infty}^{\infty} g'(t)\phi(t)\,dt = -\int_{-\infty}^{\infty} g(t)\phi'(t)\,dt\,. \tag{3.153}$$

According to the conditions defining a test function, $\psi(t) \equiv \phi'(t)$ is also a bona fide test function, so we can reexpress the derivative rule for $g(t)$:

$$\int_{-\infty}^{\infty} g'(t)\phi(t)\,dt = -\int_{-\infty}^{\infty} g(t)\phi'(t)\,dt = -\int_{-\infty}^{\infty} g(t)\psi(t)\,dt. \tag{3.154}$$

But the last element in this equality can be further developed to

$$-\int_{-\infty}^{\infty} g(t)\psi(t)\,dt = -\int_{-\infty}^{\infty} f'(t)\psi(t)\,dt = -\left[\int_{-\infty}^{\infty} f'(t)\psi(t)\,dt\right] = \int_{-\infty}^{\infty} f(t)\psi'(t)\,dt \tag{3.155}$$

where we used the first derivative property for $f(t)$. Linking (3.154) and (3.155) leads to the desired result expressed in terms of the original test function $\phi(t)$:

$$\int_{-\infty}^{\infty} f''(t)\phi(t)\,dt = \int_{-\infty}^{\infty} f(t)\phi''(t)\,dt \tag{3.156}$$

This result generalizes to derivatives of all orders (exercise).

Proposition (Scaling). Let a be a constant. Then

$$\langle f(at),\phi(t)\rangle = \frac{1}{|a|}\left\langle f(t),\phi\left(\frac{t}{a}\right)\right\rangle \tag{3.157}$$

Proof: Left as an exercise. ■

Note that (3.157) does not *necessarily* imply that $f(at) = \frac{1}{|a|}f(t)$, although such equivalence may be obtained in special cases. If this is not clear, reconsider the definition of equivalence.

Proposition (Multiplication by Constant). If a is a constant, if follows that

$$\langle af(t),\phi(t)\rangle = a\langle f(t),\phi(t)\rangle. \tag{3.158}$$

Proof: Trivial. ■

In many signal analysis applications it is common to mix distributions and classically defined functions.

Proposition (Associativity). Let $f_0(t)$ be an infinitely differentiable regular distribution. Then

$$\langle f_0(t)f(t),\,\phi(t)\rangle = \langle f(t),\,f_0(t)\phi(t)\rangle. \tag{3.159}$$

Proof: Exercise. ■

Why must we stipulate that $f_0(t)$ be infinitely differentiable? In general, the product of two distributions is *not* defined unless at least one of them is an infinitely

differentiable regular distribution. This associative law (3.159) could be established because $f_0(t)$ was a regular distribution and the product $f_0(t)\phi(t)$ has meaning as a test function.

Proposition (Derivative of Product). Let $f_0(t)$ be a regular distribution and let $f(t)$ be a distribution of arbitrary type. The derivative of their product is a distribution satisfying

$$\frac{d}{dt}[f_0(t)f(t)] = f(t)\frac{df_0}{dt} + f_0(t)\frac{df}{dt}. \tag{3.160}$$

Proof: Consider the distribution represented by the second term above, regrouping factors and then applying the derivative rule:

$$\int_{-\infty}^{\infty} f_0(t)\frac{df}{dt}\phi(t)\,dt = \int_{-\infty}^{\infty} \frac{df}{dt}\cdot f_0(t)\phi(t)\,dt = -\int_{-\infty}^{\infty} f(t)\cdot\frac{d}{dt}[f_0(t)\phi(t)]\,dt. \tag{3.161}$$

The derivative in the last equality can be unpacked using the classical product rule since both factors are regular functions,

$$-\int_{-\infty}^{\infty} f(t)\cdot\left[\phi(t)\frac{df_0}{dt} + f_0(t)\frac{d\phi}{dt}\right]dt = -\int_{-\infty}^{\infty} f(t)\cdot\phi(t)\frac{df_0}{dt}\,dt - \int_{-\infty}^{\infty} f(t)\cdot\frac{d\phi}{dt}f_0(t)\,dt. \tag{3.162}$$

The right-hand side can be rearranged by applying the derivative rule to the second term. This gives two terms with $\phi(t)$ acting as a test function:

$$-\int_{-\infty}^{\infty} f(t)\frac{df_0}{dt}\cdot\phi(t)\,dt + \int_{-\infty}^{\infty}\frac{d}{dt}[f(t)f_0(t)]\cdot\phi(t)\,dt. \tag{3.163}$$

Comparing (3.162) and (3.163) and applying the definition of equivalence gives

$$f_0(t)\frac{df}{dt} = -f(t)\frac{df_0}{dt} + \frac{d}{dt}[f(t)f_0(t)], \tag{3.164}$$

from which the desired result (3.161) follows. ■

In many applications it is convenient to scale the independent variable. Distributions admit a chain rule under differentiation.

Proposition (Chain Rule). If $f(t)$ is an arbitrary distribution, a is a constant, and $y \equiv at$, then

$$\frac{d}{dt}f(at) = a\frac{d}{dt}f(t). \tag{3.165}$$

Proof: Exercise. ■

3.5.3 The Dirac Delta

Certain signals $f(t)$ exhibit jump discontinuities. From a classical Riemannian perspective, the derivative df/dt is singular at the jump. The situation can be reassessed within the context of distributions. Consider the unit step $u(t)$. For a test function of rapid descent $\phi(t)$, integration by parts produces

$$\int_{-\infty}^{\infty} \frac{du}{dt}\phi(t)\,dt = u(t)\phi(t)\Big|_{-\infty}^{\infty} - \int_{-\infty}^{\infty} u(t)\frac{d\phi}{dt}\,dt = -\int_{-\infty}^{\infty} u(t)\frac{d\phi}{dt}\,dt. \tag{3.166}$$

This reduces to

$$-\int_{0}^{\infty} u(t)\frac{du}{dt}\,dt = -[\phi(\infty)-\phi(0)] = \phi(0), \tag{3.167}$$

so that

$$\int_{-\infty}^{\infty} \frac{du}{dt}\phi(t)\,dt = \phi(0). \tag{3.168}$$

The existence of $\frac{d\phi}{dt}$ is central to the preceding argument and is guaranteed by the definition of the test function. Consider the following definition.

Definition (Dirac Delta). The Dirac delta $\delta(t)$ is a functional that is equivalent to the derivative of the unit step,

$$\delta(t) \equiv \frac{du}{dt}. \tag{3.169}$$

From (3.168), we have

$$\langle \delta(t),\phi(t)\rangle = \left\langle \frac{du}{dt},\phi(t)\right\rangle = \phi(0) \tag{3.170}$$

so the value returned by the distribution $\delta(t)$ is the value of the test function at the origin. It is straightforward to show that the Dirac delta satisfies the conditions of continuity and linearity; it therefore belongs to the class of functionals defined as distributions. Appearances are deceiving: despite its singular nature, the Dirac delta is a distribution of slow growth since it is defined on the (dual) space consisting of the test functions of rapid descent.

By simple substitution of variables we can generalize further:

$$\langle \delta(t-\tau),\phi(t)\rangle = \int_{-\infty}^{\infty} \frac{d}{dt}u(t-\tau)\phi(t)\,dt = \phi(\tau). \tag{3.171}$$

This establishes the Dirac delta as a *sifting* operator which returns the value of the test function at an arbitrary point $t = \tau$. In signal analysis, the process of sampling, whereby a the value of a function is determined and stored, is ideally represented by an inner product of the form (3.171).

Remark. Unfortunately, it has become common to refer to the Dirac delta as the "delta function." This typically requires apologies such as "the delta function is not a function", which can be confusing to the novice, and imply that the Dirac delta is the result of mathematical sleight of hand. The term delta distribution is more appropriate. The truth is simple: The delta function is not a *function*; it is a *functional* and if the foregoing discussion is understood thoroughly, the Dirac delta is (rightly) stripped of unnecessary mathematical mystique.

The sifting property described by (3.171) can be further refined through a test compact support on the interval $t \in [a, b]$. The relevant integration by parts,

$$\int_a^b \frac{du}{dt}\phi(t)\, du = u(t)\phi(t)\Big|_a^b - \int_a^b u(t)\frac{d\phi}{dt}\, dt, \tag{3.172}$$

takes specific values depending on the relative location of the discontinuity (in this case, located at $t = 0$ for convenience) and the interval on which the test function is supported. There are three cases:

(i) $a < 0 < b$:

$$\int_a^b \frac{du}{dt}\phi(t)\, du = u(t)\phi(t)\Big|_a^b - \int_0^b 1 \cdot \frac{d\phi}{dt}\, dt = \phi(b) - [\phi(b) - \phi(0)] = \phi(0). \tag{3.173}$$

(ii) $a < b < 0$: Since the unit step is identically zero on this interval,

$$\int_a^b \frac{du}{dt}\phi(t)\, du = 0 - \int_a^b 0 \cdot \frac{d\phi}{dt}\, dt = 0. \tag{3.174}$$

(iii) $b > a > 0$: on this interval, $u(t) = 1$, so that

$$\int_a^b \frac{du}{dt}\phi(t)\, du = \phi(t)\Big|_a^b - \int_a^b 1 \cdot \frac{d\phi}{dt}\, dt = 0. \tag{3.175}$$

Remark. In general, it is not meaningful to assign a pointwise value to a distribution since by their nature they are defined by an integral over an interval specified by the test function. Cases (ii) and (iii) assert that $\delta(t)$ is identically zero on the interval $[a, b]$. The above arguments can be applied to the intervals $[-\infty, -\varepsilon]$ and $[\varepsilon, \infty]$ where ε is arbitrarily small, demonstrating that the Dirac delta is identically

zero at all points along the real line except the origin, consistent with expected behavior of $\frac{du}{dt}$.

The general scaling law (3.157) relates two inner products. But when the distribution is a Dirac delta, there are further consequences.

Proposition (Scaling). If $a \neq 0$, then

$$\delta(at) = \frac{1}{|a|}\delta(t). \tag{3.176}$$

Proof: Note that

$$\int_{-\infty}^{\infty} \delta(at)\phi(t)\, dt = \frac{1}{|a|}\int_{-\infty}^{\infty} \delta(t)\phi\left(\frac{t}{a}\right) dt = \frac{1}{|a|}\phi(0). \tag{3.177}$$

The right-hand side can be expressed as

$$\frac{1}{|a|}\phi(0) = \frac{1}{|a|}\int_{-\infty}^{\infty} \delta(t)\phi(t)\, dt. \tag{3.178}$$

Applying the definition of equivalence leads to the scaling law (3.176). ■

The special case $a = -1$ leads to the relation $\delta(-t) = \delta(t)$, so the Dirac delta has even symmetry. Some useful relations follow from the application of (3.159) to the Dirac delta.

Proposition (Associative Property). We have

$$\delta(t)f_0(t) = \delta(t)f_0(0). \tag{3.179}$$

Proof: Since

$$\int_{-\infty}^{\infty} \delta(t)f_0(t)\phi(t)\, dt = f_0(0)\phi(0) \equiv \int_{-\infty}^{\infty} \delta(t)f_0(0)\phi(t)\, dt, \tag{3.180}$$

this establishes the equivalence (3.179). ■

Note this does *not* imply $f_0(t) = f_0(0)$, since division is not an operation that is naturally defined for arbitrary singular distributions such as $\delta(t)$. However, (3.179) leads to some interesting algebra, as shown in the following example.

Example. Suppose $f_0(t) = t$. According to (3.179),

$$t\delta(t) = 0 \tag{3.181}$$

for all t. This implies that if $f(t)$ and $g(t)$ are distributions, and $tg(t) = tf(t)$, then

$$g(t) = f(t) + a_0\delta(t), \tag{3.182}$$

where a_0 is constant. Note that (3.182) applies equally well to regular and singular distributions; it is central to establishing important relations involving the generalized Fourier transform in Chapter 6.

The inner product defining the derivative,

$$\int_{-\infty}^{\infty} \frac{df}{dt}\phi(t)\,dt = -\int_{-\infty}^{\infty} f(t)\frac{d\phi}{dt}\,dt, \tag{3.183}$$

also leads to a sifting property.

Proposition (Differentiation)

$$\int_{-\infty}^{\infty} \delta'(t-\tau)\phi(t)\,dt = -\phi'(\tau). \tag{3.184}$$

Proof: Using a prime to denote differentiation with respect to t, we obtain

$$\int_{-\infty}^{\infty} \delta'(t)\phi(t)\,dt = -\int_{-\infty}^{\infty} \delta(t)\phi'(t)\,dt = -\phi'(0). \tag{3.185}$$

For an arbitrary Dirac delta centered at $t = \tau$, this generalizes to (3.184). ■

3.5.4 Distributions and Convolution

The convolution operation is central to analyzing the output of linear systems. Since selected signals and system impulse responses may be expressed in terms of the Dirac delta, some of our applications may involve the convolution of two singular distributions, or singular and regular distributions. Given that the product of two singular distributions is not defined, it may come as an unexpected result to define a convolution operation. As before, we will base the development on an analogous result derived from Riemannian calculus.

First, consider the convolution of a distribution with a test function. This problem is straightforward. Let $f(t)$ be an arbitrary distribution. Then the convolution

$$(f*\phi)(u) = \int_{-\infty}^{\infty} f(t)\phi(u-t)\,dt = \int_{-\infty}^{\infty} f(u-t)\phi(t)\,dt \tag{3.186}$$

is a function in the variable u.

Next, consider the convolution of two test functions. If $\phi(t)$ and $\psi(t)$ are test functions, their convolution presents no difficulty:

$$(\phi^*\psi)(u) \equiv \int_{-\infty}^{\infty} \phi(u-t)\psi(t)\,dt = \int_{-\infty}^{\infty} \phi(t)\psi(u-t)\,dt = (\psi^*\phi)(u)\,. \tag{3.187}$$

Remark. If $(\phi^*\psi)(u)$ is to be a test function of compact support, both $\phi(t)$ and $\psi(t)$ must also be compactly supported. When this consideration impacts an important conclusion, it will be noted.

Now reconsider this convolution in terms of a Hilbert space inner product. If we define

$$\psi_{\text{ref}} \equiv \psi(-t)\,, \tag{3.188}$$

then

$$(\phi^*\psi_{\text{ref}})(u) = \int_{-\infty}^{\infty} \phi(t)\psi(u+t)\,dt\,. \tag{3.189}$$

This leads to a standard inner product, since

$$(\phi^*\psi_{\text{ref}})(0) = \int_{-\infty}^{\infty} \phi(t)\psi(t)\,dt = \langle \phi(t), \psi(t) \rangle\,. \tag{3.190}$$

Because $(\phi^*\psi)(t)$ is a test function, it follows that

$$\langle \phi^*\psi, \eta \rangle = ((\phi^*\psi)^*\eta_{\text{ref}})(0) = (\phi^*(\psi_{\text{ref}}{}^*\eta)_{\text{ref}})(0)\,. \tag{3.191}$$

However,

$$(\phi^*(\psi_{\text{ref}}{}^*\eta)_{\text{ref}})(0) = \langle \phi, \psi_{\text{ref}}{}^*\eta \rangle\,. \tag{3.192}$$

Comparing the last two equations gives the desired result:

$$\langle \phi^*\psi, \eta \rangle = \langle \phi, \psi_{\text{ref}}{}^*\eta \rangle\,. \tag{3.193}$$

The purpose of this exercise was to allow the convolution to migrate to the right-hand side of the inner product. This leads naturally to a definition that embraces the convolution of two singular distributions.

Definition (Convolution of Distributions). Using (3.193) as a guide, if $f(t)$ and $g(t)$ are distributions of any type, including singular, their convolution is defined by

$$\langle f^*g, \phi \rangle \equiv \langle f, g_{\text{ref}}{}^*\phi \rangle\,. \tag{3.194}$$

Example (Dirac Delta). Given two delta distributions $f(t) = \delta(t-a)$ and $g(t) = \delta(t-b)$, we have

$$g_{\text{ref}} = \delta(-t-b) = \delta(-(t+b)) = \delta(t+b). \tag{3.195}$$

So

$$g_{\text{ref}} * \phi = \int_{-\infty}^{\infty} \phi(u-t)\delta(t+b)\, dt = \phi(u+b), \tag{3.196}$$

and the relevant inner product (3.194) takes the form

$$\langle f^* g, \phi \rangle = \int_{-\infty}^{\infty} \delta(u-a)\phi(u+b)\, dt = \phi(a+b). \tag{3.197}$$

So the desired convolution is expressed,

$$f^* g = \delta(t-(a+b)). \tag{3.198}$$

Later developments will lead us derivatives of distributions. An important result involving convolution is the following. A similar result holds for standard analog signals (functions on the real line).

Proposition (Differentiation of Convolution). Let f and g be arbitrary distributions. Then,

$$\frac{d}{dt}(f^* g) = f^* \frac{dg}{dt} = \frac{df}{dt} * g \ . \tag{3.199}$$

Proof: The proof of (3.199) requires the usual inner product setting applicable to distributions and is left as an exercise. (You may assume that convolution of distributions is commutative, which has been demonstrated for standard functions and is not difficult to prove in the present context.) ■

3.5.5 Distributions as a Limit of a Sequence

Another concept that carries over from function theory defines a functional as a limit of a sequence. For our purposes, this has two important consequences. First, limits of this type generate approximations to the Dirac delta, a convenient property that impacts the wavelet transform (Chapter 11). Second, such limits make predictions of the high-frequency behavior of pure oscillations (sinusoids) which are the foundations of Fourier analysis (Chapters 5 and 6). This section covers both topics.

Definition. Let $f(t)$ be a distribution of arbitrary type, and suppose $f_n(t)$ is a sequence in some parameter n. Then if

$$\lim_{n \to \infty} \langle f_n(t), \phi(t) \rangle \to \langle f(t), \phi(t) \rangle, \tag{3.200}$$

then the sequence $f_n(t)$ approaches $f(t)$ in this limit:

$$\lim_{n \to \infty} f_n(t) = f(t). \tag{3.201}$$

3.5.5.1 Approximate Identities for the Dirac Delta. The Dirac delta has been introduced as the derivative of the unit step, a functional which is identically zero along the entire real line except in an infinitesimal neighborhood of the origin. A surprising number of regular distributions—such as the square pulse, suitably scaled functions involving trigonometric functions, and another family generated by Gaussians—approach the Dirac delta when sufficiently scaled and squeezed in the limit in which the scaling factor becomes large. Intuitively, we need normalized, symmetric functions with maxima at the origin and that approach zero on other points along the real line as the appropriate limit (3.201) is taken. This leads to the following theorem.

Theorem (Approximating Identities). Let $f(t)$ be a regular distribution satisfying the criteria:

$$f(t) \in L^1(R), \tag{3.202}$$

$$\int_{-\infty}^{\infty} f(t)\, dt = 1. \tag{3.203}$$

Define

$$f_a(t) \equiv a f(at) \tag{3.204}$$

and stipulate

$$\lim_{a \to \infty} \int_{\tilde{R}} |f_a(t)| = 0, \tag{3.205}$$

where $\tilde{R}$ denotes the real line minus a segment of radius ρ centered around the origin: $\tilde{R} \equiv R / [-\rho, \rho]$.

Then $\lim_{a \to \infty} f_a(t) = \delta(t)$, and $f_a(t)$ is said to be an *approximating identity.*

Proof: First,

$$\left| \langle f_a(t), \phi(t) \rangle - \langle \delta(t), \phi(t) \rangle \right| = \left| \int_{-\infty}^{\infty} a f(at) \phi(t)\, dt - \phi(0) \right|. \tag{3.206}$$

From (3.203) a simple substitution of variables shows $\int_{-\infty}^{\infty} a f(at)\, dt = 1$. We can thus recast the right-hand side of (3.206) into a more convenient form:

$$\left| \int_{-\infty}^{\infty} a f(at) \phi(t)\, dt - \phi(0) \right| = \left| \int_{-\infty}^{\infty} a f(at) \phi(t)\, dt - \int_{-\infty}^{\infty} a f(at) \phi(0)\, dt \right|. \tag{3.207}$$

Dividing the real line into regions near and far from the origin, a change of variables $u \equiv at$ gives

$$\left| \int_{-\infty}^{\infty} f(u) \left[\phi\left(\frac{u}{a}\right) - \phi(0) \right] du \right| = I_1 + I_2 , \tag{3.208}$$

where

$$I_1 = \left| \int_{-\rho/a}^{\rho/a} f(u) \left[\phi\left(\frac{u}{a}\right) - \phi(0) \right] du \right| \tag{3.209}$$

and

$$I_2 = \left| \int_{R/\left(\frac{-\rho}{a}, \frac{\rho}{a}\right)} f(u) \left[\phi\left(\frac{u}{a}\right) - \phi(0) \right] du \right| . \tag{3.210}$$

Since $\phi(t)$ is continuous, for some t suitably close to the origin, we have

$$\left| \phi\left(\frac{u}{a}\right) - \phi(0) \right| < \varepsilon . \tag{3.211}$$

Thus, I_1 is bounded above:

$$I_1 \le \varepsilon \int_{-\rho/a}^{\rho/a} |f(u)| \, du . \tag{3.212}$$

In the second integral, note that there exists some ρ such that

$$\int_{R/\left(\frac{-\rho}{a}, \frac{\rho}{a}\right)} |f(u)| \, du \le \varepsilon . \tag{3.213}$$

Equation (3.210) can be expressed as

$$I_2 \le \int_{R/\left(\frac{-\rho}{a}, \frac{\rho}{a}\right)} \phi\left(\frac{u}{a}\right) |f(u)| \, du - |\phi(0)| \int_{R/\left(\frac{-\rho}{a}, \frac{\rho}{a}\right)} |f(u)| \, du . \tag{3.214}$$

Furthermore, by definition, $\phi(t)$ is bounded above. Consequently,

$$I_2 \le \left| \phi\left(\frac{u}{a}\right) \right|_{\max} \int_{R/\left(\frac{-\rho}{a}, \frac{\rho}{a}\right)} |f(u)| \, du - |\phi(0)| \varepsilon , \tag{3.215}$$

which reduces to

$$I_2 \le \varepsilon \left[\left| \phi\left(\frac{u}{a}\right) \right|_{\max} - |\phi(0)| \right] . \tag{3.216}$$

Returning to (3.206), we have

$$\left|\langle f_a(t),\phi(t)\rangle - \langle \delta(t),\phi(t)\rangle\right| \le \varepsilon\left[\int_{R/\left(\frac{-\rho}{a},\frac{\rho}{a}\right)} |f(u)|\ du + \left|\phi\left(\frac{u}{a}\right)\right|_{\max} - |\phi(0)|\right]. \quad (3.217)$$

In the limit of large a, we have

$$\lim_{a\to\infty} \varepsilon = 0, \quad (3.218)$$

so that

$$\lim_{a\to\infty} \left|\langle f_a(t),\phi(t)\rangle - \langle \delta(t),\phi(t)\rangle\right| = 0 \quad (3.219)$$

and we obtain the desired result. ■

The decay condition (3.205) is equivalent to

$$\lim_{t\to\infty} f(t) = 0, \quad (3.220)$$

which can be stated: for each $\lambda > 0$ there exists $T_\lambda > 0$ such that $|f(t)| < \lambda$ for all $|t| > T_\lambda$. This is equivalent to stating that if $\lambda/a > 0$ there exists $T_{\lambda/a} > 0$ such that $|f(at)| < \lambda/a$ for $|at| > T_{\lambda/a}$. The scaling required to convert $f(t)$ to an approximate identity implies that

$$|af(at)| = a|f(t)| < a\frac{\lambda}{a} < \lambda \quad (3.221)$$

so that

$$\lim_{|t|\to\infty} af(at) = 0. \quad (3.222)$$

Remark. Functions $f(t)$ that satisfy (3.202)–(3.205) are commonly called *weight functions*. They are of more than academic interest, since their localized atomistic character and ability to wrap themselves around a selected location make them useful for generating wavelets (Chapter 11). Such wavelets can zoom in on small-scale signal features. The class of weight functions is by no means small; it includes both uniformly and piecewise continuous functions.

There are several variations on these approximating identities. For example, (3.203) can be relaxed so that if the weight function has arbitrary finite area

$$\Gamma \equiv \int_{-\infty}^{\infty} f(t)\ dt, \quad (3.223)$$

then (3.125) reads

$$\lim_{a \to \infty} f_a(t) = \Gamma\delta(t) . \tag{3.224}$$

The scaling of the amplitude can be modified so that

$$f_a(t) \equiv \sqrt{a} f(at) \tag{3.225}$$

is an approximating identity. The proofs are left as exercises. These approximating identities give the wavelet transform the ability to extract information about the local features in signals, as we will demonstrate in Chapter 11.

We consider several common weight functions below.

Example (Gaussian). Let

$$f(t) = A_0 e^{-t^2/2}, \tag{3.226}$$

where A_0 is a constant. The general Gaussian integral

$$\int_{-\infty}^{\infty} e^{-\alpha y^2} dy \equiv \sqrt{\frac{\pi}{\alpha}} \tag{3.227}$$

implies that

$$A_0 = \frac{1}{\sqrt{2\pi}} \tag{3.228}$$

if $f(t)$ is to have unit area. Note that the ability to normalize the area is proof that $f(t)$ is integrable, so two of the weight function criteria are satisfied. Figure 3.7 illustrates a Gaussian approximate identity

$$f_a(t) = \frac{a}{\sqrt{2\pi}} e^{-(at)^2/2} \tag{3.229}$$

for increasing values of a. The Gaussian is a powerful tool in the development of the continuous wavelet transform. We shall review its role as an approximating identity when we cover the small-scale resolution of the wavelet transform.

Example (Abel's Function). In this case the weight function permits an arbitrary positive-definite parameter β,

$$f(t) = A_0 \frac{\beta}{1 + \beta^2 t^2} . \tag{3.230}$$

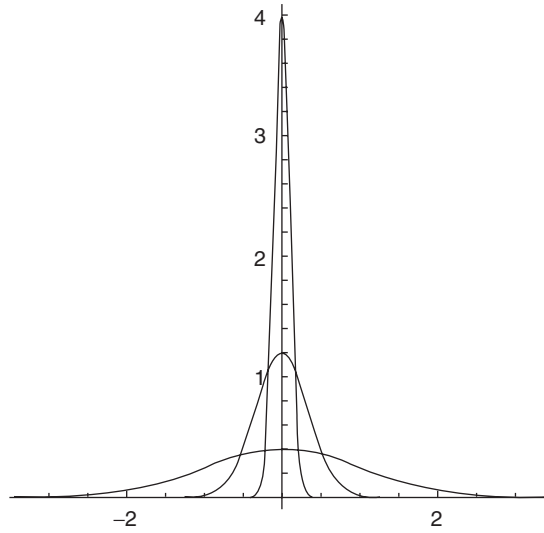

Fig. 3.7. The evolution of the scaled Gaussian (3.229) for $a = 1$ (widest), $a = 3$, and $a = 10$. In the limit $a \to \infty$, the scaled Gaussian approaches a Dirac delta.

It is left as an exercise to show that the condition of unit area requires

$$A_0 = \frac{1}{\pi}. \tag{3.231}$$

For this purpose it is convenient to use the tabulated integral,

$$\int_0^\infty \frac{x^{\mu-1}}{1+x^\nu} dx = \frac{\pi}{\nu} \csc\frac{\mu\pi}{\nu}, \tag{3.232}$$

where $Re\nu > Re\mu > 0$. The resulting approximate identity has the form

$$f_a(t) = \frac{a}{\pi} \frac{\beta}{1 + \left(\frac{\beta}{a}\right)^2 t^2}. \tag{3.233}$$

Example (Decaying Exponential). This weight function is piecewise continuous, but fulfills the required criteria:

$$f(t) = A_0 e^{-|t|}. \tag{3.234}$$

It is left as an exercise to show that $A_0 = 1$, so that $f_a(t) = ae^{-|t/a|}$.

Example (Rectangular Pulse). The unit-area rectangular pulse described by

$$f(t) = \frac{1}{\sigma}[u(t) - u(t-\sigma)] \tag{3.235}$$

approximates a Dirac delta (exercise).

Remark. The weight functions described in this section embody properties that are sufficient to generate approximate identities. These conditions are by no means necessary. The family of sinc pulses

$$f(t) = \frac{1}{\pi}\frac{\sin t}{t} \tag{3.236}$$

does not qualify as a weight function (why not?), yet it can be shown that

$$\lim_{a \to \infty} \frac{1}{\pi}\frac{\sin at}{t} = \delta(t). \tag{3.237}$$

Note that the scale is applied only in the numerator. The properties of this approximate identity are explored in the exercises.

3.5.5.2 The Riemann–Lebesgue Lemma. Much of signal analysis involves the study of spectral content—the relative contributions from individual pure tones or oscillations at given frequency ω, represented by $\sin(\omega t)$ and $\cos(\omega t)$. The behavior of these oscillations as $\omega \to \infty$ is not predicted classically, but by treating the complex exponential $e^{j\omega t}$ as a regular distribution, the foregoing theory predicts that $\sin(\omega t)$ and $\cos(\omega t)$ vanish identically in the limit of high frequency. This result is useful in several subsequent developments.

Theorem (Riemann–Lebesgue Lemma). Let $f(t) \equiv e^{-j\omega t}$. If $\phi(t)$ is a test function of compact support on the interval $t \in [t_1, t_2]$, then

$$\lim_{\omega \to \infty} \int_{-\infty}^{\infty} f(t)\phi(t)\, dt = 0. \tag{3.238}$$

Proof: It is convenient to define a $g(t)$ such that

$$\frac{dg}{dt} \equiv f(t) = e^{-j\omega t} \tag{3.239}$$

and apply integration by parts to obtain

$$\int_{t_1}^{t_2} \frac{dg}{dt}\phi(t)\, dt = g(t)\phi(t)\Big|_{t_1}^{t_2} - \int_{t_1}^{t_2} g(t)\frac{d\phi}{dt}\, dt. \tag{3.240}$$

Then

$$\int_{t_1}^{t_2} e^{-j\omega t}\phi(t)\, dt = \frac{1}{j\omega}[\phi(t_2)e^{-j\omega t_2} - \phi(t_1)e^{-j\omega t_1}] + \frac{1}{j\omega}\int_{t_1}^{t_2} e^{-j\omega t}\frac{d\phi}{dt}\, dt. \tag{3.241}$$

By definition, the test function is bounded. Hence,

$$\left|\phi(t)e^{-j\omega t}\right| \le |\phi(t)|\left|e^{-j\omega t}\right| \le |\phi(t)|, \tag{3.242}$$

and the numerator of the first term in (3.241) is bounded. Consequently, in the limit $\omega \to 0$, this first term vanishes. The integral in the second term is also finite (it is the Fourier transform of $\frac{d\phi}{dt}$), and we defer proof of its boundedness until Chapter 5. Finally,

$$\lim_{\omega \to \infty} e^{-j\omega t} = 0. \tag{3.243}$$

By extension, the real and imaginary parts of this exponential ($\cos(\omega t)$ and $\sin(\omega t)$) also vanish identically in this limit. ■

Remark. Test functions of compact support, as used herein, greatly simplify matters. When $(t_1, t_2) \to (-\infty, \infty)$, thus generalizing the result to all t, the same result obtains; we omit the complete proof, which is quite technical.

3.6 SUMMARY

Analog signal processing builds directly upon the foundation of continuous domain function theory afforded by calculus [6] and basic topology of sets of real numbers [22]. An analog system accepts an input signal and alters it to produce an output analog signal—a simple concept as long as the operations involve sums, scalar multiplications, translations, and so on. Linear, translation-invariant systems appear in nature and engineering. The notion is a mix of simple operations, and although there was a very straightforward theory of discrete LTI systems and discrete impulse response $\delta(n)$, replacing the n by a t stirs up serious complications.

Informal arguments deliver an analog equivalent of the convolution theorem, and they ought to be good enough justification for most readers. Others might worry about the analog impulse's scaling property and the supposition that an ordinary signal $x(t)$ decomposes into a linear combination of Diracs. But rigorous justification is possible by way of distribution theory [8–10].

Analog signals of certain classes, of which the L^p signals are especially convenient for signal processing, form elegant mathematical structures: normed spaces, Banach spaces, inner product, and Hilbert spaces. The inner product is a natural measure of similarity between signals. Completeness, or closure under limit operations, exists in Banach and Hilbert spaces and allows for incremental approximation of signals. Many of the results from discrete theory are purely algebraic in nature; we have been able to appropriate them once we show that analog signals—having rightly chosen a norm or inner product definition, of course—reside in one of the familiar abstract function spaces.

3.6.1 Historical Notes

Distribution theory dates from the mid-1930s with the work of S.L. Sobolev. Independent of the Soviet mathematician, L. Schwartz formalized the notion of a distribution and developed a rigorous delta function theory [7]. Schwartz's lectures are in fact the inspiration for Ref. 8.

Splines were first studied by Schoenberg in 1946 [14]. It is interesting to note that while his paper preceded Shannon's more famous results on sampling and signal reconstruction [50], the signal processing research community overlooked splines for many years.

Mathematicians developed frame theory in the early 1950s and used it to represent functions with Fourier series not involving the usual sinusoidal harmonics [41, 42]. Only some 30 years later did applied mathematicians, physicists, and engineers discover the applicability of the concept to signal analysis [43].

Details on the origins of signal theory, signal spaces, and Hilbert spaces can be found in mathematically oriented histories [51, 52]. Advanced treatments of functional analysis include Refs. 53 and 54.

Lebesgue's own presentation of his integral is given in Ref. 55. This book also contains a short biography of Lebesgue. Lebesgue's approach was the best of many competing approaches to replace the Riemannian integral [56, 57].

3.6.2 Looking Forward

The next chapter covers time-domain signal analysis. Taking representative signal interpretation problems, Chapter 4 attempts to solve them using the tools we have developed so far. The time-domain tools we can formulate, however, turn out to be deficient in analyzing signals that contain periodicities. This motivates the frequency-domain analysis of signals, beginning with the analog Fourier transforms in Chapter 5.

In Chapter 6, the formal development of the Dirac delta as a functional will help build a Fourier transform theory for periodic, constant, and otherwise untransformable analog signals.

3.6.3 Guide to Problems

This chapter includes many basic problems (1–46) that reinforce the ideas of the text. Some mathematical subtleties have been covered but casually in the main text, and the problems help the interested reader pursue and understand them. Of course, in working the problems, the student should feel free to consult the mathematical literature for help. The advanced problems (47–56) require broader, deeper investigation. For example, the last few problems advance the presentation on frames. Searching the literature should provide a number of approaches that have been considered for these problems. Indeed, investigators have not satisfactorily answered all of the questions posed.

REFERENCES

1. A. V. Oppenheim, A. S. Willsky, and S. H. Nawab, *Signals and Systems*, 2nd ed., Upper Saddle River, NJ: Prentice-Hall, 1997.
2. J. A. Cadzow and H. F. Van Landingham, *Signals, Systems, and Transforms*, Englewood Cliffs, New Jersey: Prentice-Hall, 1983.
3. H. Baher, *Analog and Dignal Signal Processing*, New York: Wiley, 1990.
4. R. E. Ziemer, W. H. Tranter, and D. R. Fannin, *Signals and Systems: Continouous and Discrete*, 3rd ed., New York: Macmillan, 1993.
5. L. B. Jackson, Signals, *Systems, and Transforms*, Reading, MA: Addison-Wesley, 1991.
6. M. Rosenlicht, *An Introduction to Analysis*, New York: Dover, 1978.
7. L. Schwartz, *Théorie des Distributions*, vols. I and II, Paris: Hermann, 1950–1951.
8. I. Halperin, *Introduction to the Theory of Distributions*, Toronto: University of Toronto Press, 1952.
9. M. J. Lighthill, *Introduction to Fourier Analysis and Generalized Functions*, New York: Cambridge University Press, 1958.
10. A. H. Zemanian, *Distribution Theory and Transform Analysis*, New York: Dover, 1965.
11. A. Friedman, *Generalized Functions and Partial Differential Equations*, Englewood Cliffs, NJ: Prentice-Hall, 1963.
12. E. M. Stein and G. Weiss, *Introduction to Fourier Analysis on Euclidean Spaces*, Princeton, NJ: Princeton University Press, 1971.
13. L. Debnath and P. Mikusinski, *Introduction to Hilbert Spaces with Applications*, 2nd ed., San Diego, CA: Academic Press, 1999.
14. I. J. Schoenberg, Contribution to the problem of approximation of equidistant data by analytic functions, *Quarterly of Applied Mathematics*, vol. 4, pp. 45–99, 112–141, 1946.
15. J. H. Ahlberg, E. N. Nilson, and J. L. Walsh, *The Theory of Splines and Their Applications*, New York: Academic Press, 1967.
16. D. Hearn and M. P. Baker, *Computer Graphics*, Englewood Cliffs, NJ: Prentice-Hall, 1986.
17. R. H. Bartels, J. C. Beatty, and B. A. Barsky, *Splines for Use in Computer Graphics*, Los Altos, CA: Morgan Kaufmann, 1987.
18. M. Unser, A. Aldroubi, and M. Eden, B-spline signal processing: Part I—theory, *IEEE Transactions on Signal Processing*, vol. 41, no. 2, pp. 821–833, February 1993.
19. M. Unser, A. Aldroubi, and M. Eden, B-spline signal processing: Part II—efficient design and applications, *IEEE Transactions on Signal Processing*, vol. 41, no. 2, pp. 834–848, February 1993.
20. S. Sakakibara, A practice of data smoothing by B-spline wavelets, in C. K. Chui, et al., eds., *Wavelets: Theory, Algorithms, and Applications*, San Diego, CA: Academic Press, pp. 179–196, 1994.
21. M. Unser, Splines: A perfect fit for signal and image processing, *IEEE Signal Processing Magazine*, vol. 16, no. 6, pp. 22–38, November 1999.
22. A. N. Kolmogorov and S. V. Fomin, *Introductory Real Analysis*, translator R. A. Silverman, New York: Dover, 1975.
23. R. Beals, *Advanced Mathematical Analysis*, New York: Springer-Verlag, 1987.

24. H. L. Royden, *Real Analysis*, 2nd ed., Toronto: Macmillan, 1968.
25. A. W. Naylor and G. R. Sell, *Linear Operator Theory in Engineering and Science*, New York: Springer-Verlag, 1982.
26. G. Birkhoff and S. MacLane, *A Survey of Modern Algebra*, New York: Macmillan, 1965.
27. E. Kreysig, *Introductory Functional Analysis with Applications*, New York: Wiley, 1989.
28. H. Dym and H. P. McKean, *Fourier Series and Integrals*, New York: Academic, 1972.
29. N. Young, *An Introduction to Hilbert Space*, Cambridge: Cambridge University Press, 1988.
30. A. Rosenfeld and A. C. Kak, *Digital Picture Processing*, 2nd ed., vol. II, Orlando, FL: Academic, 1982.
31. R. O. Duda and P. E. Hart, *Pattern Classification and Scene Analysis*, New York: Wiley, 1973.
32. S. Haykin, *Communication Systems*, 3rd ed., New York: Wiley, 1994.
33. J. L. Flanagan, A. C. Surendran, and E.-E. Jan, Spatially selective sound capture for speech and audio processing, *Speech Communication*, vol. 13, pp. 207–222, 1993.
34. F. Glazer, G. Reynolds, and P. Anandan, Scene matching by hierarchical correlation, *Proceedings of the IEEE Conference on Computer Vision and Pattern Recognition*, June 19–23, Washington, D.C., pp. 432–441, 1983.
35. P. J. Burt, C. Yen, and X. Xu, Local correlation measures for motion analysis: a comparative study, *Proceedings of the IEEE Conference on Pattern Recogniton and Image Processing*, pp. 269–274, 1982.
36. A. Haar, Zur theorie der orthogonalen Functionensysteme, *Mathematics Annalen*, vol. 69, pp. 331–371, 1910.
37. P. Wojtaszczyk, *A Mathematical Introduction to Wavelets*, Cambridge: Cambridge University Press, 1997.
38. I. Daubechies, *Ten Lectures on Wavelets*, Philadelphia: SIAM Press, 1992.
39. S. Mallat and Z. Zhang Matching pursuits with time-frequency dictionaries, *IEEE Transactions on Signal Processing*, vol. 41, no. 12, pp. 3397–3415, December 1993.
40. Goodwin and M. Vetterli, Matching pursuit and atomic signal models based on recursive filter banks, *IEEE Transactions on Signal Processing*, vol. 47, no. 7, pp. 1890–1902, July 1999.
41. R. J. Duffin and A. C. Schaeffler, A class of nonharmonic Fourier series, *Transactions of the American Mathematical Society*, vol. 72, pp. 341–366, 1952.
42. R. M. Young, *An Introduction to Nonharmonic Fourier Series*, New York: Academic Press, 1980.
43. I. Daubechies, A. Grossmann, and Y. Meyer, Painless nonorthogonal expansions, *Journal of Mathematical Physics*, vol. 27, pp. 1271–1283, 1986.
44. W. Rudin, *Real and Complex Analysis*, 2nd ed., New York: McGraw-Hill, 1974.
45. E. Hewitt and K. Stromberg, *Real and Abstract Analysis*, New York: Springer, 1991.
46. P. R. Halmos, *Naive Set Theory*, New York: Van Nostrand, 1960.
47. J. H. Richards and H. K. Youn, *Theory of Distributions: A Nontechnical Introduction*, New York: Cambridge University Press, 1990.
48. A. Papoulis, *The Fourier Integral and Its Application*, New York: McGraw-Hill, 1962.

49. N. Wiener, *The Fourier Integral and Certain of Its Applications*, New York: Dover Publications, 1958.
50. C. E. Shannon, Communication in the presence of noise, *Proceedings of the Institute of Radio Engineers*, vol. 37, pp. 10–21, 1949.
51. J. Dieudonne, *History of Functional Analysis*, Amsterdam: North-Holland, 1981.
52. J. Stillwell, *Mathematics and Its History*, New York: Springer-Verlag, 1989.
53. K. Yosida, *Functional Analysis*, 6th ed., Berlin: Springer-Verlag, 1980.
54. W. F. Rudin, *Functional Analysis*, 2nd ed., New York: McGraw-Hill, 1991.
55. H. L. Lebesgue, *Measure and the Integral*, edited, with a biography by K. O. May, San Francisco: Holden-Day, 1966.
56. J.-P. Pier, *Development of Mathematics: 1900–1950*, Basel: Birkhaeuser Verlag, 1994.
57. T. Hawkins, *Lebesgue's Theory of Integration: Its Origin and Development*, New York: Chelsea, 1970.

PROBLEMS

1. Find the domain and range of the following analog systems; if necessary, narrow the problem domain to a particular analog signal space.

(a) The amplifier (or attenuator, $|A| < 1$) system: $y(t) = Ax(t)$

(b) A translation system: $y(t) = x(t - a)$

(c) The system on real-valued signals, $y(t) = x(t)^{1/2}$

(d) The system on complex-valued signals, $y(t) = x(t)^{1/2}$

(e) The adder: $y(t) = x(t) + x_0(t)$

(f) Termwise multiplication: $y(t) = x(t) \times x_0(t)$

(g) Convolution: $y(t) = x(t)*h(t)$

(h) Accumulator:

$$y(t) = \int_{-\infty}^{t} x(s)\, ds. \tag{3.244}$$

2. Let $x(t)$ be an analog signal and let H be an analog accumulator system. Show that:

(a) If $x(t)$ has finite support, then $x(t)$ is in the domain of H.

(b) If $x(t)$ is absolutely integrable, then it is in the domain of H.

(c) There are finite energy signals are not in the domain of H. (*Hint*: Provide an example based on the signal $x(t) = t^{-1}$.)

3. Consider the systems in Problem 1.

(a) Which of them are linear?

(b) Which of them are translation-invariant?

(c) Which of them are stable?

4. Suppose that the analog systems H and G are LTI. Let $T = aH$ and $S = H + G$. Show that both T and S are LTI systems.

5. Which of the following systems are linear? translation-invariant? stable? causal?

(a) $y(t) = x(t/2)$

(b) $y(t) = x(2t)$

(c) $y(t) = x(0) + x(t)$

(d) $y(t) = x(-t)$

(e) The system given by

$$y(t) = \int_{-\infty}^{\infty} x(s)\cos(s)\, ds. \tag{3.245}$$

6. Consider the cross-correlation system $y = x^{\circ}h = Hx$, where

$$y(t) = (x^{\circ}h)(t) = \int_{-\infty}^{\infty} x(s)h(t+s)\, ds\,. \tag{3.246}$$

(a) Prove or disprove: H is linear.

(b) Prove or disprove: H is translation-invariant.

(c) Prove or disprove: H is stable.

(d) Is $h(t)$ the impulse response of H? Explain.

(e) Answer these same questions for the autocorrelation operation $y = x^{\circ}x$.

7. An analog LTI system H has impulse response $h(t) = 2e^{t}u(2-t)$, where $u(t)$ is the unit step signal. What is the response of H to $x(t) = u(t+3) - u(t-4)$?

8. Analog LTI system G has impulse response $g(t) = u(t+13) - u(t)$; $u(t)$ is the unit step. What is the response of G to $x(t) = u(t)e^{-t}$?

9. Analog LTI system K has impulse response $k(t) = \delta(t+1) + 2\delta(t-2)$, where $\delta(t)$ is the Dirac delta. What is K's response to $x(t) = u(t-1) - u(t)$?

10. Show that convolution is linear:

(a) $h^{*}(ax) = ah^{*}x$.

(b) $h^{*}(x+y) = h^{*}x + h^{*}y$.

11. Show that if H and G are LTI systems, then $H(G(x)) = G(H(x))$.

12. Show that convolution is associative: $h^{*}(x^{*}y) = (h^{*}x)^{*}y$.

13. Give an alternative argument that $\delta(t) = u'(t)$, the derivative of the unit step [3].

(a) Let $x(t)$ be a signal; show that integration by parts implies

$$\int_{-\infty}^{\infty} x(t)\frac{d}{dt}u(t)\, dt = x(t)u(t)\Big|_{-\infty}^{\infty} - \int_{-\infty}^{\infty} x'(t)u(t)\, dt. \tag{3.247}$$

(b) Remove $u(t)$ from the final integrand in (3.247) and correct the limits of integration.

(c) Show that

$$\int_{-\infty}^{\infty} x(t)\frac{d}{dt}u(t)\,dt = x(0)\,, \tag{3.248}$$

which is the sifting property once again; hence, $\delta(t) = \frac{d}{dt}u(t)$.

14. Suppose the function (an analog signal) $x(t)$ is uniformly continuous over some real interval $I = (a, b)$. This means that for every $\varepsilon > 0$, there is a $\Delta > 0$ such that if s, $t \in I$ with $|s - t| < \Delta$, then $|x(s) - x(t)| < \varepsilon$. We allow the cases that $a = -\infty$, $b = \infty$, or both.

(a) Show that the signal $\sin(t)$ is uniformly continuous on $\mathbb{R}$.

(b) Show that $\exp(t)$ is not uniformly continuous on $\mathbb{R}$.

(c) Show that $x(t) = t^2$ is uniformly continuous on any finite interval (a, b), but not on any unbounded interval ($a = -\infty$, $b = \infty$, or both).

(d) Show that $x(t) = \sqrt{|t|}$ is not uniformly continuous on any interval that includes the origin.

(e) Prove or disprove: If $x(t)$ is continuous and differentiable and has a bounded derivative in the interval (a, b), then $x(t)$ is uniformly continuous on (a, b).

15. Suppose the sequence $\{x_n(t) \in \mathbb{N}\}$ converges uniformly on some real time interval (a, b). That is, every $\varepsilon > 0$ there is an $N_\varepsilon > 0$ such that $m, n > N_\varepsilon$ implies that for all $t \in I$ we have $|y_n(t) - y_m(t)| < \varepsilon$.

(a) Show that if each $x_n(t)$ is continuous, then the limit $x(t) = \lim_{n \to \infty} x_n(t)$ is also continuous.

(b) Show that $x(t)$ may not be continuous if the convergence is not uniform.

(c) Prove or disprove: If each $x_n(t)$ is bounded, then $x(t)$ is also bounded.

16. This problem explores interchanging limit and integration operations [6]. Suppose the signal $x_n(t)$ is defined for $n > 0$ by

$$x_n(t) = \begin{cases} 4n^2 t & \text{if } 0 \le t \le \dfrac{1}{2n}, \\ 4n - 4n^2 t & \text{if } \dfrac{1}{2n} \le t \le \dfrac{1}{n}, \\ 0 & \text{if otherwise.} \end{cases} \tag{3.249}$$

(a) Show that $x_n(t)$ is continuous and integrates to unity on (0, 1).

$$\int_0^1 x_n(t)\,dt = 1 \tag{3.250}$$

(b) Let $x(t) = \lim_{n \to \infty} x_n(t)$. Show that $x(t) = 0$ for all $t \in \mathbb{R}$.

(c) Conclude that

$$\int_0^1 x(t)\, dt \neq \lim_{n \to \infty} \int_0^1 x_n(t)\, dt. \tag{3.251}$$

17. Let $\{x_n(t)\}$ be continuous and converge uniformly on the real interval $[a, b]$ to $x(t)$.

(a) Show that $x(t)$ is continuous and therefore Riemann integrable on $[a, b]$.

(b) Using the uniform continuity, find a bound for the integral of $x_n(t) - x(t)$.

(c) Finally, show that

$$\lim_{n \to \infty} \int_a^b x_n(t)\, dt = \int_a^b x(t)\, dt. \tag{3.252}$$

18. Prove (3.252) assuming that $\{x_n(t)\}$ converge uniformly and are Riemann-integrable (but not necessarily continuous) on $[a, b]$.

(a) Approximate $x_n(t)$ by step functions.

(b) Show that the limit $x(t)$ is Riemann-integrable on $[a, b]$.

(c) Conclude that the previous problem applies and (3.252) holds once again [6].

19. Suppose that the sequence $\{x_n(t) \in \mathbb{N}\}$ converges uniformly on some real interval $I = (a, b)$ to $x(t)$; that each $x_n(t)$ is continuously differentiable on I; that for some $c \in I$, $\{x_n(c)\}$ converges; and that the sequence $\{x_n'(t)\}$ converges uniformly on I.

(a) Show that for all $n \in \mathbb{N}$ and all $t \in I$,

$$x_n(t) - x_n(a) = \int_a^t x_n'(s)\, ds. \tag{3.253}$$

(b) By the previous problem, $\lim [x_n(t) - x_n(a)]$ exists and

$$\lim_{n \to \infty} [x_n(t) - x_n(a)] = \int_a^t \lim_{n \to \infty} x_n'(s)\, ds = x(t) - x(a). \tag{3.254}$$

(c) So by the fundamental theorem of calculus [6], we have

$$\lim_{n \to \infty} x_n'(t) = x(t). \tag{3.255}$$

20. Using informal arguments, show the following properties of the Dirac delta:

(a) $\delta(-t) = \delta(t)$.

(b)

$$\int_{-\infty}^{\infty} x(t)\frac{d}{dt}u(t)\ dt = x(0). \tag{3.256}$$

(c) Assuming the Dirac is differentiable and that interchange of differentiation and integration is permissable, show that

$$\int_{-\infty}^{\infty} x(t)\frac{d^n}{dt^n}\delta(t)\ dt = (-1)^n \frac{d^n}{dt^n}x(t)\bigg|_{t=0}. \tag{3.257}$$

21. Show that the nth-order B–spline $\beta_n(t)$ has compact support.

22. Let $\beta_n(t)$ be the nth-order B-spline. Show the following [21]:

(a)

$$\frac{d}{dt}\beta_n(t) = \beta_{n-1}\left(t+\frac{1}{2}\right) - \beta_{n-1}\left(t-\frac{1}{2}\right). \tag{3.258}$$

(b)

$$\int_{-\infty}^{t} \beta_n(s)\ ds = \sum_{k=0}^{\infty} \beta_{n+1}\left(t-\frac{1}{2}-k\right). \tag{3.259}$$

23. Assuming that $\|x\|_1 < \infty$ and $\|y\|_\infty < \infty$, show that $\|xy\|_1 \le \|x\|_1\|y\|_\infty$.

24. If $\|x\|_\infty < \infty$ and $\|y\|_\infty < \infty$, show $\|x+y\|_\infty \le \|x\|_\infty + \|y\|_\infty$.

25. Let X be the set of continuous, p-integrable signals x: $[a, b] \to \mathbb{K}$, where $a < b$ and $\mathbb{K}$ is either $\mathbb{R}$ or $\mathbb{C}$. Show that $(X, \|x\|_p, {}_{[a,b]})$ is a normed linear space.

26. Let X be a normed linear space. Show that the norm is a continuous map: For any $x \in X$ and $\varepsilon > 0$ there is a $\delta > 0$ such that for any $y \in X$, if $\|y - x\| < \delta$, then $|\,\|y\| - \|x\|\,| < \varepsilon$. Show continuity for the algebraic operations on X: addition and scalar multiplication.

27. Show that the map $d(x, y) = \|x - y\|_p$ is a metric. How must the set of signals $x(t)$ be restricted in order to rigorously show this result? Explain how to remove the restrictions.

28. Suppose $a \sim b$ is an equivalence relation on a set S. Show that $\{[a]: a \in S\}$ partitions S.

29. Consider the analog signals having at most a finite number of discontinuities on $[a, b]$, where $a < b$, and let $1 \le p < \infty$. We restrict ourselves to the Riemann integral, suitably extended to handle piecewise continuous functions.

(a) Show that the set of all such signals does not constitute a normed linear space. In particular, exhibit a signal $x(t)$ which is nonzero and yet $\|x\|_p = 0$.

(b) Show that the relation $x \sim y$ if and only if $\|y\|_p = \|x\|_p$ is an equivalence relation.

(c) Let $[x] = \{y(t): \|y\|_p = \|x\|_p\}$. Show that $[x] = [y]$ if and only if $x(t)$ and $y(t)$ are identical except at a finite number of points.

(d) Define $\underline{\mathbf{L}}^p[a, b] = \{[x] \mid x \in L^p[a, b]\}$. Further define an addition operation on these equivalence classes by $[x] + [y] = [s(t)]$, where $s(t) = x(t) + y(t)$. Show that this addition operation makes $\underline{\mathbf{L}}^p[a, b]$ into an additive Abelian group: it is commutative, associative, has an identity element, and each element has an additive inverse. Explain the nature of the identity element for $\underline{\mathbf{L}}^p[a, b]$. For a given $[x] \in \underline{\mathbf{L}}^p[a, b]$, what is its additive inverse, $-[x]$? Explain.

(e) Define scalar multiplication for $\underline{\mathbf{L}}^p[a, b]$ by $c[x] = [cx(t)]$. Show that $\underline{\mathbf{L}}^p[a, b]$ thereby becomes a vector space.

(f) Define a norm on $\underline{\mathbf{L}}^p[a, b]$ by $\|[x]\|_p = \|x\|_p$. Show that this makes $\underline{\mathbf{L}}^p[a, b]$ into a normed linear space.

(g) Apply the same reasoning to $L^p(\mathbb{R})$.

30. Suppose X is a normed linear space and $x, y \in X$. Applying the triangle inequality to the expression $x_n = x_m + x_n - x_m$, show that $\left|\|x_n\| - \|x_m\|\right| \leq \|x_n - x_m\|$.

31. Let $S = \{x_n\}$ and $T = \{y_n\}$ be Cauchy sequences in a normed linear space X. Define the relation $S \sim T$ to mean that S and T get arbitrarily close to one another, that is, $\lim_{n\to\infty}\|x_n - y_n\| = 0$.

(a) Show that ~ is an equivalence relation.

(b) Let $[S] = \{T: T \sim S\}$; set $B = \{[S]: S = \{x_n\}$ is Cauchy in $X\}$. Define addition and scalar multiplication on B. Show that these operations are well-defined; and show that B is vector space.

(c) Define a norm for B. Show that it is well-defined, and verify each property.

(d) For $x \in X$, define $f(x) = [\{x_n\}]$, where $x_n = x$ for all n, and let $Y = \text{Range}(f)$. Show that $f: X \to Y$ is a normed linear space isometry.

(e) Show that if C is any other Banach space that contains X, then C contains a Banach subspace that is isometric to $Y = f(X)$, where f is given in (d).

32. If X and Y are normed spaces over $\mathbb{K}$ and $T: X \to Y$ is a linear operator, then show the following:

(a) Range(T) is a normed linear space.

(b) The null space of T is a normed linear space.

(c) The inverse map T^{-1} : Range(T) $\to X$ exists if and only $Tx = 0$ implies $x = 0$.

33. Prove the following alternative version of Schwarz's inequality: If $x, y \in L^2(\mathbb{R})$, then $|\langle x, y\rangle| \leq \|x\|_2\|y\|_2$.

34. Suppose $F = \{f_n(t): n \in \mathbb{Z}\}$ is a frame in a Hilbert space H, and T is the frame operator T given by (3.88). Just to review the definition of the frame operator and inner product properties, please show us that T is linear. From its definition, show that the frame adjoint operator is also linear.

35. Suppose that a linear operator U is positive: $U \geq 0$. Show the following [26]:

(a) If I is the identity map, then $U + I$ is invertible.

(b) If V is a positive operator, then $U + V$ is positive.

36. Show that the following are σ-algebras:

(a) $\wp(\mathbb{R})$, the set of all subsets of $\mathbb{R}$.

(b) $\{\varnothing, \mathbb{R}\}$.

37. Let $S \subset \mathcal{P}(\mathbb{R})$. Show that there is a smallest σ-algebra that contains S. (The Borel sets is the class where S is the family of open sets in $\mathbb{R}$.)

38. Let Σ be a σ-algebra. Show Σ is closed under countable intersections.

39. Let $\Sigma = \wp(\mathbb{R})$. Show the following are measures:

(a) $\mu(\varnothing) = 0$ and $\mu(A) = \infty$ if $A \neq \varnothing$.

(b) For $A \in \Sigma$, define $\mu(A) = N$ if A contains exactly N elements and $\mu(A) = \infty$ otherwise.

(c) Show that if μ is a measure on Σ and $c > 0$, then $c\mu$ is also a measure on Σ.

40. Show the following properties of lim inf and lim sup:

(a) $\liminf\{a_n\}$ is the smallest limit point in the sequence $\{a_n\}$.

(b) $\limsup\{a_n\}$ is the largest limit point in the sequence $\{a_n\}$.

(c) $\liminf\{a_n\} = \limsup\{a_n\}$ if and only if the sequence $\{a_n\}$ converges to some limit value $a = \lim_{n\to\infty}\{a_n\}$; show that when this limit exists a = $\liminf\{a_n\} = \limsup\{a_n\}$.

(d) If $a_n \leq b_n$, then $\liminf\{a_n\} \leq \liminf\{b_n\}$.

(e) Provide an example of strict inequality in the above.

(f) $\limsup\{-a_n\} = -\liminf\{a_n\}$.

41. Show that the general differential equation governing the nth derivative of the Dirac delta is

$$f(t)\delta^{(n)}(t) = \sum_{m=0}^{n} (-1)^m \cdot \frac{n!}{(n-m)!} f^{(m)}(0)\delta^{(n-m)}(t). \tag{3.260}$$

42. Derive the following:

(a) The scaling law for an arbitrary distribution (3.157).

(b) Associativity (3.159).

43. **(a)** Calculate the amplitude for the unit-area of the Abel function (3.230).

(b) Calculate the amplitude for the unit-area of the decaying exponential (3.234).

(c) Graph each of these approximate identities for scales of $a = 1, 10, 100, 1000$.

(d) Verify that the behavior is consistent with the conditions governing an approximate identity.

44. Show that

(a) The rectangular pulse (3.235) is a weight function for any value of the parameter σ.

(b) Verify that this unit-area pulse acts as an approximate identity by explicitly showing

$$\lim_{a \to \infty} \int_{-\infty}^{\infty} f_a(t)\phi(t)\, dt = \phi(0). \tag{3.261}$$

45. Prove the differentiation theorem for convolution of distributions (3.199).

46. Demonstrate the validity (as approximating identities) of the alternative weight functions expressed by (3.224) and (3.225).

The following problems expand on the text's presentation, require some exploratory thinking, and are suitable for extended projects.

47. Let $1 \le p \le \infty$, $x \in L^p(\mathbb{R})$, and $h \in L^1(\mathbb{R})$.

(a) Show that $|y(t)| \le \int |x(t-s)||h(s)|\, ds$;

(b) $y = x * h \in L^p(\mathbb{R})$;

(c) $\|y\|_p \le \|x\|_p \|h\|_1$.

48. Consider a signal analysis matching application, where signal prototypes $P = \{p_1, p_2, ..., p_M\}$ are compared to candidates $C = \{c_1, c_2, ..., c_N\}$, using a distance measure $d(p, c)$. Explain why each of the following properties of $d(p, c)$ are useful to the application design.

(a) $d(p, c) \ge 0$ for all $p \in P, c \in C$.

(b) $d(p, c) = 0$ if and only if $p = c$.

(c) $d(p, c) = d(c, p)$ for all p, c.

(d) For any s, $d(p, c) \le d(p, s) + d(s, c)$.

Collectively, these properties make the measure $d(p, c)$ a metric. Consider matching applications where the $d(p,c)$ violates one metric property but obeys the other three. What combinations of of the three properties still suffice for a workable matching application? Explain how the deficiency might be overcome. Provide examples of such deficient match measures. Does deleting a particular metric property provide any benefit to the application—for instance, an ambiguity of analysis that could aid the application?

49. Develop the theory of half-infinite analog signals spaces. Provide formal definitions of the half-infinite L^p spaces: $L^p(-\infty, a]$ and $L^p[a, +\infty)$ and show that these are normed linear spaces. Are they complete? Are they inner product spaces? (You may use the Riemann integral to define L^p for this problem.)

50. Using Lebesgue measure to define it, show that L^∞ is complete [44].

51. Study the matched filtering technique of Section 3.3.2.3 for signal pattern detection. Assume that for computer experiments, we approximate analog convolution with discrete sums.

(a) Show that the the Schwarz inequality implies that the method gives a match measure of unit magnitude if and only if the candidate $x(t)$ and prototype $p(t)$ are constant multiples of one another.

(b) Show that we can generalize the match somewhat by subtracting the mean of each signal before computing the normalized cross-correlation, then the normalized cross-correlation has unit magnitude if and only if the signals are related by $x(t) = Ap(t) + B$, for some constants A, B.

(c) Consider what happens when we neglect to normalize the prototype signal. Show that the matching is still satisfactory but that the maximum match value must be the norm of the prototype pattern, $\|p\|$.

(d) Suppose further that we attempt to build a signal detector without normalizing the prototype. Show that this algorithm may fail because it finds false positives. Explain using examples how the match measure can be larger where $x(t)$ in fact is not a constant multiple of $p(t)$.

(e) What are the computational costs of matched filtering?

(f) How can the computational cost be reduced? What are the effects of various fast correlation methods on the matching performance? Justify your results with both theory and experimentation;

(g) Develop some algorithms and demonstrate with experiments how coarse-to-fine matching can be done using normalized cross-correlation [34].

52. Study the exponential and sinusoidal basis decompositions. Assume the exponential signals constitute an orthonormal basis for $L^2[-\pi, \pi]$.

(a) Show that any $x(t) \in L^2[-\pi, \pi]$ can be expressed as a sum of sinusoidal harmonics. From (3.76) set $a_n = c_n + c_{-n}$ and $jb_n = c_{-n} - c_n$. Show that

$$x(t) = \frac{a_0}{2} + \sum_{n=1}^{\infty} a_n \cos(nt) + \sum_{n=1} b_n \sin(nt). \tag{3.262}$$

(b) Give the spanning set for $L^2[-\pi, \pi]$ implied by (3.262).

(c) Show that the sinusoids are also orthogonal.

(d) By dividing up the real line into 2π-wide segments, $[-\pi + 2n\pi, \pi + 2n\pi]$, give an orthonormal basis for $L^2(\mathbb{R})$.

(e) Consider a square-integrable signal on $L^2(\mathbb{R})$, such as a Gaussian $\exp(-At^2)$ for some $A > 0$. Find a formula, based on the inner product on $L^2[-\pi, \pi]$ for the Fourier series coefficients that arise from the basis elements corresponding to this central interval.

(f) Consider the Fourier series expansion on adjacent intervals, say $[-\pi, \pi]$ and $[\pi, 3\pi]$. Show that the convergence of partial sums of the Fourier series to the signal $x(t)$ exhibits artifacts near the endpoints of the intervals. Explain these anomalies in terms of the periodicity of the exponentials (or sinusoids) on each interval.

(g) Does the selection of sinusoidal or exponential basis functions affect the partial convergence anomaly discovered in (e)? Explain.

(h) What happens if we widen the intervals used for fragmenting $\mathbb{R}$? Can this improve the behavior of the convergence at endpoints of the intervals?

(i) Summarize by explaining why identifying frequency components of general square-integrable signals based on sinusoidal and exponential Fourier series expansions can be problematic.

53. Section 3.3.4.4 argued that frame decompositions support basic signal analysis systems. One desirable property left open by that discussion is to precisely characterize the relation between two sets of coefficients that represent the same incoming signal. This exercise provides a partial solution to the uniqueness problem [42]. Let $F = \{f_n(t) : n \in \mathbb{Z}\}$ be a frame in a Hilbert space H, let $T = T_F$ be its associated frame operator (3.88), and let $S = T^*T$.

(a) If $x \in H$, define $a_n = \langle x, S^{-1}f_n \rangle$, and then show that $x = \Sigma a_n f_n$.

(b) If there are $c_n \in \mathbb{C}$ such that $x = \Sigma c_n f_n$, then

$$\sum_n |c_n|^2 = \sum_n |a_n|^2 + \sum_n |a_n - c_n|^2 . \tag{3.263}$$

(c) Explain how the representation of x in terms of the dual frame for F is optimal in some sense.

(d) Develop an algorithm for deriving this optimal representation.

54. Let $F = \{f_n(t): n \in \mathbb{Z}\}$ be a frame in Hilbert space H. Prove the following:

(a) If an element of the frame is removed, then the reduced sequence is either a frame or not complete (closure of its linear span is everything) in H.

(b) Continuing, let $S = T^*T$, where T^* is the adjoint of the frame operator $T = T_F$. Show that if $\langle f_k, S^{-1}f_k \rangle \neq 1$, then $F \setminus \{f_k\}$ is still a frame.

(c) Finally, prove that if $\langle f_k, S^{-1}f_k \rangle = 1$, then $F \setminus \{f_k\}$ is not complete in H.

55. Let us define some variations on the notion of a basis. If $E = \{e_n\}$ is a sequence in a Hilbert space H, then E is a *basis* if for each $x \in H$ there are unique complex scalars a_n such that x is a series summation, $x = \Sigma_n a_n e_n$. The basis E is *bounded* if $0 \leq \inf\{e_n\} \leq \sup\{e_n\} < \infty$. The basis is *unconditional* if the series converges unconditionally for every element x in H. This last result shows that the uniqueness of the decomposition coefficients in a signal processing system can in fact be guaranteed when the frame is chosen to be *exact*. Let $F = \{f_n(t): n \in \mathbb{Z}\}$ be a sequence in a Hilbert space H. Show that F is an exact frame if and only if it is a bounded unconditional basis for H.

56. Repeat Problem 52, except allow for a frame-based signal decomposition. In what ways does the presence of redundancy positively and negatively affect the resulting decompositions?

CHAPTER 4

Time-Domain Signal Analysis

This chapter surveys methods for time-domain signal analysis. Signal analysis finds the significant structures, recognizable components, shapes, and features within a signal. By working with signals as functions of a discrete or analog time variable, we perform what is called time-domain signal analysis. We view signals as discrete or analog functions. We distinguish one signal from another by the significant differences in their magnitudes at points in time. Ultimately, then, time-domain methods rely in a central way on the level of the signal at an instant, over an interval, or over the entire domain of the signal. Our analysis tools will be both crude and sophisticated, and our achievements will be both problematic and successful. From the perspective of Hilbert space analysis, we will find that our time-domain signal analysis methods often involve the use of basis functions for signal subspaces that have irregular, blocky shapes.

Signal analysis does encompass many signal processing techniques, but it ultimately goes beyond the signal-in, signal-out framework: Signal analysis breaks an input signal down into a nonsignal form. The output could be, for example, an interpretation of the input, recognition results, or a structural description of the source signal. In time-domain analysis we study signals without first deriving their frequency content. Signals are viewed simply as functions of time (or of another independent spatial variable). This chapter's methods depend upon the foundation in determinate and indeterminate signals, systems, and Hilbert space laid previously, together with some calculus, differential geometry, and differential equations. In contrast, a frequency-domain analysis finds the frequencies within a signal by way of Fourier transformation—or, in more modern vein, using the Gabor or wavelet transforms—and uses the frequency information to interpret the signal.

After some philosophical motivation, this chapter considers some elementary signal segmentation examples. This discussion identifies problems of noise, magnitude, frequency, and scale in detecting special signal regions. Signal edges are the obvious boundaries between segmentable signal regions, but detecting them reliably and optimally proves to be harder that it would seem at first glance. Matched filtering is introduced, but the theoretical justifications are postponed. Scale space decomposition gives a complete and general method for the segmentation and structural description of a signal. Pattern recognition networks offer a hybrid scheme for signal detection.

Signal Analysis: Time, Frequency, Scale, and Structure, by Ronald L. Allen and Duncan W. Mills
ISBN: 0-471-23441-9

They combine ideas from matched filtering and decomposition by scale; provide for design rules, as in conventional pattern recognition systems; and have a network training scheme similar to neural networks. Hidden Markov models (HMMs) are a statistical recognition tool applied widely in speech and text interpretation. Later chapters will expand these techniques further by showing how to use these signal decomposition tools with frequency and mixed-domain signal processing.

We shall cover in this chapter, as promised, signal analysis techniques that are not commonly found in the standard signal processing texts. But we do more than validate the title of the whole book. By confronting the deep problems involved in finding the content and structure of signals, right after basic presentations on linear systems, we will find both a motivation and a conceptual foundation for the study of frequency and scale in signals. The first three chapters embellished the traditional presentation of signal processing—discrete and analog signals, random signals, periodicity, linear systems—with an introductory development of the theory of Hilbert spaces. The important Hilbert space notion of inner product gives us a theoretical tool for finding the similarity of two signals and therefore a point of departure for finding one signal shape within another. Now the exposition tilts toward techniques for breaking an input signal down into a nonsignal form.

Time-domain signal analysis will prove to have some serious limitations. Some types of signals will prove amenable to the time-domain methods. We can engineer signal analysis solutions for many process monitoring problems using time-domain techniques. Other application areas—especially those where signals contain periodic components—will cause trouble for our methods. Speech recognition and vibration analysis are examples. For such applications, the signal level itself is not so important as the regular assumption of some set of values by the signal. If we retreat again to the abstract vantage point of Hilbert space, we will see that our methods must now rely on basis functions for signals that are regular, textured, periodic, sinusoidal, exponential, and so on. Although this discovery qualifies our successes in preliminary signal analysis applications, it leads naturally to the study of the Fourier transforms of analog and discrete signals, and later it leads to the modern mixed-domain techniques: time-frequency and time-scale transforms.

This decomposition into structural features may be passed on to higher-level interpretation algorithms. Machine recognition of digitized speech is an example. So, by this view, signal analysis is the front-line discipline within artificial intelligence. While it makes extensive use of standard signal processing techniques, the analysis of a signal into some interpretable format is a distinct, challenging, and perhaps neglected area of engineering education and practice.

A small diagram, due to Professor Azriel Rosenfeld,[1] who first formulated it for images, illustrates the relationships between data processing, image synthesis (graphics), image processing, and image analysis (computer vision) (Figure 4.1a). Reducing the dimension of the data, we arrive at a similar diagram for signals (Figure 4.1b)

[1]For many years Professor Rosenfeld has used this diagram in his computer vision courses (personal communication). The authors have often heard—and, in the absence of a contrary reference in the scientific literature, do believe—that the diagram is attributable to Azriel Rosenfeld.

(a)

Output \ Input	Data	Image
Data	Data processing	Computer vision
Image	Computer graphics	Image processing

(b)

Output \ Input	Data	Signal
Data	Data processing	Signal analysis
Signal	Signal synthesis	Signal processing

Fig. 4.1. (a) An input–output diagram of the disciplines that work with two-dimensional signals (i.e., images). Conventional data processing began as soon as programmable machines became available. Image processing (for example, enhancement) has been a successful technology since the 1960s. With the advent of parallel processing and fast reduced instruction set computers, computer graphics has reached such a level of maturity that is both appreciated and expected by the public in general (example: morphing effects in cinema). Computer vision stands apart as the one technology of the four that remains problematic. We seem to be decades away from the development of autonomous, intelligent, vision-based machines. (b) An input–output diagram of the computer technologies that use signals. The rediscovery of the fast Fourier transform in the mid-1960s gave digital signal processing a tremendous boost. Computer music is now commonplace, with an example of signal synthesis possible even on desktop computers since the 1980s. Like computer vision, though, signal analysis is still an elusive technology. Where such systems are deployed, they are greatly constrained, lack generality, and adapt poorly, if at all, to variations in their signal diets.

and reveal the input–output relationships between data processing, signal synthesis, signal analysis, and signal processing. Most computing tasks fall into the data processing categories of Figure 4.1, which covers financial and accounting programs, database applications, scientific applications, numerical methods, control programs, and so on. Signal processing occupies the other diagonal square, where signal data are output from a signal data input. The other squares, converting data to signal information and converting signal information to data, generally do not correspond to classes in the university curriculum, except perhaps in some specialized programs or big departments that offer many courses. An application that accepts abstract data inputs and produces a signal output is an example of a signal synthesis system. Courses such as this have been quite rare. Recently, though, some computer science departments are offering multimedia courses that cover some aspects of producing digital music, speech, and sounds. A computer program that accepts a signal and from it generates a data output is in essence a signal analysis system. It is really the form of the data output that is critical, of course. We envision a description—a breakdown of content, or an *analysis*—of the signal that does not resemble the original at all in form.

The great advances in mixed-domain signal transforms over the last 10 years are the primary reason for reworking the conventional approach to signals. These time-frequency and time-scale transforms cast new light on the Fourier transform, expose its limitations, and point to algorithms and techniques that were either impossible or terribly awkward using the standard Fourier tools. Moreover, advances in computer hardware and software make technologies based on this new theory practically realizable. Applications—commercial products, too—are appearing for speech understanding, automatic translation, fingerprint identification, industrial process control, fault detection, vibration analysis, and so on. An unexpected influence on these emerging signal analysis techniques comes from biology. Research into hearing, vision, the brain, psychophysics, and neurology has been supplemented and stimulated by the investigations into the mathematics of the new signal transforms, neural networks, and artificial intelligence. This book will show that a fruitful interaction of artificial intelligence and signal analysis methods is possible. It will introduce students, engineers, and scientists to the fresh, rapidly advancing disciplines of time-frequency and time-scale signal analysis techniques.

In universities, signal processing is taught in both computer science and electrical engineering departments. (Its methods often arise in other disciplines such as mathematics, mechanical engineering, chemical engineering, and physics.) The courses are often almost identical by their course descriptions. There is controversy, though, about whether signal processing even belongs in the computer science curriculum, so similar in content is it to the electrical engineering course. One point of this book is to show that mainstream computer science methods are applicable to signal analysis, especially as concerns the computer implementation of algorithms and the higher-level interpretation methods necessary for complete signal analysis applications.

Signal analysis includes such technologies as speech recognition [1–4], seismic signal analysis [5, 6], interpretation of medical instrumentation outputs [7], fault detection [8], and online handwriting recognition [9]. Computer user interfaces may

nowadays comprise all of the Rosenfeld diagram's technologies for both one-dimensional signals and two-dimensional signals (images): speech synthesis and recognition; image generation, processing, and interpretation; artificial intelligence; and conventional user shells and services [10, 11].

It is possible to slant a signal processing course to computer science course themes. Here, for example, we explore time-domain signal analysis and will see that tree structures can be found for signals using certain methods. One can also emphasize signal transforms in computer science signal processing instead of the design of digital filters which is taught with emphasis in the electrical engineering signal processing course. This too we will explore; however, this task we must postpone until we acquire an understanding of signal frequency through the various Fourier transforms. There are filter design packages nowadays that completely automate the design process, anyway. Understanding transforms is, however, essential for going forward into image processing and computer vision. Finally, one also notices that signal processing algorithms—with complex-valued functions, arrays having negative indices, dynamic tree structures, and so forth—can be elegantly implemented using modern computer languages known almost exclusively by students in the university's computer science department.

In the first sections of this chapter, we consider methods for finding basic features of signals: edges and textures. An edge occurs in a signal when its values change significantly in magnitude. The notion of texture seems to defy formal description; at an intuitive level, it can be understood as a pattern or repetition of edges. We develop several techniques for finding edges and textures, compare them, and discover some problems with their application. Edge and texture detection will not be complete in this chapter. Later, having worked out the details of the Fourier, short-time Fourier, and wavelet transforms, we shall return to edge and texture analysis to check whether these frequency-domain and mixed-domain methods shed light on the detection problems we uncover here.

4.1 SEGMENTATION

Segmentation is the process of breaking down a signal into disjoint regions. The union of the individual regions must be the entire domain of the signal. Each signal segment typically obeys some rule, satisfies some property, or has some numerical parameter associated with it, and so it can be distinguished from neighboring segments. In speech recognition, for example, there may be a segmentation step that finds those intervals which contain an utterance and accurately separates them from those that consist of nothing but noise or background sounds.

This section begins with an outline of the formal concept of segmentation. There are many approaches to the segmentation task, and research continues to add new techniques. We shall confine our discussion to three broad areas: methods based on signal levels, techniques for finding various textures within a signal, and region growing and merging strategies. Later sections of this chapter and later chapters in the book will add further to the segmentation drawer of the signal analysis toolbox.

4.1.1 Basic Concepts

Segmentation is a rudimentary type of signal analysis. Informally, segmentation breaks a signal's domain down into connected regions and assigns a type indication to each region. For signals, the regions are intervals: open, half-open, or closed. Perhaps a region is a single point. Some thinking in the design of a signal segmentation method usually goes into deciding how to handle the transition points between regions. Should the algorithm designer consider these boundaries to be separate regions or deem them part of one of the neighboring segments? This is not too difficult a question, and the next section's edge detection methods will prove useful for advanced segmentation strategies. However, for two-dimensional signals (images) the situation is extremely complex. The connected regions can assume quite complicated shapes[2]; and their discovery, description, and graphical representation by machine too often bring current computer vision systems to their practical limits.

Definition (Segmentation). A segmentation $\Sigma = (\Pi, L)$ of a signal f consists of a partition $\Pi = \{S_1, S_2, ...\}$ of $\mathrm{Dom}(f)$ into regions and a logical predicate L that applies to subsets of $\mathrm{Dom}(f)$. The predicate L identifies each S_i as a maximal region in which f is homogeneous. Precisely, then, segmentation requires the following [12]:

- $\mathrm{Dom}(f) = S_1 \cup S_2 \cup S_3 \cup ...$, where the S_i are disjoint.
- $L(S_i)$ = True for all i.
- $L(S_i \cup S_j)$ = False when S_i and S_j are adjacent in $\mathrm{Dom}(f)$ and $i \neq j$.

It is common to call the regions segments, but they are not necessarily intervals. Commonly, the segments are finite in number, only a specific region of interest within the signal domain is subject to segmentation, and some mathematical operation on the signal defines the logical predicate. It is also very much an application-specific predicate. For example, one elementary technique to segment the meaningful parts of a signal from background noise is to threshold the signal. Let $f(n)$ be a noisy signal, $T > 0$, $M = \{n: |f(n)| \geq T\}$, and $N = \{n: |f(n)| < T\}$. Let $\Pi = \{M, N\}$, and let L be the logical predicate "All signal values in this region exceed T or all signal values in this region do not exceed T." Then $S = (\Pi, L)$ is a segmentation of the signal into meaningful signal and background noise regions. Of course, different threshold values produce different segmentations, and it is possible that neither the M nor N is a connected subset of the integers. Most signal analysts, in point of fact, never formulate the logical predicate for segmentation; the predicate is implicit, and it is usually obvious from the computations that define the partition of the signal's domain.

[2]The famous Four-Color Problem is in fact a question of how many types are necessary to lable a map segmented into countries. For every map ever drawn, it had been shown to be possible to color the bounded regions with only four colors. Therefore, conjecture held that four-colorings of the plane were always possible, but for centuries this simple problem defined solution. Only recently, with a grand effort by both humans and computers, has the question been answered in the affirmative.

Definition (Labeling, Features, Pattern). Let $\Pi = \{S_1, S_2, ...\}$ be a partition of the domain of signal f. Then a labeling of f for Π is a map $\Lambda: \Pi \rightarrow \{\Lambda_1, \Lambda_2, ...\}$. $\text{Ran}(\Lambda)$ is the set of labels, which categorize subsets of $\text{Dom}(f)$ in Π. If $\Lambda(S_i) = \Lambda_j$, then S_i is called a signal feature with label Λ_j. A pattern is set of features in a signal.

Labeling often follows segmentation in signal analysis systems. The nature of the signal analysis application determines the set of labels which apply to signal regions. The segmentation operation uses some logical predicate—which embodies an algorithm or computation—to decompose the signal into homogeneous regions. The regions are distinct from one another and suitable for labeling. Together, the segmentation and labeling operations assign distinct signal regions to predetermined categories, appropriate to the application. This results in a primitive description of the signal's content known as feature detection. The task of finding an assemblage of features in a signal is called pattern detection or pattern recognition.

By associating the regions with a label, the positions and time-domain extents of signal features are known. One problem is that the regions of a general segmentation may be disconnected, in which case the feature is located in multiple parts of the signal. This is a little awkward, but, in general, we shall not demand that our segmentations produce connected sets. But the partition elements do contain intervals, and a maximal interval within a segment does specify the location of a feature. Thus, finding the maximal intervals that have a given label accomplishes the signal analysis task of registration.

Definition (Registration). Let f be a signal, $\Sigma = (\Pi, L)$ be a segmentation of f, and let $\Lambda: \Pi \rightarrow \{\Lambda_1, \Lambda_2, ...\}$ be a labeling of f with respect to Σ. If $\Lambda(S_i) = \Lambda_j$, $I \subseteq S_i$ is an (open, closed, or half-open) interval, and I is contained in no other connected subset of S_i, then I registers the feature with label Λ_j.

Higher-level algorithms may process the labeling and revise it according to rules, prior knowledge of the signal's content, or some model of what form the signal should take. Such high-level algorithms may employ a very small set of rules. But many signal analysis applications use a full rule database or implement a complete expert system for interpreting labeled signals. They often use graph and tree structures. By this point, the design of a signal analysis system is well into the realm of artificial intelligence. Without delving deeply into artificial intelligence issues, Section 4.2.4 discusses some elementary statistical measures and algorithms for refining the segmentation and labeling steps. This is called region splitting and merging. Region merging can be a basis for classification. If the goal is to find a sufficiently large signal region or a region with a particular registration, then a region merging procedure applied to the results of a first-cut segmentation might be adequate. Later, in Section 4.7, we will introduce what are called consistent labeling methods for revising the region label assignments. This strategy uses constraints on both the regions and the labels applied to them. The constraints on signal features can be formulated as a directed graph, a familiar data structure from artificial intelligence. When a signal's features can be labeled so as to obey the constraints, which might be derived from a signal prototype or model, then the signal has been classified.

4.1.2 Examples

Some examples of segmentation, labeling, and registration should help to make these abstract concepts more concrete.

Example (Signal versus Noise Detection). A logical predicate, N, for "either noise or signal," may apply to subsets of the domain of a signal, f. (To be precise, we are using the exclusive "or" here: noise or signal, but not containing both characteristics.) A region $R_n \subseteq \text{Dom}(f)$ for which $N(R_n) = \text{True}$ may be a region of noise, and another region $S_n \subseteq \text{Dom}(f)$ for which $N(S_n) = \text{True}$ may be meaningful information. Many applications involve signals whose noise component are of a much lower magnitude than their information-bearing component. (This is not always the case; signals may follow an active-low policy, and the choice of labels for low- and high-magnitude segments must reflect this.) Reasonably, then, we might apply a threshold to the signal for distinguishing signal from noise. Figure 4.2 shows examples of

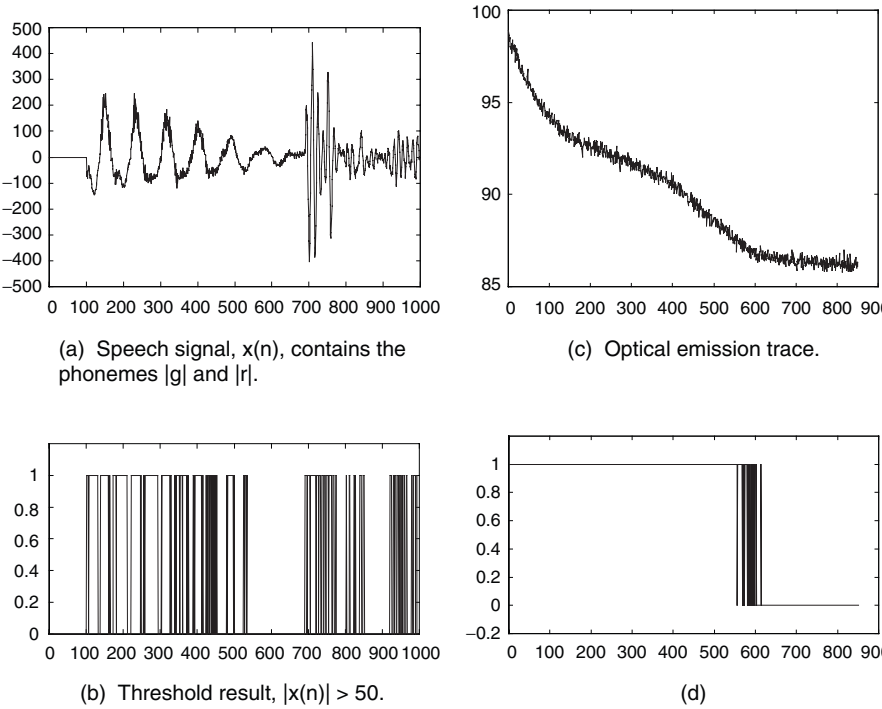

Fig. 4.2. Signal segmentation in speech recognition and industrial process control. Detecting a speaker's presence by thresholding works when the background noise level is sufficiently low (panels (a) and (b)). But background noises or artifacts of speech (tongue clicks, lip smacks, sniffs, sighs, loud breaths) will often be assigned to a speech region. Panels (c) and (d) show a representative optical trace from a plasma etching reactor. The controller monitors a carbon monoxide optical emission signal, whose high level indicates the presence of etching byproducts in the chamber.

signal segmentation based on thresholding. The goal is to separate the signal into a meaningful signal region, which has a high magnitude, and a background noise region, which has a relatively low magnitude. If the noise magnitude remains modest and the meaninful signal regions do not fade, then one-dimensional tasks like this are quite straightforward. Segmenting images into high-magnitude objects and low-magnitude background is called blob detection, an erstwhile colloquialism that has become standard technical parlance over the years. In two dimensions, because of the difficulties in tracking boundaries, blob detection is often problematic. The equivalent one-dimensional task—bump rather than blob detection—is much easier of course, because the topology of the line is simpler than the topology of the plane.

Application (Touch-Tone Telephone Pulse Detection). This example continues our discussion of digital telephony. Touch dialing telephones have largely supplanted the old rotary dialing units in the public service telephone network. Instead of a series of electromechanically generated pulses, modern telephones generate dual-tone multifrequency (DTMF) pulses for dialing [13]. The telephone company's central office (CO) equipment decodes these pulses; sets up the appropriate communication links; rings the far telephone; and sends a ringback signal, which simulates the sound a distant phone ring, to the near-end telephone. When someone lifts the far-end handset, the CO switching equipment sends a brief test tone through the circuit as a continuity check. The CO listens for facsimile (FAX) equipment tones and then for modem tones; in their absence, it initiates echo cancellation (see Chapter 2), and the call is complete. Table 4.1 shows the tone dialing scheme. Figure 4.3 illustrates a dual-tone sinusoidal pulse in noise and a sample segmentation. This segmentation produces two sets; however, due to the sinusoidal components in the pulse, there are numerous low-magnitude signal values interspersed in the time interval where we expect to detect the pulse. One strategy to improve the segmentation is to integrate the signal, and another strategy is to adjust the labeling to eliminate noise segments that are too brief.

Early telephones had two twin-tee feedback oscillators for producing DTMF signals. Later, and cheaper, designs were digital. Nowadays, digital signal processors

TABLE 4.1. DTMF Telephone Dialing Signal Specifications[a]

	1209 Hz	1336 Hz	1477 Hz	1633 Hz
697 Hz	1	2	3	A
770 Hz	4	5	6	B
852 Hz	7	8	9	C
941 Hz	*	0	#	D

[a] DTMF pulses consist of two tones from a high- and a low-frequency group. Telephones in public use do not sport the special keys on the right: A, B, C, D. The telephone company reserves them for test equipment and diagnostic signaling applications. DTMF tones pass at a 10-Hz rate. Pulse width is between 45 ms and 55 ms.

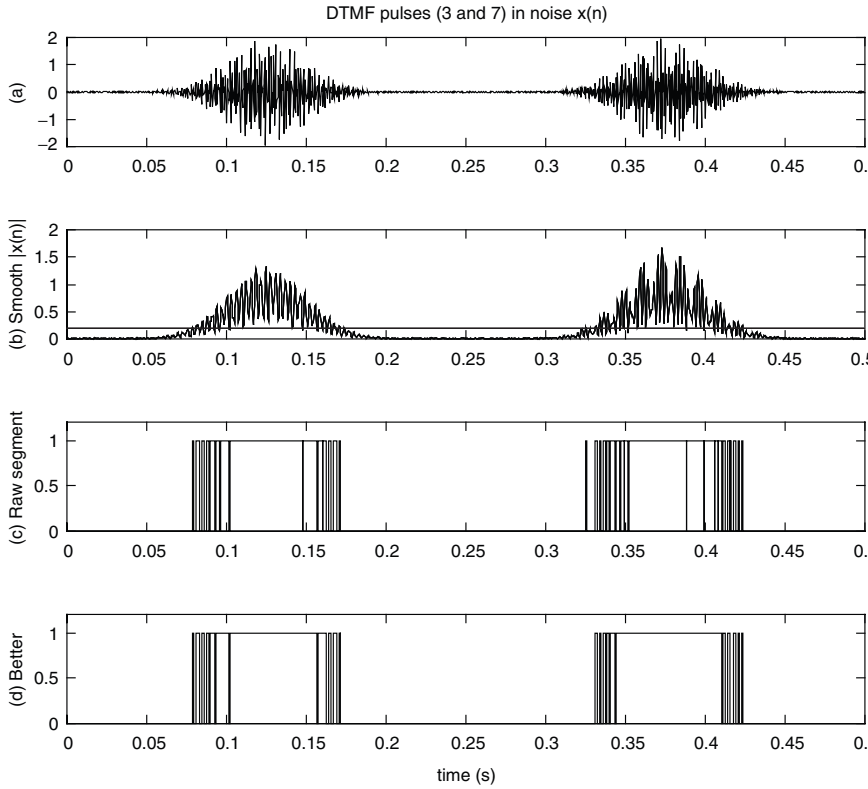

Fig. 4.3. An example of dual-tone multi-frequency (DTMF) pulse detection for telephone company dialing signals. Each number on the telephone dial is coded as a dual frequency pulse (a). Simple threshold (b) and labeling operations (c) mark tones (tone present = 1, background noise = 0). This naive, bottom-up procedure shows that no pulse segment is sufficiently long in duration to be a valid DTMF pulse; hence it finds no pulses present. The improved scheme (d) constrains the labeling operation so that short-duration noise segments are merged with signal regions, thus properly finding two 50-ms-wide pulses. It is possible—and more conventional for that matter—to filter the pulse (in this case its magnitude) for more consistent thresholding rather than rely on consistent labeling.

can be programmed to generate and decode DTMF signals [14, 15]. It is important to note that this example only considers the relatively easy problem of finding a blob-like pulse of the proper width for a DTMF pulse. A complete, practical solution must find the frequencies within the signal blob, verify that only two significant tones exist, and check that the pair of tones corresponds to a cell in Table 4.1. We will consider this more complex task in Chapter 7, after we develop methods for signal frequency analysis in Chapters 5 and 6.

4.1.3 Classification

Following segmentation and labeling, signal analysis may take a further step—classification of the entire signal. Classification is also called recognition. It is much like labeling, except that the term "labeling" in signal and image analysis parlance tends to mean a tentative classification. Labels are applied to small fragments of the signal, meant for later review, and facilitate the application of goal-driven rules. In contrast, the recognition step applies a broader signal region, which comprises several labeled, goal-directed fragments.

Definition (Classification). Let $F = \{f_1, f_2, ...\}$ be a family of signals. Then a classifier for F is a map C: $F \rightarrow \{C_1, C_2, ...\}$. The range of C is the set of classes, which categorize signals in F.

In view of our imprecise distinction between labeling and classifying, and with regard to the overlap of usage within the signal analysis community, we need to be casual about this definition. An application may break a long-term signal down into large regions and attempt to identify each chunk. While analyzing each large region, the remainder of the signal can be considered to be zero, and it is quite irrelevant about whether we deem the remaining chunks to be separate signals or just extended pieces of the original. The distinction, therefore, between labeling and classification revolves around which is the preliminary step and which is the ultimate step in the signal analysis.

The concepts of segmentation, labeling, and classification imply a scheme for constructing signal analysis systems (Figure 4.4). Most signal analysis systems work in the order: segmentation, labeling, classification. This strategy proceeds from low-level signal data, through assignment of labels to signal regions, to finally classify the entire signal. Therefore, this is a data-driven or bottom-up methodology. To impart a goal-driven or top-down aspect to the procedure, it is possible to constrain the labeling procedure. In this case, a high-level, rule-based algorithm reviews the initial labels and adjusts their assignments to signal features. The labeled regions may be too small in extent, as the narrow low-magnitude regions in the example of Fig. 4.3, and hence they are merged into the surrounding meaningful signal region.

Example (Voiced versus Unvoiced Speech Segmentation). Linguists typically classify speech events according to whether the vocal cords vibrate during the pronunciation of a speech sound, called a phone. Phones are speech fragments that represent the basic, abstract components of a natural language, called phonemes (Table 4.2). If the vocal cords do vibrate, then there is said to be a voiced speech event. If there is no vocal cord vibration, then the phoneme is unvoiced. It is also possible that a speech signal contains no speech sound; thus, it is simply background, or noise. One approach to segmenting speech classifies its portions as voiced (V), unvoiced (U), or noise (N). For example, a digital recording of the English phrase "linear fit" begins, divides the two words, and ends with noise

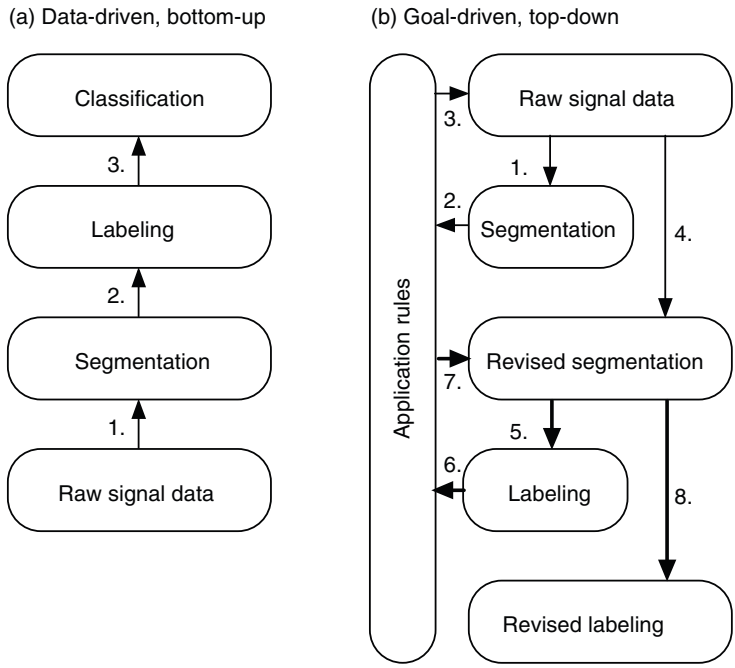

Fig. 4.4. Data-driven versus goal-driven signal analysis systems. In the data-driven, bottom-up scheme of (a), the processing proceeds from segmentation, to labeling, to classification without looking back. The goal-driven, top-down strategy in (b) revises earlier results according to rules specific to the application domain.

regions. The most apparent phonemes, then, are /l I n i ə f I t/, of which /f/ and /t/ are unvoiced. A preliminary segmentation, Σ_0, by voiced/unvoiced/noise classification is (N, V, N, U, V, U, N), respecting the stipulation that no adjacent regions have the same type. Actually, there are a number of unvoiced events that only become apparent when the speech signal is digitized and spread out over time. One may find, for example, momentary unvoiced aspirations and even periods of noise, surrounding the voiced segments. A refined segmentation, Σ_1, therefore supplies: (N, U, V, U, V, U, V, U, V, U, V, U, N, U, V, U, N). In practical speech recognition applications, surprisingly, this segmentation is too crude! Subtle periods of background noise, with no voiced or unvoiced sound present, intrude into spoken words. A modern, sophisticated segmentation algorithm finds that several *N* regions split the unvoiced regions U in the refined segmentation above. This means that several of the unvoiced intervals have much shorter time extents than Σ_1 would indicate. The benefit is that a higher-level interpretation algorithm may be better able to recognize the brief U boundaries of the V segments as trailing and leading aspirations instead

TABLE 4.2. Phonemes and Word Examples from American English [16][a]

Phoneme	Example	Class	Phoneme	Example	Class
/i/	even	Front vowel	/I/	signal	Front vowel
/e/	basis	Front vowel	/ɛ/	met	Front vowel
/ae/	at	Front vowel	/a/	father	Mid vowel
/Λ/	but	Mid vowel	/⊃/	all	Mid vowel
/schwa/	signal	Mid vowel	/u/	boot	Back vowel
/o/	boat	Back vowel	/U/	foot	Back vowel
/Ɨ/	roses	Back vowel	/ɝ/	Hilbert	Mid vowel
/a^{w}/	down	Dipthong	/a^{y}/	cry	Dipthong
/⊃^{y}/	boy	Dipthong	/y/	yet	Semivowel glide
/w/	wit	Semivowel liquid	/r/	rent	Semivowel glide
/l/	linear	Semivowel liquid	/m/	segment	Nasal consonant
/n/	nose	Nasal consonant	/ŋ/	Nguyen	Nasal consonant
/p/	partition	Unvoiced stop	/t/	fit	Unvoiced stop
/k/	kitten	Unvoiced stop	/b/	bet	Voiced stop
/d/	dog	Voiced stop	/g/	gain	Voiced stop
/h/	help	Aspiration	/f/	fit	Unvoiced fricative
/θ/	thanks	Unvoiced fricative	/s/	sample	Unvoiced fricative
/sh/	shape	Unvoiced fricative	/v/	vector	Voiced fricative
/∂/	that	Voiced fricative	/z/	zoo	Voiced fricative
/zh/	closure	Voiced fricative	/ch/	channel	Affricate
/j/	Jim	Affricate	/ʔ/	no sound	Glottal stop

[a]Vowels are voiced, and they break down further into front, mid, and back classifications, according to the location of the tongue's hump in the mouth. Other essentially vowel-like sounds are the dipthongs and the semivowels. Nasal consonants are voiced, and the affricates are unvoiced. The glottal stop is a special symbol that indicates a momentary suspension of motion by the vocal cords (glottis). For example, without the /ʔ/ symbol, the phoneme sequences for "I scream" and "ice cream" are identical. As big as it is, this table is far from panoramic; it offers but a glimpse of the natural language segmentation problem.

of, for example, unvoiced fricatives. Figure 4.5 illustrates such a speech segmentation example. We shall continue to expose the intricacies of natural language interpretation is this and the remaining chapters; there is much to cover.

Many problems involve a combination of segmentation procedures. For example, in digital telephony, it may be necessary to distinguish voice from DTMF pulses. Many commercial telephony applications that rely on DTMF detection require this capability. A pervasive—some would call it pernicious—application is the office voice mail system. The user presses telephone buttons to control the selection, playback, archival, and deletion of recorded messages. The voice mail application detects the DTMF and performs the appropriate function. Background office noise or talking confuses the DTMF classifier. Thus, a sophisticated DTMF detector sorts out the many possible natural language sounds from the dual-tone signaling pulses. Vowel sounds, such as /i/ and /u/, typically contain two sinusoidal components; and unvoiced fricatives, such as /s/ and /f/, are hard to discern from background

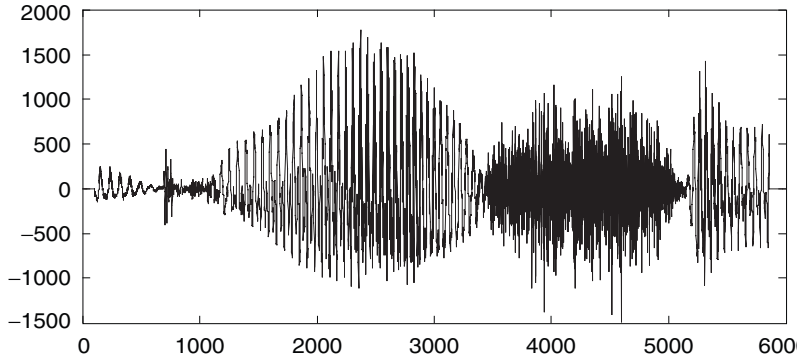

Fig. 4.5. A speech segmentation example. At a sampling rate of 16 kHz, the word "greasy" is shown. The corresponding phonemes are /g/, /r/, /i/, /s/, and /i/; of these /s/ is voiceless.

telephone line noise. Application success revolves around a careful design of segmentation, labeling, and classification algorithms. Sometimes a data-driven computational flow works, even for distinguishing DTMF signals from human voices. Where the bottom-up techniques break down, top-down constraints and goal-directed, artificial intelligence strategies become attractive.

4.1.4 Region Merging and Splitting

Once the domain of a signal f is broken down by a segmentation into a partition $\Pi = \{S_1, S_2, ...\}$, it may be necessary to combine some of the regions together. This reduction in the number of separate regions of the domain is called *region merging* (Figure 4.6). Region merging generally follows labeling. It is invoked because some goal-directed rules have discovered flaws in the labeling. We already considered this situation in the realm of speech analysis. A digitized speech fragment might receive an initial phoneme label, because of its high magnitude. However, subsequent analysis of its time-domain extent, and possibly its position at the beginning or ending of what appears to be a full-word utterance, might relegate the fragment to the category of a tongue click. Merging can also be useful when the signal segmentation must be made as simple as possible—for instance to facilitate signal compression or speed up subsequent analysis steps.

The choice of criteria for region merging depends heavily on the signal analysis application. For example, suppose that two segmentation regions have average signal values that are so close that they seem to be caused by the same physical process. Let μ_R be the mean within region R, and let be μ_S the mean within region S. If $|\mu_R - \mu_S| < \varepsilon$, where ε is an application-specific threshold, then we replace R and S in Π by $R' = R \cup S$. Merging continues by comparing the mean of R' against the mean of the remaining regions. Another statistic useful for merging two adjacent regions, especially when the segmentation is based on measures of signal texture (Section 4.3), is

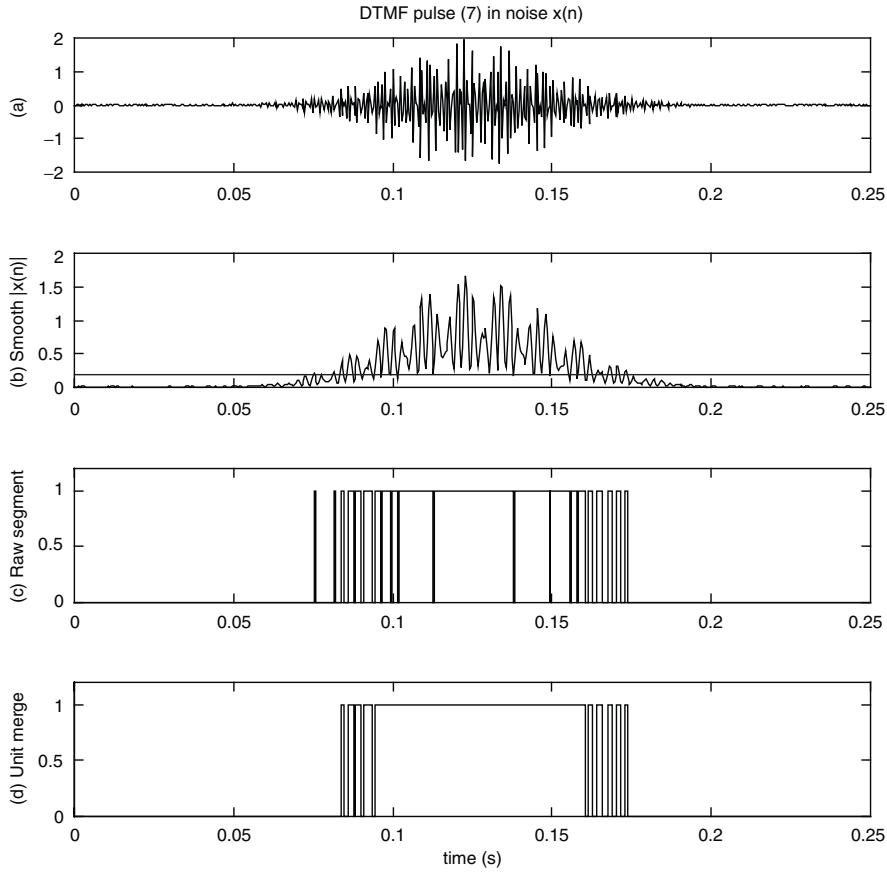

Fig. 4.6. Region merging: DTMF pulse (a), threshold operation (b), and raw labeling (c). The marked pulse segments are too small for a valid tone signal. Simply merging unit width segmented regions into their larger, differently marked neighbors isolates a valid DTMF pulse of 50-ms contiguous length (d).

a similarity in their variances. An edge detector could test the boundary between regions. If the edge detector fails to show a sufficiently distinct edge between the two areas, then they are candidates for merging. These are all low-level considerations for merging regions. If the application is so well characterized as to have a set of goal-directed rules that govern the labeling of signal regions, then the rules may be applied to the preliminary segmentation results. Regions can be joined, therefore, to better satisfy the top-down specifications. Finally, note that the results of the merging operations will supersede the original logical predicate that defined the segmentation.

Splitting a region is harder than merging. When the regions already exist, then the main problem is choosing the right criteria, out of many possibilities, for deciding whether to merge them. When a region is examined as a candidate for splitting, however, what partition of it begins the task? One possibility is to divide a region of

interest, $S = [a, b] \subseteq \text{Dom}(f)$, into segments of equal length, $S = S_1 \cup S_2 \cup S_3 \cup \cdots \cup S_N$, where the S_i are disjoint. A good choice for segment length is the smallest time interval for meaningful features of signal f. Then a statistical measure, the mean or variance for example, applied to each segment in succession, can indicate whether the segment should be set apart from the rest. With the original S now subdivided, we can consider whether to unite the various S_i, just as in the above region merging algorithm. Splitting is then a kind of inverse of merging. The end result is to split the original region $S = R_1 \cup R_2 \cup \cdots \cup R_M$, where $M \leq N$ and each R_i is a union of a different subset of $\{S_1, S_2, \ldots, S_N\}$. The obvious problem with this approach is that it directly depends upon the arbitrary partition of S into the segments, $S_1, S_2, \ldots, S_N$.

But there is a deeper problem with both the region merging and the "inverse" region splitting algorithms above. They both depend on the order in which the regions are selected for merging or splitting. This is due to the lack of transitivity in the "is similar to" relations we apply. Let's explore this. If we begin with the first segment, we may have $|\mu_1 - \mu_2| < \varepsilon$, and so we unite them, $R_1 = S_1 \cup S_2$. Now, the mean of R_1 is the statistical expectation, $E[\{f(n) \mid n \in R_1\}] = E[f(R_1)]$, and we compare it to μ_3. But it is quite possible that the criterion for merging S_3 into R_1 would be met, while at the same time we have $|\mu_1 - \mu_3| \geq \varepsilon$ and $|\mu_2 - \mu_3| \geq \varepsilon$. The merging of the subregions (and thus the splitting of the original region of interest) depends on the order in which the subregions are considered. To avoid this, we can try to cluster the subregions around some entity that does not depend on an individual region. Suppose we select M values $k_1 < k_2 < k_3 < \cdots < k_M$, where $k_i \in \text{Ran}(f)$. (Perhaps we specify $k_1 = \min\{f(n) \mid n \in [a, b]\}$, and $k_M = \max\{f(n) \mid n \in [a, b]\}$, but this is not essential.) Then we define the subregion S_i to belong to cluster j if $|\mu_i - k_j| \leq |\mu_i - k_m|$, for all m, $1 \leq m \leq M$. That is, the clusters comprise those subregions whose mean falls closest to a target signal value among $\{k_1, k_2, \ldots, k_M\}$. We take $R_j = \cup\{S_i \mid S_i \text{ belongs to cluster } j\}$.

The above approach is called *nearest-neighbor clustering*. The same method can be followed using the variance as a clustering measure. The drawback for this elementary approach is its dependence upon the target values. Another possibility is to discover the target values. We consider all possible assignments of the S_i to clusters indicated by labels $\Lambda_1, \Lambda_2, \ldots, \Lambda_M$. For each permutation, we let $R_j = \cup\{S_i \mid S_i \text{ is assigned to cluster } j\}$ and $X_j = \{\mu_i \mid \mu_i = E[f(S_i)] \text{ and } S_i \text{ is assigned to } \Lambda_j\}$. A cluster is made up of similar subregions if the average values in each X_j are close to one another. Let the target values be $k_j = E[X_j]$. Thus, if we set $\text{Var}[X_j] = E[(X_j - E[X_j])^2] = E[(X_j - k_j)^2]$, then a reasonable measure of the inhomogeneity of our cluster assignment is $\text{Var}[X_1] + \text{Var}[X_2] + \cdots + \text{Var}[X_M]$. An assignment that minimizes this measure is an optimal (i.e., minimal variance) clustering for M labels.

4.2 THRESHOLDING

The threshold system is a nonlinear, but time-invariant operation on signals. In signal analysis applications, thresholding is used to separate the signal domain into

regions according to the value that the signal assumes. Thresholding systems are a principal tool for signal segmentation. Thresholding can be applied globally or locally.

4.2.1 Global Methods

For purposes of segmentation, one of the easiest techniques is to select a single threshold value and apply it to the entire signal—global thresholding. For example, for discrete signals, $f(n)$, if $T > 0$, then $M = \{n: |f(n)| \geq T\}$ is the meaningful component, and $N = \{n: |f(n)| < T\}$ is the noise component of $f(n)$, respectively. Of course, with this division of the signal, the meaningful component will have some noise present. These jagged, low-magnitude artifacts are sometimes called "fuzz," "clutter," or "grass," and they are unavoidable for real-world signals. More precisely, the thresholding operation just picks out that part of the signal that contains something more—something relevant to the analysis application—than just the background noise.

The examples in the previous section showed that this technique works for signal features that are sufficiently distinct from the background noise. Difficulties arise, however, when the signal features of interest diminish over time, blend into the noise, or contain oscillatory components. Sometimes supplemental signal filtering helps. Sometimes a more sophisticated labeling procedure, which imposes constraints on the segmentation, corrects any flaws in the preliminary partitioning of the signal's domain. In any case, the main problem is to determine the appropriate threshold.

4.2.2 Histograms

There are several methods for finding global thresholds. Simple inspection of source signals may indeed suffice. Another method is to histogram the signal, producing a density map of the signal values. Histograms count the number of values that fall within selected ranges, or bins, over the signal domain. This is akin to segmentation, but it partitions the signal's range rather than its domain. The histogram is also an approximation of the signal level probability density function. This observation is the key idea in several of the optimal threshold selection techniques in the signal analysis literature.

Definition (Histogram). Let f be a discrete signal and let $\Pi = \{B_1, B_2, ...\}$ be a partition of the range of f. Then the B_k are *bins* for $\text{Ran}(f)$. The histogram of f with respect to Π is defined by $h(k) = \#(f^{-1}(B_k))$. In other words, the value $h(k)$ is the cardinality of $f^{-1}(B_k)$—the number of $n \in \text{Dom}(f)$ with $f(n) \in B_k$.

Even though the definition confines the histogram idea to discrete signals, it is still a very general formulation. It allows for a countably infinite number of bins as well as for infinite histogram values. It is more practical to restrict the domain of discrete signals $f(n)$ to an interval and specify a finite number of bins. That is,

suppose $f(n)$ is a digital signal with q-bit values and that f(n) is of finite support (i.e., $f(n) = 0$ outside some finite interval, I). Then $0 \leq f(n) \leq 2^q - 1$. Let $\Pi = \{\{k\} \mid 0 \leq k \leq 2^q - 1\}$. Then Π is a set of bins for Ran(f), and $h(k) = \#(\{n \in I \mid f(n) = k\}) = \#(f^{-1}(\{k\}))$ is a histogram for f. Since h counts domain elements only within I, $h(k)$ is a discrete signal with support in $[0, 2^q - 1]$.

Example (Digital Image Histograms). Many one-dimensional signal processing and analysis tasks arise in computer vision. Histograms, in particular, are fundamental to early image analysis tasks. Figure 4.7 shows a gray-scale text image and its histogram. Threshold selection is easy. But this is due to the close cropping of white background from the black text. Including larger areas of background in the image would result in an apparently unimodal histogram. A lesson in text image analysis is that successful segmentation of words into letters depends on a prior successful segmentation of the page into words or lines.

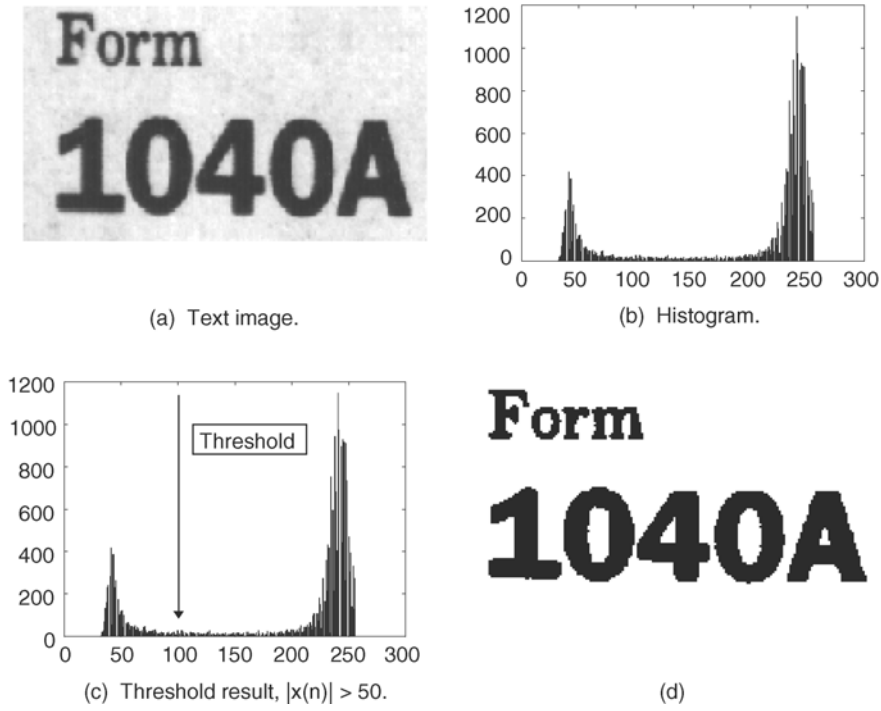

Fig. 4.7. A text image familiar to readers working in the United States. The gray-scale text image (a) has been cropped to exclude surrounding background areas. In the histogram (b), the modes correspond to the largely white and largely black picture elements. Inspection of the histogram reveals a threshold (c), and using this threshold segments the text into purely black letters and purely white background (d).

It is important, however, to automate the histogram threshold selection procedure for autonomous signal analysis systems. A valley-finding algorithm is sometimes effective. If the significant and background signal values are both large in number and different in magnitude, then two large modes appear in the histogram. Beginning from the histogram midpoint, a reverse-gradient search across the histogram should find the valley between the modes. Let $h(k)$ be the signal histogram, $T \in \text{Dom}(h)$, and search to another k as follows:

- If $T-1 \in \text{Dom}(h)$ and $h(T-1) \leq h(T)$, then continue the search at $T-1$; otherwise.
- If $T+1 \in \text{Dom}(h)$ and $h(T+1) \leq h(T)$, then continue the search at $T+1$; otherwise.
- Accept the value of T last searched as the threshold.

There are several drawbacks to this procedure, and they are common to every type of reverse-gradient technique. The algorithm stops at the first local minimum it finds. The simple valley-finding technique has a direction preference, which may not accord well with the signal analysis application. And there is no guarantee that the final T the method selects does not lie in a local minimum interior to one of the histogram's modes. The next technique offers to improve the valley-finding algorithm by building a global cost function.

If we think of the histogram as a valley, possibly containing foothills, between two mountain ranges, then selecting a threshold amounts to deciding how much effort it takes to get over the mountains to one boundary or the other. At each point on the histogram, we associate a cost of leaving the valley; it is the minimum of the cost of reaching the first and the cost of reaching the last histogram bin. Of course, only uphill walking requires effort, so we increment the separate costs to the far bins only when the histogram is decreasing on the left and increasing on the right. A point with maximal cost lies in the valley and is a feasible threshold for separating the two modes. Less metaphorically, therefore, an algorithm for finding a threshold in a histogram $h(k)$ is as follows:

$$\text{Cost}_L(t) = \sum_{\substack{k \leq t \\ h(k-1) > h(k)}} [h(k-1) - h(k)], \tag{4.1}$$

$$\text{Cost}_H(t) = \sum_{\substack{k \geq t \\ h(k) < h(k+1)}} [h(k+1) - h(k)], \tag{4.2}$$

$$\text{Cost}(t) = \min\{\text{Cost}_L(t), \text{Cost}_H(t)\}, \tag{4.3}$$

$$T = \max_t \{\text{Cost}(t)\} \tag{4.4}$$

We call the above technique a global valley-finding algorithm.

Techniques such as the above algorithm (4.1)–(4.4) furnish useful thresholds for many signal segmentation tasks. However, as the exercises show, it easy to find signals for which the algorithm fails. Furthermore, natural signals or those from engineered systems may have meaningful regions that become lost when the histogram procedure removes their time domain locality. The question therefore arises whether there is some way of inproving the histogram estimate, or, more optimistically, whether there is an optimal method for finding a threshold for segmentation of an image from its histogram.

4.2.3 Optimal Thresholding

In fact, there are several optimal methods for finding thresholds from signal histograms. Each such "optimal" method discovers the best threshold based on some particular assumption about the histogram's statistics. This is a natural thought, since the histogram approximates the probability density function of the signal values. Accordingly, let us consider some techniques for optimal threshold selection. We shall begin with work that is now classic and end with some quite recent improvements in this thread of investigation.

4.2.3.1 Parametric Approaches. Suppose that we know the some of the statistical behavior of signals that arrive as inputs to an analysis application. For example, we might have knowledge of the statistical distribution of signal values, along with knowledge of the likelihoods that signal features have certain labels; and, perhaps the most valuable information of all, we might even know the probabilities for the classification of signals. Such information on statistical parameters associated with a signal generation mechanism is the basis for the parametric approach to signal threshold determination.

Suppose that we know the probabilities that a discrete signal value is high-magnitude (meaningful), P_H, or low-magnitude (background, noise), P_L. These are called the a priori probabilities of meaningful and noise components, respectively. For example, in a digital telephony system, DTMF pulses might occur at 10 Hz with an average pulse width of 48 ms. Hence we assume a priori probabilities of $P_H = .48$ and $P_L = .52$. Some system designs rely on preliminary statistical studies to develop a priori probabilites. Other strategies are adaptive, and the probabilities change slowly while the system operates.

Segmentation errors are due to labeling a noise value as meaningful or a meaningful value as noise. Thus, if a threshold T for a signal histogram produces errors with probability $E(T)$, then

$$E(T) = P_H E_L(T) + P_L E_H(T), \tag{4.5}$$

where $E_L(T)$ and $E_H(T)$ are the probabilities of incorrectly labeling a signal value as noise and as meaningful, respectively. To find the minimum labeling error, we

differentiate (4.5) and solve the equation $dE/dT = 0$ for the threshold T:

$$\frac{dE}{dT} = P_H \frac{dE_L}{dT} + P_L \frac{dE_H}{dT} = 0. \tag{4.6}$$

Now, this scheme does not work at all unless we can find estimates for $E_L(T)$ and $E_H(T)$. The idea is to approximate the distributions of signal values in the histograms by standard statistical distributions. In the histogram of Figure 4.7, for instance, the modes resemble normal (Gaussian) density functions. From the tutorial on probability theory in Section 1.8, the Central Limit Theorem shows that whatever the distributions we observe in a histogram, then (given their bounded variance) the average of a great many of these random variables always approaches a Gaussian distribution. Let us assume, therefore, Gaussian distributions of both noise and meaningful signal. Thus,

$$q_L(t) = \frac{1}{\sqrt{2\pi}\sigma_L} e^{-(t-\mu_L)^2/(2\sigma_L^2)} \tag{4.7}$$

is the probability density function for the signal noise values, where μ_L and σ_L are the mean and standard deviation, respectively. Similarly,

$$q_H(t) = \frac{1}{\sqrt{2\pi}\sigma_H} e^{-(t-\mu_H)^2/(2\sigma_H^2)}, \tag{4.8}$$

where μ_H and σ_H are the mean and standard deviation of the signal noise values, respectively. Since noise values are on average less than meaningful signal values, we know that $\mu_L < \mu_H$. From (4.7) and (4.8), it follows that

$$E_L(T) = \int_{-\infty}^{T} q_H(t)\, dt, \tag{4.9}$$

and

$$E_H(T) = \int_{T}^{\infty} q_L(t)\, dt. \tag{4.10}$$

Differentiating (4.9) and (4.10) with respect to T shows that $dE_L/dT = q_H(T)$ and $dE_H/dT = -q_L(T)$. We substitute expressions for these derivatives—(4.7) and (4.8)—into (4.6) to obtain

$$\frac{P_H}{\sigma_H} e^{-(T-\mu_H)^2/(2\sigma_H^2)} = \frac{P_L}{\sigma_L} e^{-(T-\mu_L)^2/(2\sigma_L^2)}. \tag{4.11}$$

We take the natural logarithm on both sides of (4.11), simplify, and reveal a quadratic equation in T:

$$\left(\sigma_L^2 - \sigma_H^2\right)T^2 + 2\left(\sigma_H^2\mu_L - \sigma_L^2\mu_H\right)T + \left(\sigma_L^2\mu_H^2 - \sigma_H^2\mu_L^2\right) - 2\ln\left(\frac{P_H\sigma_L}{P_L\sigma_H}\right) = 0. \tag{4.12}$$

The quadratic equation (4.12) may have two, one, or zero solutions, depending upon the statistics of the true signal and its noise component. It may be necessary to compare the performance of two possible thresholds using (4.5). And any solution T for (4.12) must be in the range of the signal in question. The exercises further explore these ideas.

This procedure is due to Chow and Kaneko [17]. They applied the technique for finding the left ventricle cardioangiograms—x-ray images acquired after injecting a contrast-producing dye into the heart. Some observations on the method are:

- The method requires *a priori* knowledge of the signal, namely the probabilities of the true signal, P_H, and of the background, P_L.
- It is a parametric method, in that it assumes a particular model of the signal histogram and then derives parameters that best describe the model.
- To discover the parameters of the sum of Gaussian distributions in Chow and Kaneko's approach, it is necessary to fit the model to the actual histogram data.
- Thus, parameter determination requires, for example, a least-squares fit of the model to the data, and an accurate or numerically well-behaved convergence is not guaranteed.
- Moreover, as our own examples show, the model (e.g., a sum of two normal distributions) may not be appropriate for the signal histogram.

These are difficulties with any parametric technique. The next section considers a nonparametric strategy. It is an alternative that does not presuppose statistical distributions for the signal values. Then, in Section 4.2.3.3 we will revisit parametric methods. There we will examine a method inspired by information theory that avoids the assumption of *a priori* probabilities.

4.2.3.2 Nonparametric Approaches. A nonparametric approach to threshold determination assumes no knowledge of the statistical parameters that derive from a signal's values. Thus, nonparametric strategies include the valley finding tactics covered earlier. Valley finding methods do not assume any statistical distribution of meaningful signal and noise values, even though these particular algorithms are rather primitive. Methods can combine, too, for better performance. We can use a global valley-finding algorithm to split the histogram with a preliminary threshold, T. We then determine the statistical parameters of the noise and true signal by separate least-squares fits to the histogram for $t < T$ and for $t > T$. And, finally, we apply the Chow and Kaneko technique to improve the estimate of T. If the segmentation

that results from the threshold selection is unsatisfactory, goal-directed strategies are worth investigating. It may be possible to alter the preliminary threshold, recompute the mode statistics, or choose another statistical distribution for modeling the histogram.

Let us turn to a nonparametric approach for threshold determination and signal segmentation proposed by Otsu [18]. Otsu hoped to avoid some of the difficulties we noted above. The idea is to select a threshold to segment the signal into labeled regions of minimal variance in signal levels. Let $P_L(t)$ and $P_H(t)$ be the probability of background values and true signal values, respectively. In Chow and Kaneko's approach, these were needed *a priori*; in Otsu's algorithm, on the other hand, these are approximated from the histogram and are functions of the threshold value. We segment the signal values into two groups, according to the threshold. And let us suppose, again without loss of generality, that background values are low and meaningful signal values are high. Then, a measure of within group variance is

$$\sigma_w^2(t) = P_L(t)\sigma_L^2(t) + P_H(t)\sigma_H^2(t), \tag{4.13}$$

where $\sigma_L(t)$ and $\sigma_H(t)$ are the standard deviations of the noise and the meaningful signal, respectively. In order to find t so that (4.13) is minimized, we must also find the statistical distribuitons of the low-level and the high-level regions of the signal. Chow and Kaneko's parametric approach assumes that the histogram is a sum of two normal densities and that *a priori* probabilities are known.

Because it directly approximates the histogram statistics from threshold values and does not make assumptions about *a priori* noise and true signal probabilities, Otsu's method is essentially unsupervised. Let us see how the method works. Suppose that $\mathrm{Ran}(f) \subseteq [0, N-1]$, set $S_k = \{k\}$ for $0 \le k < N$, and suppose that $\mathrm{Dom}(f)$ is finite. Then $\{Sk \mid \}$ is a partition of $\mathrm{Ran}(f)$. Define

$$p_k = \frac{\#(f^{-1}(S_k))}{\#\mathrm{Dom}(f)}, \tag{4.14}$$

Then, p_k is a discrete probability density function for f. Hence,

$$P_L(t) = \sum_{k=0}^{t-1} p_k, \tag{4.15}$$

and

$$P_H(t) = \sum_{k=t}^{N-1} p_k. \tag{4.16}$$

Let $\{\Lambda_L, \Lambda_H\}$ be labels for the noise and meaningful regions of the signal. Then, the conditional probability that $f(n) = k$, given that n has label Λ_L and the threshold is t, is $P(k \mid \Lambda_L) = p_k/P_L(t)$. Similarly, $P(k \mid \Lambda_H) = p_k/P_H(t)$. This observation permits us to write down the following values for the parameters of the distributions comprising the histogram:

$$\mu_L(t) = \sum_{k=0}^{t-1} kP(k \mid \Lambda_L) = \sum_{k=0}^{t-1} k \frac{p_k}{P_L(t)}, \tag{4.17}$$

$$\mu_H(t) = \sum_{k=t}^{N-1} kP(k \mid \Lambda_H) = \sum_{k=t}^{N-1} k \frac{p_k}{P_H(t)}, \tag{4.18}$$

$$\sigma_L^2(t) = \sum_{k=0}^{t-1} (k - \mu_L(t))^2 P(k \mid \Lambda_L) = \sum_{k=0}^{t-1} (k - \mu_L(t))^2 \frac{p_k}{P_L(t)}, \tag{4.19}$$

and

$$\sigma_H^2(t) = \sum_{k=t}^{N-1} (k - \mu_H(t))^2 P(k \mid \Lambda_H) = \sum_{k=t}^{N-1} (k - \mu_H(t))^2 \frac{p_k}{P_H(t)}. \tag{4.20}$$

Having found the histogram statistics that follow from each possible threshold value, we are in a position to search over all threshold values for T which minimizes the within-group variance. Specifically, by a exhaustive search we find the optimal threshold T which satisfies

$$\sigma_w^2(T) = \min_{0 \le t < N} \sigma_w^2(t). \tag{4.21}$$

Otsu's method merits consideration in applications where human intervention in the signal analysis process must be minimized. It does not need *a priori* probability estimates. It does not make any assumptions about the distribution of histogram values. Two problems weigh on the approach, however:

- It requires a search and recomputation of the statistics (4.17)–(4.20) over all possible threshold values.
- There may not be a unique minimum in (4.21), and, unless some goal-directed are imposed, there is no criterion for selecting one variation-reducing threshold over another with the same effect.

The exercises explore some algorithm refinements that reduce the recomputation burden. But the second point is troublesome. If we knew the within-group variance to be unimodal, then the search would always identify an optimal threshold.

Experiments supported—and Otsu conjectured—variance unimodality within segmented regions, but it does not hold true in general. In summary, nonparametric strategies generally involve more computational tasks than their parametric cousins. Thus, a preliminary survey of the statistical parameters of input signals to an analysis application may be warranted. A study of the statistics within histograms, for example, may prove the feasibility of the simpler parametric strategy.

4.2.3.3 An Information-Theoretic Approach. Attempting to avoid the modality problems inherent to Otsu's algorithm, Kittler and Illingworth [19] approached the problem by trying to find the mixture of Gaussian probability distributions that best matches the signal histogram for a given threshold value. For their optimality criterion, they employed relative entropy [20, 21], an information-theoretic tool, which we introduced in Section 1.8.4. They adopted a model of the histogram as a scaled sum of two normal distributions. Thus, theirs is a parametric approach akin to Chow and Kaneko's; however, it avoids the supposition of *a priori* probabilities for noise and meaningful signal segments, and therefore it represents a significant extension to the parametric method.

Following Kittler and Illingworth, let us suppose that p_k is given by (4.14), and q_k is an alternative distribution. Then the relative entropy, $I(p, q)$, of the distribution p_k with respect to q_k is

$$\begin{aligned} I(p,q) &= \sum_{k=0}^{N-1} p_k \log_2 \frac{p_k}{q_k} = \sum_{k=0}^{N-1} p_k \log_2 p_k - \sum_{k=0}^{N-1} p_k \log_2 q_k \\ &= -H(p) - \sum_{k=0}^{N-1} p_k \log_2 q_k, \end{aligned} \tag{4.22}$$

where $H(p)$ is the entropy of p,

$$H(p) = \sum_{k=0}^{N-1} p_k \frac{1}{\log_2 p_k}. \tag{4.23}$$

It can be shown that $I(p, q) \geq 0$ for all distributions p and q. Furthermore, $I(p, q) = 0$ if and only if $p = q$. Finally, let us note that $\log_2(p_k/q_k)$ is the information increment, given that the signal $f(n) = k$, that supports the histogram $h(k)$ having distribution p_k instead of q_k. Thus, the average information in favor of $h(k)$ following distribution p_k instead of q_k is $I(p, q)$, from (4.22). If q_k is a scaled sum of two normal distributions, then

$$q_k = \frac{a_1}{\sqrt{2\pi}\sigma_1} e^{-(k-\mu_1)^2/(2\sigma_1^2)} + \frac{a_2}{\sqrt{2\pi}\sigma_2} e^{-(k-\mu_2)^2/(2\sigma_2^2)}, \tag{4.24}$$

where a_1 and a_2 are constants. Now, q_k represents the histogram $h(k)$ better when signal values $f(n) = k$ discriminate in its favor over p_k; in other words, (4.24) should

be minimized for best representing $h(k)$ with a sum of two Gaussians scaled by a_1 and a_2. Since $H(p)$ depends only upon the given histogram, this means that

$$I(p,q) + H(p) = -\sum_{k=0}^{N-1} p_k \log_2 q_k \tag{4.25}$$

should be minimized.

We can minimize (4.25) by approximating the statistical parameters of the two components of the distribution q_k for each candidate threshold, $0 < t < N-1$. If t lies between well-separated means, μ_1 and μ_2, then we should expect reasonable estimates. Thus, for each such t, we take $\mu_{1,t} = \lfloor t/2 \rfloor$ (the floor, or integer part of $t/2$). Let $a_{1,t}$ and $\sigma_{1,t}$ be the mean and standard deviation of $\{p_1, p_2, \ldots p_{t-1}\}$, respectively. We set $\mu_{2,t} = \lfloor (N-t)/2 \rfloor$, and let $a_{2,t}$ and $\sigma_{2,t}$ be the mean and standard deviation of $\{p_t, p_{t+1}, \ldots, p_{N-1}\}$, respectively. Lastly, we substitute these values into (4.24) to obtain

$$q_k(t) = \frac{a_{1,t}}{\sqrt{2\pi}\sigma_{1,t}} e^{-(k-\mu_{1,t})^2/(2\sigma_{1,t}^2)} + \frac{a_{2,t}}{\sqrt{2\pi}\sigma_{2,t}} e^{-(k-\mu_{2,t})^2/(2\sigma_{2,t}^2)}. \tag{4.26}$$

Then, the optimal threshold is T where

$$-\sum_{k=0}^{N-1} p_k \log_2 q_k(T) \leq -\sum_{k=0}^{N-1} p_k \log_2 q_k(t) \tag{4.27}$$

for all t, $0 < t < N-1$.

An extensive literature on thresholding testifies that no single technique guarantees correct signal segmentation for all applications. General surveys include [22, 23]. Others concentrate on thresholding text [24, 25] or map [26] images. Figure 4.8 shows a signal, its histogram, and the results of thresholding it using the Otsu algorithm. Simple threshold selection methods and bottom-up signal classification strategies very often work just as well as the more sophisticated techniques. When they fail, combining methods is fruitful. Many of the methods we cover can be extended, often in straightforward ways, to multiple threshold values. Such an approach looks for multiple thresholds and partitions the domain into several regions according to signal magnitude. This is also called signal quantization, since it maps signal values that spread over a wide range to a set of signal values that vary significantly less. The exercises explore this important problem. More challenging applications require some top-down, goal-directed mechanism for improving the thresholding, segmentation, and labeling of a signal.

Finally, let us confess that we have neglected an important technique for signal segmentation: local or adaptive thresholding.

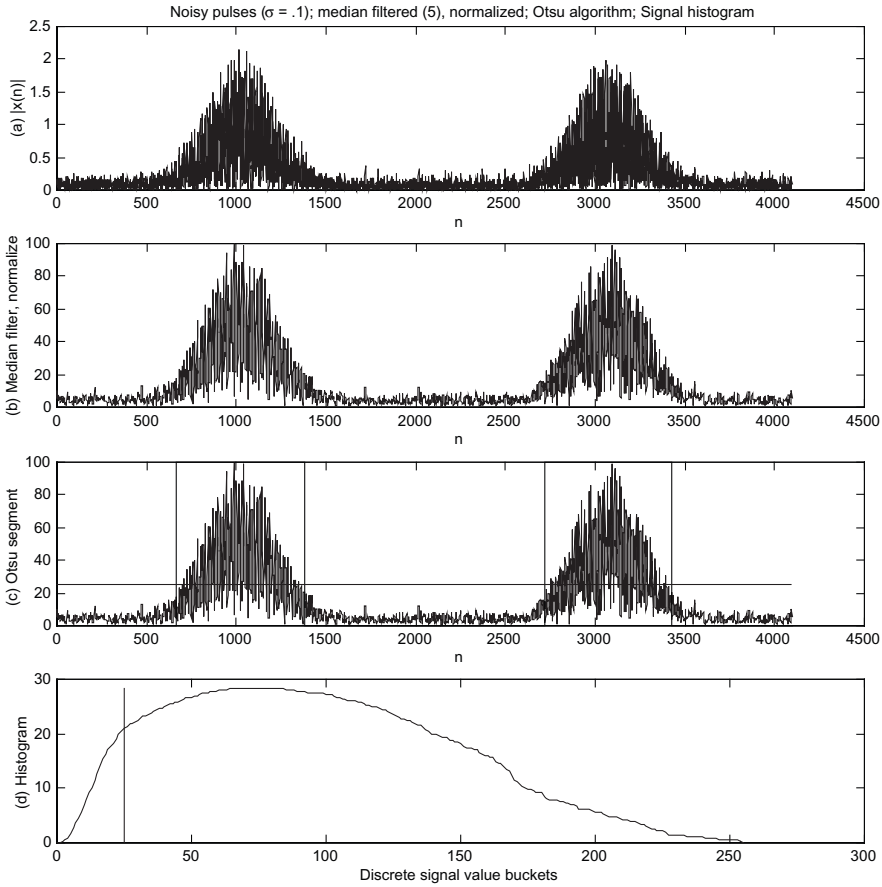

Fig. 4.8. A pulse signal (a), median filtered and normalized (b), threshold from Otsu's algorithm (c), and the signal histogram (d).

4.2.4 Local Thresholding

The methods covered above, by more or less sophisticated means, attempt to arrive at a global threshold value that will break down the signal. In many problems, the threshold that successfully segments a signal in one area fails to perform adequately in another area. But there is nothing in the global thresholding methods we have detailed above—based on histogram analysis—that prevents them from being applied to finite regions of the signal domain. When we find and apply thresholds locally within a signal's domain, the technique is called local thresholding or—since the threshold value adapts to the statistics or entropy of the signal locally—adaptive thresholding.

It may be possible, and indeed it may be essential, to vary the threshold at different places within the signal domain. This could be the case where the gain of the

signal processing elements of the system varies. Falling signal strength could cause meaningful components to be misclassified as background noise. Thus, the threshold should adapt to the overall magnitude of local regions of the signal. Varying illumination, shading, and object reflectance make adaptive thresholding vital to many image analysis applications. Optical character recognition is but one example [27]. In digital telephony, echo cancellation should be suspended during episodes of double-talk, when both the near-end and far-end speakers are talking. But the threshold level for deciding that the near-end speaker is talking needs to adapt to the signal level of the far-end speaker; otherwise, cancellation may occur when both speakers are talking softly or might not take place when the far-end speaker is very loud. One approach is to declare double-talk when the the near-end signal level $s(n) > (1/2)\max\{x(n), x(n-1), ..., x(n-N)\}$, for some $N > 0$. By comparing levels over a whole range of recent far-end speaker voice magnitudes, the algorithm accomodates the unknown echo delay in the near-end circuit [28].

4.3 TEXTURE

Signal segmentation often requires that regions with certain regular patterns of signal values be distinguished from one another. It is not the absolute signal level—as with the previous section's principal concern, thresholding—but rather the repetitive transition of the signal through some value range that is of interest in such an application. This section covers methods for segmenting a signal into regions of different texture.

A threshold-based segmentation algorithm does not easily handle signals with periodic components. Examples covered in the previous sections, such as the speech fragments and the dual-tone multifrequency telephone system signaling pulses, are cases in point. It is possible to apply a preliminary smoothing filter to the values prior to thresholding. This blends the oscillation together and reduces the average value of the signal over a region, and then the thresholding operation properly isolates the region of interest. Regions found by one threshold, T_1, but not by another threshold $T_2 \neq T_1$ constitute a distinct texture field. Perhaps several filters and thresholds are necessary. As an alternative, we might consider segmenting the large-magnitude signal regions from the low-magnitude signal regions and then estimating an overall distance between peaks or between troughs. Areas that show different average intervals between crests or troughs represent different textured signal components. We are faced with a number of algorithm design issues, though, whatever approach we select. It is desirable to arrive at some indication of texture that produces a measure directly from the signal values, without preliminary filtering followed by thresholding.

Intuitively, the notion of texture incorporates the presence of smoothness or roughness and the overall character of repetition and continuity as opposed to rupture or discontinuity. One tool in wide use by computer vision researchers is a collection of photographs of textures, originally intended for use by artists, the Brodatz textures [29]. Many pioneering researchers in the field pursued the problem of

texture characterization from psychological standpoint [30]. Some, in particular, worked with the principles of Gestalt psychology in mind [31, 32], which stipulates that pictorial features group together in such a way that the overall constellation achieves a form which cannot be expressed by descriptions of the individual elements. These pictorial features include proximity, similarity, continuation, symmetry, closure, and common fate.

Over the years, research efforts in texture analysis have been confined to three broad categories: statistical, spectral, and structural. Statistical approaches apply moment computations to the signal values: variance, skew, and kurtosis, for example [33]. Spectral approaches analyze the signal by comparing it to sinusoidal or Gabor elementary functions (Chapter 1) of varying frequencies [34]. And structural approaches endeavor to find a set of texture elements or primitives that obey a repeating pattern or a relational grammar in the signal [35].

Perhaps one of the most pressing problems is to define the type of repetitive structure, the texture regions in the signal that the application must find. Readers might well suppose that here we would introduce a formal definition of texture; this has, after all, been much the pattern of presentation so far. The U.S. industrial standard for surface metrology [36] defines it as repetitive or random deviations from the nominal surface within the three-dimensional topography of the surface. One might well object to this definition, since the terms "repetitive" and "random" contradict one another! Unfortunately, there is no suitable formal definition for texture, and there is no best approach to segmentation. The methods used are mostly ad hoc, and, if there can be anything close to a definition of texture, it is whatever the chosen method seems to find within the signal! The whole notion of what constitutes texture and what does not is quite uncertain. Let us consider the principal methods for segmenting signals according to their texture content in the next three sections. Though we lack a precise formal definition of texture, each approach constitutes a practical, working concept of what texture is—indeed it is whatever that method finds.

4.3.1 Statistical Measures

The statistical approach to texture segmentation and classification is the most widely used. However problematic the formal definition of texture is, methods to characterize and quantify it are quite important in areas such as materials science and remote sensing. In surface metrology, for example, many standard statistical measures of one- and two-dimensional textures are in use. There are also a number spectral measures of texture, and we will cover them, albeit briefly, in the next section. Some of these texture parameters are admittedly ad hoc, but they are nevertheless widely implemented and widely respected indications of the presence of texture within signals.

4.3.1.1 Basic Measures. One way to measure the amount of variation in a signal is to average the departure of the signal from its mean over a fixed interval. This statistical parameter of signal texture is the roughness average. It is the most widely

used measure in the world, especially for manufactured surface characterization, and it has been standardized in the United States and internationally [33, 36–38].

Definition (Roughness Average). Let $x(t)$ be an integrable analog signal; let $[a, b]$ an interval, $a < b$; and let μ be the mean of $x(t)$ over $[a, b]$. Then the roughness average of $x(t)$ over $[a, b]$ is

$$R_a(x(t),[a,b]) = \frac{1}{b-a}\int_a^b |\, x(t) - \mu \,|\, dt. \tag{4.28a}$$

And if $x(n)$ is a discrete signal, $[a, b]$ is an interval, $a < b$, and μ is the mean of $x(n)$ over $[a, b]$, then the roughness average of $x(n)$ over $[a, b]$ is

$$R_a(x(n),[a,b]) = \frac{1}{b-a}\sum_{n=a}^{n=b} |x(n) - \mu\,|\,. \tag{4.28b}$$

When the interval over which we compute the roughness average is understood, it is common to write this parameter as $R_a(x)$. If the signal values are also unambiguous, it is simply R_a.

The roughness average indicates a change in signal variation, but it fails to explicate the distribution of crests, troughs, and transients in the signal. Somewhat more sophisticated statistical measures can be of help. We can, for example, better understand the distribution of signal values by applying a variance measure to the signal regions of interest. As a texture measure, the variance is also a standard.

Definition (Root Mean Square (RMS) of Roughness). If $x(t)$ is an analog signal, $[a, b]$, is an interval, $a < b$, and μ is the mean of $x(t)$ over $[a, b]$, then the RMS of roughness for $x(t)$ over $[a, b]$ is

$$R_q(x(t),[a,b]) = \left(\frac{1}{b-a}\int_a^b |\, x(t) - \mu \,|^2 dt\right)^{1/2}. \tag{4.29a}$$

For analog signals, the equivalent definition is

$$R_q(x(n),[a,b]) = \left(\frac{1}{b-a}\sum_{n=a}^{b-1} |x(n) - \mu\,|^2\right)^{1/2}. \tag{4.29b}$$

It is common to omit the signal and region from the specification of R_a and R_q, since the problem context often makes it understood.

Example (Surface Profilometers and Atomic Force Microscopes). Let us look at the segmentation of surface profiles by texture characterization. Instruments such as profilometers and atomic force microscopes (AFM) acquire one-dimensional (and in many commercial instruments, two-dimensional) height profiles of a surface. Surface texture measurements from such profiles are critical for the control

and diagnosis of the fabrication processes. These measures include such aspects of surface texture as fine-scale roughness, more widely spaced regularities called waviness, and directional features called lay.

The roughness average is by far the most widely computed and reported in manufactured surface characterization. R_a detects general signal profile variations, and a significant change over one part of the signal domain indicates a fundamental change in the process that produces the signal. Nevertheless, it has limitations. To wit, the roughness average parameter fails to detect the presence or absence of widely separated signal transients. R_a completely overlooks subpatterns of texture. (Structural techniques are better suited to this type of problem; see Section 4.2.3.3.) The intervals between texture elements are also invisible to R_a. Some help in characterizing surface texture comes from the R_q parameter. It measures the distribution of deviations from the mean of the signal, so when it is large, it is an indication that the rough features of the signal have wide magnitude variability.

Other texture segmentation methods rely on peak-to-valley measurements within signal regions. Let us consider a few of these next and then proceed to some texture measures that arise from applying statistical moment ideas to a signal's values.

Definition (R_t, R_z). The total indicated reading over $[a, b]$, R_t, is the difference between the signal maximum and signal minimum over the interval. Thus, for an analog signal, $x(t)$, we define

$$R_t(x(t), [a, b]) = \max\{x(t): t \in [a, b]\} - \min\{x(t) \mid t \in [a, b]\}. \tag{4.30a}$$

The analog for a discrete signal, $x(n)$, is

$$R_t(x(n), [a, b]) = \max\{x(n): t \in [a, b]\} - \min\{x(n) \mid t \in [a, b]\}. \tag{4.30b}$$

The five-point peak parameter, R_z, is

$$R_z(x,[a,b]) = \frac{1}{5}\left(\sum_{k=1}^{5} \left(p_k - v_k \right) \right), \tag{4.31}$$

where $p_k \geq p_{k+1}$ are the five highest values x takes on $[a, b]$, and $v_{k+1} \geq v_k$ are the five lowest values x takes on $[a, b]$.

These parameters find application in diverse disciplines. Seismologists use the total indicated reading parameter to calculate earthquake magnitude according to the Richter scale.[3] Let $s(t)$ be the seismograph needle's deviation from the centerline of a paper strip chart at time t during an event. If the epicenter is 100 km

[3]Charles F. Richter (1900–1985), a seismologist at the California Institute of Technology, established the popular logarithmic scale for earthquake magnitude in 1935.

away from the instrument, then the seismologist computes the Richter magnitude, $M_L = \log_{10}[R_t(s)]$. The problem with the total indicated reading as a measure of texture is that it is sensitive to impulse noise in the signal. The R_z parameter is one of several that surface metrologists, for example, use to avoid this difficulty. An even larger average is tempting in (4.31); this provides roughness estimates with better immunity to occasional burrs and pits that blemish a generally good surface.

4.3.1.2 Higher-Order Moments. Further texture analysis measures proceed from an analysis of the signal using statistical moments. Following our histogramming discussion, suppose that we can obtain the discrete probability density function for the values of $x(n)$: $p_k = P[x(n) = k]$. For example, let $x(n)$ be a digital signal with $L \le x(n) \le M$ for $a \le n \le b$, where $a < b$. We form the histogram $h(k) = \#(\{n \in [a, b] \mid f(n) = k\})$ for each $k \in [L, M]$. If $M > L$, we then set $p_k = h(k)/(M-L)$; otherwise, $p_k = 1$. Then p_k is a discrete probability density function. The mean of x on $[L, M]$ is $\mu = (Lp_L + (L+1)p_{L+1} + \cdots + Mp_M)$. Then the variance, σ^2, skew, μ_3, and kurtosis, μ_4, are, respectively, as follows:

$$\sigma^2 = \sum_{k=L}^{M} (k-\mu)^2 p_k, \tag{4.32}$$

$$\mu_3 = \frac{1}{\sigma^3} \sum_{k=L}^{M} (k-\mu)^3 p_k, \tag{4.33}$$

$$\mu_4 = \frac{1}{4}\left(\sum_{k=L}^{M} (k-\mu)^4 p_k \right). \tag{4.34}$$

The R_q texture parameter is a variance measure. The skew measures the asymmetry of the values about the signal mean. The kurtosis measures the relative heaviness of the outlying signal values within the texture region. Some authors define kurtosis by subtracting three from (4.34); this ensures that a Gaussian distribution has zero kurtosis, but it does not affect the measure as a tool for signal segmentation.

These texture parameters supply some of the information missing from the roughness average figure. To use any of these parameters as a basis for signal segmentation, we compute the parameter over selected regions of the signal domain and label the regions according to the parameter's numerical value. A more informative segmentation of the signal is possible by calculating several of the parameters and assigning labels to the regions that represent combinations of significant texture parameters.

Notice that there is a distinct difference between the application of these texture measures and the previous section's thresholding algorithms to segmentation problems. When thresholding, the segmentation regions were discovered, signal value after signal value, by applying the thresholding criterion. On the other hand, to

apply the texture measures, an interval or region of the signal domain must be used to calculate the statistical quantity, R_a or R_q, for example. Thus, a texture segmentation commonly starts with a preliminary partition of the signal domain into intervals, called frames, with texture measures assigned to the intervals. The bounds of these preliminary texture regions may be adjusted later with split and merge criteria, as we considered in Section 4.1.4. For precise registration of texture areas, a data-driven alternative exists. An application may apply texture measures to frames of a minimum size, say $N > 0$. After applying the measure to region $[a, b]$, where $b - a = N$, the statistics are compared to one or more threshold values. If $[a, b]$ contains texture, then the measures are applied to the larger region $[a, b + 1]$; otherwise the frame becomes $[a + 1, b + 1]$ and texture finding continues. Each time a region contains texture, the application attempts to expand it on the right, until at some iteration, say $[a, b + k + 1]$, the texture indication test fails. Then $[a, b + k]$ is declared to be texture-laden, and processing continues with the next minimal frame $[b + k + 1, b + k + N + 1]$. Albeit computationally expensive, this scheme avoids any top-down split and merge procedures.

4.3.1.3 Co-occurrence Matrices. One significant drawback to the above methods for texture segmentation is that they utilize no distance measures between intensity features within the texture. The moment parameters, such as R_q, do incorporate a notion of breadth of variation. In manufactured surface characterization, R_q is often touted as an alternative to the widely quoted R_a value. Nevertheless, signal and image analysts reckon that the most powerful techniques are those that compute statistics for the distribution of signal values separated various time intervals [39]. The next definition [40] incorporates the distance between texture highlights into our statistical indicators of texture.

Definition (Co-occurence Matrix). Let $x(n)$ be a digital signal; let $L \le x(n) \le K$ for some integers L, K and for $a \le n \le b$; and let δ be a time interval. Then $M_\delta = [m_{i,j}]_{N \times N}$ is the $N \times N$ matrix defined by $m_{i,j} = \#\{(x(p), x(q)) \mid p, q \in [a, b], x(p) = i$ and $x(q) = j$, and $\delta = |p - q|\}$. The co-occurrence matrix for $x(n)$ and time interval δ is defined $P_\delta = [m_{i,j}/N_\delta]$, where $N_\delta = \#\{(x(p), x(q)) \mid p, q \in [a, b]$ and $\delta = |p - q|\}$.

Thus, $m_{i,j}$ contains a count of the number of pairs (p, q) for which $x(p) = i$, $x(q) = j$, and p and q are time δ apart. P_δ estimates the joint probability that two signal will take values i and j at a displacement δ apart. Also, it is not necessary to restrict $x(n)$ to be a digital signal; as long as its range is finite, the co-occurrence matrix can be defined.

Example (Co-occurrence Matrix). Let $x(n) = [..., 0, \underline{1}, 2, 1, 1, 2, 0, 0, 1, 0, 2, 2, 0, 1, 1, 0, ...]$ be a digital signal, and suppose we compute the co-occurrence matrices for $\delta = 1$, 2, and 3 within the interval $0 \le n \le 15$. This signal is roughly sawtooth in shape, with the ramps positioned three time instants apart. We compute the

co-occurrence matrics, P_1, P_2, and P_3 as follows:

$$15 \times P_1 = M_1 = \begin{bmatrix} 1 & 3 & 1 \\ 2 & 2 & 2 \\ 2 & 1 & 1 \end{bmatrix}, \tag{4.35a}$$

$$14 \times P_2 = M_2 = \begin{bmatrix} 1 & 2 & 2 \\ 2 & 1 & 2 \\ 2 & 2 & 0 \end{bmatrix}, \tag{4.35b}$$

$$13 \times P_3 = M_3 = \begin{bmatrix} 3 & 1 & 1 \\ 2 & 1 & 1 \\ 0 & 3 & 1 \end{bmatrix}, \tag{4.35c}$$

where $N_1 = 15$, $N_2 = 14$, and $N_3 = 13$. Notice that the values are spread out in M_1 and M_2, the main diagonal values are relatively small, and there are few outliers. In contrast, M_3 contains two large values, several small values, and a maximal probability on the diagonal. If the structures within $x(n)$ are square pulses rather than ramps, the matrices M_1, M_2, and M_3 are even more distinct. The exercises explore these ideas further.

To use the co-occurrence matrix as a texture segmentation tool, the time interval δ must be selected according to the size and spacing of the signal regions. Suppose, for instance, that the signal $x(n)$ contains high-magnitude regions approximately Δ time instants apart and that we calculate the matrix P_δ, where δ is smaller than Δ. If $|p - q| < \delta$, then the values $x(p)$ and $x(q)$ are likely to fall into the same region. Hence P_δ entries on the diagonal should be large. Large values do not concentrate on P_δ's diagonal when δ is smaller than the typical region size. If a textured signal contains features of two sizes, δ and ε, then we should expect to find matrices P_δ and P_ε to be largely diagonal. In general, many values of δ are unnecessary for good texture segmentation results.

The idea of co-occurrence measures in texture analysis dates back to the early work of Julesz [41]. The co-occurrence matrix entry on row i and column j, $P_\delta(i, j)$, gives the probability that a sampling of a signal value and its neighbor δ time instants away will have values i and j. It is also possible to sample a point and two others, δ_1 and δ_2 time instants away, to generate third-order co-occurrence statistics. Similarly, fourth- and high-order co-occurrence measures are possible. Julesz conjectured that humans cannot distinguish textures that contain identical first- and second-order co-occurrence statistics; thus, visual texture fields may differ in their third- or higher-order statistics, but this effect is too subtle for the eye–brain system to detect. Julesz's thesis was tremendously attractive to computer vision researchers. It promised to bound the ever-growing number of texture measures by invoking a discriminability criterion based on human pattern detection performance. Possibly, too, researchers could anchor a definition of texture itself in the second-order co-occurrence statistics. But counterexamples were soon found. Julesz and other investigators were able to synthesize texture fields, which humans could distinguish, that had different third- or

fourth-order co-occurrence statistics but identical first- and second-order statistics [42]. Under further scrutiny, the synthesized counterexamples themselves were shown to have different local and global co-occurrence statistics. The human visual system excels at perceiving distinct local image characteristics and can group local variations into global patterns over wide areas of the visual field. This causes many visual illusions. Thus, persons viewing the counter-example textures were able to discriminate regions within them, even though the global low-order co-occurrence statistics were identical. Ultimately, it appears that something very close to the Julesz thesis holds true and that humans cannot distinguish textures that locally have the same first- and second-order co-occurrence statistics [43].

However powerful the method of co-occurrence matrices, it evidently turns an analysis problem of a one-dimensional entity—the signal—into the two-dimensional analysis problem of analyzing the co-occurrence matrix. Hence, the key to achieving any analytical power from the method is to keep the co-occurrence matrices and their number small. For developing texture descriptors, researchers have suggested a wide variety of parameters obtained from the co-occurrence matrices [44, 45]. Briefly, let us review some of the most important ones.

Definition (Co-occurrence Matrix Texture Descriptors). Let $x(n)$ be a digital signal; $L \le x(n) \le K$ for some integers L, K and for $a \le n \le b$; let P_δ be the co-occurrence matrix for $x(n)$ with time interval δ; and denote the element at row i and column j of P_δ by $P_\delta(i, j)$. Then, the angular second moment, or energy uniformity, T_a; contrast, T_c; inverse difference moment, T_d; entropy, T_e; and maximum, T_m, descriptors are as follows:

$$T_a(\delta) = \sum_{i=L}^{K} \sum_{j=L}^{K} P_\delta^2(i, j), \tag{4.36}$$

$$T_c(\delta) = \sum_{i=L}^{K} \sum_{j=L}^{K} (i - j)^2 P_\delta(i, j), \tag{4.37}$$

$$T_d(\delta) = \sum_{i=L}^{K} \sum_{j=L}^{K} \frac{P_\delta(i, j)}{1 + (i - j)^2}, \tag{4.38}$$

$$T_e(\delta) = -\sum_{i=L}^{K} \sum_{j=L}^{K} P_\delta(i, j) \log_2 P_\delta(i, j), \tag{4.39}$$

$$T_m(\delta) = \max\{P_\delta(i, j) \mid L \le i, j \le K\}. \tag{4.40}$$

These values are easy to compute and their magnitudes shed light on the nature of the co-occurrence matrix. Note that T_a is smaller for uniform P_δ values and larger for widely varying co-occurrence matrix entries. Low-T_c and high-T_d descriptors indicate heavy groupings of values on P_δ's main diagonal. The entropy descriptor is

large when P_δ values are relatively uniform. The maximum value can be thresholded, or compared to $(T_a(\delta))^{1/2}$, to detect extreme co-occurrence matrix entries. It may also be useful to study the behavior of the descriptors when the time interval δ varies [46].

Now let us turn to another method for texture segmentation. The descriptors it generates turn out be useful for extracting different sizes of repetitiveness in a signal.

4.3.2 Spectral Methods

The spectral approach to texture segmentation applies to textured signals that are very periodic in nature. The analysis tool used in spectral approaches to texture is consequently the sinusoids, or, more generally, the complex exponential, e^{x+jy}. Rudimentary statistical measures of texture, such as the roughness average, R_a, do not adequately account for the presence of different periodic trends in the signal. For instance, a broad undulation may be modulated by a more frequent periodic phenomenon—a ripple on top of a wave. In machined surface characterization, the term for the broad undulations is waviness. Metrologists distinguish waviness from roughness, which is a variation on a finer scale. But this signal phenomenon is hardly confined to the science of characterizing manufactured surfaces. The next example explores this type of textured signal in the context of biomedicine.

Example (Waviness). Figure 4.9 shows some biomedical signals taken from an anesthetized dog: a blood pressure trace (in millimeters of mercury) and an

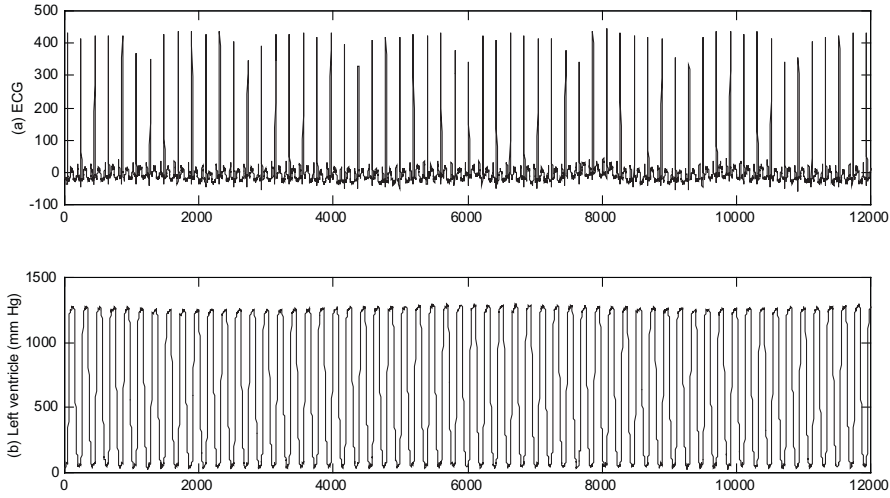

Fig. 4.9. Examples of short-term and long-term periodicities in signals. Panel (a) shows the electrocardiogram from an anesthetized dog. In panel (b) an anesthetized dog's left ventricular blood pressure indicates a short-term variation for the heart contraction and a long-term undulation due to the dog's breathing. This signal has a distinct waviness trend, a long-term undulation, which contrasts with the short-term pressure cycles.

electrocardiogram (dimensionless units). The left ventricle pressure is oscillatory, and—as expected—the histogram has two peaks, or modes, corresponding to the high- and low-pressure intervals within the heart beat. It is easy to identify a threshold that finds the individual pulses, but isolating the gentle waviness that underlies their progression is not as easy. Furthermore, the moment-based statistical methods we considered above do not help to identify the waviness. Such different periodicities in signals occur throughout signal processing and analysis. Problems in biomedicine, digitized speech, industrial control, vibration analysis, remote sensing, shape recognition, and, of course, surface characterization provide many other examples. We need to discover, for such applications, a method distinguish between the short-term periodic features from the long-term undulations in a signal. In surface characterization, the minute variations indicate the roughness of a signal profile, and large-scale, broad repetitions show the presence of waviness.

The sinusoidal functions naturally spring to mind in problems involving short-term and long-term periodicity. Not surprisingly, in order to segment signals containing both a waviness and a roughness character, signal analysts generally employ spectral measures. A comparison of the signal with sinusoids of varying frequency is the natural approach. This is the basis of the spectral method. To compare a signal to a sinusoid, we might proceed as with normalized cross-correlation, by taking the inner product of a portion of the signal with a sinusoidal function. In fact, a family of sinusoids of different frequencies can encompass the range of fine texture, medium texture, and waviness that a signal contains. This is called a spectral strategy, because in its fullest application it can expose an entire range, or spectrum, of periodicities in a signal's values. The foundation of this approach was laid, in fact, by our study of Hilbert spaces in Chapters 2 and 3. Our exploration of spectral approaches to signal texture will be introductory only. In fact, research indicates that statistical methods—and the co-occurrence matrix technique in particular—hold sway over spectral methods [39, 44, 47]. Notwithstanding the superiority of statistical approaches, there is one application for which spectral methods offer an intuitive and powerful approach to texture characterization: the identification of different periodicities—the roughness from the waviness—within a signal.

Let us contemplate the problem of discovering the various periodicities in a discrete signal $x(n)$ over an interval $[a, b] \subset \mathbb{Z}$. Let us assume that $a = 0$ and $b = N - 1$, thus translating our signal to align the beginning of the texture region of interest with the origin. Trigonometric functions, especially the sinusoids, are the natural tool with which to test $x(n)$ on $[0, N - 1]$ for periodic behavior. We know from the introduction to discrete signal frequency in Chapter 1 that the signals $\cos(2\pi nk/N)$, for $k = 0, 1, ..., \lfloor N/2 \rfloor$, range from the lowest ($k = 0$) to the highest (k = largest integer less than $N/2$) possible frequency on $[0, N - 1]$. The inner product $\langle x(n), \cos(2\pi nk/N) \rangle$ of the signals $x(n)$ and $\cos(2\pi nk/N)$ restricted to $[0, N - 1]$ measures of similarity of $x(n)$ to the sinusoid $\cos(2\pi nk/N)$. It is convenient to assume that $x(n) = 0$ outside $[0, N - 1]$. Thus, those values of k over the range $0, 1, ..., \lfloor N/2 \rfloor$, for which $\langle x(n), \cos(2\pi nk/N) \rangle$ has a relatively large magnitude, indicate the presence of a significant periodicity in $x(n)$ of frequency $\omega = 2\pi k/N$ radians per sample. Let's

capture this concept by defining the periodicity descriptors $X_c(k)$ for a signal $x(n)$ defined on $[0, N-1]$:

$$X_c(k) = \left\langle x(n), \cos\left(\frac{2\pi nk}{N}\right)\right\rangle = \sum_{n=0}^{N-1} x(n)\cos\left(\frac{2\pi nk}{N}\right). \tag{4.41}$$

Note that for values of $k = \lfloor N/2\rfloor + 1, \lfloor N/2\rfloor + 2, ..., N-1$, the descriptors repeat in reverse order; specifically, $X_c(N-k) = X_c(k)$ for $k = 1, 2, ..., \lfloor N/2\rfloor$. We can also define periodicity descriptors based on the sine function,

$$X_s(k) = \left\langle x(n), \sin\left(\frac{2\pi nk}{N}\right)\right\rangle = \sum_{n=0}^{N-1} x(n)\sin\left(\frac{2\pi nk}{N}\right). \tag{4.42}$$

In (4.42) we see that $X_s(N-k) = -X_s(k)$ for $k = 1, 2, ..., \lfloor N/2\rfloor$, so that for $k > \lfloor N/2\rfloor$, the $X_s(k)$ descriptors may be useful for detecting sign-inverted periodic signal components also.

One difficulty with the periodicity descriptors is that we do not in general know whether $x(n)$ has a maximal value at $n = 0$ as does $\cos(2\pi nk/N)$. In other words, the texture field may be shifted so that it does not align with the sinusoids used to compute the inner product periodicity measures. Suppose we shift $x(n)$ values in a circular fashion; thus, we let $y(n) = x((n+p) \bmod N)$. We desire that our texture descriptors respond equally well to $y(n)$ and $x(n)$. That is, the descriptors should support some kind of translation invariance. Equivalently, we can shift the sinusoids by amount p and compute new descriptors, $X_{c,p}(k) = \langle x(n), \cos(2\pi n(k-p)/N)\rangle$. This accounts for possible translation of the texture in the source signal $x(n)$, but now we have quite a large computation task. We must compute $X_{c,p}(k)$ for all possible offsets p and all possible frequencies $2\pi k/N$. Can we relate the shifted descriptor, $X_{c,p}(k)$, to the original $X_c(k)$ descriptor values in such a way that we avoid computation of $X_{c,p}(k)$ for multiple offsets p? We calculate,

$$\begin{aligned} X_{c,p}(k) &= \sum_{n=0}^{N-1} x(n)\cos\left(\frac{2\pi(n-p)k}{N}\right) = \sum_{n=0}^{N-1} x(n)\cos\left(\frac{2\pi nk}{N} - \frac{2\pi pk}{N}\right) \\ &= \sum_{n=0}^{N-1} x(n)\left[\cos\left(\frac{2\pi nk}{N}\right)\cos\left(\frac{2\pi pk}{N}\right) + \sin\left(\frac{2\pi nk}{N}\right)\sin\left(\frac{2\pi pk}{N}\right)\right] \\ &= X_c(k)\cos\left(\frac{2\pi pk}{N}\right) + X_s(k)\sin\left(\frac{2\pi pk}{N}\right), \end{aligned} \tag{4.43}$$

which shows that the descriptor $X_{c,p}(k)$ depends not only on $X_c(k)$ but on the sine-based descriptors as well. In other words, as the repetitive pattern of $x(n)$ shifts, both the cosine-based descriptor and the sine-based descriptor vary.

It turns out that a translation-invariant descriptor arises by combining the cosine- and sine-based descriptors into the exponential $\exp(j2\pi nk/N) = \cos(2\pi nk/N) +$

$j\sin(2\pi nk/N)$. Equation (4.43) already hints of this. We form the inner product of $x(n)$ with $\exp(j2pnk/N)$, as above, to get an exponential-based descriptor, $X(k)$:

$$X(k) = \left\langle x(n), \exp\left(\frac{2\pi jnk}{N}\right)\right\rangle = \sum_{n=0}^{N-1} x(n)\exp\left(\frac{-2\pi jnk}{N}\right)$$
$$= \sum_{n=0}^{N-1} x(n)\cos\left(\frac{2\pi nk}{N}\right) - j\sum_{n=0}^{N-1} x(n)\sin\left(\frac{2\pi nk}{N}\right) = X_c(k) - jX_s(k). \qquad (4.44)$$

Now let's consider computing $X(k)$ values for a translated texture $y(n) = x((n+p) \bmod N)$, or, equivalently, by computing the inner product, $X_p(k) = \langle x(n), \exp(2\pi jn(k-p)/N)\rangle$:

$$X_p(k) = \left\langle x(n), \exp\left(\frac{2\pi j(n-p)k}{N}\right)\right\rangle = \sum_{n=0}^{N-1} x(n)\exp\left(\frac{-2\pi j(n-p)k}{N}\right)$$
$$= \exp\left(\frac{2\pi jpk}{N}\right)\sum_{n=0}^{N-1} x(n)\exp\left(\frac{-2\pi jnk}{N}\right) = \exp\left(\frac{2\pi jpk}{N}\right)X(k). \qquad (4.45)$$

Now we have $|X_p(k)| = |\exp(2\pi jpk/N)X(k)| = |X(k)|$. In other words, we have shown the following:

Proposition (Translation Invariance of $|X(k)|$). The complex norm of the periodicity descriptor, $|X(k)|$, is invariant with respect to the modulo-N translation of the textured source signal, $x(n)$, defined by (4.44) on $[0, N-1]$.

This, then, is the tool we need to isolate periodic components within textures according to their different frequencies.

The values $X(k)$ in (4.44), for $k = 0, 1, ..., N-1$, represent the discrete Fourier transform of the signal $x(n)$ on $[0, N-1]$. We know the signals $X(k)$ already from Chapter 2. There we considered them, after a suitable normalization, as an orthonormal set on $[0, N-1]$, $\{e_k(n) \mid 0 \le k \le N-1\}$:

$$e_k(n) = \frac{\exp(j2\pi kn/N)}{\sqrt{N}}[u(n) - u(n-N)], \qquad (4.46)$$

where $u(n)$ is the unit step signal. It is common to call the values $X(k) = \langle x(n), \exp(2\pi jnk/N)\rangle$ the Fourier coefficients of $x(n)$, even though, precisely speaking, we need to normalize them according to the inner product relation on an orthonormal set (4.46). Readers must pay close attention to the definitions that textbooks provide. When discussing Hilbert space decompositions, textbooks usually normalize the coefficients according to (4.46), whereas ordinarily they omit the $N^{-1/2}$ factor in the DFT's definition.

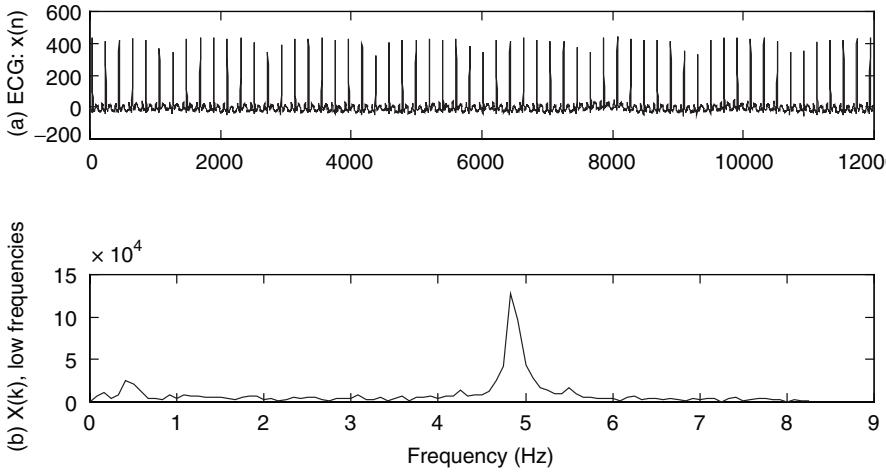

Fig. 4.10. Biomedical signal waviness extraction. The spectral method helps to identify the two sinusoidal components of the ECG signal (a). The main periodic trend is just below 5 Hz, and the waviness is the small peak below 0.5 Hz (b).

The theory and applications of the DFT will comprise much of Chapters 6 and 7. Let us content ourselves here with two applications of spectral texture analysis: first, to the biomedical signals of Fig. 4.9 and, second, to digitized speech segmentation and recognition. Figure 4.10 shows the results of applying the spectral texture descriptors $|X(k)|$ to biomedical signals.

Example (Biomedical Signal Frequency Analysis). Consider the ECG signal for the anesthesized dog.

Application (Voiced versus Unvoiced Speech Segmentation). This example continues the discussion of speech phoneme segmentation that we began in Section 4.2.2 with voiced and unvoiced consonants. Linguists typically classify speech events according to whether the vocal cords vibrate during the pronunciation of a speech sound, or phoneme (Table 4.3). If the vocal cords do vibrate, then there is said to be a voiced speech event. If there is no vocal cord vibration, then the phoneme is unvoiced. It is also possible that a speech signal contains no speech sound; thus, it is simply background, or noise. One approach to segmenting speech classifies its portions as voiced (V), unvoiced (U), or noise (N). For example, a digital recording of the English phrase "linear fit" begins, divides the two words, and ends with noise regions. The most apparent phonemes, then, are /l I n i ɜ f I t/, of which /f/ and /t/ are unvoiced. A preliminary segmentation, Σ_0, by voiced/unvoiced/noise classification is (N, V, N, U, V, U, N), respecting the stipulation that no adjacent regions have the same type. Actually, there are a number of unvoiced events that only become apparent when the speech signal is digitized and spread out over time. One may find, for example, momentary unvoiced aspirations and even periods

TABLE 4.3. More Complete Table of Phonemes and Examples from American English [12].[a]

Phoneme	Example	Class	Phoneme	Example	Class
/i/	even	Front vowel	/I/	signal	Front vowel
/e/	basis	Front vowel	/ɛ/	met	Front vowel
/ae/	at	Front vowel	/a/	father	Mid vowel
/Λ/	but	Mid vowel	/⊃/	all	Mid vowel
/schwa/	signal	Mid vowel	/u/	boot	Back vowel
/o/	boat	Back vowel	/U/	foot	Back vowel
/Ɨ/	roses	Back vowel	/ɘ/	Hilbert	Mid vowel
/a^{w}/	down	Dipthong	/a^{y}/	cry	Dipthong
/⊃^{y}/	boy	Dipthong	/y/	yet	Semivowel glide
/w/	wit	Semivowel liquid	/r/	rent	Semivowel glide
/l/	linear	Semivowel liquid	/m/	segment	Nasal consonant
/n/	nose	Nasal consonant	/ŋ/	Nguyen	Nasal consonant
/p/	partition	Unvoiced stop	/t/	fit	Unvoiced stop
/k/	kitten	Unvoiced stop	/b/	bet	Voiced stop
/d/	dog	Voiced stop	/g/	gain	Voiced stop
/h/	help	Aspiration	/f/	fit	Unvoiced fricati
/θ/	thanks	Unvoiced fricative	/s/	sample	Unvoiced fricati
/sh/	shape	Unvoiced fricative	/v/	vector	Voiced fricative
/∂/	that	Voiced fricative	/z/	zoo	Voiced fricative
/zh/	closure	Voiced fricative	/ch/	channel	Affricate
/j/	Jim	Affricate	/?/	no sound	Glottal stop

[a]Vowels are voiced, and they break down further into front, mid, and back classifications, according to t location of the tongue's hump in the mouth. Vowels typically consist of two oscillatory components, call formants. Other essentially vowel-like sounds are the dipthongs and the semivowels. The glottal stop is special symbol that indicates a momentary suspension of motion by the vocal cords (glottis). For exampl without the /?/ symbol, the phoneme sequences for "I scream" and "ice cream" are identical. As big as it this table is far from panoramic; it offers but a glimpse of the natural language segmentation problem.

of noise, surrounding the voiced segments. A refined segmentation, Σ_1, therefore supplies: (N, U, V, U, V, U, V, U, V, U, V, U, N, U, V, U, N). In practical speech recognition applications, surprisingly, this segmentation is too crude! Subtle periods of background noise, with no voiced or unvoiced sound present, intrude into spoken words. A modern, sophisticated segmentation algorithm finds that several N regions split the unvoiced regions U in the refined segmentation above. This means that several of the unvoiced intervals have much shorter time extents than Σ_1 would indicate. The benefit is that a higher-level interpretation algorithm may be better able to recognize the brief U boundaries of the V segments as trailing and leading aspirations instead of, for example, unvoiced fricatives. Figure 4.5 illustrates such a speech segmentation example. We shall continue to expose the intricacies of natural language interpretation is this and the remaining chapters. Chapter 9, in particular, introduces several frequency-domain signal analysis tools for speech interpretation.

Vowels contain two frequency components called formants. It is hard to adapt the level-based approach of thresholding to these oscillatory parts of signals. Also, the statistical measures of texture do not account well for the time intervals between transitions, and yet this is the most important aspect of signal frequency. What we need to do is to discover some way to extract the degree of similarity between some raw, noisy signal and a pure sinusoid.

4.3.3 Structural Approaches

When the precise description of local texture elements is important, then the structual approach to texture segmentation comes to the fore. The statistical and spectral methods provide numerical estimates for the amount and distribution of variability within signal regions. Simple statistical measures lose the repeating parts of the signal in the sums and integrations of their mathematical implementation. The co-occurrence matrix method retains this information when co-occurrence matrices are computed for several values of the time offset, δ. The structural approach, on the other hand, relies on texture descriptors that provide a model of a local pattern that is replicated, in one or another degree, at one or another locations across the domain of the signal. Thus, the structural approach has a pattern recognition flavor. We need to develop some basic tools for structural pattern recognition it order to cover this approach adequately, and we will do this later in Section 4.7.

4.4 FILTERING AND ENHANCEMENT

This section considers some supplementary operations that can greatly improve the performance of low-level segmentation processes before the thresholding operation: convolutional smoothing, median filtering, morphological filtering, and histogram enhancement.

4.4.1 Convolutional Smoothing

Let us here expand upon the idea of filtering a signal before it passes to a threshold operation. The purpose of preliminary filtering is to prevent labeling mistakes before they happen. Three types of filters are in common use for this purpose: convolutional filters of the type we covered in Chapters 2 and 3, for discrete and analog signals, respectively; median filters; and morphological filters.

We noted by example in the previous section that oscillatory areas of signals may contain mixtures of low- and high-magnitude signal values. Such a region may be meaningful signal in its totality, and for many applications it is not correct to separately segment the low-magnitude regions and label them as background. A linear smoothing filter proved useful for this purpose. Chapter 2 introduced the *moving average* system given by

$$y(n) = \frac{1}{2N+1} \sum_{k=-N}^{N} x(k). \tag{4.47}$$

It is also called a box filter, from the shape of its impluse response. This linear, translation-invariant (LTI) system averages the input signal values within a window of length $2N+1$ around each $x(n)$. Its effect on a oscillatory signal region, $[a, b]$, is to blur the high and low signal values together. Thus, for some threshold $T > 0$, the system's output, $y(n) = (Hx)(n)$, has magnitude $|y(n)| \geq T$ within $[a, b]$. It is also possible to smooth using an infinite impulse response filter. For example, $y(n) = ay(n - 1) + x(n)$, with impulse response $h(0) = 1$, and $0 < a < 1$ is a possibility (Section 2.4.2). Smoothing with LTI systems blends oscillations together into more blob-like, easily thresholded regions. It also reduces background noise when the signal of interest is of relatively low magnitude.

The moving average system of (4.47) is not the only filter available for smoothing signals. One problem that readers may already note (see Chapter 2) is that this filter is not causal. So it cannot be applied to a data stream as values arrive in real time. It also has sharp edges where its support ends, which, for some types of input signals, causes its output to change abruptly. We will find in Chapter 7 some problems with how this filter treats frequencies inside the input signal; in fact, this motivates us to search for alternatives. A causal box filter averages only the current and some previous samples: $y(n) = (1/3)[x(n) + x(n-1) + x(n-2)]$, for example.

Noise in signals varies widely. It is usually a detriment to signal quality; but in some interesting cases, it is actually helpful. In digital telephony, for example, comfort noise is generated and automatically inserted into the line during episodes when both talkers are quiet. The reason for this is that silent periods can be used to carry other voices. The telephone company's central office multiplexing equipment routinely disconnects the channel, fills it with other voice traffic, and swiftly provides an alternative link when someone speaks. But it is disconcerting to almost everyone to hear a silent line. Realizing this, telecommunication engineers design the multiplexers to inject a small amount of white noise onto the two ends of the interrupted link. Since the synthetic noise level is matched to the background noise present while the conversants speak, the change is imperceptible. Another example of the value of noise synthesis is in active noise cancellation.

Now let us return to our discussion of noise removal. We consider a filter that has been widely used for noise mitigation—the discrete version of the Gaussian. This filter has the impulse response

$$h(n) = \frac{1}{\sqrt{2\pi}\sigma} e^{-\frac{1}{2}\left(\frac{\tau n}{\sigma}\right)^2}, \tag{4.48}$$

where $\tau > 0$ is some sampling interval. This filter emphasizes the signal values near the value, $x(n)$. Thus, it differs from the moving average filter, which considers all quantities equally valuable in a neighborhood $[x(n - N), \ldots, x(n + N)]$ around $x(n)$. We shall investigate this type of filter carefully in the last section of this chapter. For pattern recognition applications based on signal shape over multiple scales and convolutional filtering, there are strong theoretical reasons for using Gaussian filters above all others.

4.4.2 Optimal Filtering

It is also possible to derive filters that are, in some sense at least, optimal for removing the kind of noise that affects input signals to an application. Here, we will outline two approaches for designing such filters: One method uses least-squares principles [48–50], and another involves constrained minimization—a Lagrange[4] multipliers approach [51]. Time-domain methods for noise removal, such as these, generally depend upon statistical information about the signal values.

We can pose the search for an optimal noise removal filter as a least-squares search. Suppose that the noise removal filter H is linear and translation-invariant. Then the Convolution Theorem for LTI Systems (Chapter 2) instructs us that $y = Hx$ is given by convolution of $h(n) = (H\delta)(n)$. We assume a real-valued, noisy input signal $x(n)$. Let us further seek a finite impulse response (FIR) filter, of width $M = 2p + 1$, supported on $[m - p, m + p]$, and ask what filter coefficients $h(n)$ give the best estimate of x at time instant p: $y(p) = (Hx)(p)$. We view the FIR filtering operation as a matrix operation, $Ah = b$, where the rows of matrix A are noisy samples of the input signal $x(n)$ from $n = m - p$ to $n = m + p$; h is a column vector with entries $h(-p)$, $h(-p + 1)$, ..., $h(p)$; and b is a row vector with FIR filtered values of the input. Suppose we filter N sets of noisy input windows of signal $x(n)$ around $n = p$, $(a_{1,1}, a_{1,2}, ..., a_{1,M})$, $(a_{2,1}, a_{2,2}, ..., a_{2,M})$, ..., $(a_{N,1}, a_{N,2}, ..., a_{N,M})$, with the filter $h(n)$. Suppose further that we know the true value (i.e., before corrupted by noise) of the input signal for each sample set at $n = p$; call them $b_1, b_2, ..., b_N$. Then we are in fact asking for the vector h for which the matrix product Ah is the best approximation to the ground truth vector b, representing uncorrupted input signal values $x(n)$ at $n = p$. Our quest for a best noise removal filter reduces to a problem of finding the column vector h, given a matrix A, which upon matrix multiplication Ah is closest to known signal values b. The theory of this problem is easiest if we consider the closest approximation to b in vector norm: we need to minimze $\|Ah - b\|^2$. In other words, the best filter problem reduces to a classic least squares minimization problem. The following theorem—mainly from linear algebra and numerical analysis [48, 50, 52], but drawn with a signal processing twist—summarizes this unconstrained search for the best FIR noise removal filter.

Theorem (Least-Squares Optimal Noise Removal Filters). If the vectors x, y, and b are real and the matrices A and M are real, then with the above premises and notation, the following statements are true:

1. If the columns of matrix A are linearly independent, then A^TA is symmetric and positive definite: $(A^TA)^T = A^TA$, and $x^T(A^TA)x \geq 0$ for all vectors $x \neq 0$.
2. If the square matrix M is positive definite, then the quadratic equation in a real vector x,

[4]Joseph Louis Lagrange (1736–1813), professor of mathematics at Turin, Berlin, and Paris, discovered the powerful technique of introducing new variables, subject to additional constraints, into an equation to be solved.

$$Q(x) = (1/2)x^T Mx - x^T c, \tag{4.49}$$

has a minimum of

$$Q(M^{-1}c) = (-1/2)c^T M^{-1} c, \tag{4.50}$$

when $Mx = c$.

3. The vector $h = (A^TA)^{-1}\, A^T b$ minimizes $\|Ah - b\|^2$.
4. The FIR filter $h(n) = [h(-p), h(-p+1), \ldots, \underline{h(0)}, \ldots, h(p)]$, given by the vector h of (3) is optimal for noise removal from signal $x(n)$, where matrix A in (3) is a set of noisy windows of $x(n)$, and b is the set of noise-free values of $x(n)$ corresponding to A's noisy sample sets.

Proof: To see statement 1, consider some vector x, and note that $x^T(A^TA)x = (Ax)^T(Ax) = \|Ax\|^2$. Since the columns of A are linearly independent, Ax, which is a linear combination of columns of A (the column space of A), cannot be 0 unless $x = 0$. Hence, A^TA is positive definite. Symmetry follows from the basic fact that $(AB)^T = B^TA^T$. For statement 2, observe that if $Mx = c$, then

$$Q(y) - Q(x) = (1/2)(y - x)^T M(y - x) \geq 0 \tag{4.51}$$

by the fact that M is positive definite; so $Q(y) \geq Q(x)$, and the minimum (4.50) follows. Turning to statement 3, now note that $\|Ah - b\|^2 = (Ah - b)^T(Ah - b) = x^TA^TAh - h^TA^Tb - b^TAh + b^Tb$. So minimizing $\|Ah - b\|^2$ is equivalent to minimizing $h^TA^TAh - h^TA^Tb - b^TAh$. Also, thinking of the 1×1 matrices here as real numbers, we find $h^TA^Tb = b^TAh$. So the minimization of $\|Ah - b\|^2$ reduces to a minimization of $Q(h) = (1/2)h^T(A^TA)h - h^TA^Tb$. But this is precisely (4.49) with $M = A^TA$ and $c = A^Tb$. Finally, statement 4 of the theorem simply expresses the equivalence of convolution using an FIR filter, $h(n)$, with vector dot products. Filter $h(n)$ is optimal in the sense that any other noise removal filter $g(n)$ will produce errors with respect to know values for $x(n)$ at $n = p$ that are larger in l^2 norm than those which $h(n)$ produces. ■

Example. Suppose that a signal $x(n)$ is corrupted with Gaussian noise, and we seek an optimal noise removal filter H with $(H\delta)(n) = h(n) = [h(-1), \underline{h(0)}, h(1)]$. We record a series of windows of width 3 of the input signal $x(n)$ around $n = 0$: $[a_{1,1}, a_{1,2}, a_{1,3}]$, $[a_{2,1}, a_{2,2}, a_{2,3}]$, ..., $[a_{m,1}, a_{m,2}, a_{m,3}]$. In this case, the normal equations become $Ah = b$, where, for example,

$$A^T = \begin{bmatrix} 1.12 & 0.94 & 0.77 & 0.96 & 1.83 & 0.52 & 0.91 \\ 0.86 & 1.31 & 0.94 & 1.19 & 2.15 & 0.70 & 1.03 \\ 1.19 & 2.72 & 0.32 & 0.65 & -0.04 & 0.89 & 1.21 \end{bmatrix}. \tag{4.52}$$

Upon solving the normal equations, we find $h(n) = [h(-1), \underline{h(0)}, h(1)] = [1.08, .92, 1.17]$, very close to the box or moving average filter to which our original intuition

guided us. Now let us consider the possibilty that the noise on $x(n)$ is correlated; in particular, if we assume a correlation between the noise magnitude at $x(0)$ and that at $x(-1)$ and $x(1)$, then we arrive at normal equations with the following coefficient matrix

$$A^T = \begin{bmatrix} 1.12 & 0.98 & 0.85 & 0.90 & 0.73 & -0.11 & 1.13 \\ 0.86 & 1.24 & 1.32 & 1.23 & 1.07 & 0.89 & 1.20 \\ 1.19 & 1.69 & 0.79 & 0.97 & 1.01 & 0.35 & 1.03 \end{bmatrix}. \tag{4.53}$$

The solution to the normal equations provides an estimate $h(n) = [h(-1), \underline{h(0)}, h(1)] = [0.85, 1.12, 0.93]$, emphasizing the central filter value. Thus it is the correlation between successive noise values within the input signal $x(n)$ that governs the departure of the optimal filter from the moving average filter.

It is possible to adopt a different least-squares approach for optimal noise removal. For example, a popular approach [49] is to fit quadratic (or higher-order) polynomials to the signal values to obtain families of filters of varying support. There result filters that smooth signals, but do not resemble the simple box or Gaussian filters at all. Table 4.4 shows representative finitely supported smoothing filters that derive from this procedure.

Now let's consider a constrained approach to optimal noise removal filter design. Again, we seek an LTI system H with an impulse response $h = H\delta$, of width $M = 2p + 1$, supported on $[m-p, m+p]$. Again we ask what $h(n)$ must then be to optimally remove noise from known signal $x(n)$. Since we are concerned once more with an FIR filter and a noisy source signal $x(n)$, we may view both as row vectors. We view the system output $y = Hx$ as an estimator of the random vector x which has expected value vector $\mu b = E[x]$, where b is the M-dimensional row vector of all ones. In vector terms we seek a row vector h such that $\hat{\mu} = \langle h, x \rangle$ is an estimator of $y(m) = (Hx)(m)$. Here, $\langle\ ,\ \rangle$ is the vector inner (dot) product operation. We desire the random variable $\hat{\mu}$ to be unbiased, so that its mean on $[m-p, m+p]$ is the same as $x(n)$'s value on this interval. In other words, $E[\hat{\mu}] = \mu$. This condition implies the following condition on impulse response h:

TABLE 4.4. Smoothing Filters Derived from Polynomial Fits to Signal Values[a]

Points	Quadratic Polynomial Fit:	Quartic Polynomial Fit:
5	[…, .4857, .3429, −.0857]	[…, 1.500, −.5000, .2500]
7	[…, .3333, .2857, .1429, −.0952]	[…, .5671, .3247, −.1299, .0216]
9	[…, .2554, .2338, .1688, .0606, −.0909]	[…, .4172, .3147, .0699, −.1282, .0350]
11	[…, .2075, .1958, .1608, .1026, .0210, −.0839]	[…, .3333, .2797, .1399, −.0233, −.1049, .0420]

[a]In the table, all of the impulse responses are even, and only the values for non-negative time instants are shown. Such noise removal filters are popular for smoothing data acquired from laboratory instruments [49].

Proposition (Unbiased Estimator). If the estimator $\hat{\mu}$ is unbiased, then

$$\sum_{n=m-p}^{m+p} h(n) = 1. \tag{4.54}$$

Proof: Since $E[\hat{\mu}] = \mu$, we have $E[\hat{\mu}] = E[\langle h, x\rangle] = \langle h, E[x]\rangle = \mu\langle h, b\rangle$, and therefore $\langle h, b\rangle = 1$. In terms of the impulse response of system H, this is (4.54); the proof is complete. ■

Let us continue this notational framework for the next two results. If we require the further condition that the estimator $\hat{\mu}$ have minimal variance, the following holds:

Proposition (Variance of Unbiased Estimator). If the estimator $\hat{\mu}$ is unbiased, then $\mathrm{Var}[\hat{\mu}] = \langle h, h\Sigma\rangle$, where $\Sigma = \mathrm{E}[(x - \mu b), (x - \mu b)]$ is the covariance matrix of the random vector x.

Proof: We calculate

$$\begin{aligned}\mathrm{Var}[\hat{\mu}] &= E[(\hat{\mu} - E[\hat{\mu}])^2] = E[(\langle h, x\rangle - \mu)^2] = E[(\langle h, x\rangle - \langle h, \mu b\rangle)^2] \\ &= E[\langle h, h\langle (x - \mu b), (x - \mu b)\rangle\rangle] = \langle h, hE[(x - \mu b), (x - \mu b)]\rangle = \langle h, h\Sigma\rangle. \end{aligned} \tag{4.55}$$

■

Now we wish to minimize $\mathrm{Var}[\hat{\mu}]$ subject to the constraint of the first Unbiased Estimator Proposition. The next theorem solves this is typical Lagrange multipliers problem.

Theorem (Unbiased Minimal Variance Estimator). If the estimator $\hat{\mu}$ is unbiased and has minimal variance, then

$$\mathbf{h} = \left(\frac{1}{\left\langle \mathbf{b}\Sigma^{-1}, \mathbf{b} \right\rangle} \right) \mathbf{b}\Sigma^{-1}. \tag{4.56}$$

Proof: To apply Lagrange multipliers to the optimization problem, let us introduce a function, $L(h)$, with an additional parameter, λ:

$$L(h) = \mathrm{Var}[\hat{\mu}] + \lambda(\langle h, b\rangle - 1) = \langle h, h\Sigma\rangle + \lambda(\langle h, b\rangle - 1). \tag{4.57}$$

Recall that the impulse response of the optimal filter we seek, $h(n)$, was supported on $[m-p, m+p]$. So the vector h is a $1 \times M = 1 \times (2p+1)$ row vector: $h = (h_1, h_2, \ldots, h_M)$. We next calculate the partial derivatives:

$$\left(\frac{\partial L}{\partial h_1}, \quad \frac{\partial L}{\partial h_2} \quad \ldots \quad \frac{\partial L}{\partial h_{\mathrm{M}}} \right) = 2\mathbf{h}\Sigma + \lambda \mathbf{b}. \tag{4.58}$$

Since the partial derivatives (4.58) are zero where $L(h)$ has a minimum, we solve $0 = 2h\Sigma + \lambda b$ for the vector h:

$$\mathbf{h} = -\left(\frac{\lambda}{2} \right) \mathbf{b}\Sigma^{-1}. \tag{4.59}$$

Taking the inner product of both sides of (4.59) with the all-ones vector b and applying the constraint $\langle h, b \rangle = 1$ gives

$$1 = \langle \mathbf{h}, \mathbf{b} \rangle = -\left(\frac{\lambda}{2} \right) \left\langle \mathbf{b}\Sigma^{-1}, \mathbf{b}. \right\rangle \tag{4.60}$$

and

$$\lambda = \frac{-2}{\left\langle \mathbf{b}\Sigma^{-1}, \mathbf{b} \right\rangle}. \tag{4.61}$$

Finally, substituting (4.61) into (4.59) gets us to (4.56), and the proof is complete. ■

The determination of the optimal filter $h(n)$ therefore depends entirely on the covariance matrix Σ.

Example. Suppose we seek a filter supported on $[-1, 1]$, and the random noise embedded in input signal $x(n)$ is uncorrelated. If the variances at $x(-1)$ and $x(1)$ are equal, say they are $\alpha\sigma^2$, where σ^2 is the variance of $x(0)$, then we have the following:

$$\Sigma = \sigma^2 \begin{bmatrix} \alpha & 0 & 0 \\ 0 & 1 & 0 \\ 0 & 0 & \alpha \end{bmatrix}, \tag{4.62}$$

$$h = \frac{1}{1 + 2\alpha^{-1}} \begin{bmatrix} \alpha^{-1} \\ 1 \\ \alpha^{-1} \end{bmatrix}. \tag{4.63}$$

Example. Suppose that a filter with support on [–1, 1] is again necessary, but that the random noise is correlated. Suppose that values one time instant apart have correlation ρ and values two time instants apart have correlation ρ^2. Then we have the following

$$\Sigma = \sigma^2 \begin{bmatrix} 1 & \rho & \rho^2 \\ \rho & 1 & \rho \\ \rho^2 & \rho & 1 \end{bmatrix}, \tag{4.64}$$

$$h = \frac{1}{(1-\rho)(3-\rho)} \begin{bmatrix} (1-\rho) \\ (1-\rho)^2 \\ (1-\rho) \end{bmatrix}. \tag{4.65}$$

The above development of optimal noise removal filters using Lagrange multipliers is usually presented for designing neighborhood smoothing operators in image processing [51]. We have adapted it here for one-dimensional filters. One consequence of this is that the covariance matrices (which are $M \times M$ rather than $M^2 \times M^2$, where M is the filter size) are much easier to invert.

There are some situations where convolutional filtering does not do a good job at enhancement before thresholding and segmentation. The next section considers such cases and develops some simple nonlinear smoothing filters which have proven to be very powerful and very popular.

4.4.3 Nonlinear Filters

Filtering with LTI systems may well result in an incorrect segmentation in those situations where signals contain transient phenomena, such as sharp, high-magnitude spikes. From simple faith in the principal theorems of probability, such as the Central Limit Theorem, we tend to dismiss the possibility of very high magnitude spikes in our data. After all, after repeated trials the sum of any distributions will tend toward a Gaussian distribution. Some 68.26% of the signal values should lie within one standard deviation, σ, of the signal mean, μ. Over 95% of the values should be less than 2σ from μ. And huge values should be extremely rare, using this logic. But this reasoning is flawed. Such transients may occur to severe, short-duration noise in the process that generates the source signal or result from imperfections in the signal acquisition apparatus.

The reason LTI filters become problematic is that for a very large impulse, the output of the smoothing signal $y(n)$ resembles the filter's impulse response. The linearity is the problem. Another problem with linear smoothing filters is their tendency to blur the sharp edges of a signal. Good noise removal requires a filter with a wide support. But this erodes sharp edges, too. Thus, when the thresholding operation is applied, the regions labeled as meaningful signal may be smaller in extent than they would be without the preliminary filtering. Perhaps separate regions blend together,

rendering the final form of the signal unrecognizable by the classification step in the application. The problem here is the wide support of the filter impulse response.

Two types of nonlinear filters are widely used for impulse noise removal: median and morphological filters. Properly chosen, these filter a noisy signal without leaving a large-magnitude response that interferes with the subsequent thresholding operation. Like convolutional filters, median and morphological noise removal are handy before thresholding. By dint of their nonlinearity, however, they can preserve the binary nature of a thresholded signal; they can also be used to clean out the speckle noise that often persists in a signal after thresholding.

4.4.3.1 Median Filters. A discrete median filter, H, accepts a signal $x(n)$ as input and produces $y(n)$, which is the median value of $x(n)$ in a neighborhood around $x(n)$.

Definition (Median Filter). If N is a positive integer, then the median filter $y = Hx$ for the neighborhood of width $2N+1$ is defined by $y(n) = \text{median}\{x(m) \mid n-M \le m \le n+N\}$.

To compute a median filter, the values $x(n-N)$, $x(n-N+1)$, ... , $x(n+N)$ must be sorted and the middle element selected. It is possible, and maybe useful, to have asymmetric median filters as well as to take $y(n)$ to be the median of a set that does not contain $x(n)$; nevertheless, the centered filter is the most common.

As an enhancement tool, the median filter is usually an early signal processing stage in an application, and most applications use it to improve segmentation operations that depend on some kind of thresholding. We have noted that convolutional filters tend to smear signal edges and fail to fully eradicate sharp transient noise. The main points to keep in mind about the median filter as an enhancement tool are as follows:

- It removes impulse noise.
- It smoothes the signal.
- The median can be taken over a wider interval so that the filter removes transients longer than a time instant in duration.
- Median filters preserve sharp edges.

In addition, since median filters involve no floating point operations, they are well-suited for implementation on fixed-point digital signal processors (which are much faster than their floating-point capable cousins) and in real-time applications [53]. An alternative to using wide median filters is to apply a small support median filter many times in succession. Eventually this reduces the original signal to the median root, which is no longer affected by further passes through the same filter [54].

4.4.3.2 Morphological Filters. From the very beginning of this book, all of the signal operations have been algebraic—additive, multiplicative, or based upon some extension thereof. To conceptualize analog signals, we freely adopted real- and

complex-valued functions of a real variable. To conceptualize discrete signals, we made them into vectors-without-end, as it were. Analog signal operations and analog system theory derived straight from the theory of functions of a real variable. And vector operations inspired discrete signal manipulations, too. Thus, analog and discrete systems added signals, multiplied signals by a scalar value, convolved them, and so on. This is not at all surprising. Signals are time-ordered numerical values, and nothing is more natural for numbers than arithmetic operations. But there is another, distinctly different, and altogether attractive viewpoint for all of signal processing and analysis: mathematical morphology.

Mathematical morphology, or simply morphology, relies on set-theoretic operations rather than algebraic operations on signals. Morphology first casts the concept of a signal into a set theoretic framework. Then, instead of addition and multiplication of signal values, it extends and contracts signals by union and intersection. The concept at the fore in morphology is shape, not magnitude.

It ought to be easier to understand the morphological perspective by thinking for a moment in terms of binary images in the plane, instead of signals. A binary image is a map I: $\mathbb{R} \times \mathbb{R} \to \{0, 1\}$. The binary image, I, and the subset of the plane, $A = I^{-1}(\{1\}) = \{(s, t) \in \mathbb{R} \times \mathbb{R} \mid I(s, t) = 1\}$ mutually define one another. (The image is precisely the characteristic function of the set A.) So we can think of a binary image as either a function or a set. Now suppose we have a small circle $C = \{(s, t) \mid s^2 + t^2 \leq r\}$, with $r > 0$. Suppose we place the center of C on top of a boundary point of $(a, b) \in A$; we find all of the points, (r, s) covered by C, $B = \{(r, s) \mid (r-a)^2 + (s-b)^2 \leq r^2\}$; and we set $A' = A \cup B$. We continue this placement, covering, and union operation for all of the boundary points of A. The result is the set A with a shape change effected for it by the morphological shaping element, B. This scheme works just as well for binary-valued signals: An analog binary signal is the characteristic function of a subset of the real line, and a discrete binary signal is the characteristic function of a subset of the integers.

Let's begin our brief tour of mathematical morphology with the definitions and basic properties for binary morphological operations. This will introduce the terminology and concepts as well as provide a theoretical foundation for our later extension to digital signals. Just as we can identify a binary image with a binary signal, we can also characterize a binary discrete signal with a subset of the integers or a binary analog signal with a subset of the real line. The signal is the characteristic function of the set. Although morphologists work their craft on either $\mathbb{Z}^n$ or $\mathbb{R}^n$ [55–57], we shall consider digital signals and restrict our morphological investigation to discrete n-space, $\mathbb{Z}^2$. Note that the development could proceed as well for n-tuples from an abstract normed linear space.

Definition (Translate of a Set). Let $A \subseteq \mathbb{Z}^2$ and $k \in \mathbb{Z}^2$. Then the translate of A by k is $A_k = A + k = \{a + k \mid a \in A\}$.

Definition (Dilation). Let $A, B \subseteq \mathbb{Z}^2$. Then the dilation of A by B is

$$A \oplus B = \bigcup_{b \in B} (A + \mathbf{b}). \tag{4.66}$$

The set B in (4.66) is called a structuring element; in this particular instance, it is a dilation kernel.

From this meager beginning, we see the development of diverse, interesting, useful properties.

Proposition (Dilation Properties). Let $A, B, C \subseteq \mathbb{Z}^2$ and $k \in \mathbb{Z}$. Then, $A \oplus B = \{a + b \mid a \in A \text{ and } b \in B\}$. Moreover, dilation is commutative, $A \oplus B = B \oplus A$; associative, $(A \oplus B) \oplus C = A \oplus (B \oplus C)$; translation invariant, $(A + k) \oplus B = (A \oplus B) + k$; increasing: if $A \subseteq B$, then $A \oplus D \subseteq B \oplus D$; distributive over unions: $A \oplus (B \cup C) = (A \oplus B) \cup (A \oplus C)$.

Proof: Let's show translation invariance. We need to show that the two sets, $(A + k) \oplus B$ and $(A \oplus B) + k$ are equal; thus, we need to show they contain the same elements, or, equivalently, that they are mutual subsets. If $x \in (A + k) \oplus B$, then there is $a \in A$ and $b \in B$ such that $x = (a + k) + b = (a + b) + k$. Since $a + b \in A \oplus B$, we know $(a + b) + k = x \in (A \oplus B) + k$. Thus, $(A + k) \oplus B \subseteq (A \oplus B) + k$. Now let's consider an element $x \in (A \oplus B) + k$. It must be of the form $y + k$, for some $y \in A \oplus B$, by the definition of the translate of $(A \oplus B)$. Again, there must be $a \in A$ and $b \in B$ such that $y = a + b$. This means $x = (a + b) + k = (a + k) + b \in (A + k) \oplus B$. Thus, $(A \oplus B) + k \subseteq (A + k) \oplus B$. Since these two are mutual subsets, the proof of translation invariance is complete. The other properties are similar, and we leave them as exercises. ■

Notice that the distributivity property implies that dilations by large structuring elements can be broken down into a union of dilations by smaller kernels.

How can dilation serve as a noise removal operation within a digital signal analysis application? To answer this question we adopt a set-theoretic description for discrete signals, $x(n)$, based on the graph of the signal, $\text{Graph}(x) = \{(n, x(n)) \mid n \in \mathbb{Z}\}$. $\text{Graph}(x)$ is a subset of the discrete plane, so it describes x(n) in set theory terms, but we need other tools to adequately define signal dilation. Our exposition draws the concepts of umbra and top surface from the tutorial of Haralick et al. [55].

Definition (Umbra). Let $x(n)$ be a digital signal, x: $\mathbb{Z} \to [0, N]$, for some natural number $N \geq 0$. Then the umbra of x is $\text{Umbra}(x) = \{(n, m) \in \mathbb{Z} \times [0, N] \mid m \leq x(n)\}$.

Definition (Top Surface). If $A \subseteq \mathbb{Z}^2$ and $B = \{b \in \mathbb{Z} \mid (b, k) \in A, \text{ for some } k \in \mathbb{Z}\}$, then the top surface for A is the function, $T[A]$, that has domain B and is defined $T[A](b) = \max \{k \in \mathbb{Z} \mid (b, k) \in A, \text{ for some } k \in \mathbb{Z}\}$.

Thus, the umbra of a digital signal $x(n)$ is the planar set consisting of $\text{Graph}(x)$ and all the points beneath it. The umbra operation turns a signal into a set, and the top surface operation turns a set into a function. Clearly, if $x(n)$ is a digital signal, x: $\mathbb{Z} \to [0, N]$, for some natural number $N \geq 0$, then $x = T[\text{Umbra}(x)] = T[\text{Graph}(x)]$. The next definition formally captures the idea of digital signal dilation.

Definition (Signal Dilation). Let $x(n)$ and $h(n)$ be digital signals, $x\colon \mathbb{Z} \to [0, N]$ and $h\colon \mathbb{Z} \to [0, N]$ for some natural number $N \geq 0$. Then the dilation of f by h, is $f \oplus h = T[\text{Umbra}(f) \oplus \text{Umbra}(h)]$.

Dilation is useful for removing transient signal features, such as splintering, when a signal contains a sharp gap within the overall blob-like structure. This can occur due to noise in the signal acquisition equipment. It may even be a genuine aspect of the signal, but its presence disturbs subsequent analysis algorithms. From our earlier examples of electrocardiography, recall that one occasional characteristic of electrocardiograms (ECGs) is such splintering. Its presence should not only be detected, but for purposes of heart rate monitoring, the application should not misread the ECG's splinters as individual ventricular contractions. Linear smoothing spreads the splinter into a large canyon in the signal. Using a dilation kernel on the umbra of the signal erases the splintering, although it produces a signal with an overall higher mean. If the dilation kernel is not as wide as the gap, then it has an insignificant enhancement effect. For digital signals, this decreases the effective dynamic range of the signal. However, rudimentary dilation kernels do a good job of filling gaps in signal structures.

There is a dual operation to dilation—called erosion; the dilation of A by B is equivalent to erosion of the complement, $A^c = \mathbb{Z}^2 \setminus A = \{b \in \mathbb{Z}^2 \mid b \notin A\}$, by the reflection of B across the origin.

Definition (Erosion). Let $A, B \subseteq \mathbb{E}^n$. Then the erosion of A by B is

$$A \ominus B = \bigcap_{b \in B} (A - b). \tag{4.67}$$

The structuring element B is also called an erosion kernel. The next proposition collects some properties of erosion. Note the symmetry between these properties and those in the Dilation Properties Proposition.

Proposition (Erosion Properties). If $A, B, C \subseteq \mathbb{Z}^2$, and $k \in \mathbb{Z}$, then, $A \ominus B = \{d \in \mathbb{Z}^2 \mid d + b \in A \text{ for all } b \in B\} = \{d \in \mathbb{Z}^2 \mid B_d \subseteq A\}$; $(A + k) \ominus B = (A \ominus B) + k$; $A \ominus (B + k) = (A \ominus B) - k$; $A \subseteq B$ implies $A \ominus C \subseteq B \ominus C$; $(A \cap B) \ominus C = (A \ominus B) \cap (B \ominus C)$; and, finally, $(A \ominus B)^c = A^c \oplus (-B)$, where $-B = \{-k \mid k \in B\}$.

Proof: Exercises. ■

The last of the Erosion Properties illustrates the dual nature of dilation and erosion. Note that erosion is neither commutative nor associative. Note also that translation invariance does not hold true for a translated erosion kernel. Let's continue with a definition of signal erosion and its application to enhancement.

Definition (Signal Erosion). Let $x(n)$ and $h(n)$ be digital signals, $x\colon \mathbb{Z} \to [0, N]$ and $h\colon \mathbb{Z} \to [0, N]$ for some natural number $N \geq 0$. Then the dilation of f by h, is $f \ominus h = T[\text{Umbra}(f) \ominus \text{Umbra}(h)]$.

Erosion can remove spike transients. Such transients present difficulties for linear enhancement filters. The convolution operation tends to blur the spike. Linear smoothing superimposes a replica of its kernel's impulse response on the signal and can obliterate small local features in the process. An erosion kernel removes the spike without spreading it into the rest of the signal's values. If the kernel is narrower than the transient, then it treats the transient as a blob, part of the main signal structure.

The following points summarize the behavior of dilation and erosion enhancement operators:

- (Splinter removal) Dilation blends signal structures separated by gaps narrower than the kernel width.
- (Spike removal) Erosion removes sharp, narrow, upward transients in the signal.
- Dilation has the undesirable effects of adding to the overall signal level and creating new, fine-scale signal features.
- Erosion has the undesirable effects of reducing the overall signal level and destroying existing, fine-scale signal features.

The drawbacks for both dilation and erosion as enhancement tools seem to be counterposed. They modify the signal mean in opposite ways. The have opposite effects on small signal features. These observations have led morphologists to compose dilation and erosion operations while using the same kernel. The operations are not inverses, and it turns out that this composition benefits later analysis steps, such as histogram derivation, thresholding, labeling, and region merging and splitting operations.

Definition (Opening). If $A, B \subseteq \mathbb{Z}^2$, then the opening of A by structuring element B is $A \circ B = (A \ominus B) \oplus B$. If $x(n)$ and $h(n)$ are digital signals, $x\colon \mathbb{Z} \to [0, N]$ and $h\colon \mathbb{Z} \to [0, N]$ for some natural number $N \geq 0$, then the opening of f by h, is $f \circ h = (f \ominus h) \oplus h$.

Definition (Closing). If $A, B \subseteq \mathbb{Z}^2$, then the closing of A by structuring element B is $A \bullet B = (A \oplus B) \ominus B$. If $x(n)$ and $h(n)$ are digital signals, $x\colon \mathbb{Z} \to [0, N]$ and $h\colon \mathbb{Z} \to [0, N]$ for some natural number $N \geq 0$, then the closing of f by h, is $f \bullet h = (f \oplus h) \ominus h$.

4.5 EDGE DETECTION

The edges of a signal mark the significant changes of its values, and edge detection is the process of determining the presence or absence of such significant changes. This is not a very satisfying definition, of course, since there is much room for disagreement over what makes a change in a signal significant or insignificant. It is most often the nature of the edge detection application that resolves such disputes. As we have already noted in segmentation problems, goal-directed considerations play a considerable role in designing edge detectors. Not all of the operations involved can proceed directly from the signal data to the edge detection result without some overall perspective on what the problem under study requires for a correct

result. Thus, in edge detection there is again an interaction between bottom-up (or data-driven) approaches and top-down (or goal-driven) methods. Whatever the tools employed—edge detectors, texture analysis, local frequency components, scale-based procedures—this interplay between data-driven and goal-driven methods will continue to be at work in our signal interpretation efforts.

Despite the apparent simplicity of formulating the problem, edge detection is quite difficult. Among the first attempts to analyze signals and images were edge detection techniques. We will explore these methods in some depth, and this study will bring us up to an understanding of the current research directions, performance issues, and debates surrounding derivative-based edge finding. A second main approach is to fit members of a collection of edge models to a signal. Note that edge models are simply primitive shapes to be found in a signal. Since, as numerical analysts well know, finding an approximation to the derivative of a quantized function is a problematic undertaking, many researchers regard this approach as inherently more robust. Let us look a little further at these two approaches and their advocates.

Remembering that our signals are just one-dimensional functions of a discrete or continuous independent variable, we can take the magnitude of the signal derivative as a starting point for building an edge detector. Furthermore, since the second derivative changes sign over the extent of an edge, it is feasible to base an edge detector on approximations of the second derivative of a signal. Many of the early experiments in edge detection relied upon derivative-based approaches [58–62].

Another approach to edge detection is to fit selected edge-shaped masks or patterns to the signal. The edge detection patterns are signals themselves and (reasonably assuming that we are working with finite-energy signals) are elements of a Hilbert space. For a conceptualization of the edge detection problem, we can resort to our Hilbert space theory from Chapters 2 and 3. The edge detection operators can be orthonormalized. Thus, the edge detection masks become the basis elements $\{e_i: i \in I\}$ of a subspace of linear combinations of perfect edge-containing signals. The whole edge detection problem becomes one of finding the inner products of a signal $x(t)$ with edge detector basis elements $e_i(t)$. Notice, however, that the basis elements are not smoothly undulating functions such as the sinusoids or exponentials as used in the discrete Fourier transform (e.g., Section 4.3.2). Rather, the basis elements contain sharp discontinuities in the first- or higher-order derivatives. These sharp breaks in the basis functions match the shape of the edges to be detected. Thus, large values of $\langle x(t), e_i(t - t_0)\rangle$ indicate the presence of an edge of type i at location t_0 in $x(t)$. This too was a popular path of edge detection pioneers [61, 63–65]. Again, the edge basis elements are simply templates that contain elementary shapes, and this method, therefore, can be considered as a type of template matching. Section 4.6 of this chapter furnishes some basic template matching tools; the inner product operation lies at the heart of such methods.

These references are but a few of those that have appeared in the research literature over the last 30 years. Even at this writing, near the turn of the twenty-first century, investigators twist the interpretation of what is significant in a signal, adjust the mix of top-down and bottom-up goals, optimize in yet another way, and append a new variant to the vast edge detection literature [66–69]. Indeed, in this book we

will continue to remark upon and deepen our understanding of edge detection with each new signal processing and analysis tool we develop.

Edge detection is a basic step in signal analysis. The output of an edge detector is a list of the location, quality, and type of edges in a signal. Interpretation algorithms could be designed to work on the list of edges. For an example from speech analysis, between certain pairs of edges, and based on the signal values therein, the interpretation could be that this portion of the signal represents irrelevant background noise. Other parts of the voice signal, bounded by edges, represent human speech. Further analysis may reveal that one significant section is a voiced consonant, another a fricative, and so on. In general, we find the edges in signals as a first step in analysis because the edges mark the transition between important and unimportant parts of a signal or between one and another significant part of a signal. Edge detection draws the boundaries within which later, more intricate algorithms must work. Edge guidelines allow interpretation processes to work in parallel on distinct parts of the signal domain. Finally, preliminary edge detection prevents the waste of processing time by higher-level algorithms on signal fragments that contain no useful information.

4.5.1 Edge Detection on a Simple Step Edge

To introduce the many problems that arise—even in the most elementary detection problem—let us consider a simple step edge in a signal. The unit step signal provides a natural example of a step edge. For discrete signal analysis, $u(n)$, the discrete unit step is a perfect step edge located at $n = 0$. What do we expect that a step edge detector should look like?

This much is obvious: the step edge we consider may not have unit height, and it may not be located at the origin. If the amplitude of the edge diminishes, then it is a less pronounced change in the signal, and our edge detector ought to produce a smaller response. Thus, a first consideration is that our edge detector should be linear: Its output is greater, given a larger amplitude in the edge and therefore a larger amplitude in the underlying signal. The second consideration is that an edge should be detected by the operator wherever it happens to be located within the signal. In other words, whether the step is at the origin or not is irrelevant: We should detect the edge at any time. The implication of our second consideration is that a first-cut edge detector is translation invariant. It is thus linear and translation invariant and, by the results of Chapters 2 and 3, must be convolutional.

Let us suppose that we are working with discrete signals. If the edge detector is $y = Hx$, then the output y is given by convolution with the impulse response, $h(n)$, of the detector system, H:

$$y(n) = (x * h)(n) = \sum_{k=-\infty}^{\infty} x(k)h(n - k). \tag{4.68}$$

There may be noise present in the signal $x(n)$ so that the sum in (4.68) does not readily simplify and the response is irregular. Noisy or not, the response of the

system H to input $x(n)$ will be a signal $y(n)$ with discrete values:

$$\{..., y(-3), y(-2), y(-1), y(0), y(1), y(2), y(3), ...\}. \tag{4.69}$$

To find the edge, then, we have to threshold the output, supposing that an edge is present in $x(n)$ whenever $|y(n)| \geq T$. If we are very lucky, then there will be only one value that exceeds the threshold, along with a single detection result for a single step edge. If there is a range of high response values, then it may be necessary to select the maximum or a set of maximal responses.

In the case of an analog edge detection problem, the output of the convolution integral (4.70) will be continuous. There will be no hope of thresholding to discover a single detection result unless the threshold coincides with the maximum response value. We must be content with seeking a maximum or a set of maximal responses.

$$y(t) = (x * h)(t) = \int_{-\infty}^{+\infty} x(t-s)h(s)\,ds = \int_{-\infty}^{+\infty} h(t-s)x(s)\,ds. \tag{4.70}$$

It might seem that at this early stage in conceptualizing an edge detector that it is wrong to settle so quickly on a convolutional operator. For example, if the input signal is attenuated to $Ax(t)$, $|A| < 1$, then the response of the detector to the attenuation will be $y(t) = A(x*h)(t)$. The same edges—no matter how insignificant they become because of the attenuation—will still be detected as maximal responses due to the linearity of the operator H. So if the goals of our application change, and it becomes necessary to ignore sufficiently small changes in the input signal, then our edge detector will fail by falsely indicating significant transitions in $x(t)$. Sometimes top-down specifications demand non-linearity. Note, however, that we can accommodate such a top-down scheme by adjusting the threshold parameter. If certain jumps should be detected as edges and others should be passed, then the kind of nonlinearity we need can be implemented by thresholding all responses and then selecting the maximal response from those that exceed the threshold. In other words, if Edges[x] is a predicate or list of edges of input signal $x(t)$, then Edges[x] = $\{(t, x(t)) : |y(t)| \geq T$ and t is a local maximum of $y = x*h\}$.

There is a further difficulty with uncritical convolutional edge detection. If the input signal contains spike noise, then the output of the edge operator will have a large response to the spike. In fact, around an isolated impulse, the response will tend to look like the impulse response of the edge detector itself.

Example (Difference of Boxes Operator). One of the earliest edge detectors is the Difference of Boxes (DOB) filter [60], defined by $y = h_{\mathrm{DOB}}*x$, where, for some $L > 0$,

$$h_{\mathrm{DOB}}(t) = \begin{cases} -1, & -L \leq t < 0, \\ 1, & 0 \leq t \leq L. \end{cases} \tag{4.71}$$

Clearly, the DOB operator is designed to smooth the data on both sides of a possible edge and subtract the earlier values from the later ones. Any sudden transition at

time $t = 0$ appears in the output as a large-magnitude value. The DOB operator emphasizes values near $t = 0$ just as much as values near $|t| = L$. It is also typical to zero the center value of the DOB operator, $h_{\mathrm{DOB}}(0) = 0$.

Example (Derivative of Gaussian Operator). Another popular operator for convolutional edge detection is the first derivative of the Gaussian (dG). The impulse response of this system is given by $h_{\mathrm{dG}}(t) = -t\exp[-(t/\sigma)^2/2]$. The dG operator is an alternative to the DOB convolution kernel; it emphasizes values near the edge over values further away. A disadvantage is that it has an infinite extent. Practically, of course, the kernel can be truncated, since the signal diminishes rapidly.

We can add some normally distributed noise to the analog unit step signal to produce noisy step edges. Convolution with DOB and dG operators produces satisfactory results (Figure 4.11).

Application (Plasma Etch Endpoint Detection). Consider an example from a problem of controlling an industrial process, Figure 4.2. A spectrometer monitors the carbon monoxide (CO) optical discharge from a plasma reactor that is etching an oxide layer on a silicon wafer [70]. This is a critical step in the production of integrated circuit chips. The CO is a chemical byproduct of the plasma reaction with the silicon dioxide on the wafer. When the CO spectral line falls abruptly, the layer of silicon dioxide that is exposed to the plasma has been cleared by the plasma reaction.

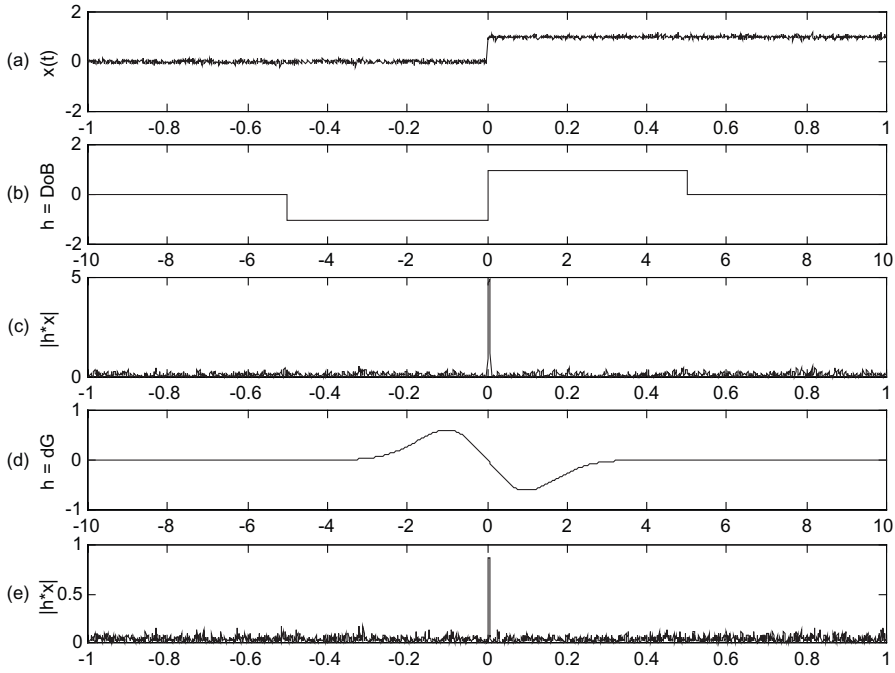

Fig. 4.11. An analog step edge in noise (a). The DOB and dG operators are shown in (b) and (d), respectively. Panels (c) and (e) show the result of convolving the signal with the DOB and dG operators, respectively.

It is essential to stop the plasma reaction as close as possible to the time when the CO intensity falls to avoid plasma damage to circuit layers underneath the target oxide. Thus, plasma etch endpoint detection can be largely viewed as a real-time edge detection problem. Plasma processes are very much subject to transients in the optical emissions. These can be caused by a reactor or acquisition fault or process instability. Transients can result in anomalous edge detection and an incorrect identification of etch process endpoint. As we found in Section 4.3.3, one the solution is to introduce a nonlinear filter that removes impulse noise prior to the linear filtering and application of a convolutional edge detection operator [e.g., the DOB operator (4.71)].

Most plasma etch endpoint detection algorithms rely on simple signal thresholding and first- and second-derivative estimates on the optical emission signal. When variability arises in the endpoint trace, perhaps due to imprecise control of previous thin film deposition steps or to the presence of different circuit configurations on the etched wafers, then strategies that consider the shape of the optical emission signal become attractive [71]. We will consider this aspect later in Section 4.7. In other processes, the signal edge is more difficult to discern, and endpoint detection methods that model the real-time optical emission and detect out-of-trend conditions become important [72]. Lastly, there is the top-down consideration that complete translation invariance is not appropriate for the edge detector. In fact, the process control application of Figure 4.2 is such a case. Typically, it is known in advance, by the process's nature, that the edge cannot occur except within a certain time range. In the case of plasma etching reactor control, it is common to specify an initiation of etch period during which no collapse in the emission spectral line should be detected. The upshot is that the convolutional operator is only applied within in the region known to contain valid edges. An alternative is to run the edge detector over the entire domain of the input signal and, in a further post-processing step, delete edges that occur outside the appropriate interval as spurious.

The next proposition sheds some further light on the nature of convolutional edge detectors [66]. We state and prove this proposition for analog signals and leave the discrete case for an exercise.

Proposition (Maximal Response Edge Detector). If a step edge detection operator locates edges from the maximal responses of a convolutional operator, H, and provides a unique maximum for $u(t)$ at $t = 0$, then

(i) $h(t)$ can only have one zero, at $t = 0$.
(ii) The impulse response of system H, $h(t)$, must be odd.

Proof: The first part of the proposition follows from the fundamental theorem of calculus. Since

$$y(t) = \int_{-\infty}^{+\infty} u(t-s)h(s)\,ds = \int_{-\infty}^{t} h(s)\,ds, \tag{4.72}$$

we know that $dy/dt = h(t)$. Since the response $y(t)$ has a maximum at $t = 0$, its derivative must be zero; therefore $h(0) = 0$. If the detector, H, responds correctly to the perfect step edge of $u(t)$ at $t = 0$, then this can be the only maximal point of the response, and it follows that $h(t)$ has precisely one zero.

For (ii) we can decompose $h(t)$ into its even and odd parts and then apply the fundamental theorem of calculus to get the result. Let $h(t) = h_e(t) + h_o(t)$ where $h_e(t)$ is even and $h_o(t)$ is odd. Applying the convolution theorem for analog LTI systems, let $t > 0$, and note that

$$y(t) = \int_{-\infty}^{+\infty} u(t-s)h(s)\,ds = \int_{-\infty}^{t} h(s)\,ds = \int_{-\infty}^{t} h_e(s)\,ds + \int_{-\infty}^{t} h_o(s)\,ds, \tag{4.73}$$

$$y(t) = \int_{-\infty}^{-t} h_o(s)\,ds + \int_{-t}^{0} h_o(s)\,ds + \int_{-\infty}^{-t} h_e(s)\,ds + \int_{-t}^{0} h_e(s)\,ds + \int_{0}^{t} h_o(s)\,ds + \int_{0}^{t} h_e(s)\,ds. \tag{4.74}$$

The finite integrals over $h_o(t)$ cancel, and the finite integrals over $h_e(t)$ are identical; thus,

$$y(t) = \int_{-\infty}^{-t} h_o(s)\,ds + \int_{-\infty}^{-t} h_e(s)\,ds + 2\int_{0}^{t} h_e(s)\,ds = \int_{-\infty}^{-t} h(s)\,ds + 2\int_{0}^{t} h_e(s)\,ds. \tag{4.75}$$

Now from (4.75) we may write

$$y(t) - y(-t) = 2\int_{0}^{t} h_e(s)\,ds. \tag{4.76}$$

Let us now differentiate (4.76), applying the chain rule to the left-hand side and the fundamental theorem to the right-hand side. This gives $2h_e(t) = 0$. Since t was arbitrary, $h_e(t) = 0$ for all $t > 0$. Moreover, since $h_e(t)$ is even, $h_e(t) = 0$ for all t. ■

4.5.2 Signal Derivatives and Edges

At first glance, finding the abrupt changes, or edges, in a signal amounts to finding the points at which the signal has a large derivative. Since we are familiar with analog differentiation from calculus and discrete differentiation from numerical analysis, it would seem that we should already possess the proper tools to begin a formal study of edge detection as a task within signal analysis. But the presence of even a minute amount of noise in a signal can lead to wild variations in its derivative at a time instant. Differentiation is known as a classical ill-posed problem or unstable process; in systems that perform differentiation, small differences in the input signal lead to large differences in the output signal [73]. The standard approach to such ill-posed

problems is to convert them to well-posed problems by smoothing the input data. Thus, for signal analysis systems, some preliminary signal conditioning is appropriate.

We recall how to take the derivative of signals from calculus as a limit,

$$x'(t_0) = \left.\frac{dx}{dt}\right|_{t=t_0} = \lim_{t \to t_0} \frac{x(t) - x(t_0)}{t - t_0}. \tag{4.77}$$

This limit leads to standard formulas for differentiation of polynomials, algebraic functions, and trigonometic and exponential functions. Thus, we can obtain estimates for derivatives of discrete signals by finding an interpolating polynomial among a set of discrete vaues. The error estimates that this procedure gives are not as good as when the time-domain signal is approximated; this is a practical manifestation of the ill-posed nature of the differentiation process [74].

Deriving discrete derivatives for the analysis of digital signals by first developing an interpolating function, however, is not necessary for an approximate slope value near a point. We can derive discrete derivative formulas for a signal $x(n)$ by assuming that $x(n)$ arises from sampling an analog signal $x_a(t)$: $x(n) = x_a(nT)$, where T is the sampling interval. To get a formula for the discrete first and second derivatives around time instant $n = 0$, we expand $x_a(t)$ in a Taylor series and neglect the error terms:

$$x(1) = x(0) + x_a'(0) + \frac{1}{2}x_a''(0), \tag{4.78a}$$

$$x(-1) = x(0) - x_a'(0) + \frac{1}{2}x_a''(0). \tag{4.78b}$$

Subtracting (4.78b) from (4.78a) gives a simple formula for the first derivative:

$$x_a''(0) = \frac{1}{2}[x(1) - x(-1)]. \tag{4.79}$$

Adding (4.78a) from (4.78b) gives a simple formula for the second derivative:

$$x_a''(0) = x(1) - 2x(0) + x(-1). \tag{4.80}$$

Thus, the system $y = Hx$ with impulse response $h(n) = [1/2, \underline{0}, -1/2]$ approximates a discrete first derivative. And the system $y = Gx$ with impulse response $g(n) = [1, \underline{-2}, 1]$ approximates the second derivative. Recall that the system $y = Gx$ from Chapter 2 is called the discrete Laplacian operator. There we noted that it detected edges in signals, producing a zero response within flat and linearly sloped signal regions. Now we discover the discrete Laplacian's true nature: It is just a discrete version of the second derivative. The above analysis easily generalizes to approximate discrete derivatives with wider support. We find $x(2)$ and $x(-2)$ in terms of the Taylor series

of $x_a(t)$, apply (4.79) and (4.80), and find that

$$x_a'(0) = \frac{1}{12}[x(-2) - 8x(-1) + 8x(1) - x(2)], \tag{4.81}$$

$$x_a''(0) = \frac{1}{12}[-x(-2) + 16x(-1) - 30x(0) + 16x(1) - x(2)]. \tag{4.82}$$

The above rudimentary edge detectors are intuitive, but they turn out to be less than ideal. To see this, we need an appropriate mathematical foundation. Thus, let's formally define signal edges and motivate the conditions on edge detectors that should constitute opimality. This will provide us with some initial results on optimal edge detectors.

Definition (Analog Signal Edge). Let $x(t)$ be an analog signal. Then $x(t)$ has an edge at $t = t_0$ if for some $n > 0$, there is a discontinuity in the nth derivative of $x(t)$. (We consider the 0th derivative of $x(t)$ to be the signal itself.)

It requires a little care to correctly define edges for a discrete signal. By their nature, discrete signals are composed entirely of discontinuities. So we adopt the following definition.

Definition (Discrete Signal Edge). Let $x(n)$ be a discrete signal. Then there is an edge in $x(n)$ at a point n_0 if there is a discontinuity in the derivative of the signal $x_a(t) = x(\lfloor t \rfloor) + (t - \lfloor t \rfloor)x(\lceil t \rceil) - x(\lfloor t \rfloor)$, where $\lfloor t \rfloor$ is the floor of t, and $\lceil t \rceil$ is the ceiling of t.

These definitions do encompass the variety of edge shapes that we find in signals. Of course, the step edge is a discontinuity in the signal itself. When the signal assumes a dihedral or "roof" shape, then the discontinuity lies in the first derivative. Thus, we shall concentrate on step edges in our theoretical development, since other edge shapes can be analyzed by computing the signal derivative and then applying our step edge analysis methods.

4.5.3 Conditions for Optimality

Let us now return to the simple step edge and complete an analysis of the edge detection problem. Specifically, three conditions for an edge detector H are as follows:

(i) The detector should have a high signal-to-noise ratio (SNR). This means that a better edge detector has a higher response to the edge within a signal than to the surrounding noise.

(ii) H should be well-localized about the true signal edge. The output maxima of H should cluster around the true edge, and better edge detectors show a tighter group of maximal responses.

(iii) There should be only one response to a single edge. If H is good, then it should present a number of apparently valid alternatives for the precise location, or registration, of the edge.

Canny chose the overall goals of (i)–(iii) for his detector design [75], which became the overwhelming favorite in research literature and signal analysis applications for many years. His strategy is to develop mathematical formulations for the goals and then to find convolution kernels that maximize the products of individual criteria.

Let's consider just the first two criteria above and see how this analysis unfolds. Let $h(t)$ be the convolution kernel that we seek and let $u(t)$ be the unit step. We will need to compute convolution integrals, $y(t) = (h * u)(t)$, so we must limit the time-domain extent of both $h(t)$ and $s(t)$, or assume that they belong to a signal space (Chapter 3) that supports closure under convolution. To achieve this, we assume that the edge detection filter has support on a finite interval $[-L, L]$. Now we define one form of the signal-to-noise ratio for analog systems and prove a property for the SNR under white Gaussian noise (Chapter 3).

Definition (Signal-to-Noise Ratio). Let $y = Hx$ be an analog system and let $n(t)$ be a noise signal. Then the signal-to-noise ratio (SNR) for H at $t = 0$ is

$$\mathrm{SNR}_{H,t=0} = \frac{|y(0)|}{\left(E\left[\int_{-\infty}^{+\infty} h(t)n(-t)\,dt\right]^2\right)^{\frac{1}{2}}}, \tag{4.83}$$

where $E[y]$ is the expectation operator.

That is, the SNR is a ratio of the system output without noise present to the system's expected output when the input is pure noise.

Proposition (SNR under White Gaussian Noise). Suppose H is an analog system and $n(t)$ is white Gaussian noise. Then $\mathrm{SNR}_{H,t=0} = |y(0)|/(n_0\|h\|_2)$, where n_0 is the standard deviation of $n(t)$.

Proof: From stochastic processes theory [76], we have that

$$E\left[\int_{-\infty}^{+\infty} h(t)n(-t)\,dt\right]^2 = E\left[\int_{-\infty}^{+\infty} h^2(t)n^2(-t)\,dt\right] = n_0^2\int_{-\infty}^{+\infty} h^2(t)\,dt; \tag{4.84}$$

hence,

$$\begin{aligned}\mathrm{SNR}_{H,t=0} &= \frac{|y(0)|}{\left(E\left[\int_{-\infty}^{+\infty} h(t)n(-t)\,dt\right]^2\right)^{\frac{1}{2}}} = \frac{|y(0)|}{\left(n_0^2\int_{-\infty}^{+\infty} h^2(t)\,dt\right)^{\frac{1}{2}}} \\ &= \frac{|y(0)|}{n_0\left(\int_{-\infty}^{+\infty} h^2(t)\,dt\right)^{\frac{1}{2}}} = \frac{|y(0)|}{n_0\|h\|_2}\end{aligned} \tag{4.85}$$

and the proof is complete. ■

This observation allows Canny [75] to specify a signal-to-noise performance measure for the edge detection system H which does not depend on the input signal $x(t)$; in particular, the optimal edge detector must maximize (4.85). It turns out the convolution kernel that provides a maximum SNR, given that the underlying step edge contains noise, is just the reversed step itself. This result is known as the Matched Filter Theorem. We introduce matched filtering in Section 4.6.2, but we need to have the tools of Fourier transform analysis at our disposal in order to complete its theoretical justification. Granting the Matched Filter Theorem, then, the convolutional kernel that is optimal for finding step edges is precisely the DOB operator. Canny attempted to prove that the DOB operator enjoyed an optimal localization property as well. The development proceeds as follows.

Let $y = Hx = H(u + n)$, where $u(t)$ is the (noiseless) unit step signal and $n(t)$ is white Gaussian noise. Then $y = Hu + Hn$ by linearity. Let $w = Hu$ and let $m = Hn$. If a maximum of the detector output appears at time $t = t_0$, then $y'(t_0) = w'(t_0) + m'(t_0) = 0$. Differentiation of the convolution integral for $w = h * u$ gives $w'(t_0) = h(-t_0) = -h(t_0)$, since h must be odd (by the Maximal Response Edge Detector Proposition, Section 4.5.1). If t_0 is close to the ideal edge at $t = 0$, then by a Taylor series expansion for $h(t)$, we know that $h(t_0) \approx h(0) + t_0 h'(0)$. Since $h(0)$ must be zero by the same Proposition, it follows that $t_0 h'(0) = m'(t_0)$. This implies that $h'(0)^2 E[(t_0)^2] = E[m'(t_0)^2]$. But, as in (4.84),

$$E\left[m'(t_0)^2\right] = n_0^2 \int_{-\infty}^{+\infty} h'(t)^2\, dt. \tag{4.86}$$

Thus,

$$E\left[(t_0)^2\right] = \frac{E\left[m'(t_0)^2\right]}{h'(0)^2} = \frac{n_0^2 \int_{-\infty}^{+\infty} h'(t)^2\, dt}{h'(0)^2}, \tag{4.87}$$

and the optimal localization criterion that Canny proposes is $(E[(t_0)^2])^{-1/2}$. Canny argued that the DOB operator remains optimal for both this localization criterion and the SNR criterion, for instance by seeking to maximize the product of (4.85) and (4.87). Canny adduced the third criterion, namely that there should be no multiple responses around a noisy edge in order to derive his optimal edge detection kernel. It turns out, after some lengthy calculus of variations, that the operator is very similar to the dG kernel [75].

Some time later, Tagare and deFigueiredo [66] pointed out some flaws in the reasoning above. The principal points are that

- There can be multiple time values $t = t_0$ for which a maximum occurs and $y'(t_0) = w'(t_0) + m'(t_0) = 0$. The performance measure must account for the distribution of all such maxima, and there is no reason to prefer one above the others.
- Equation (4.87) computes the variance of the maximum time $t = t_0$. But, by the previous point, the value of t_0 varies with every realization of the white noise process, and the substitution of (4.86) into $h'(0)^2 E[(t_0)^2] = E[m'(t_0)^2]$ to get (4.87) is invalid.

Tagare and deFigueiredo propose an alternative localization criterion. They propose that an optimal edge detector $y = h * x$ should maximize the quantity

$$J_{H,t=0} = \frac{\int_{-\infty}^{+\infty} t^2 h(t)^2 \, dt}{\int_{-\infty}^{+\infty} \omega^2 \left\| H(\omega) \right\|^2 \, d\omega}, \tag{4.88}$$

where $H(\omega)$ is the Fourier transform of the impulse response, $h(t)$, of the edge detector. Since we will develop Fourier transform theory in the next two chapters and outline its applications in Chapter 7, we defer the exposition of the new localization criterion. It turns out, interestingly enough, that the optimal kernel for convolutional edge detection under the criterion (4.88) is the dG function.

4.5.4 Retrospective

Edge detection has played a central role in the theoretical development of signal and image analysis since it was first applied, in the early 1950s, in attempts at image understanding with digital computers [58]. A large number of interdisciplinary researchers have worked on edge detection from the standpoint of building biologically motivated signal and image analysis systems. Edge detection at a variety of resolutions played a central role in Marr's account of animal and machine vision systems [77]. Marr[5] drew careful parallels between biological and computer vision mechanisms and inspired a generation of computer vision researchers to do the same. In particular, Marr conjectured that edge analysis across many scales would be sufficient for a characterization of a signal or image. Since biological signal analysis systems were capable of edge detection and multiscale analysis, it would appear that a major bond would then exist between electronic computers and their software on the one hand and animal brains and their experiences on the other. We will have occasion to revisit this conjecture later in the book; the theory of time-scale transforms, or wavelet theory, would shed light on the question a dozen or so years after Marr proposed it.

From a computational perspective, Canny's work [75]—which comprised his Master's thesis work [78] at the Massachusetts Institute of Technology—was thought to have essentially solved the edge detection problem. There was a period when just about everyone's research paper included a Canny edge detector, if it mentioned edge detection at all. Some practitioners used a derivative of the Gaussian operator as a close approximation to the Canny kernel, which was difficult to compute. Only after the passage of several years did minor flaws in the theory become apparent; fortuitously, those many papers of those many researchers that

[5]David Courtenay Marr (1945–1980). Spurred by Marr's critique ["Artificial intelligence: a personal view," *Artificial Intelligence*, vol. 9, pp. 37–48, 1977], computer vision rose from a collection of ad hoc techniques to a broad discipline unifying ideas from biology, psychology, computer science, and robotics. One of the prominent pioneers of computer vision, Marr died quite young, in the midst of a most productive carreer.

resorted to the dG shortcut were following the optimal road after all! There has begun another round of research papers, controversies, and algorithmic emendations [66, 67, 79, 80]. The most recent research, in addition to emphasizing the dG kernel, has found interconnections between diverse methods reaching back some 20 years, and a unifying framework has been elaborated [68, 69].

4.6 PATTERN DETECTION

Many of the most important signal analysis problems involve detecting more than a single edge in a signal. There may be several edges in a signal region of interest, and ascertaining the signal levels, slopes, and transitional shapes between the edges may be critical to correctly interpreting the signal. The basic signal pattern detection or recognition problem involves finding a region $a \le t \le b$ within a candidate signal $x(t)$ that closely matches a prototype signal $p(t)$ on $[0, b-a]$. For discrete signals, the detection problem reduces to comparing finite sets of values. It seems simple; but in the presence of noise or other distortions of the unknown signals, complications do arise. The difficulties worsen when the detection problem allows the size of the prototype within the candidate to vary. Indeed, the problem can be trivial, challenging, problematic, and frustrating and may even defy robust solution. Signal pattern detection remains a topic of research journals, experimental results, and tentative solutions. This section presents three basic for pattern detection approaches: correlation methods, structural methods, and statistical methods.

4.6.1 Signal Correlation

Correlating two signals seems to be the natural approach to pattern detection. Its ultimate foundation is a dot product relation of similarity between vectors, which generalizes to the inner product operation for Hilbert spaces. Some care in the formulation is essential, however. Thus, we first explore the method of normalized cross-correlation in Section 4.6.1.1. There is a subsequent result, called the Matched Filtering Theorem, which indicates that this approach is in fact optimal. We do not, however, yet possess the theoretical tools with which to prove the matched filtering result; so we simply state it herein and postpone the proof until Chapter 7.

4.6.1.1 Normalized Cross-Correlation. The Cauchy–Schwarz Inequality, covered in Chapters 2 and 3, provides a mathematically sound approach to the signal matching problem. Let's suppose that we are dealing with an unknown, candidate signal x and a prototype signal p, which may come from a collection of model signals. The application may require a comparison of x with each prototype in the collection. Prototype signals represent patterns that we expect to find in the input to the signal analysis application; thus, it is reasonable to stipulate that the patterns are finitely supported on an interval $I = [a, b]$.

For this discussion, let us assume that we are working in the discrete realm, so that the signal space tools from Chapter 2 apply. It is useful to have a measure of

match, or distance, between two signals, $d(x, y)$, that is a metric; that is, it statisfies the following:

- The positive definite property: $d(x, y) \geq 0$ for all x, y.
- The identity property: $d(x, y) = 0$ if and only if $x = y$.
- The symmetry property: $d(x, y) = d(y, x)$ for all x, y.
- The triangle inequality: For any z, $d(x, y) \leq d(x, z) + d(z, y)$.

If we take the signals to be square-summable, then the l^2 norm is a comparison measure which is a metric, $d(x, y) = \|x - y\|_2$. Assuming that we work with l^2 signals, a measure of the mismatch between two square-summable signals is the l^2 norm; in other words, if x is an unknown signal, then we need to minimize $\|x - p\|_2$ among all prototype signals p from a family of models our application attempts to detect. If the registration of pattern $p(n)$ within candidate $x(n)$ must be found, then we seek the offset k that provides the smallest $\|x(n+k) - p(n)\|_2$ for all appropriate offsets k of $p(n)$ relative to $x(n)$.

Choosing $d(x, y) = \|x - y\|_2$ as a match measure on real-valued signals is equivalent to using the inner product $\langle x, y \rangle$. To see this, suppose we compare a square-summable candidate signal $x(n)$ to a square-summable prototype $y(n)$. Then,

$$\begin{aligned}\|x-y\|_2^2 &= \sum_{n=-\infty}^{\infty} \big(x(n)-y(n)\big)^2 = \sum_{n=-\infty}^{\infty} \big(x(n)\big)^2 + \sum_{n=-\infty}^{\infty} \big(y(n)\big)^2 - 2\sum_{n=-\infty}^{\infty} x(n)y(n) \\ &= \|x\|_2^2 + \|y\|_2^2 - 2\langle x, y\rangle. \end{aligned} \tag{4.89}$$

Thus, we see that $d(x, y)$ depends on both $\|y\|_2$ and the inner product $\langle x, y \rangle$. If we require that all prototype vectors have unit norm, $\|y\| = 1$, then the equivalence between minimizing $d(x, y)$ and maximizing $\langle x, y \rangle$ is clear.

The inner product relation inspires an important method of matching signals: normalized cross-correlation. We introduced cross-correlation for discrete signals in Chapter 2, where it was noted to be a kind of backwards convolution. Suppose that we have a real-valued pattern signal $p(n)$, supported on the interval $[0, N]$: $p(n) = [p_0, p_1, \ldots, p_N]$. We search for the best match of $p(n)$ at offset location k in real-valued signal $x(n)$. A measure of the match between the two at offset k is the inner product, $y(k) = \langle p(n-k), x(n) \rangle$. When $y(k)$ is at a maximum value, then we have found the offset k at which the prototype pattern $p(n)$ best matches the source signal $x(n)$. This operation, in effect, correlates the shifted pattern $p(n-k)$ with a window of the signal $x(n)$; this windowed function is just $x(n)[u(n-k)-u(n-k-N-1)]$, which is zero outside of the interval $[k, k+N]$. To evaluate $y(k)$, notice that

$$y(k) = \sum_{n=-\infty}^{\infty} p(n-k)x(n) = \sum_{n=k}^{n=N} p(n-k)x(n) \leq \left(\sum_{n=k}^{N} p^2(n-k) \right)^{\frac{1}{2}} \left(\sum_{n=k}^{N} x^2(n) \right)^{\frac{1}{2}}. \tag{4.90}$$

The inequality in (4.90) follows from the Cauchy–Schwarz Inequality for discrete signals applied to $p(n-k)$ and the windowed signal $x(n)[u(n-k)-u(n-k-N-1)]$.

Recall from Chapter 2 that the Cauchy–Schwarz Inequality states that if $x(n)$ and $p(n)$ are in l^2, then the product $x(n)p(n)$ is in l^1, and $\|xp\|_1 \leq \|x\|_2 \, \|p\|_2$. Recall that equality holds if and only if $x = cp$ for some constant c. Thus, in (4.90) there is equality if and only if $p(n-k) = cx(n)[u(n-k)-u(n-k-N-1)]$, where c is a constant. The problem with using $y(k)$ as a measure of the match between $p(n-k)$ and $x(n)$ over the region $[k, k+N]$ is that the second term on the right in (4.90) depends on the registration value k. Thus, we take as the measure of match between the pattern $p(n-k)$ and the signal $x(n)$ on $[k, k+N]$ to be the normalized cross-correlation,

$$C_{p(n-k),x(n)} = \frac{y(k)}{\left(\sum_{n=k}^{N} x^2(n) \right)^{\frac{1}{2}}} = \frac{\sum_{n=k}^{N} p(n-k)x(n)}{\left(\sum_{n=k}^{N} x^2(n) \right)^{\frac{1}{2}}}. \tag{4.91}$$

The match measure (4.91) assumes its maximum value $C_{p(n-k),x(n)} = 1$ when the pattern is an exact multiple of the windowed input signal $x(n)$. Thus as a pattern recognition measure, normalized cross-correlation finds patterns that match our prototypes up to an amplification or attenuation factor.

Matching by normalized cross-correlation, dependent as it is on the inner product notion, is quite intuitive. The inner product operation is closed in our Hilbert spaces of square-summable discrete and square-integrable analog signals; we thus have a rich variety of signals with which to work. The inner product generalizes the dot product relation of finite-dimensional vector spaces, which is a geometrically satisfying relation of similarity between two vectors. Without a doubt, these factors recommend normalized cross-correlation as one of the first strategies to be employed in a signal analysis application. It is not the only method, however. Depending upon the application, it may suffer from a couple of problems:

- Computing the sums of squares in to arrive at the l^2 norms is time-consuming.
- There may be a lot of near-misses to the optimal registration of the pattern $p(n)$ in the unknown candidate signal $x(n)$.

To avoid the first problem, it may be feasible to apply the l^∞ norm, taking $d(p(n-k), x(n)) = \|p(n-k) - x(n)[u(n-k)-u(n-k-N-1)]\|_\infty$ as a match measure on real-valued signals instead. Computing this distance measure involves only a comparison of the $N+1$ values of $p(n-k)$ with those of $x(n)$ on the window $[k, k+N]$. In real-time applications, using digital signal processors, for example, this tactic can often help to meet critical time constraints. The second arises when there are a number of structures present in $x(n)$ that resemble the model pattern $p(n)$. An example of this situation arises during electrocardiogram analysis. Suppose a model QRS complex pulse has been extracted. Normalized cross-correlation produces many close responses. Thus, it may be necessary to search for certain critical signal features—other than raw signal values—around which more robust pattern detection methods might be constructed. This leads to the structural techniqes we consider next.

It is also possible to develop normalized cross-correlation for analog signals. Following the derivation of discrete normalized cross-correlation very closely, along with using the Cauchy–Schwarz inequality from Chapter 3, we obtain

$$C_{p(t-s),x(t)} = \frac{y(s)}{\left(\int_I x^2(t)\,dt\right)^{\frac{1}{2}}} = \frac{\left(\int_I p(t-s)x(t)\,dt\right)^{\frac{1}{2}}}{\left(\int_I x^2(t)\,dt\right)^{\frac{1}{2}}}, \tag{4.92}$$

where s is the offset of prototype signal $p(t)$ into input signal $x(t)$, and I is the interval that contains the support of $p(t)$. Deriving this result is left as an exercise.

The next section sheds some light on the importance of cross-correlation for the detection of patterns that are embedded in noise.

4.6.1.2 Matched Filtering: A Glimpse. Understanding that real-life signals contain noise, it is natural to wonder what is the best way to match a signal against a pattern. If the detection process is a linear, translation-invariant system, H, and the input signal, $x(t)$, is corrupted by additive white noise, $s(t)$, then there is an answer to this intriguing question. It turns out that the impulse response of the system H, $h(t)$, is—up to a scaling (amplifying or attenuating) factor—none other than a reflected and translated version of the input signal $x(t)$. The impulse response $h(t)$ is called the matched filter for the signal $x(t)$. Let us state this as a theorem for analog signals, but postpone the proof until we have covered the Fourier transform theory.

Theorem (Matched Filter). Suppose $x(t) = f(t) + n(t)$, where $f(t)$ is a signal of known shape, and $n(t)$ is a zero mean white noise process. Then the optimal LTI system H for detecting $f(t)$ within $x(t)$ has impulse response $h(t) = cf(t_0 - t)$ for some constants c and t_0.

Proof: Chapter 5 prepares the foundation in analog Fourier theory. Chapter 7 proves the Matched Filter Theorem as an application of Fourier methods. ■

In developing the normalized cross-correlation method for signal matching, we found that the best possible match occurs when the pattern is identical to the source signal up to a constant scale factor on the shifted support interval of the prototype. Note that the convolution implied by the Matched Filter Theorem is the same as a cross-correlation with a reflected version of the source. Thus, matched filtering theory formulates an important converse to normalized cross-correlation, namely, that the best filter—for reasonable noise assumptions—is in fact just the target source pattern itself. Many communication theory texts cover matched filtering [81, 82], there are full reviews in the engineering literature [83], and Chapter 7 points out additional resources in print.

If matched filtering is both the obvious and optimal approach, why study anything else? One answer, as with "optimal" thresholding and "optimal" noise removal, is that the conditions that validate the optimality do not always hold. Furthermore, the

optimal methods for such problems are often computationally burdensome, even untractable. Convolution, at the heart of matched filtering, can be expensive for signals, and on images may require special-purpose computing hardware. Thus, reasonably fast suboptimal techniques are desirable; a lot of these methods arise in conference presentations, appear in print, and become the basis for practical applications.

4.6.2 Structural Pattern Recognition

A structural pattern recognition application discovers the physical relationships between labeled signal regions and unites the regions into a graph structure. Then the application compares the graph structures that it derives from candidate signals against those from prototype patterns. The structural analysis application estimates the degree of match or mismatch between these graphs. If the match measure exceeds a theoretically or empirically derived threshold, then the candidate signal matches the prototype pattern; recognition is complete.

In signal analysis, structural descriptions derived from signals tend, like their source data, to be one-dimensional entities. Commonly the structure is just a vector, and the components of the vector are numerical weights that indicate the relative presence of some expected characteristic of the signal over a time interval. In computer vision, the structural descriptions are often two-dimensional, like the images they come from. Not unexpectedly, the feature relationships are more intriguing, more varied, and more difficult to analyze. Sometimes it is important to extract features at a range of scales of the signal's domain. Then there is a family of feature vectors, and a feature at a coarse scale may resolve into a set of finer scale characteristics. This forms a two-dimensional structural description of the signal: There are large-scale or low-resolution features at the top; features of intermediate size in the middle; and high-resolution, small-scale features at the bottom. For instance, we might find a texture region when segmenting a signal into wide regions and then resolve it into small curves, edges, and flats. At the finest scale, discrete signal features are just the signal values. The discrete world limits signal resolution. With analog signals, resolution refinment need never stop. This is called a pyramid representation. Pyramidal structural descriptions for signals are an important and widely studied analysis tool. However, with their introduction into the signal analysis application, the problems become as intricate as they are in computer vision.

This section first explains how to reduce the amount of signal data subject to analysis by the pervasive strategy of feature extraction. Section 4.6.2.2 follows with some basic measures for signal matching by comparing feature vectors. The vectors contain fewer numbers than the signals, so comparisons are quick—a happy contrast to correlation-based approaches. Next, we develop some formal theory for structural descriptions of signals. The last subsection explains a comparison measure for structural descriptions. This measure turns out to be a metric, one of our fundamental theoretical results in structural pattern recognition.

4.6.2.1 Feature Extraction. Extraction of feature vectors reduces the dimensionality of the matching problem. The expense of computing the normalized

cross-correlation match measure is a drawback in its application. This is all the more the case when a candidate signal must be compared against many prototype signals.

Structural pattern recognition attempts to place input signals $\{f_1, f_2, \ldots, f_N\}$ into categories $\{C_1, C_2, \ldots, C_K\}$ by forming an intermediate, structural description of the signal and then using the structural description as the basis for classification. The simplest form of structural description is the feature vector, $v = (v_1, v_2, \ldots, v_M)$. Components of the feature vector are numerical, usually real but sometimes complex numbers. By thresholding the magnitude of the feature vector components, labels can be assigned to the features to build an abstract or symbolic description of the signal. Selecting the right feature vector is both quite open to design and quite critical to the recognition application's success.

Let's consider how we might extract a feature vector from a signal. First, suppose that we have a candidate signal, $x(n)$, and a set of model or prototype signals $\{e_i(n) \mid 1 \le i \le N\}$ defined on some interval $[a, b]$. The plan is to develop a vector $\mathbf{v} = (v_1, v_2, \ldots, v_N)$ such that its components, v_i, are a measure of the similarity between $x(n)$ and prototype e_i. Any of the norms we know from the theory of normed linear spaces in Chapter 2 are suitable; we may choose $v_i = \|x - e_i\|_p$, the l^p norm of the difference between the candidate signal and prototype e_i. This measures the mismatch between x and e_i. The l^p norm is a metric and is suitable for pattern detection applications.

But the results on normalized cross-correlation and matched filtering in Section 4.6 inspire us to use the inner product $v_i = \langle x, e_i \rangle$. Since the inner product $\langle x, e_i \rangle$ depends on the magnitude of e_i, the prototypes should all have the same magnitude; otherwise a large-magnitude prototype will skew all of the matches toward itself. Orthogonality of prototypes is important also. Suppose that $\langle e_1, e_2 \rangle \neq 0$. Without orthogonality, a signal which is a scalar multiple of e_1, say $y = ce_1$ on $[a, b]$, will have a similarity measure to e_2 of $\langle y, e_2 \rangle \neq 0$. Thus, although it is a perfect scaled (amplified or attenuated) replica of prototype e_1, y shows a similarity to e_2. The solution to this identification conundrum is to simply stipulate that the prototypes be orthogonal and of unit length. Hence, orthonomal bases—such as we developed in Chapters 2 and 3 for Hilbert spaces—play an important role in pattern recognition theory. An important problem is how to choose the basis for pattern recognition applications. Of course, we can orthogonalize any linearly independent set of signals on $[a, b]$, using, for instance, the Gram–Schmidt procedure sketched in our reflections on Hilbert space. However, the resulting basis set, $\{e_i\}$, may not resemble the original patterns. One way to ensure the construction of a pattern recognition basis set that preserves the features of input signals is to build the basis set according to candidate signal statistics. A classical technique, the Karhunen–Loève transform, can be applied to select the best possible basis [84, 85]—for instance, when the problem is a simple edge shape [65].

There are many other ways to extract feature vectors from signals. We can study a single signal region with basis functions, as above. The basis function inner products can also be applied to a series of intervals. But other processing steps are possible. The presence of a given signal level can be used as a feature vector component. The presence of a texture parameter—roughness or waviness—is a common technique in feature vector designs. Often the signal features have fixed registrations,

assigned as part of the signal analysis application's design. In other situations, an input signal is subject to an initial segmentation, perhaps by signal level (thresholding), texture analysis, or edge detection. This determines the presence and registration of useful signal content. Then the feature vector is extracted from a set of intervals that derive from the preliminary segmentation. It is common, too, to generate a single large feature vector, $\boldsymbol{v} = \{v_{i,j} \mid 1 \le i \le N, 1 \le j \le M\}$, where the components $v_{i,j}$ for $1 \le j \le M$, represent M different feature values, each applied to the same region of interest of the signal, S_i, $1 \le i \le N$. Statisitcal analysis of feature vectors may reveal correlations, and some of them can be deleted from the final application. Optimal selection of features is possible and explored fully in pattern recognition treatises [85]. Feature vector components can also be labeled. Components that exceed certain thresholds that exceed certain thersholds receive an appropriate label, and the vectors of labels are processed by higher-level, goal-directed artificial intelligence algorithms.

Let's consider some examples of feature extraction to see some of the alternatives.

Example (Plasma Etch Reactor Endpoint Detection). The semiconductor manufacturing industry uses plasma reactors to selectively remove materials from the surface of silcon or gallium arsenide wafers [70]. Plasma chemistry is notoriously complex. It is difficult to know how fast etching proceeds and when to halt the process. A popular technique for ending a plasma etch process is to monitor the optical emissions from reaction species for gross changes. The sudden disappearance of an etching byproduct emission indicates the endpoint of the etch cycle. Alternatively, the appearance of optical spectra characteristic of an underlying layer that should be preserved means that the reaction should halt. If a spectrograph monitors the appropriate emissions, its output is digitized, and a computer processes this digital signal, then this at first appears to be a simple real-time edge detection task. However, differences in plasma chemistry across runs, reactor chambers, and semiconductor wafer patterns combine to make this control strategy quite problematic. Moreover, as the semiconductor industry continues to reduce the scale of integrated circuits, etched areas get very small, targeted emission species diminish, and distinct endpoints become increasingly harder to identify. Feature extraction methods in common use for recognizing plasma etch endpoint include the following:

- Estimates of the first or second derivatives of the endpoint trace
- Approxmiations of the signal level within fixed regions of the trace
- Estimates of the departure of the endpoint signal from expected models of the optical emission trace
- Estimates of the endpoint trace curvature in fixed regions of the endpoint trace

Example (Internal Combustion Engine Knock Detection). In automobile engines there is an especially noticeable and harmful abnormal combustion situation known as knock. Knock occurs after the spark plug fires and results from a spontaneous combustion of unburned gasoline vapors in the cylinder. It produces a sharp, metallic, clanking sound, and is very harmful to engine components. By mounting an

accelerometer on the engine block and recording the engine vibration signal, Molinaro and Castanié were able to digitally analyze engine knock [86]. From a vibration signal $x_a(t)$, the researchers acquired digital samples $x(n)$, $1 \le n \le N$, and extracted feature vectors $\boldsymbol{v} = (v_1, v_2, ..., v_p)$. The researchers studied a large variety of possible features, v_i, including the signal energy averaged over N samples,

$$v_1 = E_x = \frac{\sum_{n=1}^{N} |x(n)|^2}{N}. \tag{4.93}$$

Another set of features was derived from the histogram values of $|x(n)|$,

$$v_{2+i} = \#\{x(n) \mid k_i \le |x(n)| = k_{i+1}\}, \tag{4.94}$$

where $K = \{k_0, k_1, ..., k_{q-1}\}$, $0 \le i < q$, determines a set of intervals within the range of $|x(n)|$. Another set of parameters, designed to capture the significant periodicities in the $x(n)$ values, are given by $|X(k)|^2$, where, as in our study of texture segmentation in Section 4.3.2, we have

$$X(k) = \sum_{n=0}^{N-1} x(n) \exp\left(\frac{-2\pi jnk}{N}\right). \tag{4.95}$$

Molinaro and Castanié keep $|X(k)|^2$ for $k = 1, 2, ..., \lceil N/2 \rceil$ as feature vector elements. Two other families of feature vector components are more exotic: Prony and cepstral coefficients. The investigators model the trend of $x(n)$ values with a Prony model of order P:

$$x(k) \approx \sum_{k=0}^{p} A_k e^{j\theta_k} e^{n(\alpha_k + j2\pi f_k)}. \tag{4.96}$$

The construction of the model is outside the present scope, but related to the z-transform construction of Chapter 8 [87]. The cepstral coefficients, c_i, are Fourier coefficients of the Fourier transform of |the logarithm of $X(k)$|, given in (4.95):

$$\log|X(k)|^2 \approx \sum_{n=-Q}^{Q} c_i e\left(\frac{-2\pi jnk}{N}\right). \tag{4.97}$$

Both Prony model parameters and cepstral expansion coefficients are useful for compactly encoding the frequency and stability information within a signal. Prony parameters figure in time series analysis studies [88] and cepstral expansions have been widely used in speech detection applications [89]. The Prony model parameters of A_k, θ_k, α_k, and f_k and the cepstral coefficients c_k become feature vector elements. The point of this discussion is not to erode the reader's confidence is selecting feature vectors, but, rather, to show some of the possibilities and variety of feature vector components used in a modern application. In fact, Molinaro and Castanié reduce the number of feature vectors by statistical techniques before invoking their ultimate detection criteria.

4.6.2.2 Distance Measures for Feature Vectors. Let's consider two basic methods for comparing feature vectors. In a typical signal analysis application, feature vectors for a library of prototype signals, or models, may be archived in a database. Feature vectors are similarly extracted from input signals—candidates or unknowns—and compared to the library of prototype vectors.

Once the data reduction from time-series signal to finite feature vector is finished, it is possible to apply the Euclidean norm, from finite-dimensional vector spaces, to match prototype signals to candidates. This is called the *minimum distance classifier.*

Definition (Minimum Distance Classifier). Suppose $\boldsymbol{v}$ is a feature vector extracted from a application input signal, $x(n)$, and $\{\boldsymbol{e}_m \mid 1 \leq m \leq M\}$ is the set of feature vectors of prototype patterns. Then the minimum distance classifier recognizes $x(n)$ as being of type k if $\|\boldsymbol{v} - \boldsymbol{e}_k\| \leq \|\boldsymbol{v} - \boldsymbol{e}_m\|$ for all m, $1 \leq m \leq M$.

Another popular classifier works on labeled feature vector components. Suppose that signal feature vector components are derived from a partition of the domain of signal $x(n)$; that is, each feature vector component represents a particular subset of Dom(x). Let $\Pi = \{S_1, S_2, ...\}$ be the partition of Dom(x). Suppose also that Λ is labeling of x for Π, Λ: $\Pi \rightarrow \{\Lambda_1, \Lambda_2, ...\}$. Typically, labels are applied to feature vector components if the component's magnitude exceeds a threshold associated with the feature. If feature vectors have been extracted from library prototypes as well, then candidate signals can be matched against library prototypes by comparing the labelings. One such method of comparing vectors of labels and labels applied to the vector components is the Hamming distance.

Definition (Hamming Distance Classifier). The Hamming distance between a candidate signal label vector $\boldsymbol{u} = (\alpha_1, \alpha_2, ..., \alpha_N\}$ and a prototype vector $\boldsymbol{w} = (\beta_1, \beta_2, ..., \beta_N\}$ is the number of positions in which $\boldsymbol{u}$ and $\boldsymbol{w}$ differ. We write the Hamming distance between label vectors $\boldsymbol{u}$ and $\boldsymbol{w}$ as $H(\boldsymbol{u}, \boldsymbol{w})$.

It is easy, and left as an exercise, to show that the Hamming distance is a metric.

4.6.3 Statistical Pattern Recognition

The third approach to pattern recognition that we will consider is statistical pattern recognition. It is possible to resort once again to a least-squares approach. The least-squares coefficient matrix derives from a large number of samples and represents the known knowledge of input signals to the analysis application [89, 90]. We considered this very general and very powerful approach to the problem of finding an optimal noise-removal filter in Section 4.3. The extension of the method to pattern recognition is straightforward. Of the many statistical approaches, we will examine one of the most important: the Bayes classifier.

4.6.3.1 Bayes Classifier. The Bayes classifier is a fundamental tool in pattern recognition. It is a parametric approach, in that statistical parameters associated

with the source patterns (signals or images) are assumed or approximated by the application. As the first chapter already hinted, this pattern classification method relies on Bayes's formula for conditional probabilities.

Statistical pattern recognition, like correlation-based matching and structural recognition, attempts to associate a class or category, $\{C_1, C_2, ..., C_K\}$, with each input signal $\{f_1, f_2, ..., f_N\}$. In order to develop statistics for each input signal, the signal is decomposed into a feature vector, $\boldsymbol{v} = (v_1, v_2, ..., v_M)$. Each component of the feature vector is numerical, in order to develop statistics for the likelihood of features, classes, and for features within signal classes. Selecting the right feature vector is both quite open to design and quite critical to the recognition application's success.

Standard pattern recognition texts cover the Bayes classifier [91–93]. One of the earliest applications of Bayes classifiers to the design of a character recognition system was by Chow and dates from the 1950s [94].

4.6.3.2 Statistical Decision Rules. This section explains how statistical decision rules for deciding class membership can be made based on the likelihood of each class of signal occurring and on the probability distributions of feature vectors among classes. We examine the problem in several ways. First we frame the problem as a search for a set of discriminant functions that indicate the resemblance of a signal to members of a class. Then we consider the problem of finding risk functions. That is, we seek functions that measure the risk of misclassification, and our problem transposes to one of minimizing the risk of a mistaken classification of a signal. Finally, we pose the problem in terms of the Bayes rule for conditional probabilities. We find that this provides a reasonable statistical tool for building discriminant and risk functions, although there are a number of probability density functions that must be determined.

Discriminant and risk functions are closely related. Suppose that we assigning signals $\{f_1, f_2, ...\}$ to classes $C = \{C_1, C_2, ..., C_K\}$. For each signal, $f \in \{f_1, f_2, ...\}$, a feature vector, $\boldsymbol{v} = (v_1, v_2, ..., v_M)$, is generated. We desire a set of discriminant functions, $D_1, D_2, ..., D_K$, one for each signal class. The idea is that $D_k(\boldsymbol{v})$ tells us how strongly signals with features $\boldsymbol{v}$ resemble signals from class C_k. A discriminant-based classifier assigns signal f with feature vector $\boldsymbol{v}$ to class C_k if $D_k(\boldsymbol{v}) > D_i(\boldsymbol{v})$ for all $i \neq k$. The complementary idea is the risk function. Now we seek functions, $R_1, R_2, ..., R_K$, such that $R_k(\boldsymbol{v})$ tells us the risk of classifying f with features $\boldsymbol{v}$ as belonging to class C_k. How strongly do signals with features $\boldsymbol{v}$ resemble signals from class C_k? A risk-based classifier places signal f with feature vector $\boldsymbol{v}$ into class C_k if $R_k(\boldsymbol{v}) < R_i(\boldsymbol{v})$ for all $i \neq k$. Taking $R_k(\boldsymbol{v}) = -D_k(\boldsymbol{v})$ makes an easy transition from a discriminant-based classifier to a risk-based classifier.

Now let's consider how to use statistical information about feature vectors and classes to develop statistical discriminant functions. Suppose that we know the a priori probability of occurrence of each of the classes C_k, $P(C_k)$. Suppose further that for each class, C_k, we know the probability density function for the feature vector $\boldsymbol{v}$, $p(\boldsymbol{v}|C_k)$. The conditional probability, $P(C_k|\boldsymbol{v})$, provides the likelihood that class k is present, given that the input signal has feature vector $\boldsymbol{v}$. If we could compute $P(C_k|\boldsymbol{v})$ for each C_k and $\boldsymbol{v}$, then this would constitute a statistical basis for

selecting one class over another for categorizing the input signal f. But the Bayes formula for conditional probabilities (Chapter 1) provides a tool for calculating this a posteriori probability:

$$P(C_k \mid \boldsymbol{v}) = \frac{p(\boldsymbol{v} \mid C_k)P(C_k)}{p(v)} = \frac{p(\boldsymbol{v} \mid C_k)P(C_k)}{\sum_{i=1}^{K} p(\boldsymbol{v} \mid C_i)P(C_i)}, \tag{4.98}$$

where $p(\boldsymbol{v})$ is the probability density function for feature vector $\boldsymbol{v}$. This inspires the Bayes decision rule:

Definition (Bayes Decision Rule). Given a signal f and a feature vector $\boldsymbol{v}$ derived from f, the Bayes Decision Rule is to classify f as belonging to class $C_k \in C = \{C_1, C_2, ..., C_K\}$ if $P(C_k|\boldsymbol{v}) > P(C_i|\boldsymbol{v})$ for all $i \neq k$; otherwise, classify f as belonging to some C_k where $P(C_k|\boldsymbol{v})$ is maximal.

We can also improve upon our concept of risk by incorporating the probabilistic ideas. Suppose that the cost of assigning signal f with feature vector $\boldsymbol{v}$ to class C_k, when it really belongs to class C_i is $r(k, i)$, where $r(k, i) = 0$ if $k = i$. Typically, $r(k, i)$ is a 1 or 0, for the cost of an error or the cost of no error, respectively. Then, the total cost simply counts the number of misclassifications. In a real application, it may be necessary to provide more informative risk estimates and cost counters. For example, in a character recognition system, the cost might be the time estimate for human assistance to the application. Then, incorporating the a posteriori probabilities from Bayes's formula, the risk of placing f in class k, $R(C_k, v)$, is the sum of the individual misclassification risks,

$$R(C_k, \boldsymbol{v}) = \sum_{i=1}^{K} r(k,i)P(C_k \mid \boldsymbol{v}). \tag{4.99}$$

Classifying signal f with feature vector $\boldsymbol{v}$ as belonging to class C_k according to whether $R(C_k, \boldsymbol{v}) \leq R(C_i, \boldsymbol{v})$ for all $i \neq k$ implements the Bayes decision rule (4.99).

Now let us consider possible discriminant functions based on the Bayes formula (4.98). We may begin by assigning the discriminants $D_k(\boldsymbol{v}) = P(C_k|\boldsymbol{v})$, but noting that, given feature vector $\boldsymbol{v}$, for each such k, $1 \leq k \leq K$, the denominator in (4–6.1) is identical, we can simplify the discriminants to have

$$D_k(\mathbf{v}) = p(\mathbf{v} \mid C_k)P(C_k). \tag{4.100}$$

And it will be convenient in a moment to take the natural logarithm of (4.100) to obtain the alternative discriminant function

$$D_k(\mathbf{v}) = \log(p(\mathbf{v} \mid C_k)) + \log(P(C_k)). \tag{4.101}$$

Indeed, any constant can be added to each of a family of discriminant functions without changing their characterization capability. Each of the family of discriminants may be multiplied by any positive constant. Finally, a monotonic increasing function, such as the logarithm, may be be applied to all of the discriminants

without affecting the classification results. These operations are often useful for simplifying the evaluation of discriminants.

4.6.3.3 Estimating Probabilities. Let us now turn to the practical problem of how to estimate the probabilities that are necessary for applying the Bayes rule for pattern recognition. Upon examinination of (4.98), we see that applying the Bayes formula assumes that we have knowledge of:

- The a priori probability of class occurrence C_k, $P(C_k)$
- The probability density function for the feature vector $\boldsymbol{v}$, given the presence of a signal of class C_k, $p(\boldsymbol{v}|C_k)$

How are we to estimate these probabilities?

It may be possible to know the class probabilities, $P(C_k)$, from the nature of the application. For example, in a character recognition application, the class probabilities come from known probabilities of the presence of characters in text. This could come from a broad scientific study of the problem area. To wit, the development of classifiers for the optical character recognition systems used by the United States Postal Service required the collection and analysis of hundreds of thousands of character samples [95–97]. And lacking the luxury of a broad scientific study, the character recognition classifier designer can perform a sampling of representative texts. In the case of speech phoneme recognition, these probabilities are known, but if the application concerns a special application area (i.e., spoken numbers for a telephone dialing application utilizing voice recognition), then more uniform probabilities apply. There are some subtleties, to be sure. In a spoken number recognition system, one must be alert to common alternative pronunciations for numbers. The system designer might assume that $P(C_1) = \cdots = P(C_9) = .1$, with C_n signifying the utterance of a nonzero number. But two common alternatives exist for saying "zero": "zero" and "oh." Thus, the design might posit two classes for this utterance; thus, $P(C_0) = P(C_z) = 0.05$, for saying "oh" or "zero," respectively.

The class conditional feature probabilities are a further problem. If we conduct a thorough statistical study of a large number of samples from each class, then it is possible to arrive at rough ideas of the distribution functions. But when a signal f arrives at the input to the system, and the front-end processing modules derive its feature vector v, how are we to compute the probability density functions $p(\boldsymbol{v}|C_k)$ for each class C_k? If we answer that we should once more adopt a parametric stance—that is, we assume a particular probability density function for the conditional densities required by (4.98)—then there is a elegant and practical resolution to this problem.

It should come as no surprise that the distribution of choice is the Gaussian. Not only is it justified by the Central Limit Theorem, but it provides the most tractable mathematical theory. Since we are dealing with feature vectors, we must consider the multivariate normal distribution. For the probability density function $p(\boldsymbol{v}|C_k)$, this parametric assumption is

$$p(v \mid C_k) = \frac{\exp[-\frac{1}{2}(\boldsymbol{v}-\mu_k)^T \Sigma_k^{-1}(\boldsymbol{v}-\mu_k)]}{\sqrt{\det(\Sigma_k)(2\pi)^M}}, \tag{4.102}$$

where $\boldsymbol{v} = (v_1, v_2, ..., v_M)$ is the feature vector of length M extracted from signal f; μ_k is the mean for feature vectors from signals of class C_k, $\mu_k = E[\boldsymbol{v}|C=C_k]$; $(\boldsymbol{v} - \mu_k)^T$ is the transpose of $\boldsymbol{v} - \mu_k$; and Σ_k is the $M \times M$ covariance matrix for feature vectors of C_k signals, $\det(\Sigma_k)$ is its determinant, and Σ_k^{-1} is its inverse.

The parametric assumption allows us to estimate the conditional probabilities, $p(\boldsymbol{v}|C_k)$. This requires a preliminary classifier training step in order to establish the statistical parameters that the analysis application uses to classify incoming signals. Data from a large number of signals for each of the different classes $\{C_1, C_2, ..., C_K\}$ is collected. For each such signal, its feature vector $\boldsymbol{v}$ is derived. The average of the feature vectors from class C_k is μ_k. Once we have computed the means for all of the feature vectors from signals in a class C_k, then we can compute the covariance matrices, $\Sigma_k = E[(\boldsymbol{v}-\mu_k)(\boldsymbol{v}-\mu_k)^T$. Once the covariance matrix is computed for a class C_k, its determinant and inverse can be calculated (this is problematic when the number of features is large). The feature vector averages, $\{\mu_1, \mu_2, \ldots, \mu_K\}$, and the covariance matrices, $\{\Sigma_1, \Sigma_2, \ldots, \Sigma_K\}$, are stored for analyzing the signals that the classifier accepts as inputs. This completes the training of the classifier.

The steps in running the classifier are as follows. For every signal f with feature vector $\boldsymbol{v}$, the Bayes classifier

- Computes (4.102) for each class C_k;
- Calculates the a posteriori probability $P(C_k|\boldsymbol{v})$ for each k, $1 \le k \le K$;
- Classifies signal f as belonging to class C_k where $P(C_k|\boldsymbol{v})$ is maximal.

4.6.3.4 Discriminants. Now let us consider different discriminant functions that support a Bayes classifier. Different discriminants arise from the statistics of the feature vectors of input signals to the classifier. In particular, special cases of the covariance matrix Σ_k in (4.102) result in significant simplifications to the classifier's computations.

Let us first look at an alternative discriminant function for (4.98), namely the natural logarithm. Since the natural logarithm is monotone increasing, taking $\log(P(C_k|\boldsymbol{v}))$ provides the same recognition decision as $P(C_k|\boldsymbol{v})$ itself. Thus, if we assume normally distributed feature vectors (4.102), then we have

$$\begin{aligned} D_k(\boldsymbol{v}) &= \log(p(\boldsymbol{v} \mid C_k)) + \log(P(C_k)) \\ &= -\frac{1}{2}(\boldsymbol{v}-\mu_k)^T \Sigma_k^{-1}(\boldsymbol{v}-\mu_k) - \frac{m\log(2\pi)}{2} - \frac{\log(\det(\Sigma_k))}{2} + \log(P(C_k)). \end{aligned} \quad (4.103)$$

The term $m \log(2\pi)/2$ does not depend on C_k, so it can be ignored; thus, we may set

$$D_k(\boldsymbol{v}) = -\frac{1}{2}(\boldsymbol{v}-\mu_k)^T \Sigma_k^{-1}(\boldsymbol{v}-\mu_k) - \frac{\log(\det(\Sigma_k))}{2} + \log(P(C_k)). \quad (4.104)$$

In (4.104), $\det(\Sigma_k)$ and $P(C_k)$ can be calculated from the training data, so only the vector product $(\boldsymbol{v}-\mu_k)\Sigma_k^{-1}(\boldsymbol{v}-\mu_k)^T$ needs to be calculated for the feature vector $\boldsymbol{v}$ of every input signal f.

Three simplifying assumptions make the discriminants (4.104) easier to compute:

- The a priori probabilities $P(C_k)$ of the signal classes are all equal.
- The features vectors are statistically independent and have the same variance.
- The convariance matrices are all the same.

In the first case, we may drop the $\log(P(C_k))$ term from (4.104). This helps, but the inversion and determinant of the covariance matrix pose a greater threat to computational tractability.

In the second of these special cases we find $\Sigma_k = \sigma^2 I$, where I is the $M \times M$ identity matrix. Then $\Sigma_k^{-1} = \sigma^{-2} I$, which is independent of class. This allows us to trim the discriminant functions further, so that now, having removed all class-independent terms, we arrive at

$$D_k(\boldsymbol{v}) = -\frac{1}{2\sigma^2}(\boldsymbol{v} - \mu_k)^T(\boldsymbol{v} - \mu_k) + \log(P(C_k)). \tag{4.105}$$

Making the additional assumption that class membership likelihood is the same for all C_k, we find that maximizing $D_k(\boldsymbol{v})$ in (4.105) is the same as minimizing $(\boldsymbol{v} - \mu_k)(\boldsymbol{v} - \mu_k)^T = \|\boldsymbol{v} - \mu_k\|^2$. This classifier we are already familiar with from Section 4.6.2.2. It is the minimum distance match between features drawn from the input signal f and the mean feature vectors. In other words, a Bayes classifier with statistically independent features of equal variance reduces to a minimum distance classifier. The class C_k for which feature vector $\boldsymbol{v}$ is closest to μ_k is the class to which we assign input signal f.

The Bayes classifier is optimal; and when the feature vectors obey a Gaussian distribution, the discriminant functions (4.103) are the proper tool for separating input signals into classes. There are nevertheless some important difficulties with the Bayes classifier, and we must note them. The feature vectors may not, in point of fact, be normally distributed. This makes the computation of the discriminant problematic. Sometimes, alternative features that more closely follow a Gaussian distribution can be selected. Furthermore, if the number of features is large, the computation of the determinant and inversion of the covariance matrix become intractable. There are, finally, some philosophical reasons for objecting to the Bayes classifier [98].

4.7 SCALE SPACE

This section studies a signal analysis technique known as *scale-space decomposition*. From our first studies of representative signal interpretation problems, we noted that the determination of the size of a signal component is a critical step in analyzing the signal. One task in automated electrocardiography, to recall an example from the first chapter, is to distinguish between splintered and normal contractions of the heart's left ventricle. It is the time-domain extent of the signal's jump that determines whether there is a normal contraction or an abnormal, spasmodic

contraction. And in edge detection, we noted that understanding scale is a necessary part of simple edge detection. For an edge at a fine scale could just as well be considered an insignificant signal aberration at a coarse scale.

Soon after researchers began examining the magnitude of signal derivatives in study of edges, their interest extended to signal curvature, which is a local measure of signal shape. There are several quite natural reasons for this transition. Psychological experiments revealed that a few curved line fragments suffice to impart object shape information—Attneave's famous example is a sleeping cat—to a human subject [99]. Also, from calculus, the sign of the second derivative determines the curvature of a signal: Where the second derivative is positive defines a concave up region, where it is negative defines a concave down region, and where it is zero an inflection point exists. The problem is that the second derivative information is very noisy in real signals and images, resulting in erratic segmentation in regions of different curvatures. Researchers turned increasingly toward multiple resolution methods that would support the precious information content from curvature. Hierarchical methods for image processing and recognition within natural scenes were disclosed, for example [100, 101].

We have already noted Marr's contribution to multiscale edge detection, which formed the cornerstone of a very important trend in signal and image analysis [77]. Marr oriented the attention of the scientific and engineering communities to the links between the algorithms of engineered systems and the processes within biological systems—for example, animals [102]. Marr's strategy was to study animal sensory systems, especially vision, and from them derive the inspiration for machine vision system designs. Researchers in the new field of psychophysics, which studies the brain's sensory processes at a stage where they are still independent of consciousness, had found evidence of multiple resolution, orientation-sensitive processing channels in animal vision systems [103–105]. Aware of the biological vision system research, recognizing its link to the multiple resolution image analysis efforts, and building upon their earlier work in edge detection, Marr and his coworkers proposed a three-stage architecture for vision systems:

- The raw primal sketch, which segments the signal into edges and concavity regions;
- The extraction of geometric information relative to the observer;
- The determination of geometric information independent of the observer.

While Marr's scheme is a vision system formulation, we wish to focus on signal interpretation and shall reduce his architecture into one dimension. Let's replace Marr's visual terms with auditory terms. Thus, we ought to look not for a raw primal sketch so much, perhaps, as a raw primal listen. And we ought to think of signal or sound content rather than think of geometric information, with its planar and spatial connotations. An example should help. When you hear a whistle at a railroad crossing, the raw primal sketch consists of the auditory edge at the onset of train's whistle and the increasing intensity thereafter. The sudden realization that a train is coming closer to you constitutes the observer–relative signal content. The reflection

that a train is about to cross through the intersection makes up the observer-independent information in the experience.

Computationally, the raw primal sketch begins by convolution of the signal with the second derivative of the Gaussian. If $f(t)$ is a signal and $g(t, \sigma)$ is the Gaussian of standard deviation σ and zero mean, then we let $F(t, \sigma)$ be defined by

$$F(t, \sigma) = f(t) * \frac{\partial^2}{\partial x^2} g(t, \sigma). \tag{4.106}$$

We recognize this as the edge detection operation of Marr and Hildreth [62]. The next raw primal step is to link the edges together and segment the signal into regions of concavity (concave down) and convexity (concave up). The remaining steps in Marr's schema, the development of signal information relative to the observer and signal information independent of the observer, then follow.

Note that there does not seem to be any clear direction within Marr's algorithm to decide at what scales σ the edge detection operation (4.106) should be developed. The second two steps in the algorithm are less clear than the first, and they contain a number of thresholds and parameters whose values are difficult determine without extensive experimentation. Finally, there is no clear relation between the primal sketch information in the different channels. How does the content of a large σ channel affect the processing of the conent of a small σ channel? Does processing occur from large to small or from small to large σ channels? These difficulties with the conception brought some researchers to critique Marr's architecture. Prominent among the skeptics, Pentland, deemed it to be too data-driven and lacking in its qualitative aspects [106]. Soon enough, however, in the early 1980s—beginning what would turn out to be a decade of signal analysis research breakthroughs—an important step in demonstrating qualitative computer vision strategies was taken by Witkin [107] and by Koenderink [108] with the concept of scale-space representation.

Like Marr's theory, the scale-space representation smoothes an image with a family of Gaussian filters. There are two substantive differences, however: A full set of smoothed images is maintained, and there is a critical interconnection between the regions of concavity at different scales, σ. We shall see that a complete description of the signal's shape results. The description proceeds from the smallest to the largest scale, and each concavity feature of the signal ranked according to its significance.[6]

Scale space decomposition thus furnishes a useful signal analysis paradigm. It identifies concavity as a critical feature of signals. It highlights the link that this feature shares with biological vision systems, as, for instance, a scattering of curved lines immediately suggests a shape. It shows how the features at one scale affect those at another scale. We shall soon see how to derive a complete graphical or

[6]Interestingly, the first exploration of scale-space decomposition was in the area of theoretical economics. James L. Stansfield, working at the Artificial Intelligence Laboratory at the Massachusetts Institute of Technology in the late 1970s, studied zero crossings under Gaussian smoothing while tracking commodity trends ["Conclusions from the commodity expert project," MIT AI Laboratory Memo, No. 601, November 1980].

structural description of the signal from this multiscale concavity information. Furthermore, this structural description enables us to readily build pattern recognition or object matching applications. We can nevertheless use it to perform a time-domain analysis of a signal, identify signal features of different scale, and derive a nonsignal structure that is useful for interpreting the signal. That is the goal of signal analysis, and scale space decomposition is the methodological exemplar.

We will first examine scale space as originally conceived—in analog form. We will consider the type of nonsignal structures that the scale space decomposition produces for a signal. We will state and prove (for simple, but important classes of signals) the theorems that give the method its power. And we shall highlight some of the drawbacks of the classic continuous-time form of scale-space decomposition. Interestingly enough, it was not until some years after the development of the analog scale-space theory that discrete versions of the theory were discovered. We will look at some approaches to discrete scale-space decomposition and close this section with some applications.

4.7.1 Signal Shape, Concavity, and Scale

Scale-space decomposition of a signal begins by smoothing the signal with a family of Gaussian filters. The smoothing operation is a convolution, so it is linear and translation invariant (Chapter 3). Furthermore, all of the smoothing kernels are the same, except for the standard deviation of the Gaussian, σ, which increases with the amount of smoothing performed. This procedure, quite familiar after our experiments with edge detection, produces a series of representations of the signal at different scales or resolutions. The highest resolution (and hence the smallest scale) occurs with the original signal, and we may derive coarser resolution representations of the signal by increasing σ. This collection of smoothed versions constitutes a scale space decomposition of the signal.

The next idea is to look for regions of curvature in the scale space decomposition's signals. The signal derivative remains the principal tool for recovering signal shape. Recall from calculus that the extrema of the nth derivative of a signal $d^n f/dt^n$ are the zeros of its next higher derivative, $d^{(n+1)}f/dt^{(n+1)}$. Consider in particular the sign of the second derivative of a signal. (Withhold for a moment the objection, drawn from general intuition and practical edge detection endeavors, that this derivative is noisy and misleading.) Where $d^2f/dt^2 < 0$, the signal is concave down; where $d^2f/dt^2 = 0$ and $d^3f/dt^3 \neq 0$ there is a zero crossing of the second derivative, or a point of inflection, using calculus parlance; and regions where $d^2f/dt^2 > 0$ are concave up, or convex. Thus, the sign of the second derivative is the basis for signal segmentation (Section 4.1).

Definition (Curvature). Curvature is a measure of how rapidly the graph of a signal, $G = \{(t, f(t)): t \in \text{Dom}(f)\}$ is turning in on itself. More formally, the osculating circle to the graph G at a point $(t_0, f(t_0)) \in G$ is the circle that is tangent to the curve at $(t_0, f(t_0))$. And the curvature κ equals $1/\rho$, where ρ is the radius of the osculating circle to the graph G.

Note that curvature can be obtained by fitting a polynomial to the signal values and computing the derivative of the polynomial model. Alternatively, a circle can be fitted to the signal data. A least-squares formulation of the problem exists and is widely used in the analysis of machined surfaces [33].

Proposition. The curvature has an analog signal representation as well; letting $y = f(t)$ and denoting differentiation by $y'(t)$, it is given by

$$\kappa(t) = \frac{y''(t)}{\left(1 + (y'(t))^2\right)^{3/2}}. \tag{4.107}$$

Proof: Calculus; also Ref. 109. ■

From the proposition, we can classify concave-up and concave-down regions of the signal not only by the sign of the curvature (positive and negative, respectively), but also by the magnitude of the curvature. For a candidate signal analysis method, this is an attractive concept for signal structure. It has considerable descriptive power. There is a link with animal vision systems. There is an important geometric connotation as well, via the idea of the osculating circle. The problem with curvature is that, despite its descriptive power and its link with biological vision systems, in the presence of signal noise it is quite problematic. This objection has likely occurred to many readers, and we need to address the issue now. Gaussian smoothing removes the local bumpiness of the signal. At larger scales, when the smoothing Gaussian kernel has a larger variance, the concave and convex regions of the signal that persist must be more significant.

Suppose $f(t)$ is an analog signal and $G(t, \sigma, \mu) = \sigma^{-1}(2\pi)^{-1/2}\exp(-(x-\mu)^2/(2\sigma^2))$ is the Gaussian with standard deviation σ and mean μ. Let $g(t, \sigma) = G(t, \sigma, 0)$. Convolution of $f(t)$ with $g(t, \sigma)$ gives $F(t, \sigma)$:

$$F(t,\sigma) = f(t) * g(t,\sigma) = \frac{1}{\sigma\sqrt{2\pi}} \int_{-\infty}^{+\infty} f(u)\exp\left(-\frac{(x-u)^2}{2\sigma^2}\right) du. \tag{4.108}$$

We are concerned with the behavior of concavity regions as we vary σ in (4.108). But the regions where the signal is concave down and concave up are separated by those where the second derivative of $F(t, \sigma)$ is zero:

$$\frac{\partial^2}{\partial t^2} F(t,\sigma) = F_{tt}(t,\sigma) = 0. \tag{4.109}$$

Thus, we can track the concavity regions of a signal by simply keeping track of the zero crossings of the second derivative (4.109). Notice that derivatives of $F(t, \sigma)$ can be computed by the convolution of $f(t)$ with the Gaussian's derivative of the same order:

Proposition. Let $f(t)$ be an analog signal and let $g(t, \sigma)$ be the zero mean Gaussian with variance σ^2. Then

$$\frac{\partial^n}{\partial t^n} F(t,\sigma) = f * \frac{\partial^n}{\partial t^n} g(t,\sigma). \tag{4.110}$$

Proof: Write out the convolution integral for (4.110) and interchange the order of the differentiation and integration. ■

Before this gets too abstract, let us consider an example. Consider a fourth-degree polynomial with two concave-up regions surrounding a narrow concave-down region. At each scale σ we determine the zero crossings of the second derivative (4.109), and over a range of scales we can draw a contour plot of the zero crossings. Notice that with sufficient smoothing the concave-down region disappears. As σ increases, the locations of the two zero crossings get closer together, eventually meet, and then there is only a convex region. For this example, once we mark the regions as concave or convex, this marking remains; a concave region does not merge with a convex region.

If this behavior is general, then we have a very great simplification in our task of segmenting the various smoothed versions of $f(t)$. All we have to do is follow the zero crossings. Where a pair meet, we know that smoothing has obliterated a convex (or concave) region and two surrounding concave (or convex, respectively) regions will merge. We can use this simplifying assumption if we know that Gaussian smoothing never creates new zero crossings, but may only destroy them as the scale of the smoothing increases. Let's pursue this line of thinking. Consider how the contour plot of zero crossings might look were the smoothing at some scale σ_0 to create a new zero crossing located at time t_0. In this case, we know that for coarser scales, $\sigma > \sigma_0$, there are regions of opposite concavity on either side of time t_0. On which side of t_0 does the concave-up region lie? We have to reexamine the signal smoothed at scale σ each time such a new zero crossing appears during the smoothing process. Depending on the complexity of the signal, this could be quite a chore! Could a large number of zero crossings abruptly appear at some scale? Could the number of regions we have to type according to concavity increase forever as we continue to convolve with Gaussians of ever-wider support? Indeed, what kind of "smoothing" do we have here that puts new wrinkles in our signal as we proceed?

Fortunately, there is a deep theoretical result for scale space decomposition that relieves us of all of these worries. The theorem is that Gaussian smoothing (4.108) never introduces additional structure as the scale parameter s increases. That is, new zero crossings of the second derivative of $F(t, \sigma)$ do not appear with increasing σ. There is a converse too: If a convolution kernel never introduces additional structure, then it must be the Gaussian. Together, these two results are the foundation of scale space theory.

4.7.2 Gaussian Smoothing

A variety of factors motivates the use of the Gaussian signal for smoothing a signal. Of course, tradition among signal analysts is one reason for using it. It was one of the smoothing operators used in some of the earliest edge detection efforts, and we found in Section 4.5.3 that the derivative of the Gaussian is an optimal step edge finder. But the Gaussian and its derivatives have a number of attractive properties, and these properties motivate its use for edge detection as well as for the more general scale space approach to signal analysis.

For scale-space decomposition the Gaussian is well-behaved. In particular, it has the following properties:

- (Symmetry Property) It is symmetric and strictly decreasing about its mean.
- As $\sigma \to 0$, $F(t, \sigma) \to f(t)$; that is, for small scales σ, the smoothed signal resembles the original.
- As $\sigma \to \infty$, $F(t, s) \to E(f(t))$; that is, for large scales σ, the smoothed signal approaches the mean of $f(t)$.
- The Gaussian is an $L^1(\mathbb{R})$ signal (absolutely integrable), and it is C^∞ (infinitely differentiable).
- (Causality Property) As σ increases, zero crossings of $F_{tt}(t, \sigma)$ may disappear, but new ones cannot arise.

While the first four of the above properties are quite nice, the Causality Property is so important that it elevates Gaussian smoothing, in a specific sense, to the status of the only possible choice for a scale-space smoothing kernel. And as indicated in the previous section, this property has an important converse, namely, that the Gaussian is unique in this regard.

The following Scale-Space Kernel Conditions formalize the above properties. We need to state these conditions for a general, candidate smoothing kernel $k(t, \sigma)$. We shall invoke these conditions later, in the course of proving our theorems. These are basic properties that we require for the filtering kernel of any scale-based signal decomposition, and so we state the conditions as a definition.

Definition (Scale-Space Kernel Conditions). A function $k(t, \sigma)$ is a scale-space kernel if it satisfies the following five conditions:

1. $k(t, \sigma)$ is the impulse of a linear, translation-invariant system: If $f(t)$ is an analog signal, then the smoothed version of $f(t)$ at scale σ is given by $F(t, \sigma) = f(t)*k(t, \sigma)$.
2. For different values of σ, $k(t, \sigma)$ should always maintain the same fundamental shape: $k(t, \sigma) = (1/\sigma^2)m(t/\sigma)$ for some one-dimensional signal $m(u)$.
3. As σ decreases, $k(t, \sigma)$ approaches the Dirac delta $\delta(t)$, so that $F(t, \sigma)$ approaches $f(t)$: as $\sigma \to 0$, we have $k(t, \sigma) \to \delta(t)$.

4. $k(t, \sigma)$ is an even signal; as $\sigma \to \infty$, or as $t \to \infty$, we have $k(t, \sigma) \to 0$.
5. The Causality Property holds for $k(t, \sigma)$.

While they might appear much too specific and technical upon first inspection, the Scale-Space Kernel Conditions are quite well-motivated. By requiring that the decomposition be linear and translation-invariant, the Convolution Theorem for Analog LTI Systems (Chapter 3) allows us to write the smoothing operation as a convolution.

4.7.2.1 Sufficiency of the Gaussian. Let us prove that the Gaussian is sufficient to produce a scale-space decomposition of a signal which does not create zero crossings in the smoothed second derivatives of $F(t, \sigma)$. Again, suppose $G(t, \sigma, \mu) = \sigma^{-1}(2\pi)^{-1/2}\exp(-(x-\mu)^2/(2\sigma^2))$ is the Gaussian with standard deviation σ and mean μ, and set $g(t, \sigma) = G(t, \sigma, 0)$. Suppose that the smoothed signal $F(t, \sigma)$ is given by the convolution of signal $f(t)$ with $g(t, \sigma)$:

$$F(t, \sigma) = f(t) * g(t, \sigma) = \int_{-\infty}^{+\infty} f(u)g(t-u, \sigma)\,du. \tag{4.111}$$

Our five-step proof relies on concepts from calculus:

- We consider the zero crossings of the second derivative $F_{tt}(t, \sigma)$ in (4.111) as curves in the (t, σ) plane.
- This allows us to invoke the implicit function theorem and second derivative conditions for a local maximum along the (t, σ) plane curves.
- We develop some straightforward characterizations of the Causality Property in a proposition.
- Any signal $k(t, \sigma)$ that is a solution of a particular form of the heat diffusion equation also satisfies one of the proposition's equivalent conditions for the Causality Property.
- Finally, since the Gaussian does solve the diffusion equation, we know that it provides a scale-based decomposition that eliminates structure as the scale of the signal smoothing increases.

To begin with, let us vary σ and observe the behavior of zero crossings of the second derivative of $F(t, \sigma)$. Let $E(t, \sigma) = F_{tt}(t, \sigma) = (\partial^2/\partial t^2)F(t, \sigma)$. Zero crossings are solutions of $E(t, \sigma) = 0$, and such pairs form curves in the (t, σ) plane. The curves may extend over the entire range of scales for which smoothing is performed, say from $0 \le \sigma \le \sigma_{\max}$. Possibly, the curve has a local minimum or maximum at a certain time value, $t = t_0$. This situation allows us to write σ as a function of t along the curve: $\sigma = \sigma(t)$. Our structural description for $f(t)$ at scale σ is its segmentation into regions that are concave-up and concave-down, bounded by the zero crossings where $E(t, \sigma) = 0$. The desired Causality Property tells us that such zero

crossings cannot increase with scale. Equivalently, this means that as smoothing proceeds, it continues to remove structure from the signal. This is the crucial idea: We can formulate the condition that zero crossings diminish as the scale of smoothing enlarges by examining the behavior of the curves $\sigma(t)$ where $E(t, \sigma) = 0$ is an extremum in (t, σ) space. The next result provides some elementary facts about zero crossing curves. The next proposition provides some basic results, useful for showing that when the scale of Gaussian filtering increases, the structural detail of a signal diminishes.

Proposition (Zero Crossing Conditions). Consider the curve $E(t, \sigma) = 0$ in the (t, σ) plane. Let the time variable t parameterize the curve $\sigma = \sigma(t)$, so that $E(t, \sigma) = F_{tt}(t, \sigma) = F_{tt}(t, \sigma(t))$ is parameterized by t as well. Then:

- The Causality Property holds if and only if each local extremum of $\sigma(t)$ is a local maximum: $\sigma'(t_0) = 0$ implies $\sigma''(t_0) < 0$.
- Along the curve E, $\sigma' = d\sigma/dt = -E_t/E_\sigma = -(\partial E/\partial t)/(\partial E/\partial \sigma)$.
- The Causality Property holds if and only if whenever $\sigma'(t_0) = 0$, then

$$\left.\frac{\partial^2 \sigma}{\partial t^2}\right|_{t=t_0} = -\left.\frac{E_{tt}}{E_\sigma}\right|_{t=t_0} < 0. \tag{4.112}$$

Proof: Condition (i) is a differential calculus formulation of our observation that an arch-shaped curve $E(t, \sigma) = 0$ is acceptable, while a trough-shaped curve is not.

To see the second condition, first note that we can parameterize the curve $E(t, \sigma) = 0$ with some parameter, say u. By the chain rule for vector-valued functions,

$$\frac{dE}{du} = \nabla E \cdot \left(\frac{dt}{du}, \frac{d\sigma}{du}\right) = \frac{\partial E}{\partial t}\frac{dt}{du} + \frac{\partial E}{\partial \sigma}\frac{d\sigma}{du}. \tag{4.113}$$

Since $E(t, \sigma) = 0$ along the curve, the derivative dE/du in (4.113) is also zero along the curve. Next, we may choose the parameterizing variable, $u = t$, the time variable. This little ruse produces

$$\frac{dE}{dt} = 0 = \frac{\partial E}{\partial t}\frac{dt}{dt} + \frac{\partial E}{\partial \sigma}\frac{d\sigma}{dt} = E_t + E_\sigma \frac{d\sigma}{dt}, \tag{4.114}$$

which gives condition (ii).

Condition (iii) follows from the first two. Indeed, applying the quotient rule for derivatives to condition (ii), we find

$$\frac{d^2\sigma}{dt^2} = -\frac{E_{tt}}{E_\sigma} + \frac{E_t}{(E_\sigma)^2}. \tag{4.115}$$

From (4.114), note that $\sigma'(t_0) = 0$ if and only if $E_t = 0$ at $t = t_0$. Thus, (4.115) ensures yet another equivalent condition: $\sigma''(t_0) = -(E_{tt}/E_\sigma)$ at $t = t_0$. The inequality in condition (iii) follows from condition (i), completing the proof. ■

This next theorem is a basic theoretical result in scale-space decomposition. It shows that a Gaussian filtering kernel can be the foundation for a scale-based signal decomposition method, which removes signal structure as the scale of the smoothing increases.

Theorem (Sufficiency). Suppose that convolution with the Gaussian, $g(t, \sigma) = G(t, \sigma, 0) = 2^{-1/2}\sigma^{-1}\exp(-t^2/(2\sigma^2))$, smoothes the signal $f(t)$ at scale σ to produce $F(t, \sigma)$:

$$F(t,\sigma) = f(t) * g(t,\sigma) = \int_{-\infty}^{+\infty} f(u)g(t-u,\sigma)\,du = \frac{1}{\sigma\sqrt{2}} \int_{-\infty}^{+\infty} f(u)e^{-\frac{(t-u)}{2\sigma^2}}\,du. \tag{4.116}$$

Then the Causality Property holds; that is, $F_{tt}(t, \sigma)$ zero crossings may disappear—but can never appear—as σ increases.

Proof: Consider the partial differential equation

$$\frac{\partial^2 U}{\partial t^2} = \frac{1}{\sigma}\frac{\partial U}{\partial \sigma}. \tag{4.117}$$

This is a form of the heat or diffusion equation from physics, introduced already in Chapter 1. We can easily check that the Gaussian $g(t, \sigma)$ solves (4.117) by calculating:

$$g_{tt}(t,\sigma) = \frac{\partial^2 g}{\partial^2 t} = \left(\frac{t^2}{\sigma^4} - \frac{1}{\sigma^2}\right) g(t,\sigma) \tag{4.118}$$

and

$$g_\sigma(t,\sigma) = \frac{\partial g}{\partial \sigma} = \left(\frac{t^2}{\sigma^3} - \frac{1}{\sigma}\right) g(t,\sigma). \tag{4.119}$$

so that (4.117) holds for $U(t, \sigma) = g(t, \sigma)$. However, we can show that $F(t, \sigma)$ and hence $E(t, \sigma)$ satisfy the diffusion equation as well. In fact, since

$$F_{tt}(t,\sigma) = \frac{\partial^2}{\partial t^2} \int_{-\infty}^{+\infty} f(u)g(t-u,\sigma)\,du = \int_{-\infty}^{+\infty} f(u)g_{tt}(t-u,\sigma)\,du = \int_{-\infty}^{+\infty} f(u)\frac{1}{\sigma}g_{\sigma}(t-u,\sigma)\,du$$

$$= \frac{1}{\sigma}\frac{\partial}{\partial \sigma} \int_{-\infty}^{+\infty} f(u)g(t-u,\sigma)\,du = \frac{1}{\sigma}F_{\sigma}(t,\sigma) \tag{4.120}$$

we have $E_{tt} = F_{tttt} = (1/\sigma)F_{\sigma tt} = (1/\sigma)F_{tt\sigma} = (1/\sigma)E_{\sigma}$. This shows that $E(t, \sigma)$ satisfies the diffusion equation (4.117) and the weaker inequality (4.112). A Gaussian kernel thereby guarantees that increasing the scale of smoothing creates no new signal structure. This completes the sufficiency proof. ■

4.7.2.2 Necessity of the Gaussian. It is quite a bit harder to show that the Gaussian is the only kernel that never allows new signal structure to arise as the scale of smoothing increases. The necessity proof involves several steps:

- We consider a candidate filtering kernel $k(t, \sigma)$ and represent the signal to be analyzed, $f(t)$, as a sum of Dirac delta functions.
- Because of the Sifting Property of the Dirac delta (Chapter 3), this transposes the convolution integral into a discrete sum, and, using the Zero Crossing Conditions Proposition above, there arises a set of simultaneous linear equations, $Ax = b$.
- If these simultaneous equations have a solution, then we can find a signal $f(t)$ for which the proposed kernel $k(t, \sigma)$ creates new structure as σ increases.
- We show that we can always solve the simultaneous equations unless the proposed kernel $k(t, \sigma)$ satisfies a special differential equation, which is a general form of the diffusion equation.
- We prove that the only kernel that satisfies this differential equation is the Gaussian.
- Thus, if the filtering kernel $k(t, \sigma)$ is not Gaussian, it cannot be a solution to the special differential equation; this implies that we can solve the simultaneous linear equations; and this solution at long last reveals a signal, $f(t)$, for which our proposed $k(t, \sigma)$ creates at least one new inflection point during smoothing.

Let's follow the above plan, beginning with some technical lemmas. We show how to derive a set of simultaneous equations by representing $f(t)$ as a sum of Dirac delta functions and using the Zero Crossing Conditions. From the discussion of the Dirac delta's Sifting Property (Chapter 3), $f(t)$ can be represented as the limit of such a sum.

Lemma (Zero Crossing Conditions for Dirac Sum Signals). Suppose that $k(t, \sigma)$ satisfies the Scale-Space Kernel Conditions and that the signal $f(t)$ has the following representation as a sum of Dirac delta functions:

$$f(t) = \sum_{i=1}^{n} c_i \delta(t - t_i). \tag{4.121}$$

As before we define

$$F(t,\sigma) = f(t) * k(t, \sigma) = \int_{-\infty}^{+\infty} f(u)k(t-u,\sigma)\,du, \tag{4.122}$$

and we set $E(t, \sigma) = F_{tt}(t, \sigma)$. To avoid excess subscript clutter, we also define $M(t, \sigma) = k_{tt}(t, \sigma) = (\partial^2/\partial t^2)k(t, \sigma)$. If $E(t_0, \sigma) = 0$ for some $t = t_0$, then

$$\sum_{i=1}^{n} c_i M(t_0 - t_i, \sigma) = 0, \tag{4.123}$$

and at an extremum (t_0, σ) of the curve $E(t, \sigma) = 0$ the following equations hold:

$$\sum_{i=1}^{n} c_i M_t(t_0 - t_i, \sigma) = 0 \tag{4.124}$$

and

$$\frac{\sum_{i=1}^{n} c_i M_{tt}(t_0 - t_i, \sigma) = 0}{\sum_{i=1}^{n} c_i M_{\sigma}(t_0 - t_i, \sigma) = 0} > 0. \tag{4.125}$$

Proof: Since $f(t)$ is a sum of Dirac delta functions (4.121), the Sifting Property of the delta function implies

$$\begin{aligned} E(t,\sigma) &= \frac{\partial}{\partial t^2} \int_{-\infty}^{\infty} f(u)k(t-u,\sigma)\,du = \int_{-\infty}^{\infty} \left\{ \sum_{i=1}^{n} c_i \delta(t - t_i) \right\} \frac{\partial}{\partial t^2} k(t-u,\sigma)\,du \\ &= \sum_{i=1}^{n} c_i k_{tt}(t_i,\sigma) = \sum_{i=1}^{n} c_i M(t_i,\sigma). \end{aligned} \tag{4.126}$$

At a point (t_0, σ) on a zero crossing curve, $E(t_0, \sigma) = 0$, so (4.123) follows from (4.126). Furthermore, the Zero Crossing Conditions Proposition showed that at an extreme point (t_0, σ) on the zero crossing curve we must have $E_t(t_0, \sigma) = 0$, and by

(4.126) this entails (4.124). Finally, note that (4.125) follows from equation (4.112) of the same proposition, and the proof is complete. ■

Corollary (Necessary Linear Equations). Let the lemma's assumptions still hold and let $t_0, t_1, t_2, \ldots, t_n$ be arbitrary. Then, for $P < 0$, the following four simultaneous equations,

$$\begin{bmatrix} M(t_0 - t_1,\sigma) & M(t_0 - t_2,\sigma) & \cdots & M(t_0 - t_n,\sigma) \\ M_t(t_0 - t_1,\sigma) & M_t(t_0 - t_2,\sigma) & \cdots & M_t(t_0 - t_n,\sigma) \\ M_{tt}(t_0 - t_1,\sigma) & M_{tt}(t_0 - t_2,\sigma) & \cdots & M_{tt}(t_0 - t_n,\sigma) \\ M_\sigma(t_0 - t_1,\sigma) & M_\sigma(t_0 - t_2,\sigma) & \cdots & M_\sigma(t_0 - t_n,\sigma) \end{bmatrix} \begin{bmatrix} c_1 \\ c_2 \\ \vdots \\ c_n \end{bmatrix} = \begin{bmatrix} 0 \\ 0 \\ P \\ 1 \end{bmatrix}, \tag{4.127}$$

have no solution $(c_1, c_2, ..., c_n)$.

Proof: The existence of $(c_1, c_2, ..., c_n)$ satisfying (4.127) with $P < 0$ violates (4.125). ■

Once we assume that $f(t)$ is a sum of Dirac delta functions, the lemma and its corollary show that the Causality Property imposes extremely strong conditions on the filtering kernel. In (4.127), finding $(c_1, c_2, ..., c_n)$ is equivalent to finding $f(t)$, and it would appear that solutions for such an underdetermined set of linear equations should be plentiful. If for some $t_0, t_1, t_2, \ldots, t_n, P$, with $P < 0$, we could discover a solution $(c_1, c_2, ..., c_n)$, then this would give us a signal $f(t)$ and a location in scale space (t_0, σ) at which the kernel $k(t, \sigma)$ fails the Causality Property: New structure unfolds when σ increases at (t_0, σ). The matrix of second-, third-, and fourth-order partial derivatives in (4.127) must be very special indeed if a candidate smoothing kernel is to support the Causality Property. Our goal must be to show that the Causality Property guarantees that for any $t_0, t_1, t_2, \ldots, t_n, P < 0$, (4.127) defies solution. The next proposition recalls a linear algebra result that helps bring the peculiarities of (4.127) to light.

Proposition. Let $\boldsymbol{M}$ be an $m \times n$ matrix, let $\boldsymbol{b}$ be an $m \times 1$ vector, and let $[\boldsymbol{M} \mid \boldsymbol{b}]$ be the $m \times (n+1)$ matrix whose first n columns are the same as $\boldsymbol{M}$ and whose last column is $\boldsymbol{b}$. Then the following are equivalent:

(i) The equation $\boldsymbol{Mx} = \boldsymbol{b}$ has a solution.

(ii) Rank $\boldsymbol{M}$ = rank $[\boldsymbol{M} \mid \boldsymbol{b}]$; that is,

$$\operatorname{rank} \begin{bmatrix} M_{1,1} & M_{1,2} & \cdots & M_{1,n} \\ M_{2,1} & \cdots & \cdots & M_{2,n} \\ \vdots & \cdots & \cdots & \vdots \\ M_{m,1} & M_{m,2} & \cdots & M_{m,n} \end{bmatrix} = \operatorname{rank} \begin{bmatrix} M_{1,1} & M_{1,2} & \cdots & M_{1,n} & b_1 \\ M_{2,1} & \cdots & \cdots & M_{2,n} & b_2 \\ \vdots & \cdots & \cdots & \vdots & \vdots \\ M_{m,1} & M_{m,2} & \cdots & M_{m,n} & b_m \end{bmatrix}. \tag{4.128}$$

(iii) For all vectors $\boldsymbol{y} = (y_1, y_2, ..., y_m)$: If $\langle \boldsymbol{y}, \boldsymbol{b} \rangle = 0$, then $y_1(M_{1,1}, M_{1,2}, ..., M_{1,n}) + y_2(M_{2,1}, M_{2,2}, ..., M_{2,n}) + \cdots + y_m(M_{m,1}, M_{m,2}, ..., M_{m,n}) = 0$.

Proof: Recall that the column space of the matrix $\boldsymbol{M}$ is the set of vectors spanned by the column vectors of $\boldsymbol{M}$, and the row space of is the set of vectors spanned by rows of $\boldsymbol{M}$. From linear algebra, the dimensions of these two spaces are the same—the rank of $\boldsymbol{M}$. Now, (i) is clearly equivalent to (ii), because (i) is true if and only if $\boldsymbol{b}$ is in $\boldsymbol{M}$'s column space. Also note that the row space of $\boldsymbol{M}$ must have the same dimension as the row space of $[\boldsymbol{M} \mid \boldsymbol{b}]$. So if vector $\boldsymbol{y} = (y_1, y_2, ..., y_m)$ is such that the linear combination of rows of $\boldsymbol{M}$, $y_1(M_{1,1}, M_{1,2}, ..., M_{1,n}) + y_2(M_{2,1}, M_{2,2}, ..., M_{2,n}) + \cdots + y_m(M_{m,1}, M_{m,2}, ..., M_{m,n}) = 0$, and also $y_1(M_{1,1}, M_{1,2}, ..., M_{1,n}, b_1) + y_2(M_{2,1}, M_{2,2}, ..., M_{2,n}, b_2) + ... + y_m(M_{m,1}, M_{m,2}, ..., M_{m,n}, b_m)$ is nonzero in the last component (that is, $\langle \boldsymbol{y}, \boldsymbol{b} \rangle \neq 0$), then the dimension of the row space of $[\boldsymbol{M} \mid \boldsymbol{b}]$ would exceed the dimension of the row space of $\boldsymbol{M}$, a contradiction. Thus, (ii) entails (iii). Finally, (iii) says that any vector $\boldsymbol{y} \perp \boldsymbol{b}$ must also be orthogonal to every column of $\boldsymbol{M}$. This means that $\boldsymbol{b}$ is in the column space of $\boldsymbol{M}$, $\boldsymbol{Mx} = \boldsymbol{b}$ is solvable, and the proof is complete. ■

The next proposition reveals a differential equation that scale space kernels must satisfy.

Proposition (Necessary Differential Equation). Suppose that $k(t, \sigma)$ satisfies the Scale-Space Kernel Conditions and that the signal $f(t)$ has a representation as a sum of Dirac delta functions (4.121), as in the lemma. Then there are constants, A, B, C, and D, with D/C > 0, such that

$$\frac{Ak(t,\sigma)}{\sigma^2} + \frac{Bk_t(t,\sigma)}{\sigma} + Ck_{tt}(t,\sigma) = \frac{Dk_\sigma(t,\sigma)}{\sigma}. \tag{4.129}$$

Proof: Consider the vector $\boldsymbol{b}$, where $\boldsymbol{b} = (0, 0, P, 1)$ and $P > 0$. Note that it is easy to find a vector $\boldsymbol{y} = (y_1, y_2, y_3, y_4)$ such that $\langle \boldsymbol{y}, \boldsymbol{b} \rangle = 0$. Applying the previous proposition and the Necessary Linear Equations Corollary, it follows that $y_1M_{1,1}(t_0 - t_1) + y_2M_t(t_0 - t_1) + y_3M_{tt}(t_0 - t_1) + y_4M_\sigma(t_0 - t_1) = 0$. Since (4.127) has a solution for any $t_0, t_1, t_2, \ldots, t_n$ we may write this as $y_1M_{1,1}(t) + y_2M_t(t) + y_3M_{tt}(t) + y_4M_\sigma(t) = 0$. Let $A = y_1\sigma^2$, $B = y_2\sigma$, $C = y_3$, and $D = -y_4\sigma$. Then,

$$\frac{AM(t,\sigma)}{\sigma^2} + \frac{BM_t(t,\sigma)}{\sigma} + CM_{tt}(t,\sigma) = \frac{DM_\sigma(t,\sigma)}{\sigma}. \tag{4.130}$$

Observe that $D/C = (-y_4\sigma)/y_3 = P\sigma > 0$. We require, however, that $k(t, \sigma)$, not just its second derivative, $M(t, \sigma)$, satisfy the differential equation. Any two filters with second derivatives satisfying (4.130) must differ by a function with zero second derivative. That is, their difference is a linear term. Since the Scale-Space Kernel Conditions require that as $t \to \infty$, we have $k(t, \sigma) \to 0$, this linear term must be identically zero. Thus, $k(t, \sigma)$ satisfies (4.129). ■

Equation (4.129) is a general form of the heat or diffusion equation. We have come a long way and have taken nearly all the steps toward proving that a filtering kernel which obeys the Scale-Space Kernel Conditions is necessarily Gaussian. The next theorem solves the generalized heat equation. To accomplish this, we must make use of the analog Fourier transform, the formal presentation of which will not be given until the next chapter. We fancy that many readers are already familiar with this technique for solving differential equations. We apologize to the rest for asking them to see into the future and all the more so for suggesting a premonition of the Fourier transform!

Some readers may wish to skip the proofs of the next two theorems, perhaps because the heat equation's solution through Fourier transformation is already familiar, or perhaps to return to them after assimilating Chapter 5's material. The first result solves the generalized heat equation. Because the solution involves an integration, it is less than satisfying, however. The second theorem remedies this. We apply the Scale-Space Kernel Conditions to our general solution and derive a result that clearly shows the Gaussian nature of all structure reducing scale-space filtering kernels.

Theorem (Generalized Heat Equation). If $k(t, \sigma)$ is a solution to the differential equation (4.129), then $k(t, \sigma)$ is the Gaussian

$$k(t,\sigma) = \sigma^{1+\frac{a}{d}} \sqrt{D/2\pi C} \int_{-\infty}^{+\infty} x(t-u) e^{-\frac{D}{2C}\left(\frac{u}{\sigma}+\frac{B}{D}\right)^2} du. \tag{4.131}$$

Proof: Let us first simplify (4.129) with the substitution $k(t, \sigma) = \sigma^{a/d} q(t, \sigma)$. This provides a heat equation in more familiar form,

$$\frac{Bq_t(t,\sigma)}{\sigma} + Cq_{tt}(t,\sigma) = \frac{Dq_\sigma(t,\sigma)}{\sigma}, \tag{4.132}$$

which we must solve for $q(t, \sigma)$. Further simplifications are possible, but we need to reach into the next chapter for the representation of a signal by the analog Fourier transform. The normalized radial Fourier transform of a signal $x(t)$ is given by

$$X(\omega) = \frac{1}{\sqrt{2\pi}} \int_{-\infty}^{+\infty} x(t) e^{-j\omega t}\, dt, \tag{4.133}$$

where $j^2 = -1$. Here we adopt a widely used convention that lowercase letters stand for time-domain signals and that uppercase letters stand for their Fourier transform counterpart. In the near future, we shall verify that if $x(t)$ is absolutely integrable or has finite energy, then its Fourier transform $X(\omega)$ exists (4.133). Likewise, if $X(\omega) \in l^1(\mathbb{R})$ or $X(\omega) \in l^2(\mathbb{R})$, then an inverse normalized radial Fourier transform exists, which is given by

$$x(t) = \frac{1}{\sqrt{2\pi}} \int_{-\infty}^{+\infty} X(\omega) e^{j\omega t}\, d\omega. \tag{4.134}$$

The key idea is to insert the representation of $q(t, \sigma)$ by its transform from $Q(\omega, \sigma)$ into the simplified heat equation (4.132). Then, after removing $(2\pi)^{-1}$ from each term, (4.132) becomes

$$\frac{B}{\sigma}\frac{\partial}{\partial t}\int_{-\infty}^{+\infty} Q(\omega,\sigma)e^{j\omega t}\,d\omega + C\frac{\partial^2}{\partial t^2}\int_{-\infty}^{+\infty} Q(\omega,\sigma)e^{j\omega t}\,d\omega = \frac{D}{\sigma}\frac{\partial}{\partial \sigma}\int_{-\infty}^{+\infty} Q(\omega,\sigma)e^{j\omega t}\,d\omega. \tag{4.135}$$

Interchanging the order of integration and differentiation in (4.135) gives

$$\frac{B}{\sigma}\int_{-\infty}^{+\infty} Q(\omega,\sigma)(j\omega)e^{j\omega t}\,d\omega + C\int_{-\infty}^{+\infty} Q(\omega,\sigma)(j\omega)^2 e^{j\omega t}\,d\omega = \frac{D}{\sigma}\int_{-\infty}^{+\infty} Q_\sigma(\omega,\sigma)e^{j\omega t}\,d\omega. \tag{4.136}$$

By the existence of the inverse Fourier transform, the integrands on either side of (4.136) must be equal. After a bit of algebra, the differential equation simplifies considerably:

$$\frac{B\omega j}{D}Q(\omega,\sigma) - \frac{C\sigma\omega^2}{D}Q(\omega,\sigma) = Q_\sigma(\omega,\sigma). \tag{4.137}$$

Let us now separate the variables in (4.137), to obtain

$$\left(\frac{B\omega j}{D} - \frac{C\sigma\omega^2}{D}\right)\partial\sigma = \frac{\partial Q}{Q}. \tag{4.138}$$

We integrate both sides from 0 to r,

$$\int_0^r \left(\frac{B\omega j}{D} - \frac{C\sigma\omega^2}{D}\right)\partial\sigma = \int_0^r \frac{\partial Q}{Q}. \tag{4.139}$$

where $r > 0$ is an integration limit, and remove the logarithms arising from the integration on the right-hand side of (4.139) by exponentiation. Letting $r = \sigma$ then gives

$$Q(\omega,\sigma) = Q(\omega,0)e^{\frac{jB\omega\sigma}{D}}e^{\frac{-C\omega^2\sigma^2}{2D}}. \tag{4.140}$$

Thus we have found the Fourier transform of $q(t, \sigma) = \sigma^{-a/d}k(t, \sigma)$. We can find $q(t, \sigma)$ by once again applying the inverse Fourier transform operation,

$$q(t,\sigma) = \frac{1}{\sqrt{2\pi}}\int_{-\infty}^{+\infty} Q(\omega,0)e^{\frac{jB\omega\sigma}{D}}e^{\frac{-C\omega^2\sigma^2}{2D}}e^{j\omega t}\,d\omega, \tag{4.141}$$

which is very close to the form we need. To continue simplifying, we utilize some further properties of the Fourier transform. Notice two things about the integrand in (4.141): It is a product of frequency-domain signals (i.e., their independent variable is ω), and one of the frequency-domain terms is a frequency-domain Gaussian, namely $\exp(-C\omega^2\sigma^2/2D)$. Therefore, one of the properties that we can now apply is the Convolution Theorem for Fourier Transforms. It says that the Fourier transform of a convolution, $s = x*y$, is the attenuated product of the Fourier Transforms; specifically, $S(\omega) = (2\pi)^{-1/2}X(\omega)Y(\omega)$. The second property that comes to mind from inspecting the integrand in (4.141) is the formula for the Fourier transform of the Gaussian signal. This states that if $\lambda > 0$, then the Fourier Transform of the Gaussian $g(t) = \exp(-\lambda t^2)$ is $G(\omega) = (2\lambda)^{-1/2}\exp(-\omega^2/4\lambda)$. We let $X(\omega) = Q(\omega, 0)$ and $Y(\omega, \sigma) = \exp(jB\omega\sigma/D)\exp(-C\omega^2\sigma^2/2D)$. Then $q(t, \sigma)$ is the inverse Fourier transform of $X(\omega)Y(\omega, \sigma)$, so we have $q(t, \sigma) = (2\pi)^{-1/2}x*y$. That is,

$$q(t,\sigma) = \frac{1}{\sqrt{2\pi}} \int_{-\infty}^{+\infty} x(t-u)y(u,\sigma)\, du, \tag{4.142}$$

where the Fourier transforms of $x(t)$ and $y(t, \sigma)$ are $X(\omega)$ and $Y(\omega, \sigma)$, respectively. Let us set aside the mysterious signal $x(t)$ for a moment and consider the $y(t, \sigma)$ factor in (4.142). Since the Fourier transform of $s(t, \sigma) = \sigma(D/C)^{1/2}\exp(-Dt^2/(2C\sigma^2))$ is $\exp(-C\sigma^2\omega^2/2D)$, it can easily be shown that the Fourier transform of $y(t) = s(t+B\sigma/D)$ is $Y(\omega, \sigma)$. Thus,

$$q(t,\sigma) = \sigma\sqrt{D/2\pi C} \int_{-\infty}^{+\infty} x(t-u)e^{-\frac{D}{2C}\left(\frac{u}{\sigma}+\frac{B}{D}\right)^2} du, \tag{4.143}$$

and, recalling that $k(t, \sigma) = \sigma^{a/d}q(t, \sigma)$, there follows (4.131), completing the proof of the theorem. ■

Now, the next theorem applies the Scale-Space Kernel Conditions to (4.131).

Theorem (Necessity of the Gaussian). Suppose that $k(t, \sigma)$ satisfies the Scale-Space Kernel Conditions and that the signal $f(t)$ has a representation as a sum of Dirac delta functions (4.121), as in the lemma. Then $k(t, \sigma)$ is a Gaussian of the form

$$k(t,\sigma) = \sigma^{1+\frac{a}{d}}\sqrt{D/2\pi C} \int_{-\infty}^{+\infty} x(t-u)e^{-\frac{D}{2C}\left(\frac{u}{\sigma}+\frac{B}{D}\right)^2} du. \tag{4.144}$$

Proof: Recall the time-delayed Gaussian $y(t) = s(t+B\sigma/D)$ from the previous proof. Since the smoothing filter must not permit zero crossings to shift as the scale of

smoothing varies, this Gaussian must be centered at the origin; in other words, $B\sigma/D = 0$, and hence $B = 0$. Thus,

$$k(t,\sigma) = \sigma^{1+\frac{a}{d}} \sqrt{D/2\pi C} \int_{-\infty}^{+\infty} x(t-u) e^{-\frac{Du^2}{2C\sigma^2}}\, du. \tag{4.145}$$

As the scale of smoothing decreases, the smoothed signal must resemble the original, $f(t)$, and so in the limit, as $\sigma \to 0$, the Scale-Space Kernel Conditions demand that $k(t, \sigma) \to \delta(t)$, the Dirac delta. The consequence of this condition is

$$\begin{aligned} \lim_{\sigma\to 0} k(t,\sigma) &= \lim_{\sigma\to 0} \sigma^{1+\frac{a}{d}} \sqrt{\frac{D}{2\pi C}} \int_{-\infty}^{+\infty} e^{-\frac{D(t-u)^2}{2C\sigma^2}} x(u)\, du \\ &= \lim_{\sigma\to 0} \sigma^{\frac{a}{d}} \sqrt{\frac{D}{2\pi C}} \int_{-\infty}^{+\infty} \sigma e^{-\frac{D(t-u)^2}{2C\sigma^2}} x(u)\, du = \delta(t). \end{aligned} \tag{4.146}$$

This completes the proof. ■

This proof contains a valuable lesson: A judicious application of the Fourier integral representation removes the differential equation's partial time derivatives. Higher powers of the frequency variable, ω, replace the derivatives, but this is tolerable because it leads to a simpler differential equation overall. This is a powerful—and quite typical—application of the Fourier transform. Applied mathematicians usually resort to the Fourier transformation for precisely this purpose and no others. For our own purposes, however, the Fourier transform does much more than expedite computations; it is the principal tool for studying the frequency content of analog signals. The next three chapters, no less, explore Fourier theory in detail: analog signal frequency in Chapter 5, discrete signal frequency in Chapter 7, and frequency-domain signal analysis in Chapter 9.

The efforts of many researchers have helped to elucidate the theory of scale-space decompositions. Our treatment here follows most closely the presentation of one-dimensional scale-space decomposition by Yuille and Poggio [110]. Other theoretical studies of scale-space decomposition include Ref. 111. Applications of scale space filtering include the recognition of two-dimensional shapes by extracting object boundaries, formulating the boundary as a curvature signal, and deriving the scale-space representation of the boundary curvature [112]. There results a graph structure, which can be matched against model graphs using artificial intelligence techniques, or matched level-by-level using the structural pattern detection techniques of Section 4.6.2.

Now, when an image is represented in its scale-space decomposition, no arbitrary preferred scale for the objects represented in the decomposed is used. Instead,

the set of scales at which distinct regions of different curvature sign arise and disappear is found. Then the changes in the curvature are related to one another in a structure called an interval tree by Witkin. This further abstracts the structural description of the signal from its actual value, $f(x)$, by defining an interval of scales, and an interval of space, x, over which the salient curvature features of the signal are to be found. The signal is segmented in both scale and spatial coordinates.

4.8 SUMMARY

In the introduction to this chapter, we reflected on the distinction, sometimes subtle and sometimes profound, between signal processing and signal analysis. This chapter's methods work primarily with operations on the signal values in the time domain. In some cases, such as the problem of extracting periodicities from the signal values, statistics on signal levels proved to be inadequate. We resorted to comparisons, in the form of inner products, of the given signal to sinusoidal or exponential models. This makes the break with time-domain methods into the realm of frequency-domain methods. Now, we need to look deeper into the theory of analog signal frequency, discrete signal frequency, and the applications that arise from these studies. This task will occupy us for the next five chapters. Then we will consider the combination of the methods of both domains: Time-frequency transforms are the subject of Chapter 10, and time-scale transforms are covered in Chapter 11. This chapter is preparation, with a time-domain perspective, for Chapter 9 on frequency-domain signal analysis and for Chapter 12 on mixed-domain analysis.

REFERENCES

1. F. Jelinek, Continuous speech recognition by statistical methods, *Proceedings of the IEEE*, vol. 64, no. 4, pp. 532–556, April 1976.
2. S. Young, A review of large-vocabulary continuous-speech recognition, *IEEE Signal Processing Magazine*, pp. 45–57, September 1996.
3. K. Lee and R. Reddy, *Automatic Speech Recognition*, Boston: Kluwer Academic Publishers, 1989.
4. L. Rabiner and B.-H. Juang, *Fundamentals of Speech Recognition*, Englewood Cliffs, NJ: Prentice-Hall, 1993.
5. R. L. Wesson and R. E. Wallace, Predicting the next great earthquake in California, *Scientific American*, pp. 35–43, February 1985.
6. Ö. Yilmaz, *Seismic Data Processing*, Tulsa, OK: Society for Exploratory Geophysics, 1987.
7. M. Akay, *Biomedical Signal Processing*, San Diego, CA: Academic Press, 1994.
8. R. Isermann, Process fault detection based on modeling and estimation methods—a survey, *Automatica*, vol. 20, no. 4, pp. 387–404, 1984.
9. C. C. Tappert, C. Y. Suen, and T. Wakahara, The state of the art in on-line handwriting recognition, *IEEE Transactions on Pattern Analysis and Machine Intelligence,* vol. 12, no. 8, pp. 787–808, 1990.

10. A. Marcus and A. Van Dam, User interface developments in the nineties, *IEEE Computer,* pp. 49–57, September 1991.
11. J. Preece, *Human-Computer Interaction*, Reading, MA: Addison-Wesley, 1994.
12. S. L. Horowitz and T. Pavlidis, Picture segmentation in a directed split-and-merge procedure, *Proceedings of the Second International Joint Conference on Pattern Recognition,* Copenhagen, pp. 424–433, August 1974.
13. P. D. van der Puije, *Telecommunication Circuit Design*, New York: Wiley, 1992.
14. P. Mock, Add DTMF generation and decoding to DSP-µP designs, *Electronic Design News*, March 21, 1985; also in K.-S. Lin, ed., *Digital Signal Processing Applications with the TMS320 Family*, vol. 1, Dallas: Texas Instruments, 1989.
15. A. Mar, ed., *Digital Signal Processing Applications Using the ADSP-2100 Family*, Englewood Cliffs, NJ: Prentice-Hall, 1990.
16. J. L. Flanagan, *Speech Analysis, Synthesis, and Perception*, 2nd ed., New York: Springer-Verlag, 1972.
17. C. K. Chow and T. Kaneko, Automatic boundary detection of the left ventricle from cineangiograms, *Computers and Biomedical Research*, vol. 5, pp. 388–410, 1972.
18. N. Otsu, A threshold selection method from gray-level histograms, *IEEE Transactions on Systems, Man, and Cybernetics,* vol. SMC-9, no. 1, pp. 62–66, January 1979.
19. J. Kittler and J. Illingworth, On threshold selection using clustering criteria, *IEEE Transactions on Systems, Man, and Cybernetics,* vol. SMC-15, pp. 652–655, 1985.
20. S. Kullback and R. A. Leibler, On information and sufficiency, *Annals of Mathematical Statistics,* vol. 22, pp. 79–86, 1951.
21. S. Kullback, *Information Theory and Statistics*, Mineola, NY: Dover, 1997.
22. J. S. Weszka, A survey of threshold selection techniques, *Computer Graphics and Image Processing,* vol. 7, pp. 259–265, 1978.
23. P. K. Sahoo, S. Soltani, and A. K. C. Wong, A survey of thresholding techniques, *Computer Vision, Graphics, and Image Processing*, vol. 41, pp. 233–260, 1988.
24. P. W. Palumbo, P. Swaminathan, and S. N. Srihari, Document image binarization: evaluation of algorithms, *Applications of Digital Image Processing IX*, SPIE, vol. 697, pp. 278–285, 1986.
25. M. Kamel and A. Zhao, Extraction of binary character/graphics images from grayscale document images, *CVGIP: Graphical Models and Image Processing*, vol. 55, no. 3, pp. 203–217, 1993.
26. O. D. Trier and T. Taxt, Evaluation of binarization methods for document images, *IEEE Transactions on Pattern Analysis and Machine Intelligence,* vol. 17, no. 3, pp. 312–315, March 1995.
27. J. M. White and G. D. Rohrer, Image thresholding for character image extraction and other applications requiring character image extraction, *IBM Journal of Research and Development*, vol. 27, no. 4, pp. 400–411, July 1983.
28. D. L. Duttweiler, A twelve-channel digital voice echo canceller, *IEEE Transactions on Communications*, vol. COM-26, no. 5, pp. 647–653, May 1978.
29. P. Brodatz, *Textures: A Photographic Album for Artists and Designers,* New York: Dover, 1966.
30. B. Julesz, Experiments in the visual perception of texture, *Scientific American*, vol. 232, pp. 34–43, 1975.

31. J. Beck, Similarity grouping and peripheral discrimination under uncertainty, *American Journal of Psychology*, vol. 85, pp. 1–19, 1972.
32. M. Wertheimer, Principles of perceptual organization, in *Readings in Perception*, D. C. Beardslee and M. Wertheimer, eds., Princeton, NJ: Van Nostrand-Reinhold, 1958.
33. D. J. Whitehouse, *Handbook of Surface Metrology*, Bristol, UK: Institute of Physics, 1994.
34. J. Beck, A. Sutter, and R. Ivry, Spatial frequency channels and perceptual grouping in texture segmentation, *Computer Vision, Graphics, and Image Processing*, vol. 37, pp. 299–325, 1987.
35. F. Tomita, Y. Shirai, and S Tsuji, Description of texture by a structural analysis, *IEEE Transactions on Pattern Analysis and Machine Intelligence*, vol. PAMI-4, no. 2, pp. 183–191, 1982.
36. *Surface Texture: Surface Roughness, Waviness and Lay*, ANSI B46.1, American National Standards Institute, 1978.
37. *Surface Roughness—Terminology—Part 1: Surface and its Parameters*, ISO 4287/1, International Standards Organization, 1984.
38. *Surface Roughness—Terminology—Part 2: Measurement of Surface Roughness Parameters, ISO 4287/2*, International Standards Organization, 1984.
39. R. W. Conners and C. A. Harlow, A theoretical comparison of texture algorithms, *IEEE Transactions on Pattern Analysis and Machine Intelligence*, vol. PAMI-2, no. 3, pp. 204–222, May 1980.
40. A. Rosenfeld and A. C. Kak, *Digital Picture Processing*, vol. 2, Orlando, FL: Academic Press, 1982.
41. B. Julesz, Visual pattern discrimination, *IRE Transactions on Information Theory*, vol. IT-8, no. 2, pp. 84–92, February 1961.
42. B. Julesz, E. N. Gilbert, and J. D. Victor, Visual discrimination of textures with identical third-order statistics, *Biological Cybernetics*, vol. 31, no. 3, pp. 137–140, 1978.
43. A. Gagalowicz, A new method for texture field synthesis: Some applications to the study of human vision, *IEEE Transactions on Pattern Analysis and Machine Intelligence*, vol. PAMI-3, no. 5, pp. 520–533, September 1981.
44. R. M. Haralick, K. S. Shanmugam, and I. Dinstein, Textural features for image classification, *IEEE Transactions on Systems, Man, and Cybernetics*, vol. SMC-3, no. 6, pp. 610–621, November 1973.
45. S. W. Zucker and D. Terzopoulos, Finding structure in co-occurrence matrices for texture analysis, *Computer Graphics and Image Processing*, vol. 12, no. 3, pp. 286–308, March 1980.
46. D. Chetverikov, Measuring the degree of texture regularity, *Proceedings of the International Conference on Pattern Recognition*, Montreal, pp. 80–82, 1984.
47. J. S. Weszka, C. R. Dyer, and A. Rosenfeld, A comparative study of texture measures for terrain classification, *IEEE Transactions on Systems, Man, and Cybernetics*, vol. SMC-6, pp. 269–285, 1976.
48. G. Strang, *Introduction to Applied Mathematics*, Wellesley, MA: Wellesley-Cambridge, 1986.
49. A. Savitsky and M. J. E. Golay, Smoothing and differentiation of data by simplified least squares procedures, *Analytical Chemistry*, vol. 36, pp. 1627–1639, 1964.

50. C. L. Lawson and R. J. Hanson, *Solving Least Squares Problems*, Englewood Cliffs, NJ: Prentice-Hall, 1974.
51. R. M. Haralick and L. G. Shapiro, *Computer and Robot Vision*, vol. 1, New York: Addison-Wesley, 1992.
52. A. Jennings and J. J. McKeown, *Matrix Computation*, 2nd ed., Chichester, West Sussex, England: Wiley, 1992.
53. E. R. Dougherty and P. A. Laplante, *Introduction to Real-Time Imaging*, Bellingham, WA: SPIE, 1995.
54. N. C. Gallagher, Jr. and G. L. Wise, A theoretical analysis of the properties of median filters, *IEEE Transactions on Acoustics, Speech, and Signal Processing*, vol. ASSP-29, pp. 1136–1141, 1981.
55. R. M. Haralick, S. R. Sternberg, and X. Zhuang, Image analysis using mathematical morphology, *IEEE Transactions on Pattern Analysis and Machine Intelligence*, vol. PAMI-9, no. 4, pp. 532–550, July 1987.
56. M.-H. Chen and P.-F. Yan, A multiscaling approach based on morphological filtering, *IEEE Transactions on Pattern Analysis and Machine Intelligence*, vol. 11, no. 7, pp. 694–700, July 1989.
57. P. Maragos, Pattern spectrum and multiscale shape representation, *IEEE Transactions on Pattern Analysis and Machine Intelligence*, vol. 11, no. 7, pp. 701–716, July 1989.
58. L. S. Kovasznay and H. M. Joseph, Processing of two-dimensional patterns by scanning techniques, *Science,* vol. 118, no. 3069, pp. 475–477, 25 October 1953.
59. L. G. Roberts, Machine perception of three-dimensional solids, in *Optical and Electro-optical Information Processing*, J. T. Tippet, ed., Cambridge, MA: MIT Press, 1965.
60. A. Rosenfeld and M. Thurston, Edge and curve detection for visual scene analysis, *IEEE Transactions on Computers,* vol. 20, no. 5, pp. 562–569, May 1971.
61. J. M. S. Prewitt, Object enhancement and extraction, in *Picture Processing and Psychopictorics*, B. S. Lipkin and A. Rosenfeld, eds., New York: Academic Press, 1970.
62. D. Marr and E. Hildreth, Theory of Edge Detection, *Proceedings of the Royal Society of London B.* vol. 207, pp. 187–217, 1979.
63. M. F. Heukel, An operator which locates edges in digitized pictures, *Journal of the Association for Computing Machinery*, vol. 18, pp. 113–125, 1971.
64. F. O'Gorman, Edge detection using Walsh functions, *Artificial Intelligence*, vol. 10, pp. 215–223, 1978.
65. R. A. Hummel, Feature detection using basis functions, *Computer Graphics and Image Processing*, vol. 9, pp. 40–55, 1979.
66. H. D. Tagare and R. J. P. deFigueiredo, On the localization performance measure and optimal edge detection, *IEEE Transactions on Pattern Analysis and Machine Intelligence,* vol. 12, no. 12, pp. 1186–1190, 1990.
67. K. L. Boyer and S. Sarkar, Comments on "On the localization performance measure and optimal edge detection," *IEEE Transactions on Pattern Analysis and Machine Intelligence,* vol. 16, no. 1, pp. 106–108, January 1994.
68. R. J. Qian and T. S. Huang, Optimal edge detection in two-dimensional images, *IEEE Transactions on Image Processing,* vol. 5, no. 7, pp. 1215–1220, 1996.
69. M. Gökmen and A. K. Jain, $\lambda\tau$-space representation of images and generalized edge detector, *IEEE Transactions on Pattern Analysis and Machine Intelligence,* vol. 19, no. 6, pp. 545–563, June 1997.

70. D. M. Manos and D. L. Flamm, *Plasma Etching: An Introduction*, Boston: Academic Press, 1989.

71. R. L. Allen, R. Moore, and M. Whelan, Multiresolution pattern detector networks for controlling plasma etch reactors, in *Process, Equipment, and Materials Control in Integrated Circuit Manufacturing*, Proceedings SPIE 2637, pp. 19–30, 1995.

72. C. K. Hanish, J. W. Grizzle, H.-H. Chen, L. I. Kamlet, S. Thomas III, F. L. Terry, and S. W. Pang, Modeling and algorithm development for automated optical endpointing of an HBT emitter etch, *Journal of Electronic Materials*, vol. 26, no. 12, pp. 1401–1408, 1997.

73. V. Torre and T. A. Poggio, On edge detection, *IEEE Transactions on Pattern Analysis and Machine Intelligence,* vol. PAMI-8, no. 2, pp. 147–163, March 1986.

74. C. F. Gerald and P. O. Wheatley, *Applied Numerical Analysis*, 4th ed., Reading, MA: Addison-Wesley, 1990.

75. J. Canny, A computational approach to edge detection, *IEEE Transactions on Pattern Analysis and Machine Intelligence,* vol. PAMI-8, no. 6, pp. 679–698, November 1986.

76. A. Papoulis, *Probability, Random Variables, and Stochastic Processes*, New York: McGraw-Hill, 1965.

77. D. Marr, *Vision*, New York: W. H. Freeman, 1982.

78. J. F. Canny, *Finding Edges and Lines in Images*, Technical Report No. 720, MIT Artificial Intelligence Laboratory, June 1983.

79. H. D. Tagare and R. J. P. deFigueiredo, Reply to "On the localization performance measure and optimal edge detection," *IEEE Transactions on Pattern Analysis and Machine Intelligence,* vol. 16, no. 1, pp. 108–110, January 1994.

80. J. Koplowitz and V. Greco, On the edge location error for local maximum and zero-crossing edge detectors, *IEEE Transactions on Pattern Analysis and Machine Intelligence,* vol. 16, no. 12, pp. 1207–1212, December 1994.

81. L. W. Couch II, *Digital and Analog Communication Systems*, 4th ed., Upper Saddle River, NJ: Prentice-Hall, 1993.

82. S. Haykin, *Communication Systems,* 3rd ed., New York: Wiley, 1994.

83. G. L. Turin, An introduction to digital matched filters, *Proceedings of the IEEE*, vol. 64, pp. 1092–1112, 1976.

84. A. Rosenfeld and A. C. Kak, *Digital Picture Processing,* vol. 1, 2nd ed., New York: Academic, 1982.

85. J. R. Tou and R. C. Gonzalez, *Pattern Recognition Principles,* Reading, MA: Addison-Wesley, 1974.

86. F. Molinaro and F. Castanié, Signal processing pattern classification techniques to improve knock detection in spark ignition engines, *Mechanical Systems and Signal Processing*, vol. 9, no. 1, pp. 51–62, January 1995.

87. J. G. Proakis and D. G. Manolakis, *Digital Signal Processing: Principles, Algorithms, and Applications,* 2nd ed., New York: Macmillan, 1992.

88. A. V. Oppenheim and R. W. Schafer, *Discrete-Timel Signal Processing,* Englewood Cliffs, NJ: Prentice-Hall, 1989.

89. S. S. Yau and J. M. Garnett, least-mean-square approach to pattern classification, in *Frontiers of Pattern Recognition,* S. Wantanabe, ed., New York: Academic Press, pp. 575–588, 1972.

90. N. J. Nilsson, *Learning Machines*, New York: McGraw-Hill, 1965.

91. K. Fukunaga, *Introduction to Statistical Pattern Recognition*, 2nd ed., Boston: Academic Press, 1990.
92. P. R. Devijver and J. Kittler, *Pattern Recognition: A Statistical Approach*, Englewood Cliffs, NJ: Prentice-Hall, 1982.
93. R. O. Duda and P. E. Hart, *Pattern Classification and Scene Analysis*, New York: Wiley, 1973.
94. C. K. Chow, An optimum character recognition system using decision functions, *Transactions of the IRE on Electronic Computers,* vol. EC-6, pp. 247–254, 1957.
95. J. Schürmann, Multifont word recognition system with application to postal address reading, *Proceedings of the Third International Joint Conference on Pattern Recognition*, pp. 658–662, 1976.
96. W. Doster, Contextual postprocessing system for cooperation with a multiple-choice character-recognition system, *IEEE Transactions on Computers*, vol. C-26, no. 11, pp. 1090–1101, November 1977.
97. R. Ott, Construction of quadratic polynomial classifiers, *Proceedings of the Third International Joint Conference on Pattern Recognition*, 1976.
98. Y.-H. Pao, *Adaptive Pattern Recognition and Neural Networks*, Reading, MA: Addison-Wesley, 1989.
99. F. Attneave, Some informational aspects of visual perception, *Psychological Review*, vol. 61, no. 3, pp. 183–193, 1954.
100. S. Tanimoto and T. Pavlidis, A hierarchical data structure for picture processing, *Computer Graphics and Image Processing,* vol. 4, No. 2, pp. 104–119, June 1975.
101. .R. Y. Wong and E. L. Hall, Sequential hierarchical scene matching, *IEEE Transactions on Computers,* vol. C-27, No. 4, pp. 359–366, April 1978.
102. D. Marr, T. Poggio, and S. Ullman, Bandpass channels, zero-crossings, and early visual information processing, *Journal of the Optical Society of America,* vol. 69, pp. 914–916, 1979.
103. D. H. Hubel and T. N. Wiesel, Receptive fields, binocular interaction and functional architecture in the cat's visual cortex, *Journal of Physiology,* vol. 160, pp. 106–154, 1962.
104. F. W. C. Campbell and J. Robson, Application of Fourier analysis to the visibility of gratings, *Journal of Physiology*, vol. 197, pp. 551–566, 1968.
105. D. H. Hubel, *Eye, Brain, and Vision*, New York: W. H. Freeman, 1988.
106. A. P. Pentland, Models of image formation, in *From Pixels to Predicates*, A. P. Pentland, ed. Norwood, NJ: Ablex, 1986.
107. A. P. Witkin, Scale-space filtering, *Proceedings of the 8th International Joint Conference on Artificial Intelligence,* Karlsruhe, West Germany, 1983. See also A. P. Witkin, Scale-space filtering, in *From Pixels to Predicates*, A. P. Pentland, ed., Norwood, NJ: Ablex, 1986.
108. J. Koenderink, The structure of images, *Biological Cybernetics,* vol. 50, pp. 363–370, 1984.
109. M. P. do Carmo, *Differential Geometry of Curves and Surfaces*, Englewood Cliffs, NJ: Prentice-Hall, 1976.
110. A. L. Yuille and T. A. Poggio, Scaling theorems for zero crossings, *IEEE Transactions on Pattern Analysis and Machine Intelligence,* vol. PAMI-8, no. 1, pp. 15–25, January 1986.

111. Babaud, A. P. Witkin, M. Baudin, and R. O. Duda, Uniqueness of the Gaussian kernel for scale-space filtering, *IEEE Transactions on Pattern Analysis and Machine Intelligence,* vol. PAMI-8, no. 1, pp. 26–33, January 1986.

112. F. Mokhtarian and A. Mackworth, Scale-based description and recognition of planar curves and two-dimensional shapes, *IEEE Transactions on Pattern Analysis and Machine Intelligence,* vol. PAMI-8, no. 1, pp. 34-43, January 1986.

PROBLEMS

1. Consider the analog Gaussian kernel $h(t) = \exp(-t^2)$.

(a) Show that $h(t)$ contains a concave up portion for $t < 0$, a concave-down section symmetric about $t = 0$, a concave up portion for $t > 0$, and exactly two points of inflection where the second derivative of $h(t)$ is zero.

(b) Find a logical predicate, applied to subsets of Dom(h), that segments $h(t)$ into the regions described in (a).

(c) Suppose that a system designer elects to prefilter discrete signals by an approximate, discrete version of $h(t)$ and wishes to maintain the aspects of concavity of $h(t)$ in the filter $h(n)$. What is the minimal support of the filter $h(n)$?

(d) Show that if the analog signal $f(t)$ is segmented according to whether d^2f/dt^2 is negative, zero, or positive and d^3f/dt^3 exists, then segments with $d^2f/dt^2 < 0$ cannot be adjacent to segments with $d^2f/dt^2 > 0$.

2. Consider a system $y = Hx$ that should remove impulse noise from $x(n)$ to produce $y(n)$.

(a) If H is LTI, show that the moving average, or box filter $h(n) = [1/3, \underline{1/3}, 1/3]$ can fail to do an adequate job as the impulse response of H.

(b) Show that any LTI filter can fail to do an adequate job as $h = H\delta$.

3. Suppose we filter out impulse noise by a median filter, $y = Hx$.

(a) Show that H is translation invariant.

(b) Show that H is nonlinear.

(c) Show that the median filter $(Hx)(n) = \text{median}\{x(n-1), x(n), x(n+1)\}$ can remove impulse noise.

(d) Show that when performing preliminary smoothing of a signal before thresholding, a median filter $y(n) = \text{median}\{x(n-1), x(n), x(n+1)\}$ preserves signal edges better than box filters.

4. Consider a morphological filter, $y = Hx$.

(a) Show that if H is a dilation, then H is translation invariant but not linear.

(b) Show that if H is an erosion, then H is translation invariant but not linear.

5. Suppose f(n) is a discrete signal and $T > 0$. Let $M = \{n: |f(n)| > T\}$, $N = \{n: |f(n)| \le T\}$, $\Pi = \{M, N\}$, and L be the logical predicate "(1) For all n, $|f(n)| > T$;

or (2) for all n, $|f(n)| < T$; or for all n, $|f(n)| = T$." Prove that $\Sigma = (\Pi, L)$ is a segmentation of $f(n)$.

6. Let $f(t)$ be an analog signal which is twice differentiable. Show that the sign of the second derivative is the basis for a segmentation of $f(t)$ into concave-down regions, concave-up regions, and zeros of the second derivative.

7. Consider the discrete signal $x(n)$ = [..., 0, 2, −1, 3, 1, 8, 10, 9, 11, 5, 2, −1, 1, 0, . . .].

(a) Suppose values $|x(n)| \geq T$ are labeled Object and values $|x(n)| < T$ are labeled Background. Consider the effect of thresholding this signal for T = 5 with and without preliminary filtering by the moving average filter of width $N = 3$:

$$y(n) = \frac{1}{2N+1} \sum_{k=-N}^{N} x(k).$$

(b) What happens to the segmentation as the filter width increases? Does changing the threshold help?

(c) What happens to the segmentation if a causal box filter performs the preliminary filtering operation? Does this affect the registration of the blob?

(d) Examine the effect of a high-magnitude noise impulse several time samples apart from the blob; suppose, therefore, that $x(-10) = 12$. Consider the effect of preliminary box filtering and threshold changes on segmentation and blob registration.

(e) Can a top-down rule be applied to correct the labeling of impulse noise? Does the width of the smoothing filter affect the success of the rule?

8. Prove that a discrete signal edge detector which locates edges from the maximal responses of a convolutional operator, H, satisfies the following:

(i) The impulse response of H, $h(n)$, must be odd.

(ii) $h(n)$ can only have one zero, at $n = 0$.

9. Consider the estimator $\hat{\mu}$ found in the Unbiased Minimal Variance Estimator Theorem (Section 4.3.2). Suppose that $\boldsymbol{x}$ is a random vector, representing a window $[m - p, m + p]$ of the noisy source signal $x(n)$, and that $\boldsymbol{b}$ is the unit vector of all ones of length $2p + 1$. If the estimator $\hat{\mu}$ is unbiased and has minimal variance, show that

$$\mathrm{Var}[\hat{\mu}] = \left(\frac{1}{\boldsymbol{b} \Sigma^{-1} \boldsymbol{b}^T} \right),$$

where $\Sigma = E[(\boldsymbol{x} - \mu 1), (\boldsymbol{x} - \mu 1)]$ is the covariance matrix of the random vector $\boldsymbol{x}$.

10. Develop the analog version of normalized cross-correlation. Consider an analog signal $x(t)$ input in which a pattern $p(t)$ must be found at an unknown offset s. Suppose that $p(t)$ has finite support contained in the real interval I. Show the following:

(a) The normalized cross-correlation,

$$C_{p(t-s),x(t)} = \frac{y(s)}{\left(\int_I x^2(t)\,dt\right)^{\frac{1}{2}}} = \frac{\left(\int_I p(t-s)x(t)\,dt\right)^{\frac{1}{2}}}{\left(\int_I x^2(t)\,dt\right)^{\frac{1}{2}}},$$

where s is the offset of prototype signal $p(t)$ into input signal $x(t)$ and where I is the interval that contains the support of $p(t)$, is a measure of match.

(b) The cross-correlation, $C_{p(t-s),x(t)}$, assumes a unity maximum when $x(t) = cp(t-s)$ on the interval I for some constant c.

11. Check that all signals in the family of exponentials $B = \{(2\pi)^{-1}\exp(2\pi jnt/T): n \in \mathbb{Z}\}$ have $\|(2\pi)^{-1}\exp(2\pi jnt/T)\|_1 = 1$ in the Hilbert space $L^1[0, T]$.

12. Let $g(t, \sigma, \mu) = \sigma^{-1}(2\pi)^{-1/2}\exp(-(x-\mu)^2/(2\sigma^2))$ be the Gaussian with standard deviation σ and mean μ. Show that $g(t, \sigma, \mu)$ is symmetric and strictly decreasing about its mean, μ.

13. Let $F(t, \sigma)$ be defined as in Equation (4–5c) for analog signal $f(t)$. Show that for small scales σ, the smoothed signal $F(t, \sigma)$ resembles the original as $\sigma \to 0$; that is, we have $F(t, \sigma) \to f(t)$.

14. Show that as $\sigma \to \infty$, $F(t, s) \to E(f(t))$; that is, for large scales σ, the smoothed signal approaches the mean of $f(t)$.

15. Show that the Gaussian is an $L^1(\mathbb{R})$ signal (absolutely integrable), and it is C^∞ (infinitely differentiable).

16. Show that if $f(t)$ is an analog signal and $g(t, \sigma)$ is Gaussian with zero mean and variance σ^2, then

$$\frac{\partial^n}{\partial t^n} F(t,\sigma) = f * \frac{\partial^n}{\partial t^n} g(t,\sigma).$$

17. Consider the following region merging approach to real-time signal segmentation. The application receives a digitized signal, $f(n)$, and segments it into Noise and Signal regions, with labels Λ_N and Λ_S, respectively. Three thresholds are provided: T_N, T_S, and ε. If $x(n) < T_N$, then $x(n)$ is marked as a Λ_N value. If $x(n) > T_S$, then $x(n)$ is labeled Λ_S. If $T_N \le x(n) \le T_S$, then $x(n)$ is labeled the same as $x(n-1)$ if $|x(n) - x(n-1)| < \varepsilon$, and $x(n)$ is deemed the opposite of $x(n-1)$ otherwise.

(a) Show how this real-time segmentation works for $f(n)$ = [..., 0, 2, 4, 3, 1, 8, 6, 9, 11, 7, 3, 5, 1, 0, ...], with $T_N = 4$, $T_S = 7$, and $\varepsilon = 3$.

(b) What constraints should exist on T_N, T_S, and ε for a useful algorithm?

(c) What is the effect of impulse noise on the algorithm?

(d) Let N_n and S_n be the average of the Λ_N and the Λ_S values, respectively, prior to time instant n. Suppose that the algorithm is changed so that when $T_N \leq x(n) \leq T_S$, then $x(n)$ is labeled Λ_N when $|x(n) - N_n| < \varepsilon$, and then $x(n)$ is labeled Λ_S when $|x(n) - S_n| < \varepsilon$. How does this twist affect the operation of the algorithm?

(e) Critique this algorithm for real-time speech segmentation. Consider the presence of velar fricatives, noise, and voiced and unvoiced consonants in the digitized speech signal.

(f) Explain how a delay in making the labeling decision for a new signal value $x(n)$ might help improve the segmentation for the front-end of a speech recognition application.

(g) What characteristics of digitized speech signals should be taken into account in order to size the labeling decision delay in (*f*)? Explain.

18. Critique the following region splitting algorithm. We begin with a region of interest for a discrete signal $f(n)$, $S = [a, b]$, and a partition of S into (as closely as possible) equal-length subintervals, $S = S_1 \cup S_2 \cup ... \cup S_N$. We first compute the mean over the entire region S, μ. Then we begin with the region whose mean is closest to μ; by renumbering the regions, if necessary, we may suppose that it is S_1. Then we compute all of the differences, $d(1, i) = |\mu_1 - \mu_i|$, for $i > 1$, and put $R_1 = S_1 \cup \{S_i \mid i > 1 \text{ and } d(1, i) < \varepsilon\}$. We then perform this same operation with the remaining S_i, which are disjoint from R_1, to form R_2, and so on. The process eventually halts after M iterations, and S is split into M regions: $S = R_1 \cup R_2 \cup \cdots \cup R_M$.

19. Show that if $x(n)$ is a digital signal, x: $\mathbb{Z} \rightarrow [0, N]$, for some natural number $N \geq 0$, then $x = T[\text{Umbra}(x)] = T[\text{Graph}(x)]$.

20. Consider Chow and Kaneko's optimal threshold finding method, where the quadratic equation below must be solved for T:

$$(\sigma_L^2 - \sigma_H^2)T^2 + 2(\sigma_H^2\mu_L - \sigma_L^2\mu_H)T + (\sigma_L^2\mu_H^2 - \sigma_H^2\mu_L^2) - 2\ln\left(\frac{P_H\sigma_L}{P_L\sigma_H}\right) = 0.$$

(a) Suppose that the variances of the meaningful signal and the background noise are the same. Show that there can be at most one threshold, T.

(b) Show that if the variances of the meaningful signal and the background noise are the same and the *a priori* probabilities of signal and noise are the same, then $T = (mL + mH)/2$.

(c) Can there be two solutions to the quadratic equation? Explain.

(d) If there is only one solution to the quadratic equation, is it necessarily a valid threshold? Explain.

(e) Can there be no solution to the equation? Explain.

21. Suppose a signal $f(n)$ has regions of interest with high values above a relatively low background noise level. Suppose also that a threshold T on the signal histogram produces errors with probability $E(T) = P_H E_L(T) + P_L E_H(T)$, where $E_L(T)$ and $E_H(T)$ are the likelihoods of incorrectly labeling f(n) as noise and as meaningful, respectively.

(a) Assume that the histogram modes obey a log-normal distribution, and, following the Chow–Kaneko method of the text in Section 4.2, use

$$\frac{dE}{dT} = P_H \frac{dE_L}{dT} + P_L \frac{dE_H}{dT} = 0$$

to find T for a minimal labeling error.

(b) As in (a), find a T that minimizes labeling error if the histogram modes obey a Rayleigh distribution.

22. Consider the valley-finding algorithm for finding a threshold using signal histograms.

(a) Show that the search stops when the current threshold T is a local minimum.

(b) Show by example that the algorithm has a direction preference; that is, it tends to select a threshold toward the noise mode or toward the meaningful signal mode.

(c) Find and explicate a technique for resolving the direction preference of the algorithm.

(d) Show by example that the algorithm may halt its search well within the mode of the histogram's noise mode or the true signal mode.

(e) Show that a gradient calculation based on a wider interval may alleviate somewhat the problem exposed in part (d).

(f) For what types of signals does the algorithm find a threshold that is at the limit of the domain of the histogram? Explain.

23. Let f be a discrete signal with a finite domain with $\mathrm{Ran}(f) \subseteq [0, N-1]$. For $0 \leq k < N$, define

$$p_k = \frac{\#(f^{-1}(\{k\}))}{\#\mathrm{Dom}(f)}.$$

Show that p_k is a discrete probability density function for f.

24. Let f and p_k be as in the previous problem. Let μ_L, μ_H, and μ be the low-level, high-level, and total mean of $h(k)$, the histogram for f. Let σ_L, σ_H, and σ be the low-level, high-level, and total standard deviations of $h(k)$.

(a) Show

$$\sum_{k=0}^{t-1} p_k(k-\mu_L(t))(\mu_L(t)-\mu) + \sum_{k=t}^{N-1} p_k(k-\mu_H(t))(\mu_H(t)-\mu) = 0.$$

(b) Following Otsu [18] define the between-group variance to be

$$\sigma_b^2(t) = P_L(t)(\mu_L(t) - \mu)^2 + P_H(t)(\mu_H(t) - \mu)^2 mp$$

and prove that

$$\sigma^2(t) = \sigma_w^2(t) + \sigma_b^2(t).$$

(Thus, minimizing within-group variance is equivalent to maximizing between-group variance.)

(c) Show the following for $0 \le t < N-1$:

$$p_k = \frac{\#(f^{-1}(\{k\}))}{\#\mathrm{Dom}(f)},$$

(d) Explain how the relationships in (c) reduce the computational burden of finding an optimal threshold (R. M. Haralick and L. G. Shapiro, *Computer and Robot Vision*, vol. 1, New York: Addison-Wesley, 1992).

25. Consider the likelihood ratio of the distribution q_k with respect to p_k,

$$L(p,q) = \sum_{k=0}^{N-1} p_k \log_2 \frac{p_k}{q_k} = \sum_{k=0}^{N-1} p_k \log_2 p_k - \sum_{k=0}^{N-1} p_k \log_2 q_k.$$

(a) Show that $L(p, q) \ge 0$ for all discrete probability distributions p and q. (*Hint*: Note that $\ln(t) < t - 1$ for all $t > 0$, where $\ln(t)$ is the natural logarithm; $\ln(2)\log_2(t) = \ln(t)$; and $p_0 + p_1 + \cdots + p_{N-1} = 1$.)

(b) Show that $L(p, q) = 0$ if and only if $p = q$.

(c) Show that L is not symmetric; that is, find examples for p_k and q_k such that p_k and p_k are discrete probability density functions, but $L(p, q) \ne L(q, p)$.

(d) Does the triangle inequality hold for the likelihood ratio?

26. Prove the following properties of dilation. Let $A, B, C \subseteq \mathbb{Z}^2$ and $k \in \mathbb{Z}$.

(a) $A \oplus B = \{a + b \mid a \in A \text{ and } b \in B\}$.

(b) $A \oplus B = B \oplus A$.

(c) $(A \oplus B) \oplus C = A \oplus (B \oplus C)$.

(d) If $A \subseteq B$, then $A \oplus C \subseteq B \oplus C$.

(e) $A \oplus (B \cup C) = (A \oplus B) \cup (A \oplus C)$.

(f) $A \oplus (B + k) = (A \oplus B) + k$.

27. Prove the following properties of erosion. Suppose $A, B, C \subseteq \mathbb{Z}^2$ and $k \in \mathbb{Z}$.

(a) $A \ominus B = \{d \in \mathbb{Z}^2 \mid d + b \in A \text{ for all } b \in B\}$.

(b) $A \ominus B = \{d \in \mathbb{Z}^2 \mid B_d \subseteq A\}$.

(c) $(A + k) \ominus B = (A \ominus B) + k$.

(d) $A \ominus (B + k) = (A \ominus B) - k$.

(e) If $A \subseteq B$, then $A \ominus C \subseteq B \ominus C$.

(f) $(A \cap B) \ominus C = (A \ominus B) \cap (B \ominus C)$.

(g) If we define $-B$ to be the reflection of the set B, $-B = \{-k \mid k \in B\}$, then we have $(A \ominus B)^c = A^c \oplus (-B)$.

28. Consider the Bayes classifier discriminant that we developed in (4.104):

$$D_k(\boldsymbol{v}) = -\frac{1}{2}(\boldsymbol{v} - \mu_k)^T \Sigma_k^{-1}(\boldsymbol{v} - \mu_k) - \frac{\log(\det(\Sigma_k))}{2} + \log(P(C_k)).$$

The text considered the simplifications brought from assuming that the feature vectors $\boldsymbol{v}$ are statistically independent and have equal variances. What simplification, if any, results from assuming simple statistical independence? Explain.

29. Let $x(n) = [..., \underline{0}, 1, 1, 2, 1, 2, 1, 0, 1, 2, 2, 1, 0, 1, 1, 0, ...]$ be a digital signal.

(a) Compute the co-occurrence matrices, P_1, P_2, and P_3, within the interval $0 \leq n \leq 15$.

(b) Compute the energy of values on the main diagonal of P_1, P_2, and P_3, and compare it to the energy of off-diagonal values. How do the two compare? Explain.

(c) What should one expect from co-occurrence matrices P_4, P_5, and P_6?

(d) What differences exist between the co-occurrence matrices computed for a signal with sawtooth features versus a signal with square pulse features?

30. Suppose it is required that an analysis application detect signals containing large-scale, high-magnitude regions of width N separated by low-magnitude regions of width M.

(a) What co-occurrence matrices should be computed? Explain.

(b) Describe an algorithm using these co-occurrence matrices that meets the application's needs.

(c) How do different values of M and N affect the algorithm?

31. Suppose that $f(n) = A\cos(2\pi\omega n) + B\cos(2\pi\Omega n) + Cr(n)$ is a discrete signal with $A > B > C > 0$, $\Omega > \omega$, and $r(n)$ is uniformly distributed noise. Thus, $f(n)$ consists of a sinusoidal roughness component, $A\cos(2\pi\omega n)$, and a waviness component, $B\cos(2\pi\Omega n)$.

(a) Explore the feasibility of using a co-occurrence matrix method to detect waviness versus roughness in $f(n)$. Propose and explain such an algorithm. For what time intervals, δ, does the algorithm calculate P_δ? How are the entries of the P_δ used to discover the waviness and roughness within $f(n)$?

(b) How can the size of the P_δ matrices be kept small?

(c) Explain whatever assumptions you must make on ω, Ω, A, B, and C so that the proposed algorithm works.

32. Consider a discrete signal $x(n) = x_a(nT)$, where $T > 0$ is the sampling interval.

(a) Expand $x(1)$, $x(2)$, $x(-1)$, and $x(-2)$ in terms of the Taylor series of $x_a(t)$, and show that the system with impulse response $h(n) = [-1/12, 2/3, \underline{0}, -2/3, 1/12]$ is a first-derivative operation on signals.

(b) Similarly, show that $g(n) = [-1/12, 4/3, \underline{-5/2}, 4/3, -1/12]$ is a second-derivative operator on signals.

33. Consider an application that extracts and labels feature vectors of input signals, then compares them to labeled feature vectors derived from a library of prototype signals.

(a) Show that the Hamming distance, $H(u, v)$ between two vectors of labels $\boldsymbol{u} = (\alpha_1, \alpha_2, ..., \alpha_N\}$ and $\boldsymbol{w} = (\beta_1, \beta_2, ..., \beta_N\}$ is a metric.

(b) Consider the Levenshtein distance, $L(\boldsymbol{u}, \boldsymbol{v})$, defined as the total number of substitutions into $\boldsymbol{u}$ and transpositions of components of $\boldsymbol{u}$ necessary to convert $\boldsymbol{u}$ into $\boldsymbol{v}$. Prove or disprove: $L(\boldsymbol{u}, \boldsymbol{v})$ is a metric.